



Sensitivity Analysis applied to a *Listeria monocytogenes* exposure assessment model

M. Ellouze, Jean-Pierre Gauchi, J.C. Augustin

► To cite this version:

M. Ellouze, Jean-Pierre Gauchi, J.C. Augustin. Sensitivity Analysis applied to a *Listeria monocytogenes* exposure assessment model. 6th. International Conference Predictive Modeling in Foods, Sep 2009, Washington, United States. hal-02756464

HAL Id: hal-02756464

<https://hal.inrae.fr/hal-02756464>

Submitted on 3 Jun 2020

HAL is a multi-disciplinary open access archive for the deposit and dissemination of scientific research documents, whether they are published or not. The documents may come from teaching and research institutions in France or abroad, or from public or private research centers.

L'archive ouverte pluridisciplinaire **HAL**, est destinée au dépôt et à la diffusion de documents scientifiques de niveau recherche, publiés ou non, émanant des établissements d'enseignement et de recherche français ou étrangers, des laboratoires publics ou privés.

Table of Contents

Extended Abstracts 6th ICPMF

Technical Session 1

New Applications and Neural Networks - Part 1

- 1 General regression neural network model for growth of *Salmonella* serotypes on chicken skin for use in risk assessment
- 2 Design of challenge testing experiments to assess the variability of microbial behaviors in foods
- 3 Flexible querying of Web data for predictive modeling of risk in food
- 4 An integrated model for predictive microbiology and simultaneous determination of lag phase duration and exponential growth rate. ~~(not submitted)~~
- 5 An artificial neural networks approach for the rapid detection of the microbial spoilage of beef fillets based on Fourier Transform Infrared Spectroscopy data
- 6 Concept for the implementation of a generic model for remaining shelf life prediction in meat supply chains

Technical Session 2

Yeast, Mold and Spoilage Modeling

- 7 Modeling the effect of temperature and water activity on the growth boundaries of *Byssoschlamys fulva*
- 8 Distributions of the germination time of *Aspergillus flavus*, *Penicillium expansum* and *P. chrysogenum conidia* depend on storage conditions (not submitted)
- 9 Modeling the growth/no growth interface of *Zygosaccharomyces bailii* in a viscoelastic food model system

10 Development of a model describing the effect of temperature and (gel) structure on ochratoxin A production by *Aspergillus carbonarius* in liquid media and validation

11 The Quasi-Chemical Model to *Saccharomyces cerevisiae* in co-culture with *Lactobacillus fermentum* in sugar cane must (not submitted)

12 Development of a product specific model for spoilage of pasteurized fruit juices by *Saccharomyces cerevisiae* and validation under dynamic temperature conditions

Technical Session 3

Lag phase, growth and growth/no growth

13 Growth of *Cronobacter* spp. under dynamic temperature conditions occurring during cooling of reconstituted powdered infant formula (not submitted)

14 Modeling lag time of *Bacillus cereus* spore growth after heat treatment

15 Exploring lag phase and growth initiation of a yeast culture by means of an individual based model

16 Effects of temperature adaptation during growth or sporulation on heat resistance of *Bacillus cereus* spores

17 Comparative evaluation of growth/no growth interface of *Listeria monocytogenes* growing on stainless steel surfaces or in suspension, in response to pH and NaCl

18 Modeling the effect of acid and osmotic shifts from growth to no growth conditions and vice versa on the adaptation and growth of *Listeria monocytogenes*

19 Individual cells lag time distributions of *Enterobacter sakazakii*

20 Studying the growth boundary and subsequent growth kinetics of *Escherichia coli* at different temperatures, pH and water activity levels

21 Prediction of time to growth of *Bacillus cereus* in egg as a function of lysozyme, nisin and mild heat treatment.

Technical Session 4

Mechanistic Modeling and Systems Biology

22 Detection of a local contamination within a batch of food by random or systematic sampling (not submitted)

23 Assigning distributions representing variability and uncertainty to microbiological contamination data

24 Robustness analysis of an individual based model for microbial growth: outcomes and insights

25 A hierarchical Bayesian model to estimate the growth of *Listeria monocytogenes* and natural flora in minced tuna

26 Identification of complex microbiological dynamic systems by nonlinear filtering

27 Modelling the influence of free fatty acids on heat resistance of *Bacillus cereus* spores

28 Effect of the growth environment on the strain variability of *Salmonella enterica* kinetic behavior (not submitted)

29 Predicting microbial inactivation and the correlating intracellular pH under salt and acid stress (not submitted)

Technical Session 5

Application of models to food commodities (e.g. seafood, meat, produce, beverages) - Part 1

30 Quantification of inhibition of *Listeria monocytogenes* by organic acids/pH relevant to semi-hard Dutch cheese (not submitted)

31 Modelling microbial competition in foods. Application to the behaviour of *Listeria monocytogenes* and lactic acid flora in diced bacon

32 Determination of the kinetic parameters for *Campylobacter jejuni* under dynamic conditions. (not submitted)

- 33 Bayesian modelling of *Clostridium perfringens* growth in food products
- 34 Introducing a zero-modified negative binomial regression for estimating the effect of chilling on *Escherichia coli* counts from Irish beef carcasses
- 35 Use of fish shelf life prediction (FSLP) software for monitoring fresh turbot quality in the logistic chain
- 36 Probabilistic modeling of *Listeria monocytogenes* behaviour in diced bacon along the manufacture process chain

Technical Session 6

New Applications and Neural Networks - Part 2

- 37 The effect of singular and duplicate plating on the accuracy of estimating low numbers of micro-organisms in food (not submitted)
- 38 Estimating undetectably low post-pasteurization recontamination levels of milk with pathogens using surrogate microbial variables (not submitted)
- 39 Detection and identification of Acid-Lactic bacteria in an isolated system with near-infrared spectroscopy and multivariate regression modeling
- 40 Empirical meta-modelling of *Salmonella Typhimurium* at the farm level of the pork production chain
- 41 Application of network science to analyse the proteome of *Escherichia coli* during the lag phase under acid stress (not submitted)
- 42 Is the Bigelow z-concept consistent with non-log-linear inactivation models? (not submitted)
- 43 Memory embedded structures of artificial neural networks: limitations and constraints in predictive modeling in foods

Technical Session 7

Application of models to food commodities (e.g. seafood, meat, produce, beverages) - Part 2

- 44 Development and validation of predictive models for the growth and survival of *Vibrio vulnificus* in post harvest shellstock oysters

45 Development of predictive models for *Listeria monocytogenes* in selected refrigerated ready-to-eat foods

46 Modelling the kinetics of *Listeria monocytogenes* on frankfurters and other ready-to-eat meat products from manufacturing to consumption.

47 Predicting growth and growth boundary of *Listeria monocytogenes*-an international validation study with processed meat and seafood products

48 Predicting *Staphylococcus aureus* in the dairy chain

49 Introducing stochasticity in predictive modelling of *Salmonella Typhimurium* at the farm level of the pork production chain

50 The potential of end-products metabolites on predicting the shelf life of minced beef stored under aerobic and modified atmosphere with or without the effect of essential oils

Technical Session 8

Cross-Contamination; Microbial Competition Modeling; Model Performance and Validation - Miscellaneous

51 Risking more by modelling cocktail or strain?

52 Mathematical modeling the cross-contamination of food pathogens on the surface of ready-to-eat meats while slicing

53 Modelling the response of the kinetics of the arginine deaminase pathway of *Lactobacillus sakei* CTC 494 to acid stress

54 Comparison of two optical density methods and plate counts for growth parameter estimation (not submitted)

55 Relationship between cellular esterase activity and physiological state of stressed *Listeria monocytogenes* cells

Technical Session 9

Risk Assessment

56 Application of risk evaluation techniques to achieve a food safety objective for *Listeria monocytogenes* and *Salmonella* spp. in a ready-to-eat meat

57 The use of meta-analytical tools in risk assessment modeling for food safety

58 A preliminary consumer risk assessment model of Salmonella in Irish pork sausages: transport and home refrigeration modules

59 Predictive microbiology models vs. modeling microbial growth within *Listeria monocytogenes* risk assessments: What gap? What impact?

60 Sensitivity analysis applied to a *Listeria monocytogenes* exposure assessment model

61 Developing a predictive model for quantifying the risk associated with in-factory *Listeria monocytogenes* recontamination and to identify suitable management options to reduce it.

62 Development of an online predictive modeling resource for food safety risk analysis decision making

63 Accounting for diversity of food borne pathogens. Cardinal growth parameters of the *Bacillus cereus* genetic groups and consequences for risk assessment

64 A mathematical risk model for *Escherichia coli* O157:H7 cross-contamination of lettuce during processing

65 Use of time temperature indicators as a risk management tool for *Listeria monocytogenes* in ready-to-eat foods (not submitted)

Technical Session 10

Non-Thermal and Thermal Inactivation

66 Application of QMRA to go beyond safe harbors in thermal processes. Part 1: introduction and framework

67 Application of QMRA to go beyond safe harbors in thermal processes. Part 2: quantification and examples

68 Quantification of the effect of culturing temperature on the salt-induced heat resistance of mesophilic and psychrotolerant *Bacillus* strains (not submitted)

69 Estimating probability of undetected failure of pasteurization process control using Fault Tree Analysis (not submitted)

70 microbiology approach for thermal inactivation of Hepatitis A Virus in acidified berries

71 The Enhanced Quasi-chemical Kinetics Model for the Inactivation of *Bacillus amyloliquefaciens* by High Pressure Processing (HPP) (not submitted)

72 The effect of pre-acid shock in the induced heat resistance of *Escherichia coli* K12 at lethal temperatures

73 Modeling the combined effect of osmotic dehydration, nisin and modified atmosphere packaging on the shelf life of chilled gilthead seabream fillets (11)

74 Modelling the inactivation of *Listeria monocytogenes* and enzymes in mussel using high pressure processing (not submitted)

75 Application of kinetic models to describe heat inactivation of selected New Zealand isolates of *Campylobacter jejuni* (not submitted)

Technical Session 11

Applications of Predictive Modeling in Food Industry

76 Testing the Gamma hypothesis for two different hurdles, pH and undissociated acid concentration, using *Bacillus cereus* F4810/72 (not submitted)

77 Development and use of Microbiological spoilage models by the food industry (21)

78 Biological time temperature indicators as quality indicators of refrigerated products (34)

79 The importance of growth/no growth models for specific spoilage organisms within the food industry

80 SSSP version 3.1 from 2009: new freeware to predict growth of *Listeria monocytogenes* for a wide range of environmental conditions

81 Evaluation of the microbial growth for different transport conditions of warm raw pork carcasses

82 Monte Carlo simulation for the prediction of vitamin C and shelf-life of pasteurised orange juice (not submitted)

Posters

83 Predictive modelling of *Escherichia coli* O157:H7 cross contamination during slaughter operations.

84 Evaluation of primary models to predict microbial growth by plate count and absorbance methods

85 A predictive model for the effect of temperature and water activity on the growth of pseudomonads in osmotically pretreated gilthead seabream fillets

86 Quantification of the effect of factors involved in challenge-test assays on the growth rate estimation of *Listeria monocytogenes*

87 Modeling chlorine resistance of *Penicillium expansum* in aqueous solutions (non submitted)

88 Predicting the growth of *Salmonella enterica* in fresh cilantro (not submitted)

89 Dynamic modelling of *Listeria monocytogenes* growth in vacuum packed cold smoked salmon. (not submitted)

90 Dynamic models for growth of *Salmonella* in ground beef and chicken at temperatures applicable to the cooking of meat.

91 Mathematical modeling for predicting the growth of *Listeria monocytogenes* during ripening and storage of Camembert type cheese (not submitted)

92 Using ComBase Predictor and Pathogen Modeling Program as support tools in outbreak investigation: an example from Denmark

93 Influence of sporulation conditions upon the heat resistance of *Bacillus coagulans* ATCC 7050 (not submitted)

94 Variability analysis of microbial inactivation after heat treatments and the survivor lag phase (not submitted)

95 Model for *Listeria monocytogenes* inactivation on dry cured ham by high hydrostatic pressure processing

96 Simulation of human exposure to mycotoxins in dairy milk

97 Predicting the lag phase of *Listeria monocytogenes* in fluctuating environmental conditions (not submitted)

98 Validation of predictive models for the growth and survival of total *Vibrio parahaemolyticus* in post harvest shellstock Asian oysters

99 Sampling plan optimisation: application to French diced bacon industry and *Listeria monocytogenes*

- 100 Comparative modeling study of the effect of ozone flow rate and concentration on the colour degradation of orange juice.
- 101 Probability of survival and/or growth of *Listeria monocytogenes* cells exposed to heat-shock and essential oils treatments and proteomic analysis.
- 102 A predictive model for evaluating the effects of cultivation and farm-level processing on oat β -glucan levels
- 103 A Weibull model to describe the effect of ethanol vapours on inactivation of dry harvested conidia of some *Penicillium* (not submitted)
- 104 A simple and economical dialysis method for modulation of water activity (not submitted)
- 105 Prediction of food spoilage by protease activity or lipase synthesis (not submitted)
- 106 Modelling growth of *Penicillium expansum* and *Aspergillus niger* under dynamic temperature conditions (not submitted)
- 107 Growth model of a *Yersinia* species in raw ground beef
- 108 Modelling the transport of *Salmonella* into whole-muscle meat products during marination and the subsequent lethality during thermal processing
- 109 Effect of the temperature on the inhibition of *Escherichia coli* and *Listeria monocytogenes* by lactic acid bacteria
- 110 Effects of citral, carvacrol and (E)-2-hexenal on growth inactivation of *Listeria monocytogenes* during heat treatment
- 111 Evaluation of growth boundary models - importance of data distribution and performance indices
- 112 Biological significance of predictive models for moulds (not submitted)
- 113 Validation of a predictive model for the effect of water activity and temperature on growth of *Botrytis cinerea* and *Penicillium expansum* on table grapes (not submitted)
- 114 Predictive model for growth of *Clostridium perfringens* during cooling of cooked uncured meat and poultry

115 Reconciliation of the population risk with the risk per serving in determining food safety objectives (not submitted)

116 Fatty acids composition of Polish commercial cakes as assessed by standard methods or by FT-IR spectroscopy

117 Modelling aspects of orange juice quality kinetics during ultrasound processing

General regression neural network model for growth of *Salmonella* serotypes on chicken skin for use in risk assessment

T.P. Oscar¹

¹ U.S. Department of Agriculture, Agricultural Research Service, Microbial Food Safety Research Unit, Room 2111, Center for Food Science and Technology, University of Maryland, Eastern Shore, Princess Anne, MD (thomas.oscar@ars.usda.gov)

Abstract

The objective of the present study was to develop a general regression neural network (GRNN) and Monte Carlo simulation model for growth of *Salmonella* on chicken skin with native flora and as a function of serotype, temperature and time for use in risk assessment. Poultry isolates of *Salmonella* with natural resistance to antibiotics were used to investigate and model growth from a low initial dose (0.78 to 0.95 logs) on chicken skin with native flora. Computer spreadsheet and spreadsheet add-in programs were used to develop and simulate a GRNN model. Model performance was evaluated by determining the percentage of residuals in an acceptable prediction zone from -1 log (fail-safe) to 0.5 logs (fail-dangerous). The GRNN model had an acceptable prediction rate of 92% for dependent data ($n = 464$) and an acceptable prediction rate of 89% for independent data ($n = 116$), which exceeded the performance criterion for model validation of 70% acceptable predictions. Differences among serotypes were observed with Kentucky exhibiting less growth than Typhimurium and Hadar, which had similar growth. Temperature abuse scenarios were simulated to demonstrate how the GRNN model can be integrated with risk assessment.

Keywords

Risk assessment, neural network, Monte Carlo simulation, predictive model, *Salmonella*, growth, chicken skin, strain variation.

Introduction

Salmonella are a leading cause of gastroenteritis and are often isolated from poultry (Bryan and Doyle 1995). There are over 2,300 serotypes of *Salmonella* yet only about 50 are responsible for most cases of gastroenteritis (Foley *et al.* 2008). The top three serotypes isolated from chickens are Enteritidis, Kentucky and Typhimurium. Variation of growth among serotypes of *Salmonella* has been observed (Fehlhaber and Kruger 1998; Oscar 1998). However, whether growth of Kentucky differs from other serotypes of *Salmonella* has not been reported. Performance of predictive models can be improved by using better-fitting models. It has been reported that general regression neural network (GRNN) models outperform regression models and other types of neural network models in predictive microbiology applications (Jeyamkondan *et al.* 2001; Palanichamy *et al.* 2008). With the advent of commercial software applications that perform GRNN modelling, it is now easy to use GRNN modelling in predictive microbiology studies. Moreover, GRNN modelling software is compatible with Monte Carlo simulation software. Thus, it is possible to create GRNN models that use Monte Carlo simulation to model uncertainty and variability of independent variables. Output distributions from such models can be used in risk assessment. The objective of the present study was to develop a GRNN model that employs Monte Carlo simulation to provide stochastic predictions of *Salmonella* growth from a low initial dose on raw chicken skin with native flora as a function of serotype (Typhimurium, Kentucky, Hadar), temperature (5 to 50°C) and time (0 to 8 h) for use in risk assessment.

Materials and Methods

Isolates of *Salmonella* serotypes Typhimurium, Kentucky, and Hadar were obtained from poultry. Typhimurium was resistant to chloramphenicol (C), ampicillin (A), tetracycline (T) and streptomycin (S). Kentucky was resistant to novobiocin (N), A, T and S. Hadar was

resistant to T, sulfasoxazole (U), gentamicin (G), and S. Xylose lysine tergitol 4 base agar medium without tergitol (XL) but supplemented with 25 mM HEPES (H) and 25 µg per ml of C, A, T, S, N, U or G was used for enumeration. A full 3 x 10 x 5 x 2 x 2 factorial arrangement of serotype (Typhimurium, Kentucky, Hadar), temperature (5, 10, 15, 20, 25, 30, 35, 40, 45, 50°C), time (0, 2, 4, 6, 8 h), trial (1, 2), and sample (a, b) was used for model development. Replicate trials were conducted in separate weeks with different batches of chicken skin. Chicken thigh skin portions (~0.25 g) were spot inoculated (5 µl) with an initial log number of 0.95 for Typhimurium, 0.78 for Kentucky and 0.91 for Hadar. Pulsified samples (skin portion + 9 ml buffered peptone water; BPW) were used for enumeration. A combination three-tube MPN and spiral plating method with XLH-CATS for Typhimurium, XLH-NATS for Kentucky, and XLH-TUGS for Hadar was used for *Salmonella* enumeration (Oscar 2006). A dataset was created in an Excel spreadsheet with separate columns for serotype (independent categorical variable), temperature (independent numerical variable), time (independent numerical variable) and log number (dependent variable). A GRNN model was trained by the method of Specht (1991) using Neural Tools software. Eighty percent of data were used for training and 20% were used for testing. Percentage of residuals in an acceptable prediction zone from -1 log ('fail-safe') to 0.5 logs ('fail-dangerous') with an acceptable prediction rate criterion of 70% was used for model validation (Oscar 2006). A discrete distribution was used to model serotype prevalence, whereas pert distributions were used to model temperatures and times of abuse. The GRNN model was simulated with @Risk settings of Latin Hypercube sampling, 10³ iterations, and a correlation between temperature and time of 0 or -1. The best-fitting distributions for output data (log change) were determined using the Chi-square statistic within the BestFit function of @Risk.

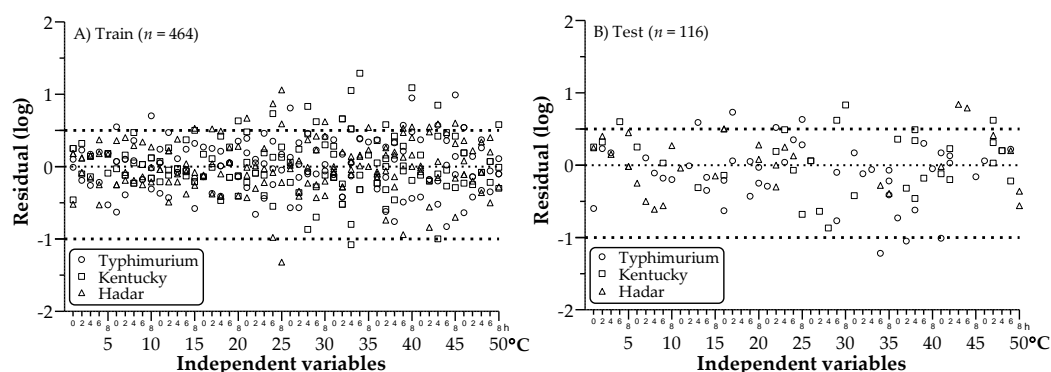


Figure 1. Residual plots for A) dependent data for training and B) independent data for testing model performance. Residuals were sorted by temperature and then time in ascending order. Major ticks correspond to temperature and 8 h of incubation whereas minor ticks to the left of major ticks correspond to incubation times of 0, 2, 4 and 6 h, respectively, for the temperature indicated on the major tick. Lower and upper dashed lines are boundaries of the acceptable prediction zone.

Results

The GRNN model was trained on 464 data points and had an acceptable prediction rate of 91.8%. There were no signs of systematic prediction bias as a function of serotype, temperature or time (Figure 1a). When tested against independent data ($n = 116$; Figure 1b), the GRNN model had an acceptable prediction rate of 88.8% and did not exhibit systematic prediction bias as a function of independent variables. Thus, the model was validated because its acceptable prediction rates for dependent and independent data exceeded 70%.

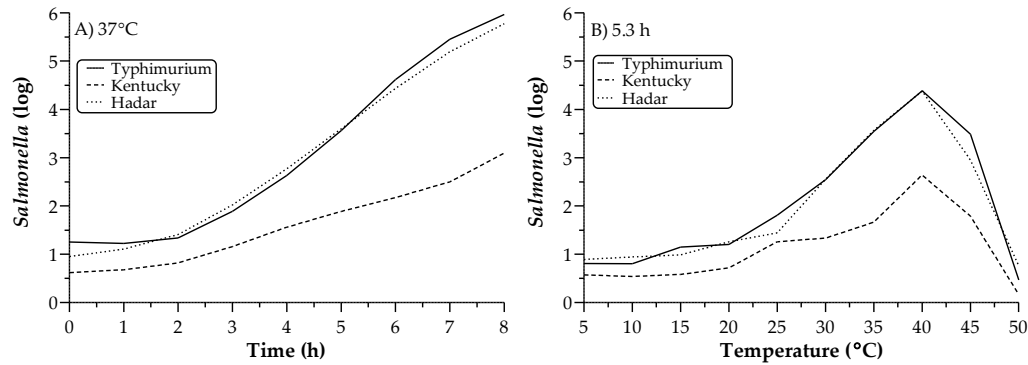


Figure 2. Output graphs from the general regression neural network model for growth of *Salmonella* on raw chicken skin as a function of A) time at 37 °C and B) temperature at 5.3 h.

The GRNN model predicted the log number of *Salmonella* for temperatures and times that were and were not investigated but that were within ranges of independent variables used in model development (e.g. Figure 2). Overall, Kentucky exhibited less growth than Typhimurium and Hadar, which had similar growth on raw chicken skin with native flora.

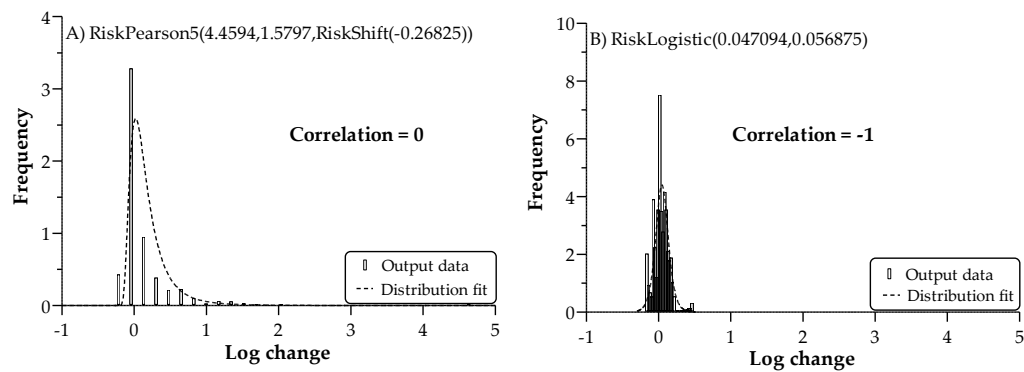


Figure 3. Output data and best-fit distributions from the general regression neural network and Monte Carlo simulation model for growth of *Salmonella* on raw chicken skin.

Temperature abuse scenarios were simulated to demonstrate how the GRNN model can be integrated with risk assessment. Examples of output distributions from the GRNN model that can be used as input distributions in a risk assessment model are shown in Figure 3.

Discussion

Accurate and unbiased predictions of pathogen growth are needed to safeguard public health. Models that under-predict pathogen growth result in consumption of unsafe food, whereas models that over-predict pathogen growth result in destruction of safe food, which is not desirable. Most studies in predictive microbiology use a mixture of pathogen strains for model development. The idea is that this will result in a ‘fail-safe’ model because the fastest-growing strain will predominate under the conditions tested. However, models developed with a cocktail of strains could be overly ‘fail-safe’. For example, if the current model had been developed with a cocktail of Typhimurium, Kentucky and Hadar, the faster-growing serotypes Typhimurium and Hadar would have predominated and the resulting model would have over-predicted growth of *Salmonella* on raw chicken skin contaminated with the slower-growing serotype Kentucky. Thus, by developing models with individual strains and then modelling growth as a function of serotype prevalence, more accurate predictions are obtained.

Models in predictive microbiology are usually developed in three stages (primary, secondary and tertiary) using regression methods. Limitations of this approach are that it is time consuming, requires significant training in regression analysis and uses regression models that are inflexible. Neural network modelling overcomes limitations of regression modelling as it is fast, requires only a basic understanding of the method, is flexible and outperforms regression modelling in predictive microbiology applications (Garcia-Gimeno *et al.* 2003; Hajmeer *et al.* 1997; Jeyamkondan *et al.* 2001; Palanichamy *et al.* 2008). The latter studies all used regression for primary modelling and neural networks for secondary modelling. In the present study, a general regression neural network was used in one-step for primary, secondary and tertiary modelling and the resulting model had acceptable and high performance (ca. 90% acceptable predictions). Thus, it does not seem necessary to use regression modelling in tandem with neural network modelling when neural network modelling is capable of developing predictive models in one-step at a considerable savings in time, effort and performance.

Risk assessment provides stochastic predictions of the risk of adverse health outcomes from food produced by different farm-to-table scenarios. Predictive models are used in risk assessment to provide stochastic predictions for individual pathogen events, such as growth. Consequently, the GRNN model developed in this study was configured for risk assessment by using Monte Carlo simulation in tandem with GRNN modelling software to provide stochastic predictions of *Salmonella* growth.

Conclusions

In the current study, a GRNN and Monte Carlo simulation model was developed and validated for making stochastic predictions of *Salmonella* growth from a low initial dose on raw chicken skin as a function of serotype, temperature and time and thus, the models' predictions can be used with confidence in risk assessment. However, because parameters of the GRNN model are not provided by the commercial software application, deployment of the model might be limited by the requirement that users possess the commercial software used to run and simulate the model and make predictions.

Acknowledgements

The author appreciates the outstanding assistance of Jacquelyn Ludwig (Agricultural Research Service) and Celia Whyte and Olabimpe Olojo (University of Maryland, Eastern Shore).

References

- Bryan, F.L. and Doyle, M.P. (1995) Health risks and consequences of *Salmonella* and *Campylobacter jejuni* in raw poultry. *Journal of Food Protection*, 58, 326-344.
- Fehlhaber, F. and Kruger, G. (1998) The study of *Salmonella enteritidis* growth kinetics using Rapid Automated Bacterial Impedance Technique. *J. Appl. Microbiol.*, 84, 945-949.
- Foley, S.L., Lynne, A.M. and Nayak, R. (2008) *Salmonella* challenges: prevalence in swine and poultry and potential pathogenicity of such isolates. *J. Anim. Sci.*, 86, E149-E162.
- Garcia-Gimeno, R.M., Hervas-Martinez, C., Barco-Alcala, E., Zurera-Cosano, G. and Sanz-Tapia, E. (2003) An artificial neural network approach to *Escherichia coli* O157:H7 growth estimation. *Journal of Food Science*, 68, 639-645.
- Hajmeer, M.N., Basheer, I.A. and Najjar, Y.M. (1997) Computational neural networks for predictive microbiology II. Application to microbial growth. *International Journal of Food Microbiology*, 34, 51-66.
- Jeyamkondan, S., Jayas, D.S. and Holley, R.A. (2001) Microbial growth modelling with artificial neural networks. *International Journal of Food Microbiology*, 64, 343-354.
- Oscar, T.P. (1998) Growth kinetics of *Salmonella* isolates in a laboratory medium as affected by isolate and holding temperature. *Journal of Food Protection*, 61, 964-968.
- Oscar, T.P. (2006) Validation of a tertiary model for predicting variation of *Salmonella* Typhimurium DT104 (ATCC 700408) growth from a low initial density on ground chicken breast meat with a competitive microflora. *Journal of Food Protection*, 69, 2048-2057.
- Palanichamy, A., Jayas, D.S. and Holley, R.A. (2008) Predicting survival of *Escherichia coli* O157:H7 in dry fermented sausage using artificial neural networks. *Journal of Food Protection*, 71, 6-12.
- Specht, D.F. (1991) A general regression neural network. *IEEE Trans. Neural. Netw.*, 2, 568-576.

Design of challenge testing experiments to assess the variability of microbial behaviors in foods

J.-C. Augustin¹, H. Bergis², G. Bourdin³, M. Cornu², O. Couvert⁴, C. Denis⁵, V. Huchet⁶, S. Lemonnier⁵, A. Pinon⁷, M. Vialette⁷, V. Zuliani⁸ and V. Stahl⁹

¹ Unité MASQ, Ecole Nationale Vétérinaire d'Alfort, 7 Avenue du Général de Gaulle – F-94704 Maisons-Alfort Cedex, France (jcaugustin@vet-alfort.fr)

² Microbiologie quantitative et estimation des risques (MQER), Agence française de sécurité sanitaire des aliments (Afssa), 23 avenue du Général de Gaulle – F-94706 Maisons-Alfort Cedex, France (m.simon-cornu@afssa.fr)

³ Agence française de sécurité sanitaire des aliments (Afssa), LERPPE, rue Huret Lagache – F-62200 Boulogne Sur Mer, France (g.bourdin@boullogne.afssa.fr)

⁴ Cellule opérationnelle Sym'Previus, ADRIA Développement, Creac'h Gwen, F-29196 Quimper Cedex, France (olivier.couvert@adria.tm.fr)

⁵ ADRIA Normandie, boulevard du 13 juin 1944, F-14310 Villers-Bocage, France (cdenis@adrianie.org)

⁶ ADRIA Développement, Creac'h Gwen, F-29196 Quimper Cedex, France (veronique.huchet@adria.tm.fr)

⁷ Institut Pasteur de Lille, 1 rue du Professeur Calmette, BP 245, F-59019 Lille Cedex, France (anthony.pinon@pasteur-lille.fr)

⁸ Ifip Institut du porc, 7 avenue du Général de Gaulle, F-94704 Maisons-Alfort Cedex, France (veronique.zuliani@ifip.asso.fr)

⁹ Aerial, Parc d'Innovation, F-67412 Illkirch, France (v.stahl@aerial-crt.com)

Abstract

The assessment of the evolution of microorganisms naturally contaminating food must take into account the variability of biological factors, food characteristics and storage conditions. A research project involving eight French laboratories was conducted to quantify the variability of growth parameters of *Listeria monocytogenes* obtained by challenge testing in five foods. The residual variability corresponded to a coefficient of variation (CV) of approximately 20% for the growth rate (μ_{\max}) and 120% for the parameter K ($=\mu_{\max}$.lag time). The between batches and between manufacturers variability was very dependent on the food tested and the CV of μ_{\max} ranged from 0 to 80%. The initial physiological state variability led to a CV of 110% for the factor K . It appeared that repeating a limited number of challenge tests in different batches/manufacturers for different initial physiological states is often sufficient to assess the variability of the behavior of *L. monocytogenes* in a given food.

Keywords

Exposure assessment, biological variability, challenge testing, *Listeria monocytogenes*

Introduction

The assessment of the evolution of microorganisms that naturally contaminate food must take into account the variability of factors influencing the microbial behavior, i.e., biological factors, physico-chemical and microbial food characteristics, and storage conditions. The probabilistic software developed in the Sym'Previus project was designed to easily perform microbial exposure assessment and to combine the different source of variability with primary and secondary predictive microbiology models (Couvert et al., 2007). The biological variability of bacterial cardinal values is already set in the software but the variability of growth parameters, initial contamination, food characteristics and storage conditions must be specified by the users. It is really challenging to specify the variability of maximum growth rate and lag time of naturally contaminating microorganisms. The estimation of these parameters in natural conditions of contamination is generally impossible for pathogenic microorganisms and operators must usually perform challenge testing. A research project involving eight French laboratories was conducted to quantify the variability of growth parameters of *L. monocytogenes* obtained by challenge testing in five different foods. The objective was to evaluate the impact of within and between batches variability, between manufacturers variability, and microbial initial physiological state variability, on the

variability of the growth parameters to optimize the challenge testing methodology applied when evaluating the variability of the behavior of microorganisms in foods.

Materials and Methods

The following foods were studied: *i*) pâté from one batch, *ii*) smoked herring from four batches of two manufacturers, *iii*) cooked ham from seven batches and three manufacturers, *iv*) cooked chicken belonging to two batches of one manufacturer, and *v*) surimi salad from different batches of one manufacturer.

Each food was studied by two or three laboratories and was artificially contaminated with exponentially growing or starved cells of one strain of *L. monocytogenes* in order to evaluate the impact of physiological state on the growth parameters. Contaminated food samples were stored at 8°C and enumerations of *L. monocytogenes* were performed on three samples at approximately 10 different times during the lag, the exponential and the stationary phases of the growth curve. Some experiments were replicated with the same batch of food, the same physiological state and the same laboratory to estimate the residual variability of growth parameters. pH and water activity (a_w) of foods were measured by laboratories to characterize the variability of physico-chemical characteristics of studied foods.

The maximum specific growth rate (μ_{\max}) and the lag time (*lag*) were estimated for each growth curve by fitting the logistic with delay growth model (Pinon et al., 2004). In a second time, the variability of μ_{\max} and of the product $K=\mu_{\max}\cdot lag$ representing the initial physiological state of contaminating cells was analyzed in order to determine the impact of the studied factors. Growth simulations were performed with the probabilistic software of Sym'Previus to combine the different variability sources in order to predict the growth curves of *L. monocytogenes* or the probabilities to exceed given concentrations in foods.

Results and Discussion

The residual variability of μ_{\max} was almost constant and a coefficient of variation (CV) of 20% was observed on average (Table 1). This variability was not explained by the variability of measured physico-chemical parameters since simulations performed for the species *L. monocytogenes* (12 strains) by only taking into account the observed variability of pH and a_w of studied foods generated less variability for μ_{\max} than the observed one (Table 1). This variability could then be linked to the variability of other not measured food characteristics or to the measurement uncertainty of μ_{\max} when performing challenge testing. This result is not surprising since Baranyi and Roberts (1995) described repeatability standard errors of approximately 10% of the estimated growth rate in synthetic media. On the contrary, the residual variability of K was more pronounced and more variable with a mean CV of 120% (Table 1). This great variability of K can be easily explained by the difficulty for laboratories to experimentally reproduce specific bacterial physiological states. Since the residual variability of μ_{\max} and K was relatively large, no significant effect of the laboratory performing the challenge test was observed for these two parameters.

The between batches and manufacturers effects on μ_{\max} were very variables with CV ranging from 0 to 23% and from 0 to 81%, respectively (Table 1). The variability of K linked to the initial physiological state was relatively constant, which is consistent with the fact that only two physiological states were studied, and the CV was 110% on average.

The growth curves of *L. monocytogenes* generated for each food taking into account the biological variability, the variability of food characteristics and the variability of growth parameters summing the means of residual, between batches, between manufacturers and physiological state variances are shown in Figure 1. For pâté we observed that, the mean residual variability of K being larger than the observed one, the lag time was sometimes overestimated but the predicted behavior was relevant on the whole. For smoked herring, the mean between manufacturers variability lead to an overestimation of the observed variability while for the cooked ham, this mean variability was not sufficient to describe the observed one.

Table 1. Variability sources for growth parameters of *L. monocytogenes*.

| | | | | μ_{\max} | | | | K | |
|----------------|-----------|----------------|-------------|------------------|----------|-------|----------|----------|---------------|
| | pH | a _w | Variability | Physico-chemical | | | Manu- | | Physio- |
| Food | (mean±SD) | (mean±SD) | (CV%) | characteristics | Residual | Batch | facturer | Residual | logical state |
| Pâté | 5.94±0.10 | 0.976±0.004 | Input | — | 16 | ND* | ND | 44 | 115 |
| | | | Output | 9 | 17 | — | — | — | — |
| Smoked herring | 6.37±0.08 | 0.966±0.009 | Input | — | 19 | 23 | 0 | 103 | ND |
| | | | Output | 26 | 32 | 40 | 40 | — | — |
| Cooked ham | 6.08±0.07 | 0.975±0.007 | Input | — | 20 | 0 | 81 | 135 | 103 |
| | | | Output | 15 | 25 | 25 | 75 | — | — |
| Cooked chicken | 6.30±0.19 | 0.974±0.008 | Input | — | 22 | 17 | ND | 141 | 88 |
| | | | Output | 17 | 23 | 29 | — | — | — |
| Surimi salad | 6.30±0.25 | 0.984±0.010 | Input | — | 21 | 0 | ND | 196 | 137 |
| | | | Output | 17 | 26 | 26 | — | — | — |
| Mean input | | | | | 20 | 10 | 41 | 124 | 111 |

* ND not determined.

It seems thus that the residual variability of 20% for μ_{\max} and 120% for K can be used to describe the variability of growth parameters for a given batch and a given physiological state but these parameters are too much varying for between batches and between manufacturers variability. Their impact on growth parameters is thus difficult to predict and several challenge tests are need. Furthermore it is hazardous to set the expected values of growth parameters with only one challenge test.

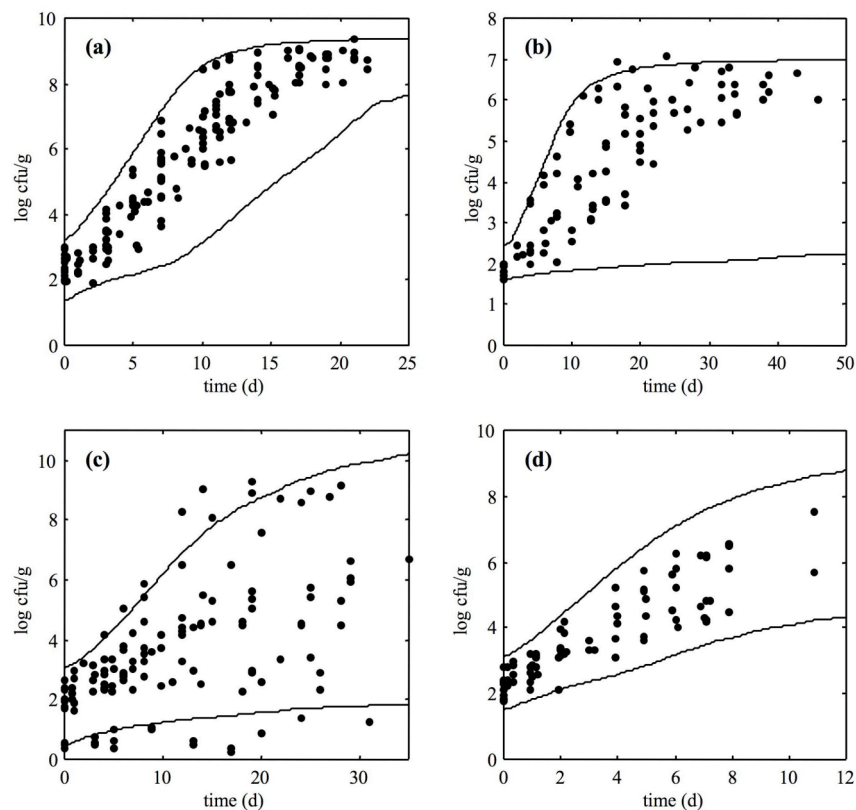


Figure 1. Observed (●) and simulated (95% confidence bands) growth of *L. monocytogenes* at 8°C in (a) pâté, (b) smoked herring, (c) cooked ham, and (d) surimi salad.

Then we proposed to perform three different challenge tests to estimate the expected values and standard deviations of μ_{\max} and K . Depending on the studied factors influencing the growth, the challenge tests can be performed with three different batches or manufacturers and with three different physiological states. The Table 2 reports the results obtained when comparing this approach with the one consisting to use only one challenge test and fixing theoretical variances. The typical prediction errors (MARE) when predicting the probability to exceed a given concentration were lower when three challenge tests were performed and the dispersions of the relative errors (SDRE) were also lower.

Table 2. Mean absolute relative errors (MARE) and standard deviations of relative errors (SDRE) for predictions of probabilities P to exceed given concentrations of *L. monocytogenes* in foods stored at 8°C. The reference probabilities are those obtained by using all the challenge tests performed.

| Food | Variability sources | 1 kinetic | | 3 kinetics | |
|--|--|-----------|----------|------------|----------|
| | | MARE (%) | SDRE (%) | MARE (%) | SDRE (%) |
| Pâté ($P > 7$ log cfu/g 8 days) | residual | 99 | 135 | 60 | 71 |
| Smoked herring ($P > 6$ log cfu/g 15 days) | residual, batch, manufacturer | 63 | 86 | 42 | 41 |
| Cooked ham ($P > 6$ log cfu/g 10 days) | residual, batch, manufacturer, physiological state | 126 | 154 | 35 | 20 |
| Cooked chicken ($P > 6$ log cfu/g 8 days) | residual, batch, physiological state | 55 | 67 | 24 | 14 |
| Surimi salad ($P > 7$ log cfu/g 10 days) | residual, batch, physiological state | 37 | 43 | 4 | – |

Conclusion

The implementation of challenge tests to assess the variability of the growth parameters of foodborne pathogens is a keystone because the impact of the different sources of variability is unpredictable. By reproducing challenge tests in three different conditions it seems possible to satisfactorily evaluate the impact of between batches, between manufacturers and initial physiological state on growth parameters.

Acknowledgements

This work is part of the national research program ACTIA 05.9 and was supported by a grant from ACTIA, the French Ministry of Agriculture and food business operators. This project is part of the National French Technological Network (RMT) “Expertise on determination of food products microbial shelf-life”.

References

- Baranyi J. and Roberts T.A. (1995) Mathematics of predictive food microbiology. *International Journal of Food Microbiology* 26, 199-218.
- Couvert O., Augustin J.-C., Buche P., Carlin F., Coroller L., Denis C., Jamet E., Mettler E., Pinon A., Postollec F., Stahl V., Zuliani V. and Thuault D. (2007) Optimising food process and formulation through Sym'Previous.. 5th International Conference Predictive Modelling in Foods, September 16-19, 2007, Athens, Greece.
- Pinon A., Zwietering M., Perrier L., Membré J.-M., Leporq B., Mettler E., Thuault D., Coroller L., Stahl V. and Vialette M. (2004) Development and validation of experimental protocols for use of cardinal models for prediction of microorganism growth in food products. *Applied and Environmental Microbiology* 70, 1081–1087.

Flexible querying of Web data for predictive modelling of risk in food

P. Buche¹, O. Couvert³, J. Dibie-Barthélemy^{1, 2}, E. Mettler⁴, L. Soler¹

¹INRA, UP 1204 Méthodologies d'analyse du risque alimentaire, F-75005 Paris, France
(buche@paris.inra.fr, dibie@agroparistech.fr, lsoler@paris.inra.fr)

²AgroParisTech, UP 1204 Méthodologies d'analyse du risque alimentaire, F-75005 Paris, France

³ADRIA Développement, Creac'h Gwen, 29196 Quimper Cedex, France (olivier.couvert@adria.tm.fr)

⁴Soredab (Groupe SOPARIND BONGRAIN), La Tremblaye, 78125 La Boissière-Ecole, France
(eric.mettler@soredab.org)

Abstract

A preliminary step to risk in food assessment is the gathering of experimental data. In the framework of the [Sym'Previus project](#), we have designed a complete data integration system opened on the Web which allows a local database to be complemented by data extracted from the Web and annotated using a domain ontology. We propose in this paper a flexible querying system using the domain ontology to scan simultaneously local and Web data in order to feed the predictive modelling tools available on the Sym'Previus platform. Special attention is paid on the way fuzzy annotations associated with Web data are taken into account in the querying process, which is an important originality of the proposed system.

Keywords

Web data, flexible querying, ontology, predictive microbiology

Introduction

A preliminary step to risk in food assessment is the gathering of experimental data (Tamplin et al. 2003, Baranyi and Tamplin 2004, McMeekin et al. 2006). In the framework of the Sym'Previus project (Couvert et al 2007 and <http://www.symprevius.org>), we have designed a complete data integration system opened on the Web which allows a local database (Buche et al. 2005) to be complemented by data extracted from the Web (Hignette et al. 2008). The local data were classified by means of a predefined vocabulary organized in taxonomy, called ontology, which is also used to extract pertinent data from the Web. Our aim is to integrate the data found on the Web with the local data by means of a flexible querying system which allows the end-user to retrieve the nearest local and Web data corresponding to his/her selection criteria. Our solution allows the end-user to query simultaneously and uniformly local and Web data in order to feed the predictive modelling tools available on the Sym'Previus platform. We first remind the semi-automatic annotation method (implemented in the @WEB tool, see [@Web demo](#)) which allows data to be retrieved from data tables found in scientific documents on the Web and to be annotated thanks to the domain ontology. Second, we present the original contribution of the paper, which consists in the design of the flexible querying system, called MIEL++, which permits to query simultaneously the local data and the semantic annotated Web data, in a transparent way to the end-user, thanks to the ontology. This system is flexible because (i) it allows the end-user to express preferences in his/her selection criteria and (ii) it takes into account, in the answers building, the different kinds of fuzziness of the semantic annotated Web data. This second point is essential to deal with the uncertainty of the Web data and with the imperfection of their annotations.

Materials and Methods

The semi-automatic annotation method

Web data have been semi-automatically classified by means of a predefined vocabulary, called ontology. This ontology is composed of data types meaningful in the domain of risk in food and semantic relations linking those data types. Data types are described in two different ways depending on whether their associated values are symbolic (*Food product*, *Microorganism* ...) or numeric (*Temperature*, *Time* ...). Symbolic types are described by

taxonomies of possible values (for example, a taxonomy of microorganisms). Numeric types are described by their possible set of units (for example, °C or °F for *Temperature*, but no unit for *pH* or *a_w*), and their possible numerical range (for example, [0, 14] for *pH*). Semantic relations are defined by a result data type and a set of access types. For example, the relation *GrowthParameterAw*, representing the growth limits of a micro-organism for any food product, has for access type the symbolic type *Microorganism* and for result types the numeric type *a_w*. Our annotation algorithm first annotates the symbolic columns and the numeric columns and then uses these annotations to determine the semantic relations present in the Web table (see Hignette et al. 2008 for more details). Figure 1 shows a part of the RDF graph which represents the annotations associated with the first line of Table 1 extracted from the Web. RDF (Resource Description Framework) is the language recommended by the W3C (World Wide Web consortium) to represent semantic annotations associated with Web resources. A particularity of our RDF annotations is to propose an explicit representation (1) of the similarity between terms of the ontology and terms of the Web and (2) of the imprecision of numerical data, using a homogeneous framework, the fuzzy set theory.

Table 1: Cardinal values.

| Organism | Aw minimum | Aw optimum | Aw maximum |
|----------------|------------|------------|------------|
| Clostridium | 0.943 | 0.95-0.96 | 0.97 |
| Staphylococcus | 0.88 | 0.98 | 0.99 |
| Salmonella | 0.94 | 0.99 | 0.991 |

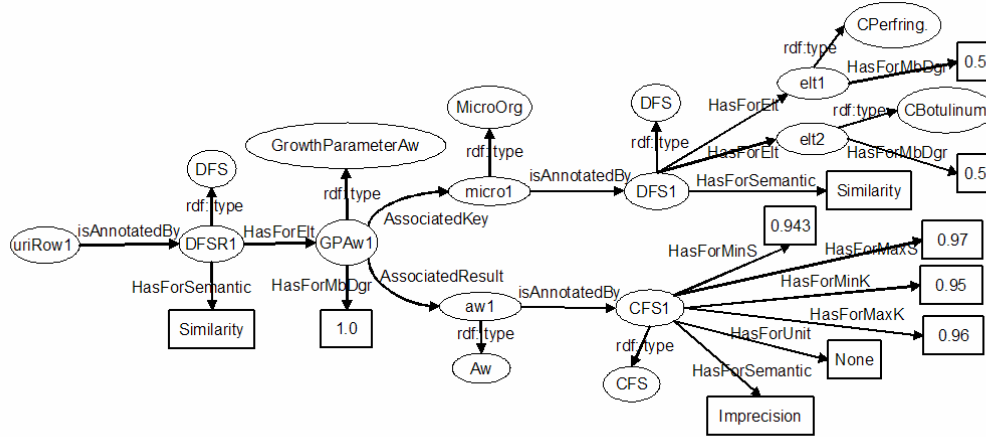


Figure 1: Annotations associated by our algorithm to the first line of Table 1

In Figure 1, the RDF annotation expresses that the row (having the identifier *uriRow1* in the RDF graph) is annotated by a discrete fuzzy set, called *DFS1*. This fuzzy set has a semantic of similarity and indicates the list of closest relations of the ontology recognized in the first row. Only the relation *GrowthParameterAw* belongs to this fuzzy set with the pertinence score of 1.0 which expresses the degree of certainty associated with the relation recognition by our semantic annotation process. The access type of the relation, which is an instance of the symbolic type *Microorganism*, is annotated by a discrete fuzzy set, called *DFS1*. This fuzzy set has a semantic of similarity and indicates the list of closest terms of the ontology compared to the term *Clostridium*. Two terms (*Clostridium Perfringens* and *Clostridium Botulinum*) belong to this fuzzy set with a membership degree of 0.5. The result type of the relation, which is an instance of the numeric type *aw*, is annotated by a continuous fuzzy set, called *CFS1*. This fuzzy set has a semantic of imprecision and indicates the possible growth limits ([0.943, 0.97]) and the possible optimal growth limits ([0.95, 0.96]).

Design of the flexible querying system MIEL++

The MIEL++ querying system relies on the domain ontology used to index the local data and to annotate the Web data. MIEL++ allows the end-user to retrieve the nearest local and Web data corresponding to his/her selection criteria expressed as fuzzy sets and representing his/her preferences. The ontology -more precisely the taxonomies of values associated with

symbolic types- is used in order to assess which data can be considered as “near” to the user’s selection criteria. A query is asked to the MIEL++ system through a single graphical user interface, which relies on the domain ontology. The query is translated into a query expressed in the query language of each data source: an SQL query in the relational local database (see Buche et al. 2005) for more details about the SQL subsystem), a SPARQL query in the RDF graph base. SPARQL is the querying language recommended by the W3C to query semantic annotations expressed in RDF graphs. Finally, the global answer to the query is the union of the local results of the two subsystems, which are ordered according to their relevance to the query selection criteria. In this paper, we focus on three original aspects of the SPARQL querying: (1) the use of the taxonomies of values associated with symbolic types to enlarge the querying, (2) the way comparisons between the user’s selection criteria and fuzzy annotations are done, (3) the total order defined to retrieve the most pertinent data to the user.

Let us consider a MIEL++ query Q expressed in the relation *GrowthParameterAw* and having for selection criteria ($aw=awPreference$) and (*Microorganism=MicroPreferences*). The continuous fuzzy set *awPreferences*, which is equal to $[0.9, 0.94, 0.97, 0.99]$, means that the end-user is first interested in *aw* values in the interval $[0.94, 0.97]$. But he/she accepts to enlarge the querying till the interval $[0.9, 0.99]$. The discrete fuzzy set *MicroPreferences*, which is equal to $\{1.0/Gram+, 0.5/Gram-\}$, means that the end-user is interested in micro-organisms which are first Gram+ and then Gram-. This fuzzy set defines implicitly user’s preferences for micro-organisms which are kinds of Gram+ and Gram-. According to the taxonomy of values associated with the symbolic type *Microorganism*, *Clostridium Botulinum* and *Staphylococcus Spp.* are kind of Gram+ and *Salmonella* is a kind of Gram-. In order to take those implicit preferences into account in the querying, we propose to perform a closure of the fuzzy set *MicroPreferences* (see Thomopoulos et al. 2006 for more details). Intuitively, the closure propagates degrees of preferences to more specific values of the taxonomy. By example, the closure of the fuzzy set *MicroPreferences* is: $\{1.0/Gram+, 0.5/Gram-, 1.0/Clostridium Botulinum, 1.0/Staphylococcus Spp., 0.5/Salmonella\}$.

In order to build the answer, selection criteria representing user’s preferences expressed as fuzzy sets must be compared with fuzzy annotations. But the fuzzy sets used in the annotations have two different semantics. We propose to realise those comparisons separately using two different measures: (i) a possibility degree of matching (noted Π) and a necessity degree of matching (noted N) which are classically used (see Dubois et Prade 1988) to compare a fuzzy set having a semantic of preference with a fuzzy set having a semantic of imprecision and (ii) an adequation degree as proposed in (Baziz et al. 2006) to compare a fuzzy set having a semantic of preference with a fuzzy set having a semantic of similarity.

Let ($a=v$) be a selection attribute of the MIEL++ query Q , v' a fuzzy annotation of the attribute a stored in a RDF graph, sem_v the semantic of v' , μ_v and $\mu_{v'}$ their respective membership functions defined on the domain Dom and cl the function which corresponds to the fuzzy set closure. The comparison result depends on the semantic of the fuzzy set v' . If $sem_v=imprecision$, the comparison result is given by the **possibility degree of matching** between v and v' noted $\Pi(v,v')=\sup_{x \in Dom}(\min(\mu_v(x), \mu_{v'}(x)))$ and the **necessity degree of matching** between v and v' noted $N(v,v')=\inf_{x \in Dom}(\max(\mu_v(x), 1 - \mu_{v'}(x)))$. If $sem_v=similarity$, the comparison result is given by the **adequation degree** between $cl(v)$ and $cl(v')$ noted $ad(cl(v), cl(v'))=\sup_{x \in Dom}(\min(\mu_{cl(v)}(x), \mu_{cl(v')}(x)))$.

The comparison results of fuzzy sets having the same semantic (similarity or imprecision) and associated with different selection criteria are aggregated using the min operator. Therefore, an answer to a query is a set of tuples composed of (i) the pertinence score ps associated with the queried relation, (ii) three comparison scores associated with the selection criteria of the query: a global adequation score ad_g and two global matching scores Π_g and N_g , and, (iii) the values associated with the projection attribute of the query. Based on those scores, we propose to define a total order on the answers which gives greater importance to the most pertinent answers compared with the ontology: ps , ad_g , N_g and Π_g .

The answer to MIEL++ query Q considered on the previous page and compared with the annotations associated with the first row of Table 1 is given below:

$\{ps=1, ad_g=0.5, N_g=1, \Pi_g=1, \text{Microorg}=(0.5/\text{Clostridium Perfringens}+0.5/\text{Clostridium Botulinum}), aw=[0.943, 0.95, 0.96, 0.97]\}$,
 $\{ps=1, ad_g=0.5, N_g=0.5, \Pi_g=0.68, \text{Microorg}=(0.5/\text{Staphylococcus spp.}+0.5/\text{Staphylococcus aureus}), aw=[0.88, 0.98, 0.98, 0.99]\}$,
 $\{ps=1, ad_g=0.5, N_g=0, \Pi_g=0.965, \text{Microorg}=(1.0/\text{Salmonella}), aw=[0.94, 0.99, 0.99, 0.991]\}$

Results and discussion

In preliminary tests performed on a RDF graph base composed of more than 22000 RDF triples (312 graphs), we have evaluated 5 queries (see Table 2) covering at least 50% of the base entries. Querying quality is assessed using two measures: precision and recall. Precision is the ratio of correct answers over the total number of computed answers. Recall is the ratio of correct computed answers over the number of expected answers. We obtain better results in the queries where the selection criterion concerns micro-organisms than in the ones concerning food products. This is due to the fact that micro-organism names are more standardized in Web tables than food product names. Therefore, the quality of the fuzzy annotations associated with the micro-organism symbolic type is better than with the food product type. Nevertheless, we obtain a precision of 100% for the two last queries concerning food product if we put a threshold of 0.7 on the terms similarity degrees.

Table 2: Evaluation of query results

| Queried relation | Selection criteria | Precision-recall | Nb of answer graphs |
|------------------|--------------------------------|------------------|---------------------|
| Lag Time | Microorganism=L. Monocytogenes | 100%-100% | 47 graphs |
| Lag Time | Microorganism=P. Fluorescens | 100%-100% | 29 graphs |
| Growth kinetics | Microorganism=E. Coli | 100%-100% | 39 graphs |
| Lag Time | FoodProduct= Egg salad | 50%-100% | 24 graphs |
| Growth kinetics | FoodProduct= Salad | 54%-100% | 26 graphs |

Conclusion

Probabilistic simulations of Sym'Previus software needs a lot of data in food products to take the food matrix into account and to assess food variability in bacterial growth simulations. A prototype of the @WEB and the MIEL++ tools will be soon integrated with the predictive modelling tools of the Sym'Previus project. These automatic links between web data and simulation tools allows a new step in risk assessment to be performed.

References

- Baranyi J. and Tamplin M. (2004). ComBase: A Common Database on Microbial Responses to Food Environments. *J. Food Prot.* 67(9):1834-1840.
- Baziz, M., Boughanem, M., Prade, H., Pasi, G. (2006) In: A fuzzy logic approach to information retrieval using a ontology-based representation of documents. in *Fuzzy logic and the Semantic Web*, Elsevier 363-377
- Buche P., Dervin C., Haemmerlé O., Thomopoulos R. (2005) Fuzzy querying of incomplete, imprecise, and heterogeneously structured data in the relational model using ontologies and rules. *IEEE Transactions on Fuzzy Systems* 13(3): 373-383.
- Buche P., Dibia-Barthélemy J., Haemmerlé O., Hignette G. (2006) Fuzzy semantic tagging and flexible querying of XML documents extracted from the Web. *Journal of Intelligent Information System.* 26(1): 25-40
- Couvert O., Augustin J.C., Buche P., Carlin F., Coroller L., Denis C., Jamet E., Mettler E., Pinon A., Stahl V., Zuliani V., Thuault D. (2007) Optimising food process and formulation through Sym'Previus, managing of the food safety. *Proceedings of 5th International Conference Predictive Modelling in Foods*
- Dubois, D., Prade, H. (1988) In: *Possibility theory- An approach to computerized processing of uncertainty*. Plenum Press, New York
- Hignette G., Buche P., Couvert O., Dibia-Barthélemy J., Doussot D., Haemmerlé O., Mettler E., Soler L. (2008). Semantic annotation of Web data applied to risk in food. *IJFM* 128, 174-180.
- McMeekin T.A., Baranyi J., Bowman J., Dalgaard P., Kirk M., Ross T., Schmid S., Zwietering M.H. (2006) Information systems in food safety management. *Int.J. Food Microbiol.* 112:181-194.
- Tamplin, M., Baranyi J. and Paoli, G. (2003). Software programs to increase the utility of predictive microbiology information. In: *Modelling Microbial responses in Foods*. (Eds: R.C McKellar, X. Lu.) CRC, Boca Raton, Fla.
- Thomopoulos R., Buche P., Haemmerlé O. (2006) Fuzzy sets defined on a hierarchical domain, *IEEE Transactions on Knowledge and Data Engineering* 18(10) 1397-1410.

An integrated model for predictive microbiology and simultaneous determination of lag phase duration and exponential growth rate

Lihan Huang, Ph.D.

USDA ARS Eastern Regional Research Center, 600 E. Mermaid Lane, Wyndmoor, PA 19038
(lihan.huang@ars.usda.gov)

Abstract

A new mechanistic growth model was developed to describe microbial growth under isothermal conditions. The development of the mathematical model was based on the fundamental phenomenon of microbial growth, which is normally a three-stage process that includes lag, exponential, and stationary phases. A differential logistic growth model was adopted to describe the competitive nature of microbial growth in the exponential and stationary phases. Incorporated with a transitional function to define the lag phase, an integrated differential logistic growth model was developed and solved analytically. The new model was capable of describing a complete three-phase growth curve or a partial growth curve that contains only lag and exponential phases.

The new integrated model was validated using *Listeria monocytogenes* in tryptic soy broth and beef frankfurters and *Escherichia coli* O157:H7 in mechanically tenderized beef. The inoculated samples were incubated at various temperature conditions and enumerated to obtain isothermal growth curves. A nonlinear regression procedure in SAS was employed to analyze each growth curve to simultaneously determine the lag phase duration and exponential growth rate. Both bias factor (B_f) and accuracy factor (A_f) were used to evaluate the performance of the new model. Results indicated that both B_f and A_f values were very close to 1.0, suggesting that the new model was very suitable for describing isothermal microbial growth. Modified Ratkowsky models were used to analyze lag phase durations and exponential growth rates and develop secondary models. The maximum and minimum temperatures obtained from the resulting secondary models matched closely with the biological nature of *L. monocytogenes* and *E. coli* O157:H7.

Keywords: growth model, kinetic analysis, mathematical modeling

Introduction

The growth of microorganisms in food systems usually exhibits three different phases – lag, exponential, and stationary phases. Several mathematical models have been used in predictive microbiology to describe the microbial growth. These models may include empirical modified Gompertz or logistic model (Gibson et al., 1987), and semi-theoretical Baranyi model (Baranyi et al., 1995). These models can be used to fit the growth curves and obtain the growth parameters, such as lag phase duration and exponential growth rate. Each of these models has both advantages and disadvantages when used to fit growth curves.

The objective of this paper was to report a new integrated kinetic model for quantitative analysis and characterization of microbial growth under isothermal conditions. The new model was a theoretical growth model, and was based on the fundamental growth phenomenon of microorganisms in foods. It clearly defined the duration of lag phase and exponential growth rate in a single equation, and was more intuitive than the traditional growth models such as modified Gompertz and Baranyi models.

Materials and methods

Model development

For a growth curve without a lag phase, the microbial culture does not need to experience an adjustment process and can multiply exponentially until the population reaches a maximum density. This process can be described by

$$\frac{dC}{dt} = kC(C_{\max} - C). \quad \text{Eq. 1}$$

In this equation, C is the cell concentration; C_{\max} is the maximum cell concentration, and kC_{\max} is equal to μ_{\max} , or specific growth rate in the exponential phase. Under isothermal conditions, it is assumed that k or μ_{\max} does not change with time and is a constant. The bacterial population would start to increase immediately. Since a lag phase is a transitional period through which bacteria enter the exponential phase of growth, a transitional function, $f(t)$, can be used to modify Eq. 1 so that it can describe a complete growth curve. A transitional function chosen for this application is

$$f(t) = \frac{1}{1 + \exp[-\alpha(t - \lambda)]} \quad \text{Eq. 2}$$

In Eq. 2, $f(t)$ is actually a unit transitional function. At $t \leq \lambda$, it equal to zero. With $f(t) = 0$, dC/dt is also zero, which mathematically describes the lag phase during which no change in the cell population occurs. At $t > \lambda$, $f(t)$ equals to 1, and the process is governed by the 1st-order kinetics. The coefficient α is a constant that allows a smooth transition from 0 to 1. The coefficient α in the new model allows a smooth but sharp transition from the lag phase to the exponential phase in a growth curve. According to Huang (2008), a value of 25 is suitable for this coefficient. With $f(t)$, a new differential growth model can be developed, and is written as

$$\frac{dC}{dt} = \frac{kC(C_{\max} - C)}{1 + \exp[-\alpha(t - \lambda)]}. \quad \text{Eq. 3}$$

Denoting $y(t)$ as the natural logarithm of C , Eq. 3 can be solved analytically to produce a new growth model:

$$y(t) = y_0 + y_{\max} - \ln\{\exp(y_0) + [\exp(y_{\max}) - \exp(y_0)]\exp[-\mu_{\max}B(t)]\},$$
$$\text{and, } B(t) = t + \frac{1}{\alpha} \ln \frac{1 + \exp(-\alpha(t - \lambda))}{1 + \exp(\alpha\lambda)} \quad \text{Eq. 4}$$

With an incomplete growth curve that does not include a stationary phase, a reduced model can be obtained for this special case.

$$y(t) = y_0 + \mu_{\max} \left\{ t + \frac{1}{\alpha} \ln \frac{1 + \exp[-\alpha(t - \lambda)]}{1 + \exp(\alpha\lambda)} \right\} \quad \text{Eq. 5}$$

Growth curves and curve fitting

Growth curves of *Listeria monocytogenes* and *Escherichia coli* O157:H7, obtained from broth and meat samples, were analyzed and compared with modified Gompertz and Baranyi models. A nonlinear regression procedure based on Gauss-Newton method in Windows-based SAS Version 9.1.3 (SAS Institute Inc., Cary, NC) was used for curve fitting.

Listeria monocytogenes

A four-strain cocktail of *L. monocytogenes* was inoculated in tryptic soy broth (TSB, BD/Difco Laboratories, Sparks, MD) or beef frankfurters. For growth studies in TSB, *L. monocytogenes* with four different initial concentration levels (1, 2, 3, and 4 log CFU/ml, labeled as G1 to G4) was inoculated into 200 ml broth and incubated at 37°C. For growth studies in beef frankfurters, *L. monocytogenes* was inoculated onto samples and incubated at 15, 25, 30, 37, or 40 °C.

E. coli O157:H7

For the growth studies of *E. coli* O157:H7, a cocktail of 5 rifampicin-resistant (rifr) strains or 3 randomly selected wild strains was inoculated into mechanically tenderized beef meat (MTBM). The inoculated samples were incubated at 5, 10, 15, 20, 25, and 37 °C.

Model evaluation

The bias factor (B_f) and accuracy factor (A_f) proposed by Ross (1996) were used to evaluate the performance of each growth model. RMSE, or root mean square error, an estimate of the standard error of a model, was also calculated for evaluation of the models.

Secondary model

The growth rate was fitted to two secondary models modified from the Ratkowskysquare-root model:

$$\sqrt{\mu_{\max}} = a(T - T_{\min}) \quad \text{Eq. 6}$$

$$\mu_{\max} = a(T - T_{\min}) \quad \text{Eq. 7}$$

Results and Discussion

New primary model

Figures 1-3 clearly illustrate that the new model can accurately describe complete growth curves with all three phases. It is also suitable for describing incomplete growth curves with only lag and exponential phases (Figure 4). The A_f and B_f values of the new model were almost identical to 1.0, suggesting the growth data calculated by the new model closely matched the experimental values. The RMSE values of the new model were very close to those of modified Gompertz and Baranyi models. All three phases were directly identified by the new model.

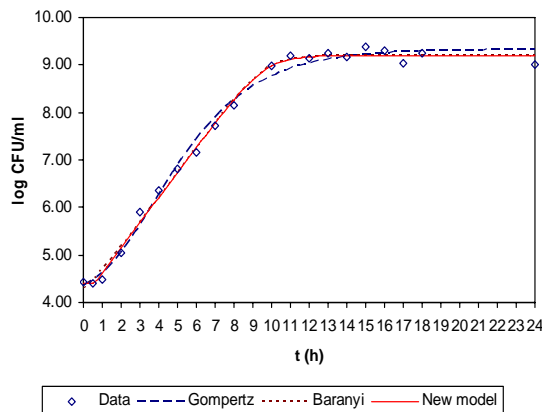


Figure 1: Growth of *L. monocytogenes* in TSB.

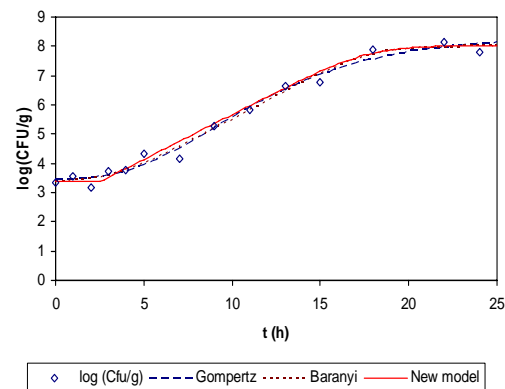


Figure 2: Growth of *L. monocytogenes* in beef frankfurters.

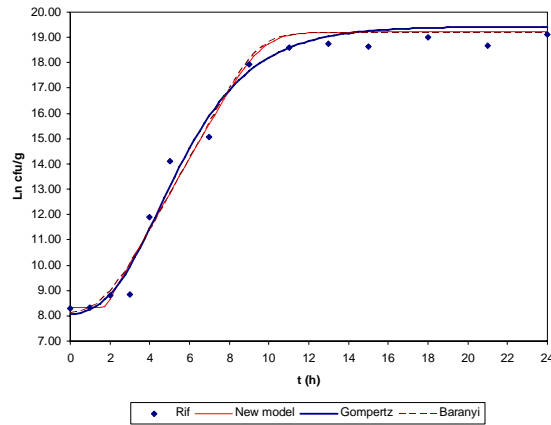


Figure 3: Growth of rif^f strains of *E. coli* O157:H7 in MTBM.

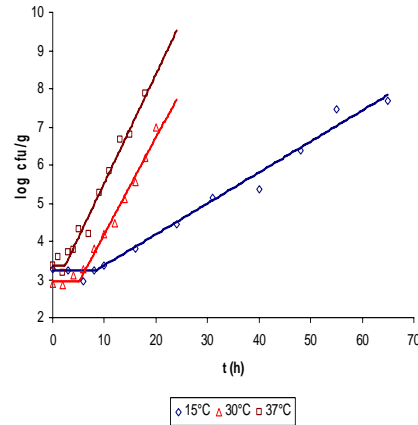


Figure 4: Partial growth curves fitted with the new model (*L. monocytogenes* in frankfurters).

Secondary model

The equation (Eq. 6), $\sqrt{\mu_{\max}} = a(T - T_{\min})$, was not suitable for describing the temperature dependence of growth rates of *L. monocytogenes* in frankfurters and *E. coli* in MTBM, as the estimated T_{\min} was very close to -18°C for *Listeria* and 0°C *E. coli*, which was not in agreement of the biological nature of the bacteria. Eq. 7 was more suitable. For *L. monocytogenes* in beef frankfurter, Eq. 7 becomes $\mu_{\max} = 0.00816(T - 2.73)$. For *E. coli* O157:H7 in MTBM, the secondary model was $\mu_{\max} = 0.0549(T - 12.39)$ for the rif^f strains and $\mu_{\max} = 0.0667(T - 13.70)$ for the wild strains. The minimum temperatures (T_{\min}) estimated from Eq. 7 matched closely with the biological nature of both *Listeria* and *E. coli*.

Conclusion

This study clearly demonstrated that the new integrated model was very accurate in describing the isothermal growth kinetics of microorganisms in foods. This study also discovered that the linear non-square-root secondary model was more suitable for describing the temperature dependence of growth rates.

References

- Baranyi J., Robinson T.P., Kaloti A. and Mackey B.M. (1995) Predictive growth of *Brochothrix thermosphacta* at changing temperature. *International Journal of Food Microbiology* 27, 61–75.
- Gibson A.M., Bratchell N. and Roberts, T.A. (1987) The effect of sodium chloride and temperature on the rate and extent of growth of *Clostridium botulinum* type A in pasteurized pork slurry. *Journal of Applied Microbiology* 62, 479-90.
- Huang, L. 2008. Growth kinetics of *Listeria monocytogenes* in broth and beef frankfurters – Determination of lag phase duration and exponential growth rate under isothermal conditions. *Journal of Food Science* 73, E235-242.
- Ross, T. 1990. Indices for performance evaluation of predictive models in food microbiology. *Journal of Applied Bacteriology* 81, 501–508.

An artificial neural networks approach for the rapid detection of the microbial spoilage of beef fillets based on Fourier transform infrared spectroscopy data

A. Argyri¹, F. Mohareb², E.Z. Panagou¹, C. Bessant² and G.-J.E. Nychas¹

¹Agricultural University of Athens, Department of Food Science and Technology, Laboratory of Microbiology and Biotechnology of Foods, Iera Odos 75, 118 55 Athens, Greece (stathispanagou@aua.gr)

²Bioinformatics Group, Cranfield Health, Cranfield University, MK43 0AL, UK (c.bessant@cranfield.ac.uk)

Abstract

The applicability of artificial neural networks (ANNs) was investigated to differentiate the quality of beef samples and predict their microbiological load based on FTIR metabolic fingerprinting. Beef fillets were stored aerobically at 0, 5, 10, 15, and 20°C from freshness to spoilage (*ca.* 3 to 15 days). Duplicate packages from each storage temperature were subjected to FTIR measurements in the spectral range of 4.000 to 400 cm⁻¹. Additional samples were analyzed to allow for the determination of total viable counts (TVC) and sensory characteristics, based on a three point hedonic scale namely, fresh (F), semi-fresh (SF), and spoiled (S). A three layer network was developed with seven nodes in the input layer and two nodes in the output layer (one for class and total viable counts). The number of neurons in the hidden layer was empirically determined based on the performance of the network. ANN training was based on the steepest-descent gradient learning algorithm and validation was carried out using the leave-1-out cross validation method. The overall correct classification of the network was 90.5% in a 74-sample population (24 F, 16 SF, 34 S). Classification accuracies were 91.7%, 81.2%, and 94.1% for fresh, semi-fresh, and spoiled beef samples, respectively. The network was able to predict the microbiological load (TVC) of beef samples quite satisfactorily. Specifically, the values of bias and accuracy factors were 0.991 and 1.123, respectively, indicating good agreement between observed and predicted bacterial counts. The average differences between predictions and observations were 12.3% as inferred by the value of the accuracy factor. The % RE values fall within the $\pm 20\%$ zone for 75%, 87.5%, and 97.1% for fresh, semi-fresh, and spoiled beef samples, respectively.

Keywords: artificial neural networks, aerobic storage, beef fillets, FTIR, spoilage

Introduction

In most developed countries meat consumption is very high mainly due to its high nutritional value in the human diet. The great variability in raw meat in terms of chemical composition, technological and chemical attributes results in highly variable end products which are marketed without a desired and controlled level of quality. In order to maintain quality standards, control procedures must be carried out on meat comprising chemical analyses, instrumental methods, organoleptic evaluation, and molecular screening methods. However, these techniques are invasive, time consuming, labour intensive, demand highly trained personnel, and thus they are unsuitable for online application. Recently, some interesting analytical approaches have been implemented for the rapid and quantitative monitoring of meat spoilage based on vibrational spectroscopy methods (e.g. FTIR, Raman spectroscopy) (Ellis et al. 2005; Herrero 2008). In contrast to conventional methods, Fourier transform infrared (FTIR) spectroscopy is rapid, non-invasive, requires no specific consumable or reagent permitting users to collect full spectra in a few seconds allowing simultaneous assessment of numerous meat properties. The basic concept underlying this method stipulates that as bacteria grow on meat, they utilize nutrients and produce by-products. The quantification of these metabolites represents a fingerprint characteristic of any biochemical substance, providing thus information about the rate of spoilage (Ellis et al. 2004; Ammor et al. 2009). However the enormous amount of information provided by the last mentioned technology makes the data produced unmanageable. The application of advanced statistical

methods (e.g. discriminant function analysis, clustering analysis, partial least square regression) and intelligent methodologies (neural networks, fuzzy logic, evolutionary algorithms, genetic programming) can be used as qualitative indices rather quantitative since their primary target is to distinguish objects or groups or populations (Goodacre et al. 2004). Nowadays, machine learning strategies are based on supervised learning algorithms. The last mentioned approach together with the development of artificial neural networks (ANN) could be used effectively in the evaluation of meat spoilage.

Materials and methods

Fresh deboned pieces of beef were purchased from a local retailer and transported to the laboratory within 30 min. On arrival, the samples were prepared by cutting the meat pieces into portions (40 mm wide x 50 mm long x 10 mm thick) and maintained at 4°C for 1 h until use. The portions were subsequently placed into 90 mm Petri dishes and stored at 0, 5, 10, 15, and 20°C in high-precision ($\pm 0.5^\circ\text{C}$) incubation chambers for an overall period of 350 h depending on storage temperature until spoilage was pronounced. For the FT-IR measurements, a thin slice of the aerobic upper surface of the fillet was excised and used for further spectral analysis. For microbiological analysis a portion (40 mm wide x 50 mm long x 10 mm thick) was added to 150 ml sterile quarter strength Ringer's solution, and homogenized in a stomacher for 60 s at room temperature. Further decimal dilutions were prepared with the same diluent, and duplicate 0.1 ml samples of three appropriate dilutions were spread in triplicate on plate count agar for counts of total viable bacteria, which was incubated at 30°C for 48 h. Duplicate samples from each storage temperature were analyzed at appropriate time intervals to allow for efficient kinetic analysis of total viable counts. Sensory evaluation of meat samples was performed during storage, based on the perception of colour, smell, and odour before and after cooking (20 min at 180°C in preheated oven). Each sensory attribute was scored on a three-point hedonic scale corresponding to: 1=*Fresh*; 2=*Marginal*; and 3=*Spoiled*. Score of 1.5 was characterized as *Semi-fresh* and it was the first indication of meat spoilage. FT-IR spectra were collected using a ZnSe 45° ATR (Attenuated Total Reflectance) crystal on a Nicolet 6700 FT-IR Spectrometer, collecting spectra over the wavenumber range of 4,000 to 400 cm^{-1} , by accumulating 100 scans with a resolution of 4 cm^{-1} . The collection time for each sample spectrum was 2 min.

Results and discussion

The classification performance of the MLP network with variable number of neurons in the hidden layer and different transfer functions (logistic sigmoid and hyperbolic tangent) is presented in Figure 1. Generally, the classification performance of the network obtained for the meat samples stored at different temperatures and cross validated with leave-1-out method was lower when the selected transfer function was hyperbolic tangent despite the fact that the algorithm converged faster. The highest overall correct classification with hyperbolic tangent transfer function (86.5%) was obtained with 20 neurons in the hidden layer (Figure 1b), however within the individual classes performance was low, especially for semi-fresh meat samples (62.5%). The best performance of the classifier was obtained with 10 neurons in the hidden layer and a logistic sigmoid transfer function (Figure 1a) providing a 90.5% overall correct classification, which within the selected classes corresponded to 91.7%, 94.1%, and 81.3% for fresh, spoiled, and semi-fresh meat samples, respectively. The classification accuracies obtained from this network, designated as 7-10-2, are presented in the form of a confusion matrix in Table 1. The sensitivities, i.e. how good the network is at correctly identifying positive samples, for fresh and spoiled meat samples were 91.7% and 94.1%, respectively, representing 2 misclassifications out of 24 fresh meat samples, and also 2 misclassifications out of 34 spoiled samples. In the case of semi-fresh samples the respective figure was somehow lower (81.2%). In this case 3 samples were misclassified (out of 16), 1 as fresh and 2 as spoiled. The specificity index, i.e. how good the network is at correctly identifying negative samples, was also high especially in fresh and spoiled samples, indicating satisfactory discrimination between these two classes.

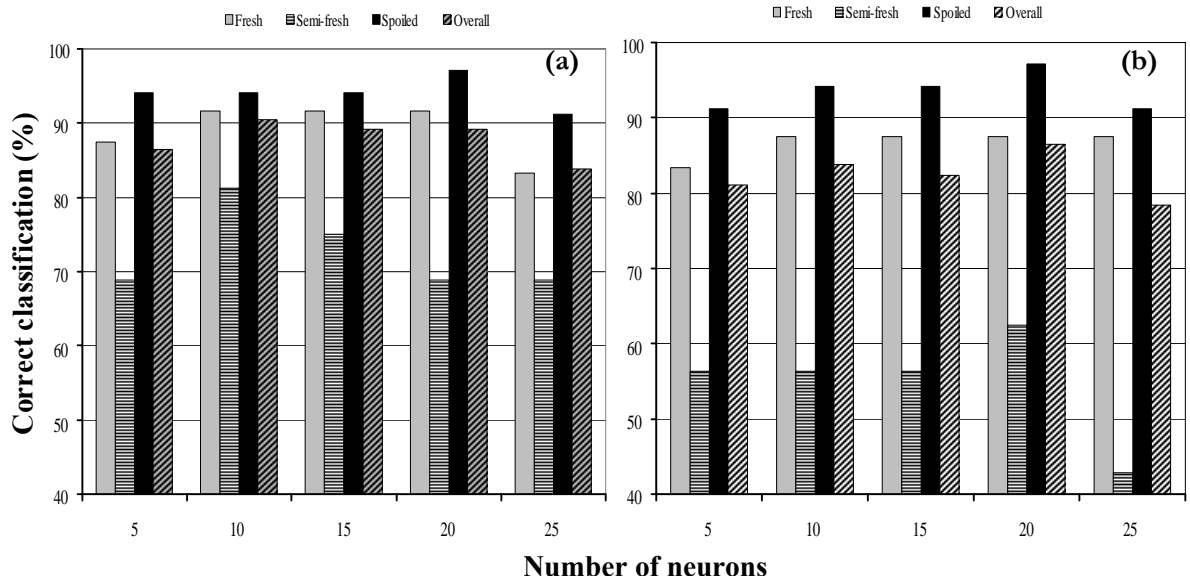


Figure 1: Classification performance of neural networks with variable number of neurons in the hidden layer according to logistic sigmoid (a) and hyperbolic tangent activation transfer functions.

Table 2: Confusion matrix of the 7-10-2 MLP classifier performing the task of discrimination of meat samples based on the leave-1-out cross validation method.

| True class | Predicted class | | | Row Total (n_i) | Sensitivity (%) |
|------------------------|-----------------|------------|-----------|------------------------|-----------------|
| | Fresh | Semi-fresh | Spoiled | | |
| Fresh ($n=24$) | 22 | 2 | 0 | 24 | 91.7 |
| Semi-fresh ($n=16$) | 1 | 13 | 2 | 16 | 81.2 |
| Spoiled ($n=34$) | 0 | 2 | 32 | 34 | 94.1 |
| Column Total (n_j) | 23 | 17 | 34 | 74 | |
| Specificity (%) | 95.6 | 76.5 | 94.1 | | |

Overall correct classification (accuracy): 90.5%.

The plot of the predicted versus the observed total viable counts (Figure 2a) showed reasonably good distribution around the line of equity without any particular trend, with the majority of data (*ca.* 78%) included within the ± 1 log unit area, although some over-prediction was evident in the case of fresh meat samples with low observed initial counts. A better picture of the prediction performance of the neural network is given in Figure 2b where the % relative error of prediction is depicted against the observed microbial population. Based on this plot, data were almost equally distributed above and below 0, with approximately 88% of predicted microbial counts included within the $\pm 20\%$ RE zone. However, the network over-estimated the bacterial population for certain fresh samples, especially at lower observed microbial counts, corresponding to low temperature (0°C) and short storage time. The performance of the neural network to predict total viable counts in meat samples in terms of statistical indices is presented in Table 2. Based on the calculated values of the bias factor (B_f) it can be inferred that the network under-estimated total viable counts in semi-fresh and spoiled samples ($B_f < 1$), whereas for fresh samples over-estimation of microbial population was evident ($B_f > 1$). In addition, the values of the accuracy factor (A_f) indicated that the

predicted total viable counts were 18.1%, 12.2%, and 8.4% different (either above or below) from the observed values for fresh, semi-fresh, and spoiled meat samples, respectively.

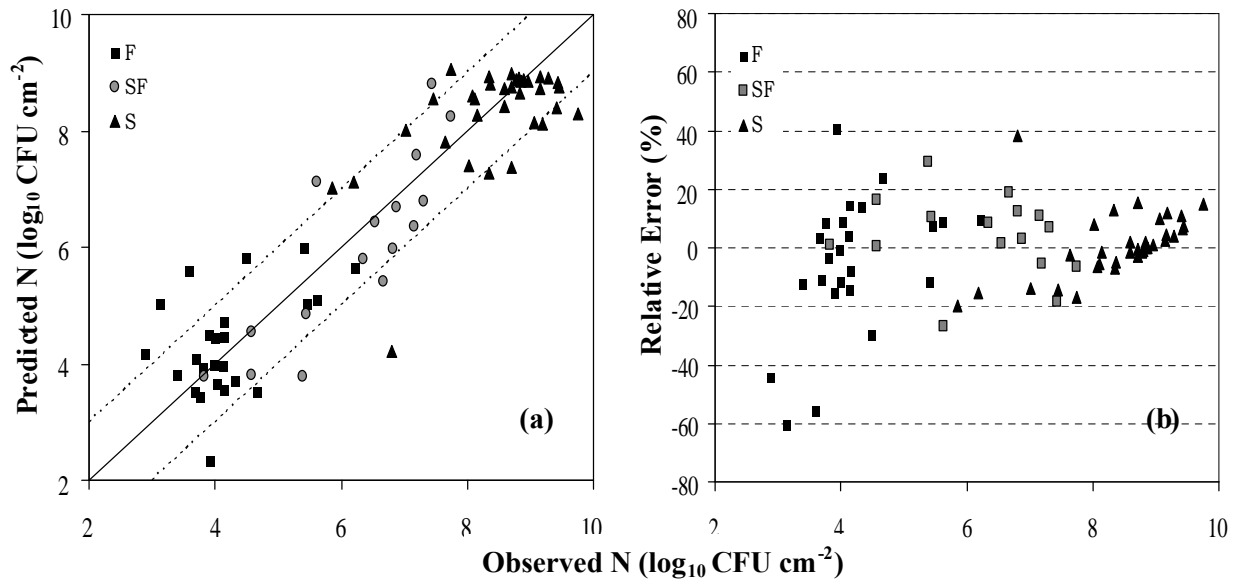


Figure 2: Comparison of total viable counts (a) and percent relative errors (b) between observed and predicted values by the neural network (F: fresh; SF: semi-fresh; S: spoiled meat samples).

Table 2: Performance of the 7-10-2 MLP classifier for the prediction of total viable counts in meat samples (fresh, semi-fresh, spoiled, overall) analyzed by FTIR.

| Statistical index | Fresh | Semi-fresh | Spoiled | Overall |
|---------------------------|-------|------------|---------|---------|
| Bias factor (B_f) | 1.031 | 0.951 | 0.982 | 0.991 |
| Accuracy factor (A_f) | 1.181 | 1.122 | 1.084 | 1.123 |

Conclusion

In conclusion, these data demonstrate the utility of the analytical approach based on FTIR spectroscopy which in combination with an appropriate machine learning strategy could become an effective tool for monitoring beef fillets spoilage during aerobic storage.

Acknowledgements

The authors acknowledge the Symbiosis-EU (www.symbiosis-eu.net) project financed by the European Commission under the 7th Framework Programme for RTD.

References

- Ammor M.S., Argyri A. And Nychas G.-J.E. (2009) Rapid monitoring of the spoilage of minced meat stored under conventionally and active packaging conditions using Fourier transform infrared spectroscopy in tandem with chemometrics. *Meat Science* 81, 57-514.
- Ellis D.I., Broadhurst D., Kell D.B., Rowland J.J. and Goodacre R. (2002) Rapid and quantitative detection of the microbial spoilage of meat by Fourier transform infrared spectroscopy and machine learning. *Applied and Environmental Microbiology* 68, 2822-2828.
- Ellis D.I., Broadhurst D., Clarke S.J. and Goodacre R. (2005) Rapid identification of closely related muscle foods by vibrational spectroscopy and machine learning. *Analyst* 130, 1648-1654.
- Goodacre R., Vaidyanathan S., Dunn W.B., Harrigan G.G. and Kell D.B. (2004) Metabolomics by numbers: acquiring and understanding global metabolite data. *Trends in Biotechnology* 22, 245-252.
- Herrero A.M. (2008) Raman spectroscopy a promising technique for quality assessment of meat and fish: a review. *Food Chemistry* 107, 1642-1651.

Concept for the implementation of a generic model for remaining shelf life prediction in meat supply chains

S. Bruckner, V. Raab and J. Kreyenschmidt

Institute of Animal Science, University of Bonn, Katzenburgweg 7-9, 53115 Bonn, Germany (bruckner@uni-bonn.de)

Abstract:

An overall concept for the implementation of a generic model to predict the remaining shelf life of meat at different steps in the supply chain was developed. The concept includes three different models: a shelf life model, an inter-organizational cold chain model and a temperature control model including a heat transfer model. Shelf life prediction is based on the growth of *Pseudomonas* sp., taking into account organizational structure, inspection scheme, technical circumstances and temperature conditions in different supply chains.

Keywords: cold chain management, meat spoilage, shelf life, temperature control

1. Introduction

During the last years, several models have been developed for shelf life prediction of perishable products, most of them based on the growth of specific spoilage organisms (SSO) (e.g. Koutsoumanis *et al.*, 2006; Gospavic *et al.*, 2008, Kreyenschmidt *et al.*, 2009). To estimate the remaining shelf life in different steps of the supply chain, rapid methods for determination of the microbiological count of the SSO are needed. Some of the rapid methods already exist but some of them are still not applicable for certain kinds of microorganisms. Another possibility is to predict remaining shelf life from the temperature history of the product - which requires a continuous control of the product's temperature. Several solutions have been developed in recent years for continuous temperature monitoring but an efficient application of such solutions, which is a prerequisite for the calculation of the remaining shelf life in meat supply chains, is in general, absent. Additionally, satisfactory concepts for the implementation of predictive shelf life models in real supply chains are still lacking. Thus, the objective of the study was the development of a generic model, which facilitates the calculation of remaining shelf life in different cold supply chains. The development and implementation of a generic model has to take into account practical requirements and inter- as well as the intra-organizational complexity of pork and poultry supply chains.

2. Materials and Methods

To develop a concept for the implementation of a generic model in meat supply chains, three approaches were combined: microbiological analysis, empirical supply chain assessment and analysis of temperature conditions in differing supply chains.

The shelf life model has been developed for fresh pork and poultry: Skinless chicken breast fillets (150 - 170 g) and sliced pork loins (150 - 200 g) were packed aerobically. Immediately after packaging, pork and poultry samples were stored at five different isothermal temperatures (2°C, 4°C, 7°C, 10°C and 15°C) in high precision low temperature incubators (Sanyo model MIR 153, Sanyo Electric Co., Ora-Gun, Gumma, Japan). Furthermore, three dynamic storage trials were performed to estimate the effectiveness of *Pseudomonas* sp. as a SSO (also under non-isothermal conditions) and to analyze the influence of dynamic temperature conditions on growth parameters in different growth phases: a periodically changing temperature cycle (24 h cycle of 4 h at 12°C, 8 h at 8°C and 12 h at 4°C), a trial with short temperatures abuses in the exponential growth phase (4 shifts for 4 h from 4°C to 7°C and 15°C, respectively) and a trial with short temperatures abuses in the beginning of storage (3 shifts for 4 h in the first 60 h of storage from 4°C to 7°C and 15°C, respectively). In parallel to the scenarios with short temperature abuses, additional samples were stored at 4°C

as controls. During storage samples of pork and poultry were analyzed for total viable count, the number of *Pseudomonas* sp., sensory changes and pH-value at appropriate time intervals. The time between slaughtering and the first investigation was 24 h for both meat types. TVC, *Pseudomonas* sp. and sensory characteristics were analyzed as described by Raab *et al.* (2008). The growth data from the enumeration of *Pseudomonas* sp. and TVC were fitted with the modified Gompertz model.

The empirical supply chain assessment consisted of three approaches: a questionnaire approach, expert workshops as well as a focus group meeting. The empirical supply chain assessment aimed firstly at the investigation of practical conditions (organizational structure, inspection schemes as well as system architecture of information and cold chain management). Secondly problems and challenges regarding temperature monitoring (e.g. placement of novel temperature monitoring solutions, sojourn times in each step of the chain) in pork and poultry supply chains in Germany were investigated (pork supply chain: n=28; poultry supply chain: n=23).

For the implementation of shelf life models, a detailed knowledge about temperature variations in supply chains is of great relevance. Consequently temperature conditions were investigated in a national poultry supply chain in Germany both in summer and winter. Furthermore, temperature variation at different places within the transport vehicles, at different levels of the pallet as well as at single packages (surface temperature of the meat) during transportation were analyzed by using Verdict ® 2K:T temperature loggers.

All calculations and figures were performed using the Origin software 8G (OriginLab Cooperation, USA) and Microsoft Excel 2003.

3. Results and Discussion

Pseudomonas sp. was identified as a SSO for both meat types at constant and dynamic temperature conditions. Based on sensory investigations, the end of shelf life was defined when *Pseudomonas* sp. reached a population of 7.5 log₁₀ cfu/g for pork and poultry. The calculated shelf life of pork was always longer than shelf life of poultry. Under non-isothermal conditions, short temperature abuses had a bigger impact on the growth of *Pseudomonas* sp. on pork than on poultry, which led to a higher reduction of shelf life for pork than for poultry. But for both meat types the influence on shelf life was greater when the temperature abuses took place in the first 60 h of storage than in the exponential phase. The results also showed, that besides temperature and initial bacterial count, other factors must have an influence on the growth of *Pseudomonas* sp. in fresh meat, because differences in shelf life also appeared when the initial counts were mostly the same. First data analysis showed no differences between the initial pH-value in all scenarios for both meat types and no definite trend was observed during storage. An additional growth experiment in broth with *Pseudomonas* sp. isolated from meat showed no difference in growth behavior at three different pH-values (5.3; 5.8 and 6.3).

The empirical supply chain analysis revealed that the application of temperature monitoring systems varies - as some systems support the temperature control at a company level (incoming inspection, process control, final inspection) and other solutions focus on control of the temperature during the whole supply chain from production to the retailer or end consumer. Most frequently mentioned methods at the incoming inspection are random checking of the product temperature and random microbiological investigations of specific food pathogens and the total viable count. During transportation temperature is mostly monitored using data loggers. Further on the results indicate that several factors for the practical implementation of predictive shelf life models are not fulfilled. Especially continuous control of product temperature over the whole chain is still absent. In parts of the supply chain novel temperature monitoring solutions are used (e.g. wireless technologies with temperature sensors) which permits the collection of real-time information on temperature data as well as digital storage of the data over the whole supply chain.

Temperature mapping within a national supply chain showed huge temperature variations between environmental temperature, temperature at the packaging material level (cardboard

boxes) and surface temperature of the meat within the cardboard boxes (Figure 1). Furthermore, environmental temperature fluctuated at different locations within the truck (differences up to +10.3°C within the summer period).

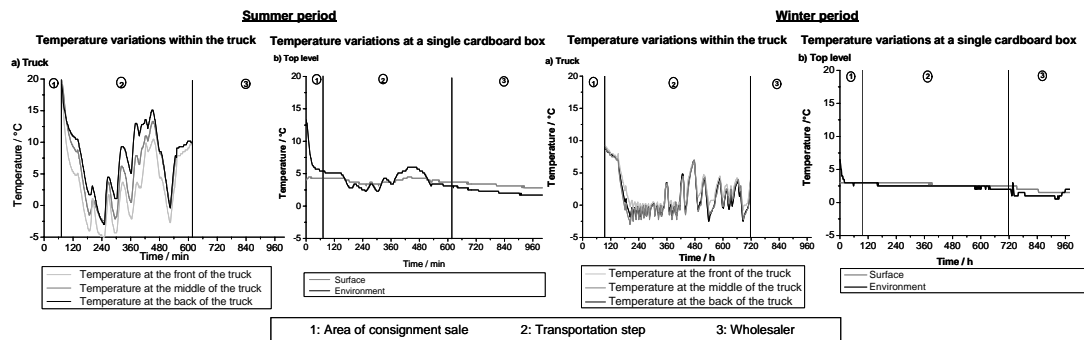


Figure 1 Temperature variations within the transport vehicle and at a single cardboard box during transportation in a national poultry supply chain in Germany (Raab and Kreyenschmidt, 2008)

The temperature mappings showed that the temperature inside the truck varied within the summer period between -3°C and +15°C and in the winter period between 2.5°C and +7.5°C. Further on there were substantial variations between the environmental temperature inside the truck and the surface temperature of the meat. Even if the environmental temperature was often outside the temperature limits required by law, the surface temperature was mostly under 4°C (also in the summer experiment). The results showed that the product temperature can differ from the environmental temperature but in practice mostly only the environmental temperature is recorded. Thus, calculations on a basis of these data can lead to an underestimation of remaining shelf life, as product temperature often varies considerably from the environmental temperature. Therefore it has to be taken into account that the calculation of the remaining shelf life based on the temperature history of a product requires careful placement of the temperature monitoring system - and the packaging material of a product is also an important factor.

4. Conclusions

Based on these results, an overall concept for the development and implementation of a generic model to predict the remaining shelf life of different kinds of meat in different cold chains has been developed (Figure 2). The generic model consists of three different models: a shelf life model, an inter-organizational cold chain model and a temperature control model including a heat transfer model. The shelf life tests showed that it is generally possible to develop a combined shelf life model for fresh pork and poultry based on the growth of *Pseudomonas* sp. But for an accurate prediction of remaining shelf life at different stages of the supply chain, the influence of parameters of the food matrix (e.g. a_w -value, lactate or glucose content) as well as the influence of temperature abuses during the cold chain on remaining shelf life have to be considered in the model. Investigations of different food matrix parameters have already been conducted and data analysis is in progress. Then, the shelf life model will allow the calculation of remaining shelf life for different types of meat. The inter-organizational cold chain model provides information for the optimal implementation of the shelf life model in specific chains with regard to organizational structures, technical circumstances, inspection schemes and information management. The output of the model is the definition of an optimal feedback control scheme for a chain specific adaptation in inter-organizational supply chains. The temperature control model includes chain specific information regarding an optimal temperature monitoring as an important requirement for the calculation of the remaining shelf life. Since most temperature monitoring systems only measure the environmental temperature, a heat transfer model is also included in this model. The integration of a heat transfer model can be useful in some chains to obtain a more precise prediction of the remaining shelf life. The combined output of the three models allows the prediction of remaining shelf life in different cold chains.

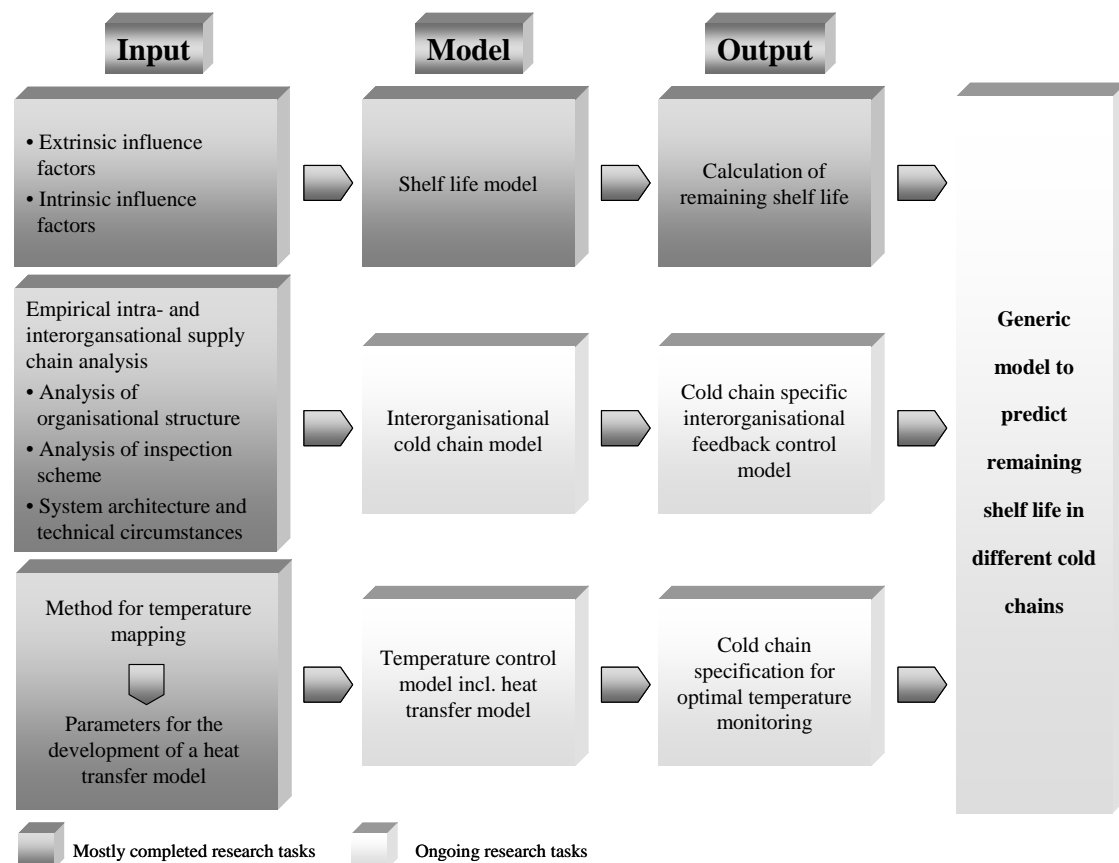


Figure 2 Conceptual steps of the development of a generic model to predict remaining shelf life in different cold supply chains (modified after Raab *et al.*, 2008)

Acknowledgments

The study was partly financed by the InterregIIIC project PromSTAP and the EU project Chill-On (FP6-016333-2). Thanks to all companies involved as well as to students and technical assistants for supporting the study.

References

- Gospavic, R., Kreyenschmidt, J., Bruckner, S., Popov, V. and Haque, N. (2008), "Mathematical modelling for predicting the growth of *Pseudomonas* spp. in poultry under variable temperature conditions", *International Journal of Food Microbiology*, 127(3), 290-297.
- Koutsoumanis, K.; Stamatiou, A.; Skandamis, P. and Nychas, G.-J. E. (2006). "Development of a Microbial Model for the Combined Effect of Temperature and pH on Spoilage of Ground Meat, and Validation of the Model under Dynamic Temperature Conditions", *Applied and Environmental Microbiology*, 72(1), 124-134.
- Kreyenschmidt, J., Hübner, A., Beierle, E., Chonsch, L., Scherer, A. and Petersen, B. (2009), "Determination of the shelf life of sliced cooked ham based on the growth of lactic acid bacteria in different steps of the chain", *Journal of Applied Microbiology*, in press.
- Raab V., Bruckner S., Beierle E., Kampmann Y., Petersen B. and Kreyenschmidt, J. (2008), "Generic model for the prediction of remaining shelf life in support of cold chain management in pork and poultry supply chains", *Journal on Chain and Network Science*, 8 (1), 59-73.
- Raab, V. and Kreyenschmidt, J. (2008), „Requirements for the effective implementation of innovative tools for temperature monitoring supporting cold chain management in poultry supply chains”, in: Kreyenschmidt J. (Ed.): *Cold Chain-Management - Conference Proceedings*, University of Bonn, Germany (ISBN 978-3-9812345-0-3) [3rd International Workshop Cold Chain-Management, Bonn (Germany), June 2-3, 2008], 259-264.

Modelling the effect of temperature and water activity on the growth boundaries of *Byssochlamys fulva*

E.Z. Panagou¹, S. Chelonas², I. Chatzipavlidis³ and G.-J.E. Nychas¹

¹Agricultural University of Athens, Department of Food Science and Technology, Laboratory of Microbiology and Biotechnology of Foods, Iera Odos 75, 118 55 Athens, Greece (stathispanagou@aua.gr)

²University of Ioannina, School of Natural Resources and Enterprises, Department of Business Administration of Food and Agricultural Products, G. Seferi 2, 301 00 Agrinio, Greece

³Agricultural University of Athens, Department of Agricultural Biotechnology, Laboratory of General and Agricultural Microbiology, Iera Odos 75, 118 55 Athens, Greece

Abstract

Byssochlamys species have been responsible for degradation and spoilage of processed fruit products due to the outgrowth of heat-resistant ascospores after thermal processing. Spoilage is manifested by the production of mycelium in fruit products and softening of processed fruit tissues. *B. fulva* was grown on malt extract agar at different temperatures (10, 15, 20, 25, 30, 35, 40, and 45°C) and water activity levels (0.88, 0.90, 0.92, 0.94, 0.96, and 0.99). Growth was determined over time in terms of colony diameter extension and the primary model of Baranyi and Roberts was used to fit growth data and estimate the maximum specific growth rates, which were further modelled as a function of temperature and water activity using the Rosso cardinal model. Linear logistic regression was also applied to predict the probability of growth over storage time. No growth was observed at 0.88 a_w regardless of storage temperature, as well as at 0.90 and 0.92 a_w /10, 15, 45°C, and 0.94 a_w /10°C. Based on the estimated parameters of the Rosso cardinal model, the optimum specific growth rate (μ_{opt}) was 26.4 mm day⁻¹, the T_{max} , T_{min} , and T_{opt} for growth were 46.4°C, 9.1°C, and 32.1°C, respectively. In addition, the estimated optimum a_w for growth was 0.985, whereas the minimum and maximum a_w values were 0.893 and 0.993, respectively. Regarding growth boundaries, the degree of agreement between predictions and observations was 98.8% concordant and 1.2% discordant. The erroneously predicted growth cases were 3.5% false-positives and 4.2% false-negatives.

Keywords: *Byssochlamys*, fungi, probabilistic modelling, Rosso cardinal model

Introduction

Byssochlamys species are responsible for spoilage and degradation of processed fruit juices and silages, since they can grow at low oxygen partial pressures and in acidic environments. They produce ascospores which can withstand thermal processing normally given to fruit juices and are also capable of producing pectinolytic enzymes modifying thus fruit texture. Besides the spoilage effect of thermally treated products, *Byssochlamys* species can also produce mycotoxins including patulin, byssotoxin A and byssochlamic acid (Houbraken et al. 2006). So far, very little has been published on the effect of environmental factors (e.g. temperature, water activity, pH, etc.) on the growth of this fungus, and heat-resistant fungi in general. The aim of this work was to provide quantitative information on the effect of temperature and water activity on the growth rates and growth boundaries (growth-no growth interface) of *B. fulva* ascospores on a synthetic growth medium.

Materials and methods

Byssochlamys fulva DSM 1808 from the fungal collection of the Deutsche Sammlung von Mikroorganismen und Zellkulturen was used in this study. The fungus was routinely grown on malt extract agar (MEA 1.05398; Merck, pH 5.7) at 30°C for 10 days in the dark. Ascospores were harvested as described previously (Panagou et al. 2003). Their density was determined by means of a counting chamber and it was found to be about 10⁶ ascospores ml⁻¹. The a_w of the MEA basal medium was 0.99 and it was modified to 0.88, 0.90, 0.92, 0.94, and 0.96 by adding different amounts of glycerol. Petri dishes containing about 20 ml of the

solidified growth medium were needle inoculated centrally with the ascospore suspension and incubated at 10, 15, 20, 25, 30, 35, 40, and 45°C. The effect of temperature and water activity on fungal growth was investigated by means of a full factorial design with four replicated plates for each temperature/ a_w combination. Fungal growth was established by diameter measurements at right angles on a daily basis. Estimates of the maximum colony growth rates (μ_{\max}) were obtained by applying Baranyi's primary model and these values were subsequently used in secondary modelling using the cardinal model of Rosso (Rosso and Robinson 2001):

$$\mu_{\max}(T, a_w) = CTPM_2(T, a_w) = \mu_{opt} \cdot \tau(T) \cdot \lambda(a_w)$$

Where,

$$\tau(T) = \left(\frac{(T - T_{\min})^2 \cdot (T - T_{\max})}{(T_{opt} - T_{\min}) \cdot [(T_{opt} - T_{\min})(T - T_{opt}) - (T_{opt} - T_{\max})(T_{opt} + T_{\min} - 2T)]} \right) \text{ and}$$

$$\lambda(a_w) = \left(\frac{(a_w - a_{w\min})^2 \cdot (a_w - a_{w\max})}{(a_{wopt} - a_{w\min}) \cdot [(a_{wopt} - a_{w\min})(a_w - a_{wopt}) - (a_{wopt} - a_{w\max})(a_{wopt} + a_{w\min} - 2a_w)]} \right)$$

The terms T_{\min} , T_{\max} , $a_{w\min}$, $a_{w\max}$ correspond to the values of temperature and water activity, respectively, below and above which no growth occurs. Additionally, T_{opt} and a_{wopt} are the values of temperature and water activity at which μ_{\max} is equal to its optimal value (μ_{opt}).

The model was externally validated with three thermally treated fruit juices, namely orange, apple and peach juice obtained by a local retailer. The juices were solidified in Petri dishes by adding sterilized agar and inoculated with the ascospore suspension as previously described. The a_w of the resulting juice medium was 0.98 for all juices. The inoculated dishes were incubated at the same temperatures as above and the extension of fungal mycelium was measured in the same way.

Moreover, for each replicate response of the fungus, growth data were converted into probabilities of growth by assigning 1 to plates with visible growth and 0 in the case of no growth. Data were fitted to a logistic regression model in order to determine the growth/no growth boundaries of the fungi under the assayed environmental factors. The model employed was a second-order logistic regression model in the form shown in the following equation:

$$\log it(P) = \ln \left[\frac{P}{1-P} \right] = a_0 + a_1 t + a_2 T + a_3 a_w + a_4 t^2 + a_5 T^2 + a_6 a_w^2 + a_7 tT + a_8 t a_w + a_9 T a_w$$

where, P is the probability of growth (in the range of 0-1), a_i are coefficients to be estimated, a_w is the water activity of the medium, t (days) is incubation time, and T (°C) is temperature. The automatic variable selection option with a stepwise selection method was used to choose the significant effects ($P < 0.05$). The predicted growth/no growth interfaces for $P=0.1$, 0.5, and 0.9 were calculated using Microsoft Excel Solver.

Results and discussion

The growth curves based on colony diameters were typical of linear fungal growth after a germination (lag) period which was dependent on incubation temperature and a_w level of the medium. It is characteristic that under low water activity levels there was higher variability among replicated treatments and fitting was less accurate. Generally, the primary model of Baranyi and Roberts fitted well the experimental data as the R^2 index ranged from 0.91 to 0.99 and the standard error of fit from 0.43 to 5.17, depending on the environmental

conditions assayed. The results of secondary modelling with the Rosso equation are presented in Figure 1 and the estimated parameters with the relevant statistics are shown in Table 1. The optimum growth rate was 26.4 mm day^{-1} which is in good agreement with the value of 20.2 mm day^{-1} reported previously for another strain of the same fungus (Valík and Piecková 2001).

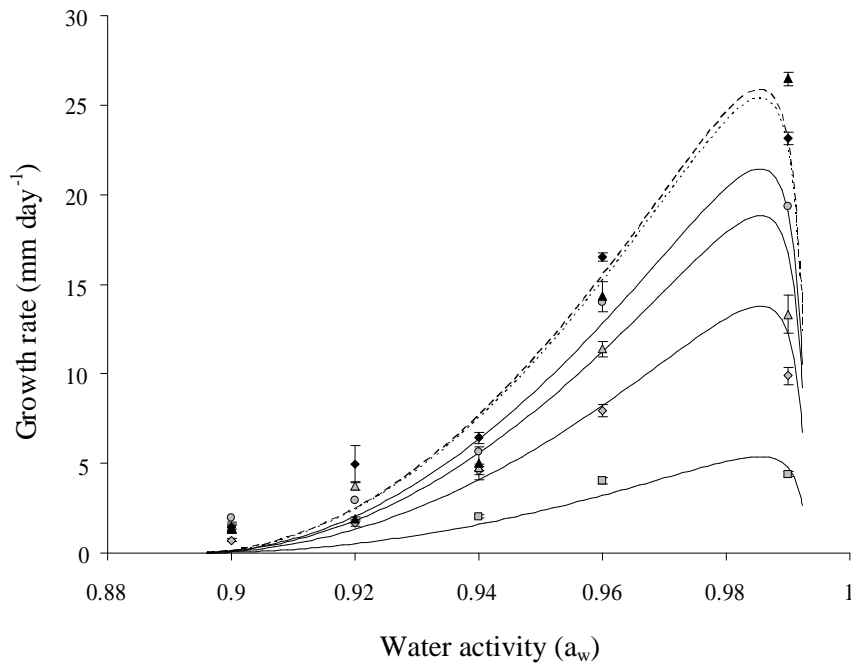


Figure 1: Fitted curves of Rosso cardinal values model describing the effect of temperature and water activity on the growth rate of *B. fulva*. (■) 15°C, (◆) 20°C, (●) 25°C, (◆) 30°C, (▲) 35°C, (▲) 40°C.

Table 1: Estimated values and statistics of the coefficients of the Rosso cardinal value model for the growth rate of *B. fulva* at different conditions of temperature and a_w .

| Parameter | Estimated value | d.f. | RMSE | R ² adjusted |
|--|-------------------|------|--------|-------------------------|
| μ_{opt} (days ⁻¹) | 26.37 ± 1.26 | 121 | 0.0681 | 0.939 |
| T_{max} (°C) | 46.45 ± 0.27 | | | |
| T_{min} (°C) | 9.11 ± 1.03 | | | |
| T_{opt} (°C) | 32.10 ± 0.36 | | | |
| $a_{w, \text{max}}$ | 0.993 ± 0.028 | | | |
| $a_{w, \text{min}}$ | 0.894 ± 0.009 | | | |
| $a_{w, \text{opt}}$ | 0.985 ± 0.002 | | | |

The graphical comparison of the observed and predicted growth rates of *B. fulva* in fruit juices is presented in Figure 2a. Overall, the model had better performance for the orange juice as the data points were closer to the line of equity. The model underestimated the growth rates at low (10, 15°C) and high (40, 45°C) temperatures, whereas for the other temperatures assayed there was reasonably good agreement between observations and predictions. Similar conclusions can be drawn from the percent relative error graph (Figure 2b).

The developed logistic regression model for the probability of growth of *B. fulva* showed that the degree of agreement between predictions and observations was 98.8% concordant and 1.2% discordant indicating successful data fitting.

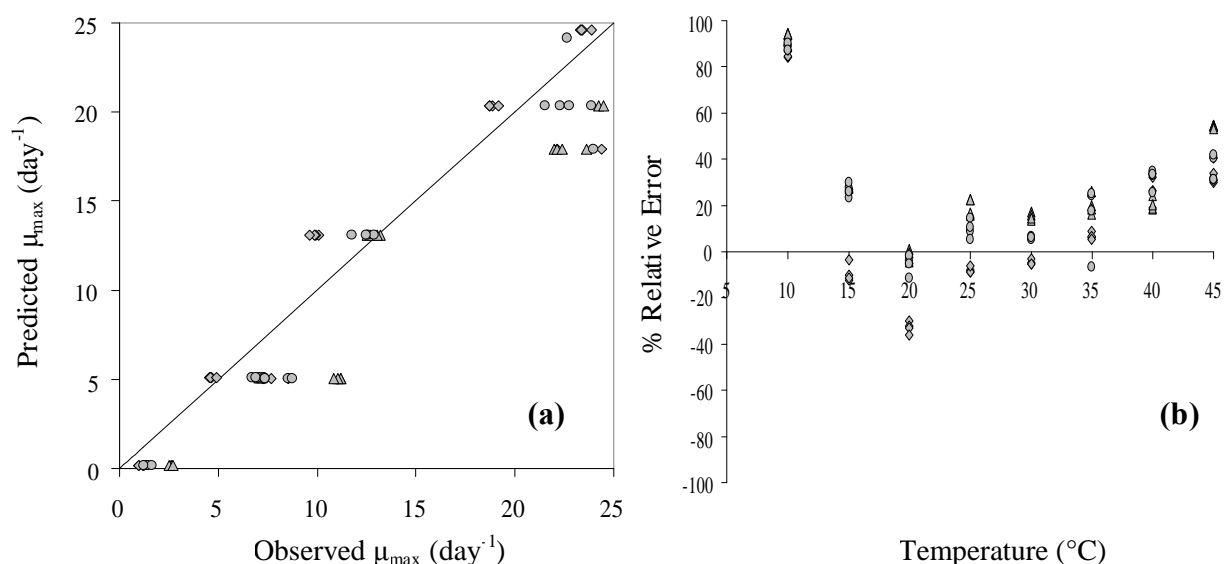


Figure 2: Comparison of predicted vs observed μ_{\max} (a) and percent relative error (b) of *B. fulva* growth by the Rosso model for orange juice (◆), apple juice (▲) and peach juice (●).

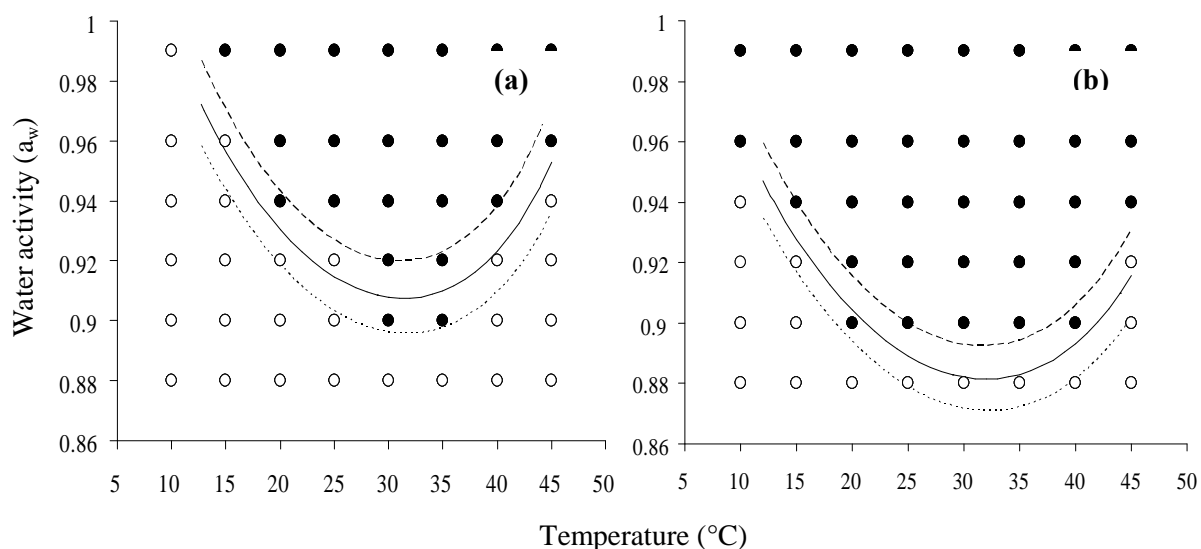


Figure 3: Growth-no growth boundaries of *B. fulva* after 5 (a) and 15 (b) days of incubation on malt extract agar. Solid symbol indicates growth; open symbol indicates no growth; solid line indicates $P = 0.9$; dotted line indicates $P = 0.5$; dashed line indicates $P = 0.1$.

Plots of probability of growth of *B. fulva* at 5 and 15 days of incubation showed that the probability was higher at 30 and 35°C for 0.90 a_w (Figure 3a) but as time increased the growth interface shifted to lower (20, 25°C) and higher (40°C) temperatures for the same a_w level.

References

- Houbraken J., Samson R.A. and Frisvad J.C. (2006) *Byssoschlamys*: significance of heat resistance and mycotoxin production. In: A.D. Hocking, J.I. Pitt, R.A. Samson, U. Thrane (Eds.), *Advances in Food Mycology*, Springer, NY, p. 211-223.
- Panagou E.Z., Skandamis, P.N. and Nychas G.-J.E. (2003) Modelling the combined effect of temperature, pH and a_w on the growth rate of *Monascus ruber*, a heat-resistant fungus isolated from green table olives. *Journal of Applied Microbiology* 94, 146-156.
- Rosso L. and Robinson T.P. (2001) A cardinal model to describe the effect of water activity on the growth of moulds. *International Journal of Food Microbiology* 63, 265-273.
- Valík L. and Piecková E. (2001) Growth modelling of heat-resistant fungi: the effect of water activity. *International Journal of Food Microbiology* 63, 11-17.

Defining the growth/no growth interface of *Zygosaccharomyces bailii* in a viscoelastic food model system

L. Mertens^{1,2}, T.D.T. Dang^{1,3}, A. Creemers^{1,2}, J. Dams^{1,2}, E. Van Derlinden^{1,2}, A.M. Cappuyns^{1,2}, A. Vermeulen^{1,3}, P. Moldenaers⁴, F. Devlieghere^{1,3}, A.H. Geeraerd^{1,5} and J.F. Van Impe^{1,2}

¹CPMF² - Flemish Cluster Predictive Microbiology in Foods – <http://www.cpmf2.be/>

²Chemical and Biochemical Process Technology and Control Section (BioTeC), Dept. of Chemical Engineering, Katholieke Universiteit Leuven, W. de Croylaen 46, B-3001 Leuven, Belgium

³Laboratory of Food Microbiology and Food Preservation, Dept. of Food Safety and Food Quality, Ghent University, Coupure Links 653, B-9000 Ghent, Belgium

⁴Applied Rheology and Polymer Processing Division, Dept. of Chemical Engineering, Katholieke Universiteit Leuven, W. de Croylaen 46, B-3001 Leuven, Belgium

⁵Division of Mechatronics, Biostatistics and Sensors (MeBioS), Dept. of Biosystems, Katholieke Universiteit Leuven, W. de Croylaen 42, B-3001 Leuven, Belgium

Abstract

In this study, a food model system based on Carbopol was used to define the growth/no growth boundary of the spoilage yeast *Zygosaccharomyces bailii* at different levels of pH, acetic acid concentration, glycerol concentration, temperature and viscoelasticity. Results show that in most cases growth domains were larger in structured media than in liquid media, which is an important contradiction to the general assumption that food structure induces an extra stress on microorganisms (Wilson *et al.* 2002).

Keywords food structure, food model system, acid sauces, growth/no growth boundary

Introduction

Within the field of predictive microbiology, the amount of experimental studies that *quantify* the effect of *food structure* on microbial growth is very limited. This is mainly due to impracticalities related to the non-liquid nature of the culture medium. Most often, agar or gelatin is used as gelling agent in this type of studies. Although both are widely used in food applications, their relevance is limited to food products with a purely gelled microstructure. Furthermore, the majority of studies only mention the concentration of the gelling agent as a quantitative measure of food structure. In this context, rheological concepts enable the evaluation of structural characteristics in a more objective way.

Among the wide range of foodstuffs, sauces are known for their complex microstructure and typical rheological properties. The group of acid sauces includes both emulsions, such as mayonnaise and salad dressings, and concentrated suspensions, such as ketchup. These sauces are viscoelastic, i.e., they have both viscous and elastic properties. Other characteristics of acid sauces are low pH, low a_w and presence of organic acid preservatives. Due to this harsh environment, spoilage is predominantly caused by lactic acid bacteria and yeasts, of which *Zygosaccharomyces bailii* is particularly troublesome.

In this study, the growth/no growth interface of the spoilage yeast *Z. bailii* is defined in a structured food model system that is relevant to this type of sauces. The model system uses a suitable thickening/gelling agent (Carbopol 980) and incorporates the main physicochemical (a_w , pH, sugar and acetic acid concentration) and rheological characteristics (viscoelastic behavior at the relevant magnitude) of acid sauces.

Material and Methods

The growth/no growth interface of *Z. bailii* was defined at different levels of pH (3.5-4.5, 3 levels), acetic acid concentration (1.5 and 2.0% (v/v)), glycerol concentration (20-32% (w/v), 5 levels), and levels of viscoelasticity (3 levels, including a purely liquid medium, covering

the whole range of gel strength of acid sauces, obtained by altering the Carbopol 980 concentration).

Growth media preparation

All media were based on Sabouraud (SAB, Oxoid) and a total sugar concentration of 15% (w/v), with glucose (G-8270, Sigma Aldrich) and fructose (F-0127, Sigma Aldrich) at a 1:1 ratio.

Growth media containing Carbopol were prepared at a proportion of 5/3 compared to the regular levels. Therefore, the media contained 50 g/liter SAB, 9.17% (w/v) glucose and 12.5% (w/v) fructose. Glycerol (24388, VWR) and Carbopol 980 (Lubrizol Corporation) concentrations were also adapted to the 5/3 ratio. All components except acetic acid were added and the mixtures were vigorously stirred for at least 30 min (OST 20 basic, IKA Werke GmbH & Co. KG). After this, the media were autoclaved at 121°C for 15 minutes. When necessary, media were centrifuged to remove entrapped air bubbles. Next, the required amount of acetic acid (818755, Merck KGaA) was aseptically added. The media were shaken and centrifuged again to remove entrapped air bubbles.

Growth media without Carbopol were prepared with the regular amounts of SAB, sugar and glycerol. The pH of these media was adjusted to the required value by adding sterile HCl (Acros organics).

Inoculation procedure

Z. bailii (strain No. 174, culture collection of LFMFP, Ghent University, Belgium) was taken from a stock culture stored at -75°C. The strain was recovered in SAB by incubating at 30°C for 48h, and afterwards it was maintained at 2°C on Yeast Glucose Chloramphenicol slants (YGC, 64104, Bio-Rad). In order to prepare the inoculum, cells from YGC slants were cultivated at 30°C in SAB for 24h. A subculture of 5 ml was taken and grown again in 200 ml SAB for 24h at 30°C. Precultures were diluted in the growth medium to provide an inoculation level of $5 \cdot 10^4$ cfu/ml. The inoculum density was verified by plating on TSA (CM131, Oxoid), supplemented with 4% (w/v) fructose.

The growth/no growth experiments were performed in 48-well microtiter plates (Greiner Bio-One) with a total volume of growth media of 500 µl per well. For the Carbopol media, this volume was obtained by adding 300 µl of inoculated growth medium and 200 µl of a sterile NaOH solution to each well (hence, the factor 5/3 for growth media preparation). The concentration of the NaOH solution was the concentration necessary to reach the required pH value, which was previously determined by obtaining calibration curves for each Carbopol concentration under study. Microtiter plate wells were filled by alternately adding 100µl of growth medium and 100µl of NaOH solution until the total volume of 500 µl per well was reached. This was done to reach an optimal level of mixing, as Carbopol solutions immediately thicken upon addition of NaOH. For the transfer of the Carbopol media, a positive-displacement pipette (Microman M100, Gilson Inc.) was used. Subsequently, microtiter plates were shaken for 2 minutes in a microplate shaker (MS 3 digital, IKA Werke GmbH & Co. KG). Sufficient mixing was verified visually as the medium within each well became completely transparent due to the addition of NaOH. For each medium, 20 replicates were performed.

Growth assessment

The microtiter plates were placed in a SpectraMax M2^c microplate reader (Molecular devices) at an incubation temperature of 22°C (for 60 days) or 30°C (for 45 days). The optical density (OD) of the media at 600 nm was measured at regular time intervals and the data were processed by the software package SoftMax Pro (Molecular devices).

For the experiments in liquid media, a single point measurement was performed in each well. For the media containing Carbopol, data collection was performed by using the well scan method, in which OD values were measured at nine different positions in a well. For each measuring point, the OD at time zero was subtracted from the OD of the suspensions and the average of the nine values per well was calculated. This value was used to construct OD

growth curves. If, at day 0, air bubbles were apparent at one (or more) of the nine measurement points of a certain well, these points were discarded. A well was considered as showing growth if the OD was higher than 0.2.

At the end of the incubation period, the strain purity was checked by looping out on TSA supplemented with 4% (w/v) fructose. Wells that were doubtful or did not show any turbidity were plated on the same agar medium to assess whether inactivation had occurred.

Results and Discussion

In this study, the G/NG boundary of *Z. bailii* was defined in a model system based on Carbopol 980 as the thickening/gelling agent. As the rheological properties of Carbopol solutions depend on pH and acetic acid concentration, the Carbopol concentration was adapted in order to reach similar levels of structure at varying values of these environmental factors. The three levels of medium structure applied in this study corresponded to a storage modulus G' of 0, 150 and 450 Pa (at 0.1 rad/s).

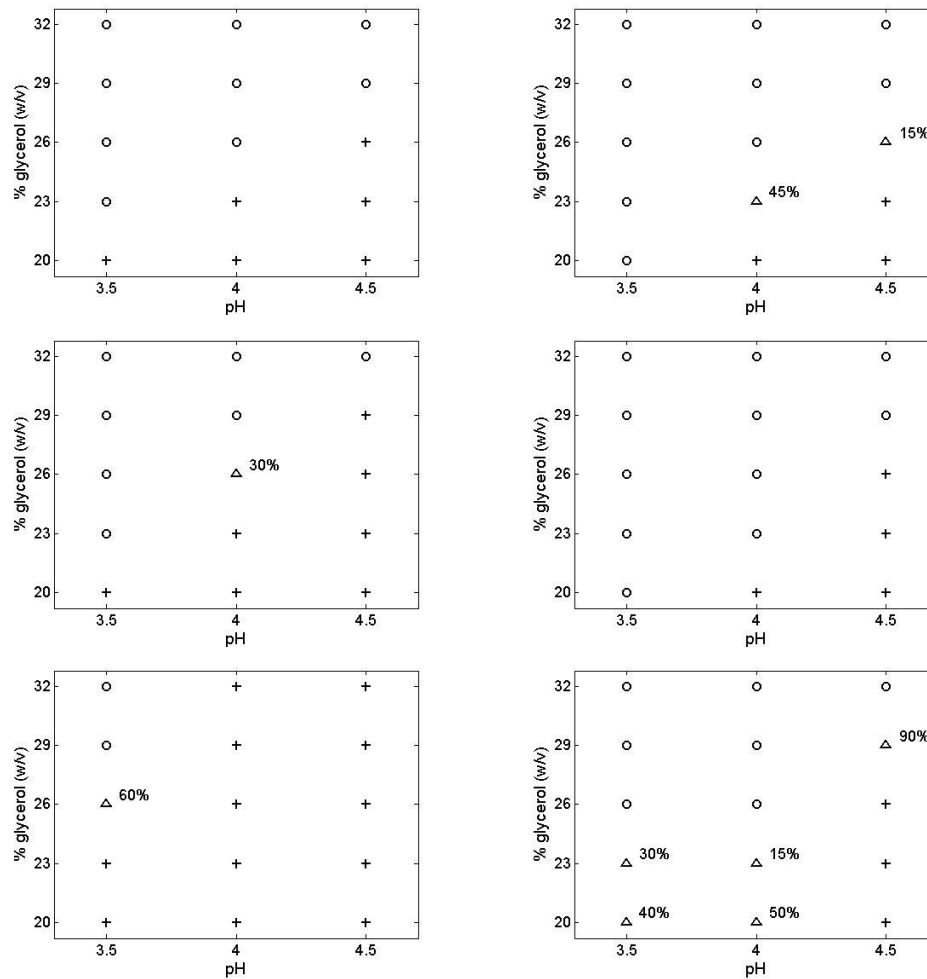


Figure 1: G/NG boundary of *Z. bailii* at 22°C after a 45-day incubation period, for liquid (upper row), moderately structured (middle row) and highly structured media (lower row), at 1.5% (v/v) (left column) and 2.0% (v/v) acetic acid (right column). Data points: $p=0\%$ (○), $p=100\%$ (+), $p \in]0, 100[$ (Δ) with the measured percentage of growth indicated.

Fig. 1 shows the growth probability of *Z. bailii* at different levels of medium structure and acetic acid concentration at 22°C and an incubation period of 45 days. A longer incubation

period (60 days) yielded higher growth probabilities, but did not result in a larger growth zone (results not shown). At each level of medium structure, growth probability generally decreased if more stringent conditions were applied. However, a peculiar effect on the G/NG boundary was observed when structure was induced. At 1.5% (v/v) acetic acid, the growth zone became larger when the level of structure was increased. A different behavior was observed at 2.0% (v/v) acetic acid, where initially a significant increase in growth zone did not occur in moderately structured media ($G'=150$ Pa). However, when the concentration of Carbopol was further increased (corresponding to a G' of 450 Pa), a more gradual and larger growth zone was observed, with possible growth at the lowest pH value of 3.5. The growth zones at 30°C were generally similar to those at 22°C (results not shown), with exception of the G/NG data at 2.0% (v/v) acetic and the highest level of structure (Figure 2), where a significantly smaller growth zone was observed.

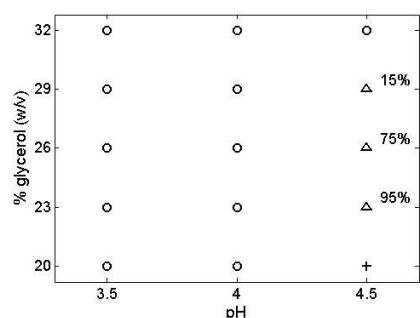


Figure 2: G/NG boundary of *Z. bailii* at 30°C after a 45-day incubation period, for highly structured media at 2.0% (v/v) acetic acid. Data points: p=0% (○), p=100% (+), p ∈]0, 100[(Δ) with the measured percentage of growth indicated.

The aforementioned results suggest that the effect of immobilisation of *Z. bailii* at stressful environmental conditions (i.e., high acetic acid concentration and low a_w) can not be explained in a straightforward way. Moreover, the fact that in most cases, larger growth domains occurred in structured media is in contradiction with the general assumption that food structure induces an extra stress on microorganisms (Wilson *et al.* 2002).

Conclusions

The results shown in this research illustrate the need for more studies that quantify the effect of food structure on microbial behavior. In order to perform such studies on a systematic and consistent basis, the experimental setup must enable careful control and appropriate methods for growth assessment.

The approach adopted here, i.e., to study microbial behavior in a food model system specifically designed for a target food product, is novel within the field of predictive microbiology. Moreover, the use of rheological concepts to assess the effect of food structure, combined with the use of optical density measurements in microtiter plates, has so far not been performed to this extent in structured media.

Acknowledgements

This project is supported by the Fund for Scientific Research – Flanders (FWO – Vlaanderen, project G.0565.06), by the Belgian Program on Interuniversity Poles of Attraction, initiated by the Belgian Federal Science Policy Office and by the K.U.Leuven-Research Council (EF/05/006 (Center-of-Excellence Optimization in Engineering) and OT/03/30).

References

- Wilson P.D.G., Brocklehurst T.F., Arino S., Thuault D., Jakobsen M., Lange M., Farkas J., Wimpenny J.W.T. and Van Impe J.F. (2002) Modelling microbial growth in structured foods: towards a unified approach. *International Journal of Food Microbiology* 73, 27-5-289.

Development of a model describing the effect of temperature and (gel) structure on ochratoxin A production by *Aspergillus carbonarius* in liquid media and evaluation in foods of different viscosity

Anastasia E. Kapetanakou^a, Anna Abavi^a, Stavros Yanniotis^b, Eleftherios H. Drosinos^a, and Panagiotis N. Skandamis^a

^aLaboratory of Food Quality and Hygiene, Department of Food Science & Technology, Agricultural University of Athens, Greece. Correspondence: pskan@aua.gr

^bLaboratory of Food Process Engineering, Processing and Preservation of Agricultural Products, Department of Food Science & Technology, Agricultural University of Athens, Greece.

Abstract

The objectives of this study were to develop a model for the combined effect of temperature (T: 15, 20 and 25°C) and micro-structure (expressed in gelatin concentration) (G: 0, 5, 10 and 20%) on growth and OTA production by *A. carbonarius* and evaluate the model in foods of different viscosity. Growth rate was expressed as the increase of fungal biomass per time. The square root of growth and OTA production rates were determined by the Baranyi model or a linear equation and were further modeled as a function of temperature and gelatin concentration by applying polynomial models. Moreover, the rate of OTA production at 20°C on two food matrices of different micro-structure, such as dairy cream and jelly, inoculated with *A. carbonarius*, were compared to the predictions of the secondary model.

Increase in gelatin concentration indicated a significant delay both, in fungal growth and OTA production rates and also reduced the maximum level of OTA production at all temperatures. The highest OTA level and rate of OTA production was observed at liquid media at 20°C, while the optimum for growth was observed at liquid media and 25°C. Coefficients of determination were 0.91 and 0.87 for the models predicting the square root ($\sqrt{\mu_{\max}}$) of growth and OTA production rate, respectively. Lag time was not influenced by the gelatin concentration, being in the range of 7-10 days. Model predictions showed good agreement with OTA production in dairy cream but over-predicted OTA production in jelly. The present findings may provide a basis for assessing the risk of fungal growth and OTA production in foods of different structure.

Keywords: ochratoxin A, modeling, gelatin, temperature.

Introduction

Ochratoxin A (OTA) constitutes a fungal secondary metabolite well known for its carcinogenic, immunosuppressive and teratogenic properties (IARC, 1993). *Aspergillus carbonarius* is one of the common ochratoxinogenic fungi. In addition to the well-established effect of a_w , pH and temperature (Esteban et al., 2006), structural properties (i.e., liquid, semi-liquid or solid) of foodstuffs are also known to highly affect the probability and rate of microbial growth. This hypothesis has been widely studied for bacteria (Skandamis et al. 2000; Wilson et al., 2002; Theys et al. 2008), while limited information is available on how food micro-structure affects fungal growth and mycotoxin production.

Mathematical models constitute a valuable tool in order to predict the responses of microorganisms to environmental conditions. In contrast to pathogenic bacteria, filamentous fungi have received less attention as far as the predictive modeling is concerned (Valik et al., 1999; Tassou et al., 2007).

Considering the above, the present study aimed: (i) to monitor fungal growth and production of OTA on laboratory media and foodstuffs of different micro-structure, expressed in gelatin concentrations, at different temperatures; and, (ii) to develop and evaluate a predictive model for the growth rate of *A. carbonarius* and the kinetics of OTA production.

Materials and methods

Growth and OTA production kinetics of *A. carbonarius* (ATHUM 5659) were determined in Malt Extract Broth (MEB; pH 5.8; initial a_w : 0.99) supplemented with different gelatin concentrations (G: 0, 5, 10 and 20%) at different temperatures (T: 15, 20 and 25°C).

Equal volumes of liquid and gelatinized media (modified pH at 5.50; a_w : 0.99) were distributed into Petri dishes and Erlenmeyer flasks for assessment of fungal growth and OTA production, respectively. Fungi were grown on Malt Extract Agar for 7 days to obtain sporulating cultures and then spores suspensions were harvested in sterile water with 0.01% Tween 80. All culture media were inoculated with 10^3 spores/ml. Inoculated media were incubated at 15, 20 and 25°C. Furthermore, OTA production was evaluated on two food matrices of different micro-structure, such as dairy cream (oil-in-water emulsion) and jelly (gel), inoculated with *A. carbonarius* and incubated at 20°C.

Fungal growth was estimated by measuring the dry fungal biomass using sterile cellophane discs, according to Pasanen et al. (1999). OTA extraction and clean up was performed according to Romer Lab immunoaffinity columns. OTA detection-quantification was performed by HPLC. The primary model of Baranyi was used to obtain the kinetic parameters of fungal growth and OTA production of *A. carbonarius*. Then, the square root ($\sqrt{\mu_{\max}}$) of specific growth rate and OTA production rate were further modeled as a function of temperature and gelatin concentration using a polynomial model.

Results and discussion

The results suggested that the combination of temperature and gelatin concentration markedly affect the growth and OTA production of *A. carbonarius*. The optimum temperature for growth was 25°C (Fig.1a), while OTA production curves clearly showed that the maximum rate and levels of OTA production were observed at 20°C (Fig.1b), in agreement with previous reports (Belli et al., 2005; Marin et al., 2006).

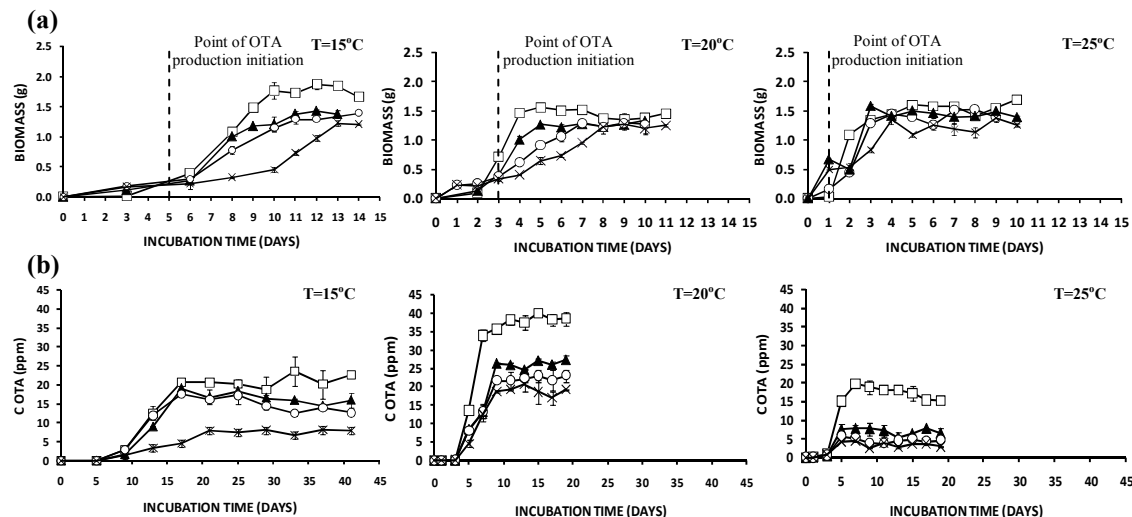


Figure 1. Graphical illustration of (a) growth and (b) OTA production kinetics of *A. carbonarius* on Malt Extract Broth using 0% (\square), 5% (\blacktriangle), 10% (\circ), and 20% (\times) gelatin as a solidified agent and incubated at 15°C, 20°C and 25°C.

With regards to micro-structure, increase of gelatin concentration seemed to constitute a hurdle for both fungal growth and OTA production, while the maximum amounts of OTA were observed in liquid media (absence of gelatin), regardless of temperature. Specifically, at all temperatures tested, growth and OTA production rate as well as maximum OTA production decreased as gelatin concentration increased from 0 to 20% (Fig. 1a, 1b). Similar results were also obtained for fungal growth rate. A possible interpretation is that the mechanisms responsible for suppressing growth rate and OTA production in structured media may be local depletion of oxygen and nutrients and local accumulation of metabolites (e.g.,

organic acids) near the hyphae (Wilson et al., 2002). Other studies support that microorganisms in structured products, are immobilized and forced to grow in a restricted space, thereby experiencing an additional stress, which reduces their growth rate (Brocklehurst et al., 1997; Theys et al., 2008).

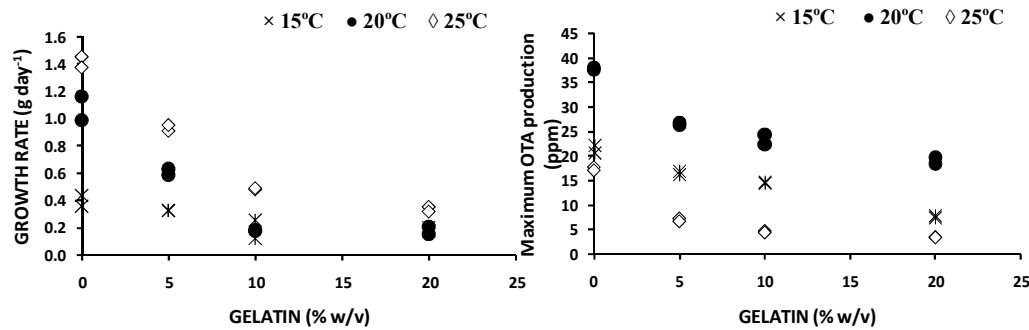


Figure 2. Comparison of *A. carbonarius* growth rate and maximum OTA production using different gelatin concentrations (0, 5, 10, and 20% w/v) and incubated at (×) 15°C, (●) 20°C, and (◇) 25°C.

The combined effect of gelatin concentration and temperature on growth and OTA production of *A. carbonarius* was modeled with a quadratic function. As far as fungal growth rate is concerned, a good agreement between the data and the model predictions was obtained ($R^2=0.91$), while poorer agreement was observed ($R^2=0.87$) for OTA production rate, possibly due to the high magnitude of OTA measurement (Table 1). The secondary model of Theys et al. (2008) and a Ratkowsky type model with the gelatin term $\sqrt{(G_{\max} - G)/(G_{\max} - G_{\text{opt}})}$ (Mejlholm and Dalgaard, 2007) were also evaluated, but resulted in R^2 of 0.72 and 0.75, respectively. Nonetheless, a realistic G_{\max} of 30.4% and a G_{opt} of 0.02% were determined. According to Figure 2, it is evident that growth rate and maximum OTA production followed a similar trend in response to gelatin concentration in the growth medium. Furthermore, Figure 2 shows that the increase of gelatin concentration caused a significant delay on growth rate and max. OTA production, regardless of temperature. Consistent with Fig. 2, the response surface (Fig. 3) also illustrated that the $\sqrt{\mu_{\max}}$ of OTA production is maximum in non gelatinized media at 20°C.

Table 1. Estimated parameters of secondary polynomial models for $\sqrt{\mu_{\max}}$ of growth and OTA production

| Parameters | Growth rate | OTA rate | Max. OTA |
|------------|-------------|----------|-----------|
| b | 0.248 | -13.859 | -21.881 |
| T | 0.019 | 1.626 | 2.917 |
| Gel | -0.018 | -0.178 | -0.180 |
| T*Gel | -0.002 | -0.002 | -8.83E-04 |
| T*T | 8.28E-04 | -0.039 | -0.076 |
| Gel*Gel | 0.002 | 0.008 | 0.005 |
| R^2 | 0.910 | 0.879 | 0.944 |
| RMSE | 0.079 | 0.260 | 0.307 |

Our findings for OTA production rates for 10-20% gelatin (15% gelatin is considered to approximate a culture medium with agar as solidified agent) are in agreement with researchers who studied the kinetics of produced OTA at similar conditions (a_w and pH) but in different culture media (Marin et al., 2006). The results also indicate that gelatin had not significant influence on lag phase, as opposed to temperature.

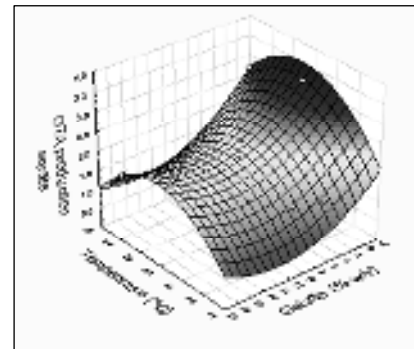


Figure 3. Quadratic response surface describing the effect of temperature and gelatin concentration on the square root of OTA production rate ($\sqrt{\mu_{\max}}$) of *A. carbonarius*.

In order to evaluate the model predictions, two foods of different micro-structure (dairy cream and jelly) were studied (fig. 4). The model agreed well with OTA production in cream but overpredicted (fail-safe) the rate of OTA in jelly (Table 2). A possible interpretation for such disagreements may be attributable to differences in intrinsic conditions (e.g., porosity and viscosity) and nutrients between laboratory media and food matrices. However, the trend of OTA production in foods was consistent with our observations on MEA.

Table 2. Observed and predicted μ_{\max} of OTA production on dairy cream and jelly.

| μ_{\max} of OTA production | | |
|--------------------------------|-----------------|----------------|
| Products | Predicted value | Observed value |
| Dairy cream | 1.963 | 2.418 |
| Jelly | 2.716 | 0.754 |

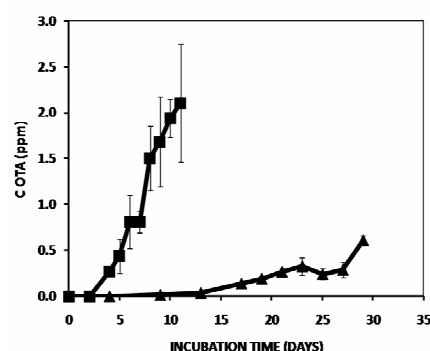


Figure 4. Kinetics of OTA production on (■) dairy cream and (▲) jelly, incubated at 20°C during 30day storage.

Conclusions

Structured environments seem to delay and suppress fungal growth and OTA production compared to more liquid environments, and such findings may assist in assessing the risk and control of OTA production in different products categories. However, the combined effect of structure with other determinants, such as pH, water content, nutrients or endogenous microflora of foods, in which OTA production is likely, is to be determined.

References

- Belli, N., A. J. Ramos, V. Sanchis and S. Marin. (2004) Incubation time and water activity effects on ochratoxin A production by *Aspergillus* section Nigri strains isolated from grapes. *Letters in Applied Microbiology* 38, 72–77.
- Brocklehurst, T. F., Mitchell, G. A., Smith, A. C., 1997. A model experimental gel surface for the growth of bacteria on foods, *Food Microbiology* 14, 303–311.
- Esteban A., M. L. Abarca, M. R. Bragulat and F. J. Cabañes. (2006) Study of the effect of water activity and temperature on ochratoxin A production by *Aspergillus carbonarius*. *Food Microbiology* 23, 634–640.
- International Agency for Research on Cancer (IARC). (1993) Monographs on the evaluation of carcinogenic risks to humans, some naturally occurring substances: Food items and constituents, heterocyclic aromatic amines and mycotoxins. Lyon, France: World Health Organization 56, 489–521.
- Marin S., Belli N., Lasram S., Chebil S., Ramos A.J., Ghorbel A., and Sanchis V. (2006) Kinetics of Ochratoxin A Production and Accumulation by *Aspergillus carbonarius* on Synthetic Grape Medium at Different Temperature Levels. *Food Microbiology and Safety* 71, M196–M200.
- Mejlholm O. and Dalgaard P. (2007) Modeling and Predicting the Growth Boundary of *Listeria monocytogenes* in lightly preserved seafood. *Journal of Food Protection* 70, 70–84.
- Pasanen, A.L., Yli-Pietila, K., Pasanen, P., Kallioikoski, P., Tarhanen, J. (1999) Ergosterol content in various fungal species and biocontaminated building materials. *Applied Environmental Microbiology* 65, 138– 142.
- Skandamis P., E. Tsigarida and G-J.E. Nychas. (2000) Ecophysiological attributes of *Salmonella typhimurium* in liquid culture and within a gelatin gel with or without the addition of oregano essential oil. *World Journal of Microbiology & Biotechnology* 16, 31–35.
- Tassou C.C., E.Z. Panagou, P. Natskoulis and N. Magan. (2007) Modeling the effect of temperature and water activity on the growth of two ochratoxigenic strains of *Aspergillus carbonarius* from Greek wine grapes. *Journal of Applied Microbiology* 103, 2267–2276.
- Theys T.E., Geeraerd A.H., Verhulst A., Poot K. , Van Bree I., Devlieghere F., Moldenaers P., Wilson D., Brocklehurst T., Van Impe J.F. (2008) Effect of pH, water activity and gel micro-structure, including oxygen profiles and rheological characterization, on the growth kinetics of *Salmonella Typhimurium*. *International Journal of Food Microbiology* 128,67–77.
- Valik L., J. Baranyi and F. Görner. (1999) Predicting fungal growth: the effect of water activity on *Penicillium roqueforti*. *International Journal of Food Microbiology* 47, 141–146.
- Wilson P.D.G., T.F. Brocklehurst, S. Arino, D. Thuaud, M. Jakobsen, M. Lange, J. Farkas, J.W.T. Wimpenny and J.F. Van Impe. (2002) Modeling microbial growth in structured foods: towards a unified approach. *International Journal of Food Microbiology*. 73, 275– 289.

Development of a product specific model for spoilage of pasteurized fruit juices by *Saccharomyces cerevisiae* and validation under dynamic temperature conditions

E.Z. Panagou¹, S. Karathanassi¹, Y. Le Marc² and G.-J.E. Nychas¹

¹Agricultural University of Athens, Department of Food Science and Technology, Laboratory of Microbiology and Biotechnology of Foods, Iera Odos 75, 118 55 Athens, Greece (stathspanagou@aua.gr)

²Institute of Food Research, Norwich Research Park, Colney, Norwich NR4 7UA, UK (yvan.lemarc@bbsrc.ac.uk)

Abstract

A product specific model was developed and validated under dynamic temperature conditions for predicting the growth of *S. cerevisiae* in pasteurized fruit juices. Commercially prepared fruit juices were inoculated with *S. cerevisiae* (initial inoculum *ca.* $2.8 \log_{10}$ CFU ml⁻¹), and stored at 4, 8, 12, and 16°C for up to 50 days. The growth kinetic parameters at each temperature were determined by the primary model of Baranyi and Roberts, and the maximum specific growth rate was further modelled as a function of temperature by a square root-type model. The performance of the model in predicting the growth of the yeast under dynamic temperature profiles was based on two temperature scenarios with periodic changes from 4 to 12°C. Model performance was based on the calculation of the bias (B_f) and accuracy (A_f) factors, the goodness-of-fit (*GoF*) index and the percent relative errors between observed and predicted growth. Moreover, fruit juice spoilage was sensory evaluated by observing gas production in the packages and subsequent swelling. It was observed that package deformation due to swelling was evident when the population of *S. cerevisiae* reached the level of $7 \log_{10}$ CFU ml⁻¹ for the higher isothermal temperatures (12 and 16°C), whereas for the lower temperatures (4 and 8°C) package deformation was noticeable at $6 \log_{10}$ CFU ml⁻¹. Spoilage was observed at 28 and 15 days, respectively, at 4 and 8°C for pasteurized apple juice. However, at higher temperatures (12 and 16°C) shelf-life was drastically reduced at 6 and 4 days, respectively. The respective values for strawberry juice were 32, 11, 5, and 3 days at 4, 8, 12, and 16°C, respectively. The shelf-life for the aforementioned temperatures was calculated via the Monod equation providing realistic estimates of the shelf-life of fruit juices stored under isothermal conditions. Specifically, for apple juice estimated shelf-life was 23.4, 15.1, 5.9, and 3.7 days at 4, 8, 12, and 16°C, respectively.

Keywords: dynamic modelling, fruit juices, *S. cerevisiae*, spoilage, yeasts

Introduction

Yeasts can generally withstand extreme conditions better than bacteria and consequently they are found in low pH products and products containing preservatives in concentrations where bacteria cannot grow (Deak and Beuchat 1996). The main factor to control microbial growth in fruit juices is pH, with the exception of certain fruit juices which contain benzoate or are carbonated (Loureiro 2000). The pH value of juices varies, but in most cases it is sufficiently low to select for yeasts, moulds, lactic acid bacteria and acetic acid bacteria. Fruit juice concentrates, fruit pulps, packaged fruit juices and soft drinks are especially prone to spoilage by yeasts, namely *S. cerevisiae*, *S. bayanus*, and *S. pastorianus* to a lesser extend (Fleet 2006). The principal spoilage reaction of *Saccharomyces* species is the fermentation of sugars (e.g. glucose, fructose, sucrose, maltose) with the production of mainly ethanol and carbon dioxide. The latter gives the product a gassy appearance and caused packages to swell with the concurrent development of a distinctive alcoholic, fermentative taste and smell. The aim of this work was to develop and validate a product specific model to predict the growth of *S. cerevisiae* in pasteurized fruit juices under isothermal and dynamic (fluctuating) temperature conditions. Based on the developed model, the shelf-life of fruit juices was determined using the Monod equation (for isothermal conditions) and Monte Carlo approach (for fluctuating temperature profiles).

Materials and methods

Packages (1 l volume) of commercially prepared and thermally treated fruit juices (green apple, peach, and strawberry juice) were obtained directly from a local manufacturer. Fruit juices taken after the processing line were inoculated with *S. cerevisiae* (initial inoculum of $2.8 \log_{10}$ CFU ml⁻¹), and stored at 4, 8, 12, and 16°C for up to 50 days. Uninoculated fruit juices were also incubated at the same temperatures and served as control. At appropriate time intervals depending on each incubation temperature, fruit juice samples were analyzed to allow for efficient kinetic analysis of microbial growth on YPD medium as well as on plate count agar for total viable counts. The growth kinetic parameters at each temperature were determined by the primary model of Baranyi and Roberts (1994). The performance of the model in predicting the growth of the yeast under dynamic temperature profiles was based on two temperature scenarios: (i) 12 h at 4°C, 6 h at 8°C and 6 h at 12°C, and (ii) 12 h at 4°C and 12 h at 8°C. Model performance was based on the calculation of the bias (B_f) and accuracy (A_f) factors, the goodness-of-fit (GoF) index and the percent relative errors between observed and predicted growth. In order to determine the product's shelf-life at each isothermal temperature, the equation of Monod was employed. Initially, shelf-life was determined by a sensory panel as the time needed for the package to swell. The shelf-life was subsequently correlated linearly with the temperature, using the modified Arrhenius equation. In the case of fluctuating temperature profiles, shelf-life was determined using a Monte-Carlo simulation, a technique that allows for the calculation of the desired output (shelf-life) based on input described by distributions instead of mean values.

Results and discussion

The population dynamics of *S. cerevisiae* in green apple and peach juices are presented in Figure 1. Similar results were obtained for the strawberry juice. A typical growth pattern was observed, comprising an initial lag phase, an exponential growth phase and finally a stationary phase. It is characteristic that the lag phase was very short in all juices even at the lowest storage temperatures as yeasts did not seem to be affected by these temperatures.

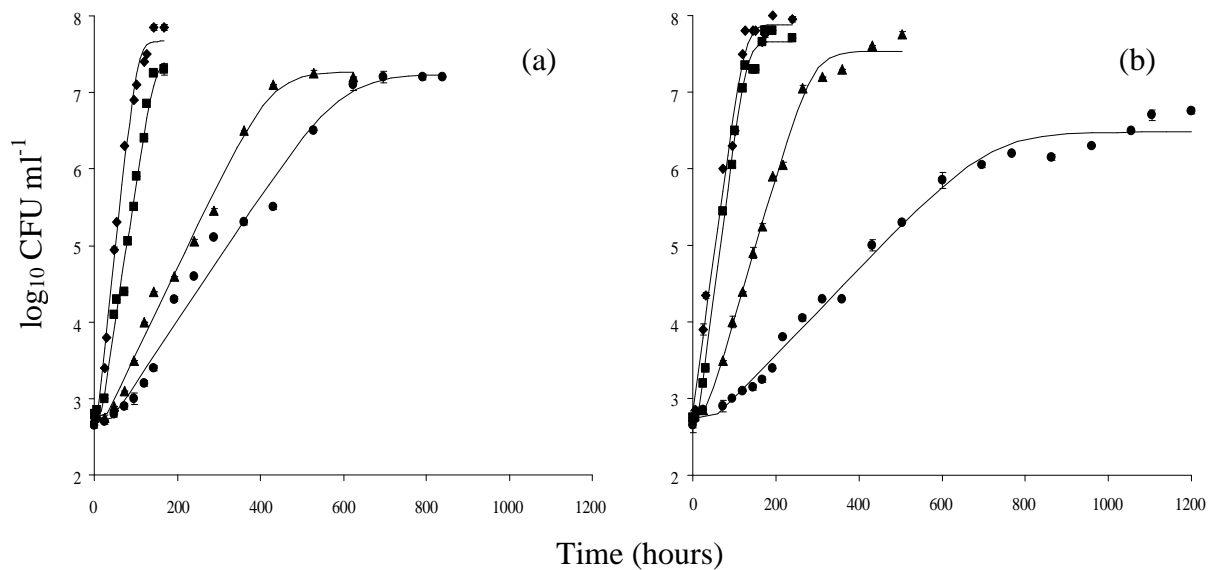


Figure 1: Growth curves of *S. cerevisiae* in green apple juice (a) and peach juice (b) stored at different isothermal conditions (●, 4°C; ▲, 8°C; ■, 12°C; ◆, 16°C).

No yeasts were enumerated in any of the control samples stored under the same conditions. The estimated kinetic parameters and statistical indices are shown in Table 1. The effect of storage temperature on μ_{\max} was further quantified by means of a secondary square-type model (Table 2). The model developed under isothermal conditions was validated against observed growth of the spoilage yeast for the dynamic temperature profile using two fluctuating temperature scenarios with periodic changes from 4 to 12°C. A typical example of the predicted growth of *S. cerevisiae* in peach juice is

shown in Figure 2. The average values of the performance indices for apple fruit juice were 1.021, 1.047, and 0.274 for B_f , A_f , and GoF , respectively for both temperature scenarios assayed. The respective values for strawberry juice were 0.98, 1.03, and 0.22 for B_f , A_f , and GoF .

Table 1: Parameters and statistics of the model of Baranyi and Roberts for the growth of *S. cerevisiae* in pasteurized fruit juices under different isothermal conditions.

| Product | Temp. (°C) | μ_{max} (h ⁻¹) | λ (h) | $h_0^{(1)}$ | $N_0^{(2)}$ | $N_{max}^{(3)}$ | SE of fit | R^2 |
|-------------------|------------|--------------------------------|---------------|-------------|-------------|-----------------|-----------|-------|
| Peach juice | 4 | 0.0129 | 52.9 | 0.682 | 2.7 | 6.7 | 0.1551 | 0.989 |
| | 8 | 0.0424 | 31.3 | 1.327 | 2.8 | 7.5 | 0.1375 | 0.994 |
| | 12 | 0.0958 | 12.3 | 1.178 | 2.7 | 7.7 | 0.1576 | 0.994 |
| | 16 | 0.0919 | - | - | 2.8 | 7.9 | 0.2446 | 0.984 |
| Green apple juice | 4 | 0.0187 | 33.8 | 0.632 | 2.7 | 7.2 | 0.2097 | 0.986 |
| | 8 | 0.0260 | 26.4 | 0.686 | 2.7 | 7.3 | 0.1643 | 0.991 |
| | 12 | 0.0841 | 18.7 | 1.570 | 2.8 | 7.5 | 0.1846 | 0.987 |
| | 16 | 0.1171 | 6.8 | 0.795 | 2.7 | 7.7 | 0.1988 | 0.990 |
| Strawberry juice | 4 | 0.0120 | 44 | 0.532 | 2.7 | 6.5 | 0.1259 | 0.993 |
| | 8 | 0.0458 | 36.2 | 1.658 | 2.8 | 7.1 | 0.1012 | 0.996 |
| | 12 | 0.0976 | 14.7 | 1.435 | 2.8 | 7.4 | 0.0971 | 0.996 |
| | 16 | 0.0942 | 0.8 | 0.075 | 2.7 | 7.4 | 0.2086 | 0.986 |

⁽¹⁾ Adaptation work parameter estimated as $\mu_{max} \times \lambda$.

^{(2), (3)} Initial and final population (\log_{10} CFU ml⁻¹) of *S. cerevisiae* determined by fitting.

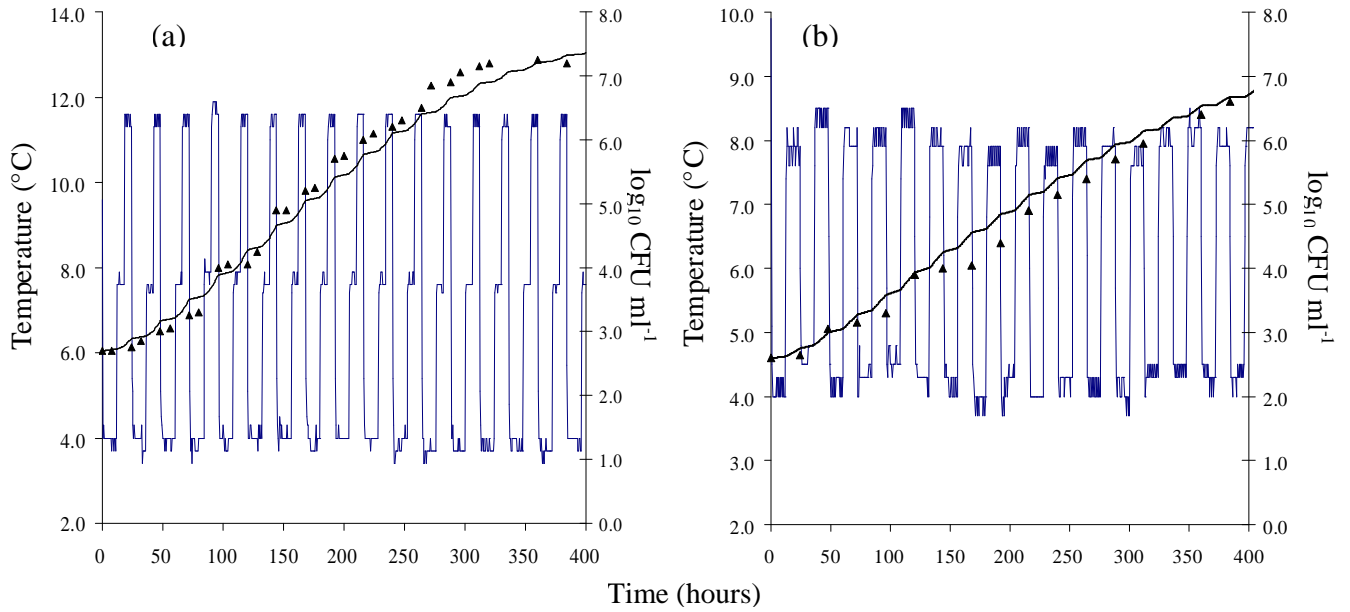


Figure 2: Comparison between observed (points) and predicted (lines) growth of *S. cerevisiae* in pasteurized peach juice under periodically changing temperature conditions (a: 12 h at 4°C, 6 h at 8°C and 6 h at 12°C; b: 12 h at 4°C and 12 h at 8°C).

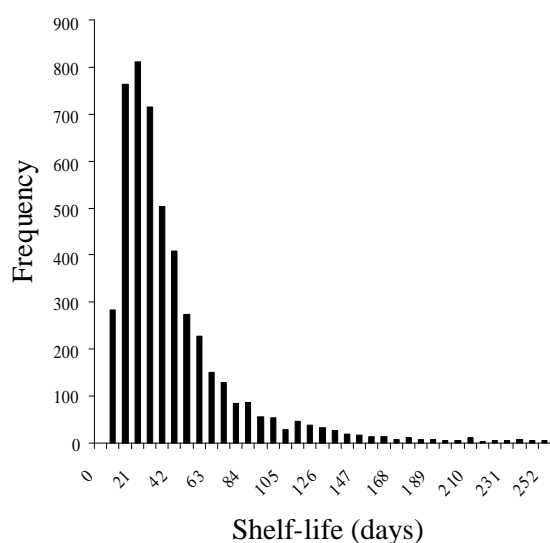
The shelf life of pasteurized fruit juices determined (a) sensorially, i.e. as the time elapsed for package swelling ($SL_{sensory}$), (b) using the Monod's equation (SL_{obs}), and (c) using the Arrhenius equation (SL_{pred}) are summarized in Table 2. Generally, the samples of pasteurized fruit juices stored at 4 and 8°C demonstrated increased shelf life compared with those stored at 12 and 16°C, which presented higher growth rate of *S. cerevisiae* resulting in a drastically decreased shelf-life. The observed shelf-life of fruit juices stored at fluctuating temperatures was 13 days for peach and strawberry juice and 17

days for green apple juice for the two temperature profile (12 h at 4°C and 12 h at 8°C). In the case of the three temperature profile (12 h at 4°C, 6 h at 8°C and 6 h at 12°C) the respective observed shelf-life was 9 and 11 days for peach and strawberry juices, and green apple juice, respectively.

Table 2: Shelf-life determination of pasteurized fruit juices during isothermal storage at 4, 8, 12, and 16°C.

| Product | Temp. (°C) | Ns ⁽¹⁾ | Sensory SL (days) | Observed SL (days) | Predicted SL (days) |
|-------------------|------------|-------------------|----------------------|-----------------------|------------------------|
| Peach juice | 4 | 6.2 | 29 | 28.2 | 24.7 |
| | 8 | 7.1 | 11 | 11.0 | 12.1 |
| | 12 | 7.1 | 5 | 4.9 | 5.8 |
| | 16 | 6.0 | 3 | 3.3 | 2.8 |
| Green apple juice | 4 | 7.0 | 28 | 23.4 | 24.5 |
| | 8 | 6.5 | 15 | 15.1 | 12.8 |
| | 12 | 7.3 | 6 | 5.9 | 6.7 |
| | 16 | 6.9 | 4 | 3.7 | 3.5 |
| Strawberry juice | 4 | 6.3 | 32 | 30.6 | 25 |
| | 8 | 6.8 | 11 | 9.8 | 12 |
| | 12 | 7.1 | 5 | 4.8 | 5.8 |
| | 16 | 6.0 | 3 | 3.4 | 2.7 |

⁽¹⁾ Yeast population at spoilage (log₁₀ CFU ml⁻¹)



Monte-Carlo simulation was employed to estimate the shelf-life of fruit juices at fluctuating temperature profiles using the following distributions for the parameters of the model: *Initial concentration of the yeast (N₀)*: Normal (-1.4, 1); *Storage temperature*: LogLogistic (-2.91, 9.33, 4.83); *Yeast population at spoilage (N_s)*: ExtValue (6.73, 0.17). The results of the simulation for 5,000 runs for strawberry juice are presented in Figure 3, showing the highest frequency, and hence shelf-life, between 14 to 28 days of storage. This estimation is more conservative than the stated shelf-life by fruit juices manufacturers, which is 60 days.

Figure 3: Shelf-life determination of strawberry fruit juice based on Monte Carlo simulation.

Acknowledgements

This work was funded by TRUEFOOD, an Integrated Project financed by the EU under the 6th Framework Programme for RTD (contract no FOOD-CT-2006-016264).

References

- Baranyi J. and Roberts T.A. (1994) A dynamic approach to predicting bacterial growth in food. *International Journal of Food Microbiology* 23, 277-294.
- Deak T. and Beuchat L.R. (1996) Handbook of food spoilage yeasts. CRC Press, New York, USA.
- Fleet G.H. (2006) *Saccharomyces* and related genera. In *Food Spoilage Microorganisms* (ed. C.W. Blackburn), pp. 306-335. Woodhead Publishing Ltd., Cambridge, United Kingdom.
- Loureiro V. (2000) Spoilage yeasts in foods and beverages: characterization and ecology for improved diagnosis and control. *Food Research International* 33, 247-256.

Modeling lag time of *Bacillus cereus* spore growth after heat treatment

O. Couvert², C. Denis³, D. Thuault², L. Coroller¹, P. Mafart¹, I. Leguerinel*¹

¹ Université Européenne de Bretagne France – Université de Brest– LUBEM EA 3882 - UMT Physiopt 08.3
6 rue de l'Université, 29334 Quimper cedex, France (guerinel@univ-brest.fr)

² ADRIA Développement - UMT Physiopt 08.3 Creac'h Gwen F29186 Quimper Cedex France

³ ADRIA Normandie Boulevard 13 juin 1944 B.P.2 14310 Villers Bocage France

Introduction

Bacillus cereus is a sporulated bacteria which resist mild heat treatments and is able to grow at low temperatures which make this bacteria of special interest in REPFED products.

Many heat treatments are insufficient to completely inactivate bacterial spore population. For example pasteurized products are heat treated to a temperature close to ninety degrees. These heat treatments decrease population size and increase lag time of spore survivor growths. These effects are influenced by time and temperature treatment, and also by recovery or incubation temperature. Thus the objective of the study was to model the impact of heat treatment and incubation temperature on spore lag time of *Bacillus cereus* spores.

Material and methods

Three strains of *Bacillus cereus* were studied. *Bacillus cereus* ATCC 14579 which is the reference strain for *Bacillus cereus* species, *Bacillus cereus* KBAB4 which is a psychotropic strain, belonging to *Bacillus cereus* genetic group 6, also named *Bacillus weihenstephanensis*. Finally *Bacillus cereus* INRA 399 has been chosen as a psychotropic strain belonging to genetic group 2. For each strain studied experimental designs were composed of two monofactorial design associated in cross with 5 levels for recovery temperatures and 3 levels of heating temperatures, thus in total 7 different conditions. For each condition thermal death kinetic was recorded and lag times were determined from growth kinetics for different heating time.

Spores of four psychrophilic and mesophilic strains have been studied. Nutrient broth containing spores was introduced in capillary tubes and submitted to thermal treatments in a thermostated glycerol bath. After heating, capillary content was poured into special flask with 9mL nutrient broth and incubated under agitation at different temperatures between 4 and 20°C. Survival spores were counted, at the same time interval in nutrient agar plates.

Growth was monitored in flask by optical density at 600 nm and represented as log of the bacterial concentration versus time. The lag time, defined as the time before the first cellular division including germination, corresponds to the intersection point of the exponential growth and initial bacterial concentration. A correlation was observed between the decimal reduction number obtained after heat treatment (time/temperature) and lag time when spores were recovered in the same medium at the same temperature.

Résults and discussion

Our first observation leads to develop an overall model where the factors taken into account are heating temperature, heating time and recovery temperature.

Experimental data (Fig 1) shows linear relationship between lag time and heating time or decimal number reduction. This relation can be described by a simple equation where the first term represents the additional lag time due to the applied heat treatment and the second term represents the lag time without heat treatment.

The two terms have been developed. The first term was developed as a function of the ratio F/D^* . The second term development uses the Ratkowsky equation $\mu=b(T'-T'_{\min})^2$ where $\lambda\mu$ is considered constant. λ_0 is a function of recovery temperature and minimal growth temperature with a constant k .

The combination and the re parametration these two developed terms follow to this equation:

$$\lambda = \frac{\lambda_0 (K^* F_{0.5} + \lambda_0^*)}{(T_{\min})^2}$$

In this equation λ_0^* presents a biological significance: lag time without heat treatment at T'_{\min} plus X °C., K^* is a simple parameter without dimension and no biological significance. These model parameters were fitted on our experimental data for the 3 strains of *B. cereus*.

Figure 1 shows the quality of fit of this model for different heating and recovery temperature for *Bacillus cereus* KBAB4

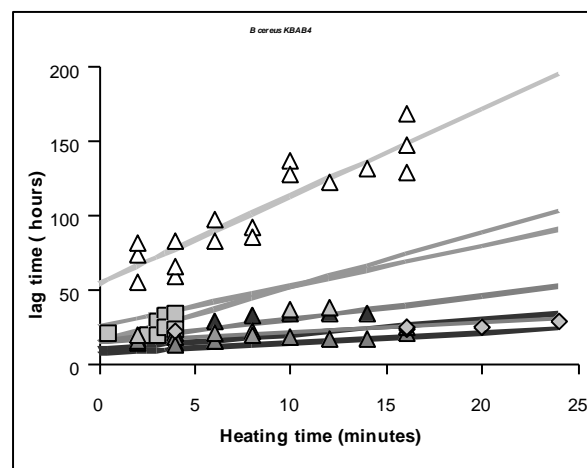


Figure 1 lag time vs heating time for different heating and recovery temperature for *Bacillus cereus* KBAB4

The parameter values fitted on experimental data are presented in table1 , The parameters z_T , T_{\min} are in the range of given values and λ_0^* values can be visually verified for $T_{\min} + 10^\circ\text{C}$.

Table1 parameter values fitted on experimental data

| <i>Bacillus cereus</i> strain | KBAB4 | INRA 399 | ATCC 14579 |
|-------------------------------|-------|----------|------------|
| T^* °C | 95,00 | 95,00 | 95,00 |
| k^* | 595 | 23,1 | 1,1 |
| λ_0^* hours | 9,47 | 53,32 | 4,52 |
| Z °C | 7,97 | 8,06 | 6,81 |
| T_{\min} °C | 5,78 | -1,14 | 11,09 |

The observation of experimental data and modelled fitted curves (Fig 1) shows the quality of this model. This presented model appears simple and robust, and be easy to use.

This work was supported by a grant from the Agence Nationale de la Recherche (ANR) (France) as part of an ANR-05-PNRA-013 *B. cereus* contrat.

Exploring lag phase and growth initiation of a yeast culture by means of an Individual-based Model

X. Portell¹, C. Prats², M. Silbert³, M. Ginovart⁴

¹ Department of Agri-Food Engineering and Biotechnology, Technical University of Catalonia, Barcelona, Spain (xavier.portell@upc.edu)

² Department of Physics and Nuclear Engineering, Technical University of Catalonia, Barcelona, Spain (clara.prats@upc.edu)

³ Institute of Food Research, Norwich Research Park Colney, Norwich, UK (moises.silbert@bbsrc.ac.uk)

⁴ Department of Applied Mathematics III, Technical University of Catalonia, Barcelona, Spain (marta.ginovart@upc.edu)

Abstract

Yeast ageing and inoculum size are factors that affect successive industrial fermentation, particularly in those processes that reuse the yeast cells. The aim of the work is to explore the effects of inocula size and aging on the dynamics of yeast population. However, only individual-based modelling (IbM) makes possible studies of small, well characterized, microbial inocula. Here we have made use of INDISIM-YEAST to carry out these studies. Several simulations were performed to analyze inoculum size and their different genealogical ages on the lag phase, first division time and specific growth rate. Shortest lag phase and time to the first division were obtained with largest inocula and with youngest inoculated parent cells.

Keywords: Individual-based model, lag phase, growth initiation, yeast inocula

Introduction

In industrial applications yeast is usually propagated in a number of steps before being inoculated into the final fermentation medium. The inoculated culture is not often well defined in spite of the fact that the physiological condition of the yeast cells may greatly affect the duration and outcome of the fermentation (Walker 1998). For instance, the production of beer reuses yeast cropped at the end of fermentation in subsequent fermentation, so yeast is maintained and reused a number of times, a process called ‘serial repitching’. When yeast cells are inoculated into a fresh growth medium, these enter a brief lag phase where they are biochemically active but they still do not divide. After this lag phase, cells go into their cell cycle and start dividing. We are concerned here with yeast budding reproduction, which leads to scar formation. The genealogical age of yeast cells and the small size of daughter cells in front of older cells are two individual characteristics that influence the evolution of a culture at the beginning of its development.

The microbial lag phase has usually been investigated with continuous population models using rather high inoculum levels. When microbial growth is considered starting from a few cells, the study of this evolution demands an individual-based approach. The two approaches, however, can converge to similar results as the size of the population increases (Gómez-Mourelo and Ginovart, 2009).

Unlike continuous models, IbM is a bottom-up approach. Of those available (Hellweger and Bucci 2009) we have used INDISIM, the simulator developed by our group (Ginovart *et al.* 2002, Ferrer *et al.* 2008), and which has already been used to study different features of the bacterial lag phase providing an ample pool of interesting results (Prats *et al.* 2006, 2008). INDISIM-YEAST constitutes the adaptation of INDISIM to study the specific characteristics of the yeast cell cycle to take care of yeast populations growing in liquid media (Ginovart *et al.* 2007, Ginovart and Cañadas 2008). This simulator has recently been used to attempt to study some aspects of the influence of cell ageing on the fermentation processes (Ginovart *et al.* 2009).

The aim of this contribution is to explore the effects of specific characteristics of the initial inocula on the dynamics of a yeast culture in liquid medium during the lag phase and the first stages of growth using the individual-based simulator INDISIM-YEAST.

Material and methods

For each yeast cell, INDISIM-YEAST implements a set of rules for uptake and metabolism of nutrient particles, excretion of end products, budding reproduction and viability. The yeast population is made up of a set of cells with individual variables defining them (position in the spatial domain, biomass, genealogical age as the number of bud scars on the cellular membrane, reproduction phase in the cellular cycle where it is the unbudded or budding phase, “start mass” or mass required to change from the unbudded to budding phase, minimum growth for the budding phase, minimum time to complete the budding phase and survival time without satisfying its metabolic requirements). The description of the principal concepts of this yeast cell modelling plus the different elements to assemble the structure system for the virtual process of glucose fermentation can be found in the works of Ginovart *et al.* (2007) and Ginovart and Cañadas (2008).

The main simulation result shown in the present study is the temporal evolution of the yeast population that grows from an inoculum, which is completely characterized. Special attention is focused during the first stages of its development until the population reaches the exponential phase. There is no nutrient limitation on the initial conditions of the simulated culture.

Two parameters are used to characterize the outcome of a given culture growth during the first stages. The first is the classic lag parameter, defined at the population level of description and calculated through its geometrical definition. When the population reaches its maximum and enters the stationary phase, a logarithmic regression of an upper interval in the exponential growth is performed to obtain the straight line $\text{Ln}N = \mu t + b$ and the maximum growth rate μ (Figure 1). The intersection of the prolongation of this straight line with the $\text{Ln}N_0$ line gives the lag time λ , where $\lambda = (\text{Ln}N_0 - b)/\mu$. In order to characterise much better the initial steps of the yeast population at an individual level of description, a second parameter is also considered, the time when the First microbial Division (t_{FD}) takes place or the first budding reproduction appears (Figure 1).

Several simulations to evaluate the above parameters have been carried out with yeast cells of different genealogical ages making up the inocula (namely samples that include daughter cells or virgin cells with 0 scars and/or parent cells with 1,2, 3,...,7 or 8 scars on their membranes), and with inocula of different sizes (the number of yeast cells to begin the evolution is set from 1 cell to 1000 cells).

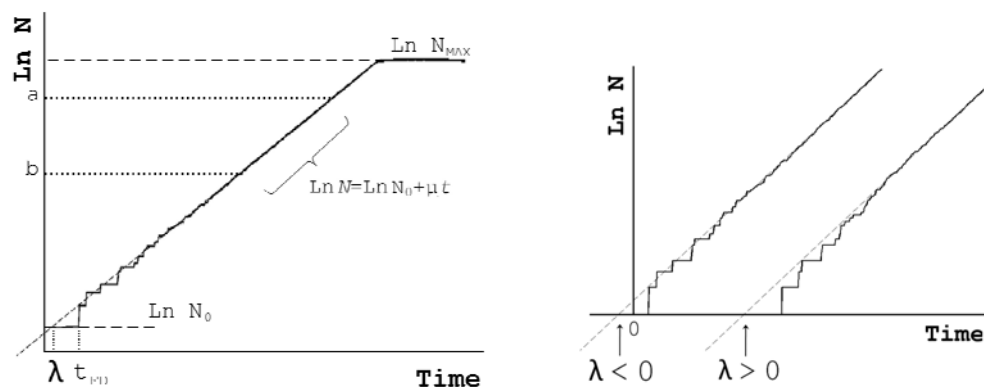


Figure 1: Calculation of the following parameters: lag time, first division time and maximum growth rate (exponential phase). *Left*: geometrical method to obtain λ and μ , where $a = \text{Ln}N_0 + 0.85(\text{Ln}N_{\text{MAX}} - \text{Ln}N_0)$ and $b = \text{Ln}N_0 + 0.60(\text{Ln}N_{\text{MAX}} - \text{Ln}N_0)$. *Right*: two different simulations to show how negative and positive lag times can be achieved.

Results and discussion

We present the results of two series of simulations carried out using INDISIM-YEAST with different virtual inocula. From a heterogeneous population of yeast cells successive inocula have been obtained which, in turn became the initial seeds to perform those simulations. The first series (with 50 runs for each case) is designed to evaluate the effect of the genealogical age of the inoculum, which is made up of a unique yeast cell, on the parameters λ , t_{FD} and μ of the growth curve (Figure 2). The second, also with 50 simulations in each case, studies yeast growth from different size inocula randomly taken from the aforementioned population (Figure 3). Low inocula growth curves have high synchronisms during the first stages of the temporal evolution. These synchronisms result in a geometrical effect that deforms the geometrical evaluation of the lag phase (Figure 1). Moreover, the fact that in some cases the lag time is shorter than its corresponding time for the first bud reproduction (Figures 2 and 3) is not consistent with the concept that lag phase desires to represent. For single-cell inocula (Figure 2) both parameters have their minimum value for youngest parent yeast. As the genealogical age of the inoculum increases, λ and t_{FD} became longer. Daughter cells also have longer lags than young parent cells. Regarding the inoculum size, large inocula reach the exponential phase sooner than small inocula do (Figure 3). A third series of simulations has been performed selecting inocula that combine the preceding two factors, size and genealogical ages. That is, different inocula sizes with only virgin cells (0 scars), middle-age cells (1-5 scars) or old cells have been chosen to perform sets of 50 runs for each combination (data not shown). All these simulations results show there is an influence of these initial features of the inocula on λ and t_{FD} , and only slight discrepancies on μ are observed.

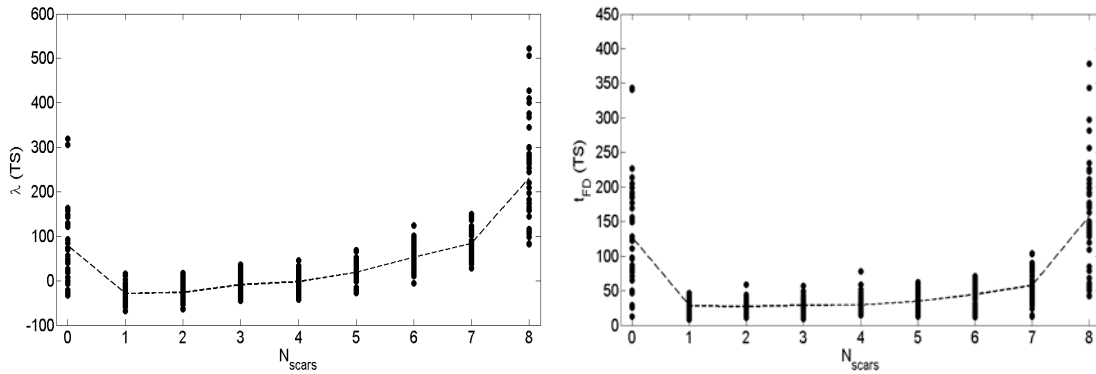


Figure 2: First simulations series (see text). Lag parameter (*left*) and first division time (*right*) versus the number of scars of the single-cell inoculum. The dashed line indicates the mean value for each genealogical age.

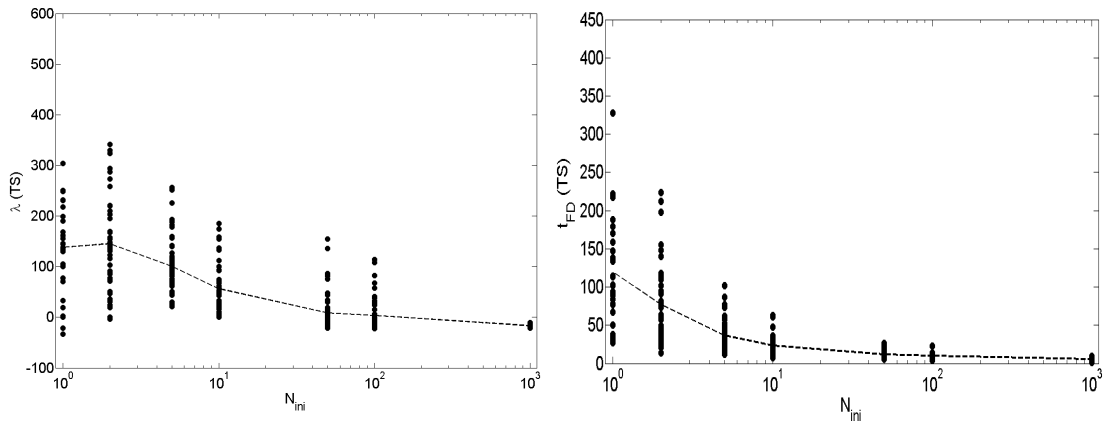


Figure 3: Second simulations series (see text). Lag parameter (*left*) and first division time (*right*) versus inoculum size. The dashed line indicates the mean value for each inoculum size.

Within the stated limitations, this study mimics the industrial production of beer, which reuses yeast cropped at the end of fermentation in subsequent fermentations, so the immediate and long term fermentation performance is conditioned by the characteristics of these reused inocula. Since the yeast *Saccharomyces cerevisiae* has a limited replicative lifespan, each cell within a population is only capable of a finite number of divisions prior to senescence and death (Powell *et al.*, 2000, 2003). Towards the end of fermentation yeast sediments and are collected within the fermenter cone. Sedimentation results in the formation of zones enriched with cells of a particular age. At the end of a fermentation a portion of the yeast is removed from the fermentation vessel for 'serial repitching'. Typically this is the centre-top portion of the yeast crop, theoretically comprising middle-aged and virgin cells (Powell *et al.*, 2003).

Conclusions

We have shown that the IbM INDISIM-YEAST is capable of distinguishing the differences in the evolution of a population that emerges from a small inocula, whether it started with a single microorganism, a population make up by different genealogical ages, or different sizes. It is particularly useful in the study of small inocula and the initial steps of the population evolution because of the excessive influence of the discrete and asymmetrical nature of yeast division. It is here that it has an edge compared to top-down continuous models, which are useful only when the initial population contains a large number of cells. The tendencies found in the simulations resemble those seen during 'serial repitching' in beer fermentation.

Acknowledgements

We thank Rosa Carbó for several comments and suggestions. We gratefully acknowledge the financial support received from the Ministry of Education and Science (Plan Nacional I+D+i) through Grant CGL2007-65142/BOS, and the Universitat Politècnica de Catalunya (UPC).

References

- Ferrer J., Prats C. and López D. (2008) Individual-based modeling: An essential Tool for Microbiology. *Journal of Biological Physics* 34 (1-2), 19-37.
- Ginovart M., López D. and Valls J. (2002) INDISIM, and individual based discrete simulation model to study bacterial cultures. *Journal of Theoretical Biology* 214 (2), 305-319.
- Ginovart M., Xifré J., López D. and Silbert M.: INDISIM-YEAST, an individual-based model to study yeast population in batch cultures. In: Méndez-Vilas A (ed) Communicating current research and educational topics and trends in applied microbiology, Microbiology book series nº1 Vol. 1, Formatex, Badajoz, 2007, 401-409.
- Ginovart M. and Cañadas, J.C. (2008) INDISIM-YEAST: an individual-based simulator on a website for experimenting and investigating diverse dynamics of yeast populations in liquid media. *Journal of Industrial Microbiology and Biotechnology* 35 (11), 1359-1366.
- Ginovart M., Portell X., Silbert M. (2009) Repitching of yeast in beer fermentations: individual-based model simulations. In I. Troch and F. Breiteneker (Eds.), *Proceedings MATHMOD 09 Vienna*, in press, ARGESIM Report no. 35 (ISBN 978-3-901608-35-3) [*MATHMOD Vienna-Vienna International Conference on Mathematical Modelling*, Vienna (Austria), February 11-13, 2009].
- Gómez-Moureló P. and Ginovart M. (2009) The differential equation counterpart of an individual-based model for yeast population growth. *Computers & Mathematics with Applications*, in press.
- Hellweger F.L. and Bucci V. (2009) A bunch of tiny individuals - Individual-based modeling for microbes. *Ecological Modelling* 220 (1), 8-22.
- Powell C.D., Van Zandyke S.M., Quain D.E. and Smart K.A. (2000) Replicative ageing and senescence in *Saccharomyces cerevisiae* and the impact on brewing fermentations. *Microbiology* 146 (5), 1023-1034.
- Powell C.D., Quain D.E. and Smart K.A. (2003) The impact of brewing yeast cell age on fermentation performance, attenuation and flocculation. *FEMS Yeast Research* 3 (2), 149-157.
- Prats C., López D., Giró A., Ferrer J. and Valls J. (2006) Individual-based modelling of bacterial cultures to study the microscopic causes of the lag phase. *Journal of Theoretical Biology* 241 (4), 939-953.
- Prats C., Giró A., Ferrer J., López D., Vives-Rego J. (2008) Analysis and IbM simulation of the stages in bacterial lag phase: Basis for an updated definition. *Journal of Theoretical Biology* 22 (1), 56-68.
- Walker G.M. (1998) *Yeast physiology and biotechnology*, JohnWiley & Sons, Chichester, UK, 350 pp. (ISBN 0-471-96446-8).

Effects of temperature adaptation during growth or sporulation on heat resistance of *Bacillus cereus* spores

E. Baril^{* 1,2}, L. Coroller², I. Leguerinel², P. Mafart²

¹ ADRIA Developpement, Z.A. de Creac'h Gwen, 29 196 Quimper, France

² Université Européenne de Bretagne, France - Université de Brest, EA3882 Laboratoire Universitaire de Biodiversité et Ecologie Microbienne, IFR148 ScInBioS, UMT 08.3 PHYSIOpt, 6 rue de l'Université, 29334 Quimper, France. (Eugenie.baril@univ-brest.fr)

Introduction

Microbiological risk assessment is modelled taking into account many environmental steps from raw ingredient to food consumption. However predictive microbiology lacks data about the bacterial sporulation behaviour (Nauta *et al.*, 2003).

The effects of the sporulation temperature on heat resistance of *Bacillus cereus* spores have been widely investigated. Sporulation temperature has been shown among the major factors that impact on spore heat resistance (Palop *et al.*, 1999). $D_{100^\circ\text{C}}$ values were 10-fold higher for *Bacillus cereus* spores when the sporulation temperature increased from 20°C to 45°C (Gonzalez *et al.*, 1999). Then, a linear relationship has been established between sporulation temperature and heat resistance of spores (Leguerinel *et al.*, 2007) :

$$\log D = \log D^* - \left(\frac{T - T^*}{z_T} \right) + \left(\frac{T_{spo} - T^*}{z_{T_{spo}}} \right)$$

Where: T^* is the reference sporulation temperature,

$z_{T_{spo}}$ is the distance of T_{spo} from T^* which leads to a ten fold reduction in decimal reduction time.

Sporulation protocols used to investigate sporulation temperature effects were biased because of allowing growth before sporulation on rich nutrient media. These last ones allowed cellular growth until nutrient depletion (occurring at stationary phase) then initiation of sporulation. Incubation temperature during growth and sporulation were kept constant and identical. Consequently in those conditions, spore properties depend on adaptation during growth as well on sporulation environment.

In contrast, synchronous sporulation consisted in transferring vegetative cells from rich nutrient medium to a poor one (Jenkinson *et al.*, 1980; Mandelstam & Higgs, 1974). It allows separating events due to adaptation during growth or sporulation processes.

In order to estimate a possible effect of stress adaptations during growth on spore heat resistance, our study compared the spore production and the spore heat resistance as a function of growth and sporulation temperatures.

Materials and methods

The studied bacterial strain was the *Bacillus cereus* psychrotrophic strain KBAB4, isolated from soil in France. Minimal, optimal and maximal growth temperatures of KBAB4 strain were estimated respectively at 7°C, 30°C and 43°C (Auger *et al.*, 2008).

Growth was carried out in nutrient broth until the beginning of stationary phase, and then cells were transferred in the sporulation media. The sporulation media were a phosphate buffer to prevent growth and ensure sporulation.

On one hand, growth (in nutrient broth) and sporulation (in phosphate buffer) were performed at the same temperature (12°C, 20°C, 30°C or 35°C). On the other hand, growth was performed at optimal temperature (30°C) in nutrient broth then sporulation occurred at stress temperature (12°C, 20°C or 35°C) in phosphate buffer. Media were incubated until more than 99% of cells were spores.

Sporulation kinetics were estimated by counting viable cells on nutrient agar. Whole population and cells resistant to heat treatment of 70°C 5 minutes (spores) were enumerated. Harvested spores were

stored one month at 4°C before use. Spore heat resistance was determined by following thermal death kinetics at 85°C and 90°C.

Results and discussion

Times to obtain more than 99% of spores were rather independent of the growth temperatures (Table 1). Whatever growth and sporulation conditions, spore concentrations were close to 10^8 spores/ml.

Table 1: Needed incubation times to standardize cellular physiological state.

| Growth temperature | Incubation time of growth | Sporulation temperature | Incubation time of sporulation |
|--------------------|---------------------------|-------------------------|--------------------------------|
| 12°C | 60 hours | 12°C | 7 days |
| 30°C | 6 hours | 12°C | 7 days |
| 20°C | 30 hours | 20°C | 6 days |
| 30°C | 6 hours | 20°C | 6 days |
| 30°C | 6 hours | 30°C | 3 days |
| 30°C | 6 hours | 30°C | 3 days |
| 35°C | 7 hours | 35°C | 3 days |
| 30°C | 6 hours | 35°C | 3 days |

$D_{85^\circ\text{C}}$ and $D_{90^\circ\text{C}}$ values of spores formed at 12°C after growth at 12°C were not significantly different from those formed at 12°C after growth at 30°C. Growth temperature does not seem to have any significant effect on spore heat resistance (Figure 1). This suggests that the spore heat resistance properties are not influenced by adaptation of the vegetative cells during growth phase.

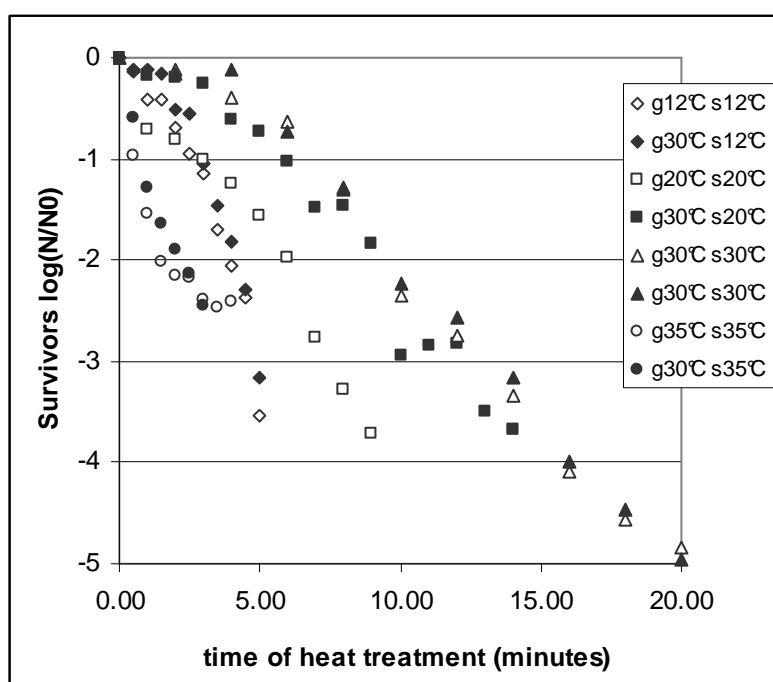


Figure 1: Log (N/N0) versus heating time at 90°C for different incubation temperatures of growth and sporulation.

Spores of *B. cereus* KBAB4 produced at 12°C, 20°C and 35°C were less resistant than spores produced at 30°C. This suggests the existence of an optimal sporulation temperature, allowing formation of highly heat resistant spores. However, this optimal temperature concept is not consistent with the linear relationship between sporulation temperature and heat resistance of spores. This linear relationship could be improved. Few studies dealt with incubation temperature higher than the optimal one. Therefore lower heat-resistance possibly induced by sporulation at temperatures close to the upper limit of growth is neglected.

This work is supported by the Agence Nationale de la Recherche (ANR) (France) as part of an ANR-07-PNRA-027-07 MEMOSPORE contract, by the industrial association Bretagne Biotechnologies Alimentaires (BBA) and the French National Association of the Technical Research (ANRT).

References

- Auger, S., Galleron, N., Bidnenko, E., Ehrlich, S. D., Lapidus, A. & Sorokin, A. (2008). The genetically remote pathogenic strain NVH391-98 of the *Bacillus cereus* group is representative of a cluster of thermophilic strains. *Applied Environmental Microbiology* 74, 1276-1280.
- Gonzalez, I., Lopez, M., Martinez, S., Bernardo, A. & Gonzalez, J. (1999). Thermal inactivation of *Bacillus cereus* spores formed at different temperatures. *International Journal of Food Microbiology* 51, 81.
- Jenkinson, H. F., Kay, D. & Mandelstam, J. (1980). Temporal dissociation of late events in *Bacillus subtilis* sporulation from expression of genes that determine them. *Journal of Bacteriology* 141, 793-805.
- Leguerinel, I., Couvert, O. & Mafart, P. (2007). Modelling the influence of the sporulation temperature upon the bacterial spore heat resistance, application to heating process calculation. *International Journal of Food Microbiology* 114, 100.
- Mandelstam, J. & Higgs, S. A. (1974). Induction of Sporulation During Synchronized Chromosome Replication in *Bacillus subtilis*. *Journal of Bacteriology* 120, 38-42.
- Nauta, M. J., Litman, S., Barker, G. C. & Carlin, F. (2003). A retail and consumer phase model for exposure assessment of *Bacillus cereus*. *International Journal of Food Microbiology* 83, 205.
- Palop, A., Manas, P. & Condon, S. (1999). Sporulation temperature and heat resistance of *Bacillus* spores: a review. *Journal of Food Safety* 19, 57-72.

Comparative evaluation of growth/no growth interface of *L. monocytogenes* growing on stainless steel surfaces or in suspension, in response to pH and NaCl

C.E.A. Belessi¹, A.S. Gounadaki¹, S. Schwartzman², K. Jordan², and P.N. Skandamis¹

¹Laboratory of Food Quality Control and Hygiene, Department of Food Science and Technology, Agricultural University of Athens, Greece. Correspondence: pskan@aua.gr.

²Teagasc, Dairy Products Research Centre, Moorepark, Fermoy, Co. Cork, Ireland.

Abstract

Several logistic regression models have been developed the last few years to describe the boundary between growth and no growth of microbial suspended cells. This study aimed to describe the growth/no growth interface of *L. monocytogenes* at all three states of growth that a bacterial cell could be found on an industrial equipment surface, namely attached, in a form of a biofilm (*B*), detached (*D*) from a biofilm and able to soil new products, or in a planktonic state (suspended; *P*). *L. monocytogenes* cells were left to form colonies on stainless steel (SS) surfaces in TSBYE at 30 different pH and NaCl concentrations at 10°C. The probability of a single cell to initiate growth (P_{in}) was evaluated, as well as the number of cells needed for growth initiation of planktonically growing *P* and *D* *L. monocytogenes* cells. Overall, pH had a more pronounced effect on the growth response of both *P* and *D* cells than a_w . Although both culture preparations demonstrated similar growth limits at populations $>10^2$ CFU/ml, the minimum pH for growth initiation of 1 to 10 of *D* cells was higher at a_w of 0.955 than those of the respective populations of *P* cells. Lower maximum P_{in} levels and longer time for an increase of $P_{in}>0$ was required at *D* over the *P* cells. As a result, higher population of *D* than *P* cells was needed, in order to initiate growth at low a_w and pH. Marginal growth of attached cells encountered at optimal conditions, whereas at 4.5-8% salt and/or pH<6.0 marked reduction of the population of enumerated cells from SS coupons was observed. The results may contribute to safety implications relevant to the potential of cells attached on contaminated surface to proliferate. Furthermore, probability of growth data may contribute to data gaps on risk assessment of *L. monocytogenes* isolates from the dairy industry.

Keywords: *L. monocytogenes*, growth/no growth interface, biofilms, planktonic, detached

Introduction

Growth/no growth modeling may serve as a means to establishing reliable critical limits. So far, available probability of growth models deal with the growth response of planktonically growing *Listeria monocytogenes* cells or cells grown as colonies on the surface of agar and foods (Koutsoumamis et al., 2004; Vermeulen et al., 2007). However, *Listeria* cells are able to attach to various surfaces and persist on processing equipments for many years, contaminating food. Thus, it is of importance to evaluate the growth potential of such cells, and even more to compare it with planktonically growing cells, which may be habituated in niches with residual food soil. This would assist in accurate modelling of growth responses.

The objectives of the present study were: (i) to comparatively evaluate the growth/no growth interface of *L. monocytogenes* cells attached on stainless steel surfaces, or in suspension, within media of different pH and NaCl levels at 10°C, and (ii) to comparatively evaluate the probability of a single cell to initiate growth as well as the number of cells needed for growth initiation of planktonically growing *L. monocytogenes*, following growth in suspension and of cells detached from stainless steel coupons.

Materials and methods

Preparation of inocula: A 3-strain composite of *L. monocytogenes*, including isolates from farmhouse cheese, dairy processing environment and farm was used to inoculate individual plastic with 40 ml of Tryptic Soy Broth supplemented with 0.6% Yeast Extract (TSBYE; pH 7.2, a_w 0.995) with or without a single sterile stainless steel (SS) coupon (2x5x2 cm). Following incubation at 20°C for 3 days, attached (*Att*: 10^{4-5} CFU/ml), planktonic (*Plan*: 10^9

cfu/ml) and detached from the SS coupons (*Det*: 10^{4-5} CFU/cm²) cells were obtained by using the “bead vortexing method” (Stopforth et al., 2002).

Experimental design: The growth/ no growth (G/NG) interface of three states (*Att*, *Plan* and *Det*) of *L. monocytogenes* cells with respect to pH and a_w was evaluated at 10°C. Specifically, a full factorial design was used to examine the effect of six pH values (6.6, 6.3, 5.9, 5.6, 5.2 and 4.8) adjusted with lactic acid, and five a_w levels (0.996, 0.982, 0.977, 0.966 and 0.955) achieved by addition of 0, 3, 4.5, 6 and 8% (w/vol) NaCl on the growth initiation of the different types (states) of *Listeria* cells. Aliquots (25 µl) of the appropriate dilution of *Plan* or *Det* cells were inoculated in triplicate wells of 96-well microplates, each one containing 225 µl of appropriate growth medium. Growth was monitored turbidimetrically at 620 nm, every day for 30 days. The ability of *Att* cells to initiate growth was evaluated with the transfer of SS coupons bearing attached cells in tubes containing 40 ml TSBYE of each pH/ a_w combination, which was renewed every 2 days. Enumeration of *Att* cells was performed on days 0 and 30 of incubation with bead vortex method (Stopforth et al., 2002). The PulseNet standardized protocol for subtyping *L. monocytogenes* by macro-restriction and PFGE was run on isolates of day 30 in order to assess the dominant strain that colonized the SS surfaces. All experiments lasted for 30 days and included at least 3 replicates each.

Model development: Ordinary logistic regression was applied with *logit* (P) described as a polynomial expression of pH and a_w (Skandamis et al., 2007). The probability of any given cell initiating growth (P_{in}) under each of the examined experimental conditions, as well as the cells needed (CN) to initiate growth at the same conditions were estimated by the fraction of wells giving growth at each condition and Most Probable Number (MPN) Tables (Razavilar and Genigeorgis 1998). P_{max} and time for increase to $P_{max}/2$ (t_{au}) were determined by a logistic model.

Results and discussion

The ability of attached *L. monocytogenes* cells on SS coupons to grow was strongly dependent on the stringency of the environmental conditions (**Table 1**). Specifically, the levels of attached cells on SS coupons demonstrated a marginal increase (< 1 Log CFU/cm²) at optimal growth conditions (pH > 5.9 and/or a_w > 0.982), whereas a significant reduction ($P < 0.05$) of the bacterial population compared to the initially attached levels occurred as the pH and a_w levels of the growth media decreased (**Table 1**).

Table 1. Levels of attached *L. monocytogenes* (mean log cfu/cm² ± SD) on SS coupons at each combination of pH/ a_w after 30 days at 10°C. Growth (dark cells), reduction (light cells or white cells) of *Listeria* cells on the SS coupons.

| pH/ a_w | 0.996 | 0.982 | 0.977 | 0.966 | 0.955 |
|-----------|--------------|---------------|--------------|---------------|-------|
| 6.6 | 4,8 Cc ± 0,3 | 5,2 Cd ± 0,2 | 3,0 Bb ± 0,3 | 2,6 Ba ± 0,3 | Bdl |
| 6.3 | 4,6 Cc ± 0,1 | 3,5 Bb ± 1,4 | 1,6 Aa ± 1,4 | 1,0 Aa ± 1,5 | Bdl |
| 5.9 | 4,9 Cc ± 0,3 | 3,2 ABb ± 1,2 | 2,5 Ba ± 0,8 | 2,8 Bab ± 0,4 | Bdl |
| 5.6 | 3,3 Bb ± 0,6 | 3,1 ABb ± 0,5 | 2,9 Bb ± 0,7 | 2,2 Ba ± 1,1 | Bdl |
| 5.2 | 2,6 Ab ± 1,2 | 2,5 Ab ± 1,3 | 1,3 Aa ± 1,4 | 0,9 Aa ± 1,2 | Bdl |
| 4.8 | Bdl | Bdl | Bdl | Bdl | Bdl |

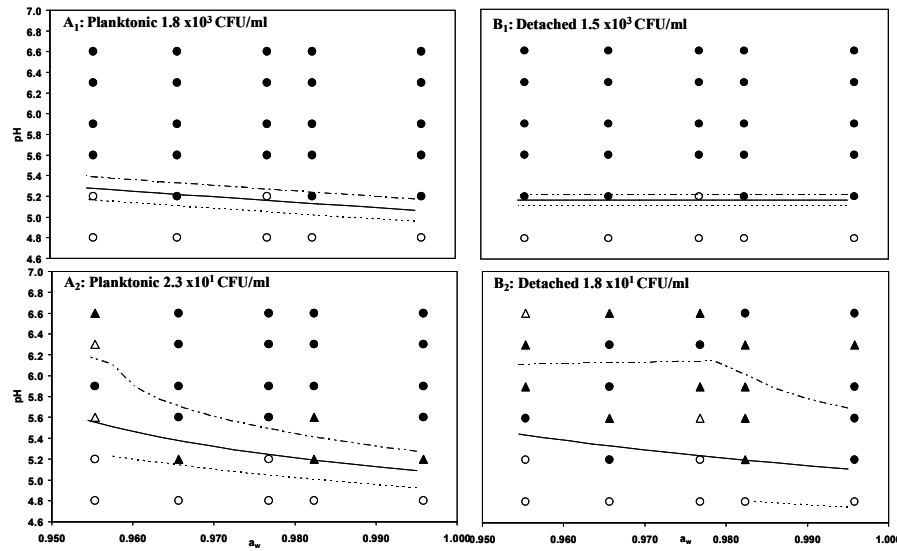
^{ABC}: means within a column sharing at least a common letter are not significantly different ($P < 0.05$).

^{abc}: means within a row sharing at least a common letter are not significantly different ($P < 0.05$).

The decrease in the attached populations of Table 1 may be associated with washing out of weakly attached cells. Furthermore, renewal (every 2 days) of the growth medium probably increased the requirements for energy expenditure of the cells to combat the homeostatic burden (either pH homeostasis or accumulation of compatible solutes) and remain attached or viable on surfaces (Skandamis et al., 2007; Tiganitas et al., 2009). PFGE patterns on 30 day isolates showed that the majority of the cells which had colonized the surfaces of SS coupons at any pH and a_w conditions belonged to one of the 3 strains, which had also been characterized as “persistent” isolate for the last 10 years in a dairy processing plant.

Consistent with previous studies, initial inoculum size exhibited a significant effect on the growth initiation of *Plan* and *Det* cells (Koutsoumanis and Sofos, 2005; Skandamis et al.,

2007). Generally, the lower the initial population, the higher the pH and a_w levels allowing growth (Fig. 1; Table 2). The variability in the growth potential of *L. monocytogenes* near the growth boundaries may be associated with variations in the abruptness of interface among strains at the different inoculation levels (Skandamis et al., 2007; van der Veen et al., 2008). G/NG interface of *Plan* and *Det* cells in response to pH and a_w were similar for populations $>10^2$ /well; however growth of *Det* cells of low initial size (1-10 cells) was inhibited at higher



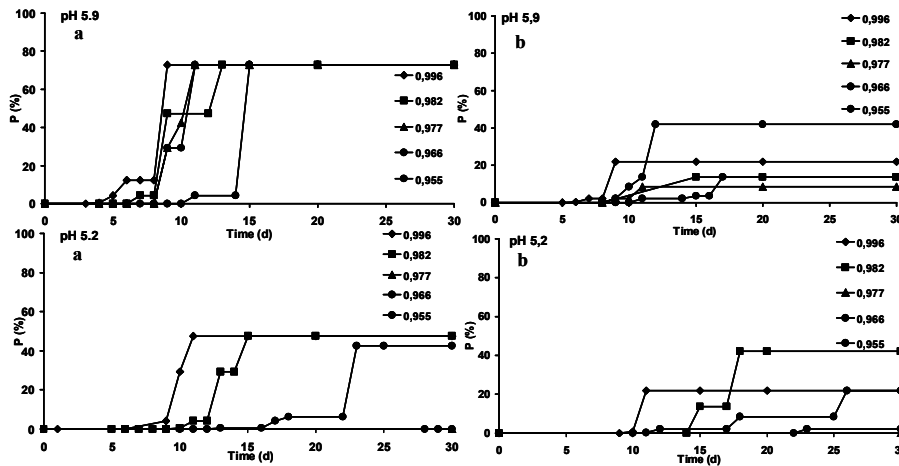
pH values compared to their *Plan* counterparts (Fig. 1; Table 2). It can be hypothesized that once detached, high populations restore their growth potential and behave similarly to suspended cells (Stopforth et al., 2002).

Figure 1: G/NG data for planktonic (A) and detached (B) *L. monocytogenes* cells with respect to pH and a_w at 10°C at inoculum levels of (1) 10^3 CFU/ml and (2) 10^1 CFU/ml compared with predictions made at probabilities 0.9 (upper dotted line), 0.5 (solid line) and 0.1 (lower dotted line). 100% Growth (●), 66.66% growth (▲), 33.33% growth (△), and (○) no growth.

Table 2: Lower pH values (positive cells out of 3 in total) at which growth of different inocula types of *L. monocytogenes* was observed

| Cell type | Initial population (CFU/well) | a_w | | | | |
|------------|-------------------------------|---------|---------|---------|---------|---------|
| | | 0.996 | 0.982 | 0.977 | 0.966 | 0.955 |
| Planktonic | 1.1×10^2 | 5.2 (3) | 5.2 (3) | 5.6 (3) | 5.2 (3) | 5.6 (3) |
| | 2.3×10^1 | 5.2 (2) | 5.2 (2) | 5.6 (3) | 5.2 (2) | 5.6 (1) |
| | 1.0×10^0 | 6.3 (1) | - | 6.3 (1) | 5.6 (1) | 5.6 (1) |
| Detached | 1.4×10^2 | 5.2 (3) | 5.2 (3) | 5.6 (3) | 5.2 (3) | 5.2 (3) |
| | 1.8×10^1 | 5.2 (3) | 5.2 (2) | 5.6 (1) | 5.2 (3) | 5.6 (3) |
| | 1.9×10^0 | 5.2 (1) | 5.2 (1) | - | 5.9 (1) | 5.9 (1) |

Regardless of inoculum size, *Plan* cells had higher P_{in} (%) compared to *Det* cells (Fig. 2) and reached significant higher maximum levels (P_{max}) (Fig. 2 & 3). In addition, the time of a



single *Det* cell to reach $P_{max}/2$ (t_{au}) was slightly higher (3-10 days) than that of their *Plan* counterparts, suggesting slower growth initiation, especially at $pH < 5.6$, $a_w < 0.997$ (Fig. 4), while such differences were minimized at less adverse environmental conditions.

Figure 2. Representative curves of P_{in} (%) of (a) *Plan* and (b) *Det* cells vs time

Table 3. Planktonic (*Plan*) and Detached (*Det*) cells needed (CN) to initiate growth at varying conditions and times

| pH | a _w | Time | <i>Plan</i> | <i>Det</i> |
|-----|----------------|------|-------------|------------------|
| 6.6 | 0.996 | 4 | 226 | >10 ⁴ |
| | | 10 | 1 | 2 |
| 6.6 | 0.977 | 6 | 2264 | >10 ⁴ |
| | | 9 | 1 | 25 |
| 6.6 | 0.955 | 6 | 22644 | >10 ⁴ |
| | | | 6 | |
| | | 11 | 2 | 476 |
| 5.6 | 0.996 | 5 | 226 | >10 ⁴ |
| | | 9 | 1 | 7 |
| 5.6 | 0.977 | 5 | 22644 | >10 ⁴ |
| | | 12 | 1 | 25 |
| | | 19 | 2 | 4 |

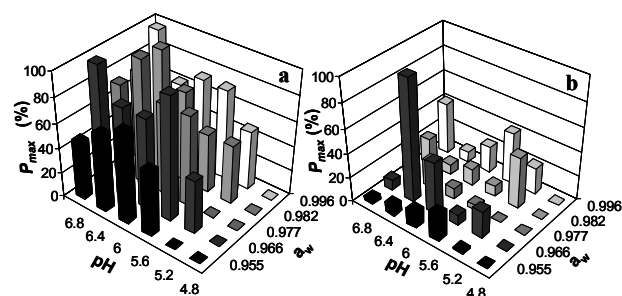


Figure 3. P_{max} (%) of (a) Planktonic and (b) Detached cells

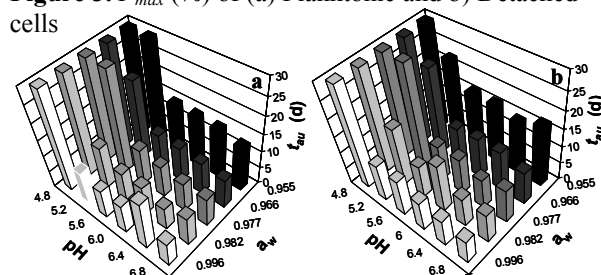


Figure 4. Time (days) for a single (a) Planktonic and/or (b) Detached cell to reach $P_{max}/2$ (t_{au}).

Moreover, the suppressed P_{in} values of *Det* cells in response to pH indicate that more *Det* cells than *Plan* cells are needed so that one to initiate growth (**Table 3**). The results suggest that detached cells from SS coupons might have been subjected to stronger metabolic suppression than suspended (never attached) cells and hence, encountered a higher burden upon transferring to low pH and a_w .

Conclusions

The significance of the present study is the comparative evaluation of the probability of growth of the three states in which a *L. monocytogenes* cell may be present on processing equipment. Attachment of *Listeria* cells in time is strongly reduced as a_w and pH decreases, even though after detachment, bacterial populations >10² cfu/cm², behave similarly to suspended cells in response to pH and a_w . Moreover, detached cells pose a lower risk as a higher population is needed to initiate growth than suspended cells, whereas low populations are generally more easily inhibited than high populations. The results may provide implications for the differences in the growth potential of different inoculum preparations and hence, be considered in development of realistic predictive models.

References

- Koutsoumanis K.P., Kendall P.A. and Sofos, J.N. (2004) A comparative study on growth limits of *Listeria monocytogenes* as affected by temperature, pH and a_w when grown in suspension or on a solid surface, *Food Microbiology* 21, 415-422.
- Koutsoumanis P., and Sofos J.N. (2005) Effect of inoculum size on the combined temperature, pH and a_w limits of growth of *Listeria monocytogenes*, *International Journal of Food Microbiology* 104, 83-91.
- Razavilar V., and Genigeorgis C. (1998) Prediction of *Listeria* spp. growth as affected by various levels of chemicals, pH, temperature and storage time in a model broth, *International Journal of Food Microbiology* 40, 149-157.
- Skandamis P.N., Stopforth J.D., Kendall P.A., Belk K.E., Scanga J.A., Smith G.C. and Sofos J.N. (2007) Modeling the effect of inoculum size and acid adaptation on growth/no growth interface of *Escherichia coli* O157:H7, *International Journal of Food Microbiology* 120, 237-249.
- Stopforth J.D., Samelis J., Sofos J.N., Kendall P.A. and Smith G.C. (2002) Biofilm formation by acid-adapted and nonadapted *Listeria monocytogenes* in fresh beef decontamination washings and its subsequent inactivation with sanitizers, *Journal of Food Protection* 65, 1717-1727.
- Tiganitis A., Zeaki N., Gounadaki A. S., Drosinos E.H., and Skandamis P.N.(2009) Study of the effect of lethal and sublethal pH and a_w stresses on the inactivation or growth of *Listeria monocytogenes* and *Salmonella* Typhimurium, *International Journal of Food Microbiology* doi:10.1016/j.ijfoodmicro.2009.02.016.
- Van der Veen, Moezelaar R., Abee T. and Wells-Bennik M.H.J. (2008) The growth limits of a large number of *Listeria monocytogenes* strains at combinations of stress show serotype-and niche-specific traits, *Journal of Applied Microbiology* 105, 1246-1258.
- Vermeulen A., Gysemans K.P.M., Bermaerts K., Geeraerd A.H., Van Impe J.F., Debevere J. and Devlieghere F. (2007) Influence of pH, water activity and acetic acid concentration on *Listeria monocytogenes* at 7°C: Data collection for the development of a growth/no growth model, *International Journal of Food Microbiology* 114, 332-341.

Modeling the effect of acid and osmotic shifts from growth to no growth conditions and *vice versa* on the adaptation and growth of *Listeria monocytogenes*

C.-I. A. Belessi¹, Y. Le Marc², S. I. Merkouri¹, A. S. Gounadaki¹, S. Schwartzman³, K. Jordan³, E. H. Drosinos, and P.N. Skandamis¹

¹Laboratory of Food Quality Control and Hygiene, Department of Food Science and Technology, Agricultural University of Athens, Greece. Correspondence: pskan@aau.gr.

²Institute of Food Research, Norwich, NR4 7UA, United Kingdom.

³Teagasc, Dairy Products Research Centre, Moorepark, Fermoy, Co. Cork, Ireland.

Abstract

In the present study, the effect of acid and osmotic shifts from growth to no growth conditions and *vice versa* on the adaptation and growth of *L. monocytogenes* was evaluated at 10°C. A *L. monocytogenes* isolate (10^2 cfu/ml), which persisted for 10 years on the environment of a dairy plant was grown to late-exponential phase in TSBYE at 7 pH (5.1-7.2) at a_w 0.995, adjusted with lactic acid and 5 NaCl concentrations (0.5-12.5%) at pH 7.2. When *L. monocytogenes* reached *ca.* 8 log cfu/ml in each of the above conditions, it was shifted to all the remaining pH and NaCl levels at 10°C. No-growth/growth shifts were also carried out by transferring *L. monocytogenes*, habituated at pH 4.9 or salt 12.5% for 1, 5 and 10 days to growth permitting conditions. Changes in viable counts were monitored on TSAYE and growth curves were fitted with the Baranyi model. A secondary model based on multiplicative terms of each factor as well as an interaction term (ξ) was used to predict μ_{max} in response to pH and/or a_w shifts. Reducing a_w from 0.995 to 0.930, resulted in linear reduction of μ_{max} and exponential increase of lag time. Shifts in the range of pH 5.5-7.0 reduced μ_{max} but did not markedly affect the lag time of cultures. Conversely, downshifts to pH 5.1 induced lag of 88-180 h. The longer the cells were incubated at no growth a_w the faster they initiated growth subsequently, suggesting adaptation to osmotic stress. Conversely, extended habituation at pH 4.9 had the opposite effect on subsequent growth of *L. monocytogenes*, suggesting potential injury of cells. We therefore, assumed the existence of an adaptation rate (ν) at no growth conditions different from μ_{max} . A global fitting of data with shifts from growth-ceasing to growth-permitting conditions enabled determination of such and adaptation rate as well as of the dependency of h_0 to a_w and pH shifts. Then, a dynamic model, describing the effect of both the magnitude and the direction of osmotic and acid shifts successfully predicted growth of *L. monocytogenes* in milk under dynamic pH (6.4-4.9) and a_w (0.98 to <0.90) conditions. Our results suggest that quantifying adaptation phenomena under growth-limiting environments is essential for reliable growth simulations.

Keywords: *L. monocytogenes*, lag time, osmotic/acid stress, shifts, dynamic modelling

Introduction

The initial lag phase of a microorganism in a new environment is affected by multiple factors, including nutrients, physiological state, etc, and is defined by the amount of work that cells need to undertake and the rate at which this work is accomplished (Robinson et al. 1998; Mellefont et al. 2003). Subsequent changes of extrinsic (e.g., temperature) or intrinsic (e.g., pH and a_w) factors induce what is called ‘intermediate’ lag phase (Swinnen et al. 2005) and this may be dependent on the magnitude and direction of environmental shift. Therefore, a key hypothesis in growth modelling is whether shifts in the environment across the growth boundaries pose additional adaptation work to microorganisms. Acid and osmotic shifts pose a higher energetic burden than temperature shifts, especially around the growth boundaries. Therefore, in order to develop a dynamic model predicting growth of *L. monocytogenes* under dynamic a_w and pH conditions, we evaluated the growth responses of the microorganism under: (i) environmental shifts within the range of growth permitting pH and a_w levels; (ii)

shifts from optimum a_w (0.995), or pH (7.2) conditions to no growth conditions for 1, 5 or 10 days and then back to growth-permitting conditions.

Materials and methods

Inoculum preparation

A *Listeria monocytogenes* isolate was maintained at -22°C in the presence of 20% glycerol. It was subcultured once by transferring 0.1 ml in 10 ml of Tryptic soy broth supplemented with 0.6% yeast extract (TSBYE) and incubation at 37°C for 24h, followed by a second subculturing for another 16 h, in order to achieve cells late exponential phase.

Media preparation

A total of 82 *Listeria monocytogenes* growth experiments were conducted in TSBYE at various pH and water activity values, adjusted by the addition of lactic acid and NaCl in 100 ml TSBYE. All bottles were autoclaved at 121°C for 15 min. The final pH of TSBYE were 7.2, 6.0, 5.8, 5.5, 5.3, 5.1 and 4.7. Due to the presence of 0.5% NaCl in commercial formulation of TSBYE, the final salt concentration of the tested media was 0.5, 5, 8, 10.5 and 12.5%. Two pairs of each tested medium were prepared for the two independent experiments.

Media inoculation and shifts

Growth media were inoculated with 10^{2-3} CFU/ml of *L. monocytogenes* inoculum and incubated at 10°C. Viable *Listeria* cells were enumerated with Spiral plater (Bio) onto Tryptic Soy Agar (Biolife, Italy) supplemented with 0.6% Yeast Extract and incubation at 30°C for 24 h. When *L. monocytogenes* reached the late exponential-early stationary phase (*ca.* 8-9 log cfu/ml) in each of the conditions tested, aliquots (1 ml) were serially diluted in MRD and transferred to all the remaining growth-permitting levels of pH (from 5.1-7.0; 36 cases) and a_w (0.93-0.995; 16 cases) and incubated at 10°C. Each factor was evaluated separately. Furthermore, cells of *L. monocytogenes* which were habituated in growth-prohibiting conditions, namely, pH 4.7 (a_w 0.995) and salt concentration 12.5% (pH 7.2) were also shifted to all growth permitting conditions of each factor after 1, 5 or 10 days at 10°C.

Analysis of the growth curves

Growth curves were fitted with the Baranyi model in order to estimate μ_{max} , lag time (λ) and “work-to-be-done” (ho). A secondary model (Le Marc et al. 2002) with multiplicative terms of each factor as well as an interaction term (ξ) was used to predict μ_{max} in response to pH and/or a_w shifts. Global fitting of the data allowed determination of the adaptation rate (ν) and the parameters controlling the dependency of ho at growth-permitting conditions following habituation at no growth conditions.

Results and discussion

(a) *Effect of shifts at growth-permitting levels of pH and a_w .* The μ_{max} was not influenced by the direction or the magnitude of a_w and pH shifts (Fig. 1). Conversely, lag time and hence, ho , seemed to increase as the conditions of a_w became harsher (Figs 1 & 2). This is in accordance with Mellefont et al. (2003), who observed increase of relative lag time (RLT) at stringent water activities for *Salmonella*, although this effect was less evident for *L. monocytogenes*. It is therefore suggested that any injury occurring is quickly repaired when a_w becomes more favorable for growth. In general, pH shifts in the range of 5.3-7.2 did not markedly affect lag times (Fig. 1) and the magnitude of ho was relatively lower (0-0.4) compared to that caused by a_w shifts (0-1.5). However, dramatic increase in lag times were caused by shifts close to the growth limiting pH values of 5.1 (Fig. 1), in agreement with Robinson et al. (1998).

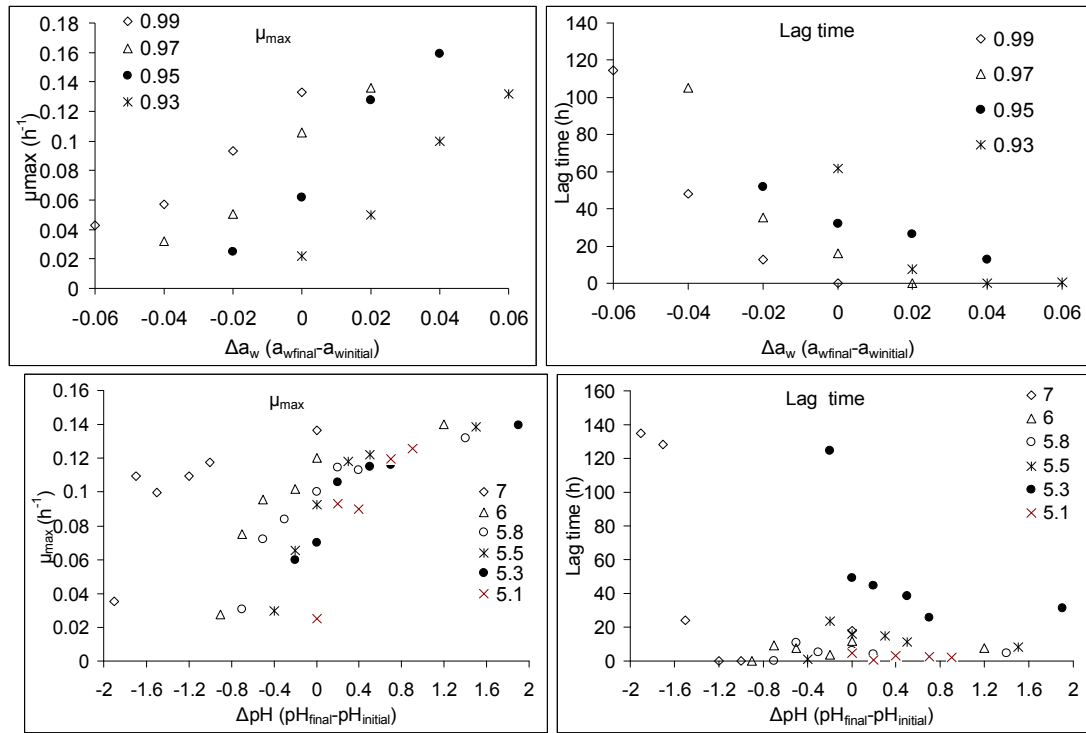


Figure 1. Effect of a_w (top) and pH (bottom) shifts on μ_{max} and lag time of *L. monocytogenes*.

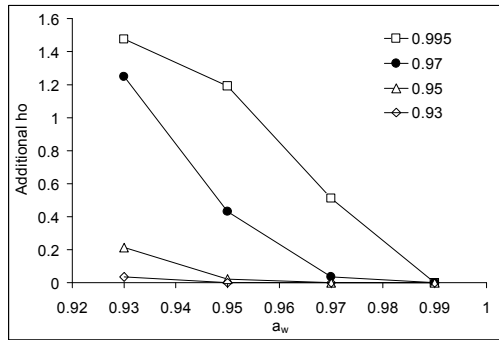


Figure 2. Additional “work-to-be done” due to shifts from different initial a_w levels. Lag time for no shift was subtracted from lag times at each shift.

(b) Effect of shifts from no growth to growth-permitting levels of pH and a_w . The duration of habituation at no growth conditions did not influence the μ_{max} of *L. monocytogenes* at subsequent shifts to growth-permitting levels (data not shown). However, an apparent effect on lag time was evident and hence, on h_0 estimates (Fig. 3). For the same level of water activity, the “work to be done” (h_0) tended to decrease as a function of the time the cells were held at 0.90 (Fig. 3b). Furthermore, lag times and h_0 estimates at a_w 0.93-0.99 after 10 days at 0.90 were lower than the respective values following growth exclusively at 0.99 (Fig. 3a).

These suggests that the cells are able to carry

out at least some of “work to be done” during habituation at 0.90. Furthermore, for the same period of incubation at no growth conditions, the lag times and h_0 values of subsequent growth decreased with increasing a_w (Fig. 3b). Therefore, h_0 seems to be inversely proportional to the magnitude of the shift up from no growth to growth conditions. Contrary to the observations with a_w , the more the cells were held at no growth pH (4.9), the higher was the work needed for growth initiation in a more favourable environment (Fig. 3c). This may be explained on the basis of the higher energetic burden posed by pH on cells compared to a_w at no growth conditions (Shabala et al. 2008). The above concepts are illustrated in Figure 4. A hypothetical adaptation rate ‘ ν ’, which is independent of μ_{max} at no growth conditions, was estimated by globally fitting the dataset of shifts from no growth to growth conditions. Then, the cardinal model of Le Marc et al. (2002); $\mu_{max} = \mu_{opt} \tau(T) \gamma(pH) \rho(a_w) \xi(T, pH, a_w)$ was used to quantify the effect of the environment on μ_{max} of *L. monocytogenes*, replacing $\gamma(pH)$ by the term $1 - 10^{(pH_{min} - pH)}$ (Presser et al. 1997) and taking into account potential synergy (ξ term). The temperature term was based on literature cardinal values, namely $T_{min} = -2.8^\circ\text{C}$, $T_{opt} = 37^\circ\text{C}$ and $T_{max} = 45.5^\circ\text{C}$.

Cardinal parameters for water activity were a_{wmin} 0.916 (based on the present data) and a_{wopt} 0.997 (from literature), whereas pH_{min} estimate was 4.96. Based on that the model showed satisfactory agreement to data obtained in pasteurized milk (Fig. 5). Ignoring the effect of shifts on adaptation of *L. monocytogenes* (i.e., using only a growth rate model) resulted in over-prediction of actual growth (Fig. 5).

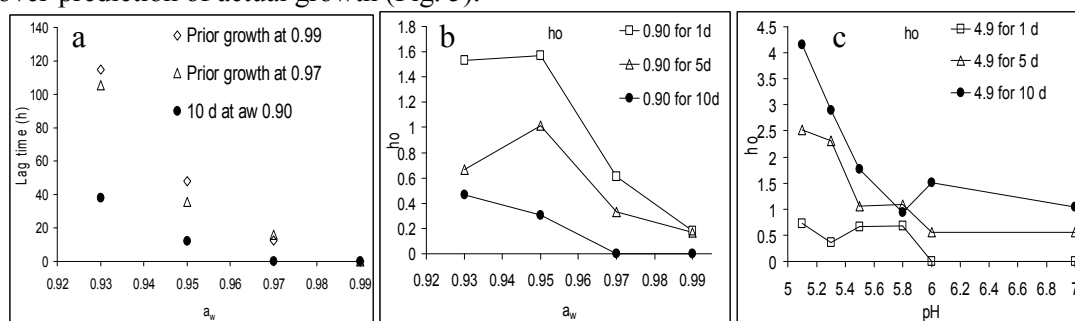


Figure 3. Lag time under different conditions (a) and h_0 (b, c) following habituation for 1, 5 or 10 days at a_w 0.90 (b) or pH 4.9 (c).

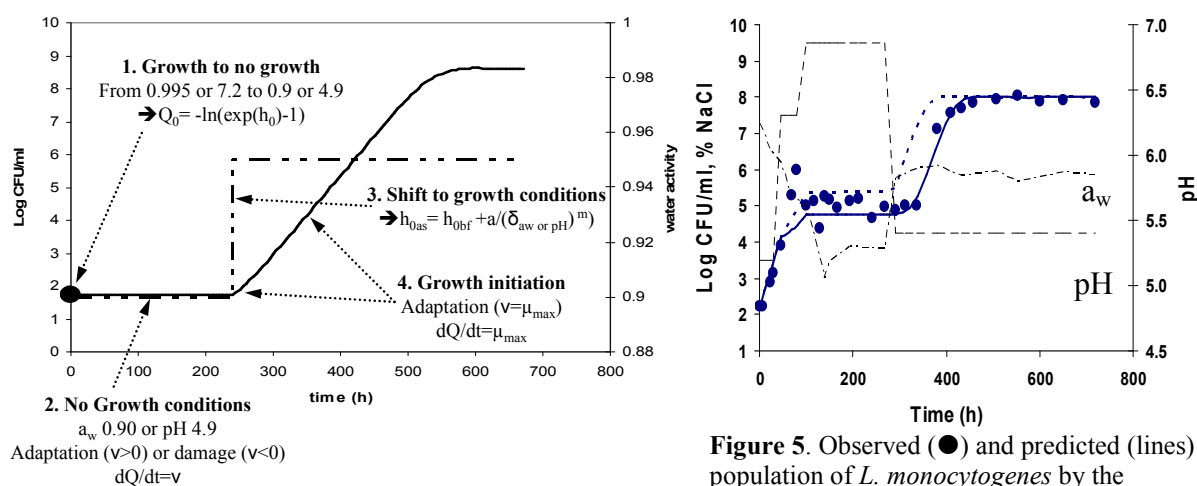


Figure 4. Conceptual basis of the dynamic model for growth of *L. monocytogenes* in response to a_w or pH shifts.

Figure 5. Observed (●) and predicted (lines) population of *L. monocytogenes* by the dynamic model considering (solid) or not (dashed) the effect of shifts on h_0 .

Conclusions

A dynamic model capable of predicting growth of *L. monocytogenes* in response to pH and a_w shifts, needs to consider: (i) the dependence of μ_{max} on pH and a_w ; (ii) the increase of h_0 in case of osmotic or pH downshifts; and, (iii) the rate of adaptation work perform during habituation at no growth a_w and the ‘rate of injury’ of cells habituated at no growth pH.

References

- Le Marc Y, Huchet V., Bourgeois C.M., Guyonnet J.P., Mafart P. and Thuault D. (2002) Modelling the growth kinetics of *Listeria* as a function of temperature, pH and organic acid concentration. *International Journal of Food Microbiology* 113, 1–15.
- Robinson T. P., Ocio M. J., Kaloti A. and Mackey B. M. (1998) The effect of the growth environment on the lag phase of *Listeria monocytogenes*. *International Journal of Food Microbiology* 44, 83–92.
- Mellfont L.A., McMeekin T.A. and Ross T. (2003) The effect of abrupt osmotic shifts on the lag phase duration of foodborne bacteria. *International Journal of Food Microbiology* 83, 281–293.
- Swinnen I.A.M., Bernaerts K., Gysemans K., and Van Impe J.F. (2005) Quantifying microbial lag phenomena due to a sudden rise in temperature: a systematic macroscopic study. *International Journal of Food Microbiology* 100, 85–96.
- Shabala L., Lee S.H., Cannesson P. and Ross, T. (2008). Acid and NaCl limits of growth of *Listeria monocytogenes* and influence of sequence of inimical acid and NaCl levels on inactivation kinetics. *Journal of Food Protection* 71, 1169–1177.
- Presser K. A., Ratkowsky, D.A. and Ross T. (1997) Modelling the growth rate of *Escherichia coli* as a function of pH and lactic acid concentration. *Applied and Environmental Microbiology* 63, 2355–2360.

Individual cells lag times distributions of *Cronobacter* (*Enterobacter sakazakii*)

R. Bennour Miled¹, L. Guillier², S. Neves¹, J.-C. Augustin³, P. Colin⁴ and N. Gnanou-Besse¹

¹Agence française de sécurité sanitaire des aliments, Afssa Laboratoire d'Etudes et de Recherches sur la Qualité des Aliments et des Procédés agro-alimentaires. Afssa LERQAP, 23 Avenue du Général de Gaulle, 94706 Maisons Alfort cedex, France. (r.miled@afssa.fr; n.besse@afssa.fr).

²Agence française de sécurité sanitaire des aliments, Afssa Direction de l'Evaluation des Risques Nutritionnels et Sanitaires (Afssa DERNS, 27-31 Avenue du Général Leclerc, 94701 Maisons Alfort cedex, France).

³Ecole Nationale Vétérinaire d'Alfort (7 Avenue du Général de Gaulle, 94706 Maisons Alfort cedex, France).

⁴Ecole Supérieure de Microbiologie et de Sécurité Alimentaire (ESMISAB, Plouzane, France).

Abstract

Cells of six strains of *Cronobacter* were submitted to a dry stress and stored for 2.5 months at ambient temperature. The individual cell lag time distributions of recovered cells were characterised at 25°C and 37°C in non selective broth. The individual cell lag times were deduced from the times for cultures issued from individual cells to reach an optical density threshold. In parallel, growth curves for each strain at high contamination levels were determined in the same growth conditions. In general, the extreme value type II distribution was the most effective to describe the 12 observed distributions of individual cell lag times. Recently, an innovating model which allowed to characterise individual cell lag time distribution from populational growth parameters was developed for other food-borne pathogenic bacteria such as *L. monocytogenes*. We verified the applicability of this model to *Cronobacter* by comparing the mean and the standard deviation of individual cell lag times to populational lag times observed with high initial concentration experiments, and then by deducing the theoretical cell lag times distributions from the observed mean and the standard deviation of cell lag times. We also validated the model in realistic conditions by studying growth in powdered infant formula decimally diluted in Buffered Peptone Water (BPW), which represents the first enrichment step of the standardised detection method for *Cronobacter*.

Keywords : *Enterobacter sakazakii*, *Cronobacter*, powdered infant food formula, individual cell lag time, pooling, growth.

Introduction

Enterobacter sakazakii recently known as *Cronobacter* (Iversen et al., 2008) is considered as an opportunistic pathogen and has been implicated in outbreaks causing meningitis or bacteraemia, especially in neonates and infants with mortality rates of 20 to 50% (Anonymous, 2006a). In most cases, powdered infant formula (PIF) has been identified as the source of infection.

In PIF, contamination levels are extremely low and generally much lower than 1 cfu per 100g (Anonymous, 2006a, 2008). Mistakes in biberon-preparation practices, such as improper holding temperatures, may lead to a critical cell level, and the occurrence of the infection. In such conditions of very low contamination levels, individual cells variability can have an important impact on the pathogen growth.

Knowing how long-term presence in PIF, and subsequent stress, affect the variability of single-cell lag times is extremely important in assessing the risk of cell recovery and growth in reconstituted milk or in enrichment broth, where low numbers of stressed cells of pathogenic bacteria may be distributed among PIF samples. Recently, a model which allowed to characterise individual cell lag time distribution from populational growth parameters has been developed for *L. monocytogenes* (Guillier and Augustin, 2006, 2008).

The first objective of the present work was to verify the applicability of this model to *Cronobacter* submitted to a dry stress for different regrowth conditions and strains. The second objective was to study single-cell lag times in a realistic condition such as the first enrichment of the standardised detection method (ISO/TS 22964, Anonymous, 2006b) which is performed in non selective Buffered Peptone Water (BPW). The log count distribution, or vertical distribution (D'Arrigo *et al.*, 2006) was applied to estimate the distribution of the single-cell lag times in BPW. This study also allowed us to evaluate the impact of pooling samples on *Cronobacter* growth and detection. Indeed, to reduce analytic cost and heaviness, common practice in food industry consists in pooling samples at constant dilution rate, in order to perform a single pre-enrichment and subsequent analysis. Consequences on *Cronobacter* detection are not established.

Materials and methods

Six strains of *Cronobacter* were used in this study: 4 strains belonged to different species of *Cronobacter* (*C. malonaticus*, *C. muytjensii* and *C. turicensis*) and 3 to the same species (*C. sakazakii*). Strains were submitted to desiccation: *Cronobacter* strains grown in an equal mixture of BHI and sterile infant formula for 24 h at 37°C were freeze-dried using the CHRIST LOC-2M apparatus (Bioblock Scientific, Ile de France, Vanves cedex, France). Contaminated powder was further 1 in 100 diluted in PIF intended for infants below 6 months of age (previously tested not contaminated with *Cronobacter* and with a very low level of total microflora), and stored for 2.5 months at ambient temperature before use. The individual cell lag time distributions were characterised at 25°C and 37°C in non selective Brain Heart Infusion (BHI) broth: individual cell lag times were deduced from the times for cultures issued from individual cells to reach an optical density threshold, by measuring optical density (OD) at 600 nm using an automated spectrophotometer (Bioscreen C reader). In parallel, growth curves for each strain at high contamination levels (100-1000 cfu/g) were determined in triplicate in BHI broth, at 25°C and 37°C. Growth was monitored by direct plating enumeration, and curves were fitted to the Baranyi model using MicroFit software (<http://www.ifr.ac.uk/MicroFit/>).

For validation purpose, the distribution of *Cronobacter* log counts at given times during first-age PIF pre-enrichment was applied to estimate the distribution of the single-cell lag times. 40 bags of 10g and 40 bags of 100g (mimicking a pooling of 10*10g samples) first-age PIF were prepared and homogenised in sterile BPW diluent (1 in 10 dilution). Each sample was inoculated with freeze-dried *C.sakazakii* type strain (ATCC 29544) at a contamination level of 4 cells per bag. All bags were incubated at 37°C and enumerated after 8h and 20h by plating on the chromogenic selective isolation agar “*Enterobacter sakazakii* Isolation Agar” (ESIA). In parallel, growth of PIF background microflora and of high *Cronobacter* populations were monitored in the same conditions.

Results and discussion

Four statistical distributions were tested in this study to describe data sets of single-cell lag time: the Gamma distribution, the Weibull distribution, the Log-Normal distribution, and the Extreme Value type II distribution. In general, the Extreme Value type II distribution provided the best fit over the whole range of growth conditions and strains tested. Guillier and Augustin (2006) investigated the individual lag times of *L.monocytogenes* cells and showed that this distribution was also the best one.

The relationships between the standard deviations and the means of individual cell lag times and between the individual cell lag times and the population lag times, were in agreement with those observed by Guillier and Augustin (2006, 2008).

In the second part of this study, these relations were applied for validation purpose: at two times of enrichment procedure of a low number of cells, *Cronobacter* log counts were both measured and estimated from growth rate and individual lag times calculated from population

growth curves. After 8 hours of enrichment, the results obtained for 10g and 100g PIF samples showed good agreement between observed and predicted values only if the variability of N_0 , individual lag times and growth rate are taken into account for predictions (Figure 1). Significant differences with observed values were found if lag time variability was not considered, which confirmed that individual cell lag times variability has a major impact on growth.

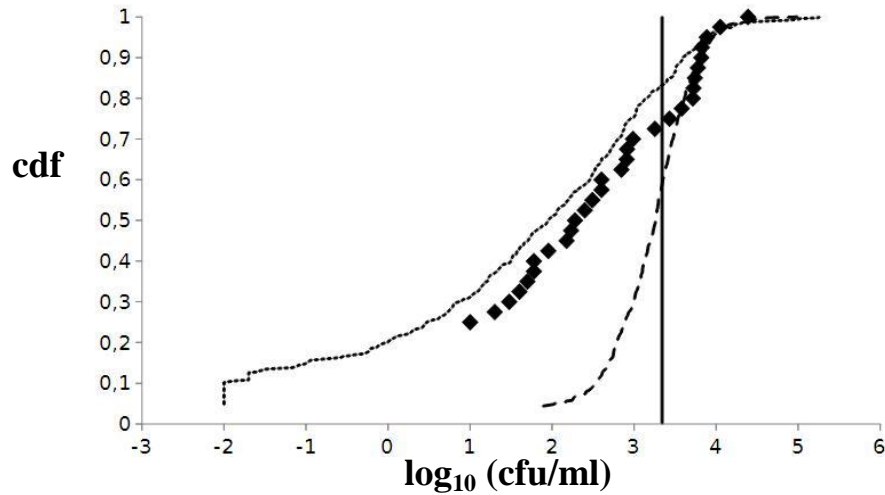


Figure 1: Cumulative distribution of *C. sakazakii* observed log counts (♦) after 8 hours (10g samples). Predicted populations: (—) N_0 , μ_{\max} and lag_i considered as constant, (--) N_0 and μ_{\max} with variability and lag_i constant, (...) N_0 , μ_{\max} and lag_i with variability.

After 20 h, vertical distributions were not in agreement with the predicted values of log counts (Figure 2). This difference can be attributed to bacterial interactions. Indeed, for population growth curves, we observed a stop of *Cronobacter* growth when background flora reached its stationary phase (approximately after 9h enrichment).

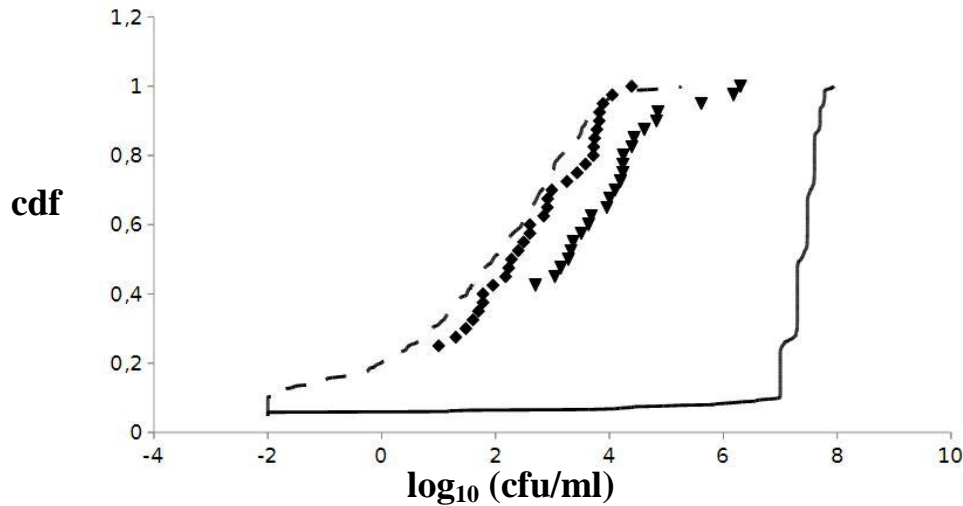


Figure 2: Cumulative distribution of observed log counts after 8 hours (♦) and 20 hours (▼) of *C. sakazakii* in enrichment medium (10g samples). Predicted concentrations after 8 hours (--) and 20 hours (—).

To better explore this phenomenon, we used the same previous simulations but with a stop of the growth at 9h, when the total microflora attained its maximum concentration. Results showed that for 10g bags and for 100g bags we obtained a good correlation between observed and predicted values (Figure 3). Furthermore, for the 100g samples, the initial concentration

is weaker than for the 10g samples which emphasized the negative impact of pooling on detection.

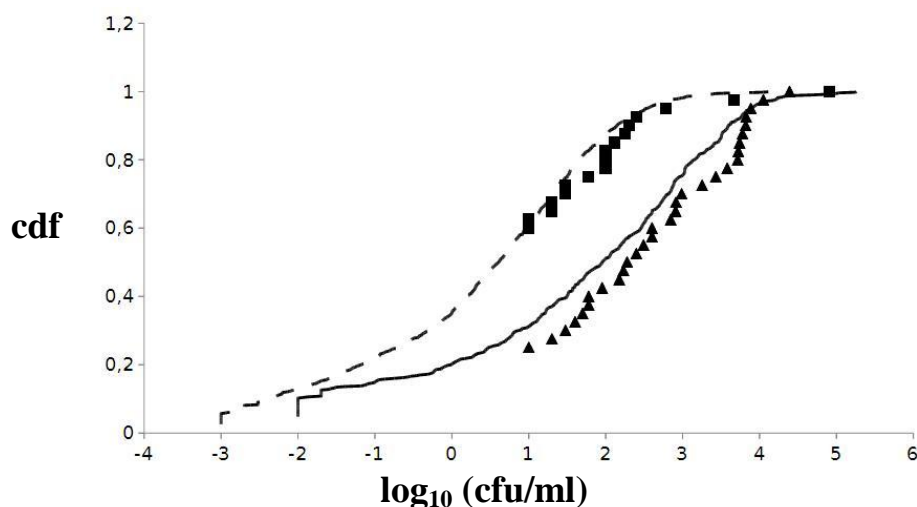


Figure 3: Cumulative distribution of observed log counts of *C. sakazakii* in enrichment medium after 20 hours in 100g samples (■) and 10g samples (▲). Predicted log counts in 100g (---) and 10g (—) bags, taking into account variability of individual lag times and microbial interaction.

Conclusion

Relationships established for *L. monocytogenes* between populational and individual parameters of growth were observed for *Cronobacter*. These relationships can thus be used for predictive modelling and risk assessment studies provided a consolidation of the data.

Relationships were validated for *Cronobacter* cells undergoing enrichment culturing in BPW for 8h and 20h provided that bacterial interactions are taken into account. This demonstrated the importance of validating the model before use especially in non-selective broth.

We also noticed a strong impact of pooling on the populations of *Cronobacter* reached at 20h which corresponds to the end of the pre-enrichment duration of the standard detection method. This effect can be explained by a combined effect of a weaker *Cronobacter* initial concentration in 100g and of a premature stop of the growth due to bacterial interactions.

Thus, from a practical point of view, pooling can have an effect on the sensitivity of the detection method.

References

- Anonymous 2006a. *Enterobacter sakazakii* and *Salmonella* in powdered infant formula: meeting report. Microbiological risk assessment series 10. World Health Organisation-Food and Agriculture Organisation of the United Nations, Geneva and Rome.
- Anonymous 2006b. Milk and milk products-Detection of *Enterobacter sakazakii*. ISO/TS 22964:2006 and IDF/RM 210:2006. International Organization for Standardization, Geneva, Switzerland.
- Anonymous 2008. Contamination microbienne des préparations lactées en poudres destinées aux nourrissons et personnes âgées. Afssa, Maisons Alfort, France.
- D'Arrigo M., García de Fernando G.D., Velasco de Diego R., Ordóñez J.A., George S.M. and Pin C. (2006). Indirect measurement of the lag time distribution of single cells of *Listeria innocua* in food. *Applied and Environmental Microbiology* 72, 2533-2538.
- Guillier L. and Augustin J.-C. (2006). Modelling the individual cell lag time distributions of *Listeria monocytogenes* as a function of the physiological state and growth conditions. *International Journal of Food Microbiology* 111, 241-251.
- Guillier L. and Augustin J.-C. (2008). Erratum to "Modelling the individual cell lag time distributions of *Listeria monocytogenes* as a function of the physiological state and the growth conditions, *International Journal of Food Microbiology* 111 (2006) 241-251". *International Journal of Food Microbiology* 124, 114.
- Iversen, C., Mullane, N., Lehner, A., Mc Cardell, B., Tall B. D., Lehner A., Fanning S., Stephan R. and Joosten H. (2008). *Cronobacter* gen. nov., a new genus to accommodate the biogroups of *Enterobacter sakazakii*, and

proposal of *Cronobacter sakazakii* gen. nov., comb. nov., *Cronobacter malonaticus* sp. nov., *Cronobacter turicensis* sp. nov., *Cronobacter muytjensii* sp. nov., *Cronobacter dublinensis* sp. nov., *Cronobacter* genomospecies 1, and of three subspecies, *Cronobacter dublinensis* subsp. *dublinensis* subsp. nov., *Cronobacter dublinensis* subsp. *lausannensis* subsp. nov. and *Cronobacter dublinensis* subsp. *lactaridi* subsp. nov. *International Journal of Systematic and Evolutionary Microbiology*, 58, 1442-1447.

Studying the growth boundary and subsequent growth kinetics of *Escherichia coli* at different temperature, pH and water activity levels

A. Valero, M. Rodríguez, R.M. García-Gimeno and G. Zurera

Department of Food Science and Technology, Faculty of Veterinary. University of Córdoba (Spain): Campus Rabanales s/n Edif. Darwin C1, Crta. Madrid-Cádiz km 396-A, 14014, Córdoba (Spain) (bt2vadia@uco.es)

Abstract

Escherichia coli has been cataloged as a microbial indicator of faecal contamination in food products when they are improperly handled or when inactivation treatments do not guarantee its inhibition. Adaptation of *E. coli* at low pH and A_w levels can vary at different temperatures depending on the strain and more detailed studies are needed. In this work, the behavior of *E. coli* was studied in a three-step process: (i) firstly, a screening of four strains of *E. coli* (serovars O55:H6; O59:H21; O158:H23 and O157:H7) was performed; (ii) secondly, growth/no growth models were elaborated with the fastest strain selected at different temperatures (8, 12 and 16°C), and inoculum levels (100, 1000 and 10000 cfu/mL) as function of pH (ranged from 7.0 to 5.0 at 0.25 levels) and A_w (five levels ranging from 0.999 to 0.960); (iii) finally, the growth kinetics of *E. coli* was described in the conditions that allowed growth. Results obtained showed that the serovars O157:H7 and O59:H21 did not grow at more stringent conditions (8°C; pH 5.5), while the serovar O158:H23 was the best adapted, resulting in a faster growth. The logistic regression models performed presented a good adjustment to data observed since more than 93.06 % of cases were correctly classified. The growth boundary was shifted to more limited conditions as the inoculum size was higher. At 8°C; pH 5.5 *E. coli* was able to grow at A_w 0.990 being the initial concentration equal to 10000 cfu/mL. Detection times (T_d , h) were calculated and the optimal pH for growth was found to be 6.75. However, an increasing variability was noted at low A_w and pH levels among the replicates. This information is valuable to be included in a risk assessment framework in order to describe the variability due to the strain and the growth kinetics of *E. coli* at various environmental conditions.

Keywords: growth/no growth, *Escherichia coli*, detection time, inoculum level, strain variability

Introduction

Verocytotoxin-producing *Escherichia coli* (VTEC) serogroups are one of the most important emerging food-borne pathogens which can be present in foods of animal origin, contaminated vegetables or ready-to-eat foods that are improperly handled up to consumption (Badri et al., 2009). The total number of pathogenic *E. coli* outbreaks within the EU increased by 38.3% in 2007 compared to 2006 being the largest number of human cases (39.4%) originated from outbreaks in catering services or restaurants (EFSA, 2009). In the last few years, predictive microbial models are focused on studying the acid adaptation of *E. coli* O157:H7 combined with the influence of various environmental factors on its growth or inactivation kinetics (Skandamis et al., 2007). However, little information is known about the behavior of other VTEC strains which can potentially cause non-reported human diseases.

On the other hand, it has been demonstrated that inoculum size influences the position of the growth/no growth interface. Generally, this interface is shifted to less stringent conditions at low microbial concentrations (Koutsoumanis and Sofos, 2005) obtaining also higher variability in growth parameters (Augustin et al., 2000). The inoculum effect has been modelled independently through the use of detection time values (T_d) (Bidlas et al., 2008). However, growth estimations can be less accurate when approaching to conditions that limit growth (Nerbrink et al., 1999). It has been suggested that a combined approach incorporating the information of growth boundaries together with growth kinetics would be more appropriate for studying microbial behavior (Ross and McMeekin 1994). In this sense it

would be important to study the interaction of environmental factors that prevent growth as well as the growth behavior at different microbial concentrations.

In this work, the behavior of *E. coli* was studied in the growth/no growth domain as a function of temperature, pH and water activity (A_w) as follows: (i) firstly, a screening of four strains of *E. coli* (serovars O55:H6; O59:H21; O158:H23 and O157:H7) was performed at different temperatures, pH and inoculum levels by turbidimetric measurements; (ii) secondly, a growth/no growth model was elaborated with the fastest strain selected as a function of pH and water activity (A_w) at different temperatures and inoculum levels during 30 days; (iii) finally, the growth kinetics of *E. coli* was studied in the conditions that produced growth.

Material and Methods

Screening of the strains

Four *E. coli* strains (serovars O55:H6; O59:H21; O158:H23 and O157:H7) obtained from the Spanish Culture Type Collection (Burjassot-Valencia, Spain) were cultured in Tryptone Soja Broth, TSB, (Oxoid, UK) at 30°C-24h. Subsequently, 0.1 mL of inoculum was transferred to a 50 mL flask until the stationary phase was reached. Growth of *E. coli* was evaluated by absorbance measurements in Bioscreen C (Labsystems, Finland) at 600 nm as a function of temperature (8 and 16°C), pH (5.5 and 7.0) and initial inoculum level (100 and 10000 cfu/mL). The Baranyi model was adjusted to obtained data for calculating the growth rates (μ_{max} , h^{-1}) and lag phases (lag, h) for each strain. The fastest and best adapted strain was selected to perform the growth/no growth models.

Growth/no growth models

The logistic regression models were performed at different levels of pH (from 7.0 to 5.0 at 0.25 levels) and A_w (five levels ranging from 0.999 to 0.960), letting constant temperature (8, 12 and 16°C) and inoculum level (100, 1000 and 10000 cfu/mL). Assessment of growth was performed by turbidity measurements in Bioscreen C (Labsystems, Finland) and checked by plating onto Plate Count agar (Oxoid, UK) at regular time intervals during 30 days. 8 replicates per condition were made and for any combination of factors, growth was recorded as “1” if it occurred and “0” if did not. A cut point of probability of growth (P) = 0.01 was taken to delimit growth and no growth.

A polynomial logistic regression model, was implemented in SPSS v15.0 (Chicago, Illinois, USA) following a stepwise process, by deleting one by one the less significant variables, until obtaining a biologically interpretable equation. To start processing data, the input variables were scaled in the range [0.1-0.9]. The new scaled variables were named pH^* and A_w^* .

$$\text{logit } P = \left(\frac{P}{1-P} \right) = a_0 + a_1 \times pH^* + a_2 \times A_w^* + a_3 \times pH^* \times A_w^* + a_4 \times pH^{*2} + a_5 \times A_w^{*2} \quad (1)$$

where P = probability of growth; and a_0 - a_5 = coefficients to be estimated by the model.

Calculation of the detection time of E. coli under growth conditions

On each day of analysis the difference between the OD and the OD_{blank} (pure medium) was recorded. For the conditions that allowed growth, the T_d (h) were calculated since the absorbance measurements as follows:

$$Td = \sum_{i=1}^n \frac{O.D_i}{n} + 3 \times \left(\sqrt{\frac{1}{n-1} \times \sum_{i=1}^n (O.D_i - \overline{O.D.})^2} \right) \quad (2)$$

where T_d (h) = detection time; OD_i is the absorbance value of the blank in the replicate i ; n = number of replicates; and $\overline{O.D.}$ is the mean absorbance value of all replicates.

Results and Discussion

Selection of the strain

Results of the screening performed showed significative differences among the behavior of *E. coli* strains. It has been observed that neither the strain O157:H7 nor O59:H21 were able to grow at 8°C-pH = 5.5, although the highest values of μ_{\max} were observed for *E. coli* O157:H7 at 16°C-pH = 7.0 (100/10000 cfu/mL = 0.030/0.038 h⁻¹). The strain O158:H23 was the best adapted since it showed the lowest lag phase values at 8°C-pH = 5.5 (100/10000 cfu/mL = 291.13/193.37 h) and at 16°C-pH = 7.0 (100/10000 cfu/mL = 31.53/16.78 h); and also the highest values of μ_{\max} at 8°C-pH = 5.5 (100/10000 cfu/mL = 0.006/0.007 h⁻¹). Therefore, this strain was selected to perform the growth/no growth models.

Growth/no growth models

Nine logistic regression models were obtained for each combination of temperature and initial inoculum level. 45 conditions of pH and Aw (8 replicates per condition = 360 cases) were evaluated for studying growth/no growth of *E. coli* O158:H23. The estimated coefficients are shown in Table 1. Transformation of the variables improved the adjustment of the models to data observed, since the percentages of correct classified cases were situated between 93.06 and 100 %. Besides, for an industrial/food safety point of view, in this model growth of *E. coli* was considered if $P > 0.01$. This provides fail-safe predictions in comparison to other published logistic regression models, in which growth was considered if $P > 0.5$.

Table 1: Estimated coefficients for the growth/no growth models of *E. coli* O158:H23 as a function of pH and Aw, at different temperatures and initial inoculum levels

| Variables | Estimated coefficients | | | | | | | | |
|--------------------------|------------------------|----------------|-----------------|---------------|----------------|-----------------|---------------|----------------|-----------------|
| | 8°C | | | 12°C | | | 16°C | | |
| | 100 cfu/mL | 1000 cfu/mL | 10000 cfu/mL | 100 cfu/mL | 1000 cfu/mL | 10000 cfu/mL | 100 cfu/mL | 1000 cfu/mL | 10000 cfu/mL |
| a_0 | -48.787 | -66.952 | -72.168 | -32.957 | -895.100 | -431.653 | -243.828 | -239.154 | -239.154 |
| a_1 (pH*) | -402.905 | 106.405 | -502.292 | NS | 1450.286 | 625.317 | NS | 169.484 | 169.484 |
| a_2 (Aw*) | NS | 60.535 | NS | 32.826 | 1189.568 | 452.017 | 303.183 | 358.379 | 358.379 |
| a_3 (pH* x Aw*) | 799.591 | NS | 1105.600 | 54.761 | -1047.388 | NS | 893.185 | 377.264 | 377.264 |
| a_4 (pH ²) | NS ¹ | -87.213 | NS | NS | -610.566 | -444.092 | NS | NS | NS |
| a_5 (Aw ²) | NS | NS | NS | NS | -151.307 | NS | NS | NS | NS |

¹ NS = not significant (p<0.05)

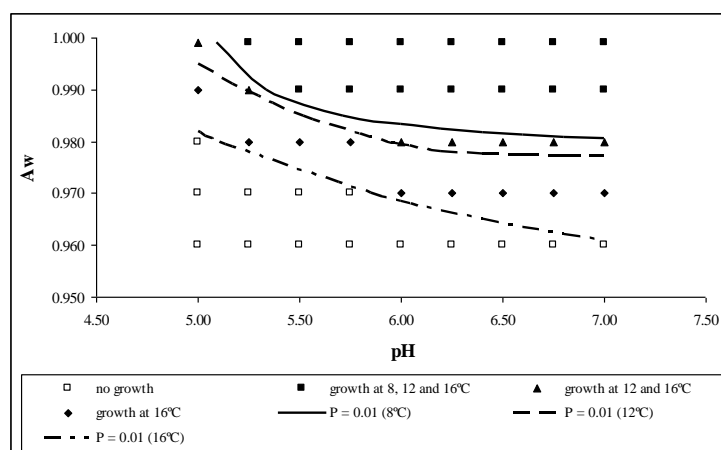
Effect of temperature, pH, Aw and initial inoculum level on the growth boundary of E. coli

Figure 1 represents the growth boundary of *E. coli* O158:H23 at 8, 12 and 16°C (10000 cfu/mL) as a function of pH and Aw. Results obtained showed that *E. coli* O158:H23 was not able to grow at low pH (5.0) at 8°C. It can be also observed that the growth/no growth interface at 16°C is closer to low levels of pH corroborating that the cell yield increases at mild growth temperatures (Salter et al., 2000). In this case, pH alone was not effective to inhibit growth, being necessary a reduction of Aw to 0.97 at pH values below 6.0.

Besides, it was shown that the position of the growth boundary was shifted at different inoculum levels. As stated by other authors, at higher microbial concentrations the growth/no growth interface was closer to low levels of environmental factors since the cells are more capable to initiate growth (Skandamis et al., 2007). However, no significant differences in the behavior of *E. coli* O158:H23 at 16°C was observed between 10000 and 1000 cfu/mL, so that an unique logistic regression model was performed for the two inoculum levels (Table 1).

Description of the growth kinetics of *E. coli*

Growth of *E. coli* O158:H23 was described through the use of Td values (h) in the conditions that allowed growth. According to the mean Td values obtained, growth of *E. coli* O158:H23 was detected later at low temperature (8°C), pH (< 6.0) and Aw (< 0.99) levels. Results have shown a variability in Td values with respect to the inoculum level, since at 100 cfu/mL (pH 5.25; Aw 0.999) Td was equal to 373.87 ± 62.38 h, while at 1000 and 10000 cfu/mL these values decreased to 327.92 ± 43.51 and 257.15 ± 16.81 h respectively. This variability was also observed by other authors (Pin and Baranyi, 2006) being also associated to the variability of the lag phase. On the contrary, at optimal conditions, reduction of pH and Aw had less influence on Td values, finding that at 10000 cfu/mL and 16°C; (Aw = 0.999) mean Td values



were situated between 29.16 and 32.34 h through the pH range 7.0-5.75.

The developed models may be viewed as tools that provide growth data of different strains of *E. coli* combined with an estimation of the growth/no growth interface and subsequent growth kinetics at various environmental conditions which may be valuable to be included in a risk assessment framework.

Figure 1: Growth/no growth interfaces ($P = 0.01$) of *E. coli* O158:H23 as a function of pH and Aw at 8, 12 and 16°C. The inoculum level was fixed at 10000 cfu/mL.

Acknowledgements

This work was partly financed by the Excellence Projects (Junta de Andalucía P06-AGR-0189; CTS-3620), MICINN- AGL2008-03298, (Department of Food Science and Technology, University of Cordoba) and by European ERDF funding.

References

- Badri, S., Filliol, I., Carle, I., Hassar, M., Fassouane, A., and Cohen, N. (2009) Prevalence of virulence genes in *Escherichia coli* isolated from food in Casablanca (Morocco). *Food Control* 20, 560-564.
- Augustin, J.C., Brouillard-Delattre, A., Rosso, L., and Carlier, V. (2000) Significance of inoculum size in the lag time of *Listeria monocytogenes*. *Applied and Environmental Microbiology*, 66 1706-1710.
- Bidlas, E., Du, T., and Lambert, R.J.W. (2008) An explanation for the effect of inoculum size on MIC and the growth/no growth interface. *International Journal of Food Microbiology* 126, 140-152.
- European Food Safety Authority (2009) The community summary report on food-borne outbreaks in the European Union in 2007. *The EFSA Journal*, 1-271.
- Koutsoumanis, K.P., and Sofos, J.N. (2005) Effect of inoculum size on the combined temperature, pH and Aw limits for growth of *Listeria monocytogenes*. *International Journal of Food Microbiology* 104, 83-91.
- Nerbrink, E., Borch, E., Blom, H., and Nesbakken, T. (1999) A model based on absorbance data on the growth rate of *Listeria monocytogenes* and including the effects of pH, NaCl, Na-lactate and Na-acetate. *International Journal of Food Microbiology* 47, 99-109.
- Pin, C., and Baranyi, J. (2006) Kinetics of single cells: observation and modeling of a stochastic process. *Applied and Environmental Microbiology* 72, 2163-2169.
- Ross, T., and McMeekin, T.A. (1994) Predictive microbiology. *International Journal of Food Microbiology* 23, 241-264.
- Salter, M.A., Ratkowsky, D.A., Ross, T., and McMeekin, T.A. (2001) Modelling the combined temperature and salt (NaCl) limits for growth of a pathogenic *Escherichia coli* strain using nonlinear logistic regression. *International Journal of Food Microbiology* 61, 159-167.
- Skandamis, P.N., Stopforth, J.D., Kendall, P.A., Belk, K.E., Scanga, J.A., Smith, G.C., and Sofos, J.N. (2007) Modeling the effect of inoculum size and acid adaptation on no growth/no growth interface of *Escherichia coli* O157:H7. *International Journal of Food Microbiology* 120, 237-249.

Prediction of time to growth of *Bacillus cereus* in egg as a function of lysozyme, nisin and mild heat treatment

P.S. Fernández^{1,2}, V. Antolinos¹, C. Pin³, M. Ros-Chumillas², P.M. Periago^{1,2}, M. Muñoz¹

¹ Department of Food Engineering and Agriculture Equipment, Polytechnic University of Cartagena, Paseo Alfonso XIII 48, 30203 Cartagena, Spain (Pablo.fernandez@upct.es)

² Laboratory of Microbial Food Safety, Institute of Plant Biotechnology, Polytechnic University of Cartagena, Campus Muralla del Mar, 30202 Cartagena, Spain (may.ros@upct.es)

³ Institute of Food Research, Norwich Research Park, Colney Lane, Norwich NR4 7UA, UK (carmen.pin@bbsrc.ac.uk)

Abstract

To establish microbial food safety based on probabilistic models it is necessary to account for stochastic data of as many microbial inactivation and growth parameters as possible. In this paper, a stochastic approach to evaluate growth of heat damaged *Bacillus cereus* cells taking into consideration germination kinetics and the influence of different stresses (mild heat treatment, presence of nisin and lysozyme separately or in combination) was performed, using an approach of growth through OD measurements. From results obtained histograms of the lag phase were generated and distributions were fitted. Histograms showed a shift to longer lag phases and an increase in variability with high stress levels. A simulation was performed to establish the time necessary for a certain increase in *B. cereus* cells in liquid egg as a function of the germination rate, initial spore numbers, inactivation and growth parameters. Results were compared with a deterministic approach to evidence the advantages of probabilistic data to establish food safety margins.

Keywords: *Bacillus cereus*; predictive modelling; heat inactivation; lag phase distributions; germinants.

Introduction

Hurdle technology advocates the synergistic combinations of various antibacterial techniques in order to drastically limit the growth of spoilage bacteria. Using an intelligent combination of hurdles (i.e. preservation factors) can effectively improve the microbial safety and maintain the sensory and nutritional quality of foods (Leistner, 1999). Nisin is a heat-stable bacteriocin produced by *Lactococcus lactis* ssp. *Lactis*, active against many Gram-positive bacteria, and prevents the outgrowth of spores of many *Clostridium* and *Bacillus* spp. (Delves-Broughton and Gasson, 1994). Lysozymes are widespread in plants and animals, where they constitute a natural defence mechanism against bacterial pathogens. The most studied lysozyme and the only one so far used commercially as a food preservative is hen egg white lysozyme (HEWL). Both compounds are classified as GRAS. Synergistic antibacterial activity between nisin and lysozyme has been reported (Nattress and Baker, 2003).

Bacillus cereus is a Gram-positive, spore-forming, obligate aerobe often associated with food spoilage and foodborne illness. The accurate number of food poisonings caused by *B. cereus* in different countries is not known because it is not a reportable illness and is not always diagnosed. *B. cereus* caused many problems in food industry by spore formation and it may survive pasteurization and heating. It is a ubiquitous microbe in the environment and can easily contaminate food production or processing equipment. Liquid egg is a heat sensitive product where the presence of sporeforming bacteria can pose a serious risk. Particularly *Bacillus cereus* can be a potential hazard and due to the maximum temperatures that can be used (in the range of 60°C) it is necessary to have additional hurdles to guarantee its safety.

Deterministic growth models describe the behaviour of bacterial populations, while ignoring individual cell variability. In small populations of cells this variability can be quite important when attempting to make accurate predictions, particularly when the cells have been exposed to stress. It is becoming clear that to develop a more complete understanding of the lag phase process, the behaviour of single or low levels of cells has to be taken into account through the

development of stochastic models (Baranyi and Pin, 1999). To achieve this, the use of optical measurement densities in automatic plate readers, once they have been adequately calibrated with standard growth curves, can be a very valuable tool (Valero et al., 2006).

Materials and methods

Bacterial strain

The strain used in the experiments was *B. cereus* TZ421AV that was kindly donated by Institut National de la Recherche Agronomique, INRA Avignon (France). It was sporulated in Fortified Nutrient Agar at 30°C and spores were harvested and stored at 4°C until use.

Chemicals

Lysozyme was obtained from Sigma-Aldrich, Switzerland (Hen egg White lysozyme, 84468U/mg). It was dissolved in sterile bidistilled water and esterilized by filtration (0.45µm Millex-HV, Millipore, Bedford, USA). It was prepared to give a final concentration of 100mg/mL and stored refrigerated until use.

Nisin was obtained from Sigma-Aldrich, Switzerland (Nisin from *Streptococcus lactis*, 2,5%). It was dissolved in ethanol 50% (v/v). It was prepared to give a final concentration of 0.13µM and stored refrigerated until use.

Combined stresses

Successive individual stresses were applied to cells in the early stationary phase of *B. cereus*. A 100µL volume of vegetative cells of *B. cereus* were inoculated in 5mL of homogenized egg with different amounts of antimicrobial compounds (lysozyme and nisin, alone or combined). Prior, a mild heat treatment was applied to inactivate 3 log cycles. Then it was incubated at 10 and 12°C. Samples were taken at different time intervals and plated on BHIA. Plates were incubated at 37°C for 24 h.

Growth curves of B. cereus measured by OD

Growth curves were made in BHI with the addition of nisin and lysozyme at different concentrations alone or combined. A dilution procedure following two-fold dilutions was applied to obtain up to single *B. cereus* cells in the wells of the microtiter plate. Serial dilutions of control or stressed cells were made and 400 µL were added into the wells of a Bioscreen plate. The plates were incubated in the Bioscreen at 10 and 12°C for different time periods. Measures were set at 15 min intervals. The time to a certain increase in cell numbers was established for each individual well (Baranyi and Pin, 1999).

Statistical data processing and distribution fitting

Statistical data processing was performed and histograms were made from every set of conditions showing the distribution of the lag phases. From each histogram, the most common statistical parameters (mean value, standard deviation, etc.) were determined.

Distributions were fitted to time to growth and were ranked using the χ^2 and the Anderson–Darling (A–D) goodness of fit statistics. The probability (p) is a measure of confidence that the fitted distribution could have generated the original data set, and ranges from zero to one, with one being the highest confidence.

A simulation was performed considering the distribution of germination of *B. cereus* (Collado et al., 2006), the initial contamination level and the distributions fitted for the different concentrations of nisin and lysozyme tested for different probabilities of time to growth where toxin could be formed and it was compared with deterministic predictions. These simulations were then contrasted with time to growth in homogenized egg determined by plate counts.

Results and discussion

Heat resistance of B. cereus

D- and z-values were obtained in the range of temperatures 55-65°C, using vegetative cells of *B. cereus* heated in homogenized egg. D values were found to be between 17.4 min at 55°C and 0.4 min at 65°C. The z-value calculated was 4.28 °C.

Effect of nisin and lysozyme on growth of B. cereus vegetative cells inBHI

The effect of nisin and lysozyme on the growth parameters of *B. cereus* vegetative cells was studied at 12°C. Concentrations of lysozyme (ranging from 0.1 to 1.0 mmol L⁻¹) or/and nisin (0.065-0.13 µmol L⁻¹) were added to BHI broth, growth was measured following OD and distributions describing growth were fitted. The average values of the main conditions tested and their combination is included in Table 1. Nisin alone or combined with lysozyme induced a significant increase in the lag phase at 12°C, whereas the maximum specific growth rate did not vary.

Growth curves in liquid egg containing lysozyme and nisin

In order to evaluate the antibacterial activity of lysozyme and nisin, individually or combined, samples of homogenized egg (5mL) containing concentrations of lysozyme (ranging from 0.5 to 4.0 mmol L⁻¹) or/and nisin (0.065-0.26 µmol L⁻¹) were inoculated with heat treated *B. cereus*. Samples were incubated at 10 and 12°C, taken at different time intervals during incubation and plated on BHIA. Plates were incubated at 37°C for 24 h. The combination of nisin and lysozyme increased the lag time of the microorganism, although individually they did not have an effect (Figure 1).

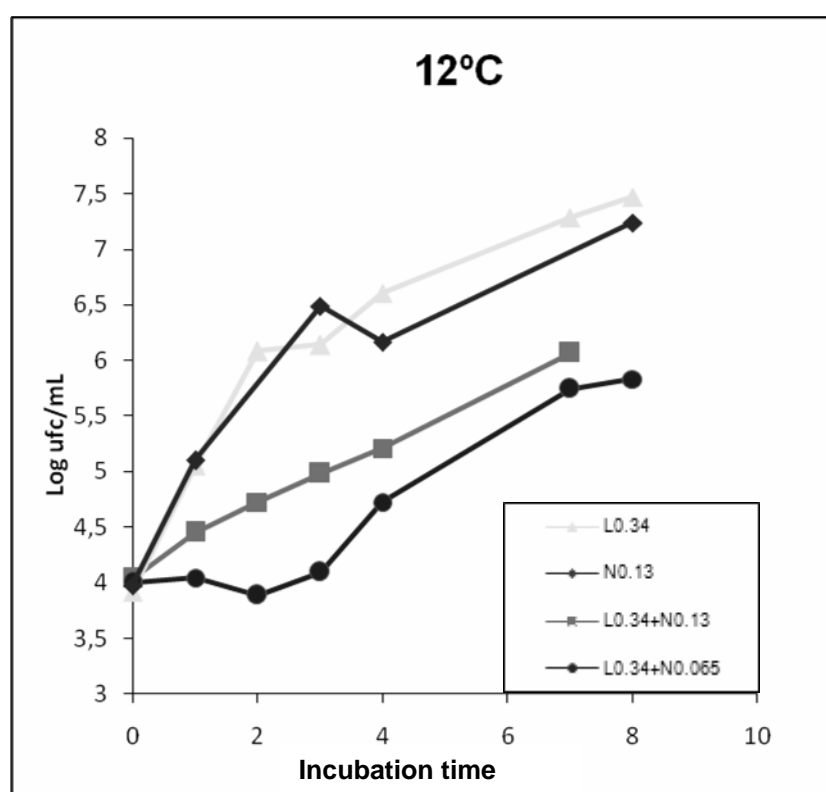


Figure 1: Growth curves of *B. cereus* exposed to lysozyme (L) and/or nisin (N) at 12°C in liquid egg

Table 1: Average estimated growth parameters of *B. cereus* TZ421 in BHI broth measured by OD at 12°C, exposed to the conditions indicated

| Treatment | μ_{\max} (h ⁻¹) | λ (h) |
|--------------------------------------|---------------------------------|---------------|
| Control | 0,099 | 16,86 |
| Lysozyme 0.5 mmol L ⁻¹ | 0,104 | 15,51 |
| Nisin 0.13 μ mol L ⁻¹ | 0,103 | 51,93 |
| Lys 0.5+Nis 0.065 | 0,118 | 35,55 |
| Lys 0.5+Nis 0.13 | 0,088 | 52,09 |

Prediction of the effect of nisin and lysozyme on B. cereus growth

A simulation was performed to establish the effect of germination, contamination level, heat inactivation and presence of nisin and/or lysozyme on *B. cereus* growth at 12°C. Distributions were fitted to describe quantitatively growth in the presence of these compounds. The simulation indicated the probability of time to growth as a function of the parameters investigated and it was compared with a deterministic prediction of time to growth.

Conclusions

The combination of lysozyme and nisin can contribute to extend the shelflife of refrigerated, liquid egg delaying growth of *B. cereus*. A probabilistic approach can help to efficiently predict the impact of different factors on time to a certain increase of *B. cereus* and to define precisely the level of risk that a consumer is exposed to for a certain food.

Acknowledgements

The work was funded by the Spanish Ministry of Science and Innovation through project AGL 2006-13320-C03-02/ALI. Marina Muñoz acknowledges Fundacion Cajamurcia for awarding her a post-doc grant and also this work is a result of the support 11154/AC/09 given to her by Fundación Séneca-Agencia de Ciencia y Tecnología de la Región de Murcia en el marco del II PCTRM 2007-2010.

References

- Baranyi J. and Pin C. (1999) Estimating growth parameters by means of detection times. *Applied and Environmental Microbiology* 65, 732–736.
- Collado J., Fernández A., Rodrigo M. and Martínez A. (2006) Modelling the effect of a heat shock and germinant concentration on spore germination of a wild strain of *Bacillus cereus*. *International Journal of Food Microbiology* 106, 85-89.
- Delves-Broughton J. and Gasson M.J. (1994) Nisin. In: V.M. Dillon and R.G. Board, (Eds.), *Natural Antimicrobial Systems and Food Preservation*, CAB International, Wallingford, Oxon, pp. 99–131.
- Leistner, L., 1999. Combined methods for food preservation. In: M.S. Rahman (Ed.), *Handbook of Food Preservation*. pp. 457-485, Marcel Dekker, New York.
- Nattress F.M., Baker L.P. (2003) Effects of treatment with lysozyme and nisin on the microflora and sensory properties of commercial pork. *International Journal of Food Microbiology* 85, 259-267.
- Valero A, Perez-Rodriguez F, Carrasco E, García-Gimeno R.M., Zurera, G. (2006) Modeling the growth rate of *Listeria monocytogenes* using absorbance measurements and calibration curves. *Journal of Food Science* 71, 257-264.

Assigning distributions representing variability and uncertainty to microbiological data

P. Busschaert^{1,2}, A.H. Geeraerd^{1,3}, M. Uyttendaele⁴ and J.F. Van Impe^{1,2}

¹ CPMF² - Flemish Cluster Predictive Microbiology in Foods, <http://www.cpmf2.be>

² Division of Chemical and Biochemical Process Technology and Control, Department of Chemical Engineering, Katholieke Universiteit Leuven, W. de Croylaan 46, B-3001 Leuven, Belgium (jan.vanimpe@cit.kuleuven.be)

³ Division of Mechatronics, Biostatistics and Sensors (MeBioS), Department of Biosystems (BIOSYST), Katholieke Universiteit Leuven, W. de Croylaan 42, B-3001 Leuven, Belgium (annemie.geeraerd@biw.kuleuven.be)

⁴ Laboratory of Food Microbiology and Food Preservation, Department of Food Safety and Food Quality, Ghent University, Coupure Links 653, B-9000 Ghent, Belgium

Abstract

In the framework of a probabilistic risk assessment, initial contamination data are often represented by a statistical distribution. However, because contamination data can consist of (combinations of) qualitative, quantitative, semiquantitative measurements and nondetects, it is not always straightforward to assign an appropriate distribution. In this research, maximum likelihood estimation (MLE) is applied to estimate the parameters of a (log)normal distribution representing various types of contamination data. Moreover, the bootstrap method is used in order to calculate uncertainty related to these estimated parameters. These techniques have been applied to two case studies, i.e., measurements of *Campylobacter* spp. contamination in chicken meat preparations, and measurements of *Listeria monocytogenes* in smoked fish samples.

Keywords: quantitative microbiological risk assessment, variability and uncertainty, maximum likelihood estimation, bootstrap method

Introduction

Outcomes of a quantitative microbiological risk assessment in food are in many situations dependent on the initial contamination of the micro-organism in the food product. In case of a probabilistic risk assessment, the initial contamination is usually represented by a distribution. However, microbiological contamination data often consist of (combinations of) qualitative, quantitative or semiquantitative measurements, or measurements below the limit of detection. As a consequence, it is not straightforward to transform the outcomes of these tests into an appropriate parametric distribution.

Materials and methods

In the case of negative presence/absence test, e.g., in 25 g of food, the concentration of the pathogen tested for in the food sample is known to be less than (a hypothetical) 0.04 CFU/g (i.e., left-censored). Similarly, in the case of a positive presence/absence test, the result is known to be greater than 0.04 CFU/g (right-censored). When a food sample results in a positive presence/absence test, a smaller portion of that same food sample could be tested again, e.g., 1 g. When the second test is negative, the pathogen concentration is between 0.04 CFU/g and 1 CFU/g. This kind of data is referred to as semi-quantitative or interval-censored.

As a first case study, laboratory analyses of *Campylobacter* in chicken meat preparations at the Belgian retail market are analyzed (Habib *et al.*, 2008a). The data set consists of direct plating results using the ISO (2006) standard method with a reduced LOD of 10 CFU/g instead of 100 CFU/g. In 387 out of 656 measurements (59%), the result is left-censored.

A set of 103 samples of smoked fish on the Belgian retail market is used as a second case study. The samples were analyzed in the period 2005-2007 for a number of food business operators (Uyttendaele *et al.*, 2009). As opposed to the *Campylobacter* data set, this data set contains merely 1 quantitative measurement. All other measurements are either interval-, left- or right-censored. Moreover, the data set contains several different LODs, depending on

the demands of the food business operator the particular food samples were supplied by, hence resulting in a rather complex data set.

In order to fit a distribution to combinations of qualitative, quantitative and semiquantitative data, the method of maximum likelihood estimation is used. It is assumed that the initial contamination (\log_{10} CFU/g) is normally distributed (Crépet *et al.*, 2007, Kilsby and Pugh, 1981, Legan *et al.*, 2001). Maximum likelihood estimation results in the parameters $\theta = (\mu, \sigma)$ of the normal distribution which is most likely to have generated the observed (censored) data. In order to express uncertainty about the obtained parameters, the bootstrap method is applied. As a result, each of the parameters is represented by an uncertainty distribution instead of single values.

The code for the simulations is programmed in R (R Development Core Team, 2009) using functions from the survival package for MLE procedures.

Results and discussions

The reading key for all figures is as follows. A large grey area in horizontal direction indicates large uncertainty about the value of the respective percentiles, i.e., the values of the percentiles differ considerably among different bootstrap iterations. A small grey area indicates that the value of each percentile doesn't alter much in between different bootstrap iterations, hence uncertainty is small. The degree of variability is indicated by the interval the median line spans from the lower percentiles to the higher percentiles.

Case study 1

Using MLE, a normal distribution with mean $\mu = 0.73 \log_{10}$ CFU/g and standard deviation $\sigma = 1.03 \log_{10}$ CFU/g is fitted to the left-censored data set of the first case study (Figure 1a). When all censored data would have been substituted by half of the LOD, the sample mean is $1.10 \log_{10}$ CFU/g. Furthermore, when all censored data would have been substituted by the LOD itself, the sample mean is $1.28 \log_{10}$ CFU/g. Substitution of nondetects by the LOD or half of the LOD clearly leads to a substantial bias, although it is a practice that has been used frequently in past research (Lorimer and Kiermeier, 2007).

The bootstrap method is applied to infer uncertainty about the estimated parameters of the variability distribution. The mean μ is represented by a normal distribution with mean $\mu_{\mu} = -0.05$ and standard deviation $\sigma_{\mu} = 0.21$. The standard deviation is represented by a gamma distribution with shape parameter $\alpha_{\sigma} = 99.4$ and scale parameter $\beta_{\sigma} = 1.87 \cdot 10^{-2}$.

This data set is subsequently employed to examine the influence of a number of conditions. In order to check the effect of using a reduced detection limit, all values below 100 CFU/g (i.e., the standard detection limit of the *Campylobacter* enumeration method) were assumed to be censored and hence regarded as nondetects. In this new data set, 589 out of 656 values are censored, i.e., 90% as opposed to 59% in the original data set. As can be seen in Figure 1b, the increased number of censored values has a high influence on the resulting distribution. This illustrates – in a reverse way – the impact a reduction of the detection limit of current detection methods (e.g., Gnanou Besse *et al.*, 2004) might have on the obtained results. To determine if measurement error (assumed to be $\pm 0.5 \log_{10}$ units) (Habib *et al.*, 2008b) would have a significant impact on the resulting distribution, another simulation is run with all quantitative data points x_i replaced by the interval $[x_i - 0.5, x_i + 0.5] \log_{10}$ CFU/g. As can be seen in Figure 1c, inclusion of this measurement error hardly affects the outcome compared to the original situation (Figure 1c). Finally, the simulation is also conducted with only half the number of data points by pseudorandomly resampling 328 data points from the original data set. When the number of data points is limited to half of the original number, the increase in uncertainty compared to the originally obtained distribution remains rather limited for this particular data set (Figure 1d). This indicates that the investment of labor and costs in a large number of additional measurements might not always have the expected impact on the resulting output distribution.

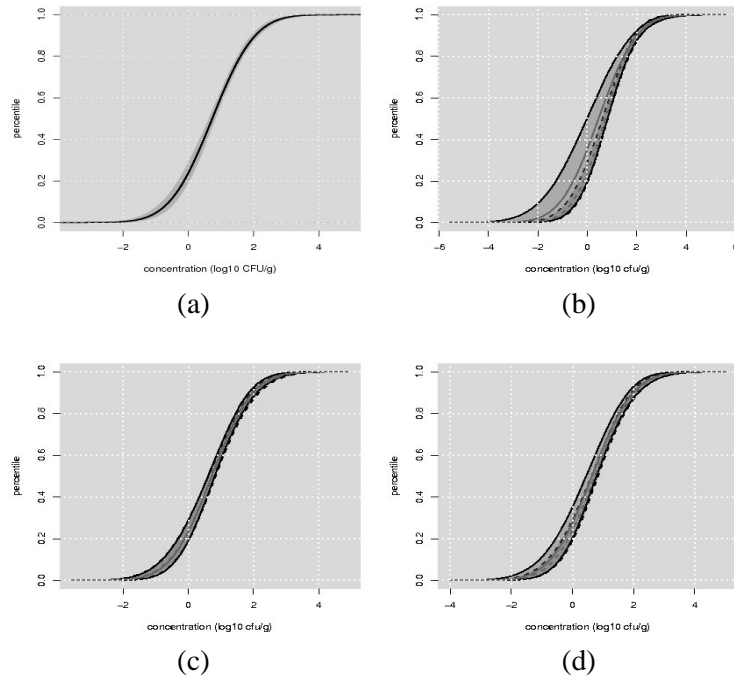


Figure 1: (a) Plot of the 95% confidence interval of the normal distribution fitted to the logarithmic *Campylobacter* spp. data; (b) with a modified LOD; (c) with measurement error included; (d) for the reduced data set.

Case study 2

The data set of *L. monocytogenes* contamination data of the second case study is represented by a normal distribution with mean $\mu = -1.58 \log_{10} \text{ CFU/g}$ and standard deviation $\sigma = 1.54 \log_{10} \text{ CFU/g}$ (Figure 2). Based on the empirical distributions of the bootstrap estimates of the distribution parameters, the normal distribution is chosen to fit both the mean and the standard deviation. A normal distribution with hyperparameters mean $\mu_{\mu} = -1.58$ and standard deviation $\sigma_{\mu} = 0.20$ is fit to the bootstrap means. The standard deviation is represented by a normal distribution with mean $\mu_{\sigma} = 1.51$ and standard deviation $\sigma_{\sigma} = 0.28$.

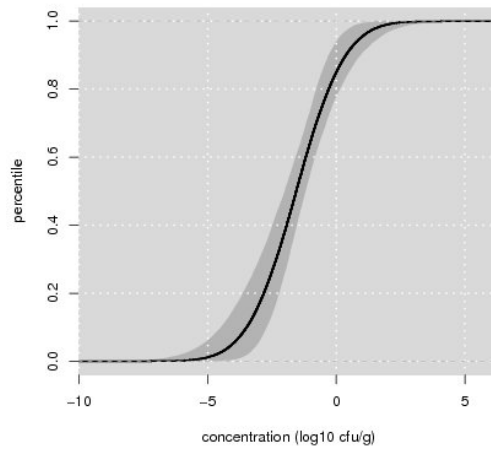


Figure 2: Plot of the 95% confidence interval of the normal distribution fitted to the logarithmic *Listeria monocytogenes* contamination data.

Conclusions

The examples presented in this text illustrate how complex data sets including nondetects, semiquantitative and qualitative measurements with multiple limits of detection can be interpreted in an appropriate way for use in microbiological risk assessment. Ignoring nondetects or substituting them with the LOD or half of it, is a classical source of bias (cfr. Lorimer and Kiermeier, 2007) that can and should be avoided using these methods. It has been demonstrated that even complex data sets including either very diverse analyses or large amounts of censored values, can lead to very satisfying outcomes.

Acknowledgements

This research is supported in part by the Research Council of the Katholieke Universiteit Leuven (projects OT/03/30 and EF/05/006 Centre-of-Excellence Optimization in Engineering), the Belgian Program on Interuniversity Poles of Attraction, initiated by the Belgian Federal Science Policy Office, and the Fund for Scientific Research-Flanders (FWO-Vlaanderen, project G.0424.09N).

We would like to thank the Ghent University cluster (Department of Veterinary Public Health and Food Safety, Department of Food Safety and Food Quality) for the *Campylobacter* data derived from a Federal Public Health Service funded project.

References

- Crépet, A., Albert, I., Dervin, C., Carlin, F., 2007. Estimation of microbial contamination of food from prevalence and concentration data: application to *Listeria monocytogenes* in fresh vegetables. *Applied and Environmental Microbiology* 73 (1), 250-258.
- Gnanou Besse, N., Audinet, N., Beaufort, A., Colin, P., Cornu, M., Lombard, B., 2004. A contribution to the improvement of *Listeria monocytogenes* enumeration in cold-smoked salmon. *International Journal of Food Microbiology* 91 (2), 119-127.
- Habib, I., Sompers, I., Uyttendaele, M., Berkvens, D., De Zutter, L., 2008a. Baseline data from a Belgium-wide survey of *Campylobacter* species contamination in chicken meat preparations and considerations for a reliable monitoring program. *Applied and Environmental Microbiology* 74 (17), 5483-5489.
- Habib, I., Sompers, I., Uyttendaele, M., Berkvens, D., De Zutter, L., 2008b. Performance characteristics and estimation of measurement uncertainty of three plating procedures for *Campylobacter* enumeration in chicken meat. *Food Microbiology* 25 (1), 65-74.
- Kilsby, D.C., Pugh, M.E., 1981. The relevance of the distribution of microorganisms within batches of food to the control of microbiological hazards from foods. *Journal of Applied Bacteriology* 51, 345-354.
- Legan, J.D., Vandeven, M.H., Dahms, S., Cole, M.B., 2001. Determining the concentration of microorganisms controlled by attributes sampling plans. *Food Control* 12 (3), 137-147.
- Lorimer, M.F., Kiermeier, A., 2007. Analysing microbiological data: Tobit or not Tobit? *International Journal of Food Microbiology* 116, 313-318.
- R Development Core Team, 2009. R: A Language and Environment for Statistical Computing. R Foundation for Statistical Computing, Vienna, Austria, ISBN 3-900051-07-0. URL <http://www.R-project.org>.
- Uyttendaele, M., Busschaert, P., Valero, A., Geeraerd, A.H., Vermeulen, A., Jacxsens, L., Goh, K.K., De Loy, A., Van Impe, J.F., Devlieghere, F., 2009. Prevalence and challenge tests of *Listeria monocytogenes* in Belgian produced and retailed mayonnaise-based deli-salads, cooked meat products and smoked fish between 2005 and 2007. *International Journal of Food Microbiology* 133, 94-104.

Robustness analysis of an individual-based model for microbial growth: outcomes and insights

A.J. Verhulst, A.M. Cappuyns, E. Van Derlinden, K. Bernaerts and J.F. Van Impe

CPMF² – Flemish Cluster Predictive Microbiology in Foods – <http://www.cpmf2.be/>

Chemical and Biochemical Process Technology and Control Section (BioTeC), Department of Chemical Engineering, Katholieke Universiteit Leuven, W. de Croylaan 46, B-3001 Heverlee, Belgium
(jan.vanimpe@cit.kuleuven.be)

Abstract

In this study, an individual-based model (IbM) for microbial growth is analyzed and validated through a robustness analysis. IbMs are discrete-event models that consider the individual cell as the modeling unit. Model analysis is an important part of the IbM modeling cycle, as it provides the opportunity to learn more about the model (e.g., effect of time resolution) and the system modeled (population and individual dynamics). Decreasing the time step leads asymptotically to a constant value for the population growth rate, regardless of the initial biomass distribution. The presented IbM is able to reproduce commonly observed microbial behavior. For example, the mean individual generation time exceeds population lag time, and the population reaches steady state in the biomass distribution during exponential growth, regardless of the initial biomass distribution.

Keywords: individual-based modeling, robustness analysis, individual and population dynamics, biomass distribution

Introduction

During the last decade, individual-based modeling (IbM) has proven to be an important tool for modeling microbial dynamics (e.g., Kreft *et al.* 1998, Dens *et al.* 2005b, and Ferrer *et al.* 2008). IbM considers the individual cell as the modeling unit (with its own specific properties), thereby providing a framework to model complex microbial dynamics like interspecies interactions, or complex dynamics induced by food structure, adaptive behavior (e.g., lag phase), ... Nevertheless, the IbM methodology is still lacking a generic set of tools for model analysis, which is an indispensable part of the IbM modeling cycle. This research aims to analyze and validate a basic IbM to obtain a thorough understanding of the model (e.g., effect of time resolution) and the system modeled (e.g., individual versus population dynamics). Information is gathered about how the model reacts to changes in the model parameters. This is achieved by a robustness analysis. Robustness analysis is similar to conventional sensitivity analysis, but a larger range of parameter values is considered. Due to their complexity, IbMs are difficult to understand and learn from. Therefore, it is important to communicate model analysis results. Communication makes other researchers familiar with the different aspects and limitations of the presented IbM.

Materials and methods

Model description

Algorithm 1 provides an overview of the model core. This IbM simulates population lag and exponential growth on the basis of individual cell growth (in a rich homogeneous liquid medium). Each individual is characterized by its growth rate ($\mu_{\text{individual}}$) [1/h] and its mass (m_i) [m*] (m* is the minimum mass at cell birth with a growth rate approaching zero). The number of bacteria is limited to $N_{\text{sim,max}}$. Stochastic elements can be included at lines 1 and 12. During the simulations, individual mass (m_i) and individual generation time (t_g) [min] are recorded at regular time intervals. Every time step the total number of bacteria N [CFU] is registered. Unless stated otherwise, the simulation values are the ones listed in Table 1. The initial biomass distribution is varied in the different simulations.

Algorithm 1: Outline of the basic simulation loop. Variables are explained in Table 1.

```

01 initialize population: randomized cell mass  $m_i$  and growth rate  $\mu_{individual}$ 
02 while  $N < N_{sim,max}$ 
03     for each cell  $i = 1 \dots N$ 
04         grow exponentially
05         if  $m_i \geq 2m^* \cdot 2^j$ 
06              $j = j + 1$  (initiate new replication round )
07         end
08     if a replication round is ended
09          $j = j - 1$ 
10         mother cell ( $m_i$ )  $\rightarrow$  2 daughter cells ( $m_i / 2$ )
11          $N \rightarrow N + 1$ 
12         set random  $\mu_{individual}$  for 2 daughter cells
13     end
15      $t = t + \Delta t$ 
16 end

```

Table 1: Overview of the reference simulation input values.

| Parameter | | Units | Value | Reference |
|---------------------------------|--|-------|---------------------------|--------------------------------|
| N_0 | initial cell number | [CFU] | 10^2 | |
| $N_{sim,max}$ | maximum cell number, simulation limit | [CFU] | 1.5×10^6 | |
| Δt | time step | [min] | 0.1 (or stated otherwise) | |
| T | temperature | [°C] | 37 (or stated otherwise) | |
| $C+D$ | replication and division time | [min] | 60 | Dens <i>et al.</i> (2005a,b) |
| $\bar{\mu}_{individual}$ (37°C) | mean individual growth rate | [1/h] | 2.1553 | Bernaerts <i>et al.</i> (2002) |
| CV of $\mu_{individual}$ | coefficient of variation | - | 0.1 | Kreft <i>et al.</i> (1998) |

Biomass growth is assumed to occur exponentially at any time. DNA replication is initiated when the cell mass reaches a critical value, always a multiple of a critical mass m^* , namely, $2m^* \cdot 2^j$, with $j = 0, 1, 2, \dots$ the number of replication rounds per cell (Donachie, 1968). After completion of the ($C+D$)-period (the time required to complete DNA replication and cell division), cell division takes place. More details can be found in Dens *et al.* (2005b).

Criteria for data analysis

The maximum specific growth rate of the population $\mu_{population}$ [1/h] is determined as the slope of the upper part of the exponential phase (in the interval $[(\ln N_0 + 0.5 (\ln N_{sim,max} - \ln N_0)), \ln N_{sim,max}]$). The population lag phase is determined as the intersection of the inoculum N_0 and the extrapolation of the exponential growth phase.

Results and discussion

Results regarding the model (effect of time resolution) and the system modeled (population and individual dynamics regarding lag, mean growth rate and biomass) are highlighted in the next paragraphs.

Population versus individual lag times

The mean of the lag phase of the individuals (i.e., the mean of the first generation times) exceeds the population lag phase (Table 2). This observation is consistent with earlier publications (Baranyi, 1998, Baranyi and Pin, 2001).

Table 2: Population versus individual lag time.

| | $\bar{m}_0 = 1.7$ | $m_0 \in \text{Normal}(1.7, 0.17)$ | $m_0 \in \text{Uniform}(1.4, 2)$ |
|-------------------------|-------------------|------------------------------------|----------------------------------|
| Population lag [h] | 0.91 | 0.90 | 0.91 |
| Mean individual lag [h] | 1.08 | 1.08 | 1.08 |

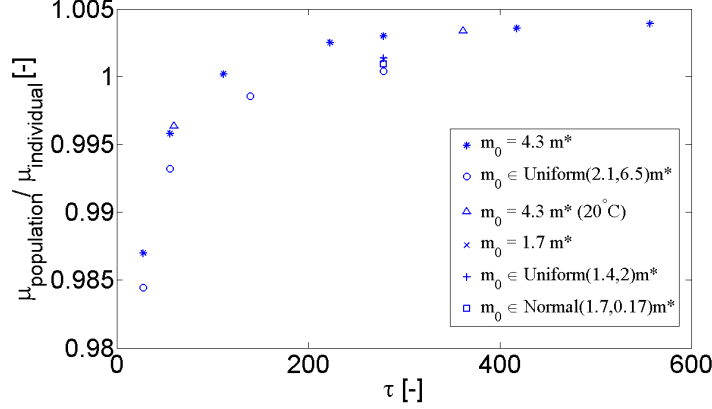


Figure 1: The effect of time resolution on the population growth rate. The graph represents the effect of the dimensionless time step τ ($\tau = (\Delta t \cdot \bar{\mu}_{individual})^{-1}$) on the dimensionless growth rate ($\mu_{population} / \bar{\mu}_{individual}$) for different conditions.

Time resolution

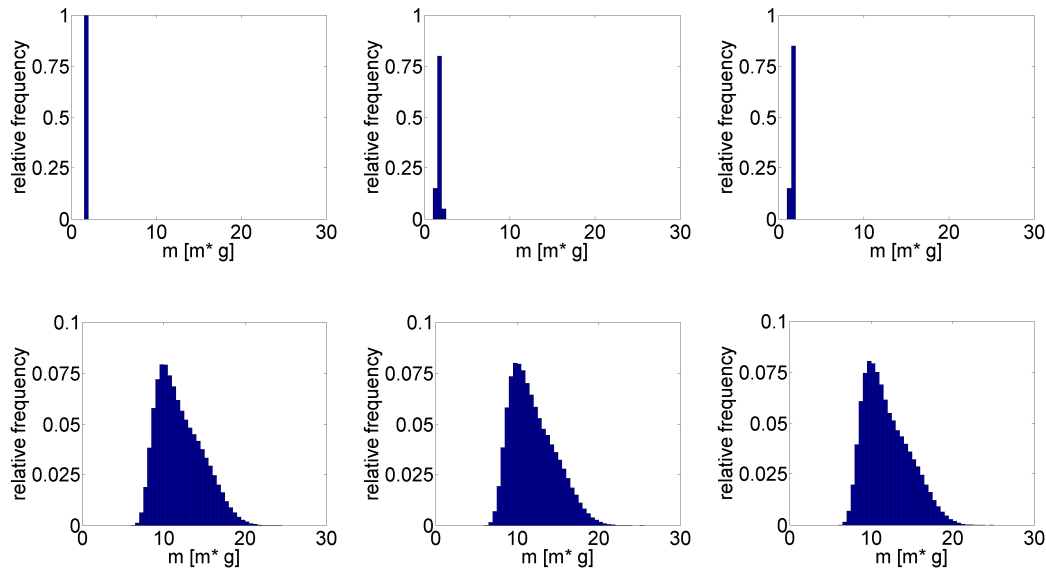
Figure 1 shows the effect of Δt on the population growth rate ($\mu_{population}$). Each symbol represents the mean of 100 simulations for a different time step and a different initial biomass distribution. For comparison, different time steps for the initial biomass distribution ($m_0 = 4.3$ m*) at 20 °C are shown ($\bar{\mu}_{individual} = 3.319 \cdot 10^{-1}$ [1/h]). Decreasing the time step leads to an increase in the population growth rate until reaching a constant value at small Δt 's. According to Baranyi (1998), the population growth rate is indeed determined by the fastest growing cells in the population. The initial biomass distribution has little impact on the outcome, which can be explained by the biomass dynamics (see next Section).

Individual biomass distribution

The biomass distribution at any time can be characterized by its mean and its shape. In the exponential growth phase, balanced growth occurs and the biomass distribution reaches a stable distribution. Regardless of the initial biomass distribution, the culture reaches the same distribution with a mean of 12.04 m* (Figure 2). This characteristic shape of the biomass distribution is also observed by Prats *et al.* (2008). Since the population reaches a steady state, independent of the initial biomass distribution, the populations seem to be in similar conditions during exponential growth, thereby exhibiting similar population dynamics. Hence, it is impossible to infer initial mass distributions from an exponentially growing population.

Conclusions

Model analysis checks for model performance, inconsistencies, possible needs for improvement, and defines the limits of the model. In the presented research, it leads to insights in the model (effect of time resolution) and the system modeled (population versus individual dynamics regarding lag and biomass). Time resolution is clearly an aspect that can not be ignored in individual-based modeling, as it has an impact on output values. Decreasing the time step leads to more accurate values for the population growth rate, regardless of the initial biomass distribution. Large time steps will reduce the simulation time and computational load, but result in erroneous output values.



(a) $m_0 = 1.7 \text{ m}^*$ (b) $m_0 \in \text{Normal}(1.7, 0.17) \text{ m}^*$ (c) $m_0 \in \text{Uniform}(1.4, 2) \text{ m}^*$
 Figure 2: Initial (top) and exponential (bottom) biomass distribution for (a) $m_0 = 1.7 \text{ m}^*$,
 (b) $m_0 \in \text{Normal}(1.7, 0.17) \text{ m}^*$, and (c) $m_0 \in \text{Uniform}(1.4, 2) \text{ m}^*$.

The simple IbM is able to reproduce commonly observed microbial behavior. For example, the mean individual generation time exceeds population lag time. Regardless of the initial biomass distribution, the biomass distribution reaches a common stable state during exponential growth.

Acknowledgements

Research is conducted utilising high performance computational resources provided by the Katholieke Universiteit Leuven, <http://ludat.kuleuven.be/hpc/>. Work supported in part by Projects OT/03/30 and EF/05/006 (Center-of-Excellence Optimization in Engineering) of the Research Council of the Katholieke Universiteit Leuven, and by the Belgian Program on Interuniversity Poles of Attraction, initiated by the Belgian Federal Science Policy Office. K. Bernaerts is a Postdoctoral Fellow with the Fund for Scientific Research Flanders (FWO-Vlaanderen). The scientific responsibility is assumed by its authors.

References

- Baranyi, J. (1998) Comparison of stochastic and deterministic concepts of bacterial lag. *Journal of Theoretical Biology* 192, 403-408.
- Baranyi, J., and Pin, C. (2001) A parallel study on bacterial growth and inactivation. *Journal of Theoretical Biology* 210, 327-336.
- Bernaerts, K., Servaes, R.D., Kooyman, S., Versyck, K.J., and Van Impe, J.F. (2002) Optimal temperature input design for estimation of the Square Root model parameters: parameter accuracy and model validity restrictions. *International Journal of Food Microbiology* 73, 145-157.
- Dens, E.J., Bernaerts, K., Standaert, A.R., and Van Impe, J.F. (2005a) Cell division theory and individual-based modeling of microbial lag, Part I. The theory of cell division. *International Journal of Food Microbiology* 101, 303-318.
- Dens, E.J., Bernaerts, K., Standaert, A.R., Kreft, J.-U., and Van Impe, J.F. (2005b) Cell division theory and individual-based modeling of microbial lag, Part II. Modeling lag phenomena induced by temperature shifts. *International Journal of Food Microbiology* 101, 319-332.
- Donachie, W.D. (1968) Relationship between cell size and time of initiation of DNA replication. *Nature* 219, 1077-1079.
- Ferrer, J., Prats, C., López, D., and Vives-Rego, J. (2009) Individual-based modelling: an essential tool for microbiology. *Journal of Biophysics* 34, 19-37.
- Kreft, J.-U., Booth, G., and Wimpenny, J.W.T. (1998) BacSim, a simulator for individual-based modelling of bacterial colony growth. *Microbiology* 144, 3275-3287.
- Prats, C., Giró, A., Ferrer, J., López, D., and Vives-Rego, J. (2008) Analysis and IbM simulation of the stages in bacterial lag phase: basis for an updated definition. *Journal of Theoretical Biology* 252, 56-68.

A hierarchical Bayesian model to estimate the growth of *Listeria monocytogenes* and natural flora in minced tuna

S. Koseki¹, Y. Takizawa², H. Takahashi², and B. Kimura²

¹National Food Research Institute, 2-1-12, Kannondai, Tsukuba, Ibaraki 305-8642, Japan (koseki@affrc.go.jp)

² Department of Food Science and Technology, Tokyo University of Marine Science and Technology, 4-5-7, Konan, Minato-ku, Tokyo 108-8477, Japan (kimubo@kaiyodai.ac.jp)

Abstract

A Bayesian state space model examining the growth of *Listeria monocytogenes* in minced tuna was developed. A total of 28 growth curves of *L. monocytogenes* ranging from 2 to 30°C with different initial competitive natural flora levels were used to develop the model. The influence of competitive natural flora on the growth of *L. monocytogenes* was also modelled. The developed model described the effect of time, temperature, competitive flora, and maximum population density of each bacterial strain on the growth of *L. monocytogenes* and natural flora. The results obtained from the developed model were used to simulate the simultaneous growth of *L. monocytogenes* and natural flora in minced tuna with variability and uncertainty.

Key words: competitive flora; time series model; hierarchical Bayesian state space model

Introduction

Sushi is a widely known Japanese traditional food that essentially comprises raw fish. Tuna is one of the most popular sushi ingredients, with minced tuna also being a popular sushi ingredient. It has recently been reported that raw seafood is contaminated with *Listeria monocytogenes* (Handa, et al., 2005), and that minced tuna in particular was contaminated with *L. monocytogenes* in 14.3% of Japanese retail stores. Consequently, the consumption of raw minced tuna is fraught with the potential risk of food poisoning by listeriosis. However, the behaviour of *L. monocytogenes* in minced tuna has not been investigated in detail. In this study, we investigated the responses of *L. monocytogenes* and the interactions with natural flora in minced tuna.

Numerous bacterial growth models have been developed in the area of predictive microbiology. Conventional deterministic growth models based on kinetics are problematic given the difficulty in separating model variability and uncertainty. We attempted to develop an alternative predictive model based on a time series modelling technique commonly applied in ecological modelling. Appropriate treatment of uncertainty can be especially important for time series data, since process errors propagate forward with processing, unlike the case with observation errors (Clark, 2007). Among the most general and flexible model alternatives is the Bayesian state space model. In the present study, we aimed to develop a Bayesian state space model for the prediction of *L. monocytogenes* growth in minced tuna with the simultaneous growth of natural flora.

Materials and methods

Preparation of Microorganisms and sample

Minced tuna (pH = 6.28, aw = 0.986) was purchased from a local wholesale market and stored at -40°C until use. Dominant natural micro flora of minced tuna were isolated and identified by examination of 16S rRNA as follows: *Serratia grimesii*, *Kurthia zopfii*, *Acinetobacter* sp., and *Pantoea agglomerans*. These four bacterial strains were cultured individually and then combined to give approximately equal populations of each strain for use as an inoculum comprising a natural flora mixture. *Listeria monocytogenes* (29-10-1, serotype 1/2b), which was isolated from seafood and stocked in the laboratory in the Department of Food Science and Technology, Tokyo University of Marine Science and Technology, was used in this study. This strain shows the fastest growth rate among stock culture collection

isolated from seafood in the laboratory. *L. monocytogenes* was inoculated into minced tuna sample (10 g) to give an inoculum level of 10^2 CFU/g. The natural flora mixture was also inoculated into minced tuna to give three different levels (10^2 , 10^4 , and 10^6 CFU/g). The inoculated tuna samples (10 g) were aseptically divided into 400-ml stomacher bags at each sampling interval, and stored at 2, 5, 10, 15, 20, 25, and 30°C until they reached the stationary phase. Sampling was generally carried out at 3-h intervals for the 15, 20, 25 and 30°C experiments, although longer sampling intervals were used for the 2, 5 and 10°C experiments.

Enumeration of *L. monocytogenes* and total natural flora

Each 10-g sample of tuna was combined with 90 ml of 0.9% saline in a 400-ml stomacher bag and pummelled for 2 min in the stomacher. The sample was then serially diluted using 0.9% saline and plated onto PALCAM Listeria selective agar (Merck) for *L. monocytogenes* and tripticase soy agar (Merck) supplemented with 1.5% sodium chloride for total natural flora using a spiral plating system. Plates were then incubated at 30°C for 48 h.

Model development

A Bayesian state space model was examined in this study. State space models comprise a parameter model, process model, and data model (Fig. 1). As an observation model, we assumed that the observed bacterial counts data follows a log normal distribution.

$$\begin{aligned} \log.NF &\sim N(xNF, \tau^2) \\ \log.LM &\sim N(xLM, \tau^2) \end{aligned}$$

where $\log.NF$ and xNF represent the observed cell counts data of natural flora (log CFU/g) and the unobservable real population density of natural flora (log CFU/g) in the latent process model, respectively. In the same way, $\log.LM$ and xLM were also specified. τ^2 represents the variance of the data. In the process model, xNF and xLM were also assumed to follow a normal distribution as follows:

$$\begin{aligned} xNF &\sim N(\text{mean}.xNF, \sigma^2) \\ xLM &\sim N(\text{mean}.xLM, \sigma^2) \end{aligned}$$

where $\text{mean}.xNF$ and $\text{mean}.xLM$ represent the mean value of natural flora and *L. monocytogenes* in the process model, respectively. σ^2 represents the variance of the latent variables in the process model. The mean value of $xAPC$ and xLM were described as a function of temperature and the effect of bacterial number on each other as follows:

$$\begin{aligned} \text{mean}.xNF[t] = xNF[t-1] + \text{Delta.time}[t] \times & \left(pN[1] + pN[2] \times \text{Temp}[t] + pN[3] \times \text{Temp}[t]^2 \right) \\ & \times \left(1 - \frac{(xNF[t-1] + pN[4] \times xLM[t-1])}{xNF.\text{max}} \right) \end{aligned} \quad (1)$$

$$\begin{aligned} \text{mean}.xLM[t] = xLM[t-1] + \text{Delta.time}[t] \times & \left(pL[1] + pL[2] \times \text{Temp}[t] + pL[3] \times \text{Temp}[t]^2 \right) \\ & \times \left(1 - \frac{(xLM[t-1] + pL[4] \times xNF[t-1])}{xLM.\text{max}} \right) \end{aligned} \quad (2)$$

where t and Temp represent time (h) and temperature (°C), respectively, and $pN[i]$ and $pL[i]$ were parameters to be estimated. Since we do not have prior knowledge regarding the

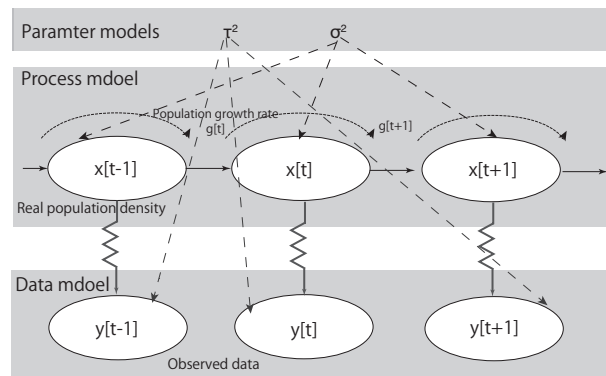


Figure 1. A diagram of the state space model of a random walk where observations y are drawn from the underlying process x .

parameters to be estimated, the distribution for each parameter of fixed effects ($pN[i]$ and $pL[i]$) is assumed as a non-informative prior distribution. All functional forms were adopted with a Gaussian distribution of mean zero and a variance of 10^4 . Hyper prior distribution for each variance parameter (τ^2 and σ^2) comprised a non-informative inverse Gamma distribution of mean one and a variance of 10^2 .

Computing posterior distribution

In Bayesian inference, all parameters (including missing data) are generated by prior distributions (Clark, 2007). To obtain the parameter values, Gibbs sampling methods driven by the Markov Chain Monte Carlo (MCMC) calculation generate sample sets from the joint posterior distribution of all parameters. Sampling from the posterior distributions of the parameters using MCMC methods was performed using WinBUGS 1.4.3 in the R2WinBUGS package (Sturtz et al. 2005) in statistical language R 2.8.1. Posterior samples were obtained from three independent Markov chains in which 50,000 values were sampled with a 10 iteration interval after a burn-in of 20,000 iterations. The convergence of the Markov chains was evaluated using \hat{R} (Gelman et al. 2003) for each parameter by comparing the variance within each chain and among chains.

Results and discussion

Growth of *L. monocytogenes* and natural flora

Representative data on the growth of *L. monocytogenes* and natural flora in minced tuna at 5°C is shown in Fig. 2. As the competitive initial natural flora increased in number, the maximum population density of *L. monocytogenes* was suppressed under all temperature conditions examined. In contrast, the number of competitive natural flora had no affect on the growth rate of *L. monocytogenes*. No interaction between the number of natural flora and the number of *L. monocytogenes* was evident except for the maximum population density. In most cases, when the natural flora reached maximum product levels, the product would become spoiled. Prediction of the number of natural flora and *L. monocytogenes* in the product up to the point where maximum population density is reached is therefore important in preventing food poisoning by listeriosis.

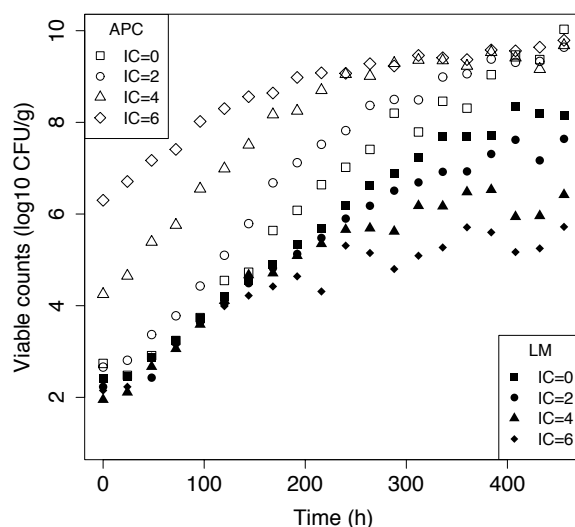


Figure 2. Changes in number of natural flora (APC) and *L. monocytogenes* in minced tuna with initial different competitive natural flora during 5°C storage

Model convergence

The estimates and variance calculated by MCMC in the hierarchical Bayesian model are listed in Table 1. All estimates for parameters were close enough to unity that the Markov chains for all parameters had sufficiently converged. The $pN[4]$ and $pL[4]$ parameters are those that influence the number of *L. monocytogenes* and natural flora, respectively. The inference of posterior distribution did not clearly affect each strain, since the 95% credible interval of these parameters included zero.

Growth simulation of natural flora and *L. monocytogenes*

Predictive simulation under fluctuating temperature condition was conducted using Eq. (1) for natural flora and Eq. (2) for *L. monocytogenes* employing the estimated parameters shown in Table 1. The result of simulation for growth under fluctuation temperature is shown in Fig. 3.

Table 1. Estimated posterior distributions of parameters

| Parameter | Mean | Credible interval | | | \hat{R} |
|-----------|--------|-------------------|--------|--------|-----------|
| | | 2.5% | 50.0% | 97.5% | |
| pNF[1] | 0.023 | 0.004 | 0.022 | 0.042 | 1.001 |
| pNF[2] | 0.010 | 0.003 | 0.010 | 0.017 | 1.001 |
| pNF[3] | 0.001 | 0.001 | 0.001 | 0.001 | 1.001 |
| pNF[4] | -0.065 | -0.132 | -0.064 | -0.003 | 1.001 |
| pLM[1] | 0.006 | -0.006 | 0.006 | 0.019 | 1.002 |
| pLM[2] | 0.007 | 0.001 | 0.007 | 0.012 | 1.004 |
| pLM[3] | 0.001 | 0.001 | 0.001 | 0.001 | 1.004 |
| pLM[4] | -0.019 | -0.090 | -0.018 | 0.043 | 1.001 |
| τ | 0.129 | 0.279 | 0.153 | 0.068 | 1.013 |
| σ | 0.766 | 0.828 | 0.770 | 0.702 | 1.002 |

Both the number of natural flora and *L. monocytogenes* were successfully simulated, representing a good fit to the observed data. The root mean square error (RMSE) of the simulation for *L. monocytogenes* and natural flora were 0.37 and 0.45, respectively. Since the developed model in the present study did not take into account of the lag time, the discrepancy between observed data and the prediction tend to be large in the early stage during the storage. Nevertheless, the accuracy of the model throughout the storage periods showed generally good agreement. Appropriate modification of the model to describe the lag time would further enhance the accuracy of the prediction. Furthermore, since the parameters were estimated as probabilistic variables, the simulated growth could estimate the probability of its prediction. Although this time series approach has only just begun to be used in investigations pertaining to food microbiology, the simplicity and flexibility of this approach should prove a useful alternative in procedures concerning risk assessment.

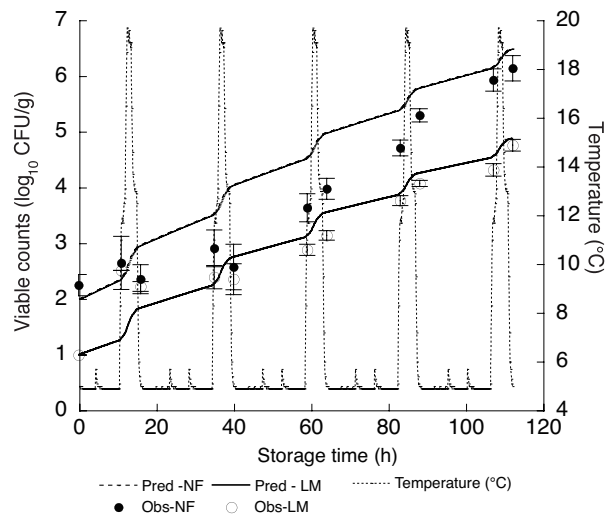


Figure 3. Simulation of the simultaneous growth of natural flora (●) and *L. monocytogenes* (○) in minced tuna during storage under fluctuating temperature. Solid and dashed lines represent the prediction by using the median of estimated parameters of the developed model for *L. monocytogenes* and natural flora, respectively.

Acknowledgements

This study was supported by Grants-in-Aid from the Food Safety Commission, Japan. (No. 0705). The authors wish to thank Takuya Kubo of Hokkaido University for the model development and computation.

References

- Clark, J. S. (2007) Models for Ecological Data: An Introduction. Princeton University Press, Princeton, New Jersey, USA.
- Gelman, A., Carlin, J.B., Stern, H.S. & Rubin, D.B. (2003) Bayesian Data Analysis (2nd ed.). Chapman & Hall/CRC.
- Handa, S., Kimura, B., Takahashi, H., Koda, T., Hisa, K., and Fujii, T. (2005) Incidence of *Listeria monocytogenes* in Raw Seafood Products in Japanese Retail Stores. *J. Food Prot.*, 68 (2), 411-415.
- Sturtz, S., Ligges, U. & Gelman, A. 2005. R2WinBUGS: A Package for Running WinBUGS from R. *Journal of Statistical Software* 12:1-16.

Identification of complex microbiological dynamic systems by nonlinear filtering

J.P. Gauchi¹, C. Bidot¹, J.C. Augustin², J.P. Vila³

¹ Unité de Mathématiques et Informatique Appliquées (UR341), INRA, Domaine de Vilvert, 78352 Jouy-en-Josas, France (Jean-Pierre.Gauchi@jouy.inra.fr, Caroline.Bidot@jouy.inra.fr)

² Laboratoire ENVA/Unité Microbiologie des Aliments – Sécurité et Qualité, 7, avenue du Général de Gaulle, 94704 Maisons-Alfort, France (jcaugustin@vet-alfort.fr)

³ UMR Analyse des Systèmes et Biométrie, INRA/SupAgro, 2, Place P. Viala, 34060 Montpellier, France (Vila@supagro.inra.fr)

Abstract

In this paper, we consider microbiological dynamic systems encountered in food processing and conservation (e.g., *Listeria monocytogenes*). In order to predict the evolution of bacteria populations to improve our microbiological knowledge or to meet other objectives such as risk analysis, the modeling and identification of such stochastic dynamic systems have to first be subjected to adapted statistical approaches. However, the specificities of such systems (nonlinear state space systems) in which the variables of interest are only indirectly observed through a complex process of sampling, dilution series and counting, make it difficult to use classical methods such as least squares or maximum likelihood. It is then necessary to resort to specialized approaches such as sequential estimation techniques. This paper describes the first results of such a promising approach that involves a new particular filter applied to simulated microbial dynamics.

Keywords

Nonlinear filters, convolution kernels, particle filters, predictive modeling, microbiology.

Introduction

The complexity of food-type microbiological systems is related to both structure (ecosystems involving several bacterial species in interaction) and to function. The latter is the result of the distribution of their dynamics according to at least three hierarchical levels that we can approximately represent here by: (a) an external level, only accessible to measurements (counts taken in culture medium after sampling and dilution series); (b) an intermediary level, corresponding to the dynamics of bacterial increases or decreases, strictly speaking, not directly measurable in the food substrate considered but normally capable of being modeled in the form of primary stochastic models; (c) a deeper level, characterized by kinetic variables that determine the preceding dynamics and that are themselves the result of the interactions of various biotic and abiotic factors (media conditions such as pH, temperature, water activity, etc.). These kinetic elements can sometimes be modeled in the form of secondary stochastic models.

These functional characteristics make all predictive modeling and identification of these bacterial dynamics particularly difficult if not impossible when using classical approaches (e.g., nonlinear least squares). Recent research (Rossi and Vila, 2003; 2005; 2006) made it possible to provide a relevant methodological response to the two problems of parametric identification of these systems and to the estimation of predicted probability densities of the evolution of bacterial concentrations in substrates of interest. This research is based on the implementation of a new nonlinear particular filtering technique using a convolution kernel approach.

The aim of this presentation is to show the results obtained by applying this new type of filtering system with two actual microbiological dynamic systems (the second one will be discussed at the conference), of great interest to the food microbiology community, using a new user-friendly procedure written in Matlab (Bidot et al., 2009; Vila et al., 2009). Rather

than go into the theoretical basis of the method, published in Rossi and Vila (2003; 2005; 2006), here, we will only provide some elements in the following section.

Method

Statistical samplings

The current data acquisition procedures are sequential: a sample is taken from a primary solution tube, diluted in cascade (Fisher dilution series), and then spread over Petri dishes. After a period of time, the bacterial units that form colonies (CFU) are counted, assuming that each colony corresponds to a single deposited bacterium. The current practice in microbiology at this time is to deduce the number of bacteria present in an initial solution of the primary tube by simple extrapolation using successive dilution factors and ignoring errors due to sampling (at the time the sample is removed), pipetting, dilution and counts on the Petri dishes. This highly approximate determinist estimation leaves room for much improvement. Using hypotheses involving spatial distributions to be validated experimentally (Poisson distributions, aggregative distributions) and hypotheses involving handling errors, we carried out probabilistic characterizations of these counts (depending on the initial numbers), taking estimates of the variances of all successive errors into account.

Conditional density estimates of countings

The dynamic systems considered here are similar to nonlinear space state systems, written as follows:

$$\begin{aligned}x_{t+1} &= f_t(x_{t+1}, \theta, \varepsilon_t) \\ y_{t+1} &= \mathcal{L}(\cdot | x_{t+1}, \theta)\end{aligned}$$

where x_{t+1} is the real vector of dimension d of state variables, f_t is a known function, y_{t+1} is the real vector of dimension q of observation variables, θ is a vector of unknown and constant parameters, ε_t is a white noise vector and \mathcal{L} is the probability distribution of y_{t+1} . In the convolution filtering approach, which is ours, we introduce the additional state equation, $\theta_{t+1} = \theta_t$, to link the estimation of conditional densities of parameters θ with those of variables x_t . On the basis of *a priori* densities at $t = 0$ for the variable vector and for the parameter vector, these estimations at time t are calculated using the formulas given by Rossi and Vila (2005; 2006). This is a non-parametric approach where the particles are generated from densities based on Parzen-Rosenblatt kernels. We will refer to Rossi and Vila (2005; 2006) for the equations and more details about this filtering algorithm and its convergence conditions.

Results and discussion

The Baranyi-Roberts (BR) model

The very well-known equation of the BR model (Baranyi and Roberts, 1994; 1995) under a discretized autoregressive form that will be our state equation is:

$$N_{t+1} = \delta N_0 \exp(\mu_{max} A_t) (1/B_t) (\mu_{max} (dA_t/dt) - (dB_t/dt) (1/B_t)) + N_t + \phi_t$$

where:

$$\begin{aligned}A_t &= t + (1/\mu_{max}) \ln(\exp(-\mu_{max} t) + \exp(\mu_{max} \lambda) - \exp(-\mu_{max} t - \mu_{max} \lambda)) \\ B_t &= 1 + (\exp(\mu_{max} A_t) - 1)/(N_{max} / N_0)\end{aligned}$$

where:

- N_t is the state variable, i.e., the bacteria number in the medium at time t ,
- N_0 is the bacteria number in the medium at the initial time t_0 ; it is a parameter to be estimated,
- N_{max} is the maximum bacteria number; it is a parameter to be estimated,
- λ is the lag time before growth; it is a parameter to be estimated,

- μ_{max} is the maximum growth rate; it is a parameter to be estimated,
- ϕ_t is an error term, a centered Poisson random $\mathcal{P}(N_t c) - (N_t c)$, where c is a fixed real constant or a parameter to be estimated and $N_t c$ the parameter of the Poisson distribution,
- δ is the discretization step.

In this case, the observation model y_{t+1} corresponds to the distribution based on the sampling-dilution process (typically Poisson distributions) and CFU counts on the Petri dishes, referred to as $\mathcal{L}(.|x_{t+1}, \theta_y)$, where θ_y is a sub-vector of θ . This distribution cannot be characterized analytically, but it can be simulated, a requirement for putting the filter into practice.

Protocol

The CFU counting data were obtained using the following protocol:

- ten sampling times = 0, 72, 120, 168, 240, 264, 288, 336, 408, 504 (hours), with three samplings at each sampling time,
- five different dilution factors: the dilution factor is equal to 1 on the 0-120 time range, equal to 0.1 at the time 168, equal to 10^{-3} on the 240-264 time range, equal to 10^{-5} on the 264-408 time range, and equal to 10^{-5} at the time 504,
- the postulated parameter intervals were: $[0.01 ; 2]$ for μ_{max} , $[20 ; 60]$ for λ , $[100 ; 400]$ for N_0 , and $[10^7 ; 10^9]$ for N_{max} ,
- discretization step $\delta = 24$ (hours),
- particle number = 10^6 .

With this protocol, we obtained (Fig. 1) the evolutions of the parameter estimations, as well as their approximated confidence intervals for the considered number of particles.

The final estimations for the four parameters, taking a computing time of about 5 minutes into account, are: $N_0 = 280$, $N_{max} = 3.44584 \times 10^8$, $\lambda = 36$, and $\mu_{max} = 0.063$.

We have shown here the application of our method to a model that is very well known to the microbiology community, but since there are only four parameters in this model, this estimation problem is too easy to fully illustrate the power of the method that we propose. We do not have adequate space here to show the results of a model with seven parameters, which would be the Baranyi model in which we would have replaced the parameter μ_{max} by its expression given by the cardinal secondary model of Rosso *et al.* (1993). Calculations were, however, made and we will present the graphs at the conference.

The advantages of the approach that we propose are highly significant and multiple. Three of them stand out in particular:

- all of the variability sources are taken into account to estimate the parameters,
- we can **directly** obtain these estimations without using the estimation of the μ_{max} of the primary model,
- it is not necessary to know the initial values for the parameters since the range of variations (even very large ones) are sufficient.

Moreover, it can be observed that the estimation in two steps by nonlinear regression for models with many parameters does not often work because of a poor choice of initial values.

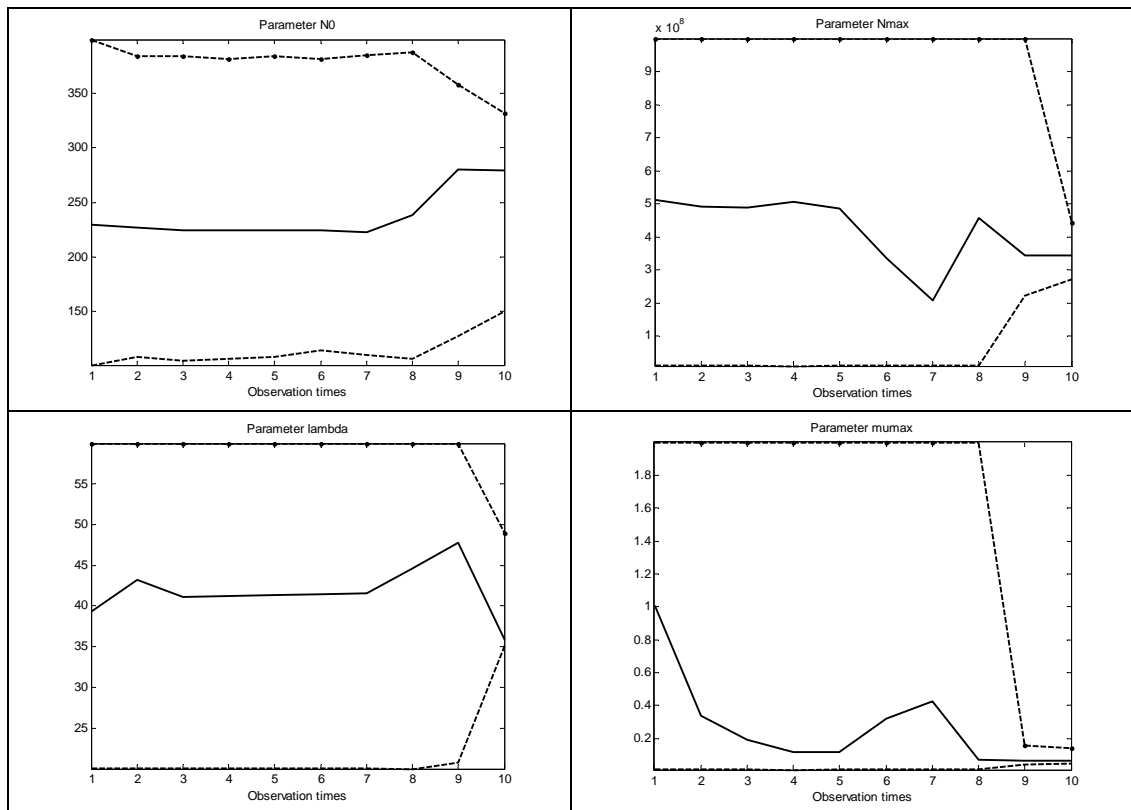


Figure 1: Evolution of the four-parameter estimates for 10^6 particles. The dashed lines represent the lower and upper bounds of a 95% confidence interval, while the central line represents the parameter estimation.

Conclusions

We think that the method described here can be used to estimate the parameters for very complicated models with many parameters, models often in demand in the food microbiology community (Augustin *et al.*, 2005). Moreover, this method is currently being generalized to resolve the following problems: comparison and selection of dynamic models by Bayes factors estimated by filtering (Vila and Saley, 2009), rupture detection in dynamic models or, on the long term, perhaps even the regulation and control (for example, by means of temperature) of microbiological systems.

References

- Augustin J.C., Zuliani V., Cornu M., Guillier L. (2005) Growth rate and growth probability of *Listeria monocytogenes* in dairy, meat and seafood products in suboptimal conditions. *Journal of Applied Microbiology*, 99, 1019-1042.
- Baranyi J. and Roberts T.A. (1994) A dynamic approach to predicting bacterial growth in food. *International Journal of Food Microbiology*, 23, 277-294.
- Baranyi J., Roberts, T.A. (1995) Mathematics of predictive food microbiology. *International Journal of Food Microbiology*, 26, 199-218.
- Bidot C., Gauchi J.P., Vila J.P. (2009) Programmation Matlab du filtrage non linéaire par convolution de particules pour l'identification et l'estimation d'un système dynamique microbiologique. *Rapport technique INRA/Jouy-en-Josas/MIA/ n°2009-1*.
- Rossi V. and Vila J.P. (2003) Filtrage non linéaire en temps discret par convolution de particules. *Actes des XXXVèmes Journées de Statistique*, 823-826.
- Rossi V. and Vila J.P. (2005) Approche non paramétrique du filtrage de système non linéaire à temps discret et à paramètres inconnus. *C.R. Acad. Sci. Paris. Ser I* 340, 759-764.
- Rossi V. and Vila J.P. (2006) Nonlinear filtering in discrete time : a particle convolution approach. *Inst. Stat. Univ. Paris*, 3, 71-102.
- Rosso L., Lobry J.R., Flandrois J.P. (1993) An unexpected correlation between cardinal temperatures of microbial growth highlighted by a new model. *Journal of Theoretical Biology*, 162, 447-463.
- Vila J.P., Saley I. (2009) Bayes Factor estimation for nonlinear dynamic state space models. *C.R. Acad. Sci., Paris, Ser. I* 347, 429-434.
- Vila J.P., Gauchi J.P., Bidot C. (2009) Identification de systèmes dynamiques microbiologiques complexes par filtrage non linéaire. *Actes des 41èmes Journées de Statistique*, Bordeaux, May 25-29, 2009.

Modelling the influence of free fatty acids on heat resistance of *Bacillus cereus* spores

Mvou Lekogo B.*¹, Coroller L.¹, Mafart P.¹, Leguerinel I.¹,

¹ Université Européenne de Bretagne, France - Université de Brest, EA3882 Laboratoire Universitaire de Biodiversité et Ecologie Microbienne, IFR148 ScInBioS, UMT 08.3 PHYST'Opt, 6 rue de l'Université, 29334 Quimper, France. (mvou@univ-brest.fr)

Introduction

Beyond temperature, pH, aw or salts are able to modify the heat resistance of bacterial spores. The influence of these factors on heat treatment or recovery efficiency was modelled (Leguerinel et al., 2005). The models describing the influence of other factors on apparent heat resistance of spore are scarce. It has been shown that free fatty acids can affect not heated pathogenic bacteria, inhibit germination and growth of micro-organisms (Ababouch et al., 1994, Lee et al., 2002). The reduction of heat resistance of spore by free fatty acids during heat treatment was described by Tremoulet et al., 2002, but these effects on recovered surviving cells were never quantified. The aims of this work was to improve the knowledge of the recovery impact of FFA and to quantify its effects on heat resistance of spores modulated by unsaturation level and pH.

Material and methods

The study was carried out with *Bacillus cereus* NTCC 11145 spores.

Heat treatment was performed in capillary tubes of 200 µl filled with 100 µl of sample (heating media), sealed, and submitted to a thermal treatment in a thermostated glycerol bath for different heating times. The heat treatment was stopped by cooling capillary tubes in water/ice bath. The viable spores were counted by duplicate plating in recovery media incubated at 37°C

Heating media used was nutrient broth and recovery media was nutrient broth and bacteriological agar with, for both media, different concentrations of free fatty acid.

Dilutions of FFA in heating and recovery media were obtained by mixing and microsonication with 0.1% TweenTM80 as dispersant. After sterilization by autoclaving at 110°C for 45 minutes as described by Marounek et al.2003.

To study the impact of insaturation number in chain of FFA added in recovery media stearic acid C18:0, oleic acid C18:1, linoleic acid C18:2 and linolenic acid C18:3 were used

To quantify of the interaction between pH and oleic acid effects in recovery media, pH of recovery media were adjusted from pH 5.5 to pH7 by addition of HCl or NaOH .

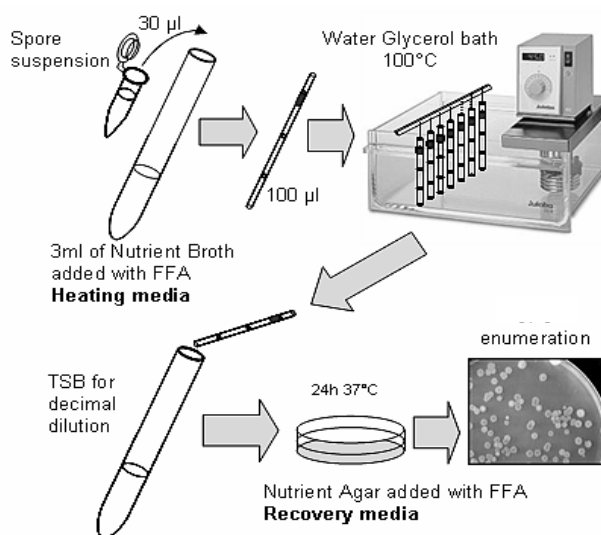


Figure 1 : schema describing the heat treatment and the recovery of *Bacillus cereus* NTCC 11145 spores

Results

Bacterial survival curves show a log linear relationship between heating time and unite forming colonies for all tested conditions. Thus the classical D values were used to quantify the bacterial heat resistance. The presence of C18 free fatty acids (stearic, oleic, linoleic or

linolenic) in the heating medium did not present significant influence on the heat resistance of spores (Fig 1 and table 2).

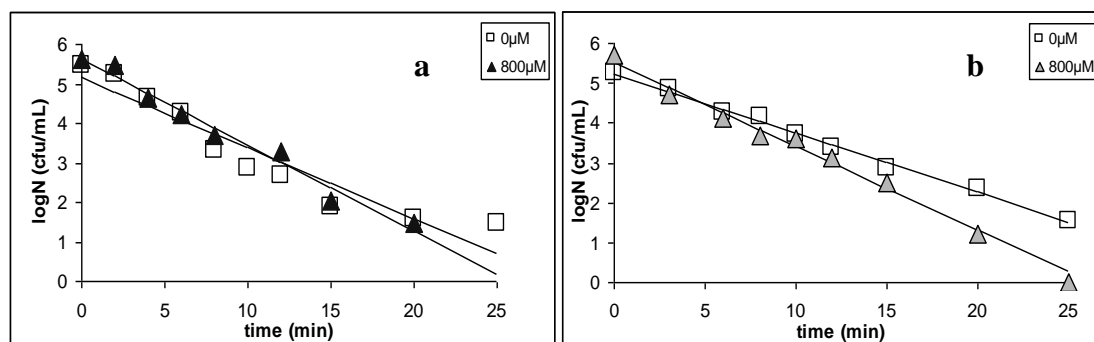


Figure 2: $\log N=f(t)$ at 100°C (\square without FFA, Δ with 800µM of stearic (a) , oleic (b), acids respectively **in heating media** for *B. cereus* NTCC 11145.

The variation of $D_{100^\circ\text{C}}$ value in presence of 800µM of C18 free fatty acids: stearic, oleic, linoleic and linolenic is presented Table2. The presence of free fatty acids in heating media present only slight effect on the apparent heat resistance of *B. cereus* spores.

Table2: D values at 100°C without FFA and with 800µM of stearic, oleic, linoleic and linolenic acids respectively in heating media for *B. cereus* NTCC 11145.

| | C18:0 | C18:1 | C18:2 | C18:3 |
|-------|-----------|-----------|-----------|-----------|
| 0µM | 5.61±1.49 | 6.74±0.41 | 5.48±1.40 | 6.33±0.68 |
| 800µM | 4.61±0.69 | 5.00±0.89 | 5.63±0.41 | 3.46±0.78 |

Oppositely, the presence of these free fatty acids in the recovery media clearly reduced the apparent heat resistance (Fig 3). No revivification was observed at 600µM with C18:2 or 400µM of C18:3 for unsaturation level.

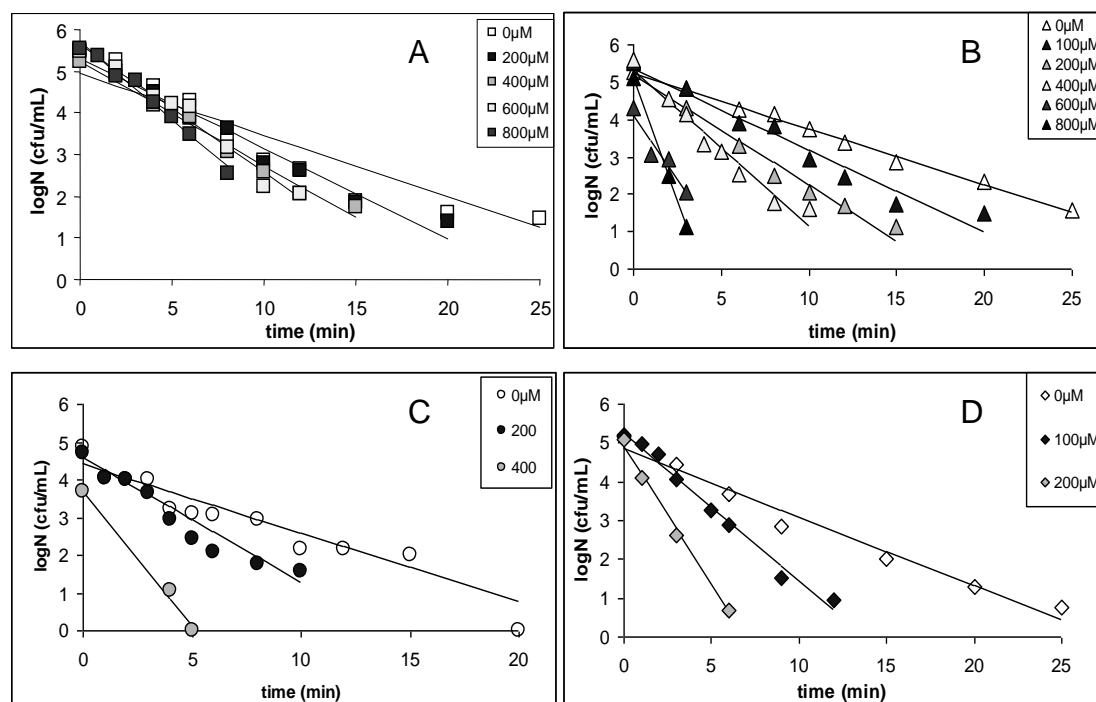


Figure 3: $\log N=f(t)$ at 100°C. with different concentrations of stearic (a) , oleic (b) , linoleic (c) and linolenic (d) acids respectively **in recovery media** for *B. cereus* NTCC 11145.

A linear relationship was observed between $\log D$ values and FFA concentration. The influence of acid concentration varies with the type of used fatty acid or pH tested with oleic acid. The effect of FFA increased proportionally to the degree of unsaturation of the carbon chain (Fig 4).

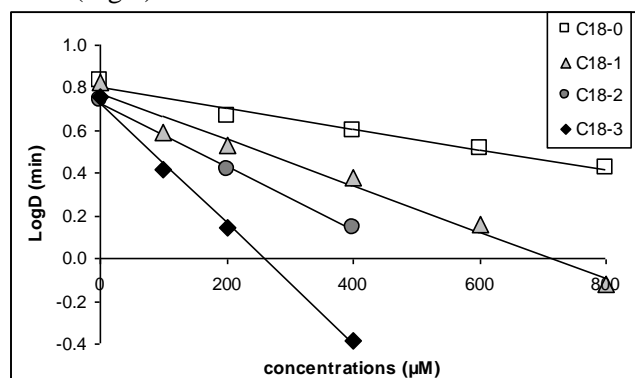


Figure 4: logarithm of $D_{100^{\circ}\text{C}}$ versus concentration in recovery media for different FFA with 18C chain length presenting different unsaturation numbers

A Bigelow type secondary model was then developed with " z'_{FFA} " value (μM) corresponds to FFA supplement which leads to a ten fold reduction of D value. This parameter quantifies the influences of FFA concentration in the recovery media on the apparent D value :

$$\log D = \log D^* - \frac{[\text{acid}]}{z'_{\text{FFA}}}$$

The z' value for the different fatty acids were 2084 μM for stearic acid, 924 μM for oleic acid, 675 μM for linoleic acid and 356 μM for linolenic acid. Thus an increase of unsaturated bound number of FFA free decrease the apparent bacterial heat resistance.

A complementary study was performed to evaluate the interaction between pH and the addition of oleic acid in recovery media. For the different pH studied, " z " values were calculated and presented Table 3. An increase of pH from 5.5 to 7 in recovery media did not affect the influence of oleic acid on spore heat resistance.

Table 3 z'_{FFA} values as function of pH of recovery media

| pH | 5.5 | 6 | 6.5 | 7 |
|-------------------|--------------------|--------------------|--------------------|-------------------|
| z'_{FFA} | 1015 μM | 1773 μM | 1215 μM | 911 μM |

Conclusion

In this study, free fatty acids had shown more pronounced effects in recovery media than in heat treatment. The influence of free fatty acid concentration in recovery media was described by a simple Bigelow like model using a " z " parameter which quantifies the influence of the free fatty acid to the bacterial heat resistance. Moreover, the apparent bacterial heat resistance decreasing as function of the unsaturation level of free fatty acid. The pH of recovery media does not affect this influence of free fatty acid. By taking in consideration the free fatty acid in food composition, the developed model and the associated parameters values can be used to optimize and reduce heat treatment in canned food industry.

References

- Ababouch, H. L., F. Bouquartacha, and F. F. Busta. 1994. Inhibition of *Bacillus cereus* spores and vegetative cells by fatty acids and glyceryl monododecanoate. *Food Microbiology*. 11, 327-336.
- Lee, J.-Y., Y.-S. Kim, and D.-H. Shin. 2002. Antimicrobial synergistic effect of linolenic acid and monoglyceride against *Bacillus cereus* and *Staphylococcus aureus*. *Journal of Food Chemistry* 50: 2193-2199.
- Leguerinel I., Spegagne I., Couvert O., S. Gaillard, P. Mafart. 2005. Validation of an overall model describing the effect on three environmental factors on the apparent D -value of *Bacillus cereus* spores. *International Journal of Food Microbiology*. 100, 223-229.
- Marounek M., E. Skřivanova, and V. Rada. (2003). Susceptibility of *Escherichia coli* to C2-C18 fatty acids. *Folia Microbiology*. 48, 731-735.
- Tremoulet, F., P. Rabier, and G. Gas. 2002. Inhibition of *Bacillus stearothermophilus* spores in liquid medium by free fatty acids with and without heat: possible mechanism for the microbiological stability of canned fat-duck liver. *Journal of Food Science*. 67, 1144-1148.

Modeling microbial competition in foods. Application to the behaviour of *Listeria monocytogenes* and lactic acid flora in diced bacon

M. Cornu¹, E. Billoir², H. Bergis¹, A. Beaufort¹, V. Zuliani³

¹ Lerqap, Afssa, 23 av. du Gal de Gaulle, F-94706 Maisons-Alfort, France (m.simon-cornu@afssa.fr)

² INRA, UR341 Mathématiques et informatique appliquées, F-78350 Jouy en Josas, France

³ IFIP, institut de la filière porcine, Pôle Viandes Fraîches et Produits Transformés, 7 av. du Gal de Gaulle, F-94704 Maisons Alfort, France (veronique.zuliani@ifip.asso.fr)

Abstract

The current models developed in predictive microbiology to describe interactions between microflora in foods are reviewed, with a special focus on the Jameson-effect and Lotka-Volterra approaches. One case-study is further explored: modelling the sparse growth of *Listeria monocytogenes* in diced bacon along the shelf-life.

Keywords

Challenge testing, Maximal Population Density, competitive growth, pork meat product.

Introduction

One of the major advances of predictive microbiology since the end of the 1990s has been the increasing interest in the fate of the hazards (e.g. *Salmonella*, *L. monocytogenes*, *Escherichia coli*, *Staphylococcus aureus*...) *in situ*, i.e. in the food itself, instead of in culture media. This has been emphasized by the creation of databases, e.g. ComBase and Sym'Previus.

In this context, different approaches have been proposed to model microbial interactions between one pathogenic micro-organism of interest and a specific microflora, or a group, i.e. lactic acid bacteria (LAB), or even mesophilic aerobic flora. They are reviewed in this paper, with a special interest for their eligibility to be integrated into simple and robust predictive models. The discussion of these different approaches is applied to the case-study of *L. monocytogenes* and LAB in diced bacon.

Jameson effect models

In the late 1990's and early 2000's, there were numerous observations that (i) many microbial interactions in foods are limited only to a reduction in the maximum population density, without any significant effect on the lag time and the growth rate [5; 6]), (ii) the minority population decelerates when the majority - or the total - population count reaches its maximum [14; 20; 33]. On this basis, Cornu [9] proposed a model relying on the hypothesis that decelerations of both populations would be simultaneous and would result from the competition for a common limiting resource. Ross *et al.* [37] proposed to call this phenomenon the Jameson effect, after Jameson [22] who had studied growth of *Salmonella* in an enrichment broth. To quote the fine comparison of Mellefont *et al.* [30], the Jameson effect "can be described as a race between species to use the resources of the environment to maximise their growth and population numbers. When those resources are depleted, the race is over, and the growth of each species in the population stops".

Since then, numerous papers have referred to the Jameson effect, concerning growth of:

- *Listeria spp.* in fishery products [2; 12; 15; 17; 29], in meat products [7; 25; 31; 35; 36], in vegetables [11; 16; 39], on surfaces [21],
- shiga-toxin producing *E. Coli* in enrichment broth [41], and in meat products [7],
- *Salmonella* in meat and poultry products [7], in broth [23] and in alfalfa sprouts [27].

This simultaneous deceleration is a simplistic principle which is of course not applicable to every interaction [9; 24; 30] but presents the major advantage to enable simple and parsimonious modelling. Thus, most modelling approaches of the Jameson effect are achieved through a modification of the standard primary growth model and can be conceptualized through the following generic system of equations, in which N_A and N_B stand respectively for

two populations, and all parameters are standard and easily obtainable in “pure cultures” (which means in absence of the other population):

$$\begin{cases} \frac{1}{N_A} \frac{dN_A}{dt} = \mu_A(t) = \mu_{max_A} \cdot \alpha_A(t) \cdot f(t) \\ \frac{1}{N_B} \frac{dN_B}{dt} = \mu_B(t) = \mu_{max_B} \cdot \alpha_B(t) \cdot f(t) \end{cases} \quad (1)$$

where $\alpha(t)$ is an acceleration function (e.g. that of the Baranyi model), and $f(t)$ is a logistic deceleration function based on the assumption that both populations inhibit each other to the same extent that they inhibit their own growth, e.g. $f(t) = \left(1 - \frac{N_A(t) + N_B(t)}{N_{max_{tot}}}\right)$ with proposals

to derive $N_{max_{tot}}$ from N_{max_A} and/or N_{max_B} [9; 10], or $f(t) = \left(1 - \frac{N_A(t)}{N_{max_A}}\right) \cdot \left(1 - \frac{N_B(t)}{N_{max_B}}\right)$ [17; 29]. All these proposed deceleration functions are equivalent when $N_A(t) \ll N_B(t)$ or $N_A(t) \gg N_B(t)$. Notice that no analytical solution can be provided for the system of equations with the above proposals, which does not help fitting.

Simpler variants of these models (based on the same empirical principle of simultaneous deceleration) consist in an abrupt deceleration function (instead of logistic) [2; 7; 12]. Another empirical variant is to keep a standard primary model for the population of interest only, and to build a secondary model on N_{max} , as a function of the temperature, and then indirectly of the extent of growth of background flora [38; 39] or as a function of N_0 [11].

Lotka-Volterra models

To circumvent cases in which the simplistic hypothesis of simultaneous deceleration is not applicable, other models have been proposed:

- i. either based on the idea that growth of the minority population is only partly inhibited after the majority population has reached its stationary phase [15]
- ii. or on the contrary based on the idea that growth of the minority population stops before the majority population reaches its stationary phase [24]

In these two last models, a new parameter, specific to the mixed culture, is introduced: (i) an inhibition coefficient of the growth rate [15], or (ii) a third N_{max} specific to the mixed culture [24]. In reference to the hypothesis underlying the Jameson effect, both models could be explained by a differential sensitivity to the unknown reason of growth limitation.

Lotka-Volterra models, historically proposed in ecology, and introduced in predictive microbiology by Dens *et al.* [13] and Vereecken *et al.* [40], are another empirical approach of the mixed cultures without referring to the simple simultaneous deceleration hypothesis. The basic scheme of primary model is the system (1) with two, instead of one, deceleration

functions:
$$\begin{cases} f_A(t) = \frac{1}{N_{max_A}} (N_{max_A} - N_A(t) - \alpha_{AB} N_B(t)) \\ f_B(t) = \frac{1}{N_{max_B}} (N_{max_B} - N_B(t) - \alpha_{BA} N_A(t)) \end{cases}$$

The parameters α_{AB} and α_{BA} (coefficients of interaction measuring the effects of one species on the other) have to be estimated in mixed culture.

Such Lotka-Volterra models have been proposed, concerning: growth of *E. Coli* O157:H7 in ground beef [34], growth of *L. monocytogenes* in salami [19], growth of LAB, coliforms, pseudomonads, *Brochothrix*, *Salmonella*, and yeasts on sliced pork shoulder [27], growth of *Aeromonas hydrophila* on fish surfaces [18], yeast-yeast and yeast-bacterium interactions during the ripening of smear cheeses [32].

Mechanistic models

Again in the late 1990's, a third class of predictive models were proposed in which the mechanism of the interaction was explicit (decrease of pH, consumption of the limiting substrate, production of an inhibitory by-product...). Such models were far from parsimonious, e.g. with 4 to 5-variable and 20-parameter models [4; 28]. In these approaches, parameters have biological meaning and can be estimated from pure cultures, but at the cost

of an intensive work, which makes them weakly eligible for extensive application *in situ*. Similar approaches published in the 2000's are reviewed by Leroy & De Vuyst [26].

Case-study: *Listeria monocytogenes* and LAB in diced bacon

Here, we propose an illustration concerning *L. monocytogenes* and LAB in two related pork meat products: (i) cooked smoked diced bacon (an ingredient used in industrially prepared dishes such as pizzas), (ii) unsmoked uncooked diced bacon (a product usually used in home cooked preparations but occasionally consumed raw by 14% of French people [1]). Both products share close physical-chemical properties.

In the first series, five growth curves were obtained at 8°C under air (*i.e.* without the modified atmosphere) in one batch of cooked smoked diced bacon: three curves for *L. monocytogenes* in “pure culture” by challenge testing in the cooked smoked product ionized at 5 kGy (Ionisos, Dagneux, France), one for *L. monocytogenes* in “mixed culture” (*i.e.* challenge testing in the non-ionized product), and one for LAB in “pure culture” by storage trial. Figure 1a presents the fitted primary model to the “pure” LAB growth curve, and various models used to predict the fate of *L. monocytogenes* in “mixed culture”, based on the median growth parameters estimated in “pure culture” and on various interactions hypotheses. The modification of the Jameson effect proposed by Le Marc *et al.* [24] appears quite promising.

For uncooked unsmoked diced bacon, nine challenge tests (9 batches, 3 from 3 producers) were performed at 8°C under the commercial modified atmosphere. Each challenge test included monitoring of *L. monocytogenes* onto ALOA, of LAB onto MRS, of pH, water activity (a_w), organic acids concentrations, and gas composition. In most cases (7/9 batches), no growth of *L. monocytogenes* was observed whereas in the 2 other ones sparse growth was observed (see example Figure 1b). The competition with LAB is likely to explain at least partly the quasi-absence of growth even if none of the tested hypotheses appears satisfactory. Stochastic modelling of the lag and stationary phases seems to be required.

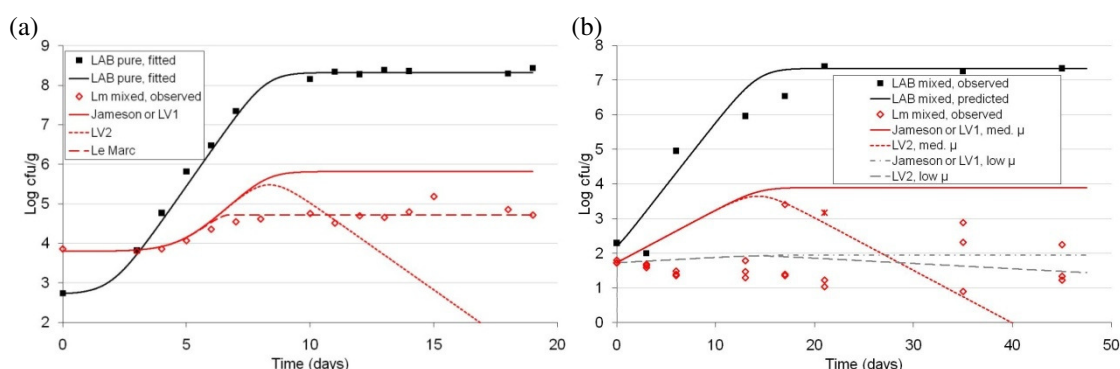


Figure 1. Fate of *L. monocytogenes* (Lm) and lactic acid bacteria (LAB) at 8°C in diced bacon (a): cooked smoked diced bacon. The 3 predicted growth curves for *L. monocytogenes* are simulated from parameters estimated in pure cultures, with different hypotheses: Jameson deceleration (“Jameson”), Lotka-Volterra with $\alpha_{AB}=1$ (“LV1”), Lotka-Volterra with $\alpha_{AB}=2$ (“LV2”) and assuming, according to Le Marc *et al.* [24] that growth of Lm stops when LAB reaches 10^7 ufc/g (instead of its own N_{max}). (b): uncooked unsmoked diced bacon. The predicted growth curve for LAB is based on parameters estimated in other batches. The 4 predicted growth curves for *L. monocytogenes* are simulated with lag = 0, and either the median (“med”) or the 5th percentile (“low”) predicted by Sym’Previus for μ_{max} using the measured pH, a_w , and lactic acid concentration, and “Jameson”, “LV1”, or “LV2”.

Conclusion

Further research appears needed to validate the various proposed alternatives to model microbial interactions, and would in particular be useful to model the fate of *L. monocytogenes* in diced bacon along the shelf-life and then to expand the on-going modeling work [3; 8] beyond the process *per se*.

References

1. AFSSA (2009). Etude individuelle nationale des consommations alimentaires (<http://www.afssa.fr/Documents/PASER-Ra-INCA2.pdf>).
2. Beaufort A., Rudelle S., Gnanou-Besse N., Toquin M.T., Kerouanton A., Bergis H., Salvat G. and Cornu M. (2007) Prevalence and growth of *Listeria monocytogenes* in naturally contaminated cold-smoked salmon. *Letters in Applied Microbiology* 44, 406-411.
3. Billoir E., Denis J-B., Commeau N., Cornu M. and Zuliani V. (2009) Probabilistic modelling of *L. monocytogenes* behaviour in diced bacon along the manufacture process chain. *Submitted to the same conference*.

4. Breidt F. and Fleming H.P. (1998) Modeling of the competitive growth of *Listeria monocytogenes* and *Lactococcus lactis* in vegetable broth. *Applied and Environmental Microbiology* 64, 3159-3165.
5. Buchanan R.L. and Bagi L.K. (1997) Microbial competition: effect of culture conditions on the suppression of *Listeria monocytogenes* Scott A by *Carnobacterium piscicola*. *Journal of Food Protection* 60, 254-261.
6. Carlin F., Nguyen The C. and Morris C.E. (1996) Influence of background microflora on *Listeria monocytogenes* on minimally processed fresh broad-leaved endive (*Cichorium endivia* var. *latifolia*). *Journal of Food Protection* 59, 698-703.
7. Coleman M.E., Sandberg S. and Anderson S.A. (2003) Impact of microbial ecology of meat and poultry products on predictions from exposure assessment scenarios for refrigerated storage. *Risk Analysis* 23, 215-228.
8. Commeau N., Parent E., Billoir E., Zuliani V. and Cornu M. (2009) Modelling contamination to build a sampling plan: application to French diced bacon industry and *Listeria monocytogenes*. *Submitted to the same conference*.
9. Cornu M. (2001). Modelling the competitive growth of *Listeria monocytogenes* and food flora in situ. *Acta Horticulturae* 566, 151-157.
10. Cornu M., Kalmokoff M. and Flandrois J.P. (2002) Modelling the competitive growth of *Listeria monocytogenes* and *Listeria innocua* in enrichment broths. *International Journal of Food Microbiology* 73, 261-274.
11. Crepet A., Stahl V. and Carlin F. (2009) Development of a hierarchical Bayesian model to estimate the growth parameters of *Listeria monocytogenes* in minimally processed fresh leafy salads. *International Journal of Food Microbiology* 131, 112-119.
12. Delignette-Muller M.L., Cornu M., Pouillot R. and Denis J.B. (2006) Use of Bayesian modelling in risk assessment: application to growth of *Listeria monocytogenes* and food flora in cold-smoked salmon. *International Journal of Food microbiology* 106, 195-208.
13. Dens E.J., Vereecken K.M. and Van Impe J.F. (1999) A prototype model structure for mixed microbial populations in homogeneous food products. *Journal of Theoretical Biology* 201, 159-170.
14. Devlieghere F., Geeraerd A.H., Versyck K.J., Vandewaetere B., Impe J.v. and Debevere J. (2001) Growth of *Listeria monocytogenes* in modified atmosphere packed cooked meat products: a predictive model. *Food Microbiology* 18, 53-66.
15. FAO-WHO (2004). Risk assessment of *Listeria monocytogenes* in ready-to-eat foods. *Microbiological risk assessment series* no. 5.
16. Geysen S., Escalona V.H., Verlinden B.E., Aertsen A., Geeraerd A.H., Michiels C.W., Van Impe J.F. and Nicolai B.M. (2006) Validation of predictive growth models describing superatmospheric oxygen effects on *Pseudomonas fluorescens* and *Listeria innocua* on fresh-cut lettuce. *International Journal of Food Microbiology* 111, 48-58.
17. Gimenez B. and Dalgaard P. (2004) Modelling and predicting the simultaneous growth of *Listeria monocytogenes* and spoilage microorganisms in cold-smoked salmon. *Journal of Applied Microbiology* 96, 96-109.
18. Giuffrida A., Ziino G., Valenti D., Donato G. and Panebianco A. (2007) Application of an interspecific competition model to predict the growth of *Aeromonas hydrophila* on fish surfaces during the refrigerated storage. *Archiv für Lebensmittelhygiene* 58, 136-141.
19. Giuffrida A., Valenti D., Ziino G., Spagnolo B. and Panebianco A. (2009) A stochastic interspecific competition model to predict the behaviour of *Listeria monocytogenes* in the fermentation process of a traditional Sicilian salami. *European Food Research and Technology* 228, 767-775.
20. Grau F.H. and Vanderlinde P.B. (1992) Occurrence, numbers and growth of *Listeria monocytogenes* on some vacuum-packaged processed meats. *Journal of Food Protection* 55, 4-7.
21. Guillier L., Stahl V., Hezard B., Notz E. and Briandet R. (2008) Modelling the competitive growth between *Listeria monocytogenes* and biofilm microflora of smear cheese wooden shelves. *International Journal of Food Microbiology* 128, 51-57.
22. Jameson J. (1962) A discussion of the dynamics of salmonella enrichment. *Journal of Hygiene* 60, 193-207.
23. Komitopoulou E., Bainton N.J. and Adams M.R. (2004) Premature *Salmonella* Typhimurium growth inhibition in competition with other Gram-negative organisms is redox potential regulated via RpoS induction. *Journal of Applied Microbiology* 97, 964-972.
24. Le Marc Y., Valik L. and Medvedová A. (2009) Modelling the effect of the starter culture on the growth of *Staphylococcus aureus* in milk. *International Journal of Food Microbiology* 129, 306-311.
25. Lecompte J.Y., Kondjoyan A., Sarter S., Portanguen S. and Collignan A. (2008) Effects of steam and lactic acid treatments on inactivation of *Listeria innocua* surface-inoculated on chicken skins. *International Journal of Food Microbiology* 127, 155-161.
26. Leroy F. and De Vuyst L. (2007). Modelling microbial interactions in foods. In: S. Brul, S. Van Gerwen and M. Zwietering (Eds.) *Modelling microorganisms in food*, Chapter 14, Woodhead Publishing Limited, Cambridge, UK (ISBN 9781845690069)
27. Liu F., Guo Y. and Li Y. (2006) Interactions of microorganisms during natural spoilage of pork at 5°C. *Journal of Food Engineering* 72, 24-29.
28. Malakar P.K., Martens D.E., Zwietering M.H., Beal C. and Van 't Riet K. (1999) Modelling the interactions between *Lactobacillus curvatus* and *Enterobacter cloacae*. II. Mixed cultures and shelf life predictions. *International Journal of Food Microbiology* 51, 67-79.
29. Mejlholm O. and Dalgaard P. (2007) Modeling and predicting the growth of lactic acid bacteria in lightly preserved seafood and their inhibiting effect on *Listeria monocytogenes*. *Journal of Food Protection* 70, 2485-2497.
30. Mellefont L.A., McMeekin T.A. and Ross T. (2008) Effect of relative inoculum concentration on *Listeria monocytogenes* growth in co-culture. *International Journal of Food Microbiology* 121, 157-168.
31. Mellefont L.A. and Ross T. (2007) Effect of potassium lactate and a potassium lactate-sodium diacetate blend on *Listeria monocytogenes* growth in modified atmosphere packaged sliced ham. *Journal of Food Protection* 70, 2297-2305.
32. Mounier J., Monnet C., Vallaes T., Arditi R., Sarthou A.-S., Helias A. and Irlinger F. (2008) Microbial Interactions within a Cheese Microbial Community. *Applied and Environmental Microbiology* 74, 172-181.
33. Palma M. and Buchanan R. (2002) The effect of *Lactococcus lactis* on the growth of *Listeria monocytogenes* in alfalfa sprout broth. *Acta Alimentaria* 31, 379-392.
34. Powell M., Schlosser W. and Ebel E. (2004) Considering the complexity of microbial community dynamics in food safety risk assessment. *International Journal of Food Microbiology* 90, 171-179.
35. Radin D., Niebuhr S.E., Dickson J.S. (2007). Spoilage microflora of vacuum-packages frankfurters and influence on the growth of *Listeria monocytogenes*. *Biotechnology in Animal Husbandry* 23, 103 - 112
36. Ross T., Rasmussen S., Fazil A., Paoli G. and Sumner J. (2009) Quantitative risk assessment of *Listeria monocytogenes* in ready-to-eat meats in Australia. *International Journal of Food Microbiology* 131, 128-137.
37. Ross T., Dalgaard P. and Tienungoon S. (2000) Predictive modelling of the growth and survival of *Listeria* in fishery products. *International Journal of Food Microbiology* 62, 231-245.
38. Koseki S. and Isobe S. (2005) Prediction of pathogen growth on iceberg lettuce under real temperature history during distribution from farm to table. *International Journal of Food Microbiology* 104, 239-248.
39. Valero A., Carrasco E., Perez-Rodriguez F., Garcia-Gimeno R.M. and Zurera G. (2007) Modeling the growth of *Listeria monocytogenes* in pasteurized white asparagus. *Journal of Food Protection* 70, 753-757.
40. Vereecken K.M., Dens E.J. and Van Impe J.F. (2000) Predictive modeling of mixed microbial populations in food products: evaluation of two-species models. *Journal of Theoretical Biology* 205, 53-72.
41. Vimont A., Vernozy-Rozand C., Montet M.P., Lazizzera C., Bavai C. and Delignette-Muller M.L. (2006) Modeling and predicting the simultaneous growth of *Escherichia coli* O157:H7 and ground beef background microflora for various enrichment protocols. *Applied and Environmental Microbiology* 72, 261-268.

Bayesian modelling of *Clostridium perfringens* growth in beef.

S. Jaloustre^{1*}, M. Cornu¹, E. Morelli¹, V. Noel¹, and M.L. Delignette-Muller²

¹ Laboratoire d'Etudes et de Recherches sur la Qualité des Aliments et sur les Procédés agro-alimentaires, Agence française de sécurité des aliments, 23 avenue du Général de Gaulle, 94706 Maisons-Alfort, France. (s.sevrin@afssa.fr)

² Université de Lyon, CNRS UMR 5558, Laboratoire de Biométrie et Biologie Evolutive, Ecole Nationale Vétérinaire de Lyon, 1 avenue Bourgelat, 69280 Marcy l'Etoile, France

* corresponding author

Introduction

Clostridium perfringens is a pathogen commonly found in meat products and often responsible for foodborne diseases in institutions and restaurants (Crouch and Golden, 2005). These outbreaks are often due to spores germination and vegetative cells growth during a too slow chilling. Many studies have been published about modelling *C. perfringens* vegetative cells growth during chilling (Juneja *et al.*, 1999, Juneja *et al.*, 2001, Huang, 2004, Juneja *et al.*, 2008, Le Marc *et al.*, 2008). The aim of this study is to estimate the parameters of a growth model using all the data published to date on beef, to be able to predict *C. perfringens* growth in beef for risk assessment, taking into account potential sources of variability and uncertainty.

Materials and methods

Growth data

Twenty five published growth curves were used from 6 experimental works published from 1980 to 2004. Each growth curve was obtained under constant thermal conditions (from 15°C to 50°C) after a heat shock (most often 75°C for 10 or 20 minutes), from one strain or a cocktail of *C. perfringens* strains inoculated in beef without modification of its natural composition. We directly used raw data, reported as measurement times (units : hour) and log counts (units : \log_{10} cfu.g⁻¹) values.

Growth model

The dataset made up of all the growth curves was modelled simultaneously by a Bayesian approach such as the ones proposed by Pouillot *et al.* (2003) and Delignette-Muller *et al.* (2006). Stochastic and logical links between nodes are displayed on the directed acyclic graph (figure 1) and defined in table 1.

Growth curves were described by the primary growth model of Baranyi and Roberts (1995) with immediate transition between exponential and stationary phase (Eq.1). The effect of temperature on maximum specific growth rate was described by the cardinal temperature model of Rosso *et al* (1995)(Eq.2). Only the effect of the temperature on the specific growth rate was explicitly modelled. The effects of the other factors were taken into account by the value of the optimal specific growth rate ($\mu_{opt-beef}$). The cardinal temperatures (T_{min} , T_{opt} , T_{max}) and the optimal specific growth rate ($\mu_{opt-beef}$) were not supposed variables. Quantity $\ln(h_0)$ (equal to the product of the lag time and the maximum specific growth rate in constant environmental conditions) was used to describe the “work to be done” during the germination-outgrowth-latence phase (Baranyi and Roberts, 1995). It was supposed variable between growth curves and described by a normal distribution $N(\mu_{\ln h_0}, \sigma_{\ln h_0})$. Input parameters of the model (table 2, figure 1) were considered as random and uncertain variables. Their prior distributions were defined from published data, that were not used in the computations (table 2). The empirical posterior distribution of each parameter was computed from its prior one and from the whole dataset. Computations were performed with JAGS.

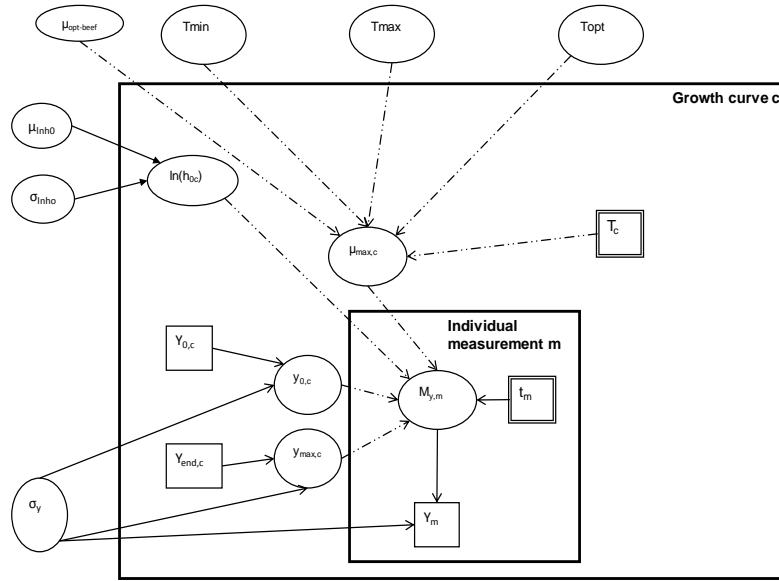


Fig. 1 : directed acyclic graph of the growth model. All model quantities are presented as nodes. Data are denoted by rectangles; covariates are denoted by double-rectangles and parameters are denoted by ellipses. Arrows run between nodes from their direct influence ('parents') to the 'descendants'. Solid arrows indicate stochastic dependences while dashed arrows indicate logical functions. Stochastic and logical links are presented in table 1.

Table 1 : links between nodes of the growth model

| Node | Type | Definition |
|----------------|------------|---|
| Y_m | stochastic | $N(M_{y,m}, \sigma_y)$ |
| $M_{y,m}$ | logical | $M_{y,m} = \min \left(y_{0,c} + \frac{\mu_{\max,c} \times t_m}{\ln(10)} + \log_{10} \left[e^{-\mu_{\max,c} \times t_m} \times (1 - e^{-h_{0,c}}) + e^{-h_{0,c}} \right], y_{\max,c} \right)$ (Eq.1) |
| $y_{\max,c}$ | stochastic | $N(Y_{\text{end},c}, \sigma_y)$ |
| $y_{0,c}$ | stochastic | $N(Y_{0,c}, \sigma_y)$ |
| $\mu_{\max,c}$ | logical | $\mu_{\max,c} = \frac{\mu_{\text{opt-beef}} \times (T_c - T_{\min})^2 (T_c - T_{\max})}{(T_{\text{opt}} - T_{\min}) \left[(T_{\text{opt}} - T_{\min}) (T_c - T_{\text{opt}}) - (T_{\text{opt}} - T_{\max}) (T_{\text{opt}} + T_{\min} - 2T_c) \right]}$ (Eq.2) |
| $\ln(h_{0c})$ | stochastic | $N(\mu_{\ln h_0}, \sigma_{\ln h_0})$ |

Validation of the model

In order to check the ability of the model to predict bacterial growth in realistic conditions, data of final cell number increase corresponding to several temperature scenarios were collected. A first personal dataset was obtained under constant temperature (6 hours at 45°C) but after a non classical heat shock chosen to mimic the cooking of beef-in-sauce products (increase from 10°C to 100°C in 40 minutes). Other datasets were obtained from published studies where the heat shock was classical but followed by an exponential cooling from 54°C to 7°C in 12 to 21 hours, depending on the study. For each temperature profile, a set of 1500 values of the growth model parameters (table 2) was randomly selected from the joint posterior distribution resulting from the Bayesian modeling, so as to take into account uncertainty on each input of the model in the simulations.

Results and discussion

Growth model parameters

Statistics of the empirical distribution of the uncertain parameters are presented in Table 2. For most of these parameters, Bayesian inference succeeded in narrowing distributions, thus giving rather precise estimations, except for T_{\max} , due to the lack of growth kinetics obtained

above 50°C. Estimated parameters of the normal variability distribution of $\ln(h_0)$ ($\mu_{\ln h_0}$ and $\sigma_{\ln h_0}$) are reflecting the great variability of germination-outgrowth-latence phase duration observed in the data.

As shown on figure 2, the model seems to reasonably describe the observed values, without clear outlier.

Table 2: Prior distributions (defined from previous publications cited below the table) and empirical posterior distributions of the inputs of *Clostridium perfringens* growth model.

| Parameter | Prior distributions | | | Posterior distributions | | |
|---------------------------------|---|---------------------------------|----------------------------------|-------------------------|---------------------------------|----------------------------------|
| | Defined distributions | 2.5 th percentile | 97.5 th percentile | Median | 2.5 th percentile | 97.5 th percentile |
| T_{\min} ^a | $N(10,2)$ | 6 | 14 | 12.7 | 12.1 | 13.1 |
| T_{opt} ^b | $N(44,2)$ | 40 | 48 | 45.1 | 44.2 | 46.2 |
| T_{\max} ^a | $N(52,1.5)$ | 49 | 55 | 53 | 51.5 | 55 |
| $\mu_{opt-beef}$ ^c | $N(4.5,1.8)$ | 1.1 | 8 | 3.8 | 3.5 | 4.2 |
| $\mu_{\ln h_0}$ ^d | $N(1.95,0.32)$ | 1.3 | 2.6 | 1.8 | 1.4 | 2.1 |
| $\sigma_{\ln h_0}$ ^e | $\sigma_{\ln h_0}^{-2} \propto \text{Gamma}(0.001,0.001)$ | 1.5×10^5 | ∞ | 0.9 | 0.6 | 1.2 |
| σ_y ^e | $\sigma_y^{-2} \propto \text{Gamma}(0.001,0.001)$ | 1.8×10^4 | ∞ | 0.33 | 0.3 | 0.36 |

a Blankenship *et al.* (1988), Juneja *et al.* (1994), Juneja *et al.* (2002), de Jong *et al.* (2005), Le Marc *et al.* (2008)

b de Jong *et al.* (2005)

c Schroder *et al.* (1971), Willardsen *et al.* (1978), Willardsen *et al.* (1979), Blankenship *et al.* (1988), Labbe *et al.* (1995), Juneja *et al.* (2002), Jong *et al.* (2005), Le Marc *et al.* (2008), Juneja *et al.* (2008)

d Le Marc *et al.* (2008)

e classical non informative priors on precision parameters

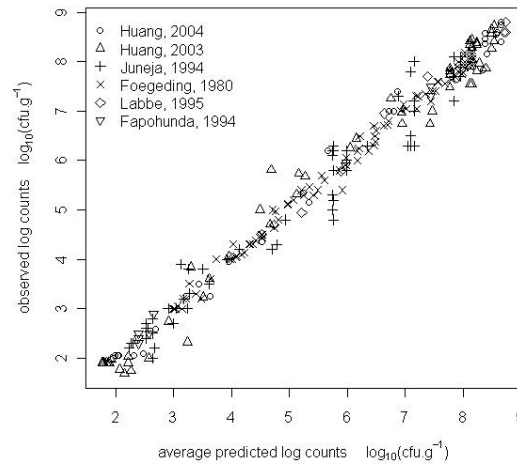


Fig. 2 : Comparison of observed log counts with the averaged predicted ones.

Validation results

Figure 3 represents simulated 95% credibility intervals and observed values of final cell number increase under different temperature scenarios. The credibility intervals reflect the overall uncertainty combining variability and uncertainty. This uncertainty seems great but is for most part due to variability on $\ln(h_0)$ and is consistent with the variability observed on the validation data, especially when data come from various authors, which is the case for scenarios d and e.

Discussion

Cardinal temperatures and optimal growth rate were not considered as variable in the proposed model due to the lack of available data enabling the characterization of this

variability. It would be of interest to explore in particular the inter strain variability by individually culturing various strains.

In our modeling approach, different alternatives were compared for parameter $\ln(h_0)$, first assumed not variable, then assumed variable between studies and at last variable between curves. The last alternative was chosen for its far better description of data. The source of this observed variability seems hard to biologically explain without any further investigation, as data collected for Bayesian modeling were all obtained on uncured beef, mostly with the same classical heat shock and with only one strain or cocktail for each study. Nevertheless, the impact of this variability on the overall uncertainty of growth model predictions should be taken into account in risk assessment.

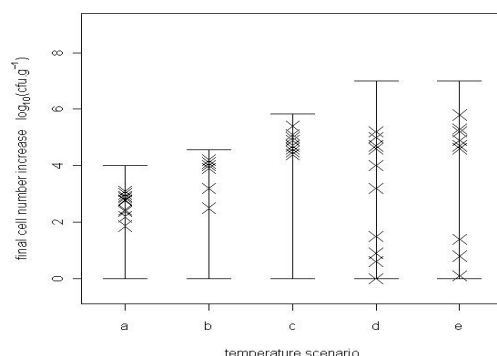


Fig. 3 : Simulated intervals and observed values of final cell number increase under different temperature scenarios (a: cooking-like heat shock followed by 6 hours at 45°C, b to e : classical heat shock followed by exponential cooling from 54°C to 7 °C within 12 hours (b), 15 hours (c), 18 hours(d), 21 hours (e)). Dark lines represent the 95% credibility interval obtained by simulation, while crosses represent observed values. Data corresponding to scenarios b to e were collected from Thippareddi *et al.* (2003), Smith *et al.* (2004), Sanchez Plata *et al.* (2005), Juneja *et al.* (2006), Juneja *et al.* (2007), Juneja *et al.* (2008)

Acknowledgements

We would like to thank the ANR for providing financial support, and the COMBASE and the SYM'PREVIUS projects for their contribution by the availability of the data.

References

- Baranyi, J., Roberts, T.A. (1995). Mathematics of predictive microbiology. *International Journal of Food Microbiology* 26 : 199-218.
- Crouch, E. and Golden, N. (2005) A Risk Assessment for *Clostridium perfringens* in Ready-To-Eat and Partially Cooked Meat and Poultry Products, USDA, Food Safety Inspection Service, September 2005.
- Delignette-Muller, M.L., Cornu, M., Pouillot, R. and Denis, J.B. (2006) Use of Bayesian modelling in risk assessment: Application to growth of *Listeria monocytogenes* and food flora in cold-smoked salmon. *International Journal of Food Microbiology* 106, 195–208
- Juneja, V. K., Whiting, R. C., Marks, H. M. and Snyder, O. P. (1999) Predictive model for growth of *Clostridium perfringens* at temperatures applicable to cooling of cooked meat. *Food Microbiology* 16, 335-349
- Juneja, V.K., Novaka, J.S., Marks, H.M. and Gombas, D.E. (2001) Growth of *Clostridium perfringens* from spore inocula in cooked cured beef: development of a predictive model. *Innovative Food Science & Emerging Technologies* 2, 289-301
- Juneja, V.K., Marks, H. and Thippareddi, H. (2008) Predictive model for growth of *Clostridium perfringens* during cooling of cooked uncured beef. *Food Microbiology* 25, 42–55
- Huang, L. (2004) Numerical analysis of the growth of *Clostridium Perfringens* in cooked beef under isothermal and dynamic conditions. *Journal of Food Safety* 24, 53-70.
- Le Marc, Y., Plowman, J., Aldus, C.F., Munoz-Cuevas, M., Baranyi, J. and Peck, M.W. (2008). Modelling the growth of *Clostridium perfringens* during the cooling of bulk meat. *International Journal of Food Microbiology* 128, (1) 41-50.
- Pouillot, R., Albert, I., Cornu, M. and Denis, J.-B. (2003). Estimation of uncertainty and variability in bacterial growth using Bayesian inference. Application to *Listeria monocytogenes*. *International Journal of Food Microbiology* 81(2): 87-104.
- Rosso, L., Lobry, J.R., Bajard, S., Flandrois, J.P. (1995) Convenient Model To Describe the Combined Effects of Temperature and pH on Microbial Growth. *Applied and Environmental Microbiology* 61 (2), 610–616

Introducing a zero-modified negative binomial regression for estimating the effect of chilling on *Escherichia coli* plate counts from Irish beef carcasses

U. A. Gonzales-Barron, J. J. Sheridan, and F. Butler

Biosystems Engineering, UCD School of Agriculture, Food Science and Veterinary Medicine. University College Dublin, Dublin 4, Ireland (ursula.gonzalesbarron@ucd.ie, f.butler@ucd.ie)

Abstract

This work introduces an alternative conceptual framework based on zero-modified count data distributions for the conduction of inferential statistics on microbial data characterized by relatively high numbers of zero counts. The effect of chilling on *Escherichia coli* plate counts from beef carcasses ($n=620$) was elucidated by two zero-modified negative binomial regressions, at group level and at carcass level. In such regressions, the individual plate count Y_i (whole number of colonies as enumerated in Petri dishes) can originate from two stochastic processes, a binomial process determining if a plate count is zero or non-zero (logit component), and a truncated-at-zero negative binomial (heterogeneous Poisson) component for count data determining all the positive counts. The group-level model, with a coded variable (pre-chill/post-chill) as treatment, confirmed that chilling had a decreasing effect ($p<0.01$ for both logit and negative binomial components) on the overall recovery of *Escherichia coli*. The second regression, with the pre-chill count value as covariate and the post-chill count as response variable, further elucidated that, for the positive counts (negative binomial component), chilling does not necessarily decrease the recovery of *Escherichia coli*, however, the proportion of zero counts (ω_0) in the post-chill group can be predicted ($p<0.01$) from the plate counts of the pre-chill carcasses. The predicted ω_0 (0.79) was in close agreement with the actual value of 0.81. This conceptual framework can find interesting applications in stochastic risk assessment and in the development of more realistic microbiological criteria and performance objectives.

Keywords: Zero-inflated, hurdle, negative binomial, chilling, *Escherichia coli*, carcass.

Introduction

In the evaluation of microbiological quality of foodstuffs, bacterial load is conventionally expressed in terms of $\log \text{CFU cm}^{-2}$ or g^{-1} . Logarithmic transformation is believed to approximate data normality, which is fundamental for the application of parametric statistical data analysis such as analysis of variance. While logarithmic transformation can be suitable for bacterial counts of high occurrence, such as mesophile or total viable counts, this approach may be unsuitable for bacterial counts of lower occurrence, for which an alternative conceptual framework should be explored.

In recent years, there have been considerable developments in regression models for count data (Boucher et al., 2008). Whereas the Poisson distribution is often used as a baseline for count data, its assumption of equi-dispersion (variance equals its mean) is too restrictive for many applications. In practice, heterogeneity or clustering causes a condition called over-dispersion, meaning that the variance of the observed count data normally exceeds the mean. A heterogeneous Poisson model loosens Poisson restriction by allowing the expected number of events (λ) to be a function of some random variable. If this random variable follows a gamma distribution, the resulting heterogeneous Poisson will be a negative binomial. However, with some types of data, over-dispersion may also stem from a high percentage of zero counts, for which the variance function of the heterogeneous Poisson (negative binomial) model may be insufficient. To model the excess of zeros, a mixture model of two data generation processes – one generating always zero counts (point mass at zero) and the other generating positive counts (either a Poisson or a negative binomial process) – may be

appropriate. Zero-inflated (Lambert, 1992), and hurdle (Mullahy, 1986) heterogeneous Poisson models are two types of zero-modified count data regression models. The objective of this work was to introduce an alternative count data framework to conduct inferential statistics on microbial data that did not approximate to a normal distribution after logarithmic transformation due to the relatively high numbers of zero counts. Specifically, the effect of chilling on *Escherichia coli* plate counts recovered from Irish beef carcasses was assessed by fitting a group-level and carcass-level zero-modified negative binomial regression models.

Methodology

Assuming that the bacterial cells extracted from a carcass swab i is randomly distributed in the 200-ml neat homogenate, the number of bacterial cells present in a 1-ml aliquot (poured to the Petri dish) should follow a Poisson distribution with mean λ_i (CFU/ml). Assuming that each of the plated cells will become a colony after incubation, Y_i can be defined as the bacterial count on the Petri dish or the number of cells present in the aliquot. Thus, the predicted probability of the plate count Y_i (CFU) can then be expressed as,

$$\Pr(Y_i) = \frac{\text{Exp}(-\lambda_i) \times \lambda_i^{Y_i}}{Y_i!}$$

The baseline Poisson model is then generalized by including a dispersion parameter to accommodate the heterogeneity in the count data. Thus, a generalised Poisson model lets the expected number of cells λ_i (CFU/ml) be a function not only of the covariate X_i but also of some unobserved random variable e_i ,

$$\lambda_i = \exp(\beta_0 + \beta_1 X_i) \exp(e_i) \quad (1)$$

The random variable $\exp(e_i)$ is assumed to follow a gamma distribution $\Gamma(1/\alpha, \alpha)$ with expected value 1 and variance α , so that the above modification yields a more flexible model, the negative binomial. As the negative binomial regression could not account for the amount of zeros in the data (results not shown here), a zero-modified negative binomial of the hurdle type (Boucher et al., 2008) was considered. A hurdle-type model assumes that the count outcome Y_i is generated by two different stochastic processes, a binomial process determining if Y_i is zero or non-zero, and a truncated-at-zero negative binomial process governing all positive counts (CFU). The probability of the count Y_i can be expressed as,

$$\Pr(Y_i) = \begin{cases} \omega_0 & \text{for } Y_i = 0 \\ (1 - \omega_0) \left[\frac{\frac{\Gamma(Y_i + \alpha^{-1})}{\Gamma(Y_i + 1)\Gamma(\alpha^{-1})} (1 + \alpha\lambda_i)^{-(Y_i + \alpha^{-1})} (\lambda_i \alpha)^{Y_i}}{1 - \left(\frac{\alpha^{-1}}{\alpha^{-1} + \lambda_i} \right)^{\alpha^{-1}}} \right] & \text{for } Y_i \geq 1 \end{cases} \quad (2)$$

where the membership of the fixed-zero group is estimated by a probability ω_0 , which is calculated by a logistic model with b_0 as intercept and b_1 as regressor for the covariate X_i .

$$\text{Log} \left[\frac{\omega_0}{1 - \omega_0} \right] = b_0 + b_1 X_i \quad (3)$$

A group-level and an animal-level zero-modified negative binomial regression model were fitted on *Escherichia coli* plate count (CFU) data that was available for Irish beef carcasses

($n=620$) sampled before and after chilling (24 hours at $\sim 5^{\circ}\text{C}$). In the first model, differences in the proportion of zeros (logit component) and counts (negative binomial component) between the pre-chill and post-chill groups were assessed by defining Y_i as the plate count for both pre-chill and post-chill and the covariate X_i (Eq. (1) and (3)) as a coded variable for pre-chill (1) and post-chill (2) carcasses. In the second model, the possibility to predict the proportion of zero counts in the post-chill group and the positive counts using the pre-chill counts was assessed by defining the response variable Y_i as the post-chill plate count and the covariate X_i (Eq. (1) and (3)) as the pre-chill count.

Results and discussion

The group-level zero-modified negative binomial regression model showed that there were significant differences in both the logit component ($p<0.01$) and in the negative binomial component ($p<0.01$) between the pre-chill and the post-chill plate counts (Table 1). Whereas the probability of encountering a zero count (ω_0) from a pre-chill carcass was on average 0.42 (95% CI: 0.39-0.44), in the case of a post-chill carcass it was significantly higher at 0.81 (95% CI: 0.79-0.83). Explained in other terms, the odds ratio (OR) for the treatment covariate was significant, and indicated that, chilling increases the odds of producing a zero count from a carcass swab in about 6 times (Table 1). For the positive counts, the model indicated that the expected value λ of the negative binomial component for the post-chill plate counts was numerically higher (7.80 CFU/ml) than the one for pre-chill plate counts (4.97 CFU/ml). To elucidate the reason for this, the animal-level regression model was fitted. The statistical difference between the pre-chill and post-chill groups is illustrated in Figure 1. As no other covariate apart from the treatment coded variable is present in this analysis (Eq. 1), the probabilities of Eq. (2) (as calculated from the regression parameter estimates) take the shape of a probability mass function of a zero-modified negative binomial distribution for pre-chill and post-chill plate counts. Notice that the flexibility of the zero-modified negative binomial is advantageous to model plate counts from microbial data of low recovery that are highly heterogeneous (producing a highly skewed negative binomial) and with extra zero counts.

Table 1: Chilling effect on the plate counts (CFU) of *Escherichia coli* from beef carcasses, as described by the group-level and carcass-level zero-modified negative binomial regression models.

| Regression parameters | Group-level regression model | | | Carcass-level regression model | | |
|--------------------------|------------------------------|-----------|---------|--------------------------------|-----------|---------|
| | Estimate | St. error | Pr > t | Estimate | St. error | Pr > t |
| Neg Bin | | | | | | |
| β_0 (int) | 1.151 | 0.381 | ** | 2.042 | 0.701 | ** |
| β_1 (covariate) | 0.451 | 0.160 | ** | -0.004 | 0.004 | ns |
| Logit | | | | | | |
| b_0 (int) | -2.131 | 0.131 | *** | 1.564 | 0.078 | *** |
| b_1 (covariate) | 1.797 | 0.089 | *** | -0.006 | 0.002 | ** |
| Other estimates | | | | | | |
| OR (int) | 0.118 | 0.015 | *** | 4.777 | 0.373 | *** |
| OR (treat) | 6.034 | 0.542 | *** | 0.993 | 0.002 | *** |
| λ_1 (pre-chill) | 4.965 | 1.606 | ** | - | - | - |
| λ_2 (post-chill) | 7.795 | 2.648 | ** | 6.916 | 4.854 | ns |
| ω_0 (pre-chill) | 0.417 | 0.013 | *** | - | - | - |
| ω_0 (post-chill) | 0.812 | 0.011 | *** | 0.798 | 0.013 | *** |

The second regression analysis resulted in a non-significant negative binomial component (for the positive counts) and a significant ($p<0.01$) logit component of the model (Table 1). The non-significance of the negative binomial component implies that the pre-chill *Escherichia coli* plate count did not have any effect on the post-chill plate count (in other words, the value of the pre-chill positive count from a carcass could not predict its post-chill count). This is not

unexpected as many other important variables such as carcass surface dryness, extent and site of swabs, proximity to contaminated carcasses, etc. play a role on microbial detection. However, at least in this model, the post-chill positive count is governed only by randomness, and, on this basis, the expected λ of the negative binomial component for the post-chill counts can be higher or lower than the one of the pre-chill counts (in accordance with the previous group-level regression showing the expected value λ higher for the post-chill carcasses). Conversely, the statistically-significant logit part of the regression model showed that it is possible to predict the proportion of zero counts (ω_0) in the post-chill group from the plate counts of the pre-chill carcasses. Thus, using the pre-chill counts, the carcass-level regression model predicted a proportion of zero counts of 0.79 (ω_0) in the post-chill group, which was very close to the actual value of 0.81 (Table 1). In terms of odds ratio (OR), the probability of having a zero count from a post-chill carcass decreases ($p < 0.01$) 0.99 times for a one-colony increase in pre-chill plate count. Finally, it was the larger number of zero counts (significant logit) – and not a potential lower positive count (non-significant negative binomial), which explained the decrease in the expected value $E(Y)$ from 10.85 CFU in the pre-chill group to 5.05 CFU in the post-chill group (Figure 1).

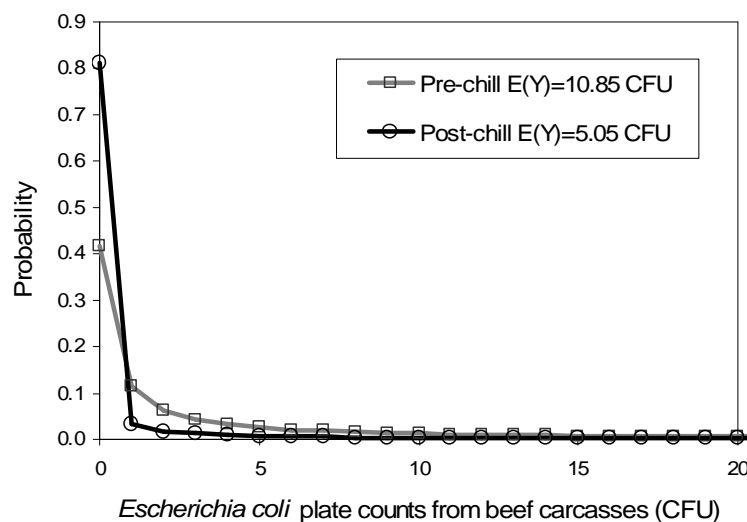


Figure 1: *Escherichia coli* plate counts from Irish beef carcasses as modeled by the group-level zero-modified negative binomial regression showing expected values.

Conclusions

This work showed an alternative framework to conduct inferential statistics on plate count data from microorganisms of low recovery, and assessed probabilistically the decreasing effect that chilling has on *Escherichia coli* counts from beef carcasses by means of two zero-modified negative binomial regressions. The utility of the approach in stochastic risk assessment modelling remains to be appraised.

Acknowledgments

The authors wish to acknowledge the Food Institutional Research Measure (FIRM) administered by the Irish Department of Agriculture, Fisheries and Food. The partial financial support of *ProSafeBeef*, an EU 6th Framework project, is also acknowledged.

References

- Boucher J.P., Denuit M., Guillén M. (2008) Risk classification for claim counts: a comparative analysis of various zero-inflated mixed Poisson and hurdle models. *North American Actuarial Journal* 11, 110-131.
- Lambert D. (1992) Zero-inflated Poisson regression, with an application to defects in manufacturing. *Technometrics* 34, 1-14.
- Mullahy J. (1986) Specification and testing of some modified count data models. *Journal of Econometrics* 33, 341-365.

Use of Fish Shelf Life Prediction (FSLP) software for monitoring fresh turbot quality in the logistic chain

Alfaro B.^a, Nuin M.^a, Pin C.^b and Le Marc Y.^b

^aAZTI-Tecnalia, Parque Tecnológico de Bizkaia, Astondo Bidea, Edf.609, 48160 Derio, Bizkaia, Spain (balfaro@azti.es)

^bInstitute of Food Research, Norwich Research Park, Norwich NR4 7UA, UK (carmen.pin@bbsrc.ac.uk)

Abstract

Fish and fish products are now transported over long distances due to continued globalization. The quality of a fish product and its shelf life is strongly dependent on the temperature history, from production to distribution and storage until consumption. Temperature abuse during any stage of the distribution chain usually affects both, the safety and quality of seafood. In this context, the “Fish Shelf Life Prediction (FSLP)” software was developed to predict the shelf life of farmed fresh fish according to the microbial growth and sensory changes in constant and fluctuating temperature conditions. The aim of this work was to evaluate the use of FSLP program as shelf life monitoring of fresh turbot in a real scenario during international transport under fluctuating temperature conditions. Results showed that FSLP program is a useful tool for monitoring fish quality in the cold chain.

Keywords: shelf life prediction, fresh fish, logistic chain, FSLP software

Introduction

Fish trade in general is paying increasing attention to aquaculture products as a source of fish and other seafood products (FAO, 2003; Josupeit *et al.*, 2001). Such is the case of turbot (*Psetta maxima*) a highly valued flat fish species appreciated for its firm, white and flavourful flesh. Recently, increasing production of this specie as an aquaculture product has raised its availability.

In the global food marketplace, the distribution of chilled fish is a long logistic chain from the origin to the destination, involving handling, intermediate points, and also includes air and road transport. Temperature monitoring along the complete logistic fresh fish chain plays an important role to ensure the quality and safety of these perishable foods. The break of the chill chain results in a rapid decrease of shelf life of fresh food products. In this context, it could be very useful for fresh fish sector to have tools for monitoring the shelf life of the product during the distribution chain. In the last decade, advance of predictive microbiology has allowed significant progress in monitoring the quality and safety status of food products. In particular, in fresh fish products several growth models for spoilage bacteria have been successfully used to predict the shelf-life (Dalgaard *et al.*, 1997; Taoukis *et al.*, 1999; Koutsoumanis 2001; Nuin *et al.*, 2008). Some of these models have been included in available software application, as “Seafood Spoilage and Safety Predictor software” developed by the Danish Institute for Fisheries Research (Dalgaard *et al.*, 2002) and for aquaculture products “Fish Shelf life Prediction (FSLP)” program (Nuin *et al.*, 2008). Other studies are focused on the development of management system (Giannakourou *et al.*, 2001) as “Shelf Life Decision System”, which was demonstrated to be an effective tool for food chill chain management leading to reduce the probability of products consumed past after shelf life end.

The main objective of the present work was the validation of the FSLP program to monitoring the quality of the fresh turbot products during transport in an international logistic chain from Spain to Italy.

Materials and methods

FSLP prediction program

Kinetic models were developed in a previous work (Nuin *et al.*, 2008) to predict the microbial spoilage and sensory quality in fresh fish and to evaluate the efficacy of two-time temperature integrator (TTI) labels to monitor shelf life. The models were implemented in a Visual Basic add-in for Excel called “Fish Shelf Life Prediction (FSLP)”. The FSLP software allows prediction in fresh fish products of the growth of spoilage bacteria, sensory quality and TTI responses at constant and fluctuating-temperatures. The program is freely available at AZTI web site <http://www.azti.es/fish-shelf-life-predictions.html>.

Application of FSLP software for monitoring fish logistic chain

For the validation of FSLP software an international fresh turbot logistic chain was selected. This real distribution chain, started with the turbot capture in an aquaculture company in Spain, then the fish was packed into polystyrene boxes and loaded into the first refrigerated truck. The field test involved monitoring the time- temperature of the fish travelling from Spain to Italy into different refrigerated trucks. The whole logistic chain took about 3 days from the capture of the fish in Spain to the local distribution point in Italy. For time-temperature monitoring, 177-T4 data loggers (TESTO, Spain) were placed in different points inside the pallet and were used to record the time-temperature during transport. At the end of the distribution chain all temperature data loggers were collected and send back to AZTI facilities.

In a second step, a simulated field test was performed; turbot samples were stored in climatic chambers (Ibercex V-450, Spain) at the real time-temperature profile. Laboratory studies were carried out to determinate the shelf-life of fresh turbot based on microbiological parameters and sensory tests. For enumeration of total aerobic viable counts, at each sampling time, samples were plate onto plate count agar (PCA, Pronadisa, Spain) and were incubated for 3 days at 31°C. Sensory evaluation was carried out by a 8 trained panel using a 6-point descriptive scale where 9 is absolutely fresh, 6 rejection limit and 4 completed spoiled (ISO 4121:1987). Shelf life determinations were set on the increase of the total aerobic bacteria and the response of a trained sensory panel.

Results and discussion

The FSLP software allows the prediction and the visualization of sensory acceptability, growth of spoilage bacteria in fish products and the response of TTIs at constant and fluctuating temperature conditions. Moreover, the software allows the graphical comparison of experimental, microbiological or sensory raw data with the respective model at either constant or fluctuating temperature. Optionally, the predictions and plots can be saved as an Excel workbook.

The application of the FSLP software for monitoring the fresh turbot logistic chain is showed in figure 1. In this case, the time and temperature profile during the international transport (72 hours) was fluctuating between 0°C and 2°C. The initial level of total bacteria was considered as 10^1 CFU g⁻¹. Moreover, figure 1 included the comparison of experimental microbiological and predicted data, figure shows good correlation between both data.

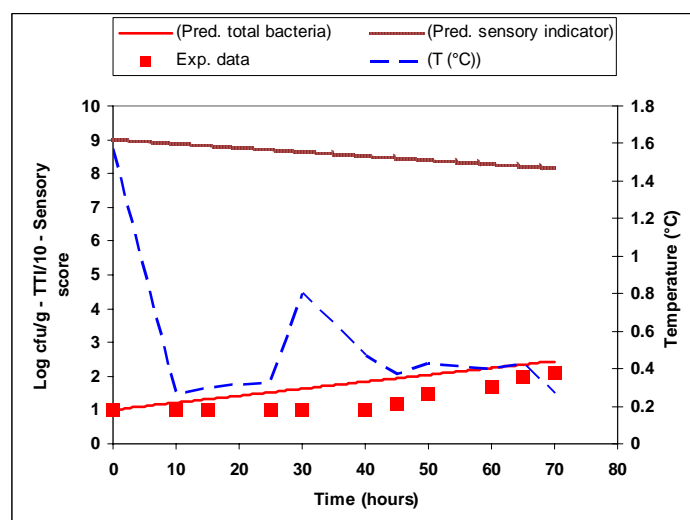


Figure 1. “Fish Shelf Life Prediction Program (FSLP)” software was used to predict the growth of total bacteria and the response of a sensory panel for fresh turbot during the international transport.

In order to determinate the quality of the turbot at the end of this logistic chain in Italy, after 70 hours, the FSLP program was used to predict the growth of total aerobic bacteria and the response of a sensory panel at this time. According to figure 2, the predicted bacterial load was $2.4 \log_{10} \text{CFU g}^{-1}$, that value indicated the high quality of the turbot at the end of this distribution chain. Regarding predicted sensory score, in a scale from 9 (fresh) to 4 (spoiled), the score of 8.2 indicating that the turbot was absolutely fresh at this point of the cold chain. Sensory results (n=8) obtained from the laboratory test agreed with predicted sensory score.

| Predictions for a given time | |
|--|--------------------------------------|
| Write here time in hours and click "Predict" | 70 |
| Predicted total bacterial load | 2.4 $\log_{10} \text{cfu/g}$ |
| Predicted sensory score - According to a trained sensory panel. Rejection limit is 6 in a scale from 9 (fresh) to 4 (spoiled) | 8.2 |
| Predicted colour scores for the TTIs. Rejection limit is below 51.5 for the Fresh Check and over 44 for the Monitor Mark. | 57.1 Fresh Check 4.7 Monitor Mark |
| Notice that the total bacteria load and the Monitor Mark scores increase with time while the sensory scores and the Fresh Check scores decrease! | |

Figure 2. Turbot quality predicted data generated from “FSLP” program. All data were obtained from the time-temperature profile field test along the cold chain logistic transport for 70 hours.

Conclusions

The use of “Fish Shelf Life Predictor” software for quality and safety data simulation can be a valuable tool to a wide variety of companies in fish industry for monitoring the quality in the distribution chain. In the future, the software FSLP will be applied as a tool for the assessment of seafood safety and quality and may be combined with seafood traceability systems. The software will be also used for educational purposes.

Acknowledgements

This work was funded by the Basque Government (Department of Agriculture and Fisheries, and Department of Presidency).

References

- Dalgaard, P., Mejlholm, O., Huss, H.H., 1997. Application of an iterative approach for development of a microbial model predicting the shelf-life of packed fish. *Int J Food Microbiol* 38, 169-179.
- Dalgaard, P., Buch, P., Silberg, S., 2002. Seafood Spoilage Predictor-development and distribution of a product specific application software. *Int J Food Microbiol* 73, 343-349.
- FAO .2003. Fishery statistics. Capture production. Food Agriculture Organization of the United Nations, Rome (Italy). Yearbook 2001. Vol. 92/1, pp. 250-252.
- Josuweit, H., Lem, A. and Lupin, H. 2001. Aquaculture products: quality, safety, marketing and trade. Presented at Conference on Aquaculture in the Third Millennium. Rome (Italy):FAO.
- Giannakourou M., Koutsoumanis K. , Nychas G.J.E. and Taoukis P.S.. 2001. Development and assessment of an intelligent Shelf life Decision System (SLDS) for quality optimization of the food chill chain. *Journal of Food Protection* 64 , pp. 1051–1057.
- ISO 4121:1987. Sensory analysis - Methodology - Evaluation of food products by methods using scales. The International Organization for Standardization. Geneva, Switzerland
- Koutsoumanis, K., 2001. Predictive modeling of the shelf life of fish under nonisothermal conditions. *Appl Environ Microbiol* 67, 1821-1829.
- Nuin M., Alfaro B., Cruz Z., Argartate N. George S. Le Marc Y., Olley J., Pin C .2008. Modelling spoilage of fresh turbot and evaluation of a time-temperature integrator (TTI) label under fluctuating temperature. *Int J Food Microbiol*. 127: 193-199.
- Taoukis, P.S., Koutsoumanis, K., Nychas, G.J., 1999. Use of time-temperature integrators and predictive modelling for shelf life control of chilled fish under dynamic storage conditions. *Int J Food Microbiol* 53, 21-31.

Probabilistic modeling of *Listeria monocytogenes* behaviour in diced bacon along the manufacture process chain.

E. Billoir¹, J.-B. Denis¹, N. Commeau^{2,3}, M. Cornu², and V. Zuliani⁴

¹ INRA, UR341 Mathématiques et informatique appliquées, F-78350 Jouy en Josas (elise.billoir@jouy.inra.fr)

² Afssa, Microbiologie quantitative et estimation des risques, 23 av. du Général de Gaulle, F-94706 Maisons-Alfort Cedex (m.simon-cornu@afssa.fr)

³ UMR 518, Mathématiques et Informatique Appliquées, AgroParisTech/INRA, 16 rue Claude Bernard F-75005 Paris, France

⁴ IFIP, Institut de la Filière Porcine, Pôle Viandes Fraîches et Produits Transformés, 7 av. du Général de Gaulle, F-94704 Maisons-Alfort Cedex (veronique.zuliani@ifip.asso.fr)

Abstract

To assess the impact of the manufacturing process on the fate of *L. monocytogenes*, we built a probabilistic model describing successively the different steps of the process. The model was actually designed as a hierarchical Bayesian network leading to the elicitation of human expertise. Contamination evolution was modelled in the adequate units (breasts, dices, then packaging units through the successive process steps). The use of probabilistic modeling allowed taking into account both the process intrinsic variability and parameter variability or uncertainty. Global statistics were deduced, diagrams showing the variability were drawn, and changes on the process were tested to look at the consequences on the final product.

Keywords

Process chain modeling; Bayesian network; *Listeria monocytogenes*; diced bacon;

Introduction

In France, 50% of the pork belly is transformed into diced bacon, and this production increases every year. The most recent data show that the *L. monocytogenes* prevalence for pork pieces decreased from 2001 to 2004 to reach about 25%. This level of prevalence remains however alarming when the pork pieces are used for the manufacture of raw meat products such as diced bacon. Indeed, during the diced bacon manufacturing, there is no physical or chemical treatment sufficiently drastic to eliminate the possibly present population of *L. monocytogenes*. Moreover diced bacon is occasionally consumed raw by 14% of French people (AFSSA, 2009).

In this work, we propose a basic model for the diced bacon process chain, from incoming breasts to outgoing packaging units, in order to evaluate the impact of each step on the contamination. Following the principles of Nauta's MPRM (2001), we adapted the model to the studied process, and to the specificity of the product, that is its solid and heterogeneity characteristics. Indeed, bacteria were assumed to be located only on the surface of the breasts, with a higher affinity for the lean areas than for the fat ones. By the mean of simulations, we exemplified the potential of the model. Simulations were performed with both a baseline calibration and alternative scenarios, in order to assess the impact of changes in the process and of accidental events.

Material and methods

Overview of the model

The model we built to study the behaviour of bacteria during the diced bacon manufacture process chain is a sequence of various steps: arrival, brining-and-tumbling, steaming, dicing and finally packaging. In the real process chain, storage steps occur between these steps. However, basing on reasonable assumptions concerning physico-chemical conditions and duration of the different storage steps, the bacterial contamination is expected not to evolve during them. Consequently we neglected the storage steps in the modeling, to focus on the other steps. During the process chain, the observation scale evolves, so we successively

followed the contamination of the breasts, the dices, then the packaging units. At every step, the contaminations were assumed to only depend on the state of the units at the end of the previous step and on modeling parameters. Thus we built our model as a Bayesian network. We introduced process intrinsic variability and, when available, parameter variability or uncertainty. In the diced bacon process chain, the batches considered at the different steps do not always match, they can be divided from one step to the following and they can overlap. For instance, a tumbling batch can be divided into several steaming batches and a dicing batch can gather several steaming batches. However in this study it was decided to follow-up the fate of tumbling batches of 1000 breasts, without overlaps later in the process.

Successive steps

(1) At **arrival**, *L. monocytogenes* contamination (Colony Forming Unit) on every breast was assumed to follow a conditional Poisson distribution of parameter equal to the breast concentration times the breast mass. (2) During the **tumbling-and-brining** step the breasts gathered in a batch were assumed to swap bacteria during the tumbling step. A part of the bacteria were assumed to be released from the breasts during this step. Then some bacteria were assumed to be lost because of staying hanging on the tumbler surface, whereas the others were assumed to be reallocated on the breasts of the tumbling batch. These two events (release and loss) were simulated by the mean of binomial drawings. Finally, the reallocated bacteria were distributed to the batch breasts using a multinomial distribution, in order to ensure the conservation of bacteria. Besides, the breasts were supposed to absorb the brine, so that their mass slightly increased. (3) To model the **steaming** step we used classical deterministic predictive microbiology tools for inactivation. (4) For the **dicing** step, we had to estimate how many dices would result from each breast. We began with geometrical considerations, assuming that every breast had a parallelepiped shape with dimensions proportional to the cubic root of their volume. The bacteria of each breast were shared between the resulting dices by a multinomial drawing, with allocation probability proportional to the exterior area, weighted by a fat/lean affinity ratio. Indeed, the bacteria are known to have a lower affinity with fat areas than with lean areas and we considered that one of the main faces of the breast was fat. Also we assumed that an additional contamination can come from the dicing machine, where bacteria can grow in some surfaces inaccessible for cleaning. (5) To model the **packaging** step, we cumulated the dice contaminations (CFU) by packaging units.

Baseline calibration of the model

To calibrate the model, the parameter estimation was carried out (i) from data given by partner business operators for the contamination at arrival and for the process parameters, (ii) from data given by IFIP for the geometrical parameters, (iii) from the literature for the inactivation parameters or (iv) basing on expert's opinions.

Alternative scenarios

In addition to the baseline calibration, we tested the following alternative scenarios: (S1) packaging units of 200g instead of 100g in the baseline, (S2) dice section of 5 mm instead of 8 mm in the baseline, (S3) steaming at an equivalent temperature of 50°C instead of 45°C in the baseline, (S4) initial contamination ten times higher than baseline, and (S5) initial contamination one hundred times higher than baseline.

Results and discussion

Results

As an example, Figure 1 shows the results of one simulation performed using the baseline calibration. The contamination distribution after brining-and-tumbling was narrower than after arrival. During the brining-and-tumbling step, the contamination was homogenized within the breasts. Then steaming reduced the contamination. This simulation predicted that a large proportion of dices were not contaminated by *L. monocytogenes*. In the packaging units,

L. monocytogenes prevalence was not negligible, however the contamination level remained low.

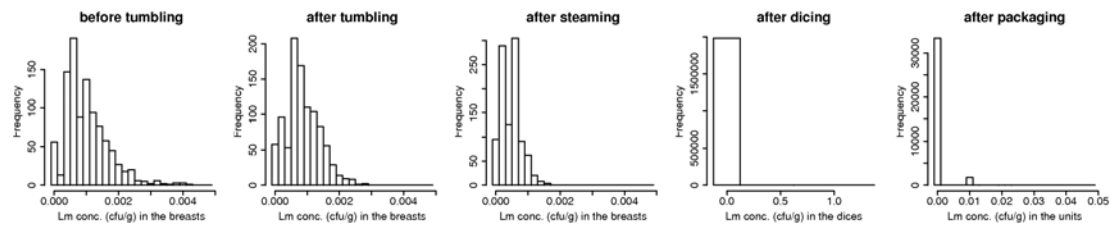


Figure 1: Results of one simulation. Bacterial concentration (CFU/g) after the five steps considered. First three graphs: on breasts, fourth graph: on dices, fifth graph: in packaging units.

Looking at the result of one simulation allows to qualitatively comment on every step. However, because our model is probabilistic, every simulation is different and numerous simulations were necessary to describe the baseline model outputs. According to the proposed model and its baseline calibration, every tumbling batch of 1000 breasts lead to 1 986 000 [1 976 000-1 996 000] dices and then 35 910 [35 610-36 210] packaging units. Figure 2 shows the results of 10,000 simulations. For each process step, the median simulation results is plotted (solid lines), as well as the 2.5% and 97.5% quantiles of the simulation results (short-dashed lines), corresponding respectively to low and high contamination levels. At every step the simulation results were quite close, indicating a low variability between simulations. In the median simulation results, at arrival about 5% of the breasts were uncontaminated by *L. monocytogenes*, 50% of the breasts had no more than 0.001 CFU/g, and 100% of the breasts had no more than about 0.005 CFU/g. After brining-and-tumbling, 100% of the breasts had no more than about 0.003 CFU/g. The steaming step reduced *L. monocytogenes* contamination so that 50% of the breasts had no more than 0.0005 CFU/g (that is 1 CFU on a breast), and 100% of the breasts had no more than about 0.002 CFU/g. In the dices, with the baseline calibration, the maximum contamination observed over all the simulations was about 1.2 CFU/g (that is 2 CFU on a dice) and 99% of the dices were predicted to be uncontaminated by *L. monocytogenes*. After the packaging step, the maximum contamination observed over all the simulations was about 0.04 CFU/g (that is 4 CFU in a packaging unit) and 95 [90-95]% of the packaging units were predicted to be uncontaminated by *L. monocytogenes*.

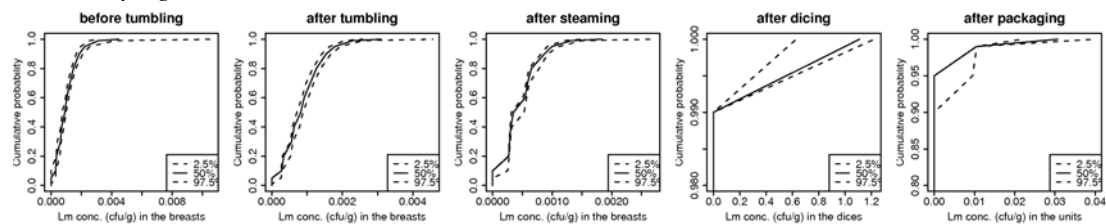


Figure 2: Cumulative distributions of the bacterial concentration (CFU/g) after the five steps already considered in Figure 1. Solid lines correspond to simulation median, long-dashed lines correspond to simulation 95% interval. The cumulative distributions must be interpreted as the repartition of items during a given step, and their variation.

The results obtained with the five scenarios alternative to the baseline calibration are summarized in Table 1. In the first three alternative scenarios, we tested changes in the process at the steaming, dicing or packaging steps. The contamination of the incoming breasts was not modified compared to the baseline calibration. Regarding the outgoing packaging units, the increase in packaging unit weight (S1) and the decrease in dice section (S2) reduced the model variability. For (S1), the 95% contamination is about $5 \cdot 10^{-3}$ UFC/g that is 1 CFU in 200g instead of $1 \cdot 10^{-2}$ for the baseline calibration (in the 2.5% most pessimistic simulations), that is 1 CFU in 100g. With the scenario (S2), the 95% contamination is about $1 \cdot 10^{-2}$, that is 1 CFU in 100g, in all the simulations, not only in the pessimistic ones. Indeed, in the scenario

(S2), much more dices were produced, and the packaging units gathered more dices than in the baseline calibration, so the contamination was homogenized within the packaging units of a batch. With the scenario (S3) the 95% contamination of the packaging units is reduced to 0. So an increase of 5°C in the steaming temperature seems to drastically inactivate the bacteria. The last two tested scenarios concerned the breast contamination at arrival. Multiplying by 10 this initial contamination (S4) lead to a 95% concentration about 2.10^{-2} , that is 2 CFU in 100g. However the median contamination of the packaging units remained null, in contrast to the scenario (S5) (one hundred times higher initial contamination), where almost all the packaging units were contaminated.

Table 1: *L. monocytogenes* 5%, median and 95% concentration (median [95% extreme] simulation) in 10^{-3} CFU/g on the breasts at arrival (process chain inputs) and in the packaging units (process chain outputs), according to the alternative scenario.

| Scenario | Incoming breasts | | | Outcoming packaging units | | |
|----------|------------------|------------------|---------------|---------------------------|------------|---------------|
| | 5% | median | 95% | 5% | median | 95% |
| Baseline | | | | | | 0 [0-9.5] |
| S1 | | | | | | 5.0 [5.0-5.1] |
| S2 | 0 [0-0.29] | 0.91 [0.73-0.99] | 2.2 [1.9-2.6] | 0 [0-0] | 0 [0-0] | 9.7 [9.6-9.8] |
| S3 | | | | | | 0 [0-0] |
| S4 | 5.3 [4.8-5.7] | 9.1 [8.6-9.6] | 17 [15-20] | | | 20 [19-20] |
| S5 | 62 [59-65] | 90 [86-94] | 170 [150-190] | 10 [10-11] | 42 [41-47] | 90 [85-95] |

Discussion

In this study, we simplified the step combination, since we followed tumbling batches without considering overlapping between them during the process. In reality, the step chain is complicated by practical constraints, both in terms of time and in terms of batch overlapping. In order to refine the step combination, it would be necessary to develop a process chain manager model, taking into account open stocks and carrying capacities at every step. To date, we neglected bacterial growth, arguing that growth was not possible during the process, given the environmental physico-chemical conditions and durations of the successive steps. However, if we want to simulate a storage step accidentally long at an accidentally high temperature, bacterial growth could occur. Also if we want to extend the model to the post-process storage until consumption, by considering further steps such as refrigerated transport and home storage, a growth model would be necessary, and potential competition between *L. monocytogenes* and the lactic acid bacteria should be considered (see Cornu et al., same conference). As this model enables us to compare various scenarios, it could be used to update the optimisation of the monitoring (see Commeau et al., same conference) and for re-engineering.

Conclusions

In this work, we propose a model for the diced bacon process chain, from incoming breasts to outcoming packaging units, in order to evaluate the impact of each step on the contamination.

Acknowledgements

This work was supported by a grant from the Agence National de la Recherche (ANR) (France), as a part of the Quant'HACCP project.

References

- Nauta M.J. (2001) A Modular Process Risk Model Structure for quantitative microbiological risk assessment and its application in an exposure assessment of *Bacillus Cereus* in a REPFED. RIVM Report, Bilthoven, 100 pp.
- Cornu M., Billoir E., Bergis H., Beaufort A. and Zuliani V. Modeling microbial competition in foods. Application to the behaviour of *Listeria monocytogenes* and lactic acid flora in diced bacon. *Submitted to the same conference.*
- Commeau N., Parent E., Billoir E., Zuliani V. and Cornu M. Modelling contamination to build a sampling plan : application to French diced bacon industry and *Listeria monocytogenes*. *Submitted to the same conference.*

Detection and identification of Acid-Lactic Bacteria in an Isolated System with Near-Infrared Spectroscopy and Multivariate regression modeling

Cámara-Martos, F., García-Gimeno, R.M., Zurera, G., Pérez-Rodríguez, F.

Departamento de Bromatología y Tecnología de los Alimentos, Universidad de Córdoba, Campus Rabanales, Edif. Darwin-Anexo, 1014 Córdoba, SPAIN

Introduction

Food industry is increasingly concerned in developing and applying rapid and non-destructive methods to offer safer foods and high quality foods to consumers.

In the last years, Fourier transform Near-Infrared (FT-NIR) has been widely used to determine food quality based on spectrum (Lopes et al. 2004). Besides this, FT-NIR has been proposed as an innovative and promising non-destructive rapid method capable to detect and identify microorganisms in foods (Alexandrakis et al, 2009); however, little progress has been made to date.

Lactic-Acid Bacteria (LAB) is a wide group which is identified as main responsible for deterioration in vacuum ready-to-eat meat (von Holy et al., 1991; Lambert et al., 1991). Indeed, spoilage flora is a concern for food industry because of the huge economic loss associated to foods deterioration. In this study, the use of FT-NIR spectroscopy in conjunction with multivariate regression modeling was evaluated for the rapid detection and identification of BAL species in water-based matrices.

Material and Methods

Test suspension

Different LAB species (*Leuconostoc mesenteroides*, *Latobacillus sakei*, and *Lactobacillus plantarum*) were selected from the Spanish Type Culture Collection (CECT). The strains were maintained at -18°C in cryovials containing bead and cryopreservative (Microbank™). Two days before the experiment, a bead of each strain was transferred to a tube containing 10 ml of Tryptone Soya Broth (TSB, Oxoid, UK) and incubated at 37°C for 24 h. Finally, 1ml of the initial subculture was pipetted into a tube containing 10 ml of TSB, and incubated at 37°C until the early stationary phase was reached (18 h). Cells were harvested by centrifugation (Micro 7; Fisher Scientific, Pittsburgh, Pa.) at 4000 rpm for 10 min and washed three times in solution saline (0,85 %). Cell pellets were re-suspended in Saline Solution and 10-fold dilutions in Saline Solution were made to obtain cells suspensions at different concentrations (~9, 8, 7, 6, 5, 4 and 3 log cfu/ml).

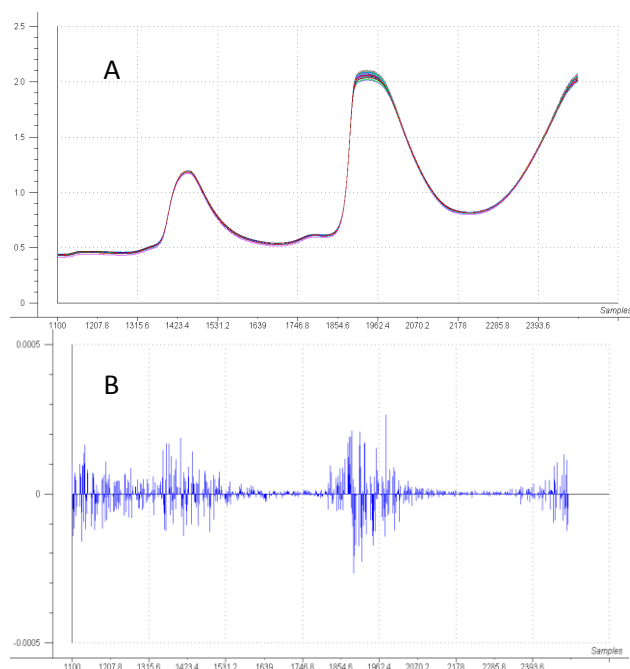


Figure 1. FT-NIR reflectance-transmittance spectra (A) and second derivative spectra (B) of different Lactic Acid Bacteria strains: *Leuconostoc mesenteroides*, *Latobacillus sakei*, and *Lactobacillus plantarum*

FT-NIR measurements

All FT-NIR spectra were recorded with a FT-NIR Perkin Elmer Spectrum One NTS (Shelton, Conn.). The FT-NIR spectra were recorded from 1100 to 2500 nm at intervals of 0.275 nm. Spectra were obtained analyzing aliquots of the test suspension for different LAB species at different concentrations ($\sim 10^9$ - 10^3 cfu/ml).

Data treatment and statistical analysis

Before statistical analysis, the FT-NIR reflectance-transmittance data were separately treated by baseline corrected, smoothed by the Savitsky-Golay smoothing function with 20 points, and first and second derivatives by difference equation with Unscrambler® v. 7.8 (Camo Technologies, Woodbridge, NJ). These three transformed-spectra sets were then used to classify the samples by applying Principal Component Analysis (PCA), PCA regression and Partial least Square (PLS) regression which was performed by using Unscrambler® v. 7.8 (Camo Technologies, Woodbridge, NJ).

Results

FT-NIR Spectra of Bacterial Strains

Figure 1 shows the characteristic absorption spectra of the different BAL strains evaluated. As the bacterial strains showed similar basic FT-NIR spectral patterns (Figure 1A), mathematical transformations were required to use the FT-NIR data for qualitative and quantitative analysis. Second derivative transformation (Figure 1B) of spectra extracted and highlighted distinct features among the bacterial strains, especially in the information-rich region of 1490-2000 nm. Using the Savitzky-Golay second derivative (optimal window size was 20 points) allowed the extraction of useful band information and reduced spectral noise.

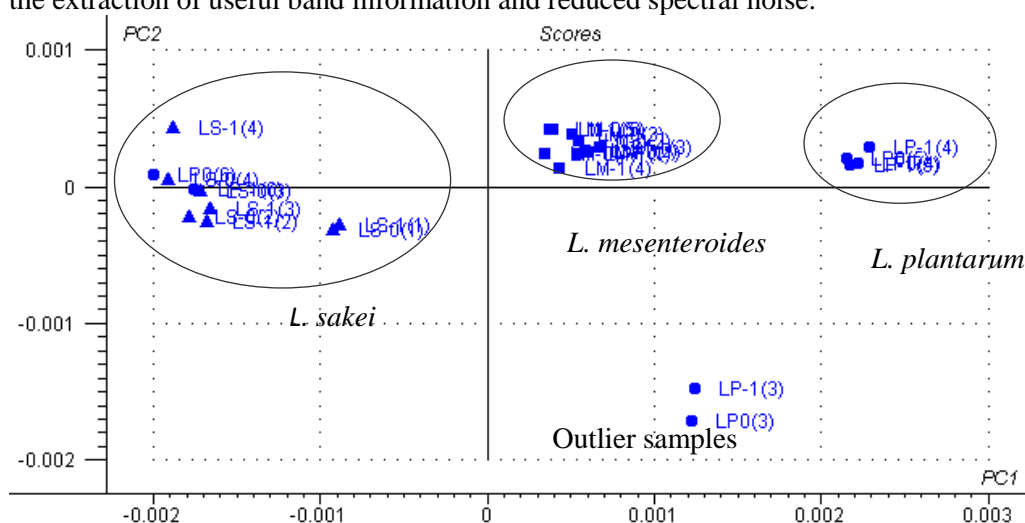


Figure 2 PC1 versus PC2 scores (PCA analysis) plot of the second-derivative transformed spectral data over the wavelength range 1490-2000 nm.

PCA analysis and Regression Models

PCA of the whole data set revealed that the best separation between bacterial strains was found using second-derivative transformed data in the wavelength 1490-2000 nm and using spectra of samples at high bacterial concentration (10^8 - 10^9 cfu/ml). The PCA explained 87% of the total variability using the first seven principal components (PC), whereas PC1 and PC2 were particularly representative of the spectral information and accounted for 70% of the total variance. The scores plot of PC1 versus PC2 displayed distinct clustering for the bacterial strains (see Figure 2). Figure 2 reveals that each bacterial strain formed a well-defined cluster. *L. mesenteroides* clustered separately from all other strains on the left-hand side, except for one sample which was misclassified on the clustering formed by *L. sakei*. The *L. sakei* clustering was formed on the right-hand side, close to *L. plantarum*, but there was not

overlapping between both. Besides, it was found two outlier samples belonging to *L. plantarum* which were removed for the PCA regression model (See Figure 2). These results strongly suggest that differentiation between the different species in isolated systems may be possible on the basis of their near-infrared spectra.

The loadings obtained from the PCA analysis for the different wavelengths studied indicated that 1100-1200 nm and 1900-2000 nm regions were the bands most contributed to bacterial variance. These regions are related to water absorption bands. Examination of the loading weights, in Figure 3, indicated which FT-NIR frequencies contribute significantly to the variation in the selected data set (1490-2000 nm). In Figure 3, it could be seen a great contribution of the water absorption band (1920 nm) which could also be an important interference source affecting the model performance. Besides this, other significant bands associated to microorganism presence could be observed around 1520 nm, corresponding with protein content, and around 1930 nm, related with C=O bond which can also be linked to microbial structures.

A regression model to differentiate the bacterial strain was performed with only samples at high bacterial concentrations based on the most important PCs generated in PCA analysis (Principal Component Regression, PCR).

The PCR model obtained a high correlation coefficient ($R = 0.98$). When the concentration range was extended to include 10^6 cfu/ml, values previously not considered, the PCR model generated lost predictive ability and the correlation coefficient dropped up to 0.6, which indicates that the differentiation capacity of bacterial strains is better performed at high concentration.

PCA analysis was also carried out to determine the potential of NIR to detect different concentration levels within each organism for enumeration purposes. The whole data set for each bacterial strain was analyzed separately and in whole, and the category variable was the dilution factor (0-6) which corresponded with concentration levels between 10^9 - 10^3 cfu/ml. However, results did not show any clusters for the six dilution factors.

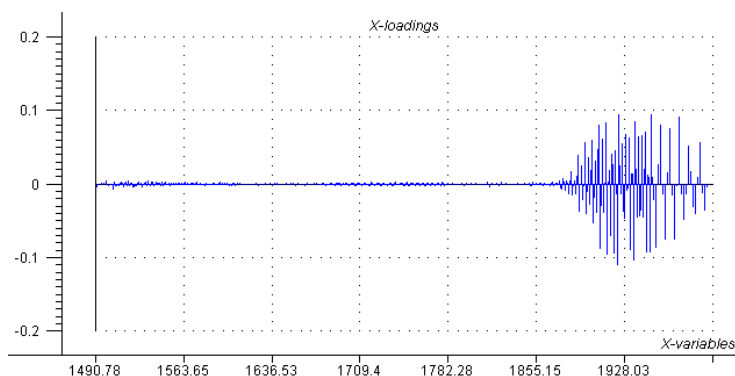


Figure 3. Loadings plot showing PC1, accounting for 60 % of the total variability in the PCA analysis performed on second – derivative transformed data in the wavelength 1490-2000 nm for spectra of samples at high bacterial concentration (10^8 - 10^9

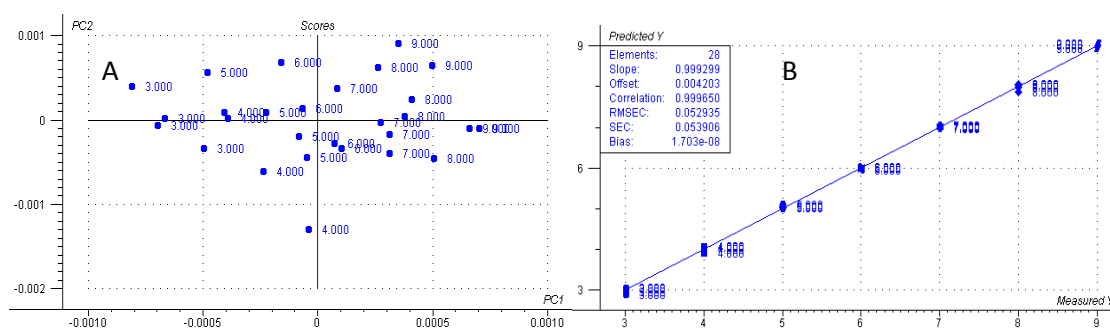


Figure 4. PC1 versus PC2 scores (PLS regression) plot of the second-derivative transformed spectral data over the wavelength range 1490-2000 nm (A) and correlation plot of measured concentration level vs. visible/near infrared predicted (B).

When a PLS regression model was developed to predict concentration level for each bacterial strain based on the whole data set, again results did not show clear clustering of dilution

factors (~concentration levels), however, it could be observed that higher dilution factors (lower concentrations) were situated at the left-hand side (low scores) in the PC1 versus PC2 plot (Figure 4A), while, lower dilution factors (higher concentrations) were found at the right-hand side (high scores). Thereby it may be stated that the higher concentration, the higher scores. As consequence of this fact, the predicted values derived from the PLS regression model showed good correlation with the measured concentration levels ($R=0.99$), as shown in Figure 4B.

Results clearly demonstrated the potential of FT-MIR spectroscopy as a tool for microbial species identification and classification; however, further investigation should be carried out so that this technique can be used on a food system and more efficient methods and mathematical models can be developed to detect and differentiate bacteria specie.

References

- Lamber, A.D., Smith, J.P. and Dobris, K.I. 1991. Shelf-life extension and microbiological safety of fresh meat- a review. *Food Microbiol.* 8, 267-297.
- Von Holy, a., Cloete, T.E. and Holzapfel, W.H. 1991. Quantification and characterization of microbial population associated with spoiled, vacuum-packed Vienna sausages. *Food Microbiol.* 8, 95-104.
- Lopes, J.A. Costa, P.F. Alves, T.P., and Menezes, J.C. 2004. Chemometrics in bioprocess engineering: process analytical technology (PAT) applications. *Chemometr. Intell.Lab. Syst.* 74, 269–275.
- Alexandrakis, D., Downey, G., and Scannelli, A.G.M. 2009. Detection and identification of Bacteria in an isolated system with near-infrared spectroscopy and multivariate analysis. *J. Agric. Food Chem.* 56, 3431–3437

Empirical meta-modeling of *Salmonella* Typhimurium at the farm level of the pork production chain

I. Soumpasis and F. Butler

School of Agriculture, Food Science and Veterinary Medicine, University College Dublin, Belfield, Dublin 4, Ireland (ilias.soumpasis@ucd.ie)

Abstract

In previous work a deterministic and a stochastic epidemic model for the compartment level of the pig farm were built. However, the stochastic model needs a lot of resources and may not be very useful as is for the risk managers and policy makers. Thus, an empirical meta-modeling approach is proposed fitting regression models to the results of the stochastic model in order to predict the prevalence of the pathogen at slaughter age. For this reason the stochastic model was run for different starting conditions of infection (SCI: 0.25% to 100% infectious pigs) and different population sizes of the compartments (TPC: 200 to 400 pigs). In a second stage the data that was produced from the stochastic model was used for the generation of secondary simpler empirical models. The results suggest that this approach can provide relatively good models for the decision makers, which are more useful and easier to use. It is stressed however that the parameterization of the primary stochastic model is a critical issue, because the secondary models simply reproduce the results of the primary model and cannot correct any underlying problems that may exist.

Keywords

Pigs, Pork, Farms, *Salmonella*, Typhimurium, Stochastic, Epidemiology, Model, Regression, Meta, Prevalence

Introduction

Human Salmonellosis is the most common foodborne disease. In previous work a stochastic mathematical model was built and run for different compartmental sizes and different starting conditions of infection in order to estimate their effect on the probability of the disease extinction, on the mean age that extinctions occur and on the prevalence of different risk groups at slaughter age. However, the stochastic model needs a lot of resources regarding computational time and storage. Moreover, it is somehow difficult to run it as is, except if a graphical user interface is built.

The objective of this work was to build simpler secondary mathematical models using different types of regression that can predict the incidence and the prevalence of the pathogen at slaughter age. In this way decision makers can use these secondary models to test and decide strategies on a more quantitative basis.

Materials and Methods

The primary stochastic model, which was developed in the first stage, was consisted by 5 classes as shown at figure 1. The S represents the susceptible class, the HI and LI the two infectious classes (High and Low Infectious), the C the carrier class and the Im the immune class. The classes of pigs were categorized in three “risk groups” of cecal-, culture- and sero-positive pigs. Cecal-positive pigs were considered to be pigs in the HI and LI classes, which carry the pathogen in the intestinal contents, culture-positive pigs in HI, LI and C classes, which carry the pathogen in the internal organs including the intestinal contents, and sero-positive pigs in the C and Im classes, which carry antibodies against the pathogen (Soumpasis and Butler, 2009). The cecal- and culture-positive risk groups may pose a risk of introducing the pathogen into the slaughterhouse, while the sero-positive risk group is frequently used for the categorization of the farms regarding the load of *Salmonella*.

The stochastic model utilized the τ -leap method for demographic stochasticity and it is summarized in table 1 (Soumpasis and Butler, 2009). In order to build the stochastic model, all the possible events should be described in the first place: The move of the pigs from the Susceptible to the High Infectious (high infection) and to the Low Infectious class (low infection), the recovery of the High Infectious (HI) class, the recovery of the Low Infectious (LI) class, the recovery for the Carriers (C) class and the loss of immunity (move from Immune (Im) class to Susceptible class). A time step was defined as one day (as in the deterministic model), in order to calculate the number of events to happen in this time step. For small time steps the number of events in each time step is given approximately by a Poisson distribution (Keeling & Rohani, 2007).

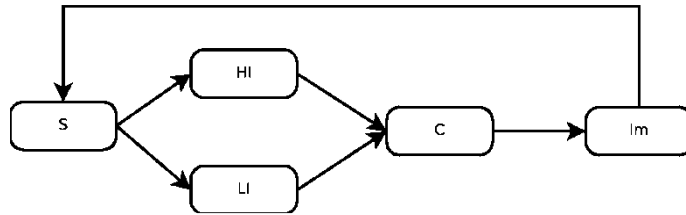


Figure 1. Conceptual representation of the model (Soumpasis and Butler, 2009).

The model was run for 113 days, which corresponds to the average day that pigs are harvested. Different Starting Conditions of Infection (SCI: 0.25-100%) and Total Population sizes of Compartments (TPC: 200-400pigs) were evaluated. For each combination of SCI and TPC, 50 iterations were run. This resulted in a large table of 139,400 rows and 9 columns. This table was used in a second stage for fitting the secondary regression models.

Table 1: Events of the model and calculation of the number of events per time step using the “ τ -leap method” (Soumpasis and Butler, 2009).

| Name | Number of events | Font style |
|------------------|--|--|
| High Infection | $M1 = \text{Poisson}(\tau * [\beta * S * (HI + \epsilon * LI) / N])$ | $S \rightarrow S - M1, HI \rightarrow HI + M1$ |
| Low Infection | $M2 = \text{Poisson}(\tau * [\beta * S * (HI + \epsilon * LI) / N])$ | $S \rightarrow S - M2, LI \rightarrow LI + M2$ |
| Recovery of HI | $M3 = \text{Poisson}(\tau * [\gamma * HI])$ | $HI \rightarrow HI - M3, C \rightarrow C + M3$ |
| Recovery of LI | $M4 = \text{Poisson}(\tau * [\gamma * LI])$ | $LI \rightarrow LI - M4, C \rightarrow C + M4$ |
| Recovery of C | $M5 = \text{Poisson}(\tau * [\Gamma * C])$ | $C \rightarrow C - M5, Im \rightarrow Im + M5$ |
| Loss of Immunity | $M6 = \text{Poisson}(\tau * [\kappa * Im])$ | $Im \rightarrow Im - M6, S \rightarrow S + M6$ |

Exponential regression using non-linear least squares method was applied for each class and risk group in question. Given that there were two trends in each graph, one decreasing for low SCI and one increasing for higher SCI, two regressions were made for each of the trends. The limit for which the data was divided in these two parts was calculated from the results of the stochastic model. Bootstrapping of the models was tried, however given the increased number of observations, uncertainty was very small. Moreover, the 95% CI of bootstrap coincided with the 95% CI provided by the standard error of the parameters of the original fitted regression model.

The model and the scenario analysis were written in Python programming language v.2.5.1, using the scientific libraries Scipy/Numpy, for numerical calculations. Optimizations were made using Pyrex python extension for translating the main algorithm to compiled x86_64 C shared library and using parallel computing with Ipython. For the statistical analysis and the fitting of the secondary meta-models, R statistical language version 2.9.1 (R Development Core Team, 2009) was used. For bootstrapping of the non linear least squares models, R package boot (Canty & Ripley, 2009; Davison & Hinkley, 1997; Venables, & Ripley, 2002) was used.

Results and discussion

The regression models that were fitted to the primary data of the stochastic model for the HI and LI classes and the risk groups of culture- and sero-positive pigs are presented in equations 1 to 4. Although, TPC had a significant effect on the probability of extinction of the infection during the fattening period (Soumpasis and Butler, 2009), the effect of TPC on all the classes and risk groups in question was insignificant.

The predicted values of the models along with the 95% CI of uncertainty and variability are plotted in figure 2. From figure 2 it is apparent that uncertainty is very small due to the large number of observations. The standard error of the parameters was very small, resulting to this very low uncertainty. On the other hand, variability that was calculated from the standard error of the model was substantial and the 95% describe relatively well the data produced from the experiment.

$$HI = \begin{cases} \text{Normal} (0.966 - 0.188 * SCI, 3.415), & \text{for } SCI \leq 5.5 \\ \text{Normal} (-0.406 - 0.037 * SCI, 0.294), & \text{for } SCI > 5.5 \end{cases} \quad (1)$$

$$LI = \begin{cases} \text{Normal} (1.804 - 0.066 * SCI, 3.622), & \text{for } SCI \leq 6.2 \\ \text{Normal} (0.875 - 0.011 * SCI, 1.234), & \text{for } SCI > 6.2 \end{cases} \quad (2)$$

$$\text{Culture} - \text{positive} = \begin{cases} \text{Normal} (3.335 - 0.273 * SCI, 17.18), & \text{for } SCI \leq 2.1 \\ \text{Normal} (3.699 - 0.004 * SCI, 4.671), & \text{for } SCI > 2.1 \end{cases} \quad (3)$$

$$\text{Sero} - \text{positive} = \begin{cases} \text{Normal} (3.609 - 0.149 * SCI, 17.24), & \text{for } SCI \leq 4.2 \\ \text{Normal} (4.087 - 0.0016 * SCI, 3.929), & \text{for } SCI > 4.2 \end{cases} \quad (4)$$

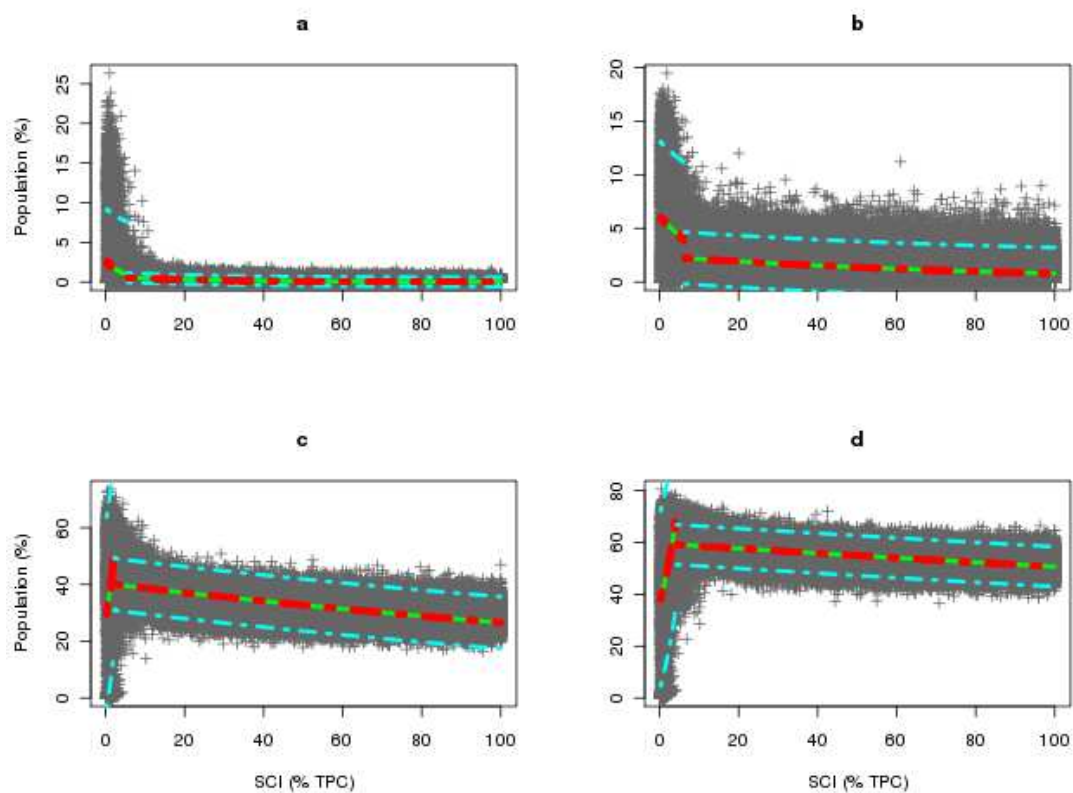


Figure 2. Scatter plot of the results of the stochastic model and the predicted prevalence (green continuous line) of the meta-model with the 95% confidence intervals of the uncertain-

ty (red dashed line) and the variability (cyan dashed line) of the Infectious classes (a) HI and (b) LI and the risk groups (c) Culture- and (d) Sero-positive (at slaughter age) over Starting Conditions of Infectious (SCI) as a percentage of the Total Population of Compartment (TPC).

The variability is bigger for the increasing part of the equations because for low SCI, there are many cases of early extinctions that could result to zero cases of all the classes and risk groups. On the other hand, starting with low SCI can lead to a low propagation rate at the beginning of the fattening period, when the infection does not go extinct. In this way there will be a large pool of pigs in the susceptible class that can get infected in the last days increasing dramatically the prevalence of the classes and risk groups of pigs up to 80% in some cases. For higher SCI, smaller variability was observed because of the lack of early extinctions. In this way the infection is established in all the cases and the prevalence of the classes is more predictable. In these cases, when extinctions are observed, these are late extinctions. Their effect on the variability of the risk groups of culture- and sero-positive is very low, because the classes that constitute these risk groups occupy a long period in the infection cycle. Although these models are capable of predicting the prevalence and the standard deviation for different SCI for the day of harvest, given that pigs were infected the first day of the fattening period, further work is ongoing to make models that can predict the prevalence for different ages of introduction of the pathogen in the compartment. Regression, non-linear least squares, splines, polynomials (simple and fractional) or even neural networks will be tested, in order to automate this procedure and provide with robust relationships of expected prevalence of risk groups and classes of pigs with SCI.

Conclusions

The secondary meta-models that were developed can predict in a good extent the prevalence of the risk groups and classes of interest, given the starting conditions of infection (SCI). They can describe efficiently the variability of the procedure, using the standard error of the model. The uncertainty of the models was very small, given the large number of observation due to the many iterations of the stochastic model. However, it has to be kept in mind, that whatever inadequacy was introduced in the parameters of the primary stochastic model will affect the results of the secondary models. Thus, it is proposed, that limited targeted experiments should take place in a first phase that they can assure parameterization and development of a stochastic model that is as accurate as possible. In a second phase, creation of data running the stochastic model and fitting of secondary regression type meta-models can provide easy to use decision tools for risk managers and policy makers.

Acknowledgment and Disclaimer

We acknowledge the 6th EU framework Integrated Project Q-Porkchains that has been the major source of information for this paper. The content of the paper reflects only the view of the authors; the Community is not liable for any use that may be made of the information contained in this paper.

References

- Canty A. and Ripley B. (2009). boot: Bootstrap R (S-Plus) Functions. R package version 1.2-36.
- Davison, A. C. & Hinkley, D. V. (1997) Bootstrap Methods and Their Applications. Cambridge University Press, Cambridge. ISBN 0-521-57391-2
- Keeling, M. J. & Rohani, P. (2007). *Modeling Infectious Diseases*. Princeton University Press. ISBN 978-0-691-11617-4.
- R Development Core Team. R (2009). A Language and Environment for Statistical Computing. R Foundation for Statistical Computing, Vienna, Austria, 2008.
- Soumpasis I. & Butler F. (2009). Development and application of a stochastic epidemic model for the transmission of *Salmonella Typhimurium* at the farm level of the pork production chain. *Risk Analysis: An International Journal*. DOI: 10.1111/j.1539-6924.2009.01274.x
- Venables, W. N. & Ripley, B. D. (2002) *Modern Applied Statistics with S*. Fourth Edition. Springer, New York. ISBN 0-387-95457-0).

Memory embedded structures of Artificial Neural Networks: power and limitations in Predictive Modelling in Foods

V.P. Valdramidis¹, Georgios N. Yannakakis², Patrick J. Cullen¹, A.H. Geeraerd³, and J.F. Van Impe⁴

¹ School of Food Science & Environmental Health, Dublin Institute of Technology, Cathal Brugha Street, Dublin 1, Ireland (vasilis.valdramidis@dit.ie)

² IT University of Copenhagen, Centre for Computer Games Research, Rued Langgaards Vej 7, 2300 Copenhagen S, Denmark.

³ Division of Mechatronics, Biostatistics and Sensors (MeBioS), Department of Biosystems (BIOSYST), Katholieke Universiteit Leuven, W. de Croylaan 42, B-3001 Leuven, Belgium.

⁴ Chemical and Biochemical Process Technology and Control (BioTeC), Department of Chemical Engineering, Katholieke Universiteit Leuven, W. de Croylaan 46, B-3001 Leuven, Belgium (jan.vanimpe@cit.kuleuven.be)

Abstract

The quantitative evaluation of (adaptive) microbial responses in food products undergoing heat processing is imperative for assessing the efficacy of such heat treatment steps. Different artificial neural network (ANN) models are constructed. A Feed Forward (FF) and a multi-step ahead Feed Forward with a Delay (FFD) that can embed microbial memory. Their input vectors were the time t_k and temperature rate $(dT/dt)_k$, while for the latter the microbial load delayed with one time unit, $\log N_{k-1}$ was also included. The predictive capability of the ANNs that had t_k as an input vector was influenced by the chosen increments of t_k therefore another multi-step ahead FFD network where the input vector of time has been replaced by the vector of temperature T_k was studied. This network appeared to be more appropriate for performing accurate microbial predictions that did incorporate the induced microbial phenomena for the off-line microbial data in hand.

Introduction

The microbial safety of thermally processed foods relies on the inactivation of pathogenic microorganisms during heating. Possible induction of an increased microbial heat resistance due to a specific time-temperature history (e.g., slowly increasing temperatures) may lead to unintentionally less efficient food heating steps. In a previous study sound differential equations that describe accurately the microbial inactivation kinetics by incorporating physiological adjustments during experiments of changing temperature conditions were developed as an independent mathematical building block (Valdramidis *et al.*, 2007). More recently, the Weibullian-log logistic inactivation model was also modified to account for heat adaptation by introducing a logistic adaptation factor (Corradini *et al.*, 2009).

Another approach to account for the induced microbial phenomena is the development of memory based models. On this line the power-law memory models incorporating a memory kernel function have been proposed to take into account memory effects associated with cumulative cell damage or progressive cell adaptation (Vaidya *et al.*, 2009). Similarly Kaur *et al* (2008), Takhar *et al* (2008) hypothesized that the effect of microbial injury at a given instant can make the physical process nonlocal in nature where destruction at a given time is also affected by the injury occurring at previous time. Therefore, they proposed a 1-term and 2-term fractional differential equation (FDE) model. Some limitations of these developed memory based models is that they are built considering that the present survival rate at time t is influenced by all the previous thermal states of the system at a temporal distance, i.e., $t-t'$. Because of this time dependency this approach appears to be more appropriate for applications that on-line microbial data are available. Nevertheless, the most classical microbiological techniques of predictive modelling in foods account for off-line microbial data for which time intervals for performing microbial predictions are not available to the user beforehand.

The objective of this study was to develop Artificial Neural Network (ANN) structures that can embed memory and evaluate their applicability in Predictive Modelling in Foods. Their time dependency and any limitations and constraints that arise for performing predictions of microbial populations were assessed. Based on these observations alternative autonomous ANN structures were also developed and a general outline on the exploitation of all these structures for on-line or off-line microbial studies is suggested.

Materials and Methods

Data

Previously generated inactivation data of *Escherichia coli* K12 MG1655 under dynamic temperature conditions were used (Valdramidis *et al.*, 2006). These experiments were performed in cell suspensions and at temperature controlled conditions. Six different heating regimes were studied, i.e., dT/dt of 0.15°C/min, 0.20°C/min, 0.40°C/min, 0.55°C/min, 0.82°C/min, and 1.64°C/min. Experiments took place in sterile glass capillary tubes (Hirschmann Laborgeräte FmbH & Co.KG, Heilbronn, Germany) in which a volume of 100µL cell suspension (cell concentration approximately 10^9 cfu/mL) was pipetted. Tubes were then sealed by a gas flame and immersed in a temperature controlled circulating water bath (GR150-S12, Grant Instruments Ltd, Shepreth, UK). At regular times, two capillaries were removed from the water bath, plunged into an ice-water bath and analysed within approximately 30 min. Decimal serial dilutions of the samples were prepared in a BHI solution and surface plated on BHI Agar (1.2 %) using a Spiral Plater (Eddy Jet, IUL Instruments, Barcelona, Spain). Plates were incubated for 24 h at 37°C and colony-forming units were enumerated. For the purposes of the ANN development these experimental sets were split on training, validation (for performing an early-stopping approach) and test set data.

Model structures

A multi-step ahead Feed Forward with a delay artificial neural network (ANN) modelling structure was constructed. In this structure there were three input vectors, namely, time t_k and temperature rate $(dT/dt)_k$, and the microbial load delayed with one time unit, $\log N_{k-1}$. Its architecture was consisting of one hidden neuron and one output neuron. The selected transfer functions for the hidden and output neuron were the logistic-sigmoid and the linear functions, respectively. All input values were linearly normalised into [0,1] before they were entered into the network. Initial values that lie within [-1, 1] are picked randomly from a uniform distribution for the ANN's connection weights. The predictive capability of these models was also compared with a Feed Forward (FF) network (with as input vectors the t_k and temperature rate $(dT/dt)_k$) while an autonomous multi-step ahead FFD network (in which the input vector of t_k of the initially developed FFD network is replaced by the temperature T_k) was also considered. The performance of this autonomous structure has also been evaluated when vector of temperature rate $(dT/dt)_k$, has been omitted and when bias parameter of the $\log N_{k-1}$ was present or not.

Results and discussion

The increased induction of the heat resistance of *Escherichia coli* K12 under treatments of decreasing heating rates was quantified for all the developed ANN structures. The developed FFD structures appear to have a non-autonomous character due to their time dependency. Consequently, the predictive capability of the ANNs that had t_k as an input vector was influenced by the chosen increments of t_k . This clearly appears in Figure 1. The results show that non-autonomous ANN structures result on different predictions depending on the chosen time increment, phenomenon which is more pronounced for the multi-step ahead FF structure. It should be mentioned that although this type of networks are a common practise for or online control applications their application in predictive microbiology that microbial

information is originating from off-line data should be reconsidered. For that purpose an autonomous ANN structure was also evaluated.

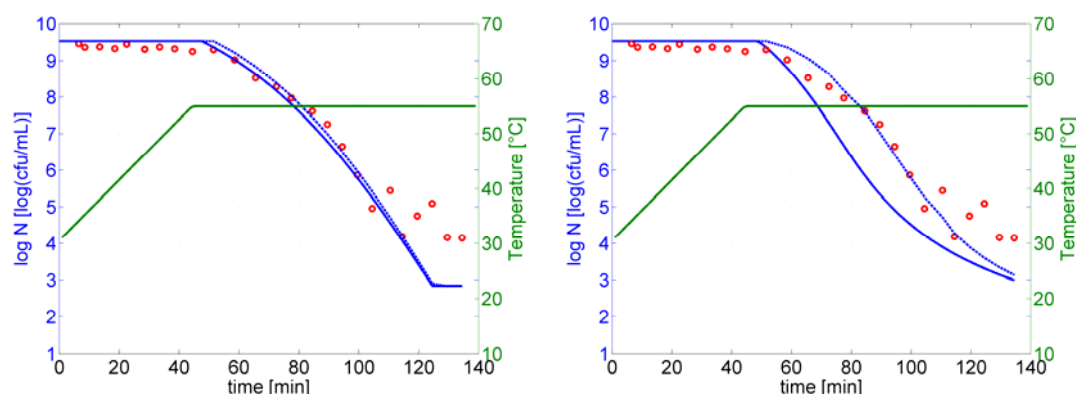


Figure 1. Examples of predictions of Feed Forward (left plot) and multi-step ahead Feed Forward with a delay (right plot) ANN architectures for t_k = experimental time of the test set (--) and t_k = 0.5 min increment (-). Microbial inactivation data (used as test set) (o) of *E. coli* K12 with their corresponding temperature profile at the studied heating rate of 0.55°C/min.

When microbial predictions were performed without presenting time explicitly as an input vector of the ANN structures (i.e., the case of the autonomous multi-step ahead FFD network) resulted in accurate microbial predictions that did incorporate the induced microbial phenomena. Results (Figure 2) show that a NN with two input variables, i.e., T_k , N_{k-1} was suffice to describe the microbial inactivation kinetics. This means that increase of the parameters of the model did not improve the generalization of the ANN. The good prediction capability of the FFD network indicates that an input incorporating past events, i.e., N_{k-1} , can improve the modelling performance by encompassing the microbial stress adaptation of the examined microbe due to the slowly increasing temperatures. This input delay can be considered as a dynamic *a priori microbiological knowledge* suitable for extracting the information contained in the microbial experimental data. Further experimental investigation of these adaptations may require studies focusing on the mechanisms influencing the microbial physiology.

A property of the currently used microbial inactivation models in Predictive Modelling in Foods (like the classical log-linear survivor curve) is memoryless, i.e., each cell inactivation event is distinct and has no information (i.e., memory) of earlier thermal events (Vaidya *et al.*, 2009). The current study outlines that quantifying adaptive microbial responses can be tackled by memory embedded modelling structures which could then assess accurately the efficacy of a heat process. The need of novel models that can incorporate the cell's history appears to be imperative for other types of food processes e.g., cooling storage (Juneja *et al.*, 2008).

Conclusions

Incorporation of past events seems to be an essential input for taking into account the observed induced microbial heat resistance and can be assessed by the development of memory embedded modelling structures. Non-autonomous ANN have implications on the prediction of the momentary microbial population. Their application should be restricted to on-line microbial measurements in which time increments are experimentally or industrially targeted. Performing predictions based on information coming from off-line techniques, like colony counts, requires the development of autonomous Neural Networks.

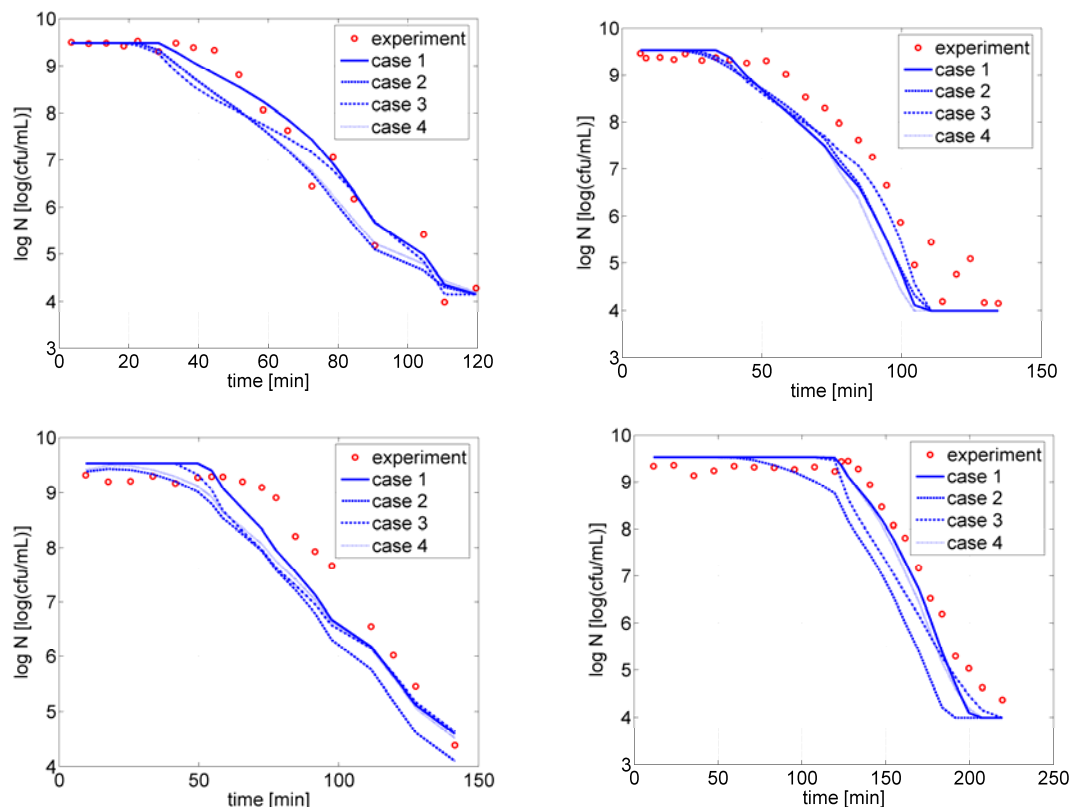


Figure 2. Predictions of autonomous multi-step ahead FFD network at heating treatments of 0.82°C/min (top left), 0.55°C/min (top right), 0.40°C/min (bottom left), 0.20°C/min (bottom right), Experiment: microbial inactivation data (used as test set) (o) of *E. coli* K12, case 1: input vectors T_k, N_{k-1} , case 2: input vectors T_k, N_{k-1} with bias factor on N_{k-1} case 3: input vectors $T_k, N_{k-1}, dT/dt_k$, case 4: $T_k, N_{k-1}, dT/dt_k$ with bias factor on N_{k-1} .

Acknowledgements

Research was supported by the National Development Plan, through the Food Institutional Research Measure, administered by the Department of Agriculture, Fisheries & Food (Ireland) and by the Research Council of the Katholieke Universiteit Leuven (Belgium). VPV is funded by the president's fund grant of the Society for Applied Microbiology (SfAM) for presenting this work at the ICPMF6.

References

- Corradini, M. G. and Peleg, M. (2009) Dynamic Model of Heat Inactivation Kinetics for Bacterial Adaptation. *Applied and Environmental Microbiology* 75(8), 2590-2597.
- Juneja, V. K., Marks, H. and Thippareddi, H. (2008) Predictive model for growth of *Clostridium perfringens* during cooling of cooked uncured beef. *Food Microbiology* 25(1), 42-55.
- Kaur, A., Takhar, P. S., Smith, D. M., Mann, J. E. and Brashears, M. M. (2008) Fractional Differential Equations Based Modelling of Microbial Survival and Growth Curves: Model Development and Experimental Validation. *Journal of Food Science* 73(8), E403-E414.
- Takhar, P. S. and Kaur, A. (2008) Modelling nonlinear microbial survival curves using one-term and two-term fractional differential equations, Shanghai, China.
- Vaidya, N. and Corvalan, C. M. (2009) An Integral Model of Microbial Inactivation Taking into Account Memory Effects: Power-Law Memory Kernel. *Journal of Food Protection* 72(4), 837-842.
- Valdramidis, V. P., Geeraerd, A. H., Bernaerts, K. and Van Impe, J. F. (2006) Microbial dynamics versus mathematical model dynamics: The case of microbial heat resistance induction. *Innovative Food Science & Emerging Technologies* 7(1-2), 80-87.
- Valdramidis, V. P., Geeraerd, A. H. and Van Impe, J. F. (2007) Stress-adaptive responses by heat under the microscope of predictive microbiology. *Journal of Applied Microbiology* 103(5), 1922-1930.

Development and validation of predictive model for the growth and survival of *Vibrio vulnificus* in post harvest shellstock

L.V. DaSilva¹, S. Parveen¹, A. DePaola², J.C. Bowers³, and M.L. Tamplin⁴

¹University of Maryland Eastern Shore, Princess Anne, MD 21853 (lvirsi@yahoo.com/ sparveen@umes.edu)

²U. S. Food and Drug Administration, Dauphin Island, AL 36528 (Angelo.Depaola@fda.hhs.gov)

³U. S. Food and Drug Administration, College Park, MD 20740 (John.Bowers@fda.hhs.gov)

⁴University of Tasmania, Tasmania 7001, Australia (Mark.Tamplin@utas.edu.au)

Abstract

Vibrio vulnificus, an opportunistic human pathogen found in the estuarine environment, is the leading cause of reported deaths in the U.S. associated with the consumption of seafood. *V. vulnificus* can cause septicemia (with 50% mortality rate) in susceptible individuals and most cases are linked to consumption of raw oysters. Post-harvest growth of *V. vulnificus* in oysters can greatly increase risk but there is limited information available on growth and survival of *V. vulnificus* in post-harvest oysters. The reliability of predictive models for the growth and survival of *V. vulnificus* in shellstock oysters harvested from Chesapeake Bay (CB) and Gulf Coast (GC) would benefit from more comprehensive information. The objective of this study was to address this existing data gap. Oysters (*Crassostrea virginica*) were collected seasonally (spring, summer and fall of 2007-2008) from the CB and then stored at 5, 10, 15, 20, 25, and 30°C. Two samples of six oysters each were analyzed at selected time intervals using a most probable number (MPN) procedure. The Baranyi D-model was fitted to the *V. vulnificus* growth data to estimate the parameters of lag phase duration (LPD), the growth rate (GR) and the maximum population density (MPD). *V. vulnificus* was slowly inactivated at 5 and 10°C with estimated GRs of -0.0043 and -0.0042 log MPN/h, respectively. The highest MPD (7.09 log MPN/g) was observed at 30°C. The estimated GRs at 15, 20, 25 and 30°C were 0.016, 0.041, 0.086 and 0.16 log MPN/h, respectively. LPD was observed at 20°C (30h) and 25°C (25h) in Spring. The *V. vulnificus* model bias (B_f) and accuracy (A_f) factors were 1.01 and 1.06, respectively. Models developed for the growth and survival of *V. vulnificus* in CB oysters were validated against a new set of model independent data, where American oysters were collected from the GC in Spring, Summer, and Fall and Asian oysters from CB in Spring-Summer, and analyzed using the same protocols as in the primary model experiments. The B_f and A_f for the GRs determined in GC American and CB Asian oysters were 1.02 and 1.09. These results suggest that the model developed for the growth of *V. vulnificus* in CB oysters are valid for, and predictive of, growth occurring in oysters harvested from the GC and CB, respectively. GRs were similar over the three seasons but were lower than predicted than by the FAO/WHO *V. vulnificus* Quantitative risk assessment. The results of this study will assist risk managers and seafood industry in designing and implementing food safety plans to minimize the risk from *V. vulnificus* in seafood consumers.

Keywords: *V. vulnificus*, shellstock oysters, predictive model, growth model

Introduction

Vibrio vulnificus is a gram-negative, halophilic, motile and curved bacterium found in marine and estuarine environments. *V. vulnificus* is the leading cause of reported deaths in the U.S. associated with the consumption of shellfish, especially oysters (Food and Nutrition Board, I.O.M., 1991). Among individuals without predisposing medical conditions, *V. vulnificus* infections due to consumption of raw or undercooked oysters are generally limited to gastroenteritis. However, among individuals with predisposing medical conditions, more extreme cases of infection can cause septic shock and skin lesions (Hlady et al., 1993, Klontz et al. 1988, and Kumamoto and Vukich, 1998). Such infections can lead to death within 24 hours and, for susceptible individuals, approximately 50% of such reported infections are fatal. Reported cases of infection follow a seasonal pattern that correlates with the temperature dependence of prevalence and post-harvest growth. To better understand the

seasonal pattern of infections, environmental surveys of *V. vulnificus* levels in relation to seawater salinity and temperature have been conducted (Motes et al. 1998, Tamplin et al. 1982) and the growth and survival of *V. vulnificus* in post-harvest oysters have been studied (Cook, 1994, Cook, 1997). Based on these studies, predictive risk models have been developed (FAO/WHO, 2004) but uncertainties remain due to the relatively narrow range of storage temperatures considered in previous post-harvest growth studies. Further studies are needed to determine predictive models for growth and survival of *V. vulnificus* in post-harvest shellstock oysters stored at temperatures relevant to commercial and consumer handling practices.

Material and methods

Sample collection, handling and storage

American Oysters (*Crassostrea virginica*) were collected seasonally (Spring, Summer and Fall 2007-2008) from the Chesapeake Bay. The temperature and salinity of the seawater where oysters were harvested were measured in the upper 0.5 m of the surface water with a dissolved oxygen conductivity meter (Model 85, Yellow Springs Instrument Co., Yellow Springs, OH). Oyster samples were shipped in an insulated chest with ice bags along with a data-logger to the Food Safety laboratory at the University of Maryland Eastern Shore. Upon arrival, oysters were stored at 5, 10, 15, 20, 25 and 30°C for analysis. At each storage temperature, two samples of six oysters each were collected at selected time intervals for bacteriological analysis.

Bacteriological analyses

Levels of *V. vulnificus* were determined by the Most Probable Number (MPN) procedure using alkaline peptone water (APW) with 3% NaCl for enrichment broth. Positive APW tubes were streaked onto modified cellobiose polymyxin colistin agar and incubated at 39°C for 18-24 hours followed by confirmation of the isolated colonies with DNA a probe technique using Alkaline Phosphatase-labeled probes for the *vhA* gene (Kaysner and DePaola, 2004).

Estimation of primary and secondary growth model

For model development, the mean and standard deviation of log MPNs of replicate observations were calculated and plotted with Excel[®] spread-sheet. The dynamic model described by Baranyi and Roberts (1994) was used to fit growth curves to the experimental data at each storage temperature and determine estimates of lag phase duration (LPD [h]), growth rate (log MPN/h) and maximum population density (MPD [log MPN/g]). The DMFit curve-fitting software kindly provided by the Institute of Food Research (Norwich, UK) was used to fit the primary model. A Secondary growth model was estimated using Table Curve 2D (SPSS Inc., Chicago, IL) with built-in and customized equations. The Ratkowsky square root model was used as the secondary model for GR as a function of storage temperature (Ratkowsky et al., 1982). Model performance was measured by bias (B_f) and accuracy (A_f) factors (Baranyi and Ross, 1999). Estimated GRs were further analyzed by an analysis of covariance (ANCOVA) to evaluate possible effect of season and harvest site conditions on the growth and survival of *V. vulnificus* in oysters. The ANCOVA was performed using the PROC GLM procedure in SAS (Statistic Analysis Software Version 9.1, SAS Institute, Cary, N.C.). Differences were considered statistically significant at $P < 0.05$.

Results and discussion

The growth and survival of natural population of *V. vulnificus* in multiple collections of oysters were measured at 5, 10, 15, 20, 25, and 30°C at selected time intervals. The *V. vulnificus* levels gradually decreased to a non-detectable level at 5 and 10°C. The inactivation rate of *V. vulnificus* at 5 and 10°C was estimated to be -0.0043 and -0.0042 log MPN/h, respectively (Table 1). While the level of *V. vulnificus* decreased at 5 and 10°C, *V. vulnificus* increased 1 to 2 log MPN in oysters stored at 20, 25 and 30°C after one day of storage. Similar results were observed by Cook and Rupple (1989) where *V. vulnificus* decreased

during storage at 10°C, but increased by 1 to 2 log cycles in oysters after one day of storage at 22°C and 30°C. The maximum MPD (7.09 log MPN/g) was observed at 30°C for oysters harvested during Summer months (Table 1). Similar results were observed for oyster collected from CB in Summer 2006 where the maximum population density of 8.16 log CFU/g was observed in samples stored at 20°C (DaSilva, L. 2007, personal communications). For all CB studies, the estimated GR at 15, 20, 25 and 30°C were 0.016, 0.041 and 0.086 and 0.16 log MPN/h, respectively. A lag phase was not observed except at 20°C (30h) and 25°C (25h) in Spring 2008.

Table 1: Inactivation/growth parameters for *V. vulnificus* in CB oysters stored at 5-30°C.

| Temperature (°C) | GR (log MPN/h) | | | LPD (h) | | | *MPD (log MPN/g) | | |
|------------------|----------------|--------|--------|---------|--------|------|------------------|--------|------|
| | Spring | Summer | Fall | Spring | Summer | Fall | Spring | Summer | Fall |
| 5 | -0.002 | -0.007 | ND | 0 | 0 | ND | ND | ND | ND |
| 10 | -0.004 | -0.005 | -0.004 | 0 | 0 | 0 | ND | ND | ND |
| 15 | 0.016 | 0.028 | ND | 0 | 0 | ND | 3.55 | 6.02 | ND |
| 20 | 0.049 | 0.144 | 0.035 | 30 | 0 | 1.33 | 5.71 | 6.19 | 6.34 |
| 25 | 0.091 | 0.098 | 0.073 | 25.21 | 0 | 3.50 | 4.77 | 6.78 | 6.40 |
| 30 | 0.064 | 0.095 | 0.215 | 0 | 0 | 0 | 5.54 | 7.09 | 6.63 |

GR= growth rate, LPD= lag phase duration, *MPD= maximum population density before oysters died, ND= not determined

For model-dependent data, the *V. vulnificus* model bias (B_f) and accuracy (A_f) factors were 1.01 and 1.06, respectively. Baranyi et al. (1994) suggested that the A_f of an acceptable model should be less than or equal to 1.15 (15% error) for one independent variable (e.g. temperature). Therefore these new models meet the definition of “acceptable.” The model for *V. vulnificus* growth in CB oysters was validated against independent data for GC, American and CB Asian oysters (*Crassostrea ariakensis*) (Figure 1). B_f and A_f for the GR in GC were 1.02 and 1.09 respectively.

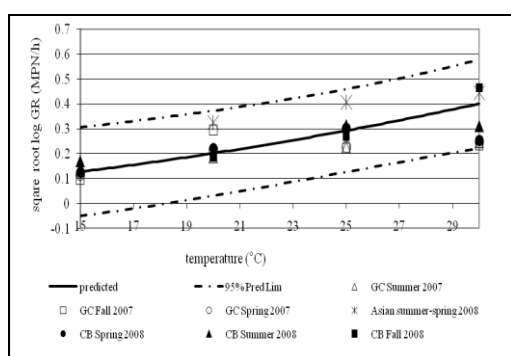


Figure 1: Observed and predicted GR of *V. vulnificus* in raw oysters stored at 15-30°C. Secondary model prediction (solid line) with upper and lower 95% confidence intervals (dashed lines).

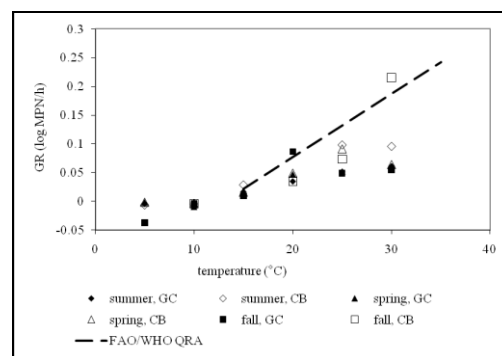


Figure 2: CB and GC growth rate estimates compared to FAO/WHO Quantitative Risk Assessment.

Generally, GRs of *V. vulnificus* were similar over the three seasons and no statistically significant differences ($P>0.05$) were identified between the GR estimates in oysters harvested from the CB versus the GC. However, relative to the expectation based on storage temperature alone, GRs did appear to be depressed at low (CB) and high (GC) salinity. The deviation from expected was small (i.e., near zero) around 20 ppt salinity, which is consistent with salinity levels found to be favorable for *V. vulnificus* in previous environmental surveys

(Motes et al. 1998). In addition, there was no apparent relationship between deviations from expected GR versus water temperature at harvest. Although consistent across sample collections, the GRs estimates for CB and GC collections held at 25 and 30°C were found to be lower than predictions of the FAO/WHO (2004) *V. vulnificus* Quantitative Risk Assessment, based on observations in studies by Cook in 1994 and 1997 (Figure 2).

Conclusions

These results indicate that the model developed for the growth of *V. vulnificus* in CB oysters are valid for, and predictive of, growth occurring in oysters harvested from GC and CB, respectively. GRs were similar over the three seasons but were systematically lower than that predicted by the FAO/WHO *V. vulnificus* Quantitative Risk Assessment at temperatures greater than 20°C. The results of this study will assist risk managers and seafood industry in designing and implementing food safety plans to minimize the risk from *V. vulnificus* in seafood consumers.

Acknowledgements

We gratefully acknowledge C. White, M. Mudoh, J. Eckroade, K. Cephas G. Rutto, J. Ngeno, P. Sang, R. Korir, K. Brohawn, T. Rippen, and J. Schwarz for their great contribution to this study. This project was supported by the National Research Initiative of the United States Department of Agriculture, Cooperative State Research, Education and Extension Service, grant # 2006-35201-16644 and University of Maryland Eastern Shore Advanced Curriculum Technology-Based Instructional Opportunities Network (ACTION).

References

- Baranyi J. and Robert T. A. (1994) A dynamic approach to predicting bacterial growth in food. *International Journal of Food Microbiology*. 23 (3-4), 277-294.
- Baranyi J., Pin C. and Ross T. (1999) Validating and comparing predictive models. *International Journal of Food Microbiology*. 48 (3), 159-166.
- Cook, D.W. and A. Ruple. 1989. Indicator bacteria and *Vibrionaceae* multiplication in post-harvest shellstock oysters. *Journal of Food Protection* 52 (5), 343-349.
- Cook D.W. (1994) Effect of time and temperature on multiplication of *Vibrio vulnificus* in postharvest Gulf Coast shellstock oysters. *Applied and Environmental Microbiology* 60 (9), 3483-3484.
- Cook D.W. (1997) Refrigeration of oyster shellstock conditions which minimize the outgrowth of *Vibrio vulnificus*. *Journal of Food Protection* 60 (4), 349-352.
- Kaysner C.A. and DePaola A. (2004) *Vibrio cholerae*, *V. parahaemolyticus*, *V. vulnificus*, and other *Vibrio* spp., Chapter 9. 8th edition, *Bacteriological Analytical Manual* (www.cfsan.fda.edu).
- FAO/WHO (2004) Joint FAO/WHO activities in risk assessment of microbiological hazards in foods: Preliminary document, hazard identification, exposure assessment, and hazard characterization of *Vibrio* spp. in seafood (Prepared by J. Sumner, A. DePaola, K. Osaka, I. Karunasager, M. Walderhaug, and J. Bowers).
- Food and Nutrition Board, I. O. M. (1991) Seafood Safety/Committee on Evaluation of the Safety of Fishery Products. *National Academy Press*, Washington, D.C.
- Hlady W. G., Mullen R.C. and Hopkin R.S (1993) *Vibrio vulnificus* from raw oysters. Leading cause of reported deaths from food-borne illness in Florida. *Journal of the Florida Medical Association* 80 (8), 536-538.
- Klontz K.C., Leib S., Schreiber M., Janowski H.T., Baldy L.M. and Gunn R.A. (1988) Syndromes of *Vibrio vulnificus* infections. Clinical and epidemiologic features in Florida cases, 1981-1987. *Annals of Internal Medicine* 109 (4), 318-323.
- Kumamoto K. S. and Vukich D.J. (1998) Clinical infections of *Vibrio vulnificus*: a case report and review of the literature. *The Journal of Emergency Medicine* 16 (1), 61-66.
- Motes M. L., DePaola A., Cook D.W., Veazey J.E., Hunsucker J.C., Garthright W.E., Blodgett R.T. and Chirtel S.J. (1998) Influence of water temperature and salinity on *Vibrio vulnificus* in Northern Gulf and Atlantic Coast oysters. *Applied and Environmental Microbiology*. 64 (4), 1459-1465.
- Ratkowsky D.A., Olley J, McMeekin T.A. and Ball A. (1982) Relationship between temperature and growth rate of bacterial cultures. *Journal of Bacteriology* 149 (1), 1-5.
- Tamplin M. L., Rodrick G.E., Blake N.J. and Cuoba T. (1982) Isolation and characterization of *Vibrio vulnificus* from two Florida estuaries. *Applied and Environmental Microbiology* 44 (6), 1466-1470.

Development of Predictive Models for *Listeria monocytogenes* in Selected Refrigerated Ready-To-Eat Foods

C.A. Hwang

Microbial Food Safety Research Unit, ERRC-ARS-USDA (Andy.Hwang@ars.usda.gov)

Abstract

Deli salads, deli ham and smoked salmon are three popular refrigerated ready-to-eat foods. These products are ready for consumption without prior cooking. If not processed and handled properly, they could be contaminated with *L. monocytogenes*, a pathogen of capable of growing at refrigerated temperature. To ensure the safety of these products, it is critical to understand the ability of *L. monocytogenes* to grow or survive in these products as affected by the product formulation and storage condition. Studies were conducted to examine the growth characteristics (lag phase duration and growth rate) of *L. monocytogenes* in seafood salad, ham and smoked salmon as affected by the mayonnaise pH in seafood salad, lactate and diacetate in ham, and salt and smoke compounds (phenols) in smoked salmon under refrigerated and abuse temperatures. Models were developed to describe the effects of formulation and storage temperature on the growth characteristics of *L. monocytogenes*, and the effects and significance of the individual factor and their interaction on *L. monocytogenes* were identified. Validation studies indicated that these models were acceptable for predicting the growth of *L. monocytogenes* in seafood salad, ham and smoked salmon. These models were examined to identify their applicability and limitation.

Keywords: *Listeria monocytogenes*, salad, ham, smoked seafood, model

Introduction

Refrigerated ready-to-eat (RTE) foods are ready for consumption without prior cooking. Deli salads, luncheon meats and smoked seafood are some of the popular RTE foods on the market. *L. monocytogenes*, a pathogen of capable of growing at refrigerated temperatures, is a concern in refrigerated RTE foods. A study found that *L. monocytogenes* was positive in 4.7% of seafood salads and in 2.4% of deli salads (Gombas *et al.* 2003). The prevalence of *L. monocytogenes* in sliced luncheon meat ranged from 4.2 to 8.0% in samples collected from federally inspected establishments between 1990 and 1999 in the U.S. (Levine *et al.* 2001). Gombas *et al.* (2003) reported that 0.89% RTE luncheon meats collected from grocery stores in California and Maryland in the U.S. between 2000-2001 were tested positive for *L. monocytogenes*. The prevalence of *L. monocytogenes* in cold-smoked salmon or smoked fish were reported to be at 13% (Nakamura *et al.* 2004), 4.3% (Gombas *et al.* 2003), and 10.3% (Beaufort *et al.* 2007). In a risk assessment reported by the U.S. FDA/USDA/CDC (2003), deli salads, RTE meat and smoke seafood had high relative risk of causing listeriosis among 20 RTE foods. Since RTE foods are normally consumed with prior heating, the high prevalence of *L. monocytogenes* in deli salads, RTE meat and smoked seafood and the ability of this pathogen to grow at refrigerated temperature render the pathogen a particular microorganism of concern in these RTE foods. The behavior of *L. monocytogenes* in seafood salad, cooked ham and smoked salmon as affected by the product formulation and processing and/or storage temperature were examined, and models were developed to describe the effects of product formulation and temperature on *L. monocytogenes*.

Materials and Methods

Product factors that are likely to affect the growth of *L. monocytogenes* in seafood salad, cooked ham and smoked salmon were examined. These factors were mayonnaise pH for seafood salad, lactate and diacetate, two common food additives which are increasingly used in RTE meat products, for cooked ham, and salt and smoke compounds (phenols) for smoked

salmon. The effects of prevalent processing/storage temperatures that these products were commonly exposed to were also examined. For seafood salad, a mixture of 5 strains of *L. monocytogenes* was inoculated onto the surface of a shrimp and crabmeat. The inoculated seafood components were mixed with mayonnaise of pH 3.7, 4.0, 4.4, 4.7 and 5.1, and then stored at 4°-12°C. Ham samples containing 1.0-4.2% lactate and 0.05-0.2% diacetate were inoculated with *L. monocytogenes* and stored at 0-45°C. Samples of minced cooked salmon containing 0-10% NaCl and 0-34 ppm phenols were inoculated with *L. monocytogenes* and stored at 0-25°C. The initial inoculum of *L. monocytogenes* in samples were 10^{2-3} cfu/g. The lag phase duration (LPD, h) and growth rate (GR, \log_{10} cfu/h) of *L. monocytogenes* were obtained and modeled as a function of the product factor and temperature.

Results and Discussion

Growth of *L. monocytogenes* occurred in seafood salad formulated with mayonnaise of pH 3.7-5.1 at 4-12°C. It is well recognized that commercial mayonnaise with pH ≤ 4.1 is sufficient to maintain its microbiological stability. The growth of *L. monocytogenes* in seafood salad formulated with mayonnaise of pH 3.7 and 4.0 indicated that the seafood components protected *L. monocytogenes* cells from the high acidity of mayonnaise. The LPD and GR of *L. monocytogenes* in seafood salad as affected by the mayonnaise pH and storage temperature can be described as:

$$\text{LPD (h)} = 620.83 + 2.916(\text{temperature}) - 186.5(\text{pH}) + 3.841(\text{temperature} \times \text{pH}) - 1.463(\text{temperature})^2 + 9.879(\text{pH})^2.$$

$$\text{GR } (\log_{10} \text{ cfu/h}) = -0.00313 + 0.00338(\text{temperature}) + 0.00214(\text{pH}) - 0.00031(\text{temperature} \times \text{pH}) - 0.000024(\text{temperature})^2 - 0.000169(\text{pH})^2.$$

Regression analyses showed that mayonnaise pH was the main factor that affected the LPD of *L. monocytogenes*, and storage temperature was the main factor on the GR.

The LPD and GR of *L. monocytogenes* in ham as a function of concentrations of lactate and diacetate at 0-36°C are:

$$\text{LPD} = 79.97 - 13.17(\text{temperature}) + 35.76(\text{lactate}) + 1059.73(\text{diacetate}) - 1.03(\text{temperature} \times \text{lactate}) - 28.55(\text{temperature} \times \text{diacetate}) - 176.53(\text{lactate} \times \text{diacetate}) + 0.31(\text{temperature})^2 + 4.93(\text{lactate})^2 + 1300.49(\text{diacetate})^2$$

$$\text{GR } (\log_{10} \text{ cfu/h}) = -0.0146 + 0.0098(\text{temperature}) - 0.0206(\text{lactate}) - 0.2220(\text{diacetate}) - 0.0013(\text{temperature} \times \text{lactate}) - 0.0392(\text{temperature} \times \text{diacetate}) + 0.0143(\text{lactate} \times \text{diacetate}) + 0.0001(\text{temperature})^2 + 0.0053(\text{lactate})^2 + 2.9529(\text{diacetate})^2$$

The LPD of *L. monocytogenes* were affected by lactate, diacetate and storage temperature, whereas the GR were affected by the temperature and the interactions of temperature and lactate and diacetate. In general, the LPD were extended by the increased concentrations of lactate and diacetate at storage temperatures $\leq 12^\circ\text{C}$, while the GR were reduced by both additives at temperatures 15°C - 36°C .

The LPD and GR of *L. monocytogenes* in smoked salmon as affected by the salt and phenol concentrations and storage temperature can be described as:

$$\text{LPD (h)} = 61.35 - 11.66(\text{temperature}) + 10.16(\text{phenol}) + 14.75(\text{salt}) - 0.15(\text{temperature} \times \text{phenol}) - 0.86(\text{temperature} \times \text{salt}) + 0.42(\text{phenol} \times \text{salt}) + 0.32(\text{temperature})^2 - 0.23(\text{phenol})^2 + 0.49(\text{salt})^2$$

$$\sqrt{\text{GR}} = -0.0639 + 0.0136(\text{temperature}) + 0.0103(\text{phenol}) + 0.0257(\text{salt}) - 0.0001(\text{temperature} \times \text{phenol}) - 0.0018(\text{temperature} \times \text{salt}) - 0.0014(\text{phenol} \times \text{salt}) + 0.0003(\text{temperature})^2 - 0.0002(\text{phenol})^2 - 0.0011(\text{salt})^2$$

The increase of salt concentrations or lower storage temperatures extended the LPD and reduced the GR of *L. monocytogenes* in smoked salmon. The growth of *L. monocytogenes* was affected by salt, phenol, storage temperature and their interactions. The LPD of *L. monocytogenes* were particularly extended by higher concentrations of phenols at lower storage temperatures. The GR of *L. monocytogenes* were reduced only at salt concentrations $>6\%$ at temperatures $<10^\circ\text{C}$.

For *L. monocytogenes* in seafood salad, ham, and smoked salmon, polynomial (quadratic) models were developed and found to be acceptable for describing the LPD and GR of *L. monocytogenes* as affected by the product factor and temperature. Polynomial models have been long used to describe the effects of food factors on the growth and survival of *L. monocytogenes* in meat products or model systems. These models were validated and reported to be acceptable in estimating the behavior of *L. monocytogenes* in food products within the product parameters that the models were developed (Devlieghere *et al.* 2001; Seman *et al.* 2002; Hwang *et al.* 2009). In addition to polynomial models, non-polynomial models that described the growth of *L. monocytogenes* in meat products, smoked seafood and other food products have also been developed (Augustin and Carlier 2000; Devlieghere *et al.* 2001; Gimenez and Dalgaard 2004). The square-root model of Ratkowsky *et al.* (1983) was a basis for most of the non-polynomial models. Two examples of non-polynomial models were proposed by Devlieghere *et al.* (2001) to describe the growth of *L. monocytogenes* in modified atmosphere-packed cooked meat products:

$$\ln(\lambda) = \ln \left\{ 1 / [b(A_w - A_{w \min})(CO_2 \max - CO_2)(T - T_{\min})^2(NaL_{\max} - NaL)] \right\}$$

$$\sqrt{\mu_{\max}} = a \cdot (T - T_{\min}) \cdot \sqrt{(A_w - A_{w \min}) \cdot (CO_2 \max - CO_2) \cdot (NaL_{\max} - NaL)}$$

Where λ is lag phase, μ_{\max} is maximum specific growth rate, T is temperature, CO_2 is carbon dioxide, NaL is sodium lactate, and min and max are the theoretical maximum and minimal, respectively, temperature/quantity of $T/CO_2/NaL$ at which the μ_{\max} of *L. monocytogenes* is zero.

Devlieghere *et al.* (2001) fitted these non-polynomial models and two polynomial models to μ_{\max} and λ of *L. monocytogenes* in cooked meat, and reported that both types of models well described the μ_{\max} and λ . This indicated that these two types of models are equally suitable for use in the development of *L. monocytogenes* growth models.

The comparison of the quadratic models of seafood salad, ham and smoked salmon to other polynomial or non-polynomial models were limited due to the different products and/or environmental factors were modeled. In general, the estimated LPD and/or GR of *L. monocytogenes* from the ham and smoked salmon models were higher than those reported by two comparable studies by Devlieghere *et al.* (2001) and Gimenez and Dalgaard (2004). This may be attributed to by the variations in product and environmental factors, notably packaging atmosphere and native microflora, in these studies. The models for seafood salad, ham and cooked ham were developed without the interference of native microflora. The estimated growth characteristics of *L. monocytogenes* by the models represent a worst-case scenario as native microflora in these products have been reported to be competitive to the growth of *L. monocytogenes* (Amezquita and Brashears 2002; Gimenez and Dalgaard 2004; Andrighetto *et al.* 2009).

References

- Amezquita, A. and Brashears, M.M. (2002) Competitive inhibition of *Listeria monocytogenes* in ready-to-eat meat products by lactic acid bacteria. *Journal of Food Protection* 65, 316–325.
- Andrighetto, C., Lombardi, A., Ferrati, M., Guidi, A., Corrain, C. and Arcangeli, G. (2009) Lactic acid bacteria biodiversity in Italian marinated seafood salad and their interactions on the growth of *Listeria monocytogenes*. *Food Control* 20, 462–468.
- Beaufort, A., Rudelle, S., Gnanou-Besse, N., Toquin, M.T., Kerouanton, A., Bergis, H., Salvat, G. and Cornu, M. (2007) Prevalence and growth of *Listeria monocytogenes* in naturally contaminated cold-smoked salmon. *Letters in Applied Microbiology* 44, 406–411.
- Devlieghere, F., Geeraerd, A.H., Versyck, K.J., Vandewaetere, B., Van Impe, J. and Debevere, J. (2001) Growth of *Listeria monocytogenes* in modified atmosphere packed cooked meat products: a predictive model. *Food Microbiology* 18, 53–66.

- Gimenez, B. and Dalgaard, P. (2004) Modelling and predicting the simultaneous growth of *Listeria monocytogenes* and spoilage microorganisms in cold-smoked salmon. *Journal of Applied Microbiology* 96, 96-109.
- Gombas, D., Chen, Y., Rocelle, S.C. and Scott, V.N. (2003) Survey of *Listeria monocytogenes* in ready-to-eat foods. *Journal of Food Protection* 66, 559-569.
- Hwang, C.A., Porto-Fett, A.C.S., Juneja, V.K., Ingham, S.C., Ingham, B.H. and J.B. Luchansky. (2009) Modeling the survival of *Escherichia coli* O157:H7, *Listeria monocytogenes* and *Salmonella typhimurium* during fermentation, drying and storage of soudjouk-style fermented sausage. *International Journal of Food Microbiology* 129, 244-252.
- Levine, P., Rose, B., Green, S., Ransom, G. and Hill, H. (2001) Pathogen testing of ready-to-eat meat and poultry products collected at federally inspected establishments in the United States, 1990 to 1999. *Journal of Food Protection* 64, 1188-1193.
- Nakamura, H., Hatanaka, M., Ochi, K., Nagao, M., Ogasawara, J., Hase, A., Kitase, T., Haruki, K. and Nishikawa, Y. (2004) *Listeria monocytogenes* isolated from cold-smoked fish products in Osaka City, Japan. *International Journal Food Microbiology* 94, 323-328.
- Ratkowsky, D.A., Lowry, R.J.K., McMeeki, T.A., Stokes, A.N. and Chandler, R.E. (1983) Model for bacterial growth rate throughout the entire biokinetic temperature range. *Journal of Bacteriology* 154, 1222-1226.
- Seman, D.L., Borger, A.C., Meyer, J.D., Hall, P.A. and Milkowski, A.L. (2002) Modeling the growth of *Listeria monocytogenes* in cured ready-to-eat processed meat products by manipulation of sodium chloride, sodium diacetate, potassium lactate, and product moisture content. *Journal of Food Protection* 65, 651-658.
- U.S. Food and Drug Administration/Department of Agriculture/Centers for Disease Control and Prevention. (2003) Quantitative assessment of relative risk to public health from foodborne *Listeria monocytogenes* among selected categories of ready-to-eat foods.
<http://www.foodsafety.gov/~dms/lmr2-toc.html>.

Modelling the kinetics of *Listeria monocytogenes* on frankfurters and other ready-to-eat meat products from manufacturing to consumption

Y. Le Marc¹, I. Geornaras², J. Baranyi¹ and J.N. Sofos²

¹ Institute of Food Research, Norwich Research Park, Norwich, NR4 7UA, UK
(yvan.lemarc@bbsrc.ac.uk)

² Colorado State University, Center for Meat Safety & Quality and Food Safety Cluster, Department of Animal Sciences, 1171 Campus Delivery, Fort Collins, CO 80523, USA

Abstract

A predictive model was created for the effects of temperature, pH, water activity, and inclusion of sodium diacetate and sodium/potassium lactate in product formulations, on growth of *Listeria monocytogenes*. The growth rate model was based on Mejlholm *et al.* (2007). The effects of several post-lethality treatments (hot water or spraying treatments) on h_0 , the “work to be done” prior to growth were evaluated on literature data. The model can be applied to predict the growth of *L. monocytogenes* on frankfurters in the presence or absence of antimicrobials.

Keywords

Listeria monocytogenes, frankfurters, ready-to-eat meat products, antimicrobials

Introduction

Contamination of ready-to-eat meat products with *Listeria monocytogenes* is recognized as an important public health issue. Mathematical models predicting growth of the pathogen during product distribution and storage can be useful in determining safety-based product shelf-life under different conditions.

To inhibit the growth of *L. monocytogenes* on ready-to-eat meat products, post-lethality inactivation treatments and/or growth inhibitors can be used. The aim of this study was to develop a predictive model for *L. monocytogenes* on frankfurters and other ready-to-eat meat products integrating i) the reduction in numbers of *L. monocytogenes* caused by post-lethality treatments, ii) the effects of these treatments on the bacterial lag time, and, iii) the growth of *L. monocytogenes* during storage. The model should also be able to deal with situations such as contamination after the application of post-lethality inactivation treatments or growth in opened packages during storage at consumer homes or food service establishments.

Materials and Methods

Inoculum preparation and product inoculation

A cocktail of 10 *L. monocytogenes* strains were used in this study: 558 (serotype 1/2, pork meat isolate), NA-1 (serotype 3b, pork sausage isolate), N-7150 (serotype 3a, meat isolate), and N1-225, N1-227, R2-500, R2-501, R2-763, R2-764, and R2-765 (serotype 4b; outbreak-related strains of food, clinical or environmental origin).

Cultures of each strain were individually suspended in autoclave-sterilized product extract, and were incubated at 7°C for approximately 72 h in order to acclimate the cells to a low temperature product environment (Lianou *et al.*, 2007). Following the habituation procedure, the 10 cultures were combined, serially diluted in freshly prepared product extract, and 0.1 ml or 0.25 ml of the diluted mixture was used to inoculate (1-2 log CFU/cm²) the surface of sliced deli meats (5 × 5 cm; 0.1-0.2 cm thick) or frankfurters, respectively. After allowing for cell attachment (4°C, 15 min), inoculated products were placed into vacuum bags (two deli meat slices or frankfurter links per bag) and were vacuum-packaged and stored at 4, 7 or 12°C for up to 90 days.

Growth data

The data used to generate the model consisted of 60 growth curves of *L. monocytogenes* on frankfurters, ham, roast beef and bologna formulated without or with antimicrobials (1.5% potassium lactate and 0.05% sodium diacetate, or 1.44% sodium lactate and 0.1% sodium diacetate). Six growth rates on bologna, calculated by Barmpalia *et al.* (2005), in the presence of sodium lactate and/or sodium diacetate were also included in the data set. Other (18) curves obtained near the growth limits were used for validation purposes.

The ability of the model to predict the growth of *L. monocytogenes* on frankfurters at various stages of storage was assessed on 14 growth curves published by Byelashov *et al.* (2008a). Frankfurters formulated with or without 1.5% potassium lactate and 0.1% sodium diacetate were inoculated with *L. monocytogenes*, vacuum-packaged, and stored at conditions simulating: storage before transportation to retail; temperature abuse during transportation and storage before purchase; and temperature abuse during transport from stores to homes. Sample packages were then opened (i.e., aerobic conditions) or held vacuum-packaged to simulate storage in the home environment.

Model development

The growth model used in this study is based on the equations proposed by Mejlholm *et al.* (2007). The terms for CO₂ concentrations, phenol and nitrite were omitted here as they were not relevant to this work. The model comprises an interaction term based on the ψ -value (Le Marc *et al.*, 2002) to predict the growth/no growth interface of *L. monocytogenes*. The final equation is written as follows:

$$\mu_{\max} = \mu_{\text{ref}} \cdot \rho(T) \cdot \gamma(pH) \cdot \theta(a_w) \cdot \tau_{\text{LAC}_U}([LAC_U]) \cdot \tau_{\text{DAC}_U}([DAC_U]) \cdot \xi \quad (1)$$

where μ_{ref} is the specific growth rate at $T_{\text{ref}}=25^\circ\text{C}$ (the other environmental conditions being optimum), $\rho(T)$, $\gamma(pH)$, $\theta(a_w)$, $\tau_{\text{LAC}_U}([LAC_U])$, $\tau_{\text{DAC}_U}([DAC_U])$ are the individual effects of temperature, pH, water activity and the concentrations of undissociated lactate $[LAC_U]$ and diacetate $[DAC_U]$, respectively, ξ is the term representing the effects of interactions between the environmental factors as defined by Le Marc *et al.* (2002). The individual effects of the environmental factors are written as:

$$\rho(T) = \left(\frac{T - T_{\min}}{T_{\text{ref}} - T_{\min}} \right)^2, \quad \gamma(pH) = \left(1 - 10^{(pH_{\min} - pH)} \right), \quad \theta(a_w) = \left(\frac{a_w - a_{w_{\min}}}{a_{w_{\text{opt}}} - a_{w_{\min}}} \right)$$

$$\tau_{\text{LAC}_U}([LAC_U]) = \left(1 - \frac{[LAC_U]}{MIC_{U \text{ LAC}}} \right), \quad \tau_{\text{DAC}_U}([DAC_U]) = \left(1 - \sqrt{\frac{[DAC_U]}{MIC_{U \text{ DAC}}}} \right)$$

where T_{\min} , pH_{\min} , $a_{w_{\min}}$ are the theoretical minimum temperature, pH and water activity, respectively, supporting the growth of *L. monocytogenes*. $MIC_{U \text{ LAC}}$ and $MIC_{U \text{ DAC}}$ are the theoretical minimum inhibitory concentrations of lactate and diacetate, respectively. The contributions of the factors to the interactions were calculated as suggested by Mejlholm *et al.* (2007). pH_{\min} , $MIC_{U \text{ LAC}}$, $MIC_{U \text{ DAC}}$ were also derived from Mejlholm *et al.* (2007) and kept constant during the fitting procedure. $a_{w_{\text{opt}}}$ was fixed to 0.997. The values for T_{\min} , $a_{w_{\min}}$, μ_{ref} (for each food product) in this study were estimated from 66 growth curves obtained on roast beef, frankfurters, bologna and ham.

The modelling was carried out in two steps. First for each curve, the specific growth rate (μ_{\max}) was calculated by fitting the primary model of Baranyi and Roberts (1994) to the experimental data. Then equation 1 was fitted to the bacterial growth rates. Before fitting, a square root transformation was performed to homogenise the variance of the growth rate.

Results and discussion

Growth rate model

The model describes satisfactorily the effects of temperature, pH, water activity, lactate, and diacetate on the growth rate of *L. monocytogenes* ($R^2_{adj} = 0.89$). The estimated values for T_{min} and aw_{min} were -3.7°C and 0.926 respectively. The values for μ_{ref} were estimated as 0.31, 0.38, 0.45, 0.49 h^{-1} for frankfurters, ham, roast beef and bologna products, respectively.

Model predictions and observed rates were compared with 18 specific rates of *L. monocytogenes* obtained in the “interaction region” as defined in equation 1. Values of 0.9 and 1.4 were obtained for the bias factor B_f and the accuracy factor A_f , respectively.

The developed model for frankfurters was validated by comparison with 14 curves of *L. monocytogenes* on frankfurters formulated with or without antimicrobials under fluctuating conditions (Byelashov *et al.*, 2008a). Figure 1 shows an example of the comparison between model predictions and experimental data. For frankfurters formulated with antimicrobials, the model was found to slightly overestimate in some cases the concentration of *L. monocytogenes* (fail safe prediction) at the end of storage. The mean of the absolute difference (MAD) between the predicted and observed viable counts was $0.6\text{ log}_{10}\text{ CFU/cm}^2$ and $0.9\text{ log}_{10}\text{ CFU/cm}^2$ for frankfurters formulated without and with antimicrobials, respectively.

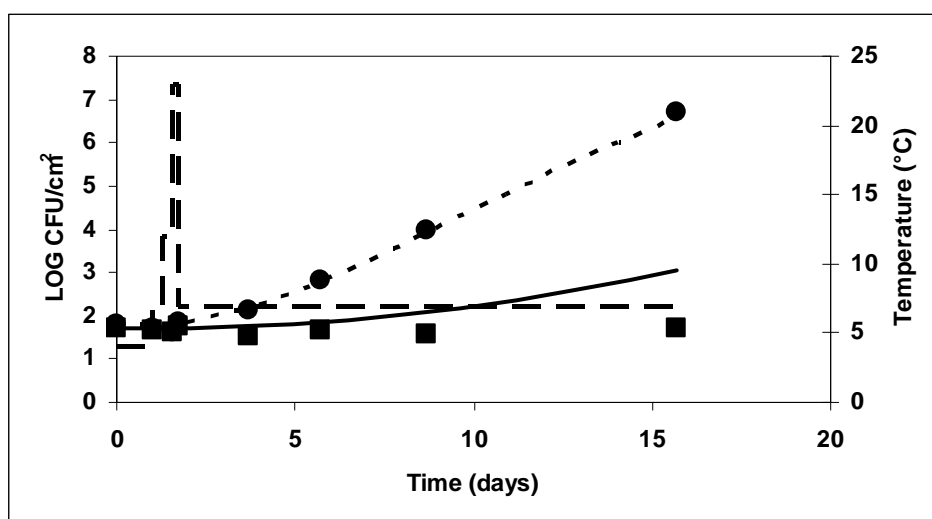


Figure 1: Predicted growth of *L. monocytogenes* on frankfurters with or without 1.5% potassium lactate and 0.1% sodium diacetate (solid and dotted lines, respectively) under fluctuating temperature (broken line) simulating storage from manufacturing to consumption. Comparison with log-counts observed with (■) and without (●) antimicrobials. Experimental data from Byelashov *et al.* (2008a).

Effects of post-lethality treatments

The “work to be done” h_0 prior to re-growth of *L. monocytogenes* were calculated for 3 antimicrobial treatments (spray with lactic acid [5% v/v], sodium lauryl sulfate [0.5% w/v] or a mixture of lactic acid [5% v/v] and sodium lauryl sulfate [0.5% w/v]). Results are summarized in Table 1.

Table 1: Effects of antimicrobial treatments on the pH of frankfurters and the “work to be done” prior to re-growth.

| Antimicrobial treatment (after inoculation) | pH reduction | “Work to be done prior” to re-growth, h_0 |
|---|--------------|--|
| A. Lactic acid (5%) | 0.2 | 6.8 |
| B. Sodium lauryl sulfate (0.5%) | 0 | 3.0 |
| C. Lactic acid (5%) + sodium lauryl sulfate (0.5%) | 0.2 | 6.7 |

These values of h_0 can be combined with the reported reduction of bacterial levels (Byelashov *et al.*, 2008b) and equation 1 to predict the kinetics of *L. monocytogenes* during storage after the application of these treatments. Table 2 shows the prediction of the time (days) to obtain an increase of 1 \log_{10} CFU/cm² in the concentration of *L. monocytogenes* after treatment C (spray with a mixture of lactic acid and sodium lauryl sulfate, reduction of 2.8 \log_{10} CFU/cm²) as a function of storage temperature.

Table 2: Predicted time to obtain a 10-fold increase in the concentration of *L. monocytogenes* after treatment C on frankfurters (initial pH 6, water activity 0.97) during storage at 4, 7 or 10°C.

| Temperature (°C) | Time to a 10-fold increase (days) |
|------------------|--------------------------------------|
| 4 | 43 |
| 7 | 23 |
| 10 | 14 |

Conclusion

The developed model may be useful in efforts to select conditions for control of *L. monocytogenes* on frankfurters and may be applicable in the development of models for other ready-to-eat meat products.

References

- Baranyi, J. and Roberts, T.A. (1994). A dynamic approach to predicting bacterial growth in food. *International Journal of Food Microbiology* 23, 277-294.
- Barmpalia, I.M., Koutsoumanis, K.P., Geornaras, I., Belk, K.E., Scanga, J.A., Kendall, P.A., Smith, G.C. and Sofos, J.N. (2005). Effect of antimicrobials as ingredients of pork bologna for *Listeria monocytogenes* control during storage at 4 or 10°C *Food Microbiology* 22, 205-211.
- Byelashov O.A., Simpson C.A., Geornaras I., Kendall P.A., Scanga, J.A. and Sofos J.N. (2008a). Evaluation of changes in *Listeria monocytogenes* populations on frankfurters at different stages from manufacturing to consumption. *Journal of Food Science* 73, M430-M437.
- Byelashov O.A., Kendall P.A., Belk K.E., Scanga, J.A. and Sofos J.N. (2008b). Control of *Listeria monocytogenes* on vacuum-packaged frankfurters sprayed with lactic acid alone or in combination with sodium lauryl sulfate. *Journal of Food Protection* 71, 728-734.
- Le Marc, Y., Huchet, V., Bourgeois, C.M., Guyonnet, J.P., Mafart, P. and Thuault, D. (2002). Modelling the growth kinetics of *Listeria* as a function of temperature, pH and organic acid concentration. *International Journal of Food Microbiology* 73, 219-237.
- Lianou, A., Geornaras, I., Kendall, P.A., Belk, K.E., Scanga, J.A., Smith, G.C. and Sofos, J.N. (2007). Fate of *Listeria monocytogenes* in commercial ham, formulated with or without antimicrobials, under conditions simulating contamination in the processing or retail environment and during home storage. *Journal of Food Protection* 70, 378-385.
- Mejlholm, O. and Dalgaard, P. (2007). Modeling and predicting the growth boundary of *Listeria monocytogenes* in lightly preserved seafood. *Journal of Food Protection* 70, 70-74.

Predicting growth and growth boundary of *Listeria monocytogenes* – an international validation study with focus on processed and ready-to-eat meat and seafood

O. Mejlholm¹, A. Gunvig², C. Borggaard², F. Hansen², L. Mellefont³, T. Ross³, F. Leroi⁴, T. Else⁵, D. Visser⁵ and P. Dalgaard^{1*}

¹ National Institute of Aquatic Resources (DTU Aqua), Technical University of Denmark, Kgs. Lyngby, Denmark (pad@aqu.dtu.dk); ² Danish Meat Research Institute (DMRI), Roskilde, Denmark; ³ Tasmanian Institute of Agricultural Research, University of Tasmania, Hobart, Australia; ⁴ Département des Sciences et Techniques Alimentaires Marines, Ifremer, Nantes, France; ⁵ PURAC biochem b.v., Gorinchem, The Netherlands

Abstract

In the present study, the performance of six predictive models for *Listeria monocytogenes* were evaluated for 971 growth responses of the pathogen in meat, seafood, poultry and dairy products. The performance of the evaluated models was closely related to their complexity i.e. the number of environmental parameters they take into account. The model of Mejlholm and Dalgaard (2009) included the effect of nine environmental parameters and it performed better than the other less complex models both with respect to prediction of growth rate (μ_{max} value) and growth boundary for *L. monocytogenes*. For this model bias and accuracy factors were 1.0 and 1.5, respectively, and a correct prediction percentage of 89 were obtained for growth/no-growth responses. The performance of the models of Zuliani et al. (2007), PURAC (2007) and Gunvig et al. (2007), including the effect of five to seven environmental parameters, were considered acceptable with bias factors of 1.2, 1.4 and 1.2, respectively. These models all included the effect of acetic acid/diacetate and lactic acid, but, the effect of CO₂, smoke components or nitrite was not always taken into account. Less complex models that did not include the effect of acetic acid/diacetate and lactic acid (Pouillot et al. 2007; Augustin et al., 2005) were unable to accurately predict growth responses of *L. monocytogenes* in the wide range of food evaluated in the present study. When the complexity of *L. monocytogenes* growth models matches the complexity of food then predictions can be accurate and useful for assessment and management of the pathogen in processed and ready-to-eat (RTE) products.

Keywords: Bias and accuracy factors, correct prediction percentage, growth/no-growth predictions, Psi (ψ) value.

Introduction

For *L. monocytogenes*, the EU regulations specifically indicate predictive models can be used to document that growth is controlled in RTE foods (EC 2073/2005) and similar criteria were recently agreed upon by the Codex Alimentarius Commission. Clearly, models that accurately predict the combined effect of product characteristics and storage conditions on growth and the growth limit of *L. monocytogenes* are interesting for the industry and food inspection authorities. Complex predictive models have been developed and they include the effect of important environmental parameters to reduce and prevent growth of *L. monocytogenes* e.g. the effect of acetic and lactic acid. However, evaluation and comparison of the performance of complex predictive models are lacking for different types of RTE foods.

Materials and methods

The performance of six existing predictive models for growth of *L. monocytogenes* was evaluated in the present study (Table 1). The number of environmental parameters included in the evaluated models varied between one and nine. The least complex models, not taking into account the effect of acetic acid, diacetate and lactic acid, were studied to determine the difference in model performance when compared to the more complex models including the effect of these organic acids.

Table 1 Environmental parameters included in the evaluated predictive models for *L. monocytogenes*

| Models | Temp. | NaCl/a _w | pH | CO ₂ | Smoke | Nitrite | Acetic acid /diacetate | Lactic acid |
|---|-------|---------------------|----|-----------------|-------|---------|------------------------|-------------|
| Pouillot et al. (2007) | + | - | - | - | - | - | - | - |
| Zuliani et al. (2007) | + | + | + | - | - | - | + | + |
| Augustin et al. (2005) | + | + | + | + | + | + | - | - |
| PURAC (2007) ^a | + | + | + | - | - | (+) | + | + |
| Gunvig et al. (2007) ^b | + | + | + | + | - | + | + | + |
| Mejlholm and Dalgaard (2009) ^c | + | + | + | + | + | + | + | + |

^a Available from: http://www.purac.com/purac_com/a5348511153c582f5bd69fd6bd64bb49.php.

^b Available from: <http://1.test.dezone.dk/>

^c Available from: <http://sssp.dtuqua.dk/>

Data from 971 experiments with growth responses of *L. monocytogenes* in processed and RTE foods were collected to evaluate the performance of the six predictive models. Data for model evaluation were collected from 34 independent sources and represented more than 20 different types of meat, seafood, poultry and dairy products. For each of the 971 experiments, information on growth of *L. monocytogenes* was obtained together with product characteristics and storage conditions of the foods. Growth of *L. monocytogenes* was described by the maximum specific growth rate (μ_{max} , h⁻¹) and by growth/no-growth responses. To differentiate between growth and no-growth, the latter was defined as an increase in the concentration of *L. monocytogenes* being less than 0.5 log CFU g⁻¹ within the experimental time. Predicted and observed μ_{max} values of *L. monocytogenes* were compared by calculation of bias and accuracy factors. Bias factor values were calculated so that numbers higher than 1 always indicated that predicted growth was faster than observed growth. To graduate the performance of the predictive models, the following interpretation of the bias factor was used (Ross, 1999): (i) 0.95-1.10 good; (ii) 0.87-0.95 or 1.10-1.43 acceptable and (iii) < 0.87 or > 1.43 unacceptable. Predicted and observed growth and no-growth responses were compared by calculating the percentage of all samples that were correctly predicted. Incorrect predictions were categorized as fail-dangerous (i.e. no-growth predicted when growth was actually observed) and fail-safe (i.e. growth predicted when no-growth was actually observed).

Results and discussion

The model of Pouillot et al. (2007), including the effect of temperature as the only environmental parameter, significantly overestimated growth of *L. monocytogenes* as shown by bias and accuracy factors of 2.1 and 2.3 for all data, and a high percentage of fail-safe predictions (Tables 2 and 3). This model was developed as part of a quantitative risk assessment of *L. monocytogenes* in French cold-smoked salmon. The effect of parameters other than temperature was considered constant and taken into account by the mean value of the reference growth rate of *L. monocytogenes*. When evaluated for seafood in the present study (with 86% of the samples being cold-smoked salmon), predicted μ_{max} values were 70% faster than the observed ones (Table 2). To explain the poor performance of this model, even for cold-smoked salmon, products with added acetic acid/diacetate and lactic acid was removed from the data set. This resulted in bias and accuracy factors of 1.5 and 1.7 for the reduced set of seafood data (n = 121). The approach of modeling the effect of storage temperature and considering other environmental parameters to be constant is therefore not supported by the present study.

For the model of Zuliani et al. (2007), bias and accuracy factors were 1.2 and 1.9 (Table 2). This model was developed for ground pork meat, but importantly, its performance was good or acceptable for other types of products with the exception of ham/cold-cuts (Table 2). The performance of this growth model may be improved by including terms for the effect of nitrite, CO₂ and smoke components. However, this will most likely increase the already high percentage of fail-dangerous predictions (Table 3).

Table 2 Comparison of predicted and observed μ_{max} values of *L. monocytogenes*

| Products | n | Bias/accuracy factors based on comparison of predicted and observed μ_{max} values | | | | | |
|----------------------|------------|--|-----------------------|------------------------|----------------|----------------------|------------------------------|
| | | Pouillot et al. (2007) | Zuliani et al. (2007) | Augustin et al. (2005) | PURAC (2007) | Gunvig et al. (2007) | Mejlholm and Dalgaard (2009) |
| Meat | | | | | | | |
| <i>Pork loin</i> | 100 | 1.8/2.3 | 0.8/1.8 | 1.5/1.9 | 1.0/1.7 | 0.9/1.5 | 0.8/1.5 |
| <i>Ham/cold-cuts</i> | 154 | 2.9/2.9 | 1.8/2.1 | 2.2/2.4 | 1.9/2.1 | 1.3/1.6 | 1.3/1.5 |
| <i>Sausages</i> | 448 | 2.2/2.4 | 1.2/2.1 | 2.2/2.7 | 1.4/1.7 | 1.0/1.5 | 1.0/1.5 |
| Seafood | 193 | 1.7/1.9 | 1.2/1.6 | 0.7/2.0 | 1.3/1.6 | 1.4/1.7 | 1.0/1.5 |
| Poultry | 64 | 1.5/1.9 | 0.9/1.5 | 2.0/2.1 | 1.0/1.4 | 1.2/1.5 | 0.9/1.5 |
| Dairy | 12 | 0.8/1.3 | 1.1/1.2 | 0.9/1.2 | 0.9/1.2 | 1.9/1.9 | 1.3/1.4 |
| All data | 971 | 2.1/2.3 | 1.2/1.9 | 1.8/2.4 | 1.4/1.7 | 1.2/1.6 | 1.0/1.5 |

Bias and accuracy factors of 1.8 and 2.4 were obtained for all data when the model of Augustin et al. (2005) was evaluated (Table 2). The conservative performance of this model was mainly explained by the fact that it did not include the effect of acetic and lactic acid. Dividing the data set, bias and accuracy factors of 1.2 and 1.9 were found for products without addition of acetic acid/diacetate and lactic acid (n = 349) whereas corresponding values of 3.3 and 3.6 were determined for products added these organic acids (n = 214). Thus, use of this model should be limited to foods without added acetic acid/diacetate and lactic acid.

For the PURAC model, bias and accuracy factors of 1.4 and 1.7 were obtained for all data. The performance of this model was good or acceptable for all types of food with the exception of ham/cold-cuts (Table 2). As discussed for the model of Zuliani et al. (2007), the performance of the PURAC model could be improved by including the effect of CO₂ and smoke components. But again, this is likely to render the model more fail-dangerous with respect to growth/no-growth predictions (Table 3).

The model of Gunvig et al. (2007) was developed for RTE meat products. For all data, bias and accuracy factors of 1.2 and 1.6 were obtained and its performance was good or acceptable except for the few dairy products studied (n=12). The model of Gunvig et al. (2007) was slightly fail-safe partly because it did not include the effect of smoke components (Table 1). When products including smoke components were removed from the data set, a small improvement of the model performance was observed as indicated by average bias and accuracy factors of 1.1 and 1.6 (n = 454).

Table 3 Comparison of predicted and observed growth/no-growth responses for *L. monocytogenes*

| Products | n | Number of fail-dangerous/fail-safe predictions | | | | | |
|-------------------------|------------|--|-----------------------|------------------------|---------------|----------------------|------------------------------|
| | | Pouillot et al. (2007) | Zuliani et al. (2007) | Augustin et al. (2005) | PURAC (2007) | Gunvig et al. (2007) | Mejlholm and Dalgaard (2009) |
| Meat | | | | | | | |
| <i>Pork loin</i> | 100 | 0/64 | 8/0 | 6/29 | 8/2 | 4/14 | 6/1 |
| <i>Ham/cold-cuts</i> | 154 | 0/52 | 27/13 | 17/26 | 10/30 | 6/29 | 8/22 |
| <i>Sausages</i> | 448 | 0/144 | 50/20 | 28/66 | 102/25 | 25/57 | 29/29 |
| Seafood | 193 | 0/33 | 12/9 | 39/18 | 21/6 | 0/27 | 1/6 |
| Poultry | 64 | 0/14 | 10/0 | 1/13 | 5/1 | 1/2 | 1/1 |
| Dairy | 12 | 0/0 | 0/0 | 0/0 | 0/0 | 0/0 | 0/0 |
| All data | 971 | 0/307 | 107/42 | 91/152 | 146/64 | 36/129 | 45/59 |
| Correct predictions (%) | | 68 | 85 | 75 | 78 | 83 | 89 |
| Fail-dangerous (%) | | 0 | 11 | 9 | 15 | 3 | 5 |
| Fail-safe (%) | | 32 | 4 | 16 | 7 | 14 | 6 |

The model of Mejlholm and Dalgaard (2009) include the effect of more environmental parameters than the other models in the present study (Table 1). On average, this model performed better than the less complex models both with respect to prediction of μ_{max} values and growth/no-growth responses of *L. monocytogenes* (Tables 2 and 3). This model was originally developed for processed and RTE seafood, but importantly, its performance was also good or acceptable for other types of products with the exception of pork loin. The good overall performance of this model suggests that it includes the effect of parameters actually controlling growth of *L. monocytogenes* in the examined foods (Fig. 1). As an example, when

the effect of smoke components was ignored for the model of Mejlholm and Dalgaard (2009), bias and accuracy factors increased to 1.4 and 1.7 for seafood. Interestingly, these values are identical to the bias and accuracy factors obtained for seafood by the model of Gunvig et al. (2007), not including the effect of smoke components (Table 2). This finding support that smoke component have an important and predictable inhibitory effect on growth of *L. monocytogenes* in smoked seafood.

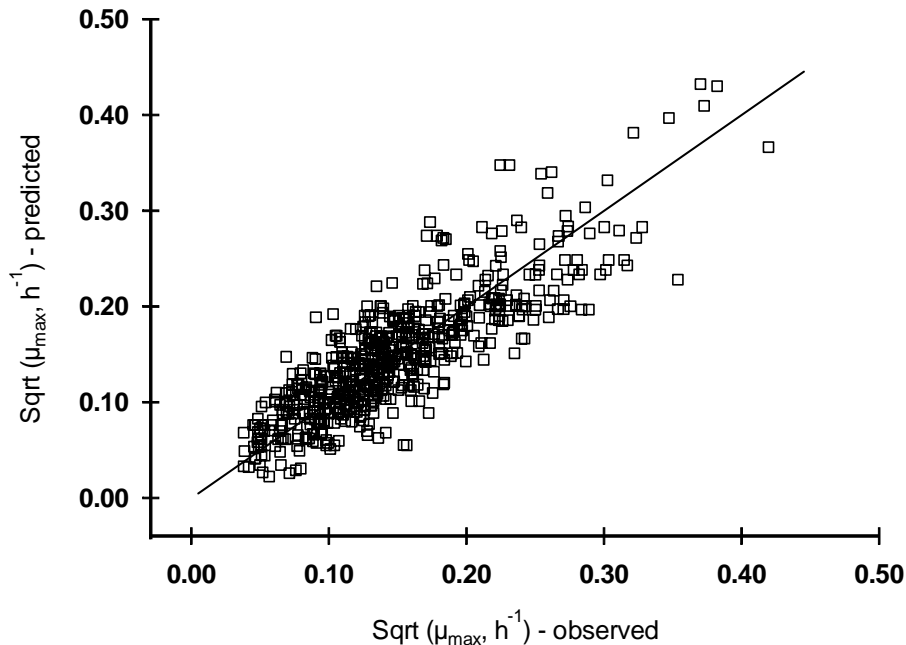


Figure 1 Comparison of observed and predicted μ_{max} values for growth of *L. monocytogenes* in meat, seafood, poultry and dairy products (n = 605). Predicted μ_{max} values were obtained by the model of Mejlholm and Dalgaard (2009) and did not included those products where growth was not observed or where no growth was predicted. The solid line represents the perfect adequacy between observed and predicted values.

Conclusions

This extensive validation study showed that μ_{max} values and growth limits of *L. monocytogenes* in processed and RTE food can be accurately predicted. Appropriate models with a relevant degree of complexity have promise for future assessment and management of *L. monocytogenes* in food.

References

- Augustin J.C., Zuliani V., Cornu M. and Guillier L. (2005). Growth rate and growth probability of *Listeria monocytogenes* in dairy, meat and seafood products in suboptimal conditions. *Journal of Applied Microbiology* 99 (5), 1019-1042.
- Gunvig A., Blom-Hansen J., Jacobsen T., Hansen F. and Borggaard C. (2007). A predictive model for growth of *Listeria monocytogenes* in meat products with seven hurdle variables. In: G.J.E Nychas et al. (Eds.), *Predictive Modelling in Foods – Conference Proceedings*, 197-200, Agricultural University of Athens, Athens, p. 553.
- Mejlholm O. and Dalgaard P. (2009). Development and validation of an extensive growth and growth boundary model for *Listeria monocytogenes* in lightly preserved and ready-to-eat shrimp. *Journal of Food Protection*, In Press.
- PURAC (2007). *Opti.Form Listeria control 2007 model*.
- Ross T. (1999). *Predictive Food Microbiology Models in the Meat Industry*. Meat and Livestock Australia, North Sydney, Australia, pp. 196.
- Zuliani V., Lebert L., Augustin J.C., Garry P., Vendevure J.L. and Lebert A. (2007). Modelling the behaviour of *Listeria monocytogenes* in ground pork as a function of pH, water activity, nature and concentration of organic acid salts. *Journal of Applied Microbiology* 103 (3), 536-550.

Predicting *Staphylococcus aureus* in the dairy chain

Carmen Pin¹, Natalia Gómez-Tomé¹ and Gary Barker¹, Moez Sanaa², Emilie Rieu³, Alexandre Maffre³, Peter Zangerl⁴, Martin Wagner⁵, Antonia Gounadaki⁶, George-John Nychas⁶ Panos Skandamis⁶

¹Institute of Food Research, Norwich, NR4 7UA, United Kingdom.

²Epidemiology and Risk Analysis Unit, National Veterinary School of Alfort, France

³National Interprofessional Center for Dairy Economy, Paris, France

⁴Federal Institute of Alpine Dairying, Vienna, Austria

⁵Department for Farm Animals and Veterinary Public Health, University for Veterinary Medicine, Vienna, Austria

⁶Department of Food Science & Technology, Agricultural University of Athens

Abstract

The population density of *S. aureus* in the dairy chain under dynamic environmental conditions (pH, a_w and temperature) that fluctuate from growth to survival/slow inactivation conditions was modelled. To do this, the dependence of the probability of growth, and of the growth and inactivation rate of *S. aureus* on the temperature, pH and A_w was modelled. Probabilistic and kinetics models were combined to give predictions on the concentration of *S. aureus* at any stage of the dairy chain under fluctuating pH, A_w and/or temperature. To validate the models, predictions were compared with observations at different stages of hard and semi-hard cheese production. Models were implemented in a user-friendly computing tool freely available from www.ifr.ac.uk

Keywords

Staphylococcus aureus, Predictive Microbiology, dairy chain, BIOTRACER

Introduction

Staphylococcus aureus is a ubiquitous bacterium and one of the most common pathogens causing mastitis in cattle. Therefore it is usually isolated from raw milk and other points of the dairy chain. Human intoxication is caused by ingesting enterotoxins produced in food by some strains.

Studying the response of *S. aureus* to the fluctuating conditions of the dairy chain is part of the tracing strategy needed to identify the sources of contamination. We have developed mathematical models able to predict the concentration of *S. aureus* at any time during the dairy chain. Probability of growth models have been integrated with kinetic models for growth and slow inactivation (or survival) at fluctuating environmental conditions.

Material and Methods

Data collection and generation

Data was selected from ComBase (www.ComBase.cc) in the range of conditions relevant to the dairy chain. This was between 0-37°C, 2.5 - 7 pH values and 0.8-1 A_w values.

505 growth curves/rates were used to model the dependence of the maximum specific growth rate on temperature, pH and A_w .

40 survival/slow inactivation curves/rates were used to study the dependence of the inactivation rates on the environmental conditions.

660 growth and 55 no growth conditions were used to fit the probability of growth model. More than 50% of the data was generated with the strain *S. aureus* 196E, which produces enterotoxins A and D.

24 of these curves were explicitly generated at temperatures below 10°C to fill the data gaps at survival/slow inactivation conditions.

Validation of the models was performed during cheese manufacturing. Hard and semi-hard cheese made from pasteurized milk inoculated with *S. aureus* was monitored during manufacturing and ripening.

In addition, observations on semi-hard cheese produced from raw milk naturally contaminated were compared to predictions. Coagulase-positive *S. aureus* were monitored after milking, before pressing the curd and during cheese manufacturing at 12 and 24 h.

Modelling

The dependence of the maximum specific growth rate, μ_{max} , on the temperature in Celsius scale, T , pH and A_w , was modelled as previously described (Presser, *et al.*, 1997).

$$\sqrt{\mu_{max}} = b(T - T_{min})\sqrt{A_w - A_{w_{min}}}\sqrt{1 - 10^{pH_{min} - pH}}$$

Where:

$$\mu_{max} = \frac{dx}{xdt} \text{ in exponential growth phase}$$

The parameters of the model, b , T_{min} , $A_{w_{min}}$ and pH_{min} were estimated by non-linear regression using SAS 9.1

The inactivation rate was modelled by an Arrhenius-type function as already reported (Ross, *et al.*, 2008)

$$\ln(-rate) = a_0 + a_1 (1/T) + a_2 (1/pH) + a_3 (1/bw)$$

Where:

$$rate = \frac{dx}{xdt} \text{ in log linear inactivation}$$

T is absolute temperature (Kelvin scale)

$$bw = \sqrt{1 - A_w}$$

a_0 , a_1 , a_2 and a_3 are the model parameters fitted by linear regression. The energy of activation, Ea , typical parameter of the Arrhenius model, can be estimated as

$$Ea = a_1/K$$

where K is the universal gas constant (8.314)

The dependence of the probability of growth, P , on the temperature in Celsius scale, T , pH and A_w , was modelled by a logistic regression model as previously described (Presser, *et al.*, 1998):

$$\ln(P/(1-P)) = b_0 + b_1 \ln(T - T_{min}) + b_2 \ln(pH - pH_{min}) + b_3 \ln(A_w - A_{w_{min}})$$

The minimum values of the environmental factors for growth were fixed according to ComBase data $T_{min} = 7$, $pH_{min} = 3.8$ and $A_{w_{min}} = 0.85$. The parameters a_0 , a_1 , a_2 and a_3 were estimated by logistic regression using SAS 9.1

Modelling at fluctuating conditions

Under fluctuating temperature, pH and A_w the differential equations were solved numerically by the Runge-Kutta method. Simulations were carried out using an in-house Excel add-in developed within this study, named "*S. aureus* Predictions" freely available at <http://www.ifr.ac.uk/>

Results and Discussion

Table 1 shows the value of the estimations for the model parameters and the coefficient of determination from the models. Estimations were robust and met the convergence criterion in all cases. The R^2 of the model for the probability of growth was relatively small. However, the predicted ability of a logistic model is given by the concordance between predictions and observation and this was ca. 93% for our model.

Table 1: Parameter estimates.

| Model | Term | Estimate | se ^a | R ² |
|-----------------------|------------|----------|-----------------|----------------|
| Growth rate | b | 0.0988 | 0.00475 | 0.92 |
| | T_{min} | 3.921 | 0.6172 | |
| | Aw_{min} | 0.8822 | 0.00673 | |
| | pH_{min} | 3.9931 | 0.0175 | |
| Inactivation rate | a_o | 0.3243 | 3.207 | 0.86 |
| | a_1 | -2480 | 894.6 | |
| | a_2 | 22.33 | 1.542 | |
| | a_3 | -0.0112 | 0.008598 | |
| Probability of growth | b_o | -0.1977 | 1.5903 | 0.60 |
| | b_1 | -1.2857 | 0.2312 | |
| | b_2 | -3.4477 | 0.4537 | |
| | b_3 | -0.6305 | 0.7578 | |

^a standard error of the parameters

In real food scenarios the growth/no growth boundary is frequently crossed. In these conditions either slow growth or slow inactivation can occur. The response of probability of growth models needs to be completed with the increase/decrease in the bacteria concentration as a result of the time under those conditions.

The predictions of the model were compared with the observations during hard-cheese manufacturing produced from pasteurized milk inoculated with *S. aureus*. Fig 1 shows that at the beginning of the process, mainly in the first 10-12 hours, the values of temperature, pH and Aw allowed *S. aureus* to grow giving ca 2 decimal log increase in the concentration. After ca. 4 days, Aw decreased to ca 0.86, pH to 5.1 and temperature was 12°C. This conditions halted growth giving place to a slow decrease of the concentration. *S. aureus* was not detected after ca. 800 hours of ripening.

In addition, the model was validated with observations on semi-hard cheese produced from raw milk naturally contaminated with *S. aureus*. Coagulase-positive *S. aureus* were monitored after milking, before pressing the curd and during cheese manufacturing at 12 and 24 h. Milk from fourteen farms was monitored and in general predictions were in good agreement with observations.

The development of user-friendly software tools is important to facilitate the practical use of predictive models. In this study, we have implemented the models developed for the growth rate, inactivation rate and probability of growth in an Excel add-in. Predictions can be obtained either at static or fluctuating temperature and the program makes it possible for users to input their own temperature, pH and Aw profiles

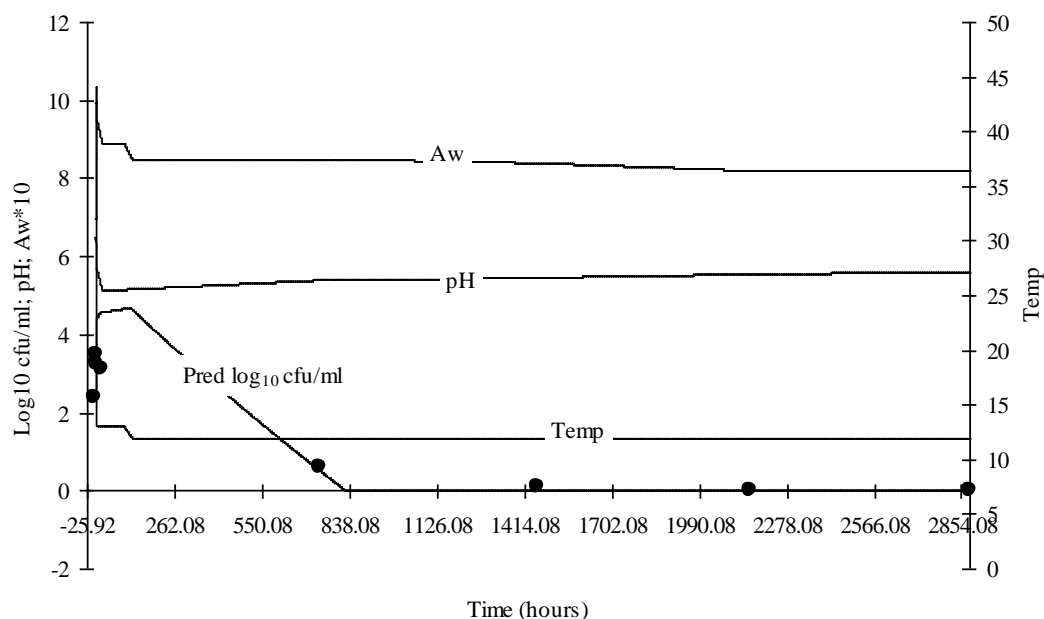


Figure 1. Predicted and observed (dots) concentration of *S. aureus* during the manufacturing of hard cheese made from pasteurized milk inoculated with *S. aureus*. Temperature, pH and Aw fluctuated during the process

Conclusions

A computing program, available as an excel Add in, has been developed to predict the concentration of *S. aureus* in the dairy chain. In the growth/no growth boundary, either slow growth or slow inactivation can occur. In real food scenarios this boundary is frequently crossed. It is desirable to know the increase or decrease in the number of bacteria as a function of the time at the boundary conditions. We have integrated probability of growth models with models for the growth and inactivation rate to give dynamic predictions of the bacteria concentration in the growth/no growth boundary

Acknowledgments

The work was supported by the European Union-funded Integrated Project BIOTRACER (contract #036272) under the 6th RTD Framework.

References

- SAS/STAT User's Guide. 2003. SAS Institute Inc, 9.1 ed. SAS Institute Inc., Cary, NC. USA.
- Presser, K.A., Ratkowsky, D.A., Ross, T., 1997. Modelling the growth rate of *Escherichia coli* as a function of pH and lactic acid concentration. *Appl Environ Microbiol* 63, 2355-2360.
- Presser, K.A., Ross, T., Ratkowsky, D.A., 1998. Modelling the growth limits (growth/no growth interface) of *Escherichia coli* as a function of temperature, pH, lactic acid concentration, and water activity. *Appl Environ Microbiol* 64, 1773-1779.
- Ross, T., Zhang, D., McQuestin, O.J., 2008. Temperature governs the inactivation rate of vegetative bacteria under growth-preventing conditions. *Int J Food Microbiol* 128, 129-135.

Introducing stochasticity in predictive modeling of Salmonella Typhimurium at the farm level of the pork production chain

I. Soumpasis and F. Butler

School of Agriculture, Food Science and Veterinary Medicine, University College Dublin, Belfield, Dublin 4, Ireland (ilias.soumpasis@ucd.ie)

Abstract

Salmonella Typhimurium is the main risk regarding foodborne human Salmonellosis attributed to pork products. The main source of the pathogen in the pork production chain is the pigs that arrive at the slaughterhouse shedding the pathogen. In this work, a stochastic model for the propagation of the pathogen at the compartment level of the pig farms was built, in order to estimate the effect of the compartmental size and the starting conditions of infection on the probability of disease extinction, mean age of extinctions and on the prevalence of infectious pigs at slaughter age.

Keywords

Pigs, Pork, Farms, Salmonella, Typhimurium, Stochastic, Epidemiology, Model, Prevalence

Introduction

Human Salmonellosis is the most common foodborne disease. Regarding the cases attributed to pork, the main risk arises from *S. Typhimurium*. *S. Typhimurium* is mainly introduced into the pork production chain from the infected pigs entering the slaughterhouse. Reducing the prevalence of positive pigs at the pre-harvest stage can help reducing the risk of introducing the pathogen into the slaughterhouse and hence reduce the incidence of human Salmonellosis. Thus, a mathematical model, that can describe the dynamics of *S. Typhimurium* in the compartment level, can help in the prediction of prevalence and in the testing of intervention strategies in order to reduce the risk arising from the high prevalence of positive pigs.

The objective of this work was to build a stochastic mathematical model that can predict the incidence and the prevalence of the pathogen at slaughter pigs. The use of different compartmental sizes and different starting conditions of infection were tested to evaluate their effect on the probability of disease extinction, on the mean age that extinctions occur and on the prevalence of different risk groups of slaughter pigs.

Materials and Methods

Using the findings of experimental infections and field experiments on *S. Typhimurium* at pig farms conducted by different researchers, an epidemic model was developed for the propagation of the pathogen in the compartment level of the pig farms. According to Fedorka-Cray & al. (1994), *Salmonella Typhimurium* in pigs may appear with two disease syndromes, depending on the dose of infection. In that work, the pigs were shedding the pathogen in higher numbers when they were challenged per os with high doses of *S. Typhimurium* than when pigs were commingled with other pigs already shedding the pathogen. Consecutively, they concluded that “their data gives evidence for a second disease syndrome. This syndrome is subclinical and may be important in establishing a carrier state.” Accordingly, in this work two syndromes were employed, a high propagation syndrome with High Infectious (HI) pigs, and a low propagation syndrome with Low Infectious (LI) pigs. The conceptual model is represented in fig. 1 (Soumpasis and Butler, 2009). Given that the low infectious pigs shed less frequently and in smaller populations the pathogen, they are expected to have smaller transmission rate, which was modeled by a reduced transmissibility factor ϵ . The decision of which of the two syndromes will be triggered, was modeled using the concept of the Infectious Equivalent (IE). When IE exceeds a critical limit (IE_{cl}), the high propagation syndrome is triggered. It was assumed that the pigs in both cases develop antibodies at the same time,

around 16 days PI (Nielsen & al., 1995). At that time pigs stop shedding and pass to a carrier stage, carrying the pathogen in internal organs, like lymph nodes and tonsils for approximately up to 12 weeks PI (Wood & Rose, 1992). After this period, the pigs clear of the pathogen but still retain antibodies for an approximate total period of sero-positivity around 110 days (Nielsen & al., 1995).

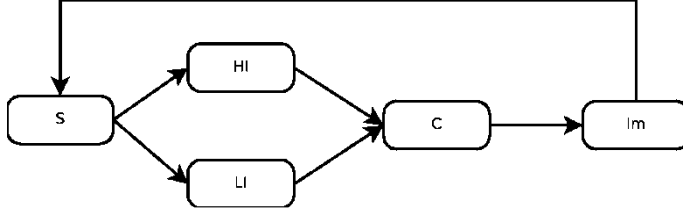


Figure 1. Conceptual representation of the model (Soumpasis and Butler, 2009).

The model is mathematically described with the following equations (Soumpasis and Butler, 2009). The frequency-dependent transmission was preferred over density-dependent (Keeling & Rohani, 2007) because of the infrastructure of the modern pig farms. This is why the population of the infectious is divided by the total population of the compartment (N).

$$\begin{aligned}
 &\text{if } \frac{HI + \varepsilon * LI}{N} \geq IE_{cl}: \\
 &\quad \frac{dS}{dt} = -\beta * S * \frac{HI + \varepsilon * LI}{N} + \kappa * Im \\
 &\quad \frac{dHI}{dt} = \beta * S * \frac{HI + \varepsilon * LI}{N} - \gamma * HI \\
 &\quad \frac{dLI}{dt} = -\gamma * LI \\
 &\quad \frac{dC}{dt} = \gamma * (HI + LI) - \Gamma * C \\
 &\quad \frac{dIm}{dt} = \Gamma * C - \kappa * Im \\
 &\text{else:} \\
 &\quad \frac{dS}{dt} = -\beta * S * \frac{HI + \varepsilon * LI}{N} + \kappa * Im \\
 &\quad \frac{dHI}{dt} = -\gamma * HI \\
 &\quad \frac{dLI}{dt} = \beta * S * \frac{HI + \varepsilon * LI}{N} - \gamma * LI \\
 &\quad \frac{dC}{dt} = \gamma * (HI + LI) - \Gamma * C \\
 &\quad \frac{dIm}{dt} = \Gamma * C - \kappa * Im
 \end{aligned}$$

In the mathematical model the parameters β , ε and IE_{cl} could not be retrieved from literature or experiments. A scenario analysis was run using the inputs of a field experiment made by Beloeil & al. (2003) in order to simulate the experiment. In that experiment three different compartments of a farm were followed bacteriologically and serologically. Using different combinations of parameters β , ε and IE_{cl} , the scenario analysis was used to find for which of the combinations the field experiment results agreed with the results produced by the simulation. The range of values resulted from this scenario analysis was for β from 0.145 to 0.19, for ε from 0.61–0.8 and for IE_{cl} from 0.10 and 0.14 (Soumpasis and Butler, 2009).

In a second phase, a stochastic model was built using an event-driven approach that is more appropriate for pig farms (Soumpasis and Butler, 2008). The τ -leap method was used in order to increase the simulation speed. The median values of β (0.165), ε (0.7) and IE_{cl} (0.12) were

used for the stochastic model, along with the other parameters already used at its deterministic counterpart. The model simulated different compartments with population ranging from 200 to 400 pigs and different starting conditions of infection from 0.25% to 100%. The probability of extinctions and the mean prevalence of each class of the model and each risk group of pigs were recorded along with the population of the compartment and the starting conditions of infection. The events and the number of events in a time step are presented in table 1 (Soumpasis and Butler, 2009).

Table 1: Events of the model and calculation of the number of events per time step using the “ τ -leap method” (Soumpasis and Butler, 2009)

| Name | Number of events | Font style |
|------------------|--|--|
| High Infection | $M1 = \text{Poisson}(\tau * [\beta * S * (HI + \epsilon * LI) / N])$ | $S \rightarrow S - M1, HI \rightarrow HI + M1$ |
| Low Infection | $M2 = \text{Poisson}(\tau * [\beta * S * (HI + \epsilon * LI) / N])$ | $S \rightarrow S - M2, LI \rightarrow LI + M2$ |
| Recovery of HI | $M3 = \text{Poisson}(\tau * [\gamma * HI])$ | $HI \rightarrow HI - M3, C \rightarrow C + M3$ |
| Recovery of LI | $M4 = \text{Poisson}(\tau * [\gamma * LI])$ | $LI \rightarrow LI - M4, C \rightarrow C + M4$ |
| Recovery of C | $M5 = \text{Poisson}(\tau * [\Gamma * C])$ | $C \rightarrow C - M5, Im \rightarrow Im + M5$ |
| Loss of Immunity | $M6 = \text{Poisson}(\tau * [\kappa * Im])$ | $Im \rightarrow Im - M6, S \rightarrow S + M6$ |

The model was run for 113 days, starting from the 61st day of life of the pigs, which it was supposed to be age that pigs lose maternal immunity. Accordingly, the last day of the model (day 174) is considered to be the average harvest day. The stochastic model was compared to the deterministic model, using the predicted mean prevalence of the stochastic model and the predicted prevalence of the deterministic model for the different classes and risk groups for the range of TPC and SCI used for validation reasons.

The model and the scenario analysis were written in Python programming language v.2.5.1, using the scientific libraries Scipy/Numpy, for numerical calculations. Parallel computing with Ipython and optimizations using Pyrex python extension resulted to an overall 86% reduction of execution time on an Intel core-duo computer clocking at 3GHz running x86_64 Linux Mint. For the graphical representations of the results Gnuplot v.4.2 was used.

Results and discussion

From the results of this work it is concluded that very low or very high starting conditions of infection can lead to increased observations of disease. However, these extinctions differ qualitatively and the impact of this difference is shown at the prevalence of the classes and risk groups with long duration in the infection cycle.

In the case of low SCI, the extinctions were early extinctions leading to a minimum of prevalence of all classes except the susceptible. In this way the distributions of prevalence of HI, LI, C and Im were highly zero-inflated and the risk of introducing the pathogen into the slaughterhouse was minimized. Thus, measures that reduce SCI like cleaning of the compartment between batches and good farming practices could have a positive effect at the reduction of the risk of introducing the pathogen at the slaughterhouse.

For SCI from 3.7% to 5.4% the extinctions almost zeroed, while the mean age of extinction maximized leading to late disease extinctions. Above this level, the cases of extinctions were increasing linearly with SCI, while the relationship of the probability of extinction and TPC was negative. Thus, the reduction of the size of the compartment has a positive effect in the reduction of the risk of *S. Typhimurium*.

For these late extinctions, although the distributions of the prevalence of the infectious classes (HI and LI) were zero-inflated, the distributions of the classes of C and Im were approximating the normal distribution. Thus, while the risk groups of culture- and sero-positive cannot predict the actual risk of introducing the pathogen into the slaughterhouse through the infectious classes, they can be used for characterization of the farm status regarding *Salmonella*, because of the property of “memory” that they have.

Indeed, this was observed for SCI above 50%, where the prevalence of the risk groups of culture- and sero-positive was relatively stable around 31% and 53% respectively. However, for

very low SCI, both risk-groups showed a lot of variation, which partly explains the big variability between consecutive serology tests of the same farm observed at national serology programs. A key point is that at least for farms that show a relatively high sero-positivity to consecutive tests are heavily contaminated. The most common scheme of farm serology monitoring programs for Salmonella, which is followed also in Ireland, is to define the index of the farm with a weighted average of three consecutive samples. There are taken 3 samples per year and in each sample 24 animals are tested (serology test with meat-juice ELISA). Having in mind the above and the hypergeometric nature of the sampling process, it is proposed that the serology monitoring programs should take into account the size of the farm, in order to define both the number of the animals tested and the frequency of the sampling.

Conclusions

In a first phase a deterministic model was developed taking into account the two different propagation syndromes, with which *S. Typhimurium* may appear in the farm and having as a modeling unit the compartment level of the farm. In a second phase, a stochastic model was built adapted to modern all-in-all-out farm systems and conditions. From the results of the model, it was concluded that cleaning and disinfection of the compartments between batches of pigs along with the reduction of the compartmental size could increase the probability of disease extinction up to 45%. On the other hand, the prevalence of the culture- and the sero-positive risk groups could be used as an indicator of the status of the farm regarding *S. Typhimurium*. A re-consideration of the Salmonella monitoring programs regarding the frequency and the sample size is proposed based on the size of the farms.

Acknowledgment and Disclaimer

We acknowledge the 6th EU framework Integrated Project Q-Porkchains that has been the major source of information for this paper. The content of the paper reflects only the view of the authors; the Community is not liable for any use that may be made of the information contained in this paper.

References

- Beloeil, P. A., Chauvin, C., Proux, K., Rose, N., Queguiner, S., Eveno, E., Houdayer, C., Rose, V., Fravallo, P., & Madec, F. (2003). Longitudinal serological responses to *Salmonella enterica* of growing pigs in a subclinically infected herd. *Preventive Veterinary Medicine*, 60(3):207-226.
- Fedorka-Cray, P. J., Whipp, S. C., Isaacson, R. E., Nord, N., & Lager, K. (1994). Transmission of *Salmonella Typhimurium* to swine. *Veterinary Microbiology*, 41(4):333-344.
- Keeling, M. J. & Rohani, P. (2007). *Modeling Infectious Diseases*. Princeton University Press. ISBN 978-0-691-11617-4.
- Nielsen, B., Baggesen, D., Bager, F., Haugegaard, J., & Lind, P. (1995). The serological response to *Salmonella* serovars Typhimurium and Infantis in experimentally infected pigs. the time course followed with an indirect anti-Ips ELISA and bacteriological examinations. *Veterinary Microbiology*, 47(3-4):205-218.
- Soumpasis I. & Butler F. (2008). A comparison of deterministic and stochastic epidemic models for the risk assessment of *Salmonella* at the preharvest level of pork production. In *FOODSIM 2008*, pages 8085. Eurosis-ETI.
- Soumpasis I. & Butler F. (2009). Development and application of a stochastic epidemic model for the transmission of *Salmonella Typhimurium* at the farm level of the pork production chain. *Risk Analysis: An International Journal*. DOI: 10.1111/j.1539-6924.2009.01274.x
- Wood, R. L. & Rose, R. (1992). Populations of *Salmonella Typhimurium* in internal organs of experimentally infected carrier swine. *American Journal of Veterinary Research*, 53(5):653-658.

The potential of end-product metabolites on predicting the shelf life of minced beef stored under aerobic and modified atmospheres with or without the effect of essential oils

A.A. Argyri^{1,2}, E.Z. Panagou¹, R. Jarvis³, R. Goodacre³, and G-J.E. Nychas¹

¹ Laboratory of Microbiology and Biotechnology of Foods, Department of Food Science and Technology, Agricultural University of Athens, Iera Odos 75, Athens 11855, Greece (author for correspondence stathispanagou@aua.gr)

² Laboratory of Applied Microbiology, Cranfield Biotechnology Centre, Cranfield Health, Cranfield University, College Road, Cranfield, Bedfordshire MK43 0AL, United Kingdom

³ University of Manchester, School of Chemistry, Lab of bioanalytical spectroscopy, PO Box 88, Sackville St, Manchester M60 1QD, UK

Abstract

In this study, the potential of using the metabolic profile of end-products, mainly organic acids, as a consequence of the evolution of the microbial association present initially in meat (minced beef), on predicting the shelf life of minced beef was evaluated, performing in parallel microbiological analysis, sensory analysis, and pH measurements. The shelf life of minced beef stored aerobically, under Modified Atmosphere Packaging (MAP) and MAP with the presence of the volatile compounds of oregano essential oil (MAP + OEO) at 0, 5, 10, and 15 °C was assessed, monitoring the microbial association of meat and the biochemical changes occurring in the meat substrate. Microbiological analysis that implicated counts of TVC, *Pseudomonas* spp., *Brochothrix thermosphacta*, lactic acid bacteria (LAB), *Enterobacteriaceae*, yeasts, and molds was performed at the same time with sensory analysis, pH measurements and HPLC analysis of organic acids. The spectral data collected from HPLC were subjected to various analyses, including Principal Components Analysis (PCA) and Factorial Discriminant Analysis (FDA), revealing qualitative classification of the samples concerning their spoilage status, as this was pre-classified from the sensory evaluation. Quantitative predictions of the TVC, *Pseudomonas* spp., *Br. thermosphacta*, LAB, *Enterobacteriaceae*, yeasts and molds were conducted using Partial Least Square-Regression (PLS-R) models, as well as Support Vector Machines (SVM) regression models with linear and non-linear kernel functions. The above classification and calibration models demonstrated that the metabolic profile of organic acids, i.e metabolic end-products derived from the microbial activity of the microbial association developed during storage, as attributed from the HPLC analysis, may be considered as a potential method to evaluate the spoilage and the microbial status of a meat sample regardless the storage conditions (e.g. packaging and temperature).

Keywords: Minced meat, Spoilage, HPLC, end-product metabolites, PLS-R, SVMs

Introduction

The relationship between microbial growth and chemical changes occurring during meat storage has been continuously recognized as a potential means to reveal indicators that may be useful for quantifying beef quality or freshness (Nychas et al. 2008). Though, the imposed different storage conditions and the preservatives could influence the production of these potential indicators, through the establishment of a transient microbial association defined as the 'Ephemeral spoilage micro-organisms' - ESO (Nychas and Skandamis 2005). As a consequence, these compounds can be formed in different concentrations depending on the storage conditions, whilst their absence or presence in low quantities, do not preclude spoilage (Nychas et al. 2008). This fact arises the need of a holistic approach in introducing shelf-life indicators that could be applied irrespective of storage temperature or packaging system and be eligible to the income of new technologies. Considering the above, the aim of the present study was to investigate the potential of HPLC analysis of organic acids as a quick analytical method for monitoring the spoilage of minced beef samples stored under different

storage conditions (i.e. packaging and temperature). Conventional packaging conditions (as aerobic storage and storage under modified atmospheres) as well as an alternative packaging technique (packaging with the presence of volatile compounds of essential oil) were used in order to explore the dynamics of the method in analysing different meat ecosystems. Moreover, different storage temperatures were tested, which represented chill (0, 5 °C) and abuse temperatures (10, 15 °C) that may occur during the chill chain of the meat.

Materials and methods

Minced beef was stored aerobically, under Modified Atmosphere Packaging (MAP) and MAP with the presence of the volatile compounds of oregano essential oil (MAP + OEO) at 0, 5, 10, and 15 °C and microbiological analysis that implicated counts of total viable counts (TVC), *Pseudomonas* spp., *Brochothrix thermosphacta*, lactic acid bacteria (LAB), *Enterobacteriaceae*, yeasts and moulds was performed in parallel with sensory analysis, pH measurements and HPLC analysis of organic acids. The spectral data collected from the HPLC (areas under peaks) were subjected to a principal component analysis (PCA) to investigate the peaks that significantly fluctuated during storage, followed by a second PCA using the selected peaks which revealed the Principal Components (PCs) that were further used for analysis. These last PCs were subjected to Factorial Discriminant Analysis (FDA) in order to predict the spoilage status of a sample belonging to a previously-defined quality group (fresh, semi-fresh, and spoiled). In an attempt to predict the different groups of microbial flora, the above PCs were regressed using a fully cross validated partial least squares regression (PLS-R) model and Support Vector Machines (SVM) regression models with linear, polynomial, radial basis and sigmoidal Kernel functions.

Results and discussion

The analysis of the chromatograms from the HPLC resulted in the selection of 17 pure peaks (purity was always greater than 99%, as calculated from the Jasco Chrompass Chromatography Data system v1.7.403.1). These peaks had Retention Times (RT) of 6.2, 6.9 (citric acid), 7.0, 7.9, 8.3, 9.7, 10.9 (lactic acid), 11.9 (formic acid), 12.9 (acetic acid), 14.9, 15.1 (propionic acid), 16.1, 17.8, 18.6, 20.5, 24.6 and 28.1. Figure 1 represents the metabolic profile of a fresh mince sample and a spoiled one as attributed from the HPLC organic acid analysis.

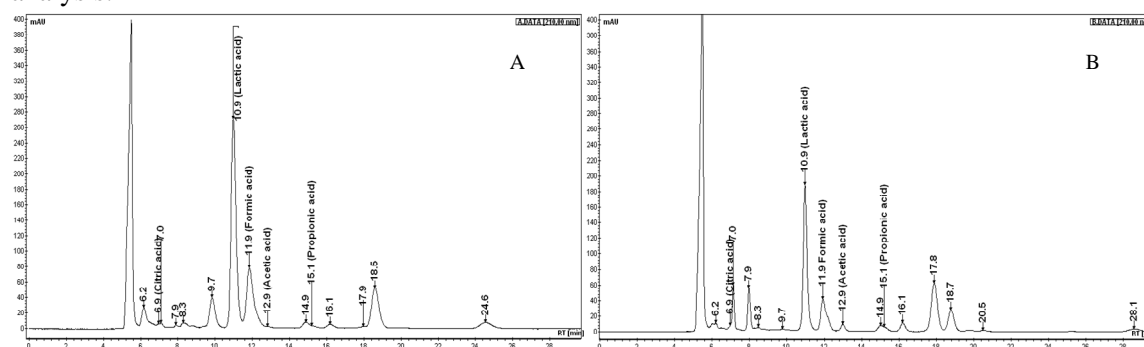


Figure 1: The metabolic profile of a fresh mince sample A) and a spoiled one B) during aerobic storage at 15 °C, as attributed from the HPLC organic acid analysis.

Qualitative classification of the samples

The FDA provided classifications of the samples regarding their spoilage status, giving a correct classification of the samples 93.3% (fit of the model) and a cross validation of 88.0%. More specifically, the classification of the samples after cross validation of the built model was 88.46% correct for the fresh samples, 81.82% for the semi-fresh and 89.47% for the spoiled ones. Figure 2 demonstrates the discrimination map of the samples regarding their spoilage status (fresh, semi-fresh and spoiled). The map reveals the transition of the meat samples from the fresh status to semi-fresh and finally to spoiled.

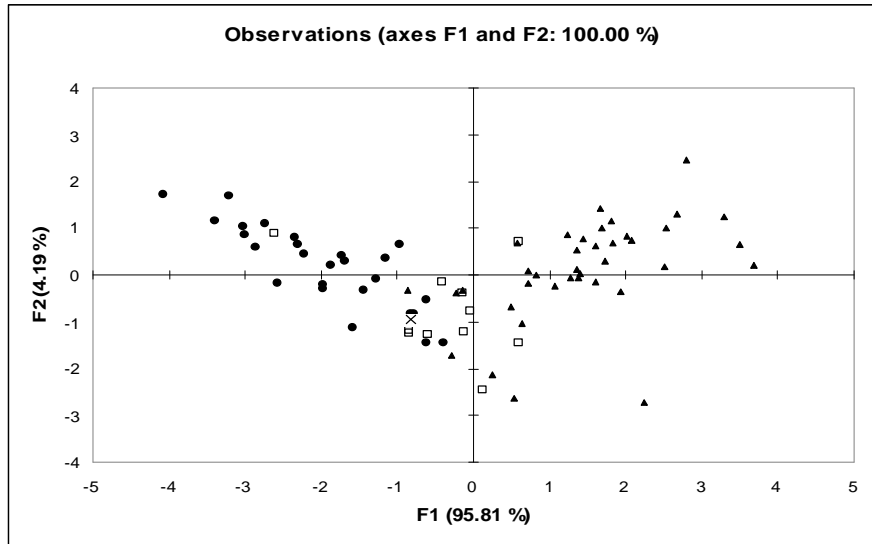


Figure 2: Discriminant analysis similarity map determined by discriminant factors 1 (F1) and 2 (F2) for HPLC spectral data of the three different minced groups: ●, fresh; □, semi-fresh; ▲, spoiled

Prediction of the microbial loads

PLS-R analysis, that employed one latent variable in all cases, as well as the SVM models with linear, polynomial, radial basis, and sigmoidal kernel functions demonstrated a predictions onto viable counts of the total microflora (TVC), *Pseudomonas* spp, *Br. thermosphacta*, LAB, *Enterobacteriaceae*, and yeasts and moulds. The values of B_f , A_f , and RMSE indices (Ross 1996; Panagou and Nychas 2008) that demonstrate the performance of the models built for every group of microorganisms are shown in Table 1 (data not shown for the polynomial models because they exhibited an overprediction trend). Figure 3 shows the distribution of the predicted cross validated values of the TVC compared to the observed ones.

Table 1: The performance of the models using the full cross validation estimates from the four built models.

| Microbial group | PLS-R | | | Linear SVM | | | Radial basis SVM | | | Sigmoid SVM | | |
|---------------------------|-------|-------|------|------------|-------|------|------------------|-------|------|-------------|-------|------|
| | B_f | A_f | RMSE | B_f | A_f | RMSE | B_f | A_f | RMSE | B_f | A_f | RMSE |
| TVC | 0.99 | 1.10 | 0.88 | 0.99 | 1.10 | 0.94 | 1.00 | 1.10 | 0.89 | 1.00 | 1.10 | 0.83 |
| <i>Pseudomonas</i> spp | 1.00 | 1.17 | 1.30 | 1.35 | 1.39 | 2.20 | 1.00 | 1.15 | 1.09 | 1.02 | 1.19 | 1.30 |
| <i>Br. thermosphacta</i> | 1.00 | 1.18 | 1.09 | 0.99 | 1.18 | 1.14 | 1.01 | 1.17 | 1.06 | 1.00 | 1.18 | 1.07 |
| LAB | 1.00 | 1.09 | 0.75 | 1.01 | 1.09 | 0.74 | 1.01 | 1.08 | 0.71 | 1.02 | 1.08 | 0.68 |
| <i>Enterobacteriaceae</i> | 0.99 | 1.16 | 1.18 | 1.00 | 1.14 | 1.08 | 1.00 | 1.14 | 0.98 | 0.98 | 1.14 | 1.05 |
| Yeasts & Molds | 0.99 | 1.15 | 1.01 | 1.00 | 1.15 | 1.03 | 0.99 | 1.11 | 0.83 | 1.02 | 1.14 | 0.97 |

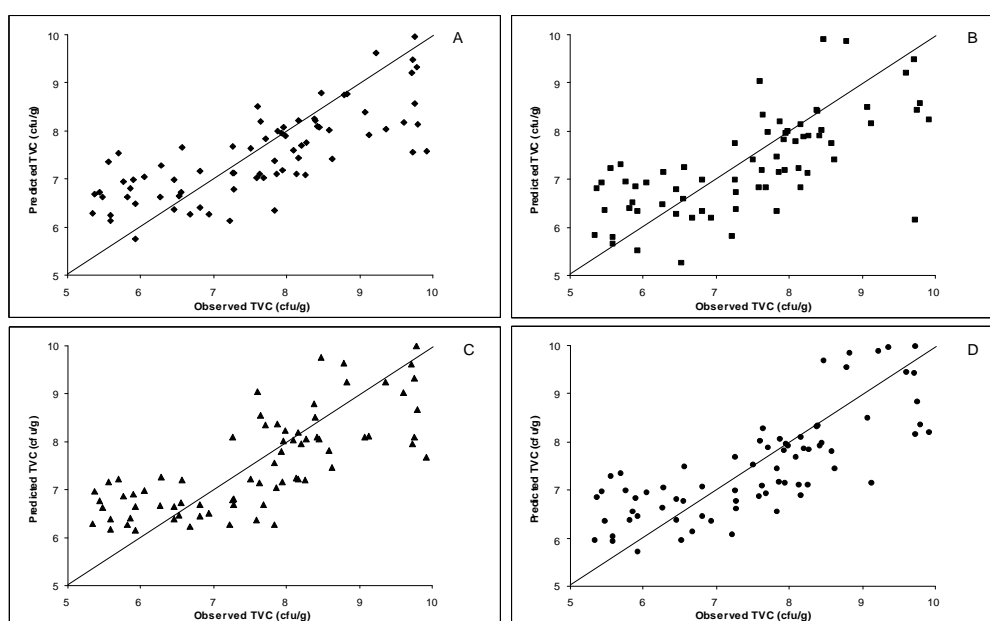


Figure 3: Observed vs Predicted counts of the total microbial flora (TVC) as estimated from the cross validated values of the PLS-R (A), linear SVM (B), radial basis SVM(C) and sigmoid SVM (D) models.

The value of B_f describing the performance of the model, was generally close to unity, indicating good agreement between observations and predictions, whilst the fact that it is slightly below unity, indicates a 'fail-safe' model (Ross, 1996). The A_f values, that were also close to unity, describe the average differences between predictions and observations, For example, the value $A_f = 1.100$ for the TVC counts indicates a 10 % average difference (either above or below). In general the PLS-R, radial basis SVM and sigmoidal SVM exhibited slightly better performance than the Linear SVM whereas the models that described the estimates of the TVC, as well as the LAB, had better performance (according to the values of Table 1), regardless of the type of the model built.

Conclusions

The above results reveal that HPLC analysis of organic acids can be proved as a potential technique for meat analysis in predicting the spoilage status and the microbial load of a meat sample regardless the type of storage conditions. A data re-processing in which the type of the packaging can be considered as a factor will strengthen the potential use of this approach. It is clear that further studies are required to investigate the eligibility of the method and update it with novel packaging and preservation techniques that are raising and sequentially change the time course and character of spoilage.

Acknowledgements

This work was co-funded by the EU projects Symbiosis (7th Framework Programme, Contr. No 21638) and ProSafeBeef (6th Framework Programme, Food-CT-2006-36241).

References

- Nychas, G.-J. E. and Skandamis, P. (2005) Fresh meat spoilage and modified atmosphere packaging (MAP). In: J. N. Sofos (Ed.), *Improving the Safety of Fresh Meat*, 461–502, CRC/Woodhead Publishing Limited, Cambridge, UK
- Nychas, G.-J. E., Skandamis, P.N., Tassou, C.C and Koutsoumanis, K.P. (2008) Meat spoilage during distribution. *Meat Science* 78, 77-89.
- Panagou, E.Z. and Nychas G.-J. E. (2008) Dynamic modeling of listeria monocytogenes growth in pasteurized vanilla cream after postprocessing contamination. *Journal of Food Protection* 71 (9), 1828-1834
- Ross, T. (1996) Indices for performance evaluation of predictive models in food microbiology. *Journal of Applied Bacteriology* (81), 501-508

Risking More by Modelling cocktail or strain?

E.Z. Panagou, M. Mataragas, D. Kagkli, G.-J.E. Nychas and P. Skandamis

Agricultural University of Athens, Department of Food Science, Technology and Human Nutrition, Laboratory of Microbiology and Biotechnology of Foods, Iera Odos 75, 118 55 Athens, Greece (gjn@aua.gr)

Abstract

In the present work, the survival of *Listeria monocytogenes* in the traditional Greek soft, spreadable cheese Katiki Domokou was studied throughout the shelf life of the product. Five strains of *Listeria monocytogenes* were aseptically inoculated individually and as a cocktail in Katiki cheese, which was then stored at 5, 10, 15, and 20°C. Pulsed-field gel electrophoresis was used to monitor strain evolution or persistence during storage at different temperatures in the case of the cocktail inoculum. The results suggested that strain survival of *L. monocytogenes* was temperature dependent since different strains predominated at different temperatures. Kinetic behavior of *L. monocytogenes* in the case of the cocktail inoculum was also studied. The applicability of a neural network approach was compared with the reparameterized Gompertz, the modified Weibull, and the Geeraerd primary models. The developed neural network described the survival of *L. monocytogenes* equally well or slightly better compared with the other models. The neural network and primary models all were validated under constant temperature storage conditions (12 and 17°C). The prediction performance of the neural network approach was equal to that of the primary models at both validation temperatures. This study underlines the usefulness of predictive modeling as a tool for realistic estimation and control of *L. monocytogenes* risk in food products. Such data are also useful when conducting risk assessment studies.

Introduction

“Katiki Domokou” is a traditional Greek Protected Designation of Origin (PDO) cheese since 1994 (pH 4.2 to 4.4). Its microflora has not been studied yet, while its structure (pseudo-emulsion) and composition may enable (or even favour) the survival and growth of several pathogens, including *Listeria monocytogenes*. The persistence of *L. monocytogenes* during storage at different temperatures has been the subject of many studies since temperature abuse of food products is often encountered (Xanthiakos et al. 2006; Sivarooban et al. 2007). The qualitative and /or quantitative risk of using single or cocktail strains is the purpose of this communication which is based on the data provided in previous publications related to Katiki cheese published from of our group (Mataragkas et al. 2008; Panagou 2008; Kakgli et al. 2009).

Materials and Methods

The strains used in the study for the inoculum consisted of two type strains of serotype 4b and three isolates belonging to our laboratory collection, isolated from soft cheese and a conveyor belt of ready-to-eat (RTE) foods. The strains were chosen on the basis of their source of isolation, since this could be crucial to the interpretation of the data. The cheese was stored at 5, 10, 15, and 20°C as temperature abused over a period of 40 days. The quantitative as well as qualitative evolution of the pathogen was monitored throughout storage. Additionally, pulsed-field gel electrophoresis (PFGE) was used to monitor the strain(s), which may survive and / or grow at different temperatures (Heir et al. 2004). Kinetic parameters related to survival and death of this cocktail of *L. monocytogenes* strains was estimated with four models [the reparameterized Gompertz model, the modified Weibull model, the Geeraerd model and an artificial neural network model – radial basis function (RBF NN)], capable of fitting linear and biphasic inactivation curves (Zwietering et al. 1990; Geeraerd et al. 2000; Albert and Mafart 2005; Panagou et al. 2007). The kinetics were then described as a function of storage temperature. The model was also validated in the actual product. The secondary

models for Katiki cheese, stored at various temperatures using a five-strain cocktail, are of great importance since the existing kinetic models for survival / inactivation of *L. monocytogenes* in different foods or food systems (e.g. broths, model systems), have been derived mainly from experiments where single strain inocula were applied.

Results and Discussion

The kinetic parameters of *L. monocytogenes* during storage at different temperatures have been the subject of many studies since temperature abuse of food products is often encountered (Mataragas et al. 2006; Xanthiakos et al. 2007). Particularly the quantitative estimation of kinetic parameters related to growth, survival, and death of a cocktail of *L. monocytogenes* strains has been described recently (Mataragas et al. 2008; Panagou 2008) by using either the reparameterized Gompertz, the modified Weibull, the Geeraerd models and artificial neural networks (ANN) approach. It was concluded that the performance of the latter (ANN) was equal to that of the primary models at both validation temperatures.

When the validation of these models was tested against the different strains used in this study a significant variation occurred. Indeed the kinetic characteristics (death rate) of individual strains displayed a different inactivation behavior at the temperatures studied, e.g. presence or absence of shoulder phase and presence or absence of a sub-population ($k_{\max 2}$). The inactivation rates of the primary population ($k_{\max 1}$) were not directly comparable between the strains at all temperatures. Therefore, the parameter of 4D reduction should be used for comparison because it takes into account the existence or not of shoulder phase or the presence or not of a sub-population (tailing). The results showed (Table 1) that there are differences between strains regarding the time needed to reach 4 logs reduction and especially at high temperatures (15 and 20°C) the parameter varied considerably. The best survivor among the strains tested was the strain TS125 (Table 1).

| T°C | <i>Listeria monocytogenes</i> strain | | | | |
|-----|--------------------------------------|-------|-------|-------|-------|
| | TS124 | TS125 | TS128 | TS131 | TS133 |
| 5 | 26.40 ^a | 29.10 | 25.20 | 25.20 | 24.60 |
| 10 | 21.90 | 24.30 | 21.00 | 21.90 | 21.90 |
| 15 | 8.60 | 17.20 | 10.60 | 11.00 | 12.20 |
| 20 | 6.24 | 9.23 | 6.37 | 3.51 | 7.41 |

^a: days needed for a 4D reduction.

Table 1: 4D reduction (in days) of different *Listeria monocytogenes* strains inoculated individually in katiki cheese and stored at different temperatures.

This was also evident with the application of PFGE, which revealed that TS125 was present in higher percentage among the other strains in the cocktail experiments (Table 2). The fact that different strains were recovered from different temperatures is of great importance *per se*. There are certainly some strains which have better survival capacity. For example the most persistent strain in all cases, both individually or mixed with other *Listeria* strains, was TS125, a serotype 4b strain, which is in accordance with previous observations regarding strain serotypes and food-borne illnesses (Cocolin et al. 2001; Borucki et al. 2003). The rest of the strains studied did not show the same behavior and, when inoculated individually, were more or less affected by the presence of other strains.

| Temperature (° C) | % contribution of <i>Listeria monocytogenes</i> strains | | | | |
|----------------------|---|-------|-------|-------|-------|
| | TS124 | TS125 | TS128 | TS131 | TS133 |
| 5 | 0 | 0 | 0 | 100 | 0 |
| 10 | 0 | 95 | 0 | 0 | 5 |
| 15 | 18 | 68 | 0 | 14 | 0 |
| 20 | 0 | 78 | 5 | 3 | 14 |

Table 2: Contribution of individual strains in the cocktail experiments at the end of storage of katiki cheese stored at different temperatures.

With this information it can be concluded that the developed model(s) could not be used for the individual strains, but the model was only accurate in the case of the cocktail inoculum. This was due to the fact that strain survival of *L. monocytogenes* was temperature-dependent since different strains managed to survive at different temperatures (Table 1).

Such information is of great importance in risk assessment studies, which typically consider only the presence or absence of the pathogen. Adopting such an approach, it can be concluded that the derived models can be useful in risk assessment studies especially when the probability of illness at the time of consumption can be assessed, in conjunction with data derived from consumption patterns of the product, retail and home time-temperature profiles, and storage times of the product. However, the strain variability should always be taken into account.

This study demonstrates the importance of the selection criteria of one strain versus another when risk assessment analysis is conducted. Whether the environment in which *Listeria* is found, e.g., cheese or meat, could influence the survival rate might be another important factor to take into consideration since it has been shown in several models that microorganisms have a different behavior in broth culture than in a complex food matrix (Xanthiakos et al. 2006; Dourou 2009). Relevant findings would contribute further to the applicability of EU regulation 2073/2005 (European Commission 2005).

Acknowledgments

The present study was part of Truefood, Traditional United Europe Food, an integrated project financed by the European Commission under the 6th Framework Programme for RTD (contract no. FOOD-CT- 2006-016264).

References

- Albert I. and Mafart P. (2005) A modified Weibull model for bacterial inactivation. *International Journal of Food Microbiology* 100, 197–211.
- Borucki M.K. and Call D.R. (2003) *Listeria monocytogenes* serotype identification by PCR. *Journal of Clinical Microbiology* 41, 5537–5540.
- Cocolin L., Manzano, M., Cantoni C. and Comi G. (2001) Denaturing gradient gel electrophoresis analysis of the 16S rRNA gene V1 region to monitor dynamic changes in the bacterial population during fermentation of Italian sausages. *Applied and Environmental Microbiology* 67, 5113–5121.
- Dourou D. (2009) Pathogens responses in food: underestimated eco-physiological factors, PhD Thesis Cranfield University, UK
- European Commission (2005) Commission regulation (EC) no. 2073/2005 of 15 November 2005 on microbiological criteria for foodstuffs. Official J. Eur. Union L338, 1–26.
- Geeraerd A.H., Herremans C.H. and Van Impe J.F. (2000) Structural model requirements to describe microbial inactivation during a mild heat treatment. *International Journal of Food Microbiology* 59, 185–209.
- Heir E., Lindstedt B.A., Røtterud O.J., Vardund T., Kapperud G. and Nesbakken T. (2004) Molecular epidemiology and disinfectant susceptibility of *Listeria monocytogenes* from meat processing plants and human infections. *International Journal of Food Microbiology* 96, 85–96.
- Kagkli D-M, Iliopoulos V, Lazaridou A, Stergiou V. and Nychas G.-J.E. (2009) *Listeria monocytogenes*: strain

- survival at different storage temperatures in Katiki, a traditional Greek soft cheese *Applied Environmental Microbiology* 75, 3621-3626.
- Mataragas M., Stergiou V. and Nychas G.-J.E. (2008) Modelling survival of *Listeria monocytogenes* in a traditional Greek soft cheese “Katiki” *Journal of Food Protection* 71, 1835-1845.
- Mataragas M., Drosinos E.H., Siana P., Skandamis P. and Metaxopoulos I. (2006) Determination of the growth limits and kinetic behavior of *Listeria monocytogenes* in a sliced cooked cured meat product: validation of the predictive growth model under constant and dynamic temperature storage conditions. *Journal of Food Protection* 69, 1312-1321.
- Panagou E.Z. (2008) A radial basis function neural network approach to determine the survival of *Listeria monocytogenes* in Katiki, a traditional Greek soft cheese. *Journal of Food Protection* 71, 750–759.
- Panagou E.Z., Kodogiannis V. and Nychas G.-J.E. (2007) Modelling fungal growth using radial basis function neural networks: the case of the ascomycetous fungus *Monascus ruber* van Tieghem. *International Journal of Food Microbiology* 117, 276–286.
- Sivarrooban T., Hettiarachchy N.S. and Johnson M.G. (2007) Inhibition of *Listeria monocytogenes* using nisin with grape seed extract on turkey frankfurters stored at 4 and 10 degrees C. *Journal of Food Protection* 70, 1017–1020.
- Xanthiakos K., Simos D., Angelidis A.S., Nychas G.-J.E. and Koutsoumanis K. (2006) Dynamic modeling of *Listeria monocytogenes* growth in pasteurized milk. *Journal of Applied Microbiology* 100, 1289–1298.
- Zwietering M.H., Jongenburger I., Rombouts F.M. and van’t Riet K. (1990) Modeling of the bacterial growth curve. *Applied and Environmental Microbiology* 56, 1875–1881.

1 **Mathematical modeling the cross-contamination of food pathogens on the**
2 **surface of ready-to-eat meats while slicing**

3
4 **Shiowshuh Sheen and Cheng-An Hwang**

5
6 *Microbial Food Safety Research Unit, Eastern Regional Research Center, Agricultural Research Service,*
7 *U.S. Department of Agriculture, 600 E. Mermaid Lane, Wyndmoor, PA 19038, USA*

8
9 Keywords: Modeling, foodborne pathogens, transfer, slicing, ready to eat meats

10
11 _____
12 Author for correspondence, Tel: (215) 836-3774; Fax: (215) 233-6581; E-mail:
13 shiowshuh.sheen@ars.usda.gov.

14 Mention of trade names or commercial products in this publication is solely for the purpose of providing
15 specific information and does not imply recommendation or endorsement by the U.S. Department of
16 Agriculture

Abstract

Foodborne pathogens including *Listeria monocytogenes*, *Escherichia coli* O157:H7 and *Salmonella* have been implicated in several food pathogens related outbreaks linked to the consumption of ready-to-eat (RTE) food products. The appearance of *L. monocytogenes* in sliced RTE deli meats has drawn considerable attention in regard to possible cross-contamination during slicing operation at retail and food service environments. Deli meats (ham and salami) were used to investigate the surface transfer of three foodborne pathogens between a meat slicer and meat slices and to understand its impact on food safety. A cocktail of each foodborne pathogen (5 to 6 strains) was inoculated onto a slicer blade to an initial level of ca. 3, 5, 6, 7 or 9 log CFU/blade (or ca. 2, 4, 5, 6 or 8 log CFU/cm² of the blade edge area), and then the deli meat was sliced to a thickness of 1-2 mm (Case I). For another cross-contamination scenario, a clean blade was used to slice the pre-surface-inoculated meat with target cocktail (ca. 3, 5, 6, 7, 8 or 9 log CFU/100 cm² area), followed by slicing the un-inoculated meat (Case II). Results showed that the developed empirical models were reasonably accurate in describing the surface transfer trend/pattern of each foodborne pathogen between the blade and meat slices when the inoculum level was > 5 log CFU on the meat or blade. With an initial inoculum at 3 or 4 log CFU, the experimental data showed a rather random pattern of bacterial transfer between blade and meat. The resulting models are microbial load, sequential slice index and contamination route dependent which might limit their applications to certain conditions. However, the models may be further applied to predict the 3 or 4 log CFU level (and below) cross-contamination of meat slicing process. The empirical models may provide a useful tool in RTE meat risk assessment.

Introduction

Ready-to-eat (RTE) meat products such as sliced deli meats (e.g. ham, salami, bologna and other restructured meat) were commonly prepared by using a slicer, which probably was the last processing step before packaging or wrapping. Those consumer products are typically available in the retail refrigerated food section, either produced by food companies or made to order in store. Sliced RTE products are also commonly sold by delicatessen and fast food restaurants, where a retail-scale slicer is commonly used on site for meal or sandwich preparations. If not properly cleaned and regularly sanitized, the slicing machine may become the potential source of microbial cross-contamination. Among the foodborne pathogens, *Listeria monocytogenes* is a psychrotrophic pathogen and has been isolated from sliced RTE meats and caused outbreaks [The Centers for Disease Control and Prevention (CDC), 2002], it is of special interest from public health protection perspective to minimize potential food hazard. It is estimated that about 2,500 cases of listeriosis occurred each year, resulting in 500 deaths, in the United States (Mead and others, 1999). The prevalence of *L. monocytogenes* in RTE meat and poultry, seafood, dairy products and produce has been reported with published data collected in the retail and food service environments (Lianou and Sofos, 2007). RTE meats also have been implicated in salmonellosis outbreaks included roast beef (Shapiro, 1999) and fermented sausage (Sauer et al., 1997). Although the contaminations of *E. coli* O157:H7 and/or *Salmonella* on RTE meats are not common, there are possibilities that these two pathogens may cause potential food hazards if the slicing equipment used for multiple products. The incidence of salmonellosis appears to be rising both in the U.S. and in other industrialized nations (FDA, 2009).

In this study, the transfer of foodborne pathogen from one contact surface to another for RTE deli meats with a delicatessen or restaurant type slicer was investigated. The objective was to develop mathematical models to describe the surface cross-contamination of *L. monocytogenes*, *E. coli* O157:H7 and *Salmonella* during slicing operation. The developed models may provide a better understanding of microbial surface transfer patterns for the three foodborne pathogens during slicing to enhance RTE meat food safety.

Materials and methods

Bacterial strains

A cocktail of 5-6 strains of targeted pathogen was used for the surface transfer studies. The foodborne pathogen strains were obtained from the Microbial Food Safety Research Unit in USDA/ARS/ERRC. A loopful of each strain was transferred from a stock culture stored at -80°C into 10 ml of Brain Heart Infusion broth (BHI, Becton, Dickinson and Company, Sparks, MD) and incubated at 37°C for 6 h. A loopful of cell suspension of each strain was then separately transferred to 10 ml of BHI broth and incubated at 37°C for 24 h. Each strain was plated on the properly selective agar plates (e.g. MOX for *L. monocytogenes*, CT-SMAC for *E. coli* O157:H7 and Rappaport for *Salmonella*) to determine the cell counts and adjusted to obtain equal cell contribution in the cocktail with 0.1% peptone water. One ml of cell suspension from each strain was combined, and the mixture was further diluted with sterile 0.1% peptone water to the targeted level.

Delicatessen slicer and deli meat slicing

A retail-scale, gravity-fed (45° angle) mechanical slicer (Model 3500, Globe Food Equipment Co., Dayton, OH) was used for ham slicing. The slicer was equipped with a 305 mm (12-inch) diameter hollow ground knife (round blade) and operated at 300 revolutions per minute (rpm). The meat holding section was equipped with a 1.36 kg (3 lb) stainless steel end weight to deliver a consistent cut weight. Deli meats (ham or salami) were sliced to 1-2 mm in thickness and individually collected in stomacher bags (one slice per bag). Each meat slice was weighed and added an equal amount of sterilized peptone water (PW), then, stomached for 2 min. One ml or 0.1 ml of “meat juice” with proper dilution (with PW) was spread on the microbial medium plate for enumeration (duplicate plates). The number of sliced meat collected was based on the initial microbial inoculation level, i.e. the higher of inoculation level, the more of sliced meat collected. Each experiment was repeated three times.

Model development and statistical analyses

Model development to describe the foodborne pathogen surface transferred patterns during slicing of RTE meats was initially investigated and reported for *L. monocytogenes* (Sheen, 2008). Due to the lack of clear understanding and complexity of the surface transfer mechanism, the empirical modeling approach was applied. TableCurve 2D version 5.01 (Systat Software Inc., Richmond, CA) software was used to derive the models where the surface transferred counts per sliced meat was the dependent variable vs. slice sequence number as the independent variable. TableCurve 2D screened hundreds of equations to fit the experimental data with regression analyses and reported the selected models in an order of either F-statistic or coefficients of determination (r^2) from high to low order. The statistic results including the t-tests for all coefficients in the fitted models, in addition to the F-statistic, were considered the key factors in selecting the best-fit model and for further model development. Model selecting criteria were F-statistic, t-test of each coefficient for parameter, simplicity, singularity, convergence and r^2 . A “best-fit” model fulfilled the following criteria was selected: (1) decaying transfer counts and approaching zero for large slice number; (2) no singularity and divergence in prediction; (3) a simple model with fewer coefficients and parameters; (4) $P > |t|$ (< 0.001) for all coefficients; (5) highly significant F-statistic results [i.e., $P > F$ (< 0.0001)]; (6) r^2 higher than 0.6. The r^2 was used as a reference since F-statistic and t-test results of all coefficients were more important for non-linear model development.

Results and Discussion

For *L. monocytogenes* surface cross-contamination during slicing, the microbial transfer followed the exponentially decaying pattern which is similar to the first-order kinetic reaction model. The transfer models were further developed to factor in the initial inoculation microbial level and presented as Eqs. LM-1 and LM-2 (Sheen, 2008).

For surface transfer from direct blade inoculation to meat (Case I):

$$Y = 0.461 \cdot \text{Exp}(0.255 \cdot n) \cdot \text{Exp}\left(\frac{-X}{0.0215 \cdot n^{4.962}}\right) \quad (\text{LM-1})$$

For surface transfer from contaminated meat to blade to meat (Case II):

$$Y = 0.495 \cdot \text{Exp}(0.244 \cdot n) \cdot \text{Exp}\left[\frac{-X}{23.98 \cdot \text{Exp}(0.413 \cdot n)}\right] \quad (\text{LM-2})$$

Models, LM-1 and LM-2 are empirical which well represented the experimental data (repeated three times) and satisfied all the modeling selecting criteria.

The *E. coli* O157:H7 surface transfer models were developed (Sheen and Hwang, 2009) and shown below. The surface transfer can be described by the non-linear models derived from the decaying power or exponential law for Case I and Case II, respectively. The model for Case II is similar to that for *L. monocytogenes*.

Case I:

$$Y = 0.017 \cdot n^{2.920} \cdot X^{-0.254} \quad (\text{EC-1})$$

Case II:

$$Y = 0.710 \cdot \text{Exp}(0.227 \cdot n) \cdot \text{Exp}\left[\frac{-X}{14.83 \cdot \text{Exp}(0.308 \cdot n)}\right] \quad (\text{EC-2})$$

For *Salmonella* surface transfer, models for Case I and Case II were found following the decaying power law which is non-linear with the inoculation level factor built in.

Case I:

$$Y = (0.301 \cdot n^{1.446}) \cdot X^{(-0.051n+0.061)} \quad (\text{SL-1})$$

Case II:

$$Y = 1.119 \cdot n^{0.713} \cdot X^{(-0.151)} \quad (\text{SL-2})$$

It is clearly demonstrated that the surface transfer of three different foodborne pathogens on RTE meat during slicing did follow the decaying trend by either a power or an exponential law. Fig. 1 and Fig. 2 showed the predicted surface transfer patterns of three pathogens at inoculation level $n=7$ for Case I and Case II, respectively. Fig. 3 and Fig.4 showed the predicted transfer patterns at inoculation level $n=4$ for Case I and Case II, respectively. Without the models, the cross-contamination of each food pathogen will be difficult to describe and predict. Furthermore, the complexities of other factors, e.g. foods, operation parameters and microbe itself (attachment, survival), make the transfer model development even more challenging. This report provides useful information for microbial cross-contamination when designing the slicing and/or other food processes in connection with food safety consideration. The transfer models may be applied to risk assessment to enhance food safety.

Conclusion

The microbial surface transfer models during slicing of three commonly found foodborne pathogens were presented for RTE meats. The models describe the microbial surface transfer patterns of any initial contamination levels and maybe used for the risk assessment to enhance food safety.

Figure 1. Transfer predictions using models with inoculation level of 7 log CFU for Lm, Ec and Sal (Case I)

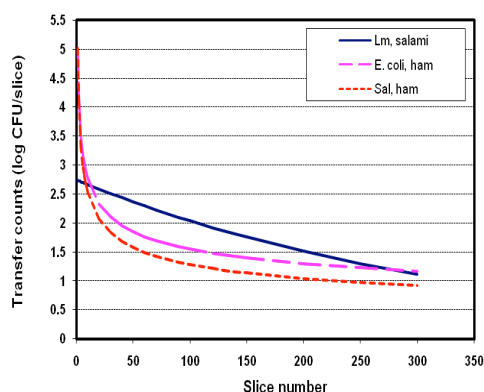


Figure 2. Transfer predictions using models with inoculation level of 7 log CFU for Lm, Ec and Sal (Case II)

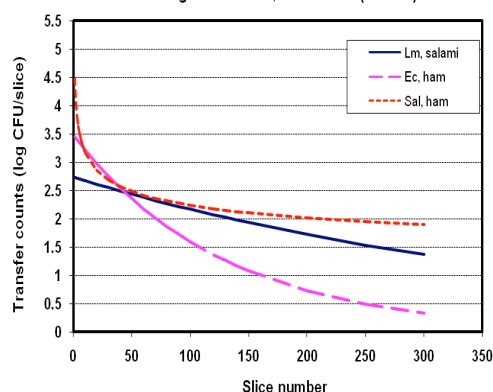


Figure 3. Transfer predictions using models with inoculation level of 4 log CFU for Lm, Ec and Sal (Case I)

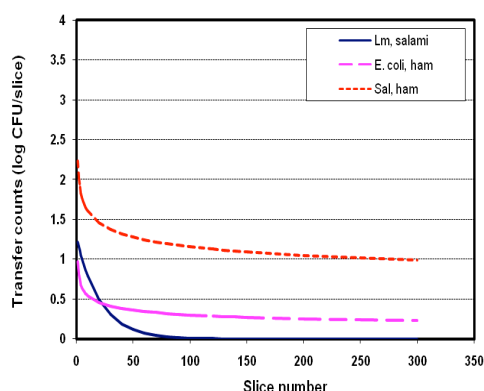
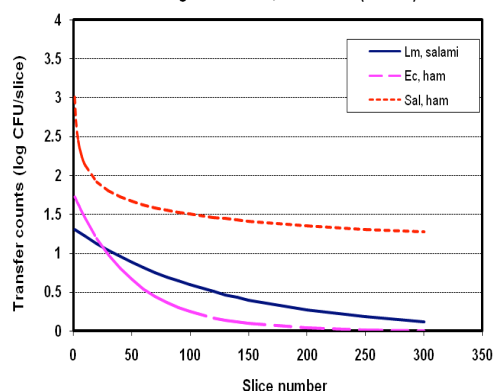


Figure 4. Transfer predictions using models with inoculation level of 4 log CFU for Lm, Ec and Sal (Case II)



References

- Centers for Disease Control and Prevention. 2002. Public health dispatch: outbreak of listeriosis- northeastern United States. *Morb Mortal Wkly Rep* 51:950-951.
- FDA. 2009. <http://www.fda.gov/Food/FoodSafety/FoodborneIllness/FoodborneIllnessFoodbornePathogensNaturalToxins/BackgroundBook/ucm069966.htm>. Accessed on July 24, 2009.
- Lianou A, Sofos J. 2007. A review of the incidence and transmission of *Listeria monocytogenes* in ready-to-eat products in retail and food service environments. *J Food Prot* 70:2172-98.
- Mead PS, Slutsker L, Dietz V, McCaig LF, Bresee JS, Shapiro C, Griffin PM, and Tauxe RV. 1999. Food-related illness and death in the United States. *Emerg Infect Dis* 5. Available at: <http://www.cdc.gov/ncidod/eid/vol5no5/mead.htm>
- Sauer, C.J., Majkowski, J., Green, S., Eckel, R. 1997. Foodborne illness outbreak associated with a semi-dry fermented sausage product. *J. Food Prot.* 60, 1612-1617.
- Shapiro, R., Ackers, M-L., Lance, S., Rabbani, M., Schaefer, L., Daugherty, J., Thelen, C., Swerdlow, D. 1999. *Salmonella* Thompson associated with improper handling of roast beef at a restaurant in Sioux Falls, South Dakota. *J. Food Prot.* 62, 118-122.
- Sheen, S., 2008. Modeling surface transfer of *Listeria monocytogenes* on salami during slicing. *J. Food Sci.* 73, E304-311.
- Sheen, S., Hwang, C.A., 2009. Mathematical modeling the cross-contamination of *Escherichia coli* O157:H7 on the surface of ready-to-eat meat product while slicing. *Food Microbiol.* (In press)

Modelling the response of the kinetics of the arginine deiminase pathway in *Lactobacillus sakei* CTC 494 to acid stress

T. Rimaux, G. Vrancken, L. De Vuyst, & F. Leroy¹.

¹ Research Group of Industrial Microbiology and Food Biotechnology (IMDO), Faculty of Sciences and Bio-engineering Sciences, Vrije Universiteit Brussel, Pleinlaan 2, B-1050 Brussels, Belgium, (fleroy@vub.ac.be).

Abstract

Lactobacillus sakei is frequently present as the dominant microorganism in spontaneously fermented meat products, demonstrating its competitiveness in and adaptation to the meat environment. Since meat is generally low in carbohydrate content, the ability to utilize other energy sources to generate ATP, such as arginine via the arginine deiminase (ADI) pathway, represents a competitive benefit. The goal of this study was to gain insight in the physiological role of the ADI pathway in *L. sakei* CTC 494, a natural dry fermented sausage isolate, through modelling of laboratory fermentation data. The results indicated that the ADI pathway was activated in the stationary growth phase. The pattern and the ratio of the end-products of the ADI pathway were influenced by different pH conditions. Arginine conversion resulted in production of both citrulline and ornithine for all pH conditions tested (pH 4.5 to pH 7.75). However, for pH values between 5.0 and 6.5, a further conversion of citrulline into ornithine was observed from the moment all arginine was depleted. Characterization of responses of the ADI pathway of *L. sakei* CTC 494 to environmental conditions will allow a better understanding and control of this potentially important starter culture in food fermentations.

Keywords: *Lactobacillus sakei*, arginine deiminase, growth, stationary phase, fermented sausage, stress response

Introduction

Lactobacillus sakei, a facultative heterofermentative lactic acid bacterium (LAB), is frequently used as a starter culture for fermented sausage production. It is the most prevalent species encountered in spontaneously fermented dry sausages, demonstrating its competitiveness in and adaptation to the meat environment (Leroy et al., 2006). *L. sakei* lacks genes encoding biosynthetic capabilities for most amino acids, naturally present in meat, but contains abundant genes encoding several transporters (Chaillou et al., 2005). Unlike other facultative heterofermentative lactobacilli, *L. sakei* and some strains of *Lactobacillus plantarum* utilize arginine via the ADI pathway (Spano et al., 2007; Zúñiga et al., 2002). In summary, this pathway results in the conversion of one mole of arginine into one mole of ornithine, with the concomitant production of two moles of ammonia, one mole of CO₂, and one mole of ATP. As is apparent from the end-products, the ADI pathway can serve several physiological functions. The ammonia released offers protection towards acid stress conditions, the ATP produced offers an improved survival in the stationary phase, and carbamoyl phosphate, an intermediate of the ADI pathway, is essential for the *de novo* pyrimidine biosynthesis (Larsen et al., 2004; Vergès et al., 1999).

The aim of the present study was to perform a detailed kinetic analysis of the ADI pathway by *L. sakei* CTC 494 as to evaluate the impact of environmental pH on the conversion of arginine into ornithine. In addition, a mathematical model, recently constructed to describe the kinetics of the ADI pathway in *Lactobacillus fermentum* IMDO 130101 was adapted and validated (Vrancken et al., 2009).

Materials and methods

Fermentation experiments and analyses

L. sakei CTC 494 was stored at -80°C in de Man-Rogosa-Sharpe (MRS) medium, supplemented with 25% (v/v) glycerol as a cryoprotectant. Fermentations were carried out in reconstituted MRS, without glucose and supplemented with 3 g/L arginine, in a 15-L Biostat[®]C fermentor (Sartorius, Göttingen, Germany). The fermentor was sterilized *in situ* at 121°C for 20 min. The fermentation temperature was kept at 30°C ; the pH was kept constant at pH 4.5, 4.75, 5.0, 5.5, 6.0, 6.5, 7.0, 7.5, and 7.75 through automatic addition of 10 M NaOH and 5 M HCl. The inoculum (1%, v/v) was prepared through three subcultures of 12 h in MRS. Cell counts (colony forming units, cfu) were obtained by plating on MRS agar (MRS plus 1.5 % agar, w/v). All measurements were performed on three independent samples. Concentrations of arginine, citrulline, and ornithine were determined using a Waters 2695 liquid chromatograph coupled to a Quattro Micro[™] mass spectrometer (Waters Corp., Milford, MA, USA) as described by Vrancken et al. (2009). Quantifications were performed through the method of standard addition.

Modelling

Following the lag phase λ (in h), biomass production $[X]$ (in cfu mL^{-1}) as a function of time t (in h) was modelled with the logistic growth equation (Vrancken et al., 2008):

$$d[X]/dt = \mu_{\max} [X] (1 - [X]/[X]_{\max}) \quad \text{if } t > \lambda \quad [1]$$

with X_{\max} the maximum obtained biomass (in cfu mL^{-1}) and μ_{\max} the maximum specific growth rate (in h^{-1}).

For certain fermentations, a decrease in the cell concentration was observed after the stationary phase was reached. To take this into account, cell death according to first order kinetics was introduced:

$$d[X]/dt = -k_D [X] \quad [2]$$

with k_D the maximum specific death rate (in h^{-1}).

Arginine [Arg] (in mM) conversion into ornithine [Orn] (in mM), via citrulline [Cit] (in mM), was modelled as (Vrancken et al., 2009):

$$d[\text{Arg}]/dt = -(k_{AC} + k_{AO}) [X] \quad [3]$$

$$d[\text{Cit}]/dt = k_{AC} [X] - k_{CO} [\text{Cit}][X] \quad [4]$$

$$d[\text{Arg}]/dt + d[\text{Cit}]/dt + d[\text{Orn}]/dt = 0 \quad [5]$$

$$\text{if } [X] \geq X_{\text{crit}}$$

where k_{AC} , k_{AO} [$\text{mM (h cfu mL}^{-1})^{-1}$], k_{CO} [$\text{in (cfu mL}^{-1} \text{ h)}^{-1}$], and X_{crit} [$\text{ln(cfu mL}^{-1})$] were model parameters. This model, describing the evolution of arginine, citrulline, and ornithine concentrations, was developed based on extracellular measurements as well as assumptions concerning the kinetics of the conversions involved. The equations were fitted to the experimental data with the numerical software package Athena Visual Studio (www.athenavisual.com) using a multiresponse approach (van Boekel, 1996).

Results and discussion

For all fermentations, growth could be modelled using the logistic growth equation (Fig. 1; examples of pH 4.5, 5.0, 6.5, and 7.5 are shown). The pH had a pronounced effect on the kinetics of arginine conversion, as well as on the final ratio of citrulline and ornithine produced. Initially, for all fermentations, no arginine conversion was observed. However,

after around 5 to 6 h of fermentation arginine conversion occurred at pH 5.5 to pH 7.0. The same was observed after 8 h for the fermentation at pH 7.5 (Fig. 1d), and after around 14 h for the fermentations at pH 4.5, pH 5.0 (Fig. 1b), and pH 7.75. At pH 5.5 to pH 6.5 (Fig. 1b, c), arginine was converted to depletion after 12-24 h of fermentation and both citrulline and ornithine were released. When all arginine was depleted, a further conversion of citrulline was found, resulting in ornithine as the main end-product at the end of the fermentation. For the fermentation at pH 7.5 (Fig. 1d), both citrulline and ornithine were produced. However, no citrulline-into-ornithine conversion was observed when all arginine was depleted, resulting in a higher ratio of citrulline to ornithine at the end of the fermentation. Finally, for the fermentation at pH 4.5 (Fig. 1a) and pH 7.75, incomplete arginine conversion took place after 50 h of fermentation. The consumption of arginine in these situations still resulted in the formation of both citrulline and ornithine, albeit at a much slower rate.

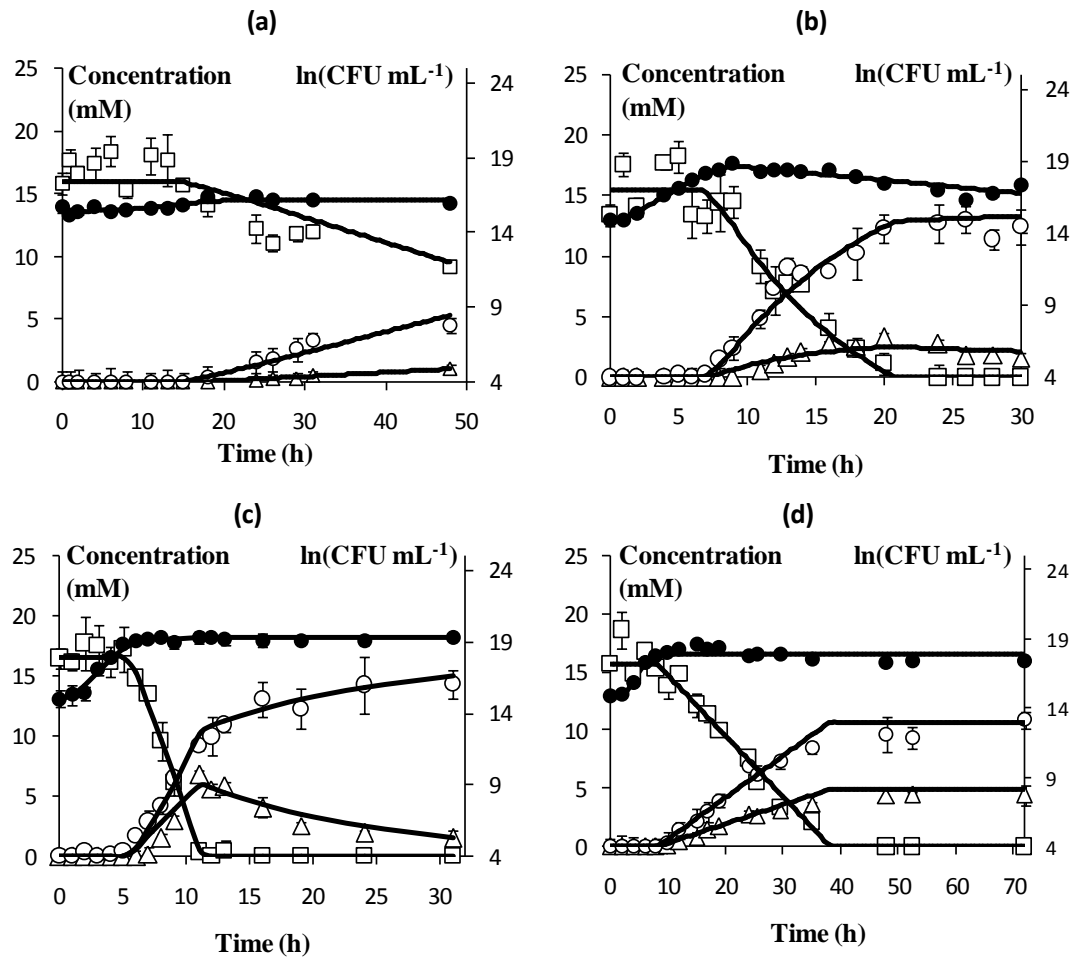


Figure 1: Growth [$\ln(\text{cfu mL}^{-1})$; ●] of *L. sakei* CTC 494 in MRS and extracellular concentrations (mM) of arginine (□), citrulline (○), and ornithine (Δ) at different pH values: (a) pH 4.5, (b) pH 5.0, (c) pH 6.5, and (d) pH 7.5. Full lines represent the predictions by the model; symbols represent the experimental data.

All fermentations were fitted using the developed model for the ADI pathway (Equations [1] to [5]). The resulting biokinetic parameters varied as a function of the pH of the fermentation medium. The parameter k_{AC} , indicating the rate of arginine conversion into citrulline, had an optimum around pH 6.0. When the pH was increased or lowered, a decrease in this parameter could be observed. The parameter k_{AO} , which is a measure of the rate of arginine conversion into ornithine, showed a less pronounced variation as a function of pH. A slight, linear increase of this parameter was observed when the pH was lowered. The parameter k_{CO} ,

representing the conversion of citrulline into ornithine, showed a similar pattern as a function of pH as for k_{AC} , with an optimum around pH 5.5. No citrulline-into-ornithine conversion was observed from pH 7.0 to pH 7.5 and thus k_{CO} was estimated as zero for these fermentation conditions. Finally, when the ratio of the parameters X_{crit} to X_{max} were plotted as a function of pH, a constant value of around 98.6% was observed, indicating that the ADI pathway started once the cell culture reached almost its final cell concentration.

Conclusions

In the present study, the effect of pH on arginine consumption by *L. sakei* CTC 494 was investigated using a modelling approach. As is shown by the present study, pH seems to be an important environmental regulator of the ADI pathway. High and low pH values resulted in a decrease of the arginine conversion rate, as reflected in the model parameters. Arginine conversion resulted in production of both citrulline and ornithine, whereby citrulline was further converted into ornithine at certain pH values, from the moment all arginine was depleted. Further research is needed to elucidate the practical significance of this pathway, and will result in an understanding of the mediators for activation or repression of genes in response to different pH conditions.

Acknowledgements

The authors acknowledge their financial support of the Research Council of the Vrije Universiteit Brussel, the Fund for Scientific Research-Flanders (FWO-Flanders), and the Institute for the Promotion of Innovation through Science and Technology in Flanders (IWT-Flanders). TR was supported by a predoctoral fellowship of the FWO-Flanders.

References

- Chaillou S., Champomier-Vergès M.C., Cornet M., Crutz-Le Coq A.M., Dudez A.M., Martin V., Beaufils S., Darbon-Rongère E., Bossy R., Loux V. and Zagorec M. (2005) The complete genome sequence of the meat-borne lactic acid bacterium *Lactobacillus sakei* 23K. *Nature Biotechnology* 23, 1527-1533.
- Larsen R., Buist G., Kuipers O.P. and Kok J. (2004) ArgR and AhrC are both required for regulation of arginine metabolism in *Lactococcus lactis*. *Journal of Bacteriology* 186, 1147-1157.
- Leroy F., Verluyten J. and De Vuyst L. (2006) Functional meat starter cultures for improved sausage fermentation. *International Journal of Food Microbiology* 106, 270-285.
- Spano G., Massa S., Arena M.E. and de Nadra M.C.M. (2007) Arginine metabolism in wine *Lactobacillus plantarum*: *in vitro* activities of the enzymes arginine deiminase (ADI) and ornithine transcarbamoylase (OTCase). *Annals of Microbiology* 57, 67-70.
- van Boekel, M. (1996) Statistical aspects of kinetic modeling for food science problems. *Journal of Food Science* 61, 477-489.
- Vergès M.C.C., Zuñiga M., Morel-Deville F., Pérez-Martínez G., Zagorec M. and Ehrlich S.D. (1999) Relationships between arginine degradation, pH and survival in *Lactobacillus sakei*. *FEMS Microbiology Letters* 180, 297-304.
- Vrancken G., Rimaux T., De Vuyst L. and Leroy F. (2008) Kinetic analysis of growth and sugar consumption by *Lactobacillus fermentum* IMDO 130101 reveals adaptation to the acidic sourdough ecosystem. *International Journal of Food Microbiology* 128, 58-66.
- Vrancken G., Rimaux T., Weckx S., De Vuyst L. and Leroy F. (2009) Environmental pH determines citrulline and ornithine release through the arginine deiminase pathway in *Lactobacillus fermentum* IMDO 130101. *International Journal of Food Microbiology*, in press.
- Zuñiga M., Miralles M.D.C. and Pérez-Martínez G. (2002) The product of *arcR*, the sixth gene of the *arc* operon of *Lactobacillus sakei*, is essential for expression of the arginine deiminase pathway. *Applied and Environmental Microbiology* 68, 6051-6058.

Relationship between cellular esterase activity and physiological state of stressed *Listeria monocytogenes* cells

C. Dupont^{1,2}, J.-C. Augustin¹

¹ Ecole Nationale Vétérinaire d'Alfort, Unité Microbiologie des Aliments – Sécurité et Qualité, 7, avenue du Général de Gaulle, F-94704 Maisons-Alfort Cedex, France (jcaugustin@vet-alfort.fr)

² AES Chemunex, Rue Maryse Bastié, Ker Lann – CS17219, F-35172 Bruz Cedex, France (cdupont@vet-alfort.fr)

Abstract

Solid phase cytometry in combination with Chemchrome V6 fluorescent probe was applied to rapidly quantify esterase activity at the cell level. The growth of stressed *Listeria monocytogenes* cells was followed simultaneously by enumeration on traditional culture media and by cell esterase activity determined by fluorescence intensity measurement.

Firstly, it was determined that cell physiological state has a great impact on the fluorescence peak-intensity distribution and that, the impact was dependent on the stress suffered by cells. Secondly, it was established that, in taking the assumption that the healthier cells, the higher fluorescence peak-intensity, the “Minimal Peak-Intensity” is an effective parameter to determine the concentration of cells able to multiply on selective or non-selective media.

These results emphasize that solid phase cytometry analysis could be an interesting tool to obtain rapid information on the efficiency of a broth to allow cell revivification.

Keywords

Cell physiological state, revivification, esterase activity, *Listeria monocytogenes*

Introduction

It is now recognized that conventional culture techniques are highly selective and underestimate true viable cell counts in natural environments as they fail to detect injured or stressed cells that are unable to reproduce on growth media. Moreover, those techniques are still time-consuming.

In contrast to culture methods, the emergence of non-culture based assays to detect activity and viability in bacteria is becoming more and more attractive. They allow the detection of metabolically-active cells and data can be obtained within a short time.

In Solid Phase Cytometry (SPC), bacteria are fluorescently labelled on the surface of a membrane filter, which is subsequently scanned by a laser beam in a ChemScan apparatus. The cellular activity detected with ChemChrome V6 probe is the esterase activity.

The aim of this research was to investigate if the esterase activity is telling of the physiological state of cells and, to observe if there is conformity between the fluorescence intensity of cells detected and their ability to multiply in culture media.

Materials and Methods

Listeria monocytogenes cells were subjected to stresses usually met in food industry. The cumulative peak-intensity distributions were characterized for 4 stressing treatments: Lactic acid pH4.2 at 25°C for 24 h, Osmotic stress in 25% (wt/vol) NaCl solution at 30°C for 48 h, Peracetic acid stress with a 200 ppm solution at 25°C for 15 min and Starvation stress for which cells were placed in physiological water with no nutritional contribution at 25°C for 24 h. Then, cell changes during revivification in nutritive broth, TSBye, and in selective broth, the half Fraser broth (1/2FB), at 30°C has been followed.

After being labelled with Chemchrome V6 probe (10 min at 40°C), cells, placed onto a membrane filter, were scanned with ChemScan cytometer. The signals produced were processed by a PC using a series of software discriminants to differentiate between valid signals (labelled bacteria) and background.

This enzymatic activity staining implies that non-charged and non-fluorescent substrate penetrates the cell, and after being modified by intracellular esterases, becomes a negatively

charged fluorophore. For live cells, free fluorescein derivate stays inside the cell without any noticeable influence on the life processes of the cells. Given plasma membrane is damage, fluorophores leaks out the cell.

For each fluorescent cell, the peak intensity which corresponds to the highest fluorescence intensity detected for the scanned event was determined and then, the results of fluorescence peak-intensity (PI) distribution obtained were compared to the cell ability to multiply in non-selective and selective media: TSBye and 1/2FB, respectively for liquid ones, TSAye and PALCAM agar for solid ones. In this purpose, the proportion of growing cells referred to the cell concentration detected before the stress was used.

Results and Discussion

Cell physiological state after stress

Figure 1a shows that the cumulative peak-intensity distributions are dependent on the stress encountered by the cell: stressed cells have a lower peak-intensity median than cells in the exponential growth phase. In the light of these results, it seems that the most active cells have the higher esterase activity and therefore, the higher fluorescence intensity.

In taking this assumption and knowing that each stressing treatment has an effect on the ability of cells to multiply in traditional media, we introduced the concept of “minimum peak intensity” (MPI) which defines the minimum PI required by a cell to be able to multiply in a particular medium, namely, cells that grow are the most fluorescent cells (Table 1).

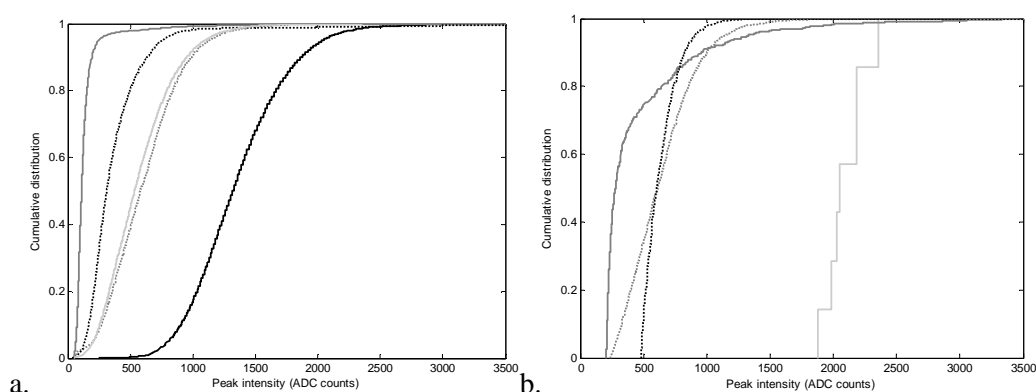


Figure 1: Cumulative distribution of peak-intensity of the bacterial population (a) and only of cells exceeding the MPI to grow on 1/2FB (b) with: cells in exponential growth phase (black), lactic acid stressed (dark-grey), peracetic acid stressed (light-grey), osmotic stressed (dash black), and starvation stressed cells (dash grey).

Distributions of stressed-cells exceeding the MPI required in 1/2FB are presented in figure 1b. The MPI obtained for peracetic acid stress is different against the others tested (1867 versus 307 on average). This is partly due to the fact that, after peracetic acid treatment, cells detected before the stress (exponentially growing cells) are still visible by cytometry. The mechanism of this disinfectant is the release of “active” oxygen, which disrupts sulfhydryl (–SH) and sulfur (S–S) bonds within enzymes contained in the cell membrane (Lefevre et al., 1992). Actually, cells that are not detected on traditional media (selective or non-selective) still have esterase activity but have lost the ability to multiply on the media tested. Consequently, cells able to multiply on traditional media represent only a fraction of the cytometry-detected population and therefore, MPI are inevitably lower on non-selective media, 1601 for TSAye, than on selective ones, 2083 for PALCAM.

On the other hand, for cells stressed by lactic acid treatment, concentration detected with non-selective media (TSBye and TSAye) are higher than the one enumerated by cytometry. Visser et al. (1979) observed that the fluorescence excitation spectrum of fluorescein is pH-dependent, for instance, the fluorescence intensity was divided by 6, from pH 7 to pH 4. Therefore, we can assume that the substrate was effectively modified by esterases insides

cells but, as intracellular pH was reduced by the stressing treatment, cell fluorescence intensity was below the detection threshold of the cytometer.

We attempted to obtain a common minimal peak-intensity in order to determine the ability for cells to grow in a given environment, whatever the cell physiological state but it seems that cells do not react to labelling in the same way by the stress suffered, meaning that, there is no simple relation between the esterase activity determined with ChemChrome V6 staining and the ability for a cell to multiply.

Fate of stressed-cells during revivification in liquid media

The behaviour of stressed cells during revivification in broth was followed by enumeration on traditional media and by fluorescent labelling.

For osmotic stressed-cells incubated in TSBye, an increase in the bacterial proportion able to grow in selective and non-selective media was observed from 120 minutes at 30°C (Figure 2I a). At the same time, a simultaneous rise was observed for concentrations determined with MPI for those media. Meanwhile, the bacterial concentrations remained steady throughout incubation in 1/2FB; and similarly, bacterial concentrations determined by MPI stood stable (Figure 2I b).

After lactic acid stress, the same behaviour was observed with a slower concentration rise throughout revivification in TSBye (Figure 2II a and b).

Concentrations obtained were concordant and evolved in the same way: the proportion of cells whether growing or exceeding MPI was enhanced throughout the revivification with a rate depending on the media and on the stress previously encountered by cells.

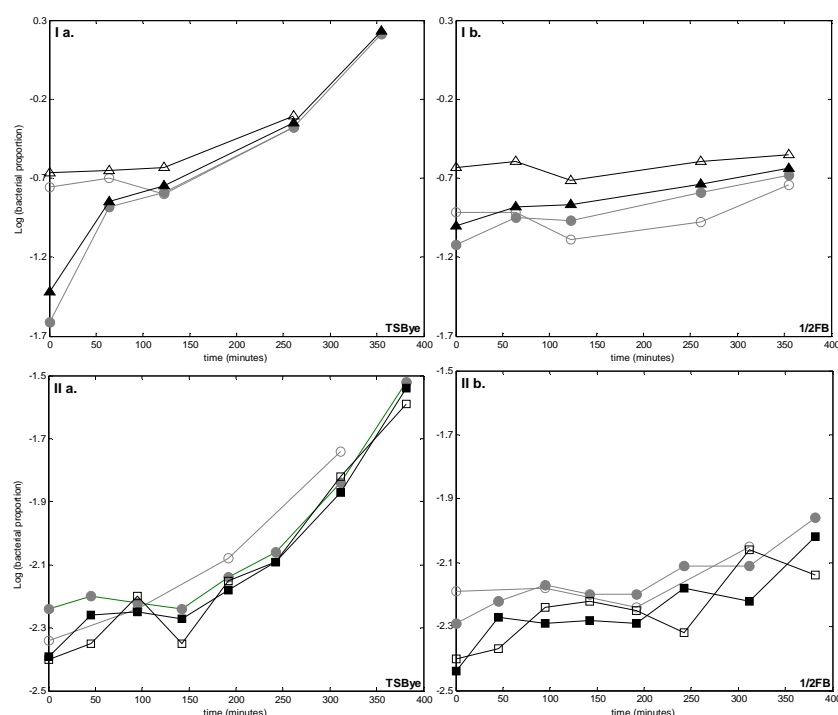


Figure 2: Logarithm of bacterial proportion of cells growing (open patterns) and of cells exceeding MPI (solid patterns) on TSBye (triangles), 1/2FB (circles) and PALCAM agar (squares) in the course of revivification in TSBye (a) and 1/2FB (b) at 30°C after osmotic stress (I) and lactic acid stress (II)

For peracetic acid stress, an immediate return to the shape of “cells in the exponential growth phase distribution” was obtained as soon as cells are introduced in broth whether TSBye or 1/2FB (data not shown). This variation could not be the result of cells repair, moreover, as MPI are very high for this stress, the bacterial proportion exceeding MPI remains low (0.01). Then, no rises were observed in fluorescence intensity or in concentrations detected on media tested throughout the revivification. Those results tend to show that, after peracetic acid

treatment, cells are more or less injured which allowing them or not to multiply in a given environment but that, physiological state does not improve regardless of the environment in which they are introduced (for those tested).

On the other hand, there seemed to be a progressive decrease in the bacterial proportions above the MPI. On light of these results, it would seem that esterase active but not cultivable cells gradually lose their esterase activity over time and that, after a while, it would remain only really viable cells.

The use of cytometry may be a useful tool in order to determine whether a medium is favourable or not to recover cell eventhough it is difficult to know if it shows the recovery of stressed cells or the genesis of newborn cells.

To determine if a broth represents an appropriate environment for cell revivification to occur, without enumerating on selective and non-selective medias, making a cell fluorescence labelling at the time of the introduction in the broth and after a long enough incubation period (e.g. 6 hours) could be efficient. Then, the ability of the media to allow cell revivification can be deduced from the difference between the peak-intensity median (ΔPI_{median}). The results presented in Table 1 clearly suggest that this parameter could rapidly give precious information on the broth efficiency for cell repair. Indeed, the higher revivification observed by enumeration on traditional media, the higher the ΔPI_{median} . Moreover, for revivification of osmotic stressed-cells in FB1/2, the cell repair (determined by the difference between enumeration on non-selective and selective broth) is reflected in the ΔPI_{median} . On the other hand, for conditions where no revivification was observed, the ΔPI_{median} is always under 100.

Table 1: Minimal peak-intensity (MPI) for cells to grow in given media and differences of fluorescence peak-intensity median (ΔPI_{median}) between the cells introduction in broth and after 6 hours of incubation at 30°C upon the stress suffered.

| Stress encountered | MPI | | | | ΔPI_{median} | |
|--------------------|-------|-------|-------|--------|----------------------|-------|
| | TSBye | TSAYe | 1/2FB | PALCAM | TSBye | 1/2FB |
| Lactic acid pH 4.2 | 0 | 0 | 206 | 459 | 1072 | 15 |
| Osmotic 25% | 415 | 364 | 477 | 789 | 771 | 325 |
| Starvation | 294 | 217 | 237 | 436 | 614 | nd |
| Peracetic acid | 948 | 1604 | 1867 | 2083 | 0 | 87 |

Conclusion

This research sought to investigate if the cell esterase activity was dependant on physiological state of cells and to observe if there was any relation between the cells fluorescence intensity and the cells ability to multiply in culture media.

We have shown that the physiological state of cells has a great impact on the fluorescence peak-intensity distribution. Moreover, in taking the assumption that the healthier cell, the higher fluorescence peak-intensity, we showed that the concept of “minimal peak intensity” could be an effective parameter to determine the cells ability to grow in a given environment. Although the impact on cell fluorescence intensity is dependent on the stress suffered, cytometry analysis could be an efficient tool to qualify broths according to their ability to allow cell revivification, and moreover to easily determine growth-no growth interface.

Acknowledgements

C. Dupont is the recipient of a doctoral fellowship from AES Chemunex and the French Association Nationale de la Recherche Technique.

References

- Lefevre F., Audic J.M. and Ferrand F. (1992) Peracetic acid disinfection of secondary effluents discharged off coastal seawater. *Water Science Technology* 25 (12), 155–164.
- Visser, J. W. M., Jongeling, A. A. M. and Tanke, H. J. (1979). Intracellular pH-Determination by fluorescence measurements. *The journal of Histochemistry and Cytochemistry* 27, 32-35.

An application of risk evaluation techniques to achieve a suggested Food Safety Objective for *Listeria monocytogenes* in a selected Ready-To-Eat meal

Z. Sosa Mejia¹, R. R. Beumer, M. H. Zwietering

Laboratory of Food Microbiology, Wageningen UR, The Netherlands

¹ zeus.sosamejia@wur.nl

Introduction

Ready-To-Eat (RTE) meals have become increasingly popular in the last two decades, particularly in metropolitan areas. The costumers of these meals have also become more knowledgeable and demanding about the nutritional content, quality and safety of these products. The objective of this work is to combine risk evaluation techniques to assess the safety of the product with risk management concepts in order to reach a suggested Performance Objective (PO) and a Food Safety Objective (FSO) (CAC, 2007). The procedure consisted of a complimentary combination of scientific literature, challenge tests (growth and inactivation), and predictive modelling. The combination of tests and predictions help to define different scenarios where practical considerations are suggested to achieve an FSO for *Listeria monocytogenes* in a Chicken Tandoori RTE meal.

Materials and methods

Growth and inactivation challenge tests were applied to a selected RTE meal: Chicken Tandoori. This meal consisted of a fresh mix of vegetables, raw chicken and semi-cooked rice in Tandoori sauce. The tests consisted of inoculating the meals with a cocktail of six different strains of *Listeria monocytogenes* pre-incubated at 12 °C till they reached their stationary phase. From these solutions, different concentrations were inoculated into the meals (500 g) for their growth (5×10^2 cfu/g) and inactivation (2×10^6 cfu/ml) experiments. After inoculation, the meals were stored at retail (7 °C) and abuse (12 °C) temperature for eight days, one day after the expiration of the shelf life. The growth of the pathogens was assessed daily on selective media, ALOA for *L. monocytogenes*, together with the spoilage organisms (TVC (PCA), LAB(MRSA)), gas composition and the pH of the meals. The heat inactivation trials of the inoculated meals consisted of heating the meals at 700 W for 7 min as suggested on the label of the product by the product manufacturer. The temperature was measured in three different points of the meal after every heating time interval. The level of the surviving bacteria after every heating time was measured in selective and PCA media. The results from the growth were compared with the results of the gamma model (Zwietering *et al.*, 1996):

$$\mu = \gamma(T) * \gamma(pH) * \gamma(aw) \quad (1)$$

μ = specific growth rate; $\gamma(T)$ = relative effect of temperature; $\gamma(pH)$ = relative effect of pH; $\gamma(aw)$ = relative effect of water activity

and ComBase® predictive program (Baranyi and Tamplin, 2004). For the gamma model, the daily measurement of pH and T from the meal were used into the model.

For the ComBase® predictor, the variables selected for the growth of both pathogens were 30 % CO₂ for 300 h, with an initial level of 3 Log CFU/ml, a physiological state of 0.7, a pH of 5.5 and temperature of 7 °C and 12 °C, were used for the whole storage period. For the inactivation predictions, only the gamma model was used, as the range of temperature in the ComBase program varied from 60-68 °C, which was limited in comparison to the range obtained from the experiments, up to 70 °C.

Further, the results from the predictions and challenge tests were adapted to the different variables of the FSO formula (ICMSF, 2002):

$$Ho - \Sigma R + \Sigma I + \leq FSO \quad (2)$$

Ho = Initial contamination concentration (Log cfu/g); ΣR = Total (cumulative) reduction of the hazard (Log cfu/g); ΣI = Total (cumulative) increase of the hazard (Log cfu/g); FSO = Food Safety Objective (Log cfu/g).

Results and Discussion

Growth of Listeria monocytogenes in a Chicken Tandoori RTE meal

No significant growth was observed for *L. monocytogenes* (Fig 1) at 7 and 12 °C. The gamma and ComBase® predictions showed similar predictions for the pathogen at both temperatures. Nevertheless, when compared with the results obtained with the challenge tests, only similarities were observed with the results from the lower temperatures.

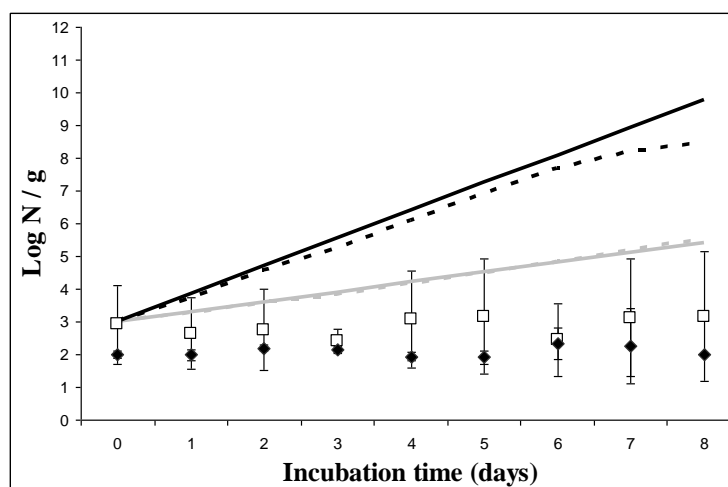


Fig 1. Growth and growth prediction of *Listeria monocytogenes* in Chicken Tandoori RTE meal. ♦ Concentration of *L. monocytogenes* in the RTE meal incubated at 12 °C; □ Concentration of *L. monocytogenes* in the RTE meal incubated at 7 °C; — gamma model prediction for storage at 12 °C; ---- prediction from the ComBase® program at 12 °C. — gamma model prediction for storage at 7 °C; ---- prediction from the ComBase® program at 7 °C.

L. monocytogenes showed no significant growth nor reduction throughout its shelf life (seven days). At this stage, the pH dropped from 5.5 to 4.4. It was observed that the gamma model and ComBase® showed similar results in the predictions, differently to the results obtained from the challenge tests.

The difference between the challenge tests and the ComBase® might be because the program does not consider changes of pH throughout the product shelf life, such as growth of spoilage bacteria and antimicrobial additives that could have influenced the pathogen growth. In the case of the gamma model, the effect of the gas composition is not taken into account.

Inactivation of Listeria monocytogenes in a Chicken Tandoori RTE meal

The objective of the inactivation tests was to assess whether the product after artificial contamination would achieve a 6D reduction. An inactivation of ± 2 Log CFU/g was observed when microwave heating was applied as recommended by the manufacturer instructions. Figure 2 illustrates the recovery of the pathogen obtained from the meals after being heated at different time intervals at constant power (700 Watts for 7 min) and their comparison with the gamma prediction. Two scenarios are presented, the first describes a fail safe approach where the inactivation was based on the temperature measured in the centre of the container. The second scenario, depicts a prediction based on the average temperature of three different measurements made in the container (centre and sides) reaching a 6D reduction at the last minutes of heating. It was noted that none of the meals was able to reach 70 °C for two minutes throughout heating.

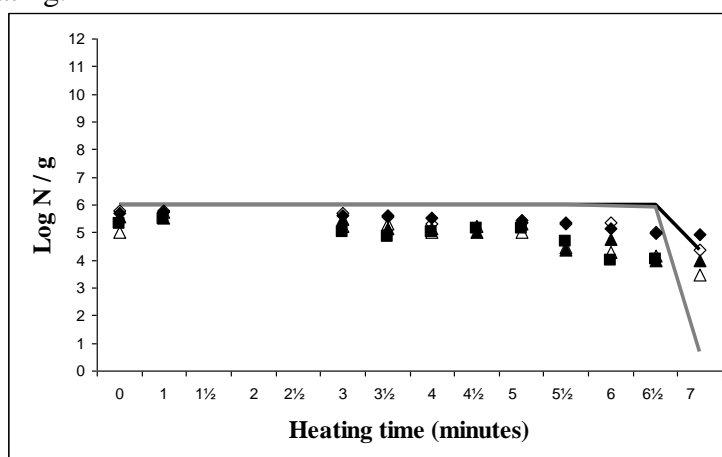


Fig 2. Inactivation of *Listeria monocytogenes* in Chicken Tandoori meals. ♦ concentration of *L. monocytogenes* after microwaving the meals briefly incubated at 7 °C on the inoculation day; ■ concentration of *L. monocytogenes* after microwaving the meals incubated at 7 °C on the expiration date; ▲ concentration of *L. monocytogenes* in the meals incubated at 7 °C on the eight day of incubation; ◇ concentration of *L. monocytogenes* after microwaving the meals briefly incubated at 12 °C on inoculation day; Δ concentration of *L. monocytogenes* in the meals incubated at 12 °C on the eight day of incubation; — gamma prediction using the temperature measured in the centre of the container; — gamma prediction using an average temperature in three locations of the container.

Achieving an FSO for *Listeria monocytogenes* in a Chicken Tandoori RTE meal

Table 1 shows two scenarios, where a hypothetical representation of a very high initial contamination (2 Log CFU/g) occurs. The first row describes a theoretical framework proposed by Perni *et al.*, (2009), where the product reaches a 6D reduction with two logs of potential growth. On the second and third rows, a description of growth and inactivation based on the results from the models and challenge tests are presented.

In both cases the reduction by microwave heating would be enough to reach the FSO suggested.

Table 1. Scenario to achieve an FSO in a ready-to-eat Chicken Tandoori

| Pathogen | Initial contamination - Raw materials | Growth during storage | PO Level before cooking | - Cooking 7 min 700Watts | Level at consumption | FSO Suggested ¹ | Conformance |
|-------------------------|---------------------------------------|-----------------------|-------------------------|--------------------------|----------------------|----------------------------|-------------|
| <i>L. monocytogenes</i> | 2 | 2 | 4 | -6 ¹ | -2 | -0.33 | Accept |
| | 2 | 0 ² | 2 | -2 ² | 0 | -0.33 | Reject |
| | 1 | 0 ² | 1 | -2 ² | -1 | -0.33 | Accept |

¹ From theoretical framework by Perni *et al.*, (2009).

² Data from challenge tests.

Conclusions

Growth of the pathogens in a Chicken Tandoori RTE meal was lower than expected for *L. monocytogenes*, particularly at abuse temperature. Inactivation of the pathogens was also lower than expected by following the manufacturer instructions. The gamma and ComBase® predictions showed similar results at different temperatures but differed from the results obtained from the challenge tests at abuse temperature. Further adaptations, e.g. including the inhibitory effect of additives, need to be included in the models. Achieving a combination of PO along the food chain will lead to reaching the targeted FSO for *L. monocytogenes* in the selected RTE meal.

Acknowledgements

This work was performed within the DoubleFresh project (contract no. FOOD-CT-2006-23182), which is a European Commission funded project within the Sixth Framework Program, Priority 5, Food Quality and Safety. The financing of the work by the European Union is gratefully acknowledged.

Reference

- Baranyi J., Tamplin M. L., 2004. ComBase: a common database on microbiol responses to food environments. Journal of Food Protection, 67, 1967-1971. Combase - www.combase.cc/toolbox.html Last visited: 23rd March 2009
- CAC (Codex Alimentarius Commission), 2007. Principles and guidelines for the conduct of microbiological risk management. Annex II: guidance on microbiological risk management metrics. Joint FAO/WHO food standards programme Codex Committee on Food Hygiene.
- ICMSF (International Commission on Microbiological Specifications for Foods), 2002. Micro-organisms in foods 7. Microbiological testing in food safety management. New York: Kluwer Academic/Plenum Publishers.
- Perni S., Beumer R., Zwietering M. H., 2009. Multi-tools approach for food safety risk management of steam meals. Journal of Food Protection. Submitted.
- Zwietering M. H., de Wit J. C., Notermans S., 1996. Application of predictive microbiology to estimate the number of *Bacillus cereus* in pasteurised milk at the point of consumption. International Journal of Food Microbiology, 30, 55-70.

The use of meta-analytical tools in risk assessment modeling for food safety

U. A. Gonzales-Barron and F. Butler

Biosystems Engineering, UCD School of Agriculture, Food Science and Veterinary Medicine. University College Dublin, Dublin 4, Ireland (ursula.gonzalesbarron@ucd.ie, f.butler@ucd.ie)

Abstract

This communication aims to demonstrate, by means of two applications, that meta-analysis can be used as a valuable tool in quantitative risk assessment for food safety. Two sets of primary studies of *Salmonella* in pork were separately combined using meta-analytical tools so as to obtain ultimately a more-informed risk assessment model. In both meta-analysis applications, relative risk was selected as the most appropriate effect size measure. As both study quality and slaughter procedures may not necessarily be uniform across primary studies, assigning weights as the inverse of the effect size variance was considered suitable in the estimation of the overall effect size. In the first meta-analysis, a relationship ($U=372$; $p<0.001$) between the proportion of *Salmonella*-carrier slaughter pigs entering the abattoir and the resulting proportion of contaminated carcasses at the point of evisceration was for the first time elucidated combining data from different studies. A stochastic weighted least squares regression was modeled after weights were corrected for heterogeneity ($Q=29.3$; $p<0.001$). In the second application, meta-analysis confirmed, on the grounds of increased statistical power, the effect of chilling on the lower recovery of *Salmonella* ($U=27.3$; $p<0.001$), and delivered a normal distribution of the overall effect of chilling (~2.4 times reduction) on *Salmonella* recovery on pig carcasses.

Keywords: Meta-analysis, *Salmonella*, slaughter, pig, pork, chilling.

Introduction

The primary aim of meta-analysis is to produce a more precise estimate of the effect of a particular intervention or treatment, with an increased statistical power than is possible using only a single study. A large collection of results from primary studies, such as experimental studies, opinion surveys and causal models, can be meta-analyzed with the purpose of combining the findings and producing an estimate that has broader generalizability.

The prevention of food-borne illnesses is complex because of the multiple stages in the production and preparation of food. On the other hand, the amount of data produced by food safety research have been growing increasingly in the last ten years, and the advances in information technology are likely to further contribute to this growth. Therefore, there is a need for conducting meta-analysis in the field of food safety, to identify, evaluate and synthesize results. Although, in principle, meta-analysis may be conducted to address a broad range of food safety research questions such as effect of pre- and post-harvest, disease incidence, prevalence of pathogens, consumer practices, etc., applications in food safety research and especially in risk assessment are still in its infancy. To date, only six published studies using meta-analysis as a tool to combine food safety data have been identified (Patil et al., 2004; Vialette et al., 2005; Sánchez et al., 2007; Bollaerts et al., 2008; Gonzales-Barron et al. 2008; and Gonzales Barron et al., 2009). This communication aims to present, by means of two applications, the methods of meta-analysis and its relevance for the synthesis of food safety research as a tool to sustain risk-based policy.

Methodology

While building a risk assessment model for predicting *Salmonella* prevalence during pork production in Ireland, Gonzales Barron et al. (2008, 2009) identified,

- (i) ten primary studies that reported results of *Salmonella*-positive cecal contents (s_C) from pigs entering the slaughter lines and *Salmonella*-positive eviscerated pig carcasses (s_E) sampled from same production batches; and
- (ii) other ten primary studies reported *Salmonella* recovery incidence from post-chill pig carcasses (s_T) in comparison to their recovery after splitting and rinsing (s_R).

In order to obtain more-informed overall effect size estimates, both data sets were separately meta-analyzed using a common methodology, whose stages are explained below. They will be referred to as ‘slaughter meta-analysis’ and ‘chilling meta-analysis’, respectively.

Systematic review and data extraction

A systematic review begins with the formulation of a focused study question for which three important facets are to be considered: population, intervention or treatment and outcome. The two principal questions addressed in both meta-analysis were: (i) is there any support in the sampled population of studies for the causal inference that the intervention (slaughter/chilling) made a statistically significant difference in the outcome (presence of *Salmonella* on a pig carcass)? And if so (ii) how large an effect or difference did the intervention make?

Parameterization of the effect size

Effect size refers to the degree to which the phenomenon is present in the population (for example, decrease in the recovery of *Salmonella* on pig carcasses due to chilling). For the primary studies to be compatible to analyze, meta-analysis converts the effect size into a ‘parameter’ that allows direct comparison and summation of the independent studies. In both meta-analyses, the effect size was parameterized as ‘relative risk’ (probability of outcome of interest in the treatment group (p_T) relative to the probability of outcome of interest in the control group (p_C)).

Estimation of the overall effect size

The next step is to combine the primary studies to compute the overall effect size estimate using a fixed-effects approach. Both meta-analyses used the common method of weighting individual estimates by means of their inverse variances (Table 1). Thus, more precise studies will have more influence in the overall estimate as compared with less precise studies. The null hypothesis of absence of effect on the ‘treated’ group was tested using the U statistic.

Assessment of heterogeneity among primary studies

The fixed-effects meta-analysis makes the strong assumption that each study is estimating the same underlying treatment effect. However, in food research, such assumption may be unrealistic given the variability of the biological systems, and also the differences in study protocols. If effect size estimates vary between studies to a greater extent than expected on the basis of chance alone (fixed-effects), the studies are considered heterogeneous and a random-effects meta-analysis is more suitable. In both meta-analyses, heterogeneity was assessed using the Q statistic to test the null hypothesis of absence of heterogeneity.

Presentation of meta-analysis results

There are a series of graphical displays to present meta-analysis results (Table 1) although the most common way to summarize the primary studies and overall effect size is by using a ‘forest plot’ which displays point estimates and confidence intervals of each primary study and the overall estimate. The results from the slaughter meta-analysis and the chilling meta-analysis were displayed as a bubble plot and a funnel plot, respectively.

Results and discussion

The first meta-analysis demonstrates how the synthesis of primary studies can help reveal a relationship between two variables. In the slaughter meta-analysis, some of the primary studies reported an statistical association (found by chi-square tests) between the proportion of *Salmonella*-positive cecal contents ($x=s_C/n_C$) from pigs entering the slaughter lines and the

proportion of positive carcass swabs ($y=s_E/n_E$) sampled from the same production batches; although no relationship at batch level (or groups of slaughter) was shown in any of the primary studies. Since these binary data were extracted from studies that used different protocols for *Salmonella* culture, it was necessary to allow for the differences by correcting the underestimated x and y values with test sensitivities for cecal culture and carcass swabs (producing then x' and y'). While the meta-analysis elucidated for the first time a relationship between x' and y' ($U=372$; $p<0.001$; Figure 1A), these data pairs could not be combined into a simple regression since they had been extracted from a series of primary studies presenting various degrees of precision. It was therefore necessary to assign weights to each of the data pairs (studies), which were calculated as the inverse variance of the relative risk. As the Q test gave evidence of presence of heterogeneity ($Q=29.3$; $p<0.001$), all weights were recalculated for a random-effects solution. The relative size of the bubbles shown in Figure 1A is proportional to the weight assigned to each primary study. This meta-analysis has shown how the body of information contained in all studies revealed a clearer picture of the state of knowledge (Figure 1A). In Gonzales Barron et al. (2009), this analysis was combined with a non-parametric bootstrap technique in order to build a stochastic regression between the *Salmonella* carriage rate in pigs entering the abattoirs and the resulting incidence on carcasses at the point of evisceration.

Table 1: Overview of commonly used numerical and graphical meta-analytical techniques.

| Numerical meta-analytical techniques | Graphical meta-analytical tools |
|---|--|
| <i>Outcomes measure – parameterization:</i> | Plot of normalized z-scores |
| Odds ratio, risk ratio, risk difference | Radial plot (Galbraith plot), forest plot, |
| Mean difference | bubble plot, funnel plot L'Abbe plot |
| Hedges' g, Cohen's d | Baujat plot |
| Correlation coefficient, Fisher's Z | Egger's regression plot |
| | Macaskill's regression plot |
| <i>Fixed-effects meta-analysis:</i> | Trim-and-fill plot |
| Inverse variance weighted method | |
| Mantel-Haenszel, Peto | |
| Maximum likelihood techniques | |
| <i>Random-effects meta-analysis and heterogeneity:</i> | |
| Weighted, normal-normal and DerSimonian-Laird methods, | |
| Cochran's Q, Higgins' H and I ² | |
| Hedges and Olkin test of homogeneity for correlation coefficients | |
| <i>Meta-regression:</i> | |
| Mixed-effect and multi-level models | |
| <i>Publication bias:</i> | |
| Trim-and-fill test, fail-safe N | |
| Egger's regression test | |
| Begg's rank correlation test | |
| Macaskill's regression test | |

The second case demonstrates the application of meta-analysis for the estimation of the overall effect of a critical process stage on the incidence of a pathogen under study. The meta-analysis conducted on the relative risk (defined as the probability of encountering *Salmonella*-positive pig carcasses after chilling relative to the probability of encountering *Salmonella*-positive carcasses before chilling), as derived from the ten primary studies, confirmed on the grounds of increased statistical power the decreasing effect that chilling has on the recovery of *Salmonella* ($U=27.3$; $p<0.001$). As there was no evidence of heterogeneity ($Q=2.9$; $p=0.96$), the fixed-effects meta-analysis was considered a suitable solution and it delivered a normal distribution of the overall effect of chilling (with a mean of ~2.4 times reduction in *Salmonella* recovery on pig carcasses).

Meta-analysis, if carefully constructed and implemented, can assist food safety researchers to determine the extent to which accumulated evidence tends to provisionally confirm or conclusively refute a specified theory of the intervention under investigation. The claimed strengths of meta-analysis are all contingent on the important condition that the measures that represent and share the same theoretical concepts within a meta-analysis be of at least satisfactory validity (related to the principle of ‘rubbish in – rubbish out’). The main limitations of meta-analysis are related to quality of primary research and publication bias. The latter exists because research with statistically significant results is potentially more likely to be published than work with non-significant results. The presence of publication bias in a meta-analysis can be assessed informally by inspection of a funnel plot, which plots the effect size of each study against some measure of its precision (1/standard error). The funnel shape of Figure 1B suggests that there is little evidence of publication bias in the chilling meta-analysis. This shape is expected because trials of decreasing size have increasingly large variation in their effect size estimates due to random variation becoming increasingly. However, if the chance of publication is greater for larger trials or trials with statistically-significant results, some small non-significant studies may not appear in the literature, leading to the omission of trials in one corner of the plot.

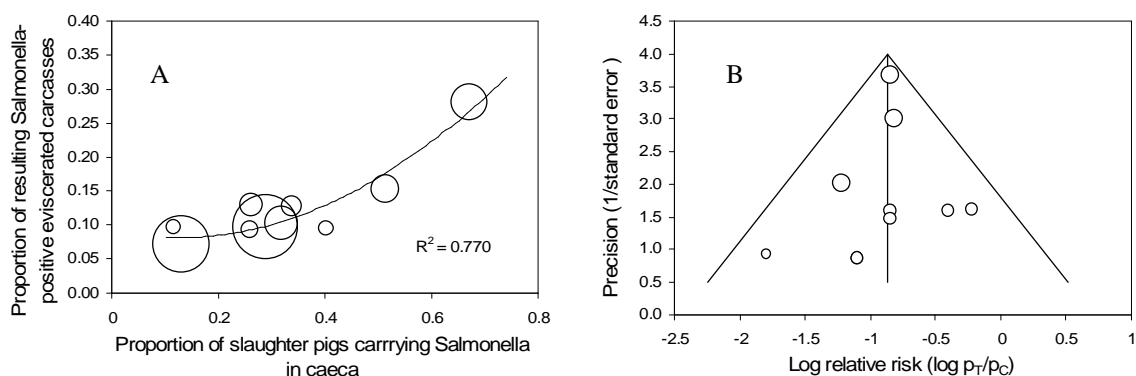


Figure 1: Bubble plot and funnel plot illustrating the meta-analysis demonstration studies.

Conclusions

These two applications demonstrate that meta-analysis can be used as a valuable tool for synthesizing food safety research and quantitative risk assessment studies.

Acknowledgments

The authors wish to acknowledge *SafeFood*, The Food Safety Promotion Board and the Food Institutional Research Measure (FIRM) administered by the Irish Department of Agriculture, Fisheries and Food.

References

- Bollaerts K., Aerts M., Faes C., Grijspeerdt K., Dewulf J., and Mintiens K. (2008) Human salmonellosis: Estimation of dose-illness from outbreak data. *Risk Analysis* 28(2),427-440.
- Gonzales Barron U., Bergin D., Butler F. (2008) A meta-analysis study of the effect of chilling on *Salmonella* prevalence on pork carcasses. *Journal of Food Protection* 71(7), 1330-1337.
- Gonzales Barron U., Soumpasis I., Butler F., Duggan S., Prendergast D., and Duffy G. (2009) Estimation of prevalence of *Salmonella* spp. on pig carcasses and pork joints using a quantitative risk assessment model aided by meta-analysis. *Journal of Food Protection* 72(2), 274-285.
- Patil S. R., Morales R., Cates S., Anderson D., and Kendall D. (2004) An application of meta-analysis in food safety consumer research to evaluate consumer behaviours and practices. *Journal of Food Protection* 67(11), 2587-2595.
- Sánchez J., Dohoo I.R., Christensen J., and Rajic A. (2007) Factor influencing the prevalence of *Salmonella* spp. in swine farms: a meta-analysis approach. *Preventive Veterinary Medicine* 81, 148-177.
- Viallette M., Pinon N., Leporq B., Dervin C., and Membré J.M. (2005) Meta-analysis of food safety information based on a combination of a relational database and a predictive modelling tool. *Risk Analysis* 25(1), 75-83.

A preliminary consumer risk assessment model of *Salmonella* in Irish fresh pork sausages: Transport and home refrigeration modules

U. A. Gonzales-Barron, I. Soumpasis, G. Redmond and F. Butler

Biosystems Engineering, UCD School of Agriculture, Food Science and Veterinary Medicine. University College Dublin, Dublin 4, Ireland (ursula.gonzalesbarron@ucd.ie, f.butler@ucd.ie)

Abstract

A stochastic risk assessment model aiming to evaluate the risk for human health posed by *Salmonella* spp. associated with consumption of fresh pork sausages in Ireland is under development. The specific objective of this work was to estimate the *Salmonella* levels in fresh pork sausages after the first two modules, transport after purchase and home refrigeration. The variability in initial level of *Salmonella* (Y_0) in retail raw pork sausages given a *Salmonella*-positive sausage pack was modeled by a lognormal distribution ($E(Y_0)=1.80 \log \text{ CFU/g}$; 95% CI: 1.17-2.30 $\log \text{ CFU/g}$) using Irish survey's data. For the entire duration of transport, the temperature profile of the centre of a sausage pack against time was modeled using transient heat transfer equations. For the refrigeration module, a simulated continuous temperature profile was obtained in two stages: a brief *temperature adjustment stage* modeled by heat transfer equations until approaching the sampled fridge average temperature, and a *temperature oscillation stage* which consisted of an actual time-temperature section randomly sampled from a parallel experiment until the completion of the total refrigeration time. The Baranyi's primary growth model and the square-root secondary model were applied to the dynamic temperature profiles to predict the *Salmonella* levels after transport and refrigeration (Y_R). While the *Salmonella* levels of fresh pork sausages prior to cooking did not increase significantly during transport and home storage ($E(Y_R)=1.85 \log \text{ CFU/g}$; 95% CI: 1.25-2.76 $\log \text{ CFU/g}$), the probability of finding hazardous *Salmonella* levels above 5 $\log \text{ CFU/g}$ from contaminated sausage packs was ~0.13%. Sensitivity analysis showed that, for the Irish conditions, the *Salmonella* levels in raw sausages are more affected by storage time ($R=0.43$) than by average temperature ($R=0.17$).

Keywords: Risk assessment, pork sausage, *Salmonella*, refrigeration, Baranyi model

Introduction

Hald et al. (2004) estimated that, between 10-30% of all cases of food-borne salmonellosis had pork and pork products incriminated as the actual source. In Ireland, a pork product that merits attention is the fresh pork sausage for being a raw comminuted product that is widely consumed – according to the Irish consumer's database (NSIFCS, 2001) 55 g of sausage per week is consumed on average per person. Assuming that approximately 65% of the population - 4.2 million (<http://www.cso.ie>) – consume pork sausages, an average of 7800 metric tons of sausages would be consumed each year. While it is true that the prevalence of *Salmonella* on Irish pork cuts is relatively low (4.0%, 95% CI: 0.3 – 12.0% in Gonzales-Barron et al., 2009) and the fresh pork sausage is a product that still undergoes cooking, there is evidence that pork sausage may become a potential hazardous product, as suggested by the 24 reported outbreaks of salmonellosis associated with sausages or sausage meat in England and Wales, corresponding to more than 1000 cases of food poisoning between 1988 and 1994 (Nichols and de Louvois, 1995). Thus, the objective of our research was to develop a stochastic risk assessment model in four modules for estimating the risk of salmonellosis from consumption of Irish-style fresh pork sausages. This communication will briefly present the methodology and results of the first two modules: transport and home refrigeration.

Methodology

The initial concentration of *Salmonella* in fresh pork sausages (λ_0) from contaminated packs produced in Ireland was approached using the MPN data compiled in Mattick et al. (2002).

Likelihood functions of CFU/g representing the uncertainty around the positive tube counts triplets were built for each of the tested sausages (6) from every pack (10). Bayesian analysis was then used to derive a more-informed posterior distribution of the initial *Salmonella* concentration in every pack. A parametric bootstrap technique was finally performed to propagate the uncertainty of the 10 posterior distributions of within-pack *Salmonella* concentration to a log-normal distribution of variability (λ_0). The distributions of uncertainty for the mean (μ) and standard deviation (σ) are shown in Table 1. Distributions for the transport time (t_T), refrigeration time (t_R) and average fridge air temperature (T_{avg}) were fitted to Irish data from Kennedy et al. (2005), while the ambient temperature during transport (T_{amb}) was modeled from Irish meteorological daily data for summer and winter (Table 1).

Table 1: Input parameters of the consumer's risk assessment model

| Notation | Description and unit | Value | Type |
|-------------|---|--|------|
| μ | Mean concentration of <i>Salmonella</i> in a contaminated sausage pack (CFU/g) | Normal (4.0389,0.1039) | Unc |
| σ | Standard deviation of the concentration of <i>Salmonella</i> in a contaminated sausage pack (CFU/g) | Normal (0.6389,0.0591) | Unc |
| λ_0 | Concentration of <i>Salmonella</i> in a contaminated sausage pack (CFU/g) | Lognormal (μ, σ) | Var |
| b | Constant of the square-root model ($1/\sqrt{h} \cdot ^\circ\text{C}$) | Normal (0.0176,0.0032) | Var |
| T_{min} | Minimum temperature for growth of <i>Salmonella</i> ($^\circ\text{C}$) | Normal (-5.0129,0.6899) | Var |
| h_0 | Lag-phase parameter in Baranyi's model (log CFU/g) | Normal (2.4538,0.0860) | Var |
| t_T | Transport time – retail to refrigerator (min) | Inverse Gaussian (36.037, 38.761) | Var |
| T_0 | Initial temperature of sausage packs at market/retail display cabinet ($^\circ\text{C}$) | Normal(5,0.8) | Var |
| T_{amb} | Ambient temperature of Ireland (summer/winter) ($^\circ\text{C}$) | Beta general (5.21, 3.68, -5.35, 25.63) Beta general (4.03, 3.19, -7.28, 18.52) | Var |
| t_R | Refrigeration time – time sausage pack is stored before preparing (h) | Gamma(1.1, 15) | Var |
| T_{avg} | Average air temperature of a refrigerator in Ireland ($^\circ\text{C}$) | Normal (5.3552, 2.49) | Var |

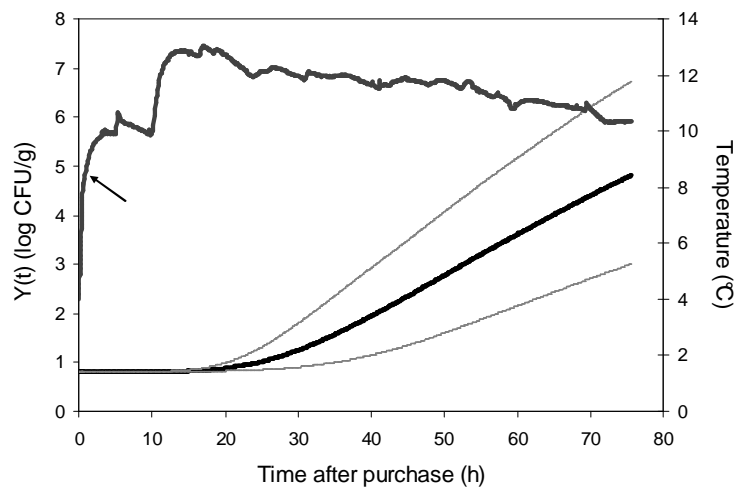


Figure 1: Simulated temperature profile of a contaminated pork sausage pack during transport and refrigeration with its respective expected *Salmonella* growth $Y(t)$ and 95% CI as predicted by the Baranyi's model. Arrow indicates the beginning of home refrigeration.

The growth of *Salmonella* spp. during transport and refrigeration was evaluated from t_0 (time of purchase) using the dynamic Baranyi's growth model for changing temperatures (Baranyi et al., 1995). The growth was calculated in small time intervals using temperature profiles ($T(t)$) that were modeled as a continuum for transport and home refrigeration (Figure 1). The estimates of *Salmonella* growth rate (μ_{\max}) in fresh bratwurst obtained from Ingham et al. (2009) were used as surrogate data, and further expressed as a function of temperature using the square-root secondary model ($p < 0.01$, $R^2 = 0.77$), $\sqrt{\mu_{\max}(T)} = b(T - T_{\min})$, where T is the product's temperature ($^{\circ}\text{C}$), b is a constant ($1/\sqrt{\text{h}} \cdot ^{\circ}\text{C}$) and T_{\min} ($^{\circ}\text{C}$) is the nominal minimum temperature for *Salmonella*. The normal distributions for b and T_{\min} (Table 1) as well as for h_0 (Baranyi's lag-phase parameter also derived from Ingham et al. (2009)) were assumed to describe the variability in *Salmonella* growth rate.

For the entire duration of transport t_T , the temperature profile ($T(t)$) of the centre of a sausage pack of half dimensions L_x (0.09 m), L_y (0.02 m) and L_z (0.06 m), was modeled using transient heat transfer equations for a one-dimensional (y) system. The initial temperature T_0 corresponded to the sausage temperature at retail (Table 1). The thermal conductivity and diffusivity of the sausage were constant at $0.48 \text{ J/m}\cdot\text{s}\cdot\text{K}$ and $1.41 \times 10^{-7} \text{ m}^2/\text{s}$, as well as the convective heat transfer coefficient (h_T) at $11.0 \text{ W/m}^2\cdot^{\circ}\text{C}$. The temperature of the air surrounding the pack (T_{∞}) was assumed to be 2°C above T_{amb} (Table 1).

For the refrigeration module, experiments were conducted to capture the oscillations in the temperature of a sausage pack stored in domestic refrigerators up to 7 days. The real temperature profiles were assigned to categories according to the average air temperature of the refrigerator (T_{avg}): $<1^{\circ}\text{C}$, $[1, 3>$, $[3, 5>$, $[5, 7>$, $[7, 9>$, and $>9^{\circ}\text{C}$. Mimicking the experimental data, $T(t)$ for the refrigeration module was modeled in two stages: a brief *temperature adjustment* stage ($\sim 2\text{-}3 \text{ h}$) governed by heat transfer equations until approaching T_{avg} , and a *temperature oscillation period*, which consisted of a temperature history section (t , T)_s randomly sampled from the above experiment within the corresponding category until the completion of the total refrigeration time (t_R). For the temperature adjustment stage, the overall convective heat transfer coefficient (h_U) of the cold air to the surface of the product was estimated from the temperature data ($h_U = 16.2 \text{ W/m}^2\cdot^{\circ}\text{C}$) and assumed to be constant for all the surfaces of the product. For the three-dimensional system, $T(t)$ was modeled using a product's initial temperature of T_T (product's temperature at the end of transport) and $T_{\infty} = T_{\text{avg}}$. Once the continuous temperature profile during transport and refrigeration was modeled for every iteration or sausage pack, the *Salmonella* growth rate was estimated for the specific temperature at time t using the square-root model, and the *Salmonella* log-concentration using the Baranyi's equation (Figure 1). The simulation model was written in Matlab 7.0 (The Mathworks, Inc) and run for 10000 iterations.

Results and discussion

Using the MPN data from Mattick et al. (2002), it was possible to model the uncertainty and variability around the initial concentration of *Salmonella* (λ_0 , CFU/g) in the contaminated pork sausage packs produced in Ireland (prevalence of ~ 0.046 with a 95% CI of 0.032-0.064). In log terms, the initial *Salmonella* level (Y_0) had an expected value of 1.80 log CFU/g with a 95% CI of 1.17-2.30 log CFU/g. While on average the *Salmonella* concentration did not increase significantly after transport and home storage ($E(Y_R) = 1.85 \text{ log CFU/g}$) because in most cases the *Salmonella* cells remained in the lag phase, the frequency distribution of *Salmonella* levels after refrigeration presented a longer right tail (95% CI: 1.25-2.76 log CFU/g). This occurred due to the possibility of temperature abuse during home storage, as illustrated in Figure 1, where the sausage pack subjected to a simulated temperature of $\sim 11^{\circ}\text{C}$ presented exponential growth around 20 hours after purchase. The normal distributions of the parameters of the square-root model, b and T_{\min} , as modelled from Ingham et al. (2009), introduced a high variability in *Salmonella* growth for a given initial concentration Y_0 , lag-phase status h_0 , and temperature profile $T(t)$ (see the extent of the 95% CI in Figure 1). While it is recognised that the total variability in these parameters is partly due to uncertainty, in this model they were assumed to represent the product of the differences between industrial

batches of pork sausages and the variability among natural strains. When the model was run for variability only, separating the uncertainty introduced by the mean and standard deviation of λ_0 , the probability of finding hazardous *Salmonella* concentration above 5 log CFU/g (that may not be inactivated sufficiently by cooking) from a contaminated sausage pack was estimated at 0.13%, with a 95% CI of 0.02-0.25% (Figure 2). Sensitivity analysis has shown that the *Salmonella* level in fresh sausages prior to cooking is highly influenced by the initial *Salmonella* load ($R=0.77$), and is more affected by storage time ($R=0.43$) than by the average fridge temperature and its oscillations ($R=0.17$). Figure 2 suggests that approximately beyond 2 days of storage, hazardous *Salmonella* concentrations are likely to occur.

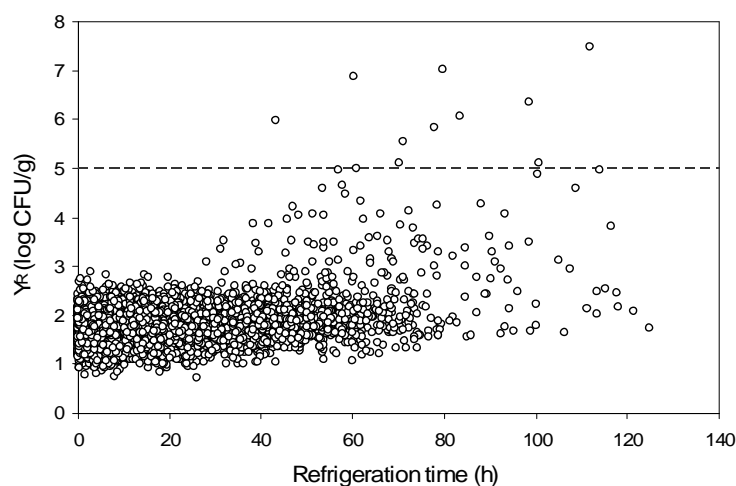


Figure 2: Influence of cold storage time on the concentration of *Salmonella* in pork sausage after refrigeration (Y_R) prior to cooking

Conclusions

The concentration of *Salmonella* in fresh pork sausages from a contaminated pack prior to cooking was estimated to be within a 95% CI of 1.25-2.76 log CFU/g, although ~0.13% of the times, hazardous levels that may not be sufficiently inactivated by cooking can be present.

Acknowledgments

The authors wish to acknowledge the Food Institutional Research Measure (FIRM) administered by the Irish Department of Agriculture, Fisheries and Food, and the partial financial support of QPORKCHAINS, an EU 6th Framework project.

References

- Baranyi J., Robinson T.P., Kaloti A., and Mackey B.M. (1995) Predicting growth of *Brochothrix thermosphacta* at changing temperature. *International Journal of Food Microbiology* 27, 61-75.
- Gonzales-Barron U., Soumpasis I., Butler F., Duggan S., Prendergast D., and Duffy G. (2009) Estimation of prevalence of *Salmonella* spp. on pig carcasses and pork joints using a quantitative risk assessment model aided by meta-analysis. *Journal of Food Protection* 72(2), 274-285.
- Hald T., Vose D., Wegener H., and Koupeev T. (2004) A Bayesian approach to quantify the contribution of animal-food sources to human salmonellosis. *Risk Analysis* 24(1), 255-269.
- Ingham S.C., Ingham B.H., Borneman D., Jaussaud E., Schoeller E.L., Hoftiezer N., Schwartzburg L., Burnham G.M., and Norback J.P. (2009) Predicting pathogen growth during short-term temperature abuse of raw sausage. *Journal of Food Protection* 72, 75-84.
- Kennedy J., Jackson V., Blair I. S., McDowell D.A., Cowan C., and Bolton D.J. (2005) Food safety knowledge of consumers and the microbiological and temperature status of their refrigerators. *Journal of Food Protection* 68, 1421-1430.
- Mattick K.L., Bailey R.A., Jorgensen F., and Humphrey T.J. (2002) The prevalence and number of *Salmonella* in sausages and their destruction by frying, grilling or barbecuing. *Journal of Applied Microbiology* 93, 541-547.
- Nichols G.L., and de Louvois J. (1995) The microbiological quality of raw sausages sold in the UK. *PHLS Microbiology Digest* 12, 236-242.
- NSIFCS (2001) Irish Universities Nutrition Alliance: The North/South Ireland food consumption survey database.

Predictive Microbiology Models vs. Modeling Microbial Growth Within *Listeria monocytogenes* Risk Assessment: What Gap? What Impact?

R. Pouillot

Center for Food Safety and Applied Nutrition/Food and Drug Administration, 5100 Paint Branch Pkwy, College Park, MD 20740. Regis.Pouillot@fda.hhs.gov

Abstract

Despite the increasing complexity of predictive microbiology models, bacterial growth in quantitative microbial risk assessments is generally predicted using very simple models. What is the impact of the choice of the model on the final risk estimates? What issues still exist for appropriate prediction of bacterial growth within risk assessments? As a partial answer to these questions, the impact of the use of various published models to predict bacterial growth during consumer storage was evaluated in a specific risk assessment for the occurrence of listeriosis from consumption of cold smoked salmon. Results underline a gap between the most studied factors in predictive microbiology modeling (lag, growth rate) and the most influential parameters in some *Listeria* risk assessments (maximum population density, bacterial competition).

Keywords

Quantitative Risk Assessment, *Listeria monocytogenes*.

Introduction

In most Microbial Quantitative Risk Assessments (MQRA), particularly those dealing with *Listeria monocytogenes* (*Lm*), bacterial growth is a key basic process that influences the evaluated risk. Some guidelines exist on how to incorporate predictive microbiology models in MQRA (DMS model, van Gerwen and Zwietering 1998; Ross and McMeekin 2003). Nevertheless, the growth models used in current MQRAs are generally very simple compared to those developed in the predictive microbiology domain. For example, the FDA/FSIS (2003) MQRA of relative risk from *Lm* in ready-to-eat foods used a single log-linear primary growth model, which did not consider either lag or competition, a simple square root model for temperature as a secondary model, and one exponential growth rate (*EGR*) distribution per food category. More recent MQRAs have modeled lag as a multiple of the generation time and may consider the effect of competition (Ross *et al.* 2009). Are the models used in these MQRAs simple or simplistic? What is the impact of the choice of the model on the final risk prediction?

To partially answer these questions, the impact of the model used to predict the growth of *Lm* during consumer storage was tested within a quantitative risk assessment of listeriosis from consumption of cold smoked salmon (CSS).

Material and Methods

The baseline parameters were adapted from a recently published MQRA of *Lm* in CSS in France (Pouillot *et al.* 2007; Pouillot *et al.* 2009). The initial \log_{10} concentration of *Lm* in contaminated CSS follows a normal distribution with a mean of $-2.57 \log_{10}$ cfu/g and a standard deviation of $1.76 \log_{10}$ cfu/g. This distribution is rounded and truncated to provide a discrete number of *Lm* per 100g package of CSS. The refrigerator temperature varied from household to household according to a normal distribution with a mean of 7.0°C and a standard-deviation of 3.0°C . The storage duration followed an exponential distribution with a mean of 4.8 days. The serving size was fixed at 35g. Dose-response for invasive listeriosis was modeled as $\text{Pr}(\text{illness}|D) = 1 - \exp(-r D)$, with $r = 1.7\text{E-}14$ ("population with decreased susceptibility", FAO/WHO 2004).

The concentration of *Lm* at consumption was predicted using various growth models obtained from the literature. All model outputs were compared to a baseline model that used an exponential growth model without lag as a primary model and a square root model with constant EGR and T_{min} as a secondary model. The alternative models used were: 1) no growth; 2) fluctuating temperature within the refrigerator (DMS model, Pouillot *et al.* 2007); 3) strain to strain variation in EGR and/or T_{min} ; 4) strain to strain variation and uncertainty in EGR and T_{min} ; 5) varying maximum population densities (MPD); 6) lag time estimated as a constant number of relative generation times (RGT); 7) strain to strain variation in lag time; 8) individual bacterial stochastic lag time; 9) competition with food flora or; 10) various secondary growth models on temperature. Temperature was considered to be the only environmental parameter that impacted the growth in this process. The results are expressed in terms of *i*) impact on the mean of the \log_{10} concentration of *Listeria* per gram at consumption and *ii*) impact on the number of expected cases of listeriosis. The code (R software) is available on request to the author.

Table 1: Impact of the growth model on the mean \log_{10} concentration of *Listeria monocytogenes* per serving and impact on the number of cases.

| | Secondary model on μ or EGR | lag | MPD | Mean \log_{10} cfu/g [95%CI] | Expected <i>n</i> cases |
|---|---|--------------------------------------|----------------------|-----------------------------------|----------------------------|
| Baseline | Square Root model, $\mu_{25} = 6.24 \text{ d}^{-1}$, $T_{min} = -2.86$ [1] | 0 | 7.27 [1] | 0 (ref) | 100 (ref) |
| 1. No growth | | | | -1.70 | 0.00007 |
| 2. Fluctuating environment | DMS model [2] | 0 | 7.27 | +0.08 | 110 |
| 3. Varying growth parameters | μ_{25} , T_{min} from [1] | 0 | 7.27 | -0.03 | 129 |
| | $T_{min} = -1.18^{\circ}\text{C}$, EGR_5 from [3] | | 7.27 | -0.41 | 66 |
| 4. Varying and uncertain growth parameters | μ_{25} , T_{min} from [1], second order simulation | 0 | 7.27 | -0.01 [-0.03, 0.00] | 136 [126, 145] |
| 5. Varying MPD | Baseline | 0 | from [1] from [3] | -0.00 +0.02 | 256 421 |
| 6. lag | Baseline | 3.09 RGT [4] 5.29 RGT [5] | 7.27 7.27 | -0.65 -0.92 | 74 60 |
| 7. Varying lag | Baseline | $\sim\text{LN}(1.3, 0.9)$ RGT [5] | 7.27 | -0.76 | 66 |
| 8. Stochastic lag | | from [6] from [7] | 7.27 7.27 | -0.63 -0.88 | 76 62 |
| 9. Competition | Jameson effect using parms. for the food flora from [1] | 0 | 7.27 | -0.07 | 33 |
| 10. Secondary growth model | [8] as in [9] [10] as in [9] | 0 0 | 7.27 7.27 | -0.37 -0.17 | 76 70 |

[1] (Delignette-Muller *et al.* 2006); [2] (Pouillot *et al.* 2007); [3] (FDA/FSIS 2003); [4] (Augustin and Carlier 2000); [5] (Ross *et al.* 2009); [6] (Standaert *et al.* 2007); [7] (Guillier and Augustin 2006); [8] Ross (FAO/WHO 2004) modified by (Gimenez and Dalgaard 2004); [9] (Cornu *et al.* 2006); [10] (Devlieghere *et al.* 2001) modified by (Gimenez and Dalgaard 2004)

Results and Discussion

The results are shown in Table 1. These results do not answer the question “which model is best” but they do show the impact of different predictive microbiology models for a specific pathogen, process and set of parameters (here, storage time and temperature at the consumer’s household and dose-response model).

The ability of the food being modeled is important for an *Lm* risk assessment. If no growth occurs in this product (or it is not modeled), no illnesses would be predicted at the initial level of contamination (see alternative 1.). Indeed, in a contaminated product that permits growth, consumer storage appears to be a critical step in determining overall risk (FDA/FSIS 2003; FAO/WHO 2004; Pouillot *et al.* 2009). This is particularly true in scenarios that include high refrigerator temperatures. The distribution of refrigerator temperatures used here was derived from a representative sample in France. In this situation, growth modeling was a significant impact on the final predicted number of illnesses.

The DMS model (Pouillot *et al.* 2007) has been used to evaluate microbial growth in a varying temperature environment. It is based on a log-linear primary growth model without lag and a square root model. The issue of this model does not significantly impact estimated risk in this context (Alternative 2.). Consideration of strain to strain variability seems to be more influential, resulting in a 29% increase in predicted risk as compared to a situation where this variability is not considered (Alternative 3a.). In this example, consideration of uncertainty in the growth parameter estimate seems to have a low impact (Alternative 4.), but this uncertainty does not consider the model uncertainty.

In this case, the use of a lag time is questionable; it is considered only as an illustration purpose. Lag time has been described as a major factor influencing overall growth. Nevertheless, no clear model exists for considering the impact of preincubation condition or the stress on lag. QMRA models sometimes assume that there is no lag as a safe assumption. It has been recommended to use a constant or a variable number of RGT (Ross and McMeekin 2003; Ross *et al.* 2009). Consideration of lag had a relatively low impact on the final estimated number of cases (Alternative 6. and 7.). It has also been suggested that the behavior of individual bacterial cells should be modeled. To test this, we used a model from Guillier and Augustin (2006) with a population relative lag time of 3.09 and one from Standaert *et al.* (2007) that leads to a median population relative lag time of 3. Both models have a low impact on the final risk, compared to a model using a population lag (Alternative 8.).

Estimating the influence of the secondary growth model is more difficult because *i*) various models exist in the literature; *ii*) some models are specifically designed for a given product or process, and may be not useful for QMRA. For CSS, the use of various secondary growth models on temperature has a little impact (Alternative 10.). Nevertheless, other results (not shown) suggest that there may be a large impact if other environmental parameters, such as phenolic content, are considered.

The maximum achievable population density (MPD) seems the most influential factor among those tested (Alternative 5.). The expected number of cases increases by a factor of 2.5 if the distribution derived by Delignette-Muller *et al.* (2006) is used and the expected number of cases increases by a factor of 4 if the FDA/FSIS (2003) assumption of a varying MPD with temperature is used, all other parameters being equal. The importance of MPD is confirmed by looking at the impact of the modeling bacterial competition using the Jameson effect. In fact, consideration of the Jameson effect leads to a decrease in the maximum density of *Listeria* for some model iterations. Maximum population density is rarely, if ever, studied in the predictive microbiology literature, but is clearly an essential consideration in QMRA modeling for *Listeria* with the current dose-response models.

Conclusions

To a large degree, these results are a consequence of the fact that the dose-response calculation considers the number of bacteria on an arithmetic scale. As a consequence, *i*) the expected number of listeriosis cases is poorly linked to the mean of the log₁₀ concentration of

Lm but is strongly linked to the arithmetic mean of *Lm*, a measure which is seldom considered in microbiology literature; *ii*) the most extreme concentrations have a large impact on the predicted risk; *iii*) the situations that either limit or increases the occurrence of these high numbers of bacteria (lower or higher MPN, bacterial competition) have the greatest influence on predicted risk.

Currently, there is an important gap between predictive microbiology models and the models used in microbial risk assessments. It is difficult for a risk assessor to find an applicable predictive microbiology model in the abundant literature. It is important for risk assessors to evaluate the impact of the choice of the model on the final output.

Acknowledgements

I thank Marie Cornu for her inputs, comments and suggestions in this study and Steven Gendel for his review of this study and abstract. This project was supported in part by an appointment to the Research Participation Program at the CFSAN administered by the ORISE through an interagency agreement between the U.S. Department of Energy and the U.S. FDA.

References

- Augustin, J.-C. and V. Carlier (2000). "Mathematical modelling of the growth rate and lag time for *Listeria monocytogenes*." *International Journal of Food Microbiology* 56(1): 29-51.
- Cornu, M., A. Beaufort, S. Rudelle, L. Laloux, H. Bergis, N. Miconnet, T. Serot and M. L. Delignette-Muller (2006). "Effect of temperature, water-phase salt and phenolic contents on *Listeria monocytogenes* growth rates on cold-smoked salmon and evaluation of secondary models." *International Journal of Food Microbiology* 106(2): 159-68.
- Delignette-Muller, M. L., M. Cornu, R. Pouillot and J. B. Denis (2006). "Use of Bayesian modelling in risk assessment: Application to growth of *Listeria monocytogenes* and food flora in cold-smoked salmon." *International Journal of Food Microbiology* 106(2): 195-208.
- Devlieghere, F., A. H. Geeraerd, K. J. Versyck, B. Vandewaelere, J. Van Impe and J. Debevere (2001). "Growth of *Listeria monocytogenes* in modified atmosphere packed cooked meat products: a predictive model." *Food Microbiology* 18(1): 53-66.
- FAO/WHO (2004). Risk assessment of *Listeria monocytogenes* in ready to eat foods - Technical report. Rome, Food and Agriculture Organization of the United Nations and World Health Organization. Microbiological Risk Assessment Series 5: 269.
- FDA/FSIS (2003). Quantitative Assessment of Relative Risk to Public Health from Foodborne *Listeria monocytogenes* Among Selected Categories of Ready-to-Eat Foods, Food and Drug Administration, United States Department of Agriculture, Center for Disease Control.
<http://www.foodsafety.gov/~dms/lmr2-toc.html>
- Gimenez, B. and P. Dalgaard (2004). "Modelling and predicting the simultaneous growth of *Listeria monocytogenes* and spoilage micro-organisms in cold-smoked salmon." *Journal of Applied Microbiology* 96(1): 96-109.
- Guillier, L. and J.-C. Augustin (2006). "Modelling the individual cell lag time distributions of *Listeria monocytogenes* as a function of the physiological state and the growth conditions." *International Journal of Food Microbiology* 111(3): 241-251.
- Pouillot, R., V. Goulet, M. L. Delignette-Muller, A. Mahe and M. Cornu (2009). "Quantitative Risk Assessment of *Listeria monocytogenes* in French Cold-Smoked Salmon: II. Risk Characterization." *Risk Analysis* 29(6): 806-819.
- Pouillot, R., N. Miconnet, A. L. Afchain, M. L. Delignette-Muller, A. Beaufort, L. Rosso, J. B. Denis and M. Cornu (2007). "Quantitative risk assessment of *Listeria monocytogenes* in French cold-smoked salmon: I. quantitative exposure assessment." *Risk Analysis* 27(3): 683-700.
- Ross, T. and T. A. McMeekin (2003). "Modeling microbial growth within food safety risk assessments." *Risk Analysis* 23(1): 179-97.
- Ross, T., S. Rasmussen, A. Fazil, G. Paoli and J. Summer (2009). "Quantitative risk assessment of *Listeria monocytogenes* in ready-to-eat meats in Australia." *International Journal of Food Microbiology*. 131(2-3): 128-37.
- Standaert, A. R., K. Francois, F. Devlieghere, J. Debevere, J. F. Van Impe and A. H. Geeraerd (2007). "Modeling individual cell lag time distributions for *Listeria monocytogenes*." *Risk Analysis* 27(1): 241-54.
- van Gerwen, S. J. C. and M. H. Zwietering (1998). "Growth and inactivation models to be used in quantitative risk assessments." *Journal of Food Protection* 61(11): 1541-1549.

Sensitivity Analysis applied to a *Listeria monocytogenes* exposure assessment model

M. Ellouze^{1,2}, J.P. Gauchi³ and J.C. Augustin²

¹ CRYOLOG SA, 58, Boulevard Gustave Roch, 44261 Nantes, France (mellouze@cryolog.com)

² Unité MASQ, Ecole Nationale Vétérinaire d'Alfort, 7, Avenue du Général de Gaulle, F-94704 Maisons-Alfort cedex, France (jcaugustin@vet-alfort.fr)

³ Unité MIA (UR341), INRA, Domaine de Vilvert, 78352 Jouy en Josas, France (jean-pierre.gauchi@jouy.inra.fr)

Abstract

In this study, the Saltelli (2002) Sensitivity Analysis method was applied to an exposure assessment model of *Listeria monocytogenes* in cold smoked vacuum packed salmon. The impact of the choice of the approach (populational or cellular) of the primary and secondary models as well as the effect of their associated factors on the final contamination level was investigated. Results provided a ranking of all the factors which revealed that the food water activity, its storage temperature and duration in the domestic refrigerator were the most important factors.

Key words

Sensitivity Analysis, Exposure Assessment, Modeling, *Listeria monocytogenes*

Introduction

Over the last years, quantitative microbial risk assessment (QMRA) has become an important tool for food safety, however criticized as an extremely data hungry and time consuming method (Havelaar *et al.*, 2008). In fact, simple and deterministic approaches are now put aside and a large variety of complexities can be found with very extensive and stochastic models. Indeed, it can be tempting to include every phenomenon that could be of relevance, but this could lead to over-parameterized models (Zwietering, 2009). Sensitivity Analysis (SA) can help solve this issue by eliminating the less influent factors. SA is defined as the study of how the output uncertainty of a model can be apportioned to different sources of uncertainty in the model input (Saltelli, 2002). Several SA methods have been previously used in QMRA, (ANOVA, Spearman regression coefficient...) (Frey & Patil, 2002; Membré *et al.*, 2008) but these methods seem to be poorly adapted to complex and non linear models like those encountered in QMRA. The Saltelli (2002) SA method, is commonly recognized in the statistical field ; its application to microbiological modeling issues will represent a major breakthrough in QMRA as it will help modelers better understand and evaluate quantitatively the effects of the inputs on the output and consequently orientate data acquisition campaigns and efforts to the most impacting factors. The aim of this study was to apply this innovative SA method to an exposure assessment model of *L. monocytogenes* in Cold Smoked Vacuum Packed Salmon (CSVPS) to identify inputs that substantially impact the final concentration of the pathogen at consumption.

Materials and methods

Experimental design

The exposure assessment model is composed of a secondary model which calculates the effects of the environmental conditions on the maximum growth rate and a primary model which computes the final contamination x given the secondary model output (μ_{\max}), the initial contamination level x_0 and the physiological state of the microorganisms K . Two approaches were considered. The first and commonly used approach is a populational approach in which all the contaminating cells are supposed to have the same physiological state K and their growth is modeled globally. The second approach is a cellular approach in which each cell is characterized by a specific physiological state k_i which is obtained by an Extreme Value type II distribution EVII(a,b) (Guillier & Augustin, 2006)

with $b = D/0.3658$ and $a = E - D(1.1642/0.3658)$ where $D = \exp(1.004 \cdot \log(E) - 0.447)$ and $E = \exp(0.0103(\log(K))^5 + 0.0065(\log(K))^4 - 0.039(\log(K))^3 + 0.0586(\log(K))^2 + 1.1941(\log(K)) + 0.1549)$. Their growth is thus modeled individually and the final contamination level is the sum of the population density reached at consumption time by each cell of the initial inoculum. The tested primary models were those of Rosso (1995) (equation 1) and Baranyi and Roberts (1994) (Baranyi & Roberts, 1994) (equation 2).

$$\ln x = \begin{cases} \ln x_0 & , t \leq lag \\ \ln x_{max} - \ln \left(1 + \left(\frac{x_{max}}{x_0} - 1 \right) \cdot \exp(-\mu_{max}(t - \frac{K}{\mu_{max}})) \right) & , t > lag \end{cases} \quad (1)$$

where x (CFU/g) is the bacterial concentration at the time t (h), x_0 (CFU/g) the initial bacterial concentration, x_{max} (CFU/g) the maximum bacterial concentration, μ_{max} (h⁻¹) the maximum specific growth rate K the physiological state of *L.monocytogenes* and lag the lag time(h).

$$\ln x = \ln x_{max} - \ln \left(1 + \left(\frac{x_{max}}{x_0} - 1 \right) \exp(-\mu_{max}(A(t))) \right) \quad \text{with} \quad A(t) = t + \frac{1}{\mu_{max}} \ln [\exp(-\mu_{max}t) + \exp(-K) - \exp(-K - \mu_{max}t)] \quad (2)$$

A multiplicative with or without interaction model (Augustin et al., 2005) was used as a secondary model to describe the effects of temperature T , pH and water activity aw on μ_{max} . The temperature and pH effects were modeled by cardinal type models (Rosso *et al.*, 1995) while the water activity effect was modeled either by a cardinal type (Rosso *et al.*, 1995) or a square root type model (Ratkowsky *et al.*, 1982).

$$\mu_{max} = \mu_{opt} \cdot CM_2(T) \cdot CM_1(pH) \cdot \begin{cases} SR(aw) \\ SR(aw) \cdot \gamma_{int} \\ CM_1(aw) \\ CM_1(aw) \cdot \gamma_{int} \end{cases} \quad (3)$$

with

$$CM_n(X) = \begin{cases} 0 & , X \leq X_{min} \\ \frac{(X - X_{max})(X - X_{min})^n}{(X_{opt} - X_{min})^{n-1} [(X_{opt} - X_{min})(X - X_{opt}) - (X_{opt} - X_{max})(X_{opt} + X_{min} - nX)]} & , X_{min} < X < X_{max} \\ 0 & , X \geq X_{max} \end{cases}$$

$$SR(aw) = \begin{cases} 0 & , X \leq X_{min} \\ \frac{X - X_{min}}{X_{opt} - X_{min}} & , X_{min} < X \leq X_{opt} \end{cases} \quad \gamma_{int} = \begin{cases} 1 & , \psi \leq 0.5 \\ 2(1 - \psi) & , 0.5 < \psi < 1 \\ 0 & , \psi \geq 1 \end{cases} \quad \psi = \sum_i \frac{\phi(i)}{2 \prod_{j \neq i} (1 - \phi(j))} \quad \phi(X) = \left(\frac{X_{opt} - X}{X_{opt} - X_{min}} \right)^3$$

where X_{min} , X_{opt} , and X_{max} are the cardinal values of *L. monocytogenes*, μ_{opt} is the optimal value of the maximum specific growth rate μ_{max} (h⁻¹) when $X = X_{opt}$ and n a shape parameter ($n=2$ for temperature and $n=1$ for pH and aw).

The parameters of these models were allowed to vary according to the ranges identified by a literature review and presented in table 1.

Table 1: Range of variations of the exposure assessment model parameters

| Microbiological parameters | Range | Distribution chain parameters | Range |
|--------------------------------|-------------|--|-----------|
| K | 0 – 8 | Duration of transport and storage $dTEP$ (h) | 4 – 96 |
| x_0 (UFC/g) | 1 – 20 | Temperature of transport and storage $TTEP$ (°C) | -2 – 7 |
| $\log x_{max}$ (log UFC/g) | 6.00 – 8.00 | Duration of storage in cold rooms dC (h) | 0 – 48 |
| μ_{opt} (h ⁻¹) | 0.60 – 1.30 | Temperature of storage in cold rooms TC (°C) | 1 – 7 |
| CSVPS pH | 5.30 – 6.30 | Duration of storage in the shelves dM (h) | 2 – 288 |
| CSVPS aw | 0.93 – 0.99 | Temperature of storage in the shelves TM (°C) | 2 – 9 |
| T_{min} (°C) | -2.5 – 0.1 | Duration of the journey back home dV (h) | 0.1 – 2.5 |
| T_{opt} (°C) | 36.5 – 39.5 | Temperature of the journey back home TV (°C) | 6 – 20 |
| T_{max} (°C) | 40.0 – 45.0 | Duration of the storage in the refrigerator dR (h) | 0 – 336 |
| pH_{min} | 4.00 – 4.40 | Temperature of the storage in the refrigerator TR (°C) | 2 – 12 |
| aw_{min} | 0.91 – 0.94 | Duration of unrefrigerated storage before consumption dD (h) | 0 – 16 |
| | | Temperature of unrefrigerated storage before consumption TD (°C) | 10 – 25 |

Sensitivity Analysis indices

This SA method is based on variance decomposition (Sobol, 2001) and computes first order indices (S_i) which represent the main effect contribution of each input factor to the variance of the output, and total effect indices (S_{ti}) which account for the total contribution to the output variance due to the first order effects (S_i) and to their non linear interactions. Several methods are available to compute these indices (Chan *et al.*, 2000). In the present study the SA was based on the Saltelli (2002) method because it is 50% cheaper than other published works in terms of required number of simulations (Saltelli, 2002). Here is a brief description of the method. Two

matrixes A and B of N lines (typically $N=10^4$ to $5 \cdot 10^4$) and F columns (F = number of factors of interest) are filled with numbers provided by a Latin Hypercube Sampling (McKay *et al.*, 1979) with respect to the range of variation of each factor. The approach (populational or cellular), the choice of the primary or secondary model were also considered as factors. A third matrix C_i containing all the columns of B but the column i which is replaced by the i^{th} column of matrix A is finally generated and the exposure assessment model is run on each row of the three matrixes to provide three vectors YA , YB and YC_i . The indices are then calculated with the following formula (Saltelli, 2002).

$$S_i = \frac{\left(\frac{1}{N} \sum_{u=1}^N YA^{(u)} YC_i^{(u)} \right) - g_0}{\left(\frac{1}{N} \sum_{u=1}^N YA^{(u)} YA^{(u)} \right) - f_0^2} \quad St_i = 1 - \frac{\left(\frac{1}{N} \sum_{u=1}^N YB^{(u)} YC_i^{(u)} \right) - f_0^2}{\left(\frac{1}{N} \sum_{u=1}^N YA^{(u)} YA^{(u)} \right) - f_0^2} \quad \text{with} \quad f_0 = \frac{1}{N} \sum_{u=1}^N YA^{(u)} \quad g_0 = \frac{1}{N} \sum_{u=1}^N YA^{(u)} YB^{(u)}$$

Results and discussion

The results of the SA are presented in table 2 where the factors were ranked according to their total effect indices (St_i). These indices are especially powerful in case of non additive and non linear model, particularly when used with their bootstrap confidence bounds estimates (Archer *et al.*, 1997). The exposure assessment model used in this study proved to be non additive and non linear. In fact, the sum of the first order indices (S_i) which account for the individual contribution of each factor into the variance of the output is less than 1 (0.72) which means that the variance of the output cannot be only explained by the sum of the individual effects of each factor but is also attributed to the effects of interactions.

Table 2. Estimates of the first order (S_i) and total effect (St_i) indices of the SA and their bootstrap confidence intervals

| Factors | St_i | S_i | Factors | St_i | S_i |
|--------------------|-------------------|------------------|-------------------|-------------------|------------------|
| CSVPS aw | 0.50 [0.47,0.54] | 0.30 [0.29,0.32] | T_{\max} | 0.02 [-0.02,0.07] | 0.00 [0.00,0.01] |
| TR | 0.21 [0.17,0.25] | 0.08 [0.07,0.09] | $\log x_{\max}$ | 0.02 [-0.02,0.07] | 0.00 [0.00,0.00] |
| dR | 0.18 [0.13,0.22] | 0.07 [0.06,0.08] | TD | 0.02 [-0.02,0.06] | 0.00 [0.00,0.01] |
| K | 0.13 [0.09,0.18] | 0.06 [0.06,0.07] | TTEP | 0.02 [-0.03,0.06] | 0.00 [0.00,0.01] |
| μ_{opt} | 0.08 [0.04,0.13] | 0.03 [0.03,0.04] | pH _{min} | 0.02 [-0.03,0.06] | 0.00 [0.00,0.00] |
| aw _{min} | 0.08 [0.03,0.12] | 0.01 [0.00,0.01] | TC | 0.02 [-0.03,0.06] | 0.00 [0.00,0.00] |
| TM | 0.08 [0.03,0.12] | 0.02 [0.02,0.03] | Approach | 0.02 [-0.03,0.06] | 0.00 [0.00,0.00] |
| dM | 0.07 [0.03,0.12] | 0.02 [0.01,0.03] | dTEP | 0.02 [-0.03,0.06] | 0.00 [0.00,0.00] |
| T_{\min} | 0.07 [0.02,0.11] | 0.02 [0.02,0.03] | dC | 0.02 [-0.03,0.06] | 0.00 [0.00,0.00] |
| x_0 | 0.06 [0.02,0.10] | 0.04 [0.04,0.05] | Primary model | 0.02 [-0.03,0.06] | 0.00 [0.00,0.00] |
| CSVPS pH | 0.05 [0.01,0.09] | 0.02 [0.01,0.02] | dV | 0.01 [-0.03,0.06] | 0.00 [0.00,0.00] |
| T_{opt} | 0.03 [-0.01,0.08] | 0.01 [0.01,0.01] | Secondary model | 0.01 [-0.03,0.06] | 0.00 [0.00,0.00] |
| dD | 0.03 [-0.02,0.07] | 0.00 [0.00,0.01] | TV | 0.01 [-0.03,0.06] | 0.00 [0.00,0.00] |

This is confirmed by the relatively important difference observed between the St_i and the S_i for all the factors. For example for the CSVPS aw, the difference between the St_i (0.5) and the S_i (0.3) flags an important role of interactions for that factor in the model final response.

The confidence intervals computed by bootstrap were used to identify the factors which indices are significantly different from 0 as the most influent factors. Figure 1 shows that the subset of these important factors is different in case the log transformation is applied or not to the model response before the SA is performed. When applying the SA directly to the concentrations (CFU/g) of *L. monocytogenes* (Figure 1a), the parameter x_{\max} appears to be the most important factor ($St_i=0.59$) while this factor is not identified in the subset of important factors when applying the SA to the log CFU/g (Figure 1b). Thus, the ranking of the factors strongly depends on the chosen model response. In the field of food microbiology, results are often expressed in log CFU/g to avoid scale effects, we therefore based our analysis on that particular response (Figure 2b) and used the ranking presented in table 2. The three most important factors are the CSVPS aw and the temperature and duration of the domestic refrigerator storage. The importance of the consumer link in the cold chain was previously reported and this study quantitatively confirms this observation, whereas the salmon aw has never been identified as a major factor influencing the growth of *L. monocytogenes* in CSVPS. This result may be due to the large range of variation that was used to assess its influence.

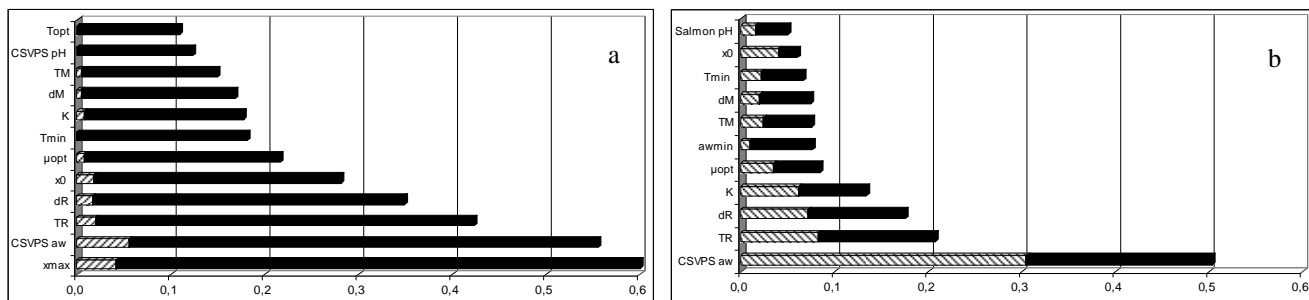


Figure 1. Indices S_i (dashed bars) and St_i (black bars) obtained for the Sensitivity Analysis when applied to (a) Y or (b) $\log_{10}(Y)$.

The factors μ_{opt} , T_{min} and x_0 also identified as important factors in this study, were previously ranked among important factors impacting the response of similar models (Pouillot, 2006). But surprisingly, neither the approach choice (populational or cellular) nor the primary or secondary model choice, impacted the studied model response. Finally, the SA showed that the physiological state of the cells K , which is scarcely used in QMRA, was twice more important than x_0 . This leads to fail safe but incorrect predictions and we therefore think that a better characterization of such a factor is worth conducting to improve model predictions in QMRA.

Conclusion

This method proved to be very efficient and relatively easy to interpret. In a further study, the impact of the range of variation of the factors will be evaluated before performing an Uncertainty Analysis which will make it possible to identify the impact of the input uncertainty on the model response.

References

- Archer G. E. B., Saltelli A. and Sobol I. M. (1997). Sensitivity measures, ANOVA-like techniques and the use of bootstrap. *Journal of Statistical Computation and Simulation* 58, 99-120.
- Augustin J.-C., Zuliani V., Cornu M. and Guillier L. (2005). Growth rate and growth probability of *Listeria monocytogenes* in dairy, meat and seafood products in suboptimal conditions. *Journal of Applied Microbiology* 99, 1019-1042.
- Baranyi J. and Roberts T. A. (1994). A dynamic approach to predicting bacterial growth in food. *International Journal of Food Microbiology*, 23, 277-294.
- Chan K., Tarantola S., Saltelli A. and Sobol I.M. (2000). Variance based methods. In A. Saltelli, K. Chan and E. M. Scott (Eds.), *Sensitivity Analysis*, Chapter 8, 167-197, John Wiley and Sons Limited, West Sussex, UK, 475 pp. (ISBN 0-471-99892-3).
- Frey H. C. and Patil S. R. (2002). Identification and Review of Sensitivity Analysis Methods. *Risk Analysis* 22, 553-578.
- Guillier L. and Augustin J. C. (2006). Modelling the individual cell lag time distributions of *Listeria monocytogenes* as a function of the physiological state and the growth conditions. *International Journal of Food Microbiology* 111, 241-251.
- Havelaar A. H., Evers E. G. and Nauta M. J. (2008). Challenges of quantitative microbial risk assessment at EU level. *Trends in Food Science and Technology* 19, S26-S33.
- McKay, M. D., Beckman, R. J. and Conover, W. J. (1979). A comparison of three methods for selecting values of input variables in the analysis of output from a computer code. *Technometrics* 21, 239-245.
- Membré J.-M., Kan-King-Yu D. and Blackburn C. d. W. (2008). Use of sensitivity analysis to aid interpretation of a probabilistic *Bacillus cereus* spore lag time model applied to heat-treated chilled foods (REPFEDs). *International Journal of Food Microbiology* 128, 23-33.
- Pouillot R. (2006). Appréciation quantitative des risques en hygiène des aliments: Développements et mises en oeuvre pour la prise en compte des recommandations internationales. PhD thesis. *Université Paris XI, Faculté de Médecine Paris-Sud*, pp. 186. Paris.
- Ratkowsky D. A., Olley J., Meekin T. A. M. and Ball A. (1982). Relationship between temperature and growth rate of bacterial cultures. *Journal of Bacteriology* 149, 1-5.
- Rosso L., Lobry J. R., Bajard S. and Flandois J. P. (1995). Convenient model to describe the combined effects of temperature and pH on microbial growth. *Applied and Environmental Microbiology* 61, 610-616.
- Saltelli A. (2002). Making best use of model evaluations to compute sensitivity indices. *Computer Physics Communications* 145, 280-297.
- Sobol I. M. (2001). Global sensitivity indices for non linear mathematical models and their Monte Carlo estimates. *Mathematics and Computers in Simulation* 55, 271-280.
- Zwietering, M. H. (2009). Quantitative Risk Assessment: Is More Complex Always Better? – Simple Is Not Stupid and Complex Is Not Always More Correct. *International Journal of Food Microbiology. in press*

Developing a predictive model for quantifying the risk associated with in-factory *Listeria monocytogenes* recontamination and to identify suitable management options to reduce it.

J.-M. Membré¹, X. Chen², and N.B. Johnson²

¹ Unilever, Safety & Environmental Assurance Centre, Colworth Park, Sharnbrook, MK44 1LQ, United Kingdom (Jeanne-Marie.Membre@Unilever.com)

² Unilever, Food and Health Research Institute, Advanced Food Microbiology, Olivier van Noortlaan 120, 3133 AT Vlaardingen, the Netherlands (Nick.B.Johnson@Unilever.com)

Abstract

Listeria monocytogenes is a serious hazard to consider during ice-cream manufacture. The aim of this study was to develop a predictive model to quantify the probability of end-product recontamination in ice cream factories, and then assess the impact of various management options to reduce the risk.

Recontamination sources identified as priority for investigation were air, drains and floors in the production area; transmission vectors were water droplets in air and food contact surfaces. Based upon factory equipment design and process operations, the model structure was built. Data to inform inputs were collected from a representative factory and were supplemented by literature information. Results were realistic enough to provide confidence to the Quality Assurance team that the model could be used to rank the impact of various scenarios and to suggest options to reduce the probability of recontamination.

A major mechanism to trigger recontamination events was localised intermittent cleaning, i.e. low pressure hose cleaning used between 'deep clean' procedures. Conversely, large improvements in quality of typical air filtration and air recycling conditions, produced negligible improvement in the probability of recontamination due to *L. monocytogenes* from air.

Introduction

Listeria monocytogenes is a pathogen that can cause serious food-borne illness, particularly in the very young and old, unborn children and immunocompromised groups. The risk of listeriosis from ice cream consumption has been clearly identified as 'the product is eaten worldwide, with a high consumption rate, particularly for some immunocompromised persons' (WHO 2004).

The pathogen is typically removed during pasteurisation, and raw material checks should eliminate the hazard from direct introduction during manufacture. However, the micro-organism is commonly found in cold environments such as those often prevailing in liquid dairy food processing operations. From such environments, the pathogen can recontaminate the final product after pasteurisation.

Understanding the underlying mechanisms and principles of recontamination during manufacture or shelf-life has attracted comparatively little attention from food technologists and risk modellers when compared to other aspects of controlling microbial contamination of products; such as heat inactivation, or inactivating or inhibitory formulations. However, recontamination is a major issue to be controlled (Reij et al., 2004) and considerable costs are involved in assuring control of recontamination through product and process designs, and operationally through adherence to 'good hygienic practices' and HACCP programmes. With the exception of some design criteria, the relative and absolute effectiveness of many practices and approaches in controlling microbial recontamination, and *L. monocytogenes* recontamination specifically, are unknown.

Therefore, there is a need for greater understanding of the main mechanisms through which products are recontaminated and, by modelling these routes, more effective and practical management strategies can be devised to reduce and manage the risks.

Developing the recontamination model

Several mathematical models have been developed to quantify the risk of recontamination during food processing, which could be used in microbiological risk assessment studies to estimate the recontamination frequency and assess the relative importance of the various scenarios. In summary, they can be classified as three types: generic (can be used as a framework or starting point for model building), route-specific (based on various routes of recontamination, i.e. via the air or surface), and site-specific (focus on certain food processing flow under industrial conditions). As examples of these categories, the following can be noted:

- A general framework of modelling proposed by Schaffner (2004), which is a generic approach to quantify the risk of *Listeria* cross-contamination. The model tracked *L. monocytogenes* concentration and prevalence from raw material or environment to finished product.
- An air-food recontamination route model devised to quantify the risk of recontamination in food processing environment (den Aantrekker *et al.*, 2003). Although the air-food recontamination route was not developed and applied, contamination via the air was described based upon the density and settling velocity of particles.
- A model developed by Ivanek *et al.* (2004), which was used to estimate the effect of cross-contamination transmission among employee's hands, food products, food contact surfaces and the environment. A compartmental mathematical model of *L. monocytogenes* cross-contamination was developed for the slicing stage (finished product area) of smoked ready-to-eat fish production. It defined and quantified *L. monocytogenes* cross-contamination dynamics in a processing plant and allowed the estimation of the prevalence of contaminated fish in a lot as a result of cross-contamination. The most significant input parameters were identified by sensitivity analysis, followed by risk reduction suggestions.

The modelling approach adopted in this study for recontamination was site-specific and thus similar to the one suggested by Ivanek *et al.* (2004). Firstly, an *in-situ* factory analysis was performed at a representative ice-cream factory, focusing on the High Care Area (HCA) in this manufacturing operation which is the area before the packaging of end-product. A conveyor was used as the main example of surfaces in contact with food. Only low-pressure water hosing was considered here as the negative impact of high-pressure water hosing on recontamination risks was already well known.

Five scenarios of recontamination were investigated in detail in this study (Figure 1):

- Air contamination (one scenario) with *Listeria monocytogenes* circulating within the air volume of the production hall, falling on the conveyor or directly onto the product; this used inputs from den Aantrekker *et al.* (2003) as well as information gathered in the representative factory (e.g. production line flow, air volume exchange, HCA volume, filtration efficacy, conveyor speed);
- Droplets from drain or from floor (two separate scenarios) splashed directly to conveyor or directly to the product; high *Listeria* concentrations in drain (10^9 cfu/ml) and moderate in floor (10^6 cfu/ml) were assumed; mapping of drains in HCA, frequency of hosing and the distances between drains and conveyors were obtained directly from *in-situ* inspection; literature information (Burfoot *et al.*, 2003) was used to provide realistic values for inputs such as size of droplets and percentage of transfer of bacteria to droplets;
- Droplets in atmosphere, produced through floor and drain hosing (two separate scenarios) are then deposited onto conveyor and directly onto product; these two scenarios included inputs from the relevant factory and from literature (den Aantrekker *et al.*, 2003; Burfoot *et al.*, 2003).

A dynamic model was built for the five recontamination scenarios. Predictions expressed as probability of recontamination (number of end-products containing at least one bacterium

divided by number of end-products during the same period of time) were compared with data collected in the same factory.

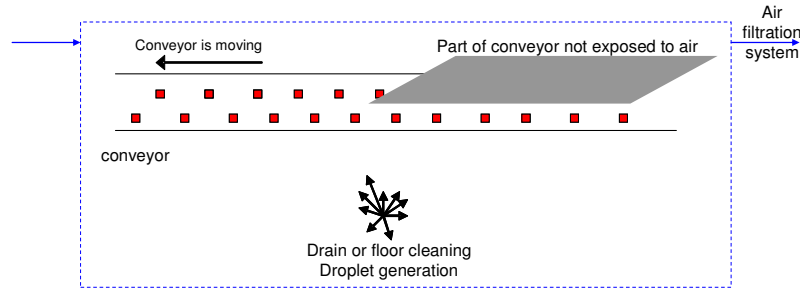


Figure 1: Schematic representation of the three main sources of contamination (drain or floor cleaning and air) studied in detail in this quantitative risk assessment study.

Results and Discussion

From the five detailed scenario analyses related to routes of recontamination (via air, direct from drain or floor cleaning, indirect from drain or floor cleaning), the followings insights have been obtained:

- the distance between floors or drains and the conveyor can make a huge difference in terms of risk due to droplet generation as a consequence of hosing and exposure of the conveyor to droplets. Figure 2 illustrates the scenario with floor to conveyor distance when hosing the floor. From this it can be seen that the direct route source-to-conveyor leads to a risk that is three fold higher when the distance is 1 m as compared to 10 m. In other words, hosing water, even on floors where low *Listeria* contamination levels and/or prevalence may be expected, close to pieces of equipment on which the food is carried, must be avoided to minimise risks;
- the time that either the floor or the drain is hosed (Figure 3 illustrates the scenario with floor) does not impact massively on the recontamination risk; however, it should be borne in mind that in this study the prevalence of the *Listeria* recontamination in the product is estimated, not its concentration;
- in most of the scenarios explored, the air recontamination route was not found to be a major issue. This is mainly due to the fact that the concentration of *L. monocytogenes* in air (at least in the absence of droplet splashing) was taken to be small (based upon 1-year data analysis). An air filtration efficiency of 90% was considered as a realistic value in the representative factory and, in this case, increasing the filtration efficiency from 90% to 99% does not significantly decrease the recontamination risk (Figure 4).

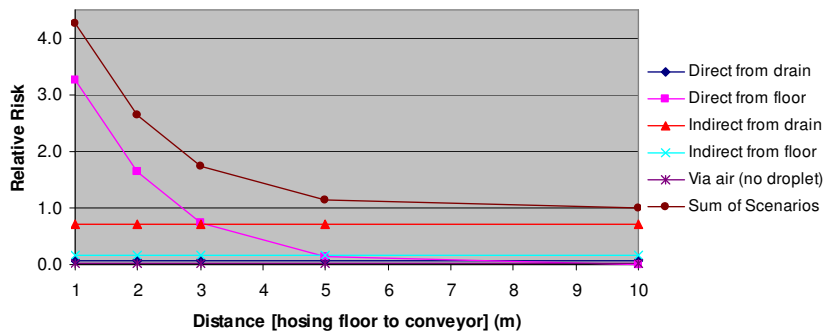


Figure 2: Effect of hosing distance on recontamination risk. Relative risk equal to 1 has been defined with distance [hosing floor to conveyor] of 10m, time of floor hosing of 2 min and air filtration system efficiency of 99%.

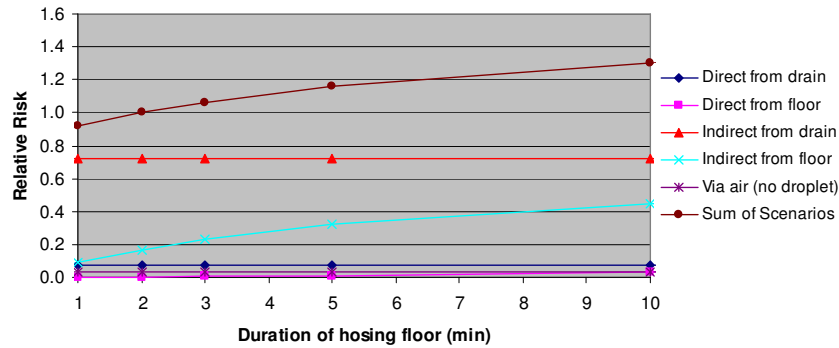


Figure 3: Effect of hosing time on recontamination risk. Same relative risk definition as in Figure 2.

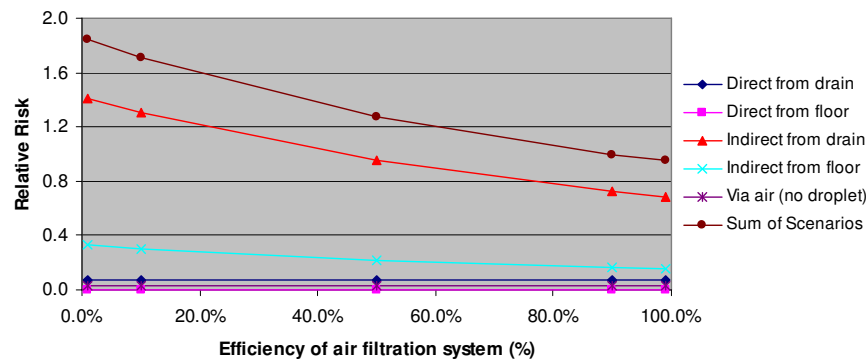


Figure 4: Effect of air filtration efficiency on recontamination risk. Same relative risk definition as in Figure 2.

In conclusion, one important mechanism of recontamination from potentially contaminated sources to final products is the result of specific cleaning operations such as hose cleaning. Indeed, hose cleaning, even at low water pressure, plays a crucial role in bringing bacteria from drains and floors to vectors such as air and conveyor-belts that directly can be in contact with final products. The model developed in this study was used to provide an informed and more quantitative definition for a "dry-floor policy" as it gave adequate evidence regarding the advantages of its implementation, despite the associated infrastructure costs. The possibility to apply or further tailor the model to other ice cream factories, and to include physical recontamination routes, is now being investigated.

References

- den Aantrekker E.D., Beumer R.R., van Gerwen S.J.C., Zwietering M.H., van Schothorst M. and Boom R.M. (2003) Estimating the probability of recontamination via the air using Monte Carlo simulations. *International Journal of Food Microbiology* 87, 1-15.
- Burfoot D., Reavell S., Tuck C. and Wilkinson D. (2003) Generation and dispersion of droplets from cleaning equipment used in the chilled food industry. *Journal of Food Engineering* 58, 343-353.
- Ivanek R., Gröhn Y.T., Wiedmann M. and Wells M.T. (2004) Mathematical model of *Listeria monocytogenes* cross-contamination in a fish processing plant. *Journal of Food Protection* 67 (12), 2688-2697.
- Reij M.W., den Aantrekker E.D., ILSI Europe Risk Analysis in Microbiology Task Force, 2004. Recontamination as a source of pathogens in processed foods. *International Journal of Food Microbiology*, 91(1), 1-11.
- Schaffner D.W. (2004) Mathematical frameworks for modelling *Listeria* cross-contamination in food-processing plants. *Journal of Food Science* 69 (6), R155-R157.
- WHO (2004) Risk assessment of *Listeria monocytogenes* in ready-to-eat foods. ISBN 92 4 156262 5. Available at <http://whqlibdoc.who.int/publications/2004/9241562625.pdf>.

Development of an Online Predictive Modeling Resource for Food Safety Risk Analysis Decision Making

G.M. Burnham¹, E. Hartnett², T. Ruthman², D.W. Schaffner³, C.A. Baxa¹, S.C. Ingham⁴, B.H. Ingham⁵, M.A. Fanslau⁶, and J.P. Norback⁵

¹United States Army Natick Soldier Research, Development & Engineering Center – Combat Feeding Directorate, 15 Kansas Street, Natick, MA 01760

²Risk Sciences International, 200-449 Sussex Drive, Ottawa, ON K1N 6Z4

³Rutgers, The State University of New Jersey, Food Science Department, 65 Dudley Road, New Brunswick, NJ 08903

⁴Wisconsin Department of Agriculture, Trade & Consumer Protection, Division of Food Safety, P.O. Box 8911, Madison, WI 53708-8911

⁵University of Wisconsin-Madison, Department of Food Science, 1605 Linden Drive, Madison, WI 53706

⁶Fair Oaks Farms, 7600 95th Street, Pleasant Prairie, WI 53158

Abstract

Information on pathogen-behavior in food is needed by risk managers in making sound food safety decisions. Ideally, this information would be obtained through controlled inoculation studies using the agent/food combination of concern during the actual processing flow of the food in its actual environment. This approach is seldom safe or practical, since it involves use of actual pathogens in the food processing environment. Alternatively, laboratory-based agent/food inoculation challenge studies can be conducted that simulate actual processing conditions. This method has been frequently used and is well accepted by risk managers. It is important to note however that processors that choose to use this approach must ensure that conditions in their process, such as food formulation and temperature, are at least as inhibitory to pathogen growth as in the laboratory study. Another way to obtain this information is to analyze processing conditions using computer generated predictive models of pathogen behavior. There is an ever increasing acceptance of this approach in food safety risk analysis decision making and there are many existing models and tools. A difficulty for risk managers however, is that they must be familiar with the benefits and limitations of appropriate models and tools which are available. Additionally, there must be adequate understanding of how to apply/direct a specific model or tool to obtain meaningful predictions. A predictive modeling resource that offers simplicity, flexibility, and an easy-to-understand means of communicating results is needed.

Our model, the Time and Temperature Pathogen Predictor (T2P2), will be easy to use, and will provide accurate-to-fail-safe predictions of pathogen behavior in relevant food matrices and laboratory media to provide sound scientific advice for the implementation of mitigation strategies and for use in other food safety risk analysis decision making.

Key Words: predictive modeling, food safety risk analysis, risk assessment, HACCP

Introduction

Since 2000, all wholesale meat processors in the United States have been required to use the hazard analysis critical control point (HACCP) system for ensuring food safety (*USDA 1996*). HACCP is also becoming increasingly utilized in other industry segments to include food processing, food service, and even retail. Under the HACCP system, processors must conduct a hazard analysis for each of their products and then develop and implement an HACCP plan for the control of identified hazards that are reasonably likely to occur. To control identified hazards critical limits must be established at critical control points to ensure the elimination (or reduction to safe levels) of the identified hazard. One way of establishing critical limits is

by using predictive modeling tools. These tools are also useful in conducting a thorough hazard analysis and evaluating system deviations (corrective actions). Today, many predictive modeling tools exist to help processors, regulators and academics evaluate microbial responses (growth, survival, and inactivation). The mathematical methodology used to describe these microbial environmental responses has evolved and many methods, some of which are quite complex, have been described. The United States Department of Agriculture (USDA) – Agricultural Research Service’s Pathogen Modeling Program (PMP) is the most recognized predictive microbiology tool in the United States. A similar tool is the Institute of Food Research’s (Norwich, UK) ComBase Growth Predictor. However both of these tools can be difficult to use and the results are not easy to interpret. A tool developed recently at the University of Wisconsin-Madison, Temperature History Evaluation for Raw Meats (THERM; in a series of papers, *Burnham 2007a, 2007b, & 2006 and Ingham 2009, 2008, & 2007*), addressed some of the limitations associated with these and other tools, but it has limited environmental condition and food matrix applicability. With the ever increasing availability of predictive modeling resources it has become necessary to establish a common resource which utilizes the predictive power of existing tools and minimizes limitations.

The objective of this work is to develop a web-based predictive modeling resource, the T2P2, which makes use of existing predictive modeling tools and provides related training materials which will provide information for use in food safety risk analysis decision making.

T2P2 will utilize the existing online THERM application, transfer the tool to the software Analytica, develop a web interface for the tool, and expand upon the functionality of the tool in terms of 1) the scope of calculations performed, 2) the level of user interaction with the tool, and 3) enhanced reporting from use of the tool. The tool will provide the user with information regarding the overall performance of the food handling system, thereby providing a scientific basis upon which to make decisions regarding the acceptability of the food produced in terms of the risk posed from bacterial pathogens of concern.

Materials and Methods

The work will be undertaken in two phases. In Phase I we will develop a prototype for T2P2 (referred to as the “T2P2-prototype” in the remainder of this abstract). This will be a functioning T2P2-prototype including Analytica based growth and inactivation models, a web-based user interface that will perform calculations, and a basic reporting system. The aim of the T2P2-prototype will be to provide a basis for the development of the key functionalities of the tool and to illustrate the features (and uses) of the final tool. The T2P2-prototype is not intended to be distributed for general use and will not reflect the full functionality of the final tool. In Phase II the T2P2-prototype developed in Phase I will be expanded and enhanced to provide full functionality.

Mathematical Functionality

The aim is to develop a common mathematical framework for all food-hazard combinations that may be used in the tool, combining lag phase, growth, and inactivation across the stages and time-temperature relationships described in the treatment chain. The mathematics of the THERM tool will be included and additional predictive models will be added from PMP to broaden the scope of food-hazard combinations that can be considered. In the final model we will include the capability to model lag phase, growth, and inactivation for *Bacillus cereus*, *Escherichia coli* O157:H7, *Listeria monocytogenes*, *Shigella*, *Staphylococcus aureus* and *Salmonella* serovars. These pathogens have been selected for the initial list as they either are already included in THERM or are considered in models available through PMP. The T2P2-prototype will incorporate at least 3 of these hazards to fully illustrate the functionality of the tool (including at least one that is migrated from PMP). In addition, given the association of

these hazards with foodborne illness, there is a high likelihood that required information not found in THERM or PMP can be found in the scientific literature.

Reporting Requirements

The user will be provided with the option to view and/or save a report. This report will include:

- Description of the user inputs, for example the food and hazard(s) selected, the stages included in the treatment chain, and the lot ID. The times and temperatures across the treatment chain will be shown as a graph rather than as a table.
- Result of the model run and a selection of graphs (presented in the results window) as an example of the types of graphs that can be included.
- Appendices or references to other documents as deemed appropriate (e.g. references to models and data used, etc.). Full appendices/references will not be included in the T2P2-prototype but instead an example of what this would look like will be included.
- Key assumptions and caveats will be provided when “generic” behavior models have been used (e.g. behavior in broth) as opposed to food specific models.

Users will also be provided with access to a description of the data, parameters, and models used in the model predictions and have the option to include these in the report.

Results and Discussion

The T2P2-prototype (Phase I), will demonstrate the types of features and functions that the final online tool will have and the potential uses of such a tool. The user will take the following steps to interact with the tool (Figure 1): 1) select the food of interest, 2) select the hazard(s) of interest, and 3) define the treatment chain (with respect to time, temperature, and processing stage). T2P2 will generate a report of the prediction (.pdf format), with an option to view or save the report. A user defined results screen will then be displayed and contain at a minimum:

- A summary of the data, including a graph of the time-temperature relationship of the treatment chain
- The overall predicted population change in the hazard (expressed in \log_{10} CFU) as a result of the defined treatment chain
- A graph of the cumulative hazard population change over the course of the treatment chain
- A table of the time, temperature and cumulative population change over the course of the treatment chain.

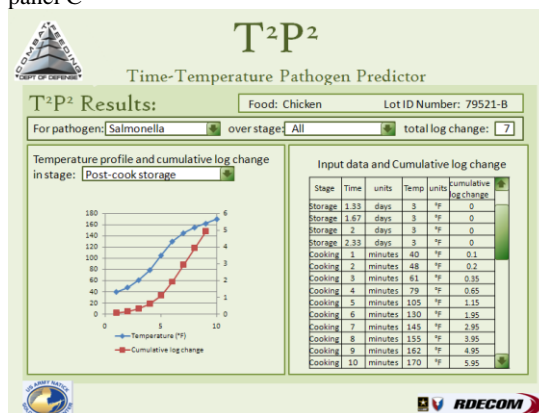
In phase II, the final T2P2 website will include a detailed User’s Guide and a Quick-Start Guide. These documents will take the user step-by-step through the process of using the tool, and will include industry-relevant examples demonstrating the use of the tool. The user will be able to download these documents from the T2P2 website. Additionally, extensive context-specific help and training modules will be available to the user on the website. The training modules will provide hands-on experience and demonstrate the power of the tool through defined temperature treatment scenarios of specific food/hazard combinations.

Figure 1. Examples of sign-in screen (panel A), user interaction screen (panel B), and results screen (panel C) proposed for the T2P2-prototype.

panel A

panel B

panel C



Conclusion

Once complete, the easy-to-use T2P2 will provide accurate-to-fail-safe predictions of pathogen behavior in relevant food matrices and laboratory media to give sound scientific advice for the implementation of mitigation strategies and for use in other food safety risk analysis decision making.

References

- Burnham, G.M., S.C. Ingham, M.A. Fanslau, B.H. Ingham, J.P. Norback, and D.W. Schaffner, 2007a, Using Predictive Microbiology to Evaluate Risk and Reduce Economic Losses Associated with Meats & Poultry Exposed to Temperature Abuse, *U.S. Army Medical Department Journal*, 3rd Quarter 2007: 57-65
- Burnham, G.M., 2007b, Predicting pathogen growth and death in raw meat and poultry: challenge studies and predictive tools, Doctoral dissertation, University of Wisconsin – Madison
- Burnham, G.M., M.A. Fanslau, and S.C. Ingham. 2006. Evaluating microbial safety of slow partial-cooking processes for bacon: use of a predictive tool based on small-scale isothermal meat inoculation studies, *J. Food Prot.* 69: 602-608
- Ingham, S.C., Vang, S., Levey, B., Fahey, L., Norback, J.B., Fanslau, M.A., Senecal, A.G., Burnham, G.M., and Ingham, B.H., 2009, Predicting behavior of *Staphylococcus aureus*, *Salmonella* serovars, and *Escherichia coli* O157:H7 in pork products during single and repeated temperature-abuse periods, *J. Food Prot.* In Press
- Ingham, S.C., B.H. Ingham, D. Borneman, E. Jaussaud, E.L. Schoeller, N. Hoftiezer, L. Schwartzburg, G.M. Burnham, and J.P. Norback, 2008, Predicting Pathogen Growth during Short-Term Temperature Abuse of Raw Sausage, *J. Food Prot.* In Press
- Ingham, S.C., M.A. Fanslau, G.M. Burnham, B.H. Ingham, J.P. Norback, and D.W. Schaffner. 2007. Predicting Pathogen Growth during Short-Term Temperature Abuse of Raw Pork, Beef and Poultry Products: Use of an Isothermal-Based Predictive Tool. *J. Food Prot.* 70: 1446-1456
- United States Department of Agriculture, Food Safety & Inspection Service (USDA), 1996, Pathogen Reduction; Hazard Analysis and Critical Control Point (HACCP) systems: final rule, Fed. Register 61: 38805-38989.

Cardinal growth parameters of the *Bacillus cereus sensu lato* phylogenetic groups and consequences for risk assessment

F. Carlin^{1,2}, C. Albagnac^{1,2}, A. Rida^{1,2}, O. Couvert³, M.-H. Guinebretière^{1,2}, C. Nguyen-the^{1,2}

¹ INRA, UMR408 Sécurité et Qualité des Produits d'Origine Végétale, F-84000 Avignon, France (frederic.carlin@avignon.inra.fr)

² Université d'Avignon et des Pays de Vaucluse, UMR408 Sécurité et Qualité des Produits d'Origine Végétale, F-84000 Avignon, France

³ ADRIA Développement, Creach Gwen, F-29196 Quimper, France

Abstract

Keywords

Bacillus cereus, Cardinal parameter model, temperature, pH, water activity, diversity, genetics

Introduction

Growth limits for temperature, pH or water activity are major characteristics of foodborne pathogenic bacteria and primary determinants of food safety hazards. Although important those growth/no growth limits are obviously not adapted to predictions of the increases in populations of the foodborne pathogens in foods. Risk characterization is partly based on the assessment of the concentrations reached in a food before consumption. Risk management options will favour conditions keeping bacterial concentrations below a critical level. Those predictions are of particular importance for the foodborne pathogenic bacterium *Bacillus cereus*, causing two types of foodborne poisonings, an emetic syndrome and a diarrheic syndrome, representing a significant part of outbreaks of foodborne poisonings in many countries, and widely distributed in food materials (Anonymous, 2005; Granum, 2007).

Several theoretical approaches have been proposed to predict microbial growth in foods. Among those Cardinal Parameter Models offer the advantage to use parameters having a biological significance. These cardinal parameters are T_{min} , T_{opt} , T_{max} , pH_{min} , pH_{opt} , $a_{w\ min}$, $a_{w\ opt}$ for the prediction of the maximum specific growth rate μ_{max} as a function of temperature pH and a_w respectively, with X_{min} and X_{max} representing the value of X_i below and above which no growth occurs, and X_{opt} the value at which μ_{max} is equal to μ_{opt} (Ross and Dalgaard, 2004).

These parameters must account for genetic variability. The *B. cereus sensu lato* phylogenetic structure was recently resolved in seven major phylogenetic groups (I-VII) using both genetic and phenotypic criteria (Table 1) (Guinebretiere *et al.*, 2008). These groups showed clear differences in their ability to grow at low or high temperatures and considering *B. cereus* globally is meaningless. Whether it is similar for growth at various pH and various low a_w – high NaCl concentrations is not known. The aim of this work was the determination of the cardinal temperature, pH and a_w of representative strains of those *B. cereus* phylogenetic groups and to study the relation with their growth limits established in growth/no growth tests.

Table 1: The seven *Bacillus cereus* phylogenetic groups (Guinebretiere *et al.*, 2008) and their main characters.

| Group | Association to currently defined species | Association to cases of food poisonings | Domain of growth temperatures | Heat resistance of spores ¹ |
|-------|--|---|-------------------------------|--|
| I | <i>B. pseudomycoides</i> | No | 10°C – 40°C | ? |
| II | <i>B. cereus</i> II, <i>B. thuringiensis</i> II | Yes | 7°C – 40°C | ++ |
| III | Emetic strains, <i>B. cereus</i> III, <i>B. thuringiensis</i> III, <i>B. anthracis</i> | Yes | 15°C – 45°C | +++ |
| IV | <i>B. cereus</i> IV, <i>B. thuringiensis</i> IV | Yes | 10°C – 45°C | ++ |
| V | <i>B. cereus</i> V, <i>B. thuringiensis</i> V | Yes | 8°C – 40°C | ++ |
| VI | <i>B. weihenstephanensis</i> , <i>B. mycoides</i> , <i>B. thuringiensis</i> VI | No | 5°C – 37°C | + |
| VII | ' <i>B. cytotoxicus</i> ' | Yes | 20°C – 50°C | +++ |

¹Ranking established from (Afchain *et al.*, 2008; Carlin *et al.*, 2006).

Materials and Methods

A collection of 42 strains representative of the seven phylogenetic groups of *B. cereus sensu lato* was selected for that work. Growth/no growth limits at a range of pH and a_w near growth limits were determined for all strains in BHI at pH 5.0, 4.8, 4.6 and 4.3 or in BHI supplemented with 5%, 7%, 8%, and 10% (wt/vol) NaCl. Growth was followed for up to 14 days at 30°C. Cardinal temperatures, pHs and a_w s were determined for two strains of groups II-VII. Filament growth of group I strains was not suitable for OD growth curves and cardinal parameters of those strains were consequently not determined. A method now commonly used in predictive microbiology method and based on optical density measurement was applied (Membré *et al.*, 2002). Briefly the OD₆₀₀ of series of binary dilution of each *B. cereus* strain were followed in (i) in BHIYG at the selected pH or a_w – NaCl concentration were incubated at 30°C, or (ii) in BHIYG incubated at the selected temperature. Time to a specific OD₆₀₀ (usually initial OD₆₀₀ + 0.05) were plotted against the natural Log of the dilution to determine the μ_{max} of each strain in each growth condition. The μ_{max} values were then plotted as a function of pH, temperature or a_w to determine the cardinal parameters according to the model of (Rosso *et al.*, 1995).

Results

Growth limits of B. cereus sensu lato phylogenetic groups

The phylogenetic groups show some marked differences in their NaCl or pH growth limits (Table 2 and Table 3). All group VII strains were able to grow at 10% NaCl. All groups II-V strains were able to grow at 7% NaCl, while none of the group I and VI were. All group VII (and group II) strains were also able to grow at pH 4.6, while only one Group VI strain out of 6 was able to grow at pH 4.6.

Table 2: Effect of water activity (NaCl concentration) on growth of *B. cereus sensu lato* genetic groups

| Genetic group | % strains ¹ growing in BHI at a NaCl concentration (a_w) of: | | | | | |
|---------------|---|------------|------------|------------|------------|-------------|
| | 0.5% (0.996) | 5% (0.965) | 6% (0.960) | 7% (0.952) | 8% (0.945) | 10% (0.929) |
| VII | 100 | 100 | 100 | 100 | 100 | 100 |
| III | 100 | 100 | 100 | 100 | 100 | 75 |
| IV | 100 | 100 | 100 | 100 | 100 | 33 |
| II | 100 | 100 | 100 | 100 | 67 | 0 |
| V | 100 | 100 | 100 | 100 | 33 | 0 |
| VI | 100 | 100 | 83 | 0 | 0 | 0 |
| I | 100 | 67 | 0 | 0 | 0 | 0 |

¹ 4-8 strains tested in each genetic group

Table 3: Effect of pH on growth of *B. cereus sensu lato* genetic groups

| Genetic group | % strains ¹ growing in BHI at a pH of: | | | | |
|---------------|---|-----|-----|-----|-----|
| | 7.4 | 5 | 4.8 | 4.6 | 4.3 |
| II | 100 | 100 | 100 | 100 | 17 |
| VII | 100 | 100 | 100 | 100 | 25 |
| III | 100 | 100 | 100 | 88 | 13 |
| I | 100 | 100 | 100 | 83 | 0 |
| IV | 100 | 100 | 100 | 67 | 0 |
| V | 100 | 100 | 100 | 33 | 0 |
| VI | 100 | 100 | 67 | 17 | 0 |

¹ 4-8 strains tested in each genetic group

Cardinal parameters of *B. cereus sensu lato* phylogenetic groups

The cardinal temperatures are in agreement with the growth limits previously recorded for the phylogenetic groups (Guinebretiere *et al.*, 2008). The psychrotrophic Group II and VI have the lowest T_{min} and their lower tolerance to temperature higher than 37°C is also expressed by lower T_{max} values (Table 4). The “moderately thermophilic” group VII has also the highest T_{min} and T_{max} and its T_{opt} is also higher than the T_{opt} of the other strains. Cardinal parameters of the mesophilic groups III and IV have intermediate values. Differences in pH_{min} are less marked than differences in temperature. The highest pH_{min} was that of group VI strains, which were also the least adapted to low pH according to their pH growth limits (Table 3). Group VI had the lowest $a_{w\ min}$, which is consistent with its lower ability to grow at increasing NaCl concentrations.

Table 4: Cardinal parameters of *B. cereus sensu lato* genetic groups¹.

| Genetic group ² | T_{min} (°C) | T_{opt} (°C) | T_{max} (°C) | pH_{min} | $a_{w\ min}$ (% NaCl) |
|----------------------------|----------------|----------------|----------------|------------|-----------------------|
| II | 2.2 | 35.6 | 41.6 | 4.65 | 0.950 (7 – 7.5) |
| III | 8.0 | 38.4 | 48 | 4.73 | 0.942 (8.5) |
| IV | 7.5 | 37.9 | 47.4 | 4.63 | 0.949 (7 – 7.5) |
| V | 5.5 | 36.1 | 43.1 | 4.72 | 0.949 (7 – 7.5) |
| VI | 4.1 | 31.3 | 42.4 | 4.88 | 0.972 (3.5 – 4) |
| VII | 11.6 | 44.2 | 58 | 4.7 | 0.953 (7) |

¹ pH_{opt} , pH_{max} , $a_{w\ opt}$ and $a_{w\ max}$ were not shown because of poor significance in a food context and/or low differences between groups

² Two strains tested in each group

Discussion

This work establishes a link between microbial genetics and predictive microbiology. This is of major interest for microbial risk assessment. In addition to the differences observed between groups in ability to grow at low temperature, pH or a_w , or in their resistance to heat, *B. cereus* strains in each genetic groups likely differ in their virulence and therefore in their potential to cause foodborne poisonings (Guinebretiere *et al.*, 2008). For instance the emetic syndrome is specifically associated to Group III strains. Psychrotrophic strains of group VI have never been associated to outbreaks of foodborne poisonings, which is not the case with psychrotrophic strains of group II. Most strains of group VII have been associated to severe outbreaks of foodborne poisonings. Prediction of the growth potential of each *B. cereus* genetic group will be easier to perform with the availability of their cardinal parameters. The technical effort to determine the genetic group of a new isolate represents either (i) one PCR and two growth tests (at 43°C, and 10°C or 7°C) in standard conditions, or a (ii) 16S rDNA sequencing or *panC* gene sequencing and a comparison to the sequences of the reference strains. A tool is available at www.tools.symprevius.org/Bcereus/ for the identification using the *panC* sequence of the relation of bacterial strains to one of the *B. cereus* phylogenetic groups. To our opinion this is a minor effort considering the importance of accounting for *B. cereus* genetic diversity in microbial risk assessment.

Acknowledgments

This work was supported by a grant from the Agence Nationale de la Recherche (ANR) (France) as part of an ANR-05-PNRA-013 *B. cereus* contract. Author AR has received a fellowship from the *Programme Assistants-Boursiers* of the France-Syria cooperation

References

- Afchain A. L., Carlin F., Nguyen-the C. and Albert I. (2008). Improving quantitative exposure assessment by considering genetic diversity of *B. cereus* in cooked, pasteurised and chilled foods. *International Journal of Food Microbiology* 128, 165-173.
- Anonymous (2005). Opinion of the scientific panel on biological hazards on *Bacillus cereus* and other *Bacillus* spp. in foodstuffs. *The EFSA Journal* 175, 1-48.
- Carlin F., Fricker M., Pielat A., Heisterkamp S., Shaheen R., Salkinoja Salonen M., Svensson B., Nguyen-the C. and Ehling-Schulz M. (2006). Emetic toxin-producing strains of *Bacillus cereus* show distinct characteristics within the *Bacillus cereus* group. *International Journal of Food Microbiology* 109, 132-138.
- Granum P. E. (2007). *Bacillus cereus*. In: M.P. Doyle and L.R. Beuchat (Eds.). *Food microbiology Fundamentals and frontiers Third Edition*, 445-455, ASM Press, Washington DC.
- Guinebretiere M. H., Thompson F. L., Sorokin A., Normand P., Dawyndt P., Ehling-Schulz M., Svensson B., Sanchis V., Nguyen-The C., Heyndrickx M. and De Vos P. (2008). Ecological diversification in the *Bacillus cereus* Group. *Environmental Microbiology* 10, 851-865.
- Membré J.-M., Leporq B., Vialette M., Mettler E., Perrier L. and Zwietering M. (2002). Experimental protocols and strain variability of cardinal values (pH and a_w) of bacteria using Bioscreen C: microbial and statistical aspects. (Eds.). *Proceedings and abstracts of the 18th International ICFMH symposium "Microbial adaptation to changing environments"*, Lillehammer, août 2002, 143-146, MATFORSK, As.
- Ross T. and Dalgaard P. (2004). Secondary models. In: R.C. McKellar and X. Lu (Eds.). *Modeling Microbial Responses in Food*, 63-150, CRC Press, Boca Raton.
- Rosso L., Lobry J. R., Bajard S. and Flandrois J.-P. (1995). Convenient model to describe the combined effects of temperature and pH on microbial growth. *Applied and Environmental Microbiology* 61, 610-616.

“A mathematical risk model for *E. coli* O157:H7 cross-contamination of lettuce during processing”

Pérez Rodríguez, Fernando¹; Campos, Danny³; Ryser, Elliot T.²; Buchholz, Annemarie L.²; Bradley, Marks P.³; Zurera, Gonzalo¹; Todd, Ewen⁴

1. Food Science and Technology, University of Córdoba, Córdoba, Spain.
2. Food Science and Human Nutrition, Michigan State University, East Lansing, MI, USA.
3. Biosystems and Agricultural Engineering, Michigan State University, East Lansing, MI, USA.
4. Advertising, Public Relations and Retailing, Michigan State University, East Lansing, MI, USA.

Introduction

Escherichia coli O157:H7 is a major pathogen capable of surviving harsh environmental conditions and refrigeration temperatures. Although it was originally associated with ground beef, the organism has more recently caused a series of outbreaks involving leafy greens including lettuce. The *E. coli* was found in the final bagged product of fresh-cut processed greens but originated somewhere along the food chain (USFDA, 2006). However, there is a lack of knowledge as to how the pathogen was transmitted through different steps and processes, though it seems that field contamination followed by cross-contamination could be a typical scenario.

Risk assessment can be applied to determine those points in food chain impacting on pathogen incidence, e.g. effect of inactivation treatments on concentration and prevalence (Lammerding and Fazil, 2000). The present study aims at performing a quantitative risk assessment to evaluate *E. coli* O157:H7 cross contamination in a processing line for fresh-cut lettuce, estimating contamination levels at factory and identifying critical control points (CCPs) in processing.

Material and Methods

Transfer data for *E. coli* O157:H7 were obtained in our laboratory simulating cross-contamination at different steps in a processing line for fresh-cut lettuce (shredding, belt, flume and shaker) (Buchholz et al., 2008). Transfer coefficients were modelled by fitting probability distributions describing the variability and uncertainty. Based on transfer coefficients distributions, a model were constructed in Excel which simulated the contamination processes from contaminated lettuce to non prevalent lettuces because of cross-contamination at processing line. In addition, the impact of different sanitation regimes, disinfection processes (i.e., irradiation and chlorination treatments), sampling plans at different steps in the processing line (e.g., shredder, shaker table, and conveyor) on the prevalence and concentration of *E. coli* O157:H7 in the bags of product could also be evaluated using the model. In order to obtain comparable data among different simulations, model process parameters were fixed to: 22 batches processed per day (at 3 batches/h); Batch size: 1000 kg; Bag size: 100 g; Number of bags per batch: 10,000.

The model considered uncertainty sources such as when contaminated lettuces entered the factory and initial contamination levels. The probabilistic model assumed that the contaminated batch could enter the processing line in any point during production being an uncertainty source in the model. The model simulated 3 different contamination levels for this contaminated batch: Low level (S1): 0.01 cfu/g; Medium level (S2): 1 cfu/g; High level (S3): 100 cfu/g.

Furthermore, the pathogen survival on surfaces was modelled to more accurately simulate transfer from contaminated equipments to non-contaminated lettuce. For this, experimental data from our laboratory were used (non-published data).

Simulations of the model were performed using @Risk Palisade© Software (consisting of 10,000 variability iterations and 10 uncertainty realizations) with the end result providing an estimate of *E. coli* O157:H7 populations in commercially bagged product.

Results

Probability distributions for E. coli O157:H7 transfer and model validation

The most suitable distributions to describe transfer data were Beta and Log normal distributions (Table 1). Results in Table 1 show that higher transfer occurred from produce to processing water and from equipment to lettuces.

Table 1. Main statistics of transfer data set and fitted probability distribution

| Transfer (%) at low level | Maximum | Minimum | Mean | Distribution |
|----------------------------------|----------------|----------------|-------------|---------------------|
| Lettuce-Shredder | 0.02 | 0.00 | 0.02 | Log-Normal |
| Lettuce-Flume | 0.02 | 0.00 | 0.01 | Log-Normal |
| Lettuce-Shaker | 0.02 | 0.00 | 0.01 | Log-Normal |
| Lettuce-Conveyor | 0.24 | 0.00 | 0.10 | Log-Normal |
| Lettuce-Water | 10.46 | 0.00 | 8.79 | Beta |
| Equipment-Lettuce | 18.83 | 9.90 | 15.33 | Log-Normal |

The cross-contamination model was satisfactorily validated based on the prediction index called SEP (Standard Error of Prediction), which ranged 0.00-35%.

Simulated model

Figure 1 shows uncertainty on the total percentage of *E. coli* O157:H7 transferred from initially contaminated lettuce to non-contaminated lettuce in the processing line for Scenario 2 ($S_2 = 1$ cfu/g). These values ranged between 0% and 0.32 %. The value 0 % was because the contaminated batch entering to processing line was the last one before finishing production. Similar total transfer percentages could be observed for S_1 and S_3 . These results indicate that cross contamination occurred at very low levels. However, the increase of prevalence derived from cross-contamination (percentage of cross-contaminated bags) showed higher values. Thus, for example, for S_2 , the uncertainty range on the increase of prevalence (from cross contamination) was between 0 and 13.89% (30566 bags), with a mean value of 3.59% (7902 bags). The ANOVA analysis performed on simulated data revealed that the initial level in the contaminated batch (S_1 ; S_2 and S_3) did not influence significantly ($=0.4$) the concentration levels in bags derived from cross- contamination (Figure 2). In turn, for prevalence, There were significant differences ($p = 0.000$) at the different levels simulated (S_1 ; S_2 and S_3).

Figure 3 reveals that the increase of number of contaminated bags by *E. coli* O157:H7 through cross-contamination decreased logarithmically along the

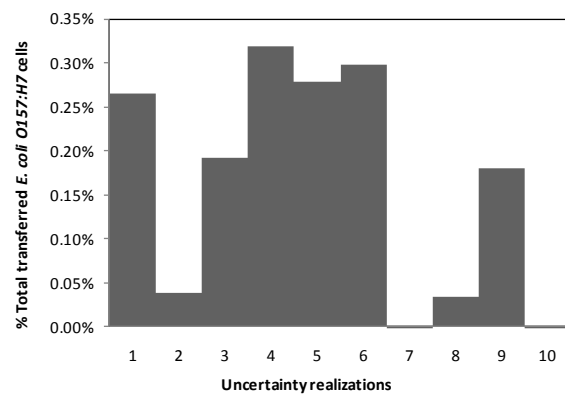


Figure 1. Percentage of transferred cells of *E. coli* O157:H7 from contaminated lettuce to non-contaminated lettuce during production (after 22 batches) for 10 uncertainty realizations.

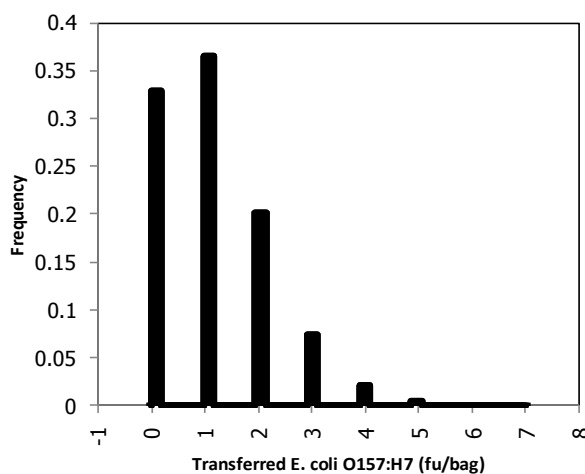


Figure 2. Example of the simulated distribution of *E. coli* O157:H7 in bags in Scenario 3 ($S_3 = 100$ cfu/g).

production for the 3 simulated scenarios. In S1 ($S1=0.01$ cfu/g) cross-contamination occurred only during the first hour (3 batches/h), immediately after the originally contaminated batch entered the processing line, showing a dramatic drop of prevalence up to 0 %. However, even at this low level, bags were cross-contaminated sporadically, resulting in very low concentration (mean: ≤ 2 cfu/bag) and prevalence levels (<1 %). At medium contamination level (S2), cross-contamination remained high for the first two batches (10,000 cross-contaminated bags/batch), then the number of cross-contaminated bags dropped significantly, in the following batch, to 100 cross-contaminated bags/batch, followed by a much more gradual decline up to 10 cross-contaminated bags in the last batch (Figure 3). With the S3 scenario (100 cfu/g) there was a gradual decline in the number of cross-contaminated bags along the whole production sequence from 10,000 to 1,000 cross-contaminated bags per batch, indicating that higher initial contamination numbers are more likely to persist in subsequent batches if not decontamination steps are used.

Effect of Control Measures

In the present model, the effect of different intervention scenarios was evaluated: decontamination by irradiation, and by chlorination and then application of a sampling plan to detect and remove contaminated batches after processing. Chlorination has long been used in the produce industry, but has not been completely effective. Recently the FDA (Food and Drug Administration) approved the use of gamma irradiation on vegetables allowing irradiation levels up to 4KGy. However, sensory characteristics in irradiated vegetables can be affected at irradiation levels above 0.5KGy (Niemira, 2008, Niemira et al., 2002, Foley et al. 2002), and so only lower irradiation levels could be used practically. In the model, by applying 0.5KGy (borderline for sensory acceptance), in S3, resulted in a prevalence average of 0.03%. For S2, the prevalence was reduced by up to an average value of 0.0005%. For S1, applying an irradiation treatment of 0.5KGy on the final product resulted in all bags being non-contaminated, i.e., eliminating fully contamination in both the originally contaminated lettuce entering to processing line and cross-contaminated lettuce occurred during production. However, when lower values (<0.5 KGy) were simulated, *E. coli* contamination could be still found in a very small number of bags (≤ 0.15 %). As to be expected, at medium levels (S2) and high levels, irradiation at 0.5KGy was not completely effective (about 0.002% and 0.03% contaminated bags respectively). When we simulated decontamination with chlorine at 200 ppm, even if chlorinated water was maintained at 200ppm throughout the washing stages ($S1=0.01\%$; $S2=14\%$; $S3=4.23\%$). Besides, at low and high levels ($S1$ and $S3$), chlorination (200 ppm) was not as effective in reducing cross-contamination as at medium levels ($S2$), i.e., chlorination reduced $S2$ prevalence levels by about 2200 % compared with 900 % and 340 % for $S1$ and $S3$ levels, respectively. However, when combination of chlorination (200ppm) and irradiation (0.5KGy) were used sequentially for lettuce contaminated at high level ($S3$), the simulated concentration was ≤ 2 cfu/bag, and prevalence ranged between 0.01 and 0.14 % (mean, 0.06 %). For medium level ($S2$), the combination of both resulted in only one cross-contaminated bag after 10 uncertainty realizations of the model. This very low value could be considered to be 0% practically. Therefore, combining both decontamination steps can be an effective intervention to reduce completely cross-contamination effect at medium contamination levels ($S2$).

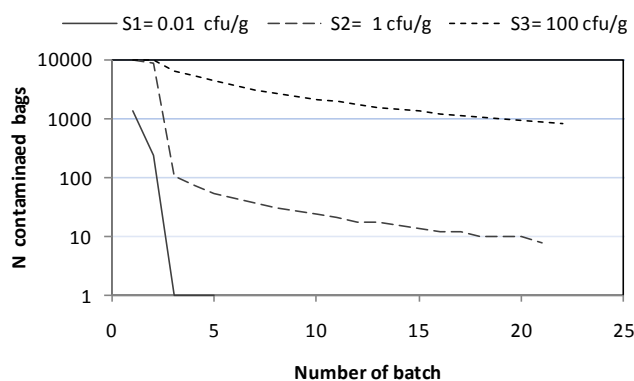


Figure 3. Simulated number of cross-contaminated bags along the production (22 batches) when one contaminated batch enters the processing line.

Table 2. Prevalence of cross-contamination bags at the different simulated scenarios

| Scenario | Prevalence (% bags) | | | |
|----------|---------------------|------------------------|----------------------|---------------------|
| | Baseline | Chlorination (200 ppm) | Irradiation (0.5KGy) | Detection (n=5;c=0) |
| S1 | 0.09 (0.23)* | 0.01 (0.05) | 0.00 (0.00) | 0.09 (0.23) |
| S2 | 3.05 (4.37) | 0.14 (0.23) | 0.002 (0.0004) | 3.05 (4.37) |
| S3 | 13.39 (25.09) | 4.23 (7.55) | 0.03 (0.09) | 9.2 (20.52) |

* mean (95th percentile)

The last intervention is having a sampling plan of n= 5 and c= 0 (sample size = 25g) to allow testing and rejection of positive batches of final product. According to the model, the prevalence would be reduced by up to 9.2% (average) for S3, if the detected contaminated batches were detected and destroyed. Performing a sampling plan (n=5) together with chlorination treatment led to a significant prevalence reduction only in S3, in which prevalence reached a mean value of 1.53%. Similarly, sampling plan had a positive effect when applied after a irradiation treatment at 0.1KGy, resulting in a mean prevalence of 0.8 %; however, at higher irradiation levels, sampling did not have significant effect on prevalence. On the other hand, the sampling plan (n=5; c=0) was not effective when the product was contaminated at low (S1) and medium levels (2).

Unfortunately, we do not know what the concentration of *E. coli* O157:H7 is when it enters the processing line, but we believe it can be as high as the S3 level on rare occasions, e. g, animal feces on several lettuce plants. Even if lower levels are more typical, once *E. coli* O157:H7 enters in a processing line, cross contamination can occur. Control measures, such as chlorination, irradiation and frequent *E. coli* testing can significantly reduce the likelihood of cross-contamination, especially if they are all considered together. At low contamination levels, the decontamination steps here simulated were especially effective reducing cross-contamination. Furthermore, results demonstrated that irradiation was a more effective decontamination step in reducing prevalence than chlorination for the simulated conditions. Nevertheless, there is always small probability that *E. coli* O157:H7 can contaminate a bag leaving the processing facility for distribution and sale.

References

- Buchholz, A.L., Z. Yan, and E.T. Ryser. 2008. Glo Germ as a cross contamination indicator during processing of leafy greens. Abst. Ann Mtg. Intern. Assoc. Food Prot. Columbus, OH, August 3 – 6.
- Foley DM, Dufour A, Rodriguez L, Caporaso F, Prakash A. (2002). Reduction of *Escherichia coli* O157:H7 in shredded iceberg lettuce by chlorination and gamma irradiation.
- Lammerding, A. & Fazil, A. (2000). Hazard identification and exposure assessment for microbial food safety risk assessment. Intl. J. Food Microbiol., Vol. 58, p. 147-157.
- Niemira BA, Sommers CH, Fan X. (2002). Suspending lettuce type influences recoverability and radiation sensitivity of *Escherichia coli* O157:H7. J Food Prot 65(9):1388–93.
- Niemira, B.A. (2008). Irradiation compared with chlorination for elimination of *Escherichia coli* O157:H7 internalized in lettuce leaves: influence of lettuce variety. J. Food Sci. 73, 208-213.
- [USFDA] U.S. Food and Drug Administration. 2006. Nationwide *E. coli* O157:H7 outbreak: questions & answers. Available from: <http://www.cfsan.fda.gov/~dms/spinacqa.html>. Accessed July 25, 2009.

Application of QMRA to go beyond safe harbors in thermal processes.

Part 1: introduction and framework

François Bourdichon¹, Mieke Uyttendaele², Annemie Geeraerd³, Marcel H. Zwietering⁴, Jeanne-Marie Membré⁵

¹ DANONE Research – Centre Daniel Carasso, Food Safety Centre, RD128, 91767 Palaiseau, France (francois.bourdichon@danone.com)

² Laboratory of Food Microbiology and Food Preservation, Ghent University, Coupure Links 653, B-9000 Gent, Belgium (mieke.uyttendaele@UGent.be)

³ Division of Mechatronics, Biostatistics and Sensors (MeBioS), Department of Biosystems (BIOSYST), Katholieke Universiteit Leuven, B-3001 Leuven, Belgium (Annemie.Geeraerd@biw.kuleuven.be)

⁴ Wageningen University and Research Centre, Laboratory of Food Microbiology, P.O. box 8129, 6700 EV Wageningen, The Netherlands (marcel.zwietering@wur.nl)

⁵ Unilever, Safety & Environmental Assurance Centre, Colworth Park, Sharnbrook, MK44 1LQ, United Kingdom (Jeanne-Marie.Membre@Unilever.com)

Abstract

Thermal processing is today probably the most well established and rationalized process of food preservation and is widely adopted by food business operators throughout the world. Thermal processing procedures are predominantly governed by safe harbors, historically set generally recognized time/temperature combinations or reduction targets to provide “safe” food. Most of currently used thermal processes are significantly ‘fail-safe’. This can lead to greater quality deterioration than necessary. The key issue of a thermal process is to find the right balance between rendering foods safe and stable, along with respecting technical constraints to ensure tasty and healthy food. There has recently been an increasing development of food products which have undergone milder heat processing. The heat treatment is still designed to reduce the numbers of pathogenic and spoilage organisms, but is used in combination with other factors (hurdles) to manage safety and stability over a designated shelf life.

Keywords

Food Safety Objectives, heat inactivation, microbial reduction, equivalence, microbial risk characterization, food safety management.

Introduction

Rationale in heat treatment of foods is recent in human history. Back in 1810, Nicolas Appert made the set up of his experiments on heat processing, which became the basis of the canning process. Peter Durand, took the process one step further and developed a method of sealing food into unbreakable tin containers (Goldblith, 1971). The rationale at this time was to process food in absence of oxygen. Louis Pasteur then put an end to the dogma of spontaneous generation by demonstrating that the spoilage of food and the process of rotting were due to the microbial activity rather than simply the presence of oxygen. In the late 19th century Samuel C. Prescott and William Lyman Underwood (Prescott & Underwood, 1897) in the United States gave canning a further scientific context by identifying bacterial spores as the main source of alteration of canned food.

Materials and methods

International Life Sciences Institute (ILSI)-Europe is a global network of scientists devoted to enhancing the scientific basis for public health decision-making. ILSI-Europe has initiated a new activity on risk assessment approaches to setting thermal processes in food manufacturing.

Results and discussion

Bacillus botulinus (then the name for *Clostridium botulinum*) was isolated in 1896 by Emile van Ermengem from a blood sausage implicated in an outbreak. Spores of mesophilic strains of *C. botulinum* were identified to be the most heat resistant form of the pathogenic organisms in low acid ambient stable products. (Bigelow, 1921) and (Esty & Meyer, 1922) proposed exponential destruction to model destruction by heat treatment of *C. botulinum*. The concept of a sterilizing value (F-value) was developed by Ball (1927) and is usually expressed in minutes at 121.1°C (250°F) to destroy an organism. Starting from the original work by Esty and Meyer (1922), Townsend et al. (1938) and finally Stumbo (1965), the F0 3 minimum botulinum cook was established and is used widely today for low-acid canned foods. Time to achieve a 12 log reduction for *C. botulinum* spores when using a decimal reduction time at 121.1°C of 0.21 minutes is equivalent to 2.52 minutes or an F value of 2.52. In the above calculation of the F value the population of *C. botulinum* was considered to be contained in an undefined unit volume or mass, which may be 1 mL, 1 gram or the volume of a container. This 12D cook thus is based on the statement that a probability of survival of not more than 1 in 10^{12} containers (or another unit) is regarded as acceptable. It therefore takes into account a certain element of risk assessment, with the conclusion that a probability of 1 in 10^{12} is an acceptable level of risk.

Considering an initial load of 100 spores per container and D121.1 of 0.21 minutes for the most resistant spores of *C. botulinum*, the F value required to achieve a 10^{-12} final number of surviving spores is $0.21 (2+12) = 2.94$ minutes. Based on these requirements the F (sterilization value) of 2.94 is again rounded up to 3 minutes, hence the F0 3 minutes process. The approach taken in North America is defined by the Food and Drugs Agency (FDA) and equates to the same F0 3 botulinum cook recommendation (http://www.fda.gov/ora/inspect_ref/itg/itg7.html). The FDA example of a 12 log reduction process gives reference to an initial population of 10,000 spores in a can of food. If a 12 D process is given, the initial 10,000 spores per can (10^4 spores) would be reduced to a theoretical 10^{-8} living spores per can, or one living spore per 10^8 cans of product. This is actually a lower level of public health safety, but in reality is still secure. The FDA example is likely to have been chosen to illustrate the principles of a 12 D reduction and the caution that must be taken if the initial spore loading is high (*i.e.* 10,000 spores in a can of food).

The F0 3 process is based on thermal resistance of *C. botulinum*. However, many sterilization treatments are designed to achieve a considerable higher process than F0 3 in order to inactivate spoilage organisms, some of which exhibit a higher heat resistance.

Heat processing in the dairy industry

Pasteurization was initially patented for the conservation of wine in France by Pasteur in the middle of the 19th century. Due to the versatile nature of the dairy process, pasteurization of raw milk became the best solution to achieve a longer shelf life and better safety of dairy products. The work of Kilbourne (Kilbourne, 1912, Kilbourne, 1913) highlighted the balance between food safety and technological constraints. From a microbiological point of view, *Mycobacterium tuberculosis* was the first identified heat-resistant pathogen of concern associated with milk (Hammer 1948). Minimal pasteurization time/temperature combinations were established in the US in 1956 to assure destruction of *Coxiella burnetti*, which was then found to be more heat resistant than *M. tuberculosis*. The highest level of *C. burnetti* in milk of infected cows from samples collected was determined to be 10,000 infective guinea pig doses (minimum number of *C. burnetii* required to infect a guinea pig by intraperitoneal inoculation of 2 mL). The goal for minimal pasteurization conditions was to provide an additional 10-fold margin of safety and seek a destruction of 100,000 infective guinea pig doses (equivalent to a 5D reduction; (Enright et al., 1957)).

Since the recognition of *Listeria monocytogenes* as a foodborne pathogen in the 1980s, the organism has become the main focus of the dairy industry. As a result, extensive investigations have been conducted on the heat resistance of *L. monocytogenes*. The current

consensus is that the D value at 72°C does not exceed 15 seconds in foods. This means that minimal heating of food, at the coldest spot, for 2 minutes at 72°C would result in a degree of lethality at least equaling 8D (Mossel & Struijk, 1991).

Ultra-heat-treated (UHT) milk was developed to meet the demand for room temperature stable dairy products. UHT comprises a heat treatment of no less than 135°C for at least 1 second (but usually between 135-150°C for 1-8 s) (Scheldeman et al., 2006). In UHT-processed milk obtained by treatment in continuous flow and subsequent packaging in presterilized containers, all micro-organisms including spores are presumably killed.

Both pasteurization and UHT heat processes induces proteolysis and thermocoagulation of proteins. In order to achieve extended storage of raw milk prior to further processing, a minimal heat treatment – thermisation – is applied (heating to a temperature of between 57°C and 68°C for at least 15 seconds). Combined with ultrafiltration, thermisation of milk has been proposed as an alternative to pasteurization (Benard et al., 1981), although providing a lower guarantee of safety. Thermisation helps finding another balance between food safety and technological parameters, with less denaturation of milk constituents.

The meat processing industry

Salmonella spp. is identified by the USDA risk assessment as the pathogen of concern for meat and poultry with an objective of 7 D reduction of *Salmonella* in Ready-to-Eat (RTE) poultry products and a 6.5D reduction of *Salmonella* in RTE beef products. The rationale is based on the establishment of a worst case population of *Salmonella* spp. by animal species and the probability of survival of *Salmonella* spp. in 100 g of finished product after the specific lethality processes was calculated.

The assumptions behind these standards are now being debated. Prerequisite programs (PRP) and HACCP rules have resulted in an improvement of global hygiene in food processing industries. Developing a standard that uses a safety margin based on a highly conservative worst-case scenario may lead to the production of over processed products of inferior quality and may place an undue burden on the processor, without significantly increasing public health safety.

In its 2007 report on safe cooking of burgers, the United Kingdom Advisory Committee on the Microbiological Safety of Food confirmed that a heat process of 70°C for 2 minutes would be sufficient to give at least 6 log reductions of pathogens of concern, namely *E. coli* 0157:H7, *Salmonella* spp. and *L. monocytogenes*.

Cooked chill foods

The requirements to ensure the safety of cooked chilled foods also referred to as REfrigerated Processed (or Pasteurized) Food with Extended Durability (REPFEDs) were described (Mossel & Struijk, 1991). Non-proteolytic psychrotrophic *C. botulinum* strains are the principal microbiological safety concern, in relation to spore-forming bacteria in the manufacture of cooked chilled foods. In 1992, ACMSF gave the recommendation in the report on «Vacuum Packaging and Associated Processes» that a heat treatment should provide a reduction of non-proteolytic *C. botulinum* by 10⁶, or a so called 6D Process.

The potential for growth and toxin formation by non-proteolytic *C. botulinum* in short shelf life commercial chilled food has been recently assessed. Examination of the literature indicates that given the correct circumstances, non-proteolytic *C. botulinum* can in theory form toxin in less than 10 days at less than 8°C. However, commercial short shelf life chilled foods have not been associated with foodborne botulism when stored correctly. The safety of some chilled foods can be attributed to the presence of one or more “unquantified controlling factors”, e.g. raw material quality, heat process, high hygiene level during manufacture, good chill chain (Peck, 2006).

Conclusions:

Nowadays, when setting thermal process criteria, a quantitative risk assessment approach to reach a safe level in the final product is conducted by the food business operators to

demonstrate the safety of its product when implementing effective process control – associated with defined performance criteria.

Established heat treatment procedures address safety issues, but take also technological, as well as economical issues in consideration. The origins of the choices made at that time are sometimes lost. Time/temperature combinations widely accepted today were historically set taking into account at the time often limited available knowledge on the microbial hazard, its expected levels and its thermal resistance. This has been illustrated above for the canning process and pasteurization of milk which are major milestones in the history of thermal processing in food preservation. They represent the inheritance we still rely on to develop performance standards for alternative thermal processes. Science based safety assessment is available presently, with ability to include the more widely available information on supply chain management and biological variability in comparison to the time these safe harbors were set. Better risk characterization helps to define modified heat treatment scenarios, enables evaluation of appropriate target levels, and eliminates the need of setting thermal processes based upon worst case situation. The hurdle concept of food chain safety management provides now an acceptable degree of protection to the consumer, where the heat process is not anymore the only/main critical point.

Acknowledgements:

Authors want to thank ILSI Europe, the Risk Analysis in Food Microbiology Task Force and the Expert Group on Thermal Processing for the preparation of this topic.

References:

- Benard, S., J. L. Maubois, and A. Tareck, 1981. [Ultrafiltration-thermisation du lait à la production: aspects bactériologiques]. *Le Lait* 61:435-457.
- Bigelow, W. D., 1921. Logarithmic Nature of Thermal-death-time Curves. *Journal of Infectious Disease* 29:528-536.
- Enright, J. B., W. W. Sadler, and R. C. Thomas, 1957. Pasteurization of milk containing the organism of Q fever. *Am. J Public Health Nations. Health* 47:695-700.
- Esty, J. R. and R. F. Meyer, 1922. The heat resistance of the spores of *B. botulinus* and allied anaerobes. *Journal of Infectious Disease* 31:650.
- Goldblith, S. A., 1971. Thermal processing of foods. A review. *World Rev Nutr. Diet.* 13:165-193.
- Kilbourne, C. H., 1912. Pasteurization of milk with suggestions as to methods and apparatus to be employed. *Am. J Public Health (N. Y.)* 2:626-634.
- Kilbourne, C. H., 1913. The control of temperatures in the pasteurization of milk. *Am. J Public Health (N. Y.)* 3:268-272.
- Mossel, D. A. and C. B. Struijk, 1991. Public health implication of refrigerated pasteurized ('sous-vide') foods. *Int. J Food Microbiol* 13:187-206.
- Peck, M. W., 2006. *Clostridium botulinum* and the safety of minimally heated, chilled foods: an emerging issue? *J Appl. Microbiol* 101:556-570.
- Prescott, S. C. and W. L. Underwood, 1897. Contributions to our knowledge of micro-organisms and sterilizing processes in the canning industries. *Science* 6:800-802.
- Scheldeman, P., L. Herman, S. Foster, and M. Heyndrickx, 2006. *Bacillus sporothermodurans* and other highly heat-resistant spore formers in milk. *J Appl. Microbiol* 101:542-555.

Application of QMRA to go beyond safe harbors in thermal processes.

Part 2: quantification and examples

Jeanne-Marie Membré¹, Mieke Uyttendaele², François Bourdichon³, Annemie Geeraerd⁴, Marcel H. Zwietering⁵

¹ Unilever, Safety & Environmental Assurance Centre, Colworth Park, Sharnbrook, MK44 1LQ, United Kingdom (Jeanne-Marie.Membre@Unilever.com)

² Laboratory of Food Microbiology and Food Preservation, Ghent University, Coupure Links 653, B-9000 Gent, Belgium (mieke.uyttendaele@UGent.be)

³ DANONE Research – Centre Daniel Carasso, Food Safety Centre, RD128, 91767 Palaiseau, France (francois.bourdichon@danone.com)

⁴ Division of Mechatronics, Biostatistics and Sensors (MeBioS), Department of Biosystems (BIOSYST), Katholieke Universiteit Leuven, B-3001 Leuven, Belgium (Annemie.Geeraerd@biw.kuleuven.be)

⁵ Wageningen University and Research Centre, Laboratory of Food Microbiology, P.O. box 8129, 6700 EV Wageningen, The Netherlands (marcel.zwietering@wur.nl)

Abstract

In the context of risk assessment approaches for setting the thermal processes in food manufacturing (see Part 1 – introduction and framework), mathematical modeling is a tool to interpret experimental data and to provide predictions on microbial inactivation.

Firstly, three examples from literature are provided to show how the scientific community has applied risk assessment (completely or partially) to setting thermal process targets (log reduction) in food manufacturing.

Secondly, generic guidelines for application of mathematical models for estimating the heat-treatment condition (temperature and time) which deliver the log reduction targeted are presented. In order to use models for prediction purposes often the more simple models can be quite easily applied, since generally applicable estimates can be used, like for example a z -value of 10°C for spores. For more complex primary and secondary models often parameters are not readily available. In specific cases, however, for which specific models are shown to be significantly better, these models are necessary to obtain sufficient accuracy. To guarantee the possibility of making predictions for a wide range of conditions, often new datasets need to be measured. In time databases can develop, such as exist currently for D and z , however still much work needs to be done to make more complex models practically workable in general conditions.

To illustrate these ideas various levels of complexity: i): a global approach making use of classical D , z values (a so-called safe harbor); ii): an approach based on database exploitation; iii): an approach based on user-specific experimental data, will be discussed.

Introduction

In the context of risk assessment approaches for setting the thermal processes in food manufacturing, quantification of microbial inactivation in one or several of the food processing steps is an important issue. This is reflected in the ΣR term in the ICMSF equation (ICMSF, 2002). Mathematical modeling is a tool to interpret experimental data on microbial inactivation, or, in other words, to extract the information present in experimental data and to translate this information into a tangible format. As such, modeling approaches enable to quantify the value of the ΣR term.

The objective of this paper (Part 2) is to review how quantitative methodology encompassing various modeling approaches can be used in the new tools of microbial risk assessment and food safety management metrics proposed by the ICMSF to assess microbial food safety risks. It will be illustrated with some examples how the quantitative methodology can best be elaborated to support more effectively targeted thermal process establishment.

Results and discussion

Moving from safe harbors, using a risk assessment approach means to work with *equivalence*: an equivalent level of safety can be reached by applying a severe heat treatment in combination with a relatively high initial level and / or potential growth, and a less severe heat treatment where growth can be prevented or low initial levels can be assured. The severity of the heat treatment can thus be balanced against the level of control in the other parts of the process, or even the level of control in preceding or subsequent steps in the food processing chain.

In such an approach, determination of initial levels, reductions to be achieved, potential growth that can occur, etc. must be based on solid information. Such data can be obtained from literature, databases, predictive models, surveys and experiments. The strongest determinations combine information from several of these sources. Microbiological analysis of raw materials, in process or finished product may be used to verify that the process is operating as needed to achieve the required Performance Objective.

This log reduction setting, using a risk assessment approach will be illustrated through the following examples:

1. 4.4 log reduction of *E. coli* O157 in frozen raw ground beef patties (ICMSF, 2002)
2. 5 log reduction of *L. monocytogenes* in shrimp (Walls, 2005)
3. *Salmonella* in pasteurized frozen foods (Membré et al., 2007)

To quantify the required heat-treatment conditions, i.e. the temperature and the time required to deliver the expected level of reduction, predictive models are necessary. In the following, we focus on *generic guidelines for application of mathematical models for prediction purposes*. In this context, we assume that the (possibly time-varying) temperature profile for a specific thermal processing step is available, either via representative monitoring devices, or via the outcome of dedicated heat transfer models. Furthermore, we assume that this temperature profile is approximated via (possibly very small) time intervals with constant temperature (static temperature). This second assumption is not essential, as we could use dynamic models, but we add this assumption for the ease of illustration.

It should be realized that often the more simple models can be quite easily applied, since generally applicable estimates can be used, like for example a z -value of 10°C for spores. For many organisms D_{ref} and z values can be estimated (van Asselt and Zwietering, 2006), meaning that quite easily one can make estimates on inactivation at various temperatures as function of time by combining the classical log-linear inactivation kinetics in combination with a Bigelow type model. If also parameters like z_{pH} and z_{aw} are known, these effects can be included. For more complex primary and secondary models often generally accepted parameters are not readily available, making it difficult to use these models in predictions. For some cases, however, for which specific models are shown to be significantly better, these models are necessary to obtain sufficient accuracy. To guarantee the possibility of making predictions for a wide range of conditions, often new datasets need to be measured. In time databases can develop, such as exist currently for D and z (ICMSF, 1996, Van Asselt and Zwietering, 2006), however, still much work needs to be done to make more complex models practically workable in general conditions.

These general statements can be exemplified as follows.

First level of complexity: a safe harbor approach

The simplest approach is to combine classical log-linear inactivation kinetics, with a Bigelow type model, describing the effect of temperature T on the decimal reduction time D . Furthermore, globally accepted parameter values such as a D_{ref} -value of 0.21 min at 121.1°C and z -value of 10°C for *C. botulinum* (A&B) are chosen. This procedure delivers responses to many questions (canning of peas, canning of ham, ...) and has proven to be at least not resulting in dangerous situations, thereby constituting a safe harbor approach. Another

example is the first record in Table 1, referring to the current consensus safe harbor for *L. monocytogenes* in RTE-foods (D -value not exceeding 15 seconds at 72°C).

It should be remarked that by following this approach, we are actually focusing on the most important variables influencing microbial inactivation, i.e., vegetative or spore type and temperature. Other influences like pH and water activity of the food product, species and strain variability and process variability are not taken into account, except for by deliberately selecting fail-safe values. It has been shown that these other effects are generally negligible in comparison with the variability on published D -values.

Second level of complexity: an approach based on database exploitation

Based on a large database of D values (van Asselt and Zwietering, 2006) one can get a more solid basis for valid parameter values in various products/product groups. Table 3, record 2a, summarizes the information on *L. monocytogenes* in various food products with a 95% prediction interval for the D value of 0.274 min at 72°C (940 data). This confirms the validity of the safe harbor. If the data specific for dairy (280) are used a smaller value of 0.104 min is obtained, and specifically for milk (226 data) 0.091 min. Such more specific information gives better targeted values, and for a specific product group a better estimate, and in this case a clearly smaller value than the safe harbor. This of course can be done quite well for *Listeria* and milk (as it contains 226 data), or fish, meat, vegetables since ample data are available, but for a product group like butter it becomes very questionable, since fewer data are available, and all from only one reference (one lab, only two strains), or potato slices (3 data, only one lab, only one strain).

This level of complexity does allow to use the stated, more specific parameter values in combination with the classical log-linear inactivation kinetics and the Bigelow type model.

In this respect, also ComBase (www.combase.cc and Baranyi and Tamplin, 2004), is a very interesting database as inactivation data, reported either as raw data or as a lumped D -value, can conveniently be searched for a specific food product/pathogen combination. If sufficient information at different temperatures is present, a z value may also be extractable, but this is not always possible.

Alternatively, this level of complexity can also include a somewhat more advanced model. Imagine that for *L. monocytogenes*, for example the Weibull model with its parameters b and δ in its re-parameterisation from Mafart et al. (2002), is valid. We can take the D value for use as δ , but what is b for a certain food product? It could be that in future we will have databases gathering rules of thumb concerning this b -value for certain conditions, but until we need for every product to do an experiment to determine the b -value, the model is not yet practically applicable for general prediction purposes (Table 3, record 2b).

Third level of complexity: an approach based on user-specific experimental data

If user-specific experimental data are available for a specific question of course these data can be used. Tools such as the freeware GInaFit (Geeraerd et al., 2005) allow the user to identify suitable primary models for user-specific experimental data. Where relevant, it may be interesting to combine this information with information from databases. It is likely that a more complex primary model is selected: imagine that this is –again– the Weibull model with its parameters b and δ . As a result, we will have an estimate for the Weibull parameter b (for which no generally accepted value or rule of thumb exists, as stated for the second level of complexity) and for values of the Weibull parameter δ (Table 3, record 3). As b is typically a temperature independent parameter for a specific strain/food product, there is generally no need to develop a secondary model for this parameter. Concerning the parameter δ , if data are available for several values of temperature, pH, water activity, ... it is possible that, for example, an extended Bigelow-type model such as the one proposed by Gaillard et al. (1998) provides a good quality of fit (replacing D by the δ parameter of the Weibull model).

The developed models give rise to the following two possibilities going beyond safe harbor approaches. Firstly, when a (possibly time-varying) temperature profile for a specific processing step is available, which was one of the assumptions in this section, the developed

models will give an accurate quantification of the number of log reductions attained via this processing step. Secondly, if, on the contrary, a specific number of log reductions to be attained is provided, by linking with the other terms in the ICMSF equation delivering equivalent performance as a whole, the developed models enable to calculate accurately the time needed at a specific treatment temperature or, conversely, the temperature needed for a specified treatment duration. As the safe harbors constitute a fail-safe approach, the treatment time or temperature needed is expected to be shorter (respectively lower) when using this third level of complexity, giving the opportunity to optimize heat treatment designs.

Table 1: Three different levels of complexity to be distinguished when quantifying the microbial inactivation through modeling approaches – illustration on *L. monocytogenes*

| Level of complexity – key word | D_{ref} [min] ^a | T_{ref} [°C] | z [°C] | b [-] |
|--|--|-----------------------|-----------------|---|
| 1 – Safe harbor | 0.25 | 72 | 7 | Not needed |
| 2a – Extended database for D and z | 0.274 (all products) 0.104 (dairy) 0.091 (milk) | 72 | 7 6.4 6.2 | Not needed |
| 2b – Extended database for D , z , and b | 0.091 (milk) | 72 | 6.2 | Needed, but databases for b not available yet |
| 3 – Case-specific | All model parameters needed are extracted from specifically designed and conducted experiments | | | |

^a 95% upper bands for $D(72)$ value for all products (except those containing high levels of salt)

Conclusions

Risk assessment is an appropriate framework to go beyond safe harbors; to do so, three routes might be explored (on their own or in combination):

1. combining in an accurate way the performance of a certain, specified thermal treatment with performances in other stages of the food production chain;
2. reducing the uncertainty on predictions, and therefore decreasing the need for being conservative;
3. calculating accurately the time needed at a specified treatment temperature or the temperature needed for a specified treatment duration using more complicated models to attain a stated performance level.

Nevertheless, if exploring none of these routes is possible, applying safe harbors to set heat-treatment is still really valuable: they are widely (even generally worldwide) known, accepted and largely used at operational level; in addition, they can be readily used by anyone to design a heat-treatment process without the need of extensive information about the food characteristics or prior knowledge on the initial microbial level.

References

- Baranyi J. and Tamplin M.L. (2004) ComBase: A common database on microbial responses to food environments. *Journal of Food Protection* 67, 1967-1971.
- Gaillard S., Leguerinel I. and Mafart P. (1998b) Model for combined effects of temperature, pH and water activity on thermal inactivation of *Bacillus cereus* spores. *Journal of Food Science* 63, 887-889.
- Geeraerd A.H., Valdramidis V. and Van Impe J.F. (2005) GInaFIT, a freeware tool to assess non-log-linear microbial survivor curves. *International Journal of Food Microbiology* 102, 95-105.
- International Commission on Microbiological Specifications for Foods (ICMSF) (2002). *Microorganisms in Foods 7: Microbiological Testing in Food Safety Management*. New York: Kluwer Academic/Plenum Publishers, ISBN 0 306 47262 7.
- Mafart P., Couvert O., Gaillard S. and Leguerinel I. (2002) On calculating sterility in thermal preservation methods: application of the Weibull frequency distribution model. *International Journal of Food Microbiology* 72, 107-113.
- Membré J.M., Bassett J. and Gorris L.G.M. (2007) Applying the food safety objective and related standards to thermal inactivation of *Salmonella* in poultry meat. *Journal of Food Protection* 70, 2036-2044.
- van Asselt E.D. and Zwietering M.H. (2006) A systematic approach to determine global thermal inactivation parameters for various food pathogens. *International Journal of Food Microbiology* 107, 73-82.
- Walls I. (2005) Achieving continuous improvement in reductions in foodborne listeriosis - A risk-based approach. *Journal of Food Protection* 68, 1932-1994.

A predictive microbiology approach for thermal inactivation of Hepatitis A Virus in acidified berries

A. Pinon¹, N. Deboosère¹, A. Delobel¹, G. Merle², S. Blaise-Boisseau², S. Perelle², S. Temmam³, T. Morin³ and M. Vialette¹

¹ Institut Pasteur de Lille, 1 rue du Prof. Calmette, BP 245, 59019 Lille, France (anthony.pinon@pasteur-lille.fr)

² AFSSA LERQAP – Unité VAE, 23 av. du Général de Gaulle, 94700 Maisons-Alfort, France (s.perelle@afssa.fr)

³ ADRIA Normandie, Bd du 13 juin 1944, BP2, 14310 Villers-Bocage, France (tmorin@adrianie.org)

Abstract

A model was developed for the inactivation of Hepatitis A Virus (HAV) in berries with different pH values. Nonlinear inactivation curves in acidified raspberries were modelled using an integrated model, with a single equation nesting secondary models of temperature and pH in the primary model. Model predictions were then confronted to experimental results obtained in another laboratory on other berries with different pH values. Excellent predictions were obtained in most cases, while failed predictions provided safe results, with the model predicting higher residual virus titres than what was observed.

Keywords

Hepatitis A Virus, thermal inactivation, pH, red berries

Introduction

Frozen berries produced in eastern Europe have been found responsible for infections linked to enteric viruses when used in unprocessed foods (Niu *et al.*, 1992; Ramsay and Upton, 1989). Thermal treatment of these fruits is used as a decontamination method, but it has to be adapted to product characteristics; indeed, factors such as sugar or pH may have an impact on the viral sensitivity to thermal treatments (Deboosère *et al.*, 2004; Scholz *et al.*, 1989). This study aims at modelling the behaviour of Hepatitis A Virus (HAV) in acidified red berries as a function of thermal treatment and pH.

Materials and methods

Strains and media

HM175/18f strain of HAV (VR-1402) and the foetal rhesus monkey kidney cell line (FRhK-4) were obtained from the American Type Culture Collection. These cells were used throughout the study for the propagation of HAV to prepare inoculums and to measure HAV infectivity. Methods of cultivation, maintenance of cells and preparation of virus pools have been described previously (Cromeans *et al.*, 1987; Flehmig, 1980; Lemon *et al.*, 1985). Quantitative measurement of the infectivity of HAV was done by plaque assay in 6-well cell-culture multiplates (Costar, VWR International, Fontenay-sous-Bois, France), following a method described previously (Deboosère *et al.*, 2004). Raspberries supplied by food industrial partners (Vergers de Boiron; Kerry Ravifruit) were ground to obtain a purée that was used as a reference matrix for the modelling step, and citric acid was added to obtain final pH values of 3.3, 3.0, or 2.5. Regarding validation of model predictions, other ground fruits were used with their natural pH: strawberries (pH 3.35), raspberries (pH 3.05) and bilberries (pH 2.87).

Thermal treatment

Each food matrix was artificially contaminated with HAV to obtain concentrations of 10^6 to 10^8 PFU.mL⁻¹; 0.5 gram of preparations were then distributed in glass tubes, 100 mm long and 0.5 mm thick (Fisher Bioblock Scientific) and left at room temperature for 3 hours, as an aggregation step. Heat treatments were performed by simultaneous immersion of the tubes in a glycerol bath set at the desired temperature (65, 70 or 75°C) for a determined period of time. A thermocouple connected to a data acquisition unit (Agilent Technologies, Actifa, France)

was inserted into an uncontaminated aliquot of preparation to monitor the internal temperature throughout the heat treatment. Individual aliquots were removed at periodic time intervals and placed immediately in an ice bath for rapid cooling. The treated media samples were 50-fold diluted in DMEM before virus titration. Each experiment was replicated 3 times. The desired temperature was reached in 2 to 3 minutes; however, since virus inactivation took place during this step, it was assumed that the target temperature was reached immediately.

Inactivation model

A primary model used to describe viral inactivation kinetics was adapted from a bacterial inactivation model proposed by Albert and Mafart (2005):

$$\text{Log}_{10}(N) = \text{Log}_{10}[(N_0 - N_{\text{res}})10^{-(t/\delta)^p} + N_{\text{res}}] \quad (1)$$

where N is the infectious virus titre, t is time, N_0 represents the initial titre (at time 0), N_{res} is the residual titre at the end of the treatment, δ is the time for first decimal reduction for the population not included in N_{res} , and p is a shape parameter for concavity or convexity of the curve.

The reduction, or abatement, in virus titre obtained at the end of the treatment was described using $A = \text{Log}_{10}(N_0) - \text{Log}_{10}(N_{\text{res}})$.

The impacts of temperature and pH on δ and A were described using the following secondary models:

$$\text{Log}_{10}(\delta) = \text{Log}_{10}(\delta^*) - \frac{T - T^*}{Z_T} - \frac{\text{pH} - \text{pH}^*}{Z_{\text{pH}}} \quad (2)$$

$$A = A^* - \frac{T - T^*}{Y_T} - \frac{\text{pH} - \text{pH}^*}{Y_{\text{pH}}} \quad (3)$$

where δ^* (respectively A^*) represents the value of δ (respectively A) in an arbitrary reference condition T^* (65°C) and pH^* (3.3), Z_T (respectively Y_T) is the temperature increase necessary for a 1-unit reduction of $\text{Log}_{10}(\delta)$ (respectively A), and Z_{pH} (respectively Y_{pH}) is the pH increase necessary for a 1-unit reduction of $\text{Log}_{10}(\delta)$ (respectively A).

It was assumed that the shape parameter p did not depend on temperature and pH, as has been observed previously for bacteria (Couvert *et al.*, 2005; van Boekel, 2002).

A complete model combining the primary and secondary models was actually used to evaluate the parameters on the full dataset: the values of δ and N_{res} in Equation 1 were substituted by their expressions from Equations 2 and 3. N_0 values were forced at $N_{(t=0)}$. Titres under the detection threshold were set at the detection threshold (safe assumption). A one-step fitting procedure was thus performed and parameters describing HAV inactivation in raspberries were obtained: p , δ^* , Z_T , Z_{pH} , A^* , Y_T , Y_{pH} .

Results and discussion

Parameters estimation

Using the combined primary and secondary models from Equations 1-3, the parameters were estimated from HAV inactivation in acidified raspberry data. Using this combined approach, the estimated values are expected to be more objective and robust, and the variability in kinetic data is taken into account (Pouillot *et al.*, 2003). Estimates are indicated in Table 1.

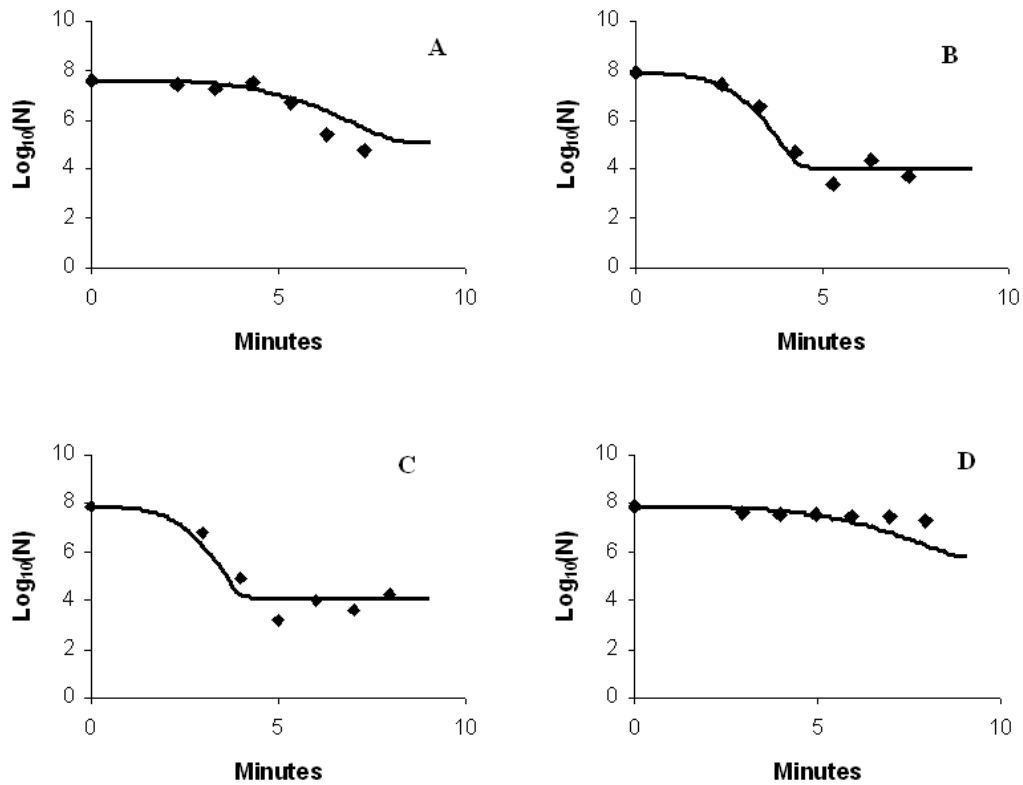


Figure 1: Inactivation kinetics of HAV in raspberries at 65°C - pH 3.0 (A), 70°C - pH 2.5 (B), 75°C - pH 3.3 (C), and 65°C - pH 3.3 (D); experimental data (symbols) and model (line).

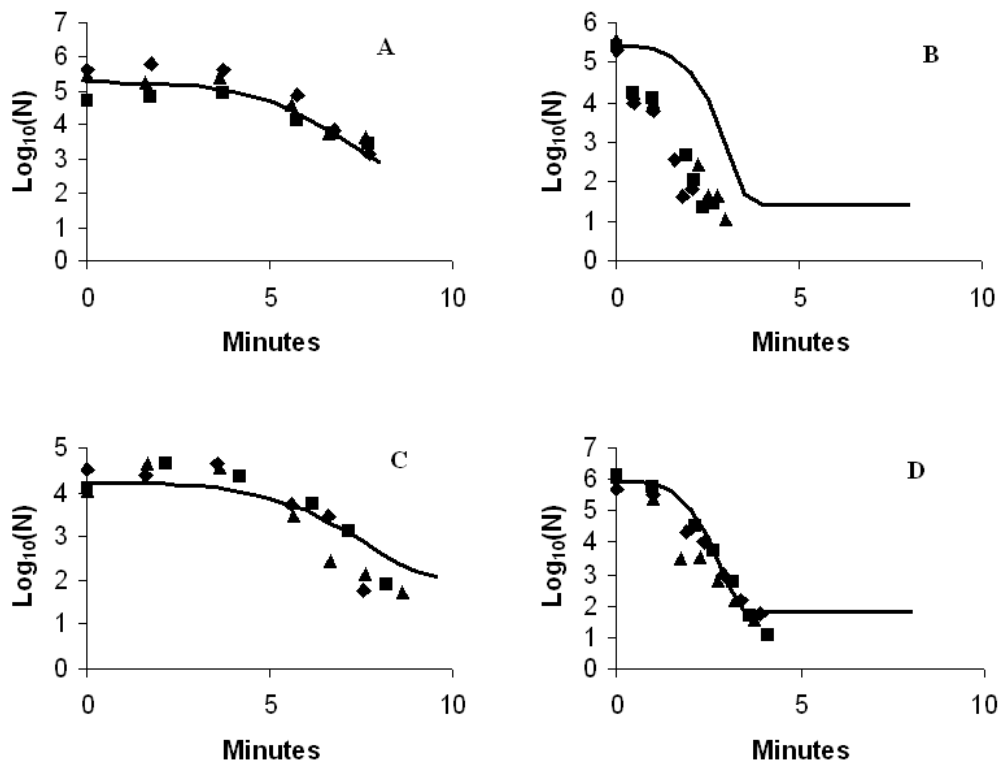


Figure 2: Inactivation kinetics of HAV in raspberries (pH 3.05) at 65°C (A), in raspberries (pH 3.05) at 75°C (B), in strawberries (pH 3.35) at 65°C (C), and in bilberries (pH 2.87) at 75°C (D); experimental data (symbols, 3 repetitions) and model prediction (line).

Table 1: Parameters estimates from acidified raspberry data.

| Parameter | Estimated value | 95% confidence interval |
|-----------------------------|-----------------|-------------------------|
| p | 3.31 | 2.56 ; 4.23 |
| $\text{Log}_{10}(\delta^*)$ | 0.83 | 0.80 ; 0.85 |
| Z_T | 24.13 | 22.19 ; 26.12 |
| Z_{pH} | -4.67 | -5.74 ; -3.86 |
| A^* | 2.25 | 1.78 ; 2.75 |
| Y_T | -6.67 | -9.78 ; -5.16 |
| Y_{pH} | 0.97 | 0.70 ; 1.68 |

From these experiments, it appeared that a reduced pH led to a faster thermal inactivation in the tested range. The final reduction in viral titre (parameter A) is greater for higher temperatures and lower pH. Examples of inactivation kinetics and model curves are shown in Figure 1.

It is worth noting that, since a global primary and secondary model was used, no individual fit was conducted on any given condition. Therefore, the model describes a global behaviour rather than a sum of individual behaviours, which explains why a “perfect fit” is not observed.

Model validation

Predictions with the model were confronted to new experimental data, obtained on other fruits in another laboratory. Examples of these comparisons are presented in Figure 2.

The model used with parameters estimated on acidified raspberries (Table 1) gave excellent predictions of HAV behaviour in the various fruits for most cases. Failed predictions provided safe results, with higher predicted N_{res} values than what was observed.

Conclusions

A model for thermal inactivation of HAV in berries with different pH values was successfully developed and validated. Yet, the phase of temperature increase was neglected, assuming that the preparations reached the target temperature immediately, while it took 2 to 3 minutes. This simplifying assumption will be addressed in future studies.

References

- Albert I. and Mafart P. (2005) A modified Weibull model for bacterial inactivation. *International Journal of Food Microbiology* 100, 197-211.
- Couvert O., Gaillard S., Savy N., Mafart P. and Leguerinel I. (2005) Survival curves of heated bacterial spores: effect of environmental factors on Weibull parameters. *International Journal of Food Microbiology* 101, 73-81.
- Cromeans T., Sobsey M.D. and Fields H.A. (1987) Development of a plaque assay for a cytopathic, rapidly replicating isolate of hepatitis A virus. *Journal of Medical Virology* 22 (1), 45-56.
- Deboosère N., Legeay O., Caudrelier Y. and Lange M. (2004) Modelling effect of physical and chemical parameters on heat inactivation kinetics of hepatitis A virus in a fruit model system. *International Journal of Food Microbiology* 93 (1), 73-85.
- Flehmg B. (1980) Hepatitis A-virus in cell culture: I. propagation of different hepatitis A-virus isolates in a fetal rhesus monkey kidney cell line (Frhk-4). *Medical and Microbiological Immunology* 168 (4), 239-248.
- Lemon S.M., Jansen R.W. and Newbold J.E. (1985) Infectious hepatitis A virus particles produced in cell culture consist of three distinct types with different buoyant densities in CsCl. *Journal of Virology* 54 (1), 78-85.
- Niu M.T., Polish L.B., Robertson B.H., Khanna B.K., Woodruff B.A., Shapiro C.N., Miller M.A., Smith J.D., Gedrose J.K., Alter M.J. and Margolis H.S. (1992) Multistate outbreak of hepatitis A associated with frozen strawberries. *Journal of Infectious Diseases* 166, 518-524.
- Pouillot R., Albert I., Cornu M. and Denis J.-B. (2003) Estimation of uncertainty and variability in bacterial growth using Bayesian inference. Application to *Listeria monocytogenes*. *International Journal of Food Microbiology* 81, 87-104.
- Ramsay C.N. and Upton P.A. (1989) Hepatitis A and frozen raspberries. *Lancet* 1, 43-44.
- Scholz E., Heinrich U. and Flehmig B. (1989) Acid stability of hepatitis A virus. *The Journal of General Virology* 70, 2481-2485.
- van Boekel M.A.J.S. (2002) On the use of the Weibull model to describe thermal inactivation of microbial vegetative cells. *International Journal of Food Microbiology* 72, 139-159.

The effect of pre-acid shock on the heat resistance of *Escherichia coli* K12 at lethal temperatures

E. G. Velliou^{1,2}, E. Van Derlinden^{1,2}, A. Cappuyns^{1,2}, E. Nikolaidou², A.H. Geeraerd^{1,3}, F. Devlieghere^{1,4}, J. Van Impe^{1,2}

¹CPMF²-Flemish Cluster Predictive Microbiology in Foods –<http://www.cpmf2.be/>

²BioTeC-Bioprocess Technology and Control, Department of Chemical Engineering, Katholieke Universiteit Leuven, W. de Croijlaan 46, B-3001, Leuven, Belgium.

³Division of Mechatronics, Biostatistics and Sensors (MeBioS), Department of Biosystems (BIOSYST), Katholieke Universiteit Leuven, W. de Croijlaan 42, B-3001, Leuven, Belgium.

⁴Laboratory of Food Microbiology and Food Preservation, Department of Food Technology and Nutrition, Ghent University, Coupure Links 653, B-9000 Ghent, Belgium.

Abstract

The objective of this work is to investigate the effect of pre-acid shock on the induced heat resistance of *E. coli* K12 MG1655 at lethal temperatures. The bacterial cells were acid shocked after exposure in acidified BHI broth, achieved after adaptation of the pH with addition of different acids each time (acetic acid, lactic acid, hydrochloric acid). The duration of the pre-acid shock is approximately 30 minutes. Generally, it is observed that rapid pre-acid shock can lead to resistance of *E. coli* to heat. The induced resistance is dependent on the type of acid used and on the quantity added, since different levels of acidification (different pH values of the broth) lead to a different level of heat resistance.

Key-words

Pre-acid shock, stress, stress adaptation, inactivation, *E. coli*, heat resistance.

Introduction

Micro-organisms reveal stress adaptation, which actually is the increase of a micro-organism's resistance to environmental conditions (like temperature, acidity, presence of chemical agents etc.) which would normally be lethal, and this by pre-exposure to a similar or a different kind of stress. The ability of stress adapted micro-organisms to resist when they are exposed to a different environmental stress is known as *cross protection* (Juneja and Novak 2003).

It is widely known that acids and temperature are stress factors for bacterial cultures. The type of acid, used during acid stress may affect the level of stress and/or cell injury. Strong acids – such as HCl- lead to trafficking of the dissociated [H⁺] in the cell via the membrane leading to an increase of the internal pH of the cell to levels that can be toxic or lethal. The weak acids – such as acetic and lactic- enter bacterial cells in their undissociated form and they partly dissociate in the cytoplasm (Foster 2004). Weak acids are less stressful for the cells compared to a strong acid.

The aim of this research is to investigate the influence of rapid pre-acid shock –with different types of acids each time- on the heat resistance of *E.coli* at lethal temperatures.

Materials and Methods

Inoculum preparation

E. coli K12 MG1655 stock culture was stored at -80°C in Brain Heart Infusion (BHI) broth (Oxoid Limited, Basingstoke, UK) with 25% (v/v) glycerol (Acros Organics, NJ, USA). For the preparation of the inoculum a loopful of the stock culture was transferred in 20 mL of BHI broth and was incubated at 37°C on a rotary shaker (175 rpm) for 9.5 h. 20 µL of the cell suspension was transferred to 20 mL of fresh BHI broth and was incubated at 37°C for 15 h. Early stationary phase cultures were harvested by centrifugation (1699 g, 2 min, 20°C) and portions of the cell suspensions were washed in acidified BHI.

Pre-acid shock

The pH value of normal BHI broth is approximately 7.5 acidified BHI of pH 5, 5.5 and 6 was prepared with addition of different acids each time, in fresh BHI broth. The acids added were hydrochloric acid 30% (v/v) (Acros Organics, NJ, USA), acetic acid 50% (v/v) (Acros Organics, NJ, USA) and lactic acid 50% (v/v) (Acros Organics, NJ, USA). The harvested cells gained from the step described in paragraph 2.1, remained in the acidified BHI for approximately 30 minutes.

Thermal Inactivation of E. coli at static temperatures

Static inactivation experiments took place in sterile glass capillary tubes in which a volume of 60 µL cell suspension of the pre-acidified inoculum was pipetted. Tubes were then sealed by a gas flame and immersed in a water bath (GR150-S12, Grant Instruments Ltd, Shepreth, UK), at static temperatures of 54°C and 58°C. At regular times one capillary was removed from the water bath, placed in an ice-water bath and analysed within approximately 45 min. Decimal serial dilutions of the samples were prepared in a BHI solution and surface plated on BHI agar (1.2% (w/v)) using a Spiral Plater (Eddy Jet IUL Instruments, Barcelona, Spain). Plates were incubated for 24 h at 37°C and colony forming units were enumerated. Each experiment was repeated in duplicate.

Data analysis

The experimental data (cell density data) were *ln*-transformed and plotted as a function of time. The inactivation model of Geeraerd et al. (2000) (Equation 1) was fitted to the data.

$$N = N_0 \cdot \exp(-k_{\max} \cdot t) \cdot \frac{\exp(k_{\max} \cdot S_t)}{1 + (\exp(k_{\max} \cdot S_t) - 1) \cdot \exp(-k_{\max} \cdot t)} \quad (1)$$

with N [cfu mL⁻¹] the cell population, $N(0)$ [cfu mL⁻¹] the initial cell population, k_{\max} [min⁻¹] the maximum specific inactivation rate, t [min] the time and S_t [min] is the shoulder period. In one case a tail was observed and for that condition an extended form of equation (1), which incorporates the tail as well was fitted to the data.

For the modelling of the data the GinaFiT (Version 1.5) software tool, a freeware Add-in for Microsoft® Excel was used (Geeraerd et al., 2005). Graphical illustrations were generated in MatLab® Version 7.4 (The Mathworks, Inc., Natick, USA).

Results and discussion

The experimental data followed a log-linear trend with a preceding shoulder and/or a preceding tail, depending on the conditions.

Experimental data were described after parameter identification using the inactivation model of Geeraerd et al. (2000). Induced thermotolerance of *E. coli* is defined as a prolongation of the shoulder and/or a reduction of the inactivation rate and/or a formation of a tail.

Acetic acid

For addition of acetic acid in the BHI broth, at 54°C for pH 6 and 5.5 an extension of the shoulder and a reduction of the inactivation rate is observed, compared to normal BHI broth. The level of the induced resistance is approximately the same for these pH values –the prolongation of the shoulder and the reduction of the inactivation rate are similar- (Figure 1). For pH 5 no shoulder is observed, the inactivation starts rapidly but the inactivation rate is similar to the rate observed for pH 6 and 5.5. At 58°C for pH 6 and 5.5 an extension of the shoulder and a reduction of the inactivation rate, compared to normal BHI broth was observed. For pH 5 only a decrease of the inactivation rate was apparent (Figure 1).

Lactic acid

For addition of lactic acid in the BHI broth, at 54°C no significant difference in the duration of the shoulder nor the inactivation rate was observed, compared to normal BHI broth for pH 5, 5.5 and 6 (Figure 1). It seems that lactic acid has no effect on the induction of heat resistance of *E. coli* when added in BHI broth, for pH at the range 5-6. At 58°C there is a similar decrease on the inactivation rate compared to normal BHI for pH 5, 5.5 and 6 but no prolongation of the shoulder is observed (Figure 1). At this temperature, lactic acid seems to trigger the cell leading to an induction of resistance and the level of the induced resistance is significantly the same for pH 5, 5.5 and 6.

HCl acid

For addition of HCl acid in the BHI broth, at 54°C a reduction of the inactivation rate is observed compared to normal BHI broth. This reduction is similar for pH 5, 5.5 and 6 (Figure 1). At 58°C for all studied pH values of the broth a decrease of the inactivation rate was observed, compared to normal BHI broth. For pH 6 also a prolongation of the shoulder is observed and there is an occurrence of a tail (Figure 1). The presence of the tail is the result of a stress resistant population. The formation of this resistant population –which is not present in non acidified conditions- is possible that occurs due to the pre-acid shock, which increases the bacterial resistance to heat. This change in the shape of magnitude of the heat inactivation curve after acid stress was also observed by Black et. al. (2009): a tail occurred during heat inactivation at 58°C after growth of *E. coli* K12 cells in acidified medium with pH levels of 6.2 and 6.5, adapted by phosphate buffer.

Conclusions

As a general conclusion, it is observed that rapid pre-acid shock can lead to resistance of *E. coli* to heat. The induced resistance is dependent on the type of acid used and on the quantity added, since different levels of acidification (different pH values of the broth) lead to a different level of heat resistance.

This work aims to provide additional knowledge on the reaction of bacterial cultures to heat after rapid pre-acid shock and, therefore, it contributes to an improved understanding of the level of the induced resistance of bacteria to heat when pre-exposed to different types of acids shortly before heat inactivation.

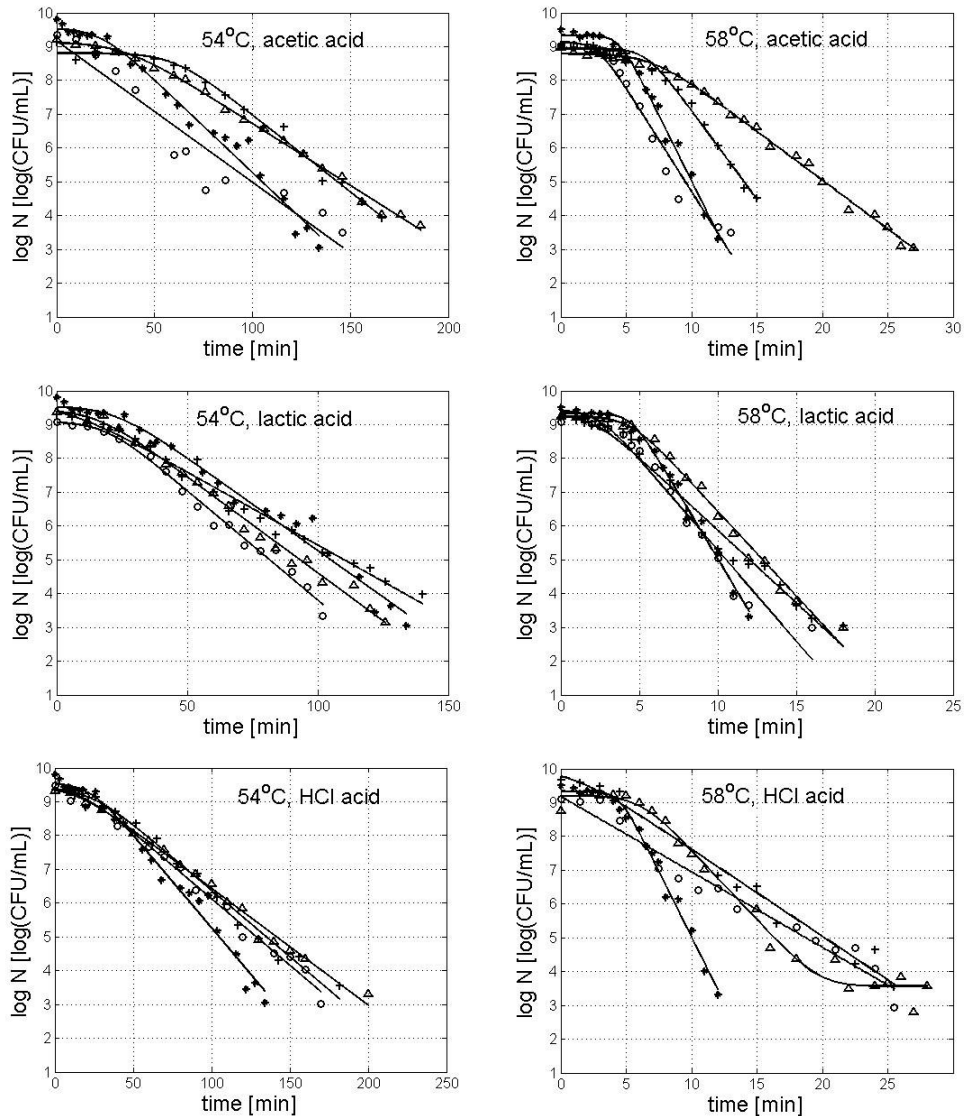


Figure 1: Thermal inactivation curves of *E. coli* and fits of Geeraerd et al. (2000) inactivation model at 54°C and 58°C for acetic, lactic and HCl acid: (*) normal BHI broth, (Δ) pH 6, (+) pH 5.5, and (o) pH 5.

Acknowledgements

This work was supported by grant DB/08/006/BM and OT/03/30 and by BOF EF/05/006 Center-of-Excellence Optimization in Engineering of the Research Council of the Katholieke Universiteit Leuven and the Belgian Program on Interuniversity Poles of Attraction, initiated by the Belgian Federal Science Policy Office.

References

- Foster, J.W., (2004) *Escherichia coli* acid resistance: Tales of an amateur acidophile, *Nature reviews* **2**, 898-907.
- Black, D. G., Harte, F., Davidson, P.M. (2009) *Escherichia coli* Thermal Inactivation Relative to Physiological State. *Journal of Food Protection* **72**, 399-402.
- Geeraerd, A.H., Herremans, C.H. and Van Impe, J.F. (2000) Structural model requirements to describe microbial inactivation during a mild heat treatment. *International Journal of Food Microbiology* **59**, 185-209.
- Geeraerd, A.H., Valdramidis, V. P., Van Impe, J.F. (2005) GinaFit, a freeware tool to assess non-log-linear microbial survivor curves. *International Journal of Food Microbiology* **102**, 95-105.
- Juneja, V.K. and Novak, J.S. (2003) Adaptation of Foodborne Pathogens to Stress from Exposure to Physical Intervention Strategies. In: Yousef, A.E. and Juneja, V.K. (eds.) *Microbial Stress Adaptation and Food Safety*, p.159-211, CRC Press, Boca Raton.

Modeling the combined effect of osmotic dehydration, nisin and modified atmosphere packaging on the shelf life of chilled gilthead seabream fillets

T.N. Tsironi, P.S. Taoukis

National Technical University of Athens, School of Chemical Engineering, Laboratory of Food Chemistry and Technology, Iroon Polytechniou 5, 15780 Athens, Greece (ftsironi@chemeng.ntua.gr)

Abstract

The objective of the study was the kinetic modeling of temperature, modified atmosphere packaging (MAP) and osmotic pre-treatment with the addition of nisin as antimicrobial agent on the shelf life of chilled fish. Gilthead seabream fillets were treated at 15°C in osmotic solution, 50:5maltodextrin(DE47):NaCl/100g with nisin (1000 IU/g fish in the osmotic solution), for 45 min. Untreated and treated slices were either packed in air or MA packed (50% CO₂-50% air) and stored at controlled isothermal conditions (0-15°C). Quality assessment and kinetic modeling was based on microbial growth, chemical indices (TVB-N, TMA-N, lipid-oxidation) and sensory scoring. The developed models were validated under dynamic conditions. Pre-treated samples were found to have improved quality stability during subsequent refrigerated storage, in terms of microbial growth, chemical changes and organoleptic degradation, resulting in a significant shelf life extension at all storage temperatures. MAP gave additional shelf-life increase of treated fillets. Osmotic pre-treatment with the addition of nisin in combination with MAP was the most effective treatment for the preservation of gilthead seabream fillets.

Keywords

Osmotic dehydration, modified atmosphere, nisin, chilled fish, kinetic modeling, shelf life

Introduction

Partial dehydration of food products by an osmotic process has received increased attention as a pre-treatment to further processing to improve nutritional, sensorial and functional properties of food. During the osmotic dehydration, water flows from the product into the osmotic solution, while osmotic solutes are transferred from the solution into the product (Raoult-Wack, 1994). By reducing the water activity of the food matrix, microbial growth is reduced or inhibited. Combined processes with OD could synergistically further increase shelf-life. The use of antimicrobial agents can effectively reduce the rate of spoilage and extend shelf-life of perishable foods. Nisin is a bacteriocin produced by *Lactococcus lactis* and it has a much broader spectrum than most other bacteriocins, being active against a wide range of Gram-positive bacteria (Thomas and Delves-Broughton, 2005). Modified atmosphere packaging (MAP) can effectively reduce the rate of spoilage and extend shelf life of perishable fish (Torrieri et al., 2006). CO₂ hinders the growth of the respiratory organisms like *Pseudomonas* spp. and *Shewanella putrefaciens* and their counts in most cases do not exceed 10⁵-10⁶ cfu/g (Gram and Huss, 1996).

Gilthead seabream (*Sparus aurata*) is a Mediterranean fish of high commercial value due to its desirable characteristics (aroma, taste, white flesh). Products like chilled fillets from marine cultured Mediterranean fish have high commercial potential if their shelf life can be extended through packaging or minimal processing.

The objective was the kinetic modeling of temperature, MAP and OD with the addition of nisin as antimicrobial agent dependence on the shelf life loss rate of chilled fish fillets.

Materials and methods

Fresh gilthead seabream (*Sparus aurata*) fillets directly obtained in ice from the filleting line of a mariculture unit were cut into rectangular slices (3x3x1cm³, 10±1g) and treated at 15°C

in osmotic solution, 50:50 maltodextrin(DE47):NaCl/100g with or without nisin (1000 IU/g fish in the osmotic solution) for 45 min. Untreated and treated slices were either packed in air or MA packed at (50% CO₂-50% air) (Boss NT42N, Bad Homburg, Germany) and stored at controlled isothermal conditions (0, 5, 10 and 5°C). Gas headspace analysis took place with the CheckMate 9900 O₂/CO₂ device (PBI Dansensor, Ringsted, Denmark).

Total viable count, *Pseudomonas* spp., lactobacilli, *Brochothrix thermosphacta*, *Enterobacteriaceae*, *Shewanella putrefaciens* and yeasts and molds were measured with appropriate sampling and plating techniques. The microbial growth was modeled using the Baranyi Growth Model (Baranyi and Roberts, 1995) and kinetic parameters such as the rate (k) of the microbial growth were estimated.

2-Thiobarbituric acid reactive substances (TBARS) assay, to evaluate lipid oxidation, was performed according to the method of Loovas (Loovas, 1992). Total volatile basic nitrogen (TVB-N) and trimethylamine nitrogen (TMA-N) analyses were conducted on a single TCA extraction by distillation in a Kjeldhal rapid distillation unit (Büchi 321 Distillation unit, Flawwil, Switzerland) and titration with sulphuric acid (Pivarnik et al., 2001).

Sensory evaluation allowed the correlation of microbial population and chemical indices with organoleptically perceived spoilage. 8 trained panellists were asked to score appearance, colour, odour, taste and texture of fish. Rating was assigned separately for each parameter on a 1 to 9 descriptive hedonic scale (9 being the highest quality score and 1 the lowest). A score of 5 of overall sensory acceptability was taken as the average score for minimum acceptability.

Quality indices were kinetically modeled and temperature dependence of quality loss rates was modeled by the Arrhenius equation. The models developed from the isothermal experiments were validated at dynamic conditions (variable temperature profile with a T_{eff}≈9°C).

Results and discussion

The osmotic pre-treatment caused a significant moisture loss from the fish flesh. After osmotic pre-treatment for 45 min at 15°C the fish flesh had 68% moisture, 2.3% solid gain and 0.95 water activity. The addition of nisin in the osmotic solution did not affect the mass transfer from and to the fish flesh.

Growth curves of microbial flora in untreated and osmotically pre-treated with and without nisin gilthead seabream fillets packed in air or under MAP were fitted to the Baranyi equation, as shown representatively in Figures 1a-f, and the growth kinetic parameters at each condition were determined. *Pseudomonas* spp. dominated the spoilage microflora of aerobically packed fillets. This was in agreement with other authors who reported that *Pseudomonas* spp. can be the dominant spoilage microorganism in aerobic storage of fresh, chilled fish (Gram and Huss, 1996; Koutsoumanis and Nychas, 2000; Tsironi et al., 2009). Lactic acid bacteria defined spoilage at the MAP conditions. Similar results referring to the growth of lactic acid bacteria in fish stored under MA or vacuum have been reported in relevant reviews (Gram and Huss 1996, Sivertsvik et al., 2002).

The microbial count reduction after the osmotic pre-treatment was 0.3-1.0 log cfu/g, depending on the bacteria species. The osmotic pre-treatment led to significantly lower microbial growth rates at all storage temperatures. Lowering the water activity to a value of 0.95, has a pronounced effect, especially on the growth rate of *Pseudomonas* spp. (Neumeyer et al., 1997). Under this context, osmotic treatment can extend the shelf life of gilthead seabream fillets, reducing the initial load and delaying microorganisms' growth.

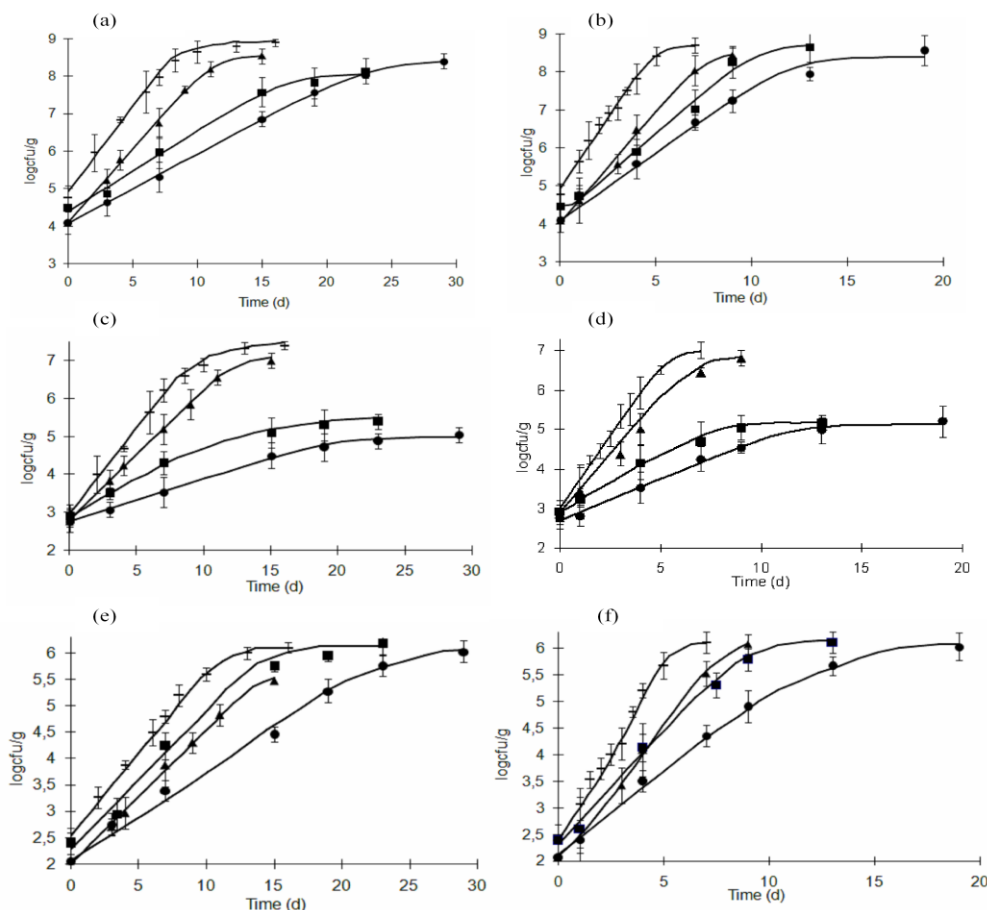


Figure 1. Development of microflora on gilthead seabream slices: untreated, stored aerobically (— Control); packed in modified atmosphere of 50% CO₂ (■ MAP); osmotically pretreated stored aerobically (▲ OD); osmotically pretreated stored in MAP (● MAP-OD). (a) TVC at 5°C (b) TVC at 10°C, (c) *Pseudomonas* sp. at 5°C, (d) *Pseudomonas* sp. at 10°C, (e) LAB at 5 °C and (f) LAB at 10°C.

Microbial growth was significantly inhibited in MAP samples at all storage temperatures compared to aerobically stored samples. It is evident that the growth rates of *Pseudomonas* spp. decreased significantly when MAP was used. *B.thermosphacta* and *S.putrefaciens* growth was significantly inhibited by MAP but not to the extent observed for *Pseudomonas* sp. The use of nisin in the osmotic solution was introduced as a means to further eliminate the growth of LAB (Gram-positive organisms) that defined spoilage at MAP conditions. Osmotically pre-treated samples with nisin stored under modified atmosphere led to the slowest bacterial growth.

The aerobically stored untreated samples showed increased TBARs value (1.20 mg malonaldehyde/kg) at 13 days of storage at 5°C, while osmotic pre-treated samples reached this value after 15 days. The use of nisin showed no difference in TBARs values, compared to the pre-treated samples. TVB-N values increased with storage time following apparent first order kinetics. Untreated samples packed in air showed significantly higher TVB-N values than osmotically pre-treated and modified atmosphere packed samples. Slow production of TMA-N was observed when sufficient O₂ for aerobic respiration was included in the package. The lowest values were observed in osmotically pre-treated with nisin samples packed under MA. The indices that could more consistently be correlated to storage time and temperature of the products were microbial growth (*Pseudomonas* spp. for aerobically packed and LAB for MAP samples) and the chemical index TVBN, showing high correlation with sensory scores, as indicated by their similar temperature dependence (65-75 kJ/mol). The processing of

gilthead seabream fillets with osmotic dehydration with nisin led to a significant shelf life extension as compared to untreated fillets (Table 1).

The specific growth rates of spoilage microorganisms and the rates of change of chemical indices and sensory scoring derived from the models was compared to those observed by experiments under dynamic conditions. The models gave satisfactory results with the predictions, with the relative errors being well below the 20% limit of applicability.

Table 1. Shelf life t_{SL} (d) of gilthead seabream slices: untreated, stored aerobically (Control); packed in MA 50% CO₂ (MAP); osmotically pre-treated and stored aerobically (OD); osmotically pre-treated and MAP (MAP-OD); osmotically pre-treated with nisin packed aerobically (ODn) and in modified atmosphere of 50% CO₂ (MAP-ODn) and stored at 5°C

| | t_{SL} (d) based on microbial growth (<i>Pseudomonas</i> sp.<10 ⁶ cfu/g for aerobically stored and LAB<10 ⁶ cfu/g for MAP fish) | t_{SL} (d) based on sensory evaluation (score for overall acceptability<5) | t_{SL} (d) based on TVB-N value (TVB-N<22 mg 100g ⁻¹) |
|---------|---|---|--|
| Control | 7±1.3 | 7±0.7 | 5±0.2 |
| OD | 9±0.9 | 9±0.4 | 9±1.1 |
| MAP | 14±1.4 | 15±2.6 | 13±0.5 |
| MAP-OD | 22±1.7 | 22±2.9 | 21±2.7 |
| ODn | 17±2.5 | 17±2.7 | 16±1.1 |
| MAP-ODn | 26±2.4 | 23±1.7 | 25±3.4 |

Conclusions

The objective of the present study was to evaluate the combined effect of osmotic dehydration with and without nisin and modified atmosphere packaging on the quality characteristics of gilthead seabream. The results of the study show the potential of using osmotic pre-treatment in combination with nisin as antimicrobial agent and MAP to extend the shelf-life and improve the commercial value of fresh chilled fish products. Models that correlate well with sensory evaluation or spoilage can be a reliable tool for predicting the shelf life of minimally treated and MA packed gilthead seabream fillets during refrigerated storage.

References

- Baranyi J., Roberts T.A. (1995). Mathematics of predictive food microbiology. *International Journal of Food Microbiology* 26, 199-218.
- Gram L., Huss H.H. (1996) Microbiological spoilage of fish and fish products. *International Journal of Food Microbiology* 33, 121-137.
- Koutsoumanis K., Nychas G.J.E. (2000) Application of a systematic experimental procedure to develop a microbial model for rapid fish shelf life predictions. *International Journal of Food Microbiology* 60, 171-184.
- Loovas E.A. (1992) Sensitive spectrophotometric method for lipid hydroperoxide determination. *JAOCs* 69, 777-783.
- Neumeyer K., Ross T., McMeekin T.A. (1997) Development of a predictive model to describe the effects of temperature and water activity on the growth of spoilage pseudomonads. *International Journal of Food Microbiology* 38, 45-54.
- Pivarnik L., Ellis P., Wang X., Reilly T. (2001). Standardization of the Ammonia electrode method for evaluating seafood quality by correlation to sensory analysis. *Journal of Food Science* 66(7), 945-952.
- Raoult-Wack A.L. (1994) Recent advances in the osmotic dehydration of foods. *Trends in Food Science & Technology* 5, 255-260.
- Sivertsvik M., Jeksrud W.K. and Rosnes J. 2002. A review of modified atmosphere packaging of fish and fishery products-significance of microbial growth, activities and safety. *International Journal of Food Science and Technology* 37, 107-127.
- Thomas L.V. and Delves-Broughton J. (2005) Nisin. In: P.M. Davidson, J.N. Sofos, A.L. Branen (Eds.), *Antimicrobials in Food*. 3rd ed. Taylor & Francis, CRC Press, Boca Raton, FL. p 237-274.
- Torrieri E., Cavella S., Villani F. and Masi P. (2006) Influence of modified atmosphere packaging on the chilled shelf life of gutted farmed bass (*Dicentrarchus labrax*). *Journal of Food Engineering* 77, 1078-1086.
- Tsironi T., Salapa I. and Taoukis P. (2009) Shelf life modelling of osmotically treated chilled gilthead seabream fillets. *Innovative Food Science and Emerging Technologies* 10, 23-31.

Development and use of Microbiological spoilage models in the food industry

L.K.Everis and G.D.Betts

Campden BRI, Chipping Campden, Glos. UK. (l.everis@campden.co.uk)

Abstract

The use of predictive models in the food industry as a quick, easy and inexpensive way of establishing the stability of product formulations and assessment of likely shelf life is increasing. The development of reliable, fully validated models is therefore of great benefit to the food industry. Campden BRI has produced many models that cover a wide range of spoilage organisms and product commodities.

Keywords

spoilage, models, food industry, Forecast, kinetic, time to growth

Introduction

Over the past few years the food industry has started to use predictive microbiological models to help in many areas of food manufacture, such as new product development, evaluation of recipe changes and determination of appropriate shelf-life and storage conditions. The type of model required will depend on the food category under consideration.

For perishable, short-shelf-life food products, kinetic growth models that are able to give reliable estimations of lag time and growth rate are most appropriate. In such products, a certain amount of growth of spoilage organisms can be tolerated provided the levels do not exceed any microbiological criteria that have been set. Use of predictive models can ensure that the product formulation or storage conditions chosen will be appropriate to control the growth, so that these criteria are achieved.

For ambient stable products such as acid preserved foods or drinks and fruit based products, it is not the rate of growth which is important but more the ability for growth to be initiated. In these long shelf-life products, the formulation conditions must be designed to prevent any growth throughout life, as once growth begins it is inevitable that the product will spoil. A different modelling approach based on growth/no growth or likelihood of growth occurring is needed for these foods. These models can be used to predict whether spoilage is likely to occur rapidly (within 0-4 weeks), slowly (within 1-6 months) or not at all.

Development of dynamic kinetic growth models for a range of spoilage groups (*Pseudomonas*, Enterobacteriaceae, lactic acid bacteria, *Bacillus*) and for specific products such as fish and meat where a mixed spoilage consortium comprising several genera of organisms are present would be of great benefit for the food industry. Making these models to be dynamic allows fluctuating temperature conditions to be considered. This allows more realistic predictions to be obtained, as it ensures that the temperature profile represents the conditions that products will encounter during distribution and sale. Development of models that allow the likelihood of spoilage of long life ambient products to be predicted can save the food industry valuable time in product development and can save the industry money by reducing both microbial testing costs and product spoilage and hence wastage.

Two of the models produced by Campden BRI, the Enterobacteriaceae model and acid preserved foods spoilage model, will be discussed in further detail.

Materials and Methods

Suitable microbiological broth media were chosen depending upon the model to be produced and the microorganisms to be used, for example Tryptone Soya Broth (TSB, Oxoid CM 0129) for Enterobacteriaceae modelling or de Mann Rogosa Sharpe Broth (MRSB, Lab M, lab 94) for modelling cocktails of spoilage yeasts, moulds and lactics. The relevant amount of salt or sugar was then added to the base medium to give the required concentration. The pH of the

broth was adjusted using hydrochloric acid or sodium hydroxide and preservatives were added where relevant.

Once prepared, these broths were inoculated with a cocktail of organisms grown to late exponential phase. The microorganisms used were appropriate to the spoilage group or product type under consideration. For the Enterobacteriaceae model the following organisms were used: *Proteus mirabilis* (CRA 615), *Klebsiella pneumoniae* (CRA 1483), *Citrobacter freundii* (CRA 3777), *Enterobacter cloacae* (CRA 4933) and *Hafnia alvei* (CRA 4936). The organisms were inoculated at a level of 10^2 - 10^3 cfu/ml and these were enumerated over time using standard microbiological procedures. This data was modelled using the Baranyi parameterisation of the four-parameter Gompertz model and a quadratic response surface model in a single global fitting approach. The single fitting approach does not require complete curves to be generated, which means that it is more data efficient.

For spoilage organisms of relevance to cold filled acidified foods the following organisms were used: yeasts: *Pichia membranefaciens* (VYAPi 01-02) and *Zygosaccharomyces bailii* (VYASa 07-01), moulds: *Monascus ruber* (VMEuMo 01-02), *Penicillium roqueforti* (VMMope 16-07) and *Penicillium verrucosum* (VMMope 20-07) and lactic acid bacteria: *Lactobacillus buchneri* (VBLLa 18-01). In this case, the organisms were inoculated at a level of approximately 10^5 cfu/ml, and the time for the broths to show turbidity as a sign of growth was assessed. A different type of modelling technique was used to develop the models for the acidified foods as no growth curves were generated (Everis and Betts, 1999). Due to the increased number of parameters involved, i.e. pH, aw, salt, sorbate and benzoate, the possible number of combinations required was large. A matrix of 1306 conditions was used to produce the cold fill spoilage model and the time to growth data was fitted using a Classification and Regression Trees approach (CART). This CART model is purely descriptive, working with classes or categories rather than with actual times to growth. So, for the purpose of fitting a CART model, times to growth were categorised as : under 15 days, under 1 month, under 3 months, under 5 months and over 5 months, i.e. no growth. The application of this technique is carried out by a computer program and the output is a logical classification tree. Each branch of the tree corresponds to a test and a decision as to whether a certain factor is above or below a critical value, calculated by the program. The tree provides a complete description of the classification scheme. The program places restrictions on the number of branches and end-point nodes so that the tree becomes manageable. It is then a question of applying the set of rules defining the tree to a new set of data, to see whether the rules still hold.

All Campden BRI spoilage models are fully food validated. Relevant foodstuffs were inoculated with the organisms used in the production of the model and were stored at the appropriate temperatures. Either the level of organisms present or the turbidity and changes in physical appearance were then noted. The data generated from these studies were then compared to the broth data.

Results and Discussion

For the Enterobacteriaceae kinetic growth model there was a good fit to the data, with a residual square (R^2) value of 80% and a root mean square value (rms) residual error of 0.86 \log_{10} (count). There was good agreement between fitted and observed \log_{10} (counts) and this is illustrated graphically in Figure 1 for the 1.0% salt conditions (Everis and Betts, 2008).

This CART model fitted the cold fill spoilage data well, with 84% of the data predicted correctly overall. It was better at predicting where growth occurred, predicting 98% of them correctly whereas only 78% of the no growth situations were correctly modelled. (Table 1). The full list of spoilage models available at Campden BRI for industrial applications is given in Table 2

Figure 1. Growth curves at salt = 1.0%

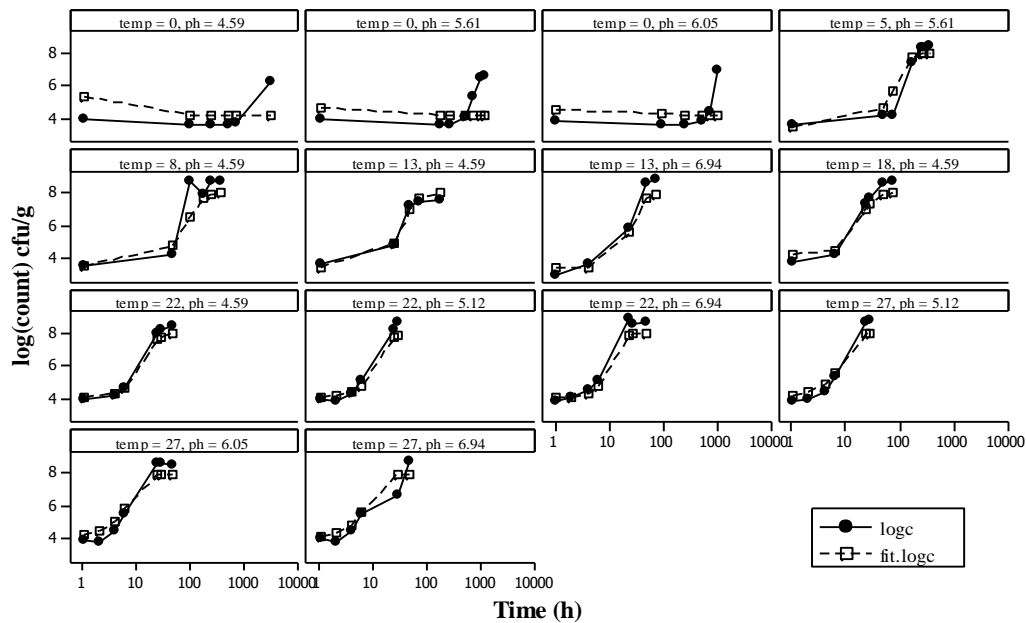


Table 1: Results for cold fill spoilage organisms in terms of predictions of growth/no growth in 270 days

| Trial result | No. of trials | | Predicted | Not predicted | |
|--------------|---------------|--|-------------|---------------|--|
| Growth | 347 | | 339 (97.7%) | 8 (2.3%) | |
| No growth | 998 | | 790 (79%) | 208 (21%) | |

| Days | 1 to 14 | 15 to 30 | 31 to 60 | 61 to 270 | No growth |
|---------------------------------|-----------|----------|----------|-----------|-----------|
| No. of broths exhibiting growth | 190 | 60 | 54 | 43 | 998 |
| No. predicted correctly | 158 (83%) | 40 (67%) | 29 (54%) | 38 (88%) | 790 (79%) |
| No. incorrectly predicted | 32 (17%) | 20 (33%) | 25 (46%) | 5 (12%) | 208 (21%) |

Conclusions

The spoilage models described here cover a wide range of spoilage organisms, groups of organisms and product types. They are suitable for use with a wide range of product types including chilled foods, meats, fish, drinks, ambient stable acidified foods and fresh produce. These models are widely used to aid the food industry with developing stable product formulations, assessing potential shelf life and in trouble shooting when there are deviations with parameters such as pH, salt or temperature of storage.

References

- Everis L. and Betts G. (2008). Modelling the increase and growth of spoilage microorganisms in food: Production of an Enterobacteriaceae model for predictions under fluctuating conditions. Campden BRI, Chipping Campden, Glos. UK R&D Report No. 269.
- Everis L. and Betts G. (1999). Unpublished. The final report of the acid preservation club. Campden BRI, Chipping Campden, Glos. UK.

Table 2: Spoilage models available in FORECAST

| Model | Temperature (°C) | NaCl (% aq) | Equivalent a_w | pH | Other Conditions |
|---|------------------|-------------|------------------|-----------|---|
| Kinetic models: | | | | | |
| <i>Pseudomonas</i> | 0 - 15 | 0.0 - 4.0 | 1.00- 0.977 | 5.5 - 7.0 | Fluctuating temperature, pH, salt |
| <i>Bacillus</i> spp. | 5 - 25 | 0.5 - 10 | 0.997 – 0.935 | 4.0 – 7.0 | Fluctuating temperature, pH, salt |
| Enterobacteriaceae | 0 - 27 | 0.5 - 10 | 0.997 – 0.935 | 4.0 - 7.0 | Fluctuating temperature, pH, salt |
| Yeasts (chilled foods) | 0 - 22 | 0.5 – 10 | 0.997 – 0.935 | 2.6 – 6.0 | Fluctuating temperature, pH, salt |
| Lactic acid bacteria | 2 - 30 | 0.5 - 10 | 0.997 – 0.935 | 3.0 – 6.0 | Fluctuating temperature |
| Meat spoilage | 2 - 22 | 0 – 6 | 1.00-0.964 | 4.6 – 7.0 | 0 – 240 KNO ₂ (ppm) Fluctuating temperature, pH, salt |
| Fish spoilage | 2 - 22 | 0 - 6 | 1.00-0.964 | 4.5– 8.0 | Fluctuating temperature, pH, salt |
| Fresh produce TVC | 2-25 | - | - | - | |
| Fresh produce Enterobacteriaceae | 2-25 | - | - | - | |
| Fresh produce lactic acid bacteria | 2-25 | - | - | - | |
| Fresh produce <i>Pseudomonas</i> | 2-25 | - | - | - | |
| Time to growth models | | | | | |
| Yeasts (fruit/drinks) | 0 - 22 | - | | 2.0 – 7.0 | 0 - 60 % Sucrose (w/v) 0 – 20% Ethanol (v/v) Potassium sorbate 0 – 1000 (ppm) |
| <i>Bacillus</i> | 8-45 | 0.5-10 | 0.997 – 0.935 | 4.0-7.0 | |
| Cold fill spoilage (yeasts, moulds, lactics) | 25 | 0.5 – 18 | 0.85 – 1.00 | 2.8 – 5.0 | Benzoate Sorbate 0–2000 (in total) |
| Cold fill pathogens (<i>E.coli</i> , <i>S.aureus</i> <i>Salmonella</i>) | 25 | 0.5 – 16 | 0.87 – 1.00 | 3.9 – 5.0 | Benzoate Sorbate 0–2000 (in total) |
| Hot fill spoilage <i>B. polymyxa</i> <i>B.coagulans</i> <i>B. cereus</i> <i>C. tyrobutyricum</i> <i>C. pasteurianum</i> <i>C. butyricum</i> | 25 | 0.5 – 18 | 0.86 – 1.00 | 3.7 – 5.2 | Benzoate Sorbate 0–2000 (in total) |
| Thermal death model | | | | | |
| Enterobacteriaceae | 52 to 64 | 0-8 | 1.00-0.95 | 4.0-7.0 | Predicts D value |

Biological Time Temperature Integrators as quality and safety indicators of refrigerated products

M. ELLOUZE^{1,2}, and J-C. AUGUSTIN²

¹ CRYOLOG S.A. 58, Boulevard Gustave Roch, 44261 Nantes, France. (mellouze@cryolog.com)

² Unité MASQ, Ecole Nationale Vétérinaire d'Alfort, 7 Avenue du Général de Gaulle F-94704 Maisons-Alfort cedex, France. (jcaugustin@vet-alfort.fr)

Abstract

The aim of this study was to evaluate (eO)[®], a biological Time Temperature Integrator (TTI) as a quality and safety indicator for three examples of refrigerated food: ground beef and chicken slices under modified atmosphere and cold smoked vacuum packed salmon. Storage trials and challenge tests were thus performed under static temperatures to model the behaviors of three pathogens (*Salmonella*, *Listeria monocytogenes* and *Staphylococcus aureus*) and the indigenous flora in the studied foods. In parallel, specific TTI prototypes were developed for each of the three products. The TTIs color evolution under static and dynamic temperatures was monitored and modeled. Using the collected data, exposure assessment models were set and used under several storage conditions to assess the distributions of the concentrations of the indigenous food flora and the distributions of the increase in the pathogens population at the end of the product shelf life or at the end point of the TTI. These distributions were compared to check if the TTI response was appropriate for monitoring the quality and safety of the studied products.

Key words

Biological TTI, Refrigerated Products, Exposure Assessment, *Listeria monocytogenes*, *Salmonella*, *Staphylococcus aureus*.

Introduction

Nowadays, refrigerated products are widely consumed but are still considered as sensitive foods. In fact, the temperature at which they are handled is a major factor determining their quality and safety as it influences the rate of the growth of pathogens or alteration microorganisms (McMeekin *et al.*, 2008). Several traceability tools have been previously proposed to keep track of the time temperature history to which perishable products are exposed (Kerry *et al.*, 2006) among which Time Temperature Indicators (TTIs) are a promising alternative. These are simple and user friendly devices which are put on the food packaging to indicate when the food is spoiled by measurable and irreversible time temperature dependent changes, usually expressed by mechanical deformations, color development or color change (Taoukis and Labuza, 1989).

In the present work, a biological TTI (eO)[®] commercialized by the French company CRYOLOG was studied. (eO)[®] is shaped like a green flower in which a selected strain of lactic acid bacteria (*C. piscicola*) is trapped. In case of inappropriate storage conditions, *C. piscicola* produces lactic acid causing a continuous pH decrease in the TTI medium leading to a color change of the TTI chromatic indicator. The green flower thus becomes red to indicate that the product is no longer fit for consumption. The aim of this study was to evaluate (eO)[®] as a quality and safety indicator through an exposure assessment model applied to three examples of refrigerated food: ground beef and chicken slices packed under modified atmosphere and cold smoked vacuum-packed salmon.

Materials and methods

The evolution of the indigenous bacteria in several batches of the studied food was monitored in iso-thermal conditions ranging from 2 to 30°C (Table1) then modeled by a primary model without lag (Baranyi and Roberts, 1994) and a square root type secondary model (Ratkowsky *et al.*, 1982). The evolutions of *L. monocytogenes*, *Salmonella* and *S. aureus* were modeled by a primary model with a lag time (Baranyi and Roberts, 1994) and a cardinal type secondary model (Rosso *et al.*, 1995). When appropriate, the evolution of the maximum population density with

temperature was modeled by a linear model. The microbial growth parameters were thus assessed, validated and implemented in the exposure assessment model.

Table 1. Food experimental design

| Foods | Nb of batches | T (°C) | Food characteristics | |
|-----------------------|---------------|---------------|--|--------------------------------|
| | | | Microbiological | Physico-chemical |
| Salmon | | | | |
| Storage trials | 4 | 2,4,8,12, 25 | Mesophilic and Psychrotrophic Aerobic Flora, Lactic Acid Bacteria, Thermotolerant Coliforms | pH : 723 measures |
| Challenge tests | 2 | 2,4,8,12, 25 | <i>L. monocytogenes</i> strains INRA 100, INRA 101, INRA 103, TQA 200 stressed by starvation | aw : 754 measures |
| | 1 | 8,12 | <i>L. monocytogenes</i> strain INRA 100 stressed by a disinfectant | |
| | 1 | 8,12 | <i>L. monocytogenes</i> strain TQA 200 stressed by a "salmon process" stress | |
| Ground beef | | | | |
| Storage trials | 4 | 2,4,8,12 | Mesophilic Aerobic Flora, Lactic Acid Bacteria, Thermotolerant Coliforms, <i>Enterobacteriaceae</i> , <i>E. coli</i> | pH : 161 measures |
| Challenge tests | 3 | 2,4,8,12 | <i>L. monocytogenes</i> strain INRA 100 stressed by starvation | aw : 235 measures |
| | | | | CO ₂ : 133 measures |
| Chicken slices | | | | |
| Storage trials | 3 | 4,8,15,20,25 | Mesophilic Aerobic Flora, Lactic Acid Bacteria, Thermotolerant Coliforms, <i>Enterobacteriaceae</i> , <i>E. coli</i> | pH : 846 measures |
| Challenge tests | 3 | 8,15,20,25,30 | <i>L. monocytogenes</i> strain INRA 100 stressed by starvation | aw : 276 measures |
| | 4 | 8,15,20,25,30 | <i>Salmonella</i> strains SOR 302 and AER 300 stressed by starvation | CO ₂ : 282 measures |
| | 1 | 15, 25 | <i>Salmonella</i> strain AER 300 stressed by a disinfectant | |
| | 4 | 8,15,20,25,30 | <i>S. aureus</i> strains S47 and S44 stressed by starvation | |
| | 1 | 15, 25 | <i>S. aureus</i> strain S44 stressed by a disinfectant | |

The temperature dependence of the color change of the TTIs was investigated by monitoring their *a* and *b* coordinates and modeled isothermally (Table 2) for three batches for each TTI setting using the following equations based on the angle of color $h = \tan^{-1}(b/a)$:

$$h = h_i + \frac{h_f - h_i}{1 - \exp(-R) + \exp(-R + \mu_h t)} \quad (1)$$

$$t_r = \frac{1}{\mu_h} \left(R + \ln \left(\exp(-R) - \frac{h_i}{h_f} \right) \right) \quad (2)$$

where *h* is the angle of color at the time *t*(h), *h_i* and *h_f* its initial and final values, respectively and *R* a constant that relates the specific rate of color change (*μ_h*) and the time of response of the TTI (*t_r*) according to equation (2). *μ_h* was further modeled by a square root type model (Ratkowsky *et al.*, 1982) to predict its evolution with temperature. The estimates of the parameters were validated under non iso-thermal conditions (Table 2) and the TTI model was used to predict the time of response of the TTI for any temperature profile. Monte Carlo simulations were finally performed using either the pathogen or the indigenous microflora parameters on several storage profiles to predict the level of microbial spoilage or the increase in the pathogen population to which a consumer may be exposed by eating a food at its use by date or at the TTI end point.

Table 2. TTI experimental design

| Food shelf life (S) | Reference Profile for TTI Setting | Isothermal temperatures (°C) | Dynamic temperature profiles |
|--------------------------|------------------------------------|------------------------------|--|
| Salmon: 28 days. | 28 days at 4°C. | | 1/3(S) at 2°C and 2/3(S) at 15°C. |
| Ground beef: 9 days. | 3 days at 4°C 6, days at 8°C. | 2, 4, 8, 15, 20, 30. | 1/3(S) at 4°C and 2/3(S) at 8°C. |
| | | | 1/3(S) at 15°C and 2/3(S) at 4°C. |
| Chicken slices: 16 days. | 5.3 days at 4°C, 10.7 days at 8°C. | | 1/3(S) at 2°C 8h at 15°C and then 4°C. |

Results and discussion

The results of the alteration exposure assessment model applied to ground beef packed under modified atmosphere are presented in Figure 1. The correspondent TTI prototype was set to reach its end point after 3 days at 4°C and 6 days at 8°C (Table 2) which represents the shelf life validation protocol for the ground beef samples used in this study. In the reference conditions (Fig 1.a) the TTI meets this specification as it changes to red exactly after 9 days, and the cumulative probability distributions obtained at its end point or at the end of the shelf life are unsurprisingly identical. These are considered as reference curves, obtained in ideal storage conditions, to which the cumulative probability distributions obtained in real storage profiles will be compared. When the cold chain is globally respected (Fig 1.b) the concentration of the indigenous microflora at the time of response of the TTI is very close to that obtained at the end of the product shelf life and is estimated to 7.4 log CFU g⁻¹ in 50% of the simulations which is slightly smaller than the concentration obtained in the reference condition (7.6 log CFU g⁻¹). In case of bad storage (Fig 1.c), the TTI response is reached after 6.6 days and there is an important difference between the concentrations obtained in 50% of the cases at the end of the 9 days shelf life (8 log CFU g⁻¹) and at the TTI end point (5.9 log CFU g⁻¹). Thus, the use of the TTI makes the consumer eat the product earlier and contributes, in 50% of the cases, to a 2 log CFU g⁻¹ reduction in the concentration of the indigenous microflora at consumption.

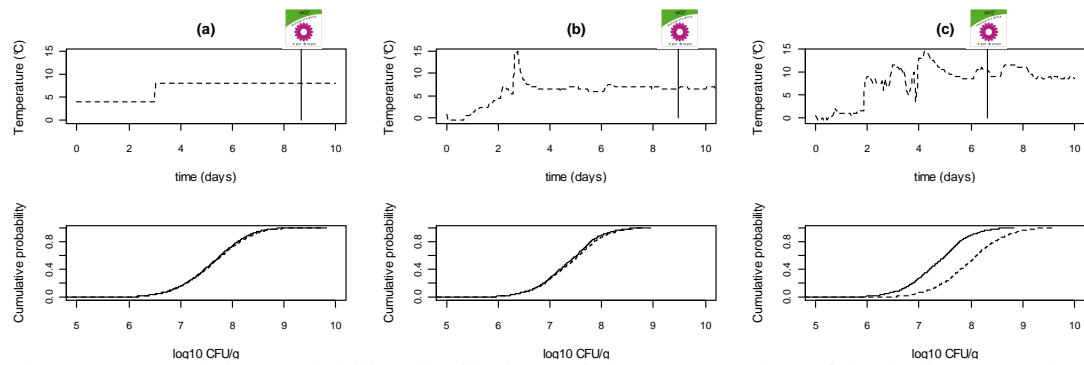


Figure 1. Cumulative probability distributions of the concentration of the indigenous microflora obtained for (a) reference (b) good and (c) bad storage conditions in ground beef at the end point of the TTI (solid lines) and at the end of the product shelf life (dashed lines).

Figure 2 depicts the results of the exposure assessment model of *L. monocytogenes* in cold smoked salmon. The end point of the TTI used for this product was based on its shelf life validation protocol of 28 days at 4°C. Figure 2.a shows that the TTI complies with the specifications as the shelf life and TTI curves of reference are identical. The cumulative probability distributions obtained in real storage profiles show a clear reduction in the increase in the *L. monocytogenes* population when applying the TTI. In fact, the TTI distributions are systematically shifted to the left compared to the use by date distributions. For example, in case of a bad storage, in 50% of the cases, the increase in the *L. monocytogenes* population at the use by date was estimated to 6.4 log CFU g⁻¹ (Fig 2.c) while only a 2.7 log CFU g⁻¹ increase was observed for the TTI distribution. Thus, in case of a single cell contamination of a 100 g slice of cold smoked salmon, in 50% of the cases, the increase in the *L. monocytogenes* population at the end of the shelf life would lead to a 25 000 CFU g⁻¹ contamination level, well above the authorized level of 100 *L. monocytogenes* g⁻¹. If the TTIs were used the product would have been consumed earlier which means that in 50% of the cases it would have only reached a 5 CFU g⁻¹ contamination level.

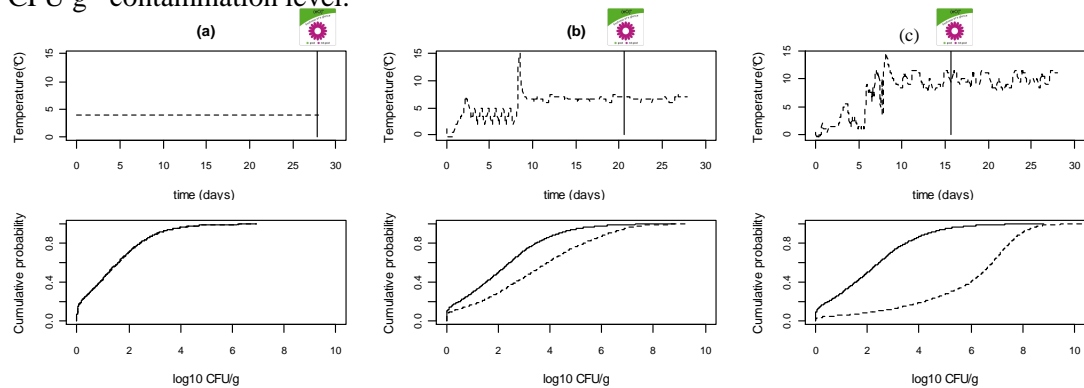


Figure 2. Cumulative probability distributions of the increase in the *L. monocytogenes* population obtained for (a) reference (b) good and (c) bad storage conditions in cold smoked salmon at the end point of the TTI (solid lines) and at the end of the product shelf life (dashed lines).

Similar results were obtained for *L. monocytogenes*, *Salmonella* and *S. aureus* in chicken slices. Figure 3 shows that the increases in the pathogen populations obtained either in good or in bad storage conditions when using the TTIs were always smaller than those obtained at the end of the shelf life (Fig 3.b and 3.c).

The TTI distributions for *L. monocytogenes* (Fig 3.b and 3.c) were very similar (0.1 log CFU g⁻¹ difference) to those obtained for the reference conditions (Fig 3.a) which proves that consuming the chicken slices at the TTI end point, whatever its time temperature history, is equivalent to consuming a product that was properly stored during its entire shelf life with regards to the *L. monocytogenes* hazard.

However, 1 and 2 log differences in the *S. aureus* and *Salmonella* population increases were respectively obtained between the reference storage conditions (Fig 3.a) and the realistic storage conditions (Fig 3.b and 3.c) at the TTI end point.

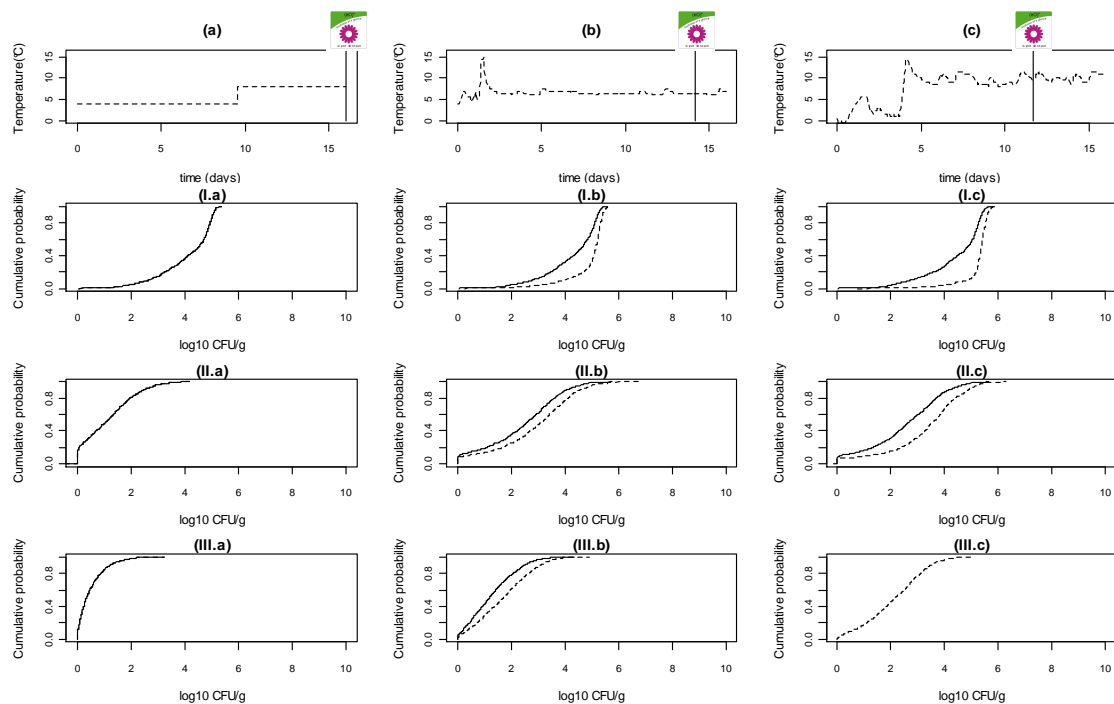


Figure 3. Cumulative probability distributions of the increase in the population of *L. monocytogenes* (I), *Salmonella* (II) and *S. aureus* (III) obtained for (a) reference (b) good and (c) bad storage conditions in cooked chicken slices at the end point of the TTI (solid lines) and at the product shelf life (dashed lines).

These differences can be explained by the behavior of the TTI micro-organism which is closer to the *L. monocytogenes* behavior but rather different from those of *Salmonella* and *S. aureus*. Despite that, the TTI also reduced the consumer exposure to these pathogens, especially in bad storage conditions. Indeed, when considering for example *S. aureus*, a 2.2 log CFU g⁻¹ increase was observed at the end of the shelf life in 50% of the cases while only a 1.2 log CFU g⁻¹ increase was obtained when using the TTI. The same result was observed for *Salmonella*. Thus, in case of bad storage conditions and in 50% of the cases, under the scenario of a single cell contaminating a 100 g portion of chicken slices, 4 *Salmonella* cells would have been found in the product at the end point of the TTI while 32 *Salmonella* cells would have developed at the end of the shelf life in the 100 g chicken slices portion.

These results show that, in case of a bad storage and in 50% of the cases, the TTIs help reduce the exposure to *S. aureus* by a factor 10, to *Salmonella* by a factor 8 and to *L. monocytogenes* by a factor 4.

Conclusion

Given the results of this study, correctly set TTIs can be considered as valuable tools to monitor the food quality and safety of refrigerated products as they significantly reduced the consumer exposure to the studied pathogens and alteration microorganisms in the considered refrigerated foods.

References

- Baranyi J. and Roberts T. A. (1994). A dynamic approach to predicting bacterial growth in food *International Journal of Food Microbiology*, 23, 277-294.
- Kerry J. P., O'Grady M. N. and Hogan S. A. (2006). Past, current and potential utilisation of active and intelligent packaging systems for meat and muscle-based products: A review. *Meat Science* 74, 113-130.
- McMeekin T., Bowman J., McQuestin O., Mellefont L., Ross T. and Tamplin M. (2008). The future of predictive microbiology: Strategic research, innovative applications and great expectations. *International Journal of Food Microbiology* 128, 2-9.
- Ratkowsky D. A., Olley J., McMeekin T. A. M. and Ball A. (1982). Relationship between temperature and growth rate of bacterial cultures. *Journal of Bacteriology* 149, 1-5.
- Rosso L., Lobry J. R., Bajard S. and Flandois J. P. (1995). Convenient model to describe the combined effects of temperature and pH on microbial growth. *Applied and Environmental Microbiology* 61, 610-616.
- Taoukis P. S. and Labuza T. P. (1989). Applicability of time-temperature indicators as shelf life monitors of food products. *Journal of Food Science* 54, 783-788.

The importance of growth/no growth models for specific spoilage organisms within the food industry

A. Vermeulen¹, T.D.T. Dang¹, J. Daelman¹, L. Mertens², A.H. Geeraerd³, J.F. Van Impe² and F. Devlieghere¹

CPMF² - Flemish Cluster Predictive Microbiology in Foods – www.cpmf2.be – (info@cpmf2.be).

¹ LFMFP – Laboratory of Food Microbiology and Food Preservation. Dept. of Food Safety and Food Quality, Ghent University, Coupure links 653, B-9000 Ghent, Belgium. (a.vermeulen@UGent.be)

² BioTeC – Chemical and Biochemical Process Technology and Control, Dept. of Chemical Engineering, KULeuven, W. de Croylaan 46, B-3001 Leuven, Belgium (jan.vanimpe@cit.kuleuven.be)

³ MeBioS – Division of Mechatronics, Biostatistics and Sensors, Dept. of Biosystems, KULeuven, W. de Croylaan 42, B-3001 Leuven, Belgium (Annemie.geeraerd@biw.kuleuven.be)

Abstract

Predictive models are often focusing on safety aspects such as growth of pathogens, toxin and mycotoxin production. Next to food safety, an additional important field of interest for the food industry is the prediction of microbial stability. There is the possibility that growth of spoilage microorganisms will lead to enormous economical losses. Nowadays, also new challenges appear for food producers as consumers and authorities adopt a more critical attitude towards food. Trends in lowering salt, sugar and fat content in different food products are observed. In this way the hurdles which assure the microbial stability of these products will approach their limits. Growth/no growth models can be very advantageous for product innovations and particularly those focusing on certain food products. In this article, two different product-specific growth/no growth models for yeast will be presented. The first model describes the growth probability of *Z. bailii* in sauces at different temperatures and the second model focuses on the growth chances of *Z. rouxii* in intermediate moisture foods. Both models are also incorporated in software programs to improve the transfer of scientific knowledge to industrial practice.

Introduction

As the consumers, retail and authorities are more focussing on healthier foods (lower fat, sugar and salt content), the food industry is confronted with new challenges. By reducing these ingredients different hurdles to inhibit growth of micro-organisms are fading away. For a lot of products this might lead to microbial instability. Product innovations combined with determination of microbial stability can be very time-consuming, labour intensive and expensive, particularly for products with a prolonged shelf-life. Therefore, the food industry is the steering force in the development of predictive (growth/no growth) models specific for their products. This will give the food business operators well-founded and practical guidelines during the process of product innovation. It will give the opportunity to estimate in advance the influence of changing ingredients and product characteristics on the microbial stability. Growth/no growth models were developed for two product types, which are looked upon as unhealthy because of their high sugar and fat content. The models for *Z. bailii* in sauces incorporate a_w , pH and acetic acid as variables (Dang et al., 2009). Chemical preservatives were deliberately excluded out of the model as these are disputed by consumers and authorities. The models were developed at two different temperatures, 22 en 30°C, and different incubation times. The models for intermediate moisture foods (such as chocolate fillings, cakes, marzipan, etc.) focused on the effect of pH, a_w , ethanol and absence/presence of acetic acid.

Material and Methods

Medium preparation

Media were prepared based on Sabouraud (SAB, Oxoid) and adapted depending on the target product. For the sauce model, glucose (G-8270, Sigma Aldrich, Steinheim, Germany) and

fructose (F-0127, Sigma Aldrich) were added to SAB to have in total 15% (w/v) sugar (1:1 ratio). This was done to mimic the high sugar content of sweet-and-sour sauces. The intrinsic factors were changed by adding NaCl (Vel 1723, VWR, Leuven, Belgium) (a_w ranging from 0.93 to 0.97, 5 levels), acetic acid (UN2789, VWR) ranging from 0 to 2.5% (6 levels). The pH was adjusted by adding HCl (5 N, VWR) and/or NaOH (5N, VWR) to levels between 3.0 and 5.0 (5 levels). Media were sterilized and stored at room temperature. More detailed information about the medium preparation can be found in Dang et al. (2009).

For the model for intermediate moisture foods 50 % sugar (1:1 ratio glucose/fructose) was added. Additionally glycerol (Sigma Aldrich) was added to lower the a_w ranging from 0.76 to 0.88 (4 levels). Ethanol (Merck, Darmstadt, Germany) was added to the media in concentrations ranging from 0 to 4.5% (w/w) (4 levels). For the model with acetic acid 1% was added to all media. Finally the pH was adjusted by adding HCl (5 N, VWR) and/or NaOH (5N, VWR) to levels between 5.0 and 6.2 (4 levels).

Inoculation procedure and growth assessment

Both strains were stored at -75°C , inoculated in SAB and incubated 24h at 30°C for *Z. bailii* and 48h at 30°C for *Z. rouxii*. Subcultures were taken in acidified SAB (pH 4.0) for *Z. bailii* and normal SAB for *Z. rouxii*. Cultures were incubated again 24h or 48h at 30°C for *Z. bailii* and *Z. rouxii*, respectively. Before inoculation, cells were washed with a saline solution (8.5 % NaCl), resuspended in one of the specific media and diluted in the same medium until the appropriate inoculation level was reached (approx. 4 log CFU/ml). The cells were inoculated in 96 well format microtiter plates (Roll s.a.s, Plove di Sacco, Italy) which were filled with the different media. Wells were filled with 180 μL specific medium and inoculated with 20 μL of the appropriate culture. Growth at each condition was checked in at least 20 replicates. Plates were incubated at their specific temperature (22 or 30°C for *Z. bailii* and 22°C for *Z. rouxii*). To avoid evaporation of acetic acid and ethanol in the media for *Z. rouxii* which had to be stored at room temperature for a long period of time) extra precautions were taken. Firstly, the microtiterplates were covered by a Breath-easy film (Fiers NV, Kuurne, Belgium). Secondly, silicone (Henkel, Belgium) was applied on the frame of the microtiterplate before the lid was closed. To avoid changes in water activity the plates were stored at constant relative humidity. To achieve this microtiterplates with the same a_w were stored in closed jars which were for at least 1/10 filled with a glycerol solution of the same a_w . Growth was checked daily by optical density measurements, using a VERSAmaxTM microtiter plate reader at 600 nm. Growth was defined as $\text{OD}_{\text{sample}}$ which is consistently higher than three times the standard deviation of OD_{blank} (Vermeulen et al., 2007). Growth was assessed in each individual well of the replicates to have a detailed percentage of growth for each combination of intrinsic factors tested.

Model development

Data were in all cases described by an ordinary logistic regression model which consisted of a polynomial (right-hand side) and logit $p = \ln\left(\frac{p}{1-p}\right)$ (left-hand side) with p the probability

that growth occurred. The models were fitted using statistical software packages (SPSS, Inc., Chicago IL., USA) using linear logistic regression.

For each model, goodness-of-fit statistics were considered: (i) $-2 \log L$ with L the likelihood in its optimum, (ii) Akaike's Information Criterion ($\text{AIC} = -2 \log L - \text{number of parameters in model}$), and (iii) Hosmer-Lemeshow statistic. The predictive power was measured by c (the concordance index) which is equal to the area under the ROC-curve (Receiver Operating Curve). It estimates the probability that the predictions and the outcomes are concordant. A value $c = 0.5$ means that the predictions are no better than random guessing and the higher the value of c , the better the prediction (Agresti, 2002).

The predicted growth/no growth interfaces for $p = 0.1$, 0.5 and 0.9 for both models were plotted in Matlab®7.3 (The Mathworks, Inc., Natick, MA, USA).

Development of software tool

To improve the transferability of the developed models towards the industry, an integrated, user-friendly software tool was developed by using Matlab®7.3 Graphical User Interface (The Mathworks, Inc., Natick, MA, USA).

Results and discussion

Three different models were developed to describe the growth probability of *Z. bailii* in acidified sauces. The parameter estimates with their standard deviation and the performance statistics of the model are given in Dang et al. (2009). Comparing the model at 22°C with the one at 30°C revealed that at 30°C the growth zone was larger than at 22°C for acetic acid concentrations higher than 1.5%. The growth rate was, however, faster at 30°C. It might be that at these elevated temperature (30°C), the higher metabolism rate of the yeast made it more susceptible to stressful conditions, resulting in a lower growth probability. At 22°C a model was made for 45 days and one for 60 days incubation. As expected, more conditions were classified as growth after a longer incubation time. The data after 60 days showed some higher growth chances at conditions close to the growth/no growth boundary. However, the no growth zone remained stable (more details see Dang et al. 2009).

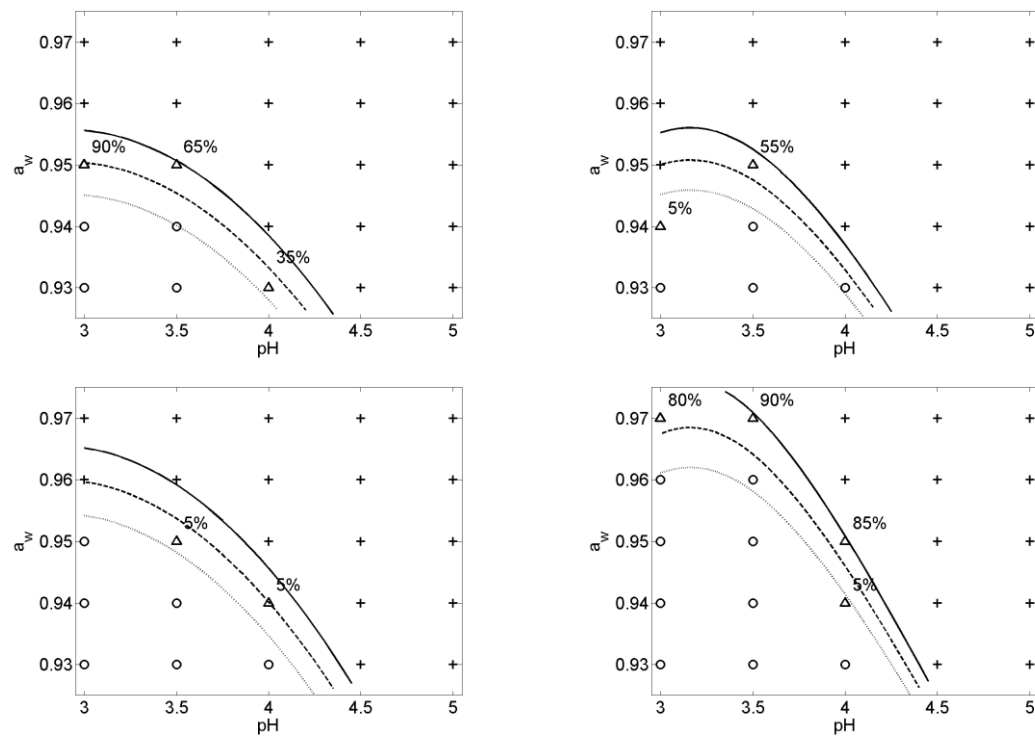


Figure 1: G/NG boundary of *Z. bailii* at 22°C (left column) and 30°C (right column) after 45-day incubation period at 1.5% (v/v) (upper row) and 2.0% (v/v) acetic acid (lower row) with (+) 100% growth, (o) no growth and (Δ) growth % $\in]0,100[$ indicated. Lines represent the ordinary logistic regression model, with $p = 90\%$ (—), $p = 50\%$ (---) and $p = 10\%$ (....).

For intermediate moisture foods two models were developed after 60 days incubation at 22°C. One model describes the G/NG interface at conditions without acetic acid while the other model includes 1% acetic acid at all conditions. The parameter estimates with their standard deviation and the performance statistics of the model are given in Table 1. Results showed that in media without acetic acid, pH had almost no influence on the growth/no boundary in the examined region (Fig 2a). This implicates that in these conditions only a very low a_w and/or high ethanol concentration was sufficient to inhibit growth. If 1% acetic acid was added to the media a significant pH effect was observed (Fig. 2b).

Table 1: Parameter estimates with their standard errors and performance statistics for the models at 22°C and 30°C.

| Parameter Statistics/predictive power | Without acetic acid | Acetic acid |
|---|---------------------|-----------------|
| Constant | -142.5 ± 37.6 | 1010.6 ± 211.9 |
| a_w | 252.6 ± 58.5 | -1339.9 ± 288.2 |
| pH | -0.74 ± 0.86 | -245.6 ± 45.3 |
| Ethanol | -13.1 ± 2.3 | 83.46 ± 16.1 |
| a_w^2 | N.S. ^a | -167.0 ± 29.0 |
| $a_w \cdot \text{pH}$ | N.S. | 349.6 ± 61.4 |
| $a_w \cdot \text{Ethanol}$ | -36.1 ± 16.0 | -50.8 ± 12.7 |
| $\text{pH} \cdot \text{Ethanol}$ | 1.4 ± 0.5 | -9.4 ± 1.3. |
| - 2 ln L | 50.388 | 225.408 |
| AIC | 56.388 | 239.408 |
| Hosmer-Lemeshow | 0.235 | 1.197 |
| | P-value = 0.999 | P-value = 0.997 |
| c-value | 0.999 | 0.996 |
| % concordant | 99.6 | 97.3 |

a Not significant (P = 0.001)

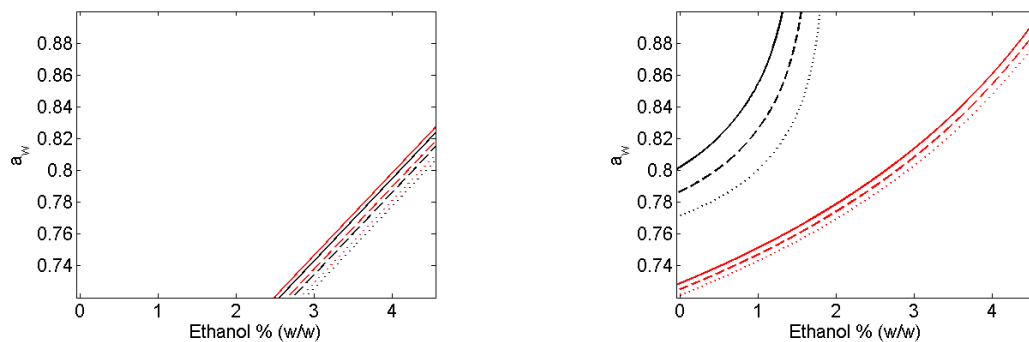


Figure 2: G/NG boundary of *Z. rouxii* at pH 5.0 (black) and pH 6.2 (red) after 60 at 0% acetic acid (left) and 1% acetic acid (right). Lines represent the ordinary logistic regression model, with $p = 90\%$ (—), $p = 50\%$ (---) and $p = 10\%$ (....).

Conclusion

Sauces as well as intermediate moisture foods are products, which will questioned more and more because of their high fat and sugar content. Besides these products can contain chemical preservatives. As lowering these factors to improve the nutritional quality of the products can compromise their microbial stability, combination technology will be unavoidable. Therefore, the industry is constantly searching for a way to quantify the effects of combination of stress factors for their products. Growth/no growth models are excellent instruments to fulfil this want. Besides the models are easily to use by food business operators during the process of product innovation when incorporated in user-friendly software, as was done during this research.

References

- Dang, T.D.T., Vermeulen, A., Ragaert, P. and Devlieghere, F. (2009). A peculiar stimulatory effect of acetic and lactic acid on growth and fermentative metabolism of *Zygosaccharomyces bailii*. Food Microbiology, 26 (3), 320-327.
- Vermeulen, A., Dang, T.D.T., Geeraerd, A.H., Bernaerts, K., Debevere, J., Van Impe, J., Devlieghere, F. (2008). Modelling the unexpected effect of acetic and lactic acid in combination with pH on the growth/no growth interface of *Zygosaccharomyces bailii*. International Journal of Food Microbiology, 124 (1), 79-90

SSSP version 3.1 from 2009: New freeware to predict growth of *Listeria monocytogenes* for a wide range of environmental conditions

P. Dalgaard¹, O. Mejlholm¹ and B. J. Cowan²

¹ Seafood & Predictive Microbiology, DTU Aqua, Technical University of Denmark, Søtofts Plads, Building 221, DK-2800 Kgs. Lyngby, Denmark. (pad@aqua.dtu.dk).

² Section for Software Development, DTU Aqua, DK-2800, Kgs. Lyngby, Denmark.

Abstract

The Seafood Spoilage and Safety Predictor (SSSP) software has been expanded by adding a new *Listeria monocytogenes* growth and growth boundary model that include the effect of temperature, NaCl/a_w, pH, CO₂, smoke intensity, nitrite, organic acids (acetic acid/diacetate, benzoic acid, citric acid, lactic acid, sorbic acid) and the interaction between all these environmental parameters. The new SSSP v. 3.1 freeware predicts growth of *L. monocytogenes* for a wide range of environmental conditions including constant and variable storage temperatures. Importantly, the new software predicts both the growth boundary and no-growth conditions with a defined distance to the growth boundary. This is important e.g. when predictions are used for development or modification of food formulations to prevent growth of *L. monocytogenes*. SSSP v. 3.1 can be used in 15 different languages to facilitate communication between the many parties interested in using predictions to manage food chains. The freeware is available from <http://sssp.dtuqua.dk>.

Keywords: Application software, growth/no-growth predictions, psi(ψ)-value, ready-to-eat foods.

Introduction

Software with predictive microbiology models is important to support decisions on safety and quality of food (Dalgaard et al. 2002; McMeekin et al. 2006; Tamplin et al. 2009). For *Listeria monocytogenes*, predictive modelling is specifically recognized in EU regulations to demonstrate control of its growth in ready-to-eat food (EC 2073/2005, EC 1441/2007). Several application software with *L. monocytogenes* growth models are available (Tamplin et al. 2009). However, complex predictive models are needed to accurately predict responses in processed and ready-to-eat food where several environmental parameters influence growth of *L. monocytogenes* (Mejlholm et al. 2009b). For practical applications of such complex mathematical models user-friendly software is needed but freeware to predict growth and the growth boundary of *L. monocytogenes* in food with organic acids including benzoic and sorbic acids is not available. The objective of the present study was to expand the existing Seafood Spoilage and Safety Predictor (SSSP) software with a flexible mathematical model that allow growth and the growth boundary of *L. monocytogenes* to be predicted for various foods and for a wide range of environmental conditions.

Materials and methods

SSSP v. 3.0 from December 2008 includes 14 different models to predict shelf-life and safety of seafood. This and previous versions of SSSP has been popular and are used world wide by more than 4000 people/institutions from 105 different countries. In 2009 SSSP has been expanded by adding an extensive *L. monocytogenes* growth and growth boundary model that includes the effect of temperature, NaCl/a_w, pH, CO₂, smoke intensity, nitrite, organic acids (acetic acid/diacetate, benzoic acid, citric acid, lactic acid, sorbic acid) and the interaction between all these environmental parameters. The new *L. monocytogenes* growth and growth boundary model was previously developed for shrimps and then both extensively and successfully validated for various seafood and meat products (Mejlholm and Dalgaard, 2009; Mejlholm et al. 2009b). The Logistic equation is used as primary growth model together with

a cardinal parameter model to predict the effect of storage conditions and product characteristics on growth and on the growth boundary of *L. monocytogenes*. Growth boundary predictions are obtained by using the Le Marc approach for interaction between environmental parameters (Le Marc et al. 2002). The new SSSP v. 3.1 software predicts the growth boundary of *L. monocytogenes* (with $\psi(\psi)$ -value of 1.0) depending on combinations of product characteristics and storage conditions. Furthermore, the new software can predict boundaries for other ψ -values. This is important to identify environmental conditions that prevent growth of *L. monocytogenes* and at the same time take into account the inherent variability in product characteristics and storage conditions (Mejlholm and Dalgaard, 2009; Mejlholm et al. 2009a).

Microsoft Visual C# .Net and Studio .Net were used to program SSSP v. 3.1. C# supports XML which was used for data handling within SSSP v. 3.1. XML also facilitated the development of a multi-language application. SSSP v. 3.1 has been translated into 15 different languages.

Results and discussion

SSSP v. 3.1 uses 2D and 3D graphs to illustrate the effect of combinations of environmental parameters on the growth boundary of *L. monocytogenes* (ψ -value of 1.0) as well as on other boundaries corresponding to ψ -values between 0.5 and 2.5 (Fig. 1 and 2). 3D graphs are useful to provide an overview of the environmental conditions that prevent growth of *L. monocytogenes* (Fig. 1). To facilitate extraction of more precise information from 3D graphs SSSP users can select specific points on these graphs and the software then provides corresponding coordinates in a dedicated results bar. This can be useful e.g. in the initial phase of developing or modifying food formulations to prevent growth of *L. monocytogenes*.

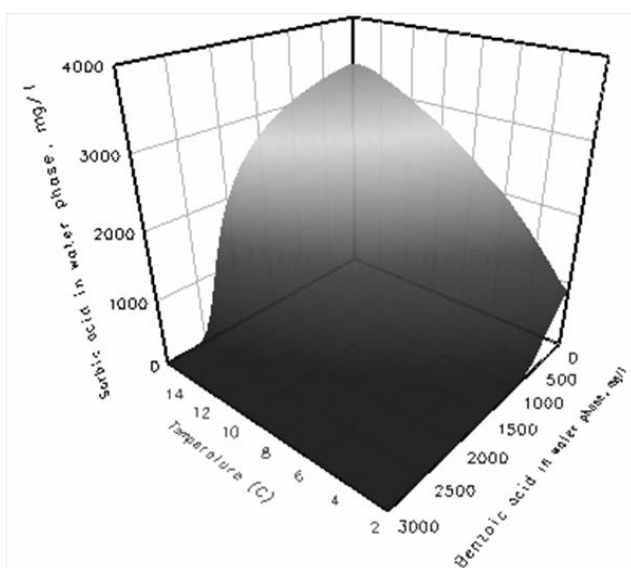


Figure 1: Predicted growth boundary for *L. monocytogenes* as influenced by different combinations of temperature and concentrations of benzoic and sorbic acids. Predictions were obtained for pH 6.0, with 4.0% water phase salt and 7000 ppm lactic acid in the water phase.

Small variations in product characteristics away from the growth boundary can result in unacceptable growth of *L. monocytogenes*. However, data from a very large validation study with seafood and meat products has shown that no-growth conditions corresponding to an ψ -value of 2.0 is sufficient to prevent growth of *L. monocytogenes* even when the inherent variability in the environmental conditions of these products are taken into account (Mejlholm et al. 2009b). To illustrate the effect of the ψ -value Figure 2 below shows predicted combinations of temperature and concentrations of diacetate and lactic acid corresponding, respectively, to ψ -values of 1.0 (growth boundaries) and 2.0 (boundaries within the no-growth space of the environmental conditions).

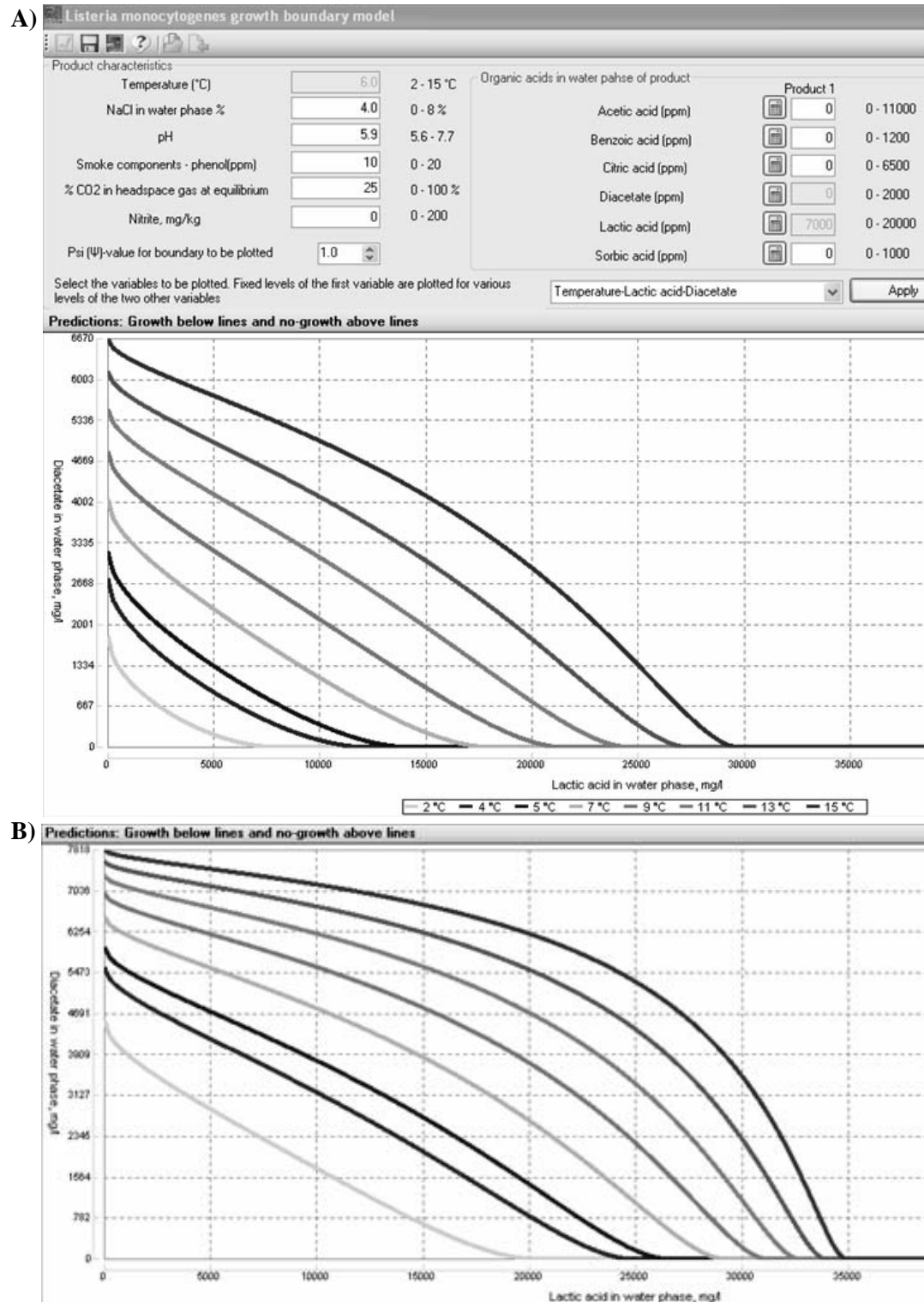


Figure 2: Predicted combinations of temperature, diacetate and lactic acid corresponding to: **A)** the growth boundary of *L. monocytogenes* with $\psi = 1.0$ and **B)** no-growth conditions with ψ -value of 2.0. This graph also shows the range of environmental conditions covered by SSSP v. 3.1.

According to EU regulations, concentrations of *L. monocytogenes* must remain below 100 cells/g within the shelf-life of ready-to eat foods (EC 2073/2005; EC 1441/2007). To meet this requirement SSSP v. 3.1 can predict appropriate combinations of storage conditions, product characteristics and safe shelf-life. Importantly, the effect of both constant and variable storage temperatures can be predicted. Figure 3 below shows the effect of a simple and fictive

temperature profile. However, SSSP v. 3.1 includes a flexible module to import product temperature profiles as collected by various types of data loggers.

To benefit the global food sector SSSP v. 3.1 has been translated into Chinese, Croatian, Danish, Dutch, English, Finnish, French, German, Greek, Italian, Spanish, Persian, Polish, Portuguese and Vietnamese by users of the freeware. This facilitates communication between the many parties interested in food chains. In fact, food chains (including raw materials, ingredients, processing, packaging and distribution to consumers) very often span wide geographical regions and various language zones. When SSSP v. 3.1 is used to determine e.g. the effect of temperature profiles during processing or distribution this information can conveniently be send to relevant food chain participants in a language that is understood not only by quality assurance personnel but also by those actually carrying out the practical processing and distribution of products.

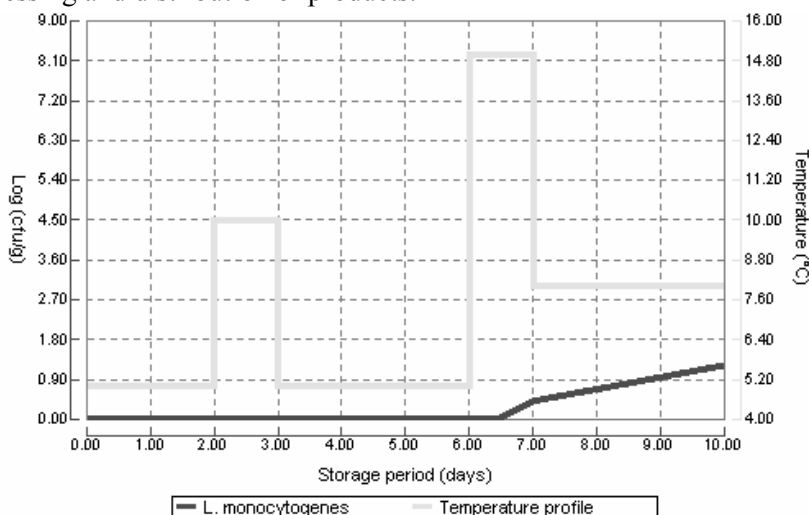


Figure 3: Effect of a simple temperature profile with variations between 5°C and 15°C on the predicted growth of *L. monocytogenes*. Predictions were obtained for pH 6.0 and with 3.0% NaCl, 1000 ppm benzoate/benzoic acid and 400 ppm sorbate/sorbic acid the water phase of the product.

Conclusions

SSSP v. 3.1 from 2009 is available for download from <http://sssp.dtuqua.dk>. This new version of the freeware can be used in 15 different languages and includes a growth and growth boundary model to predict growth responses of *L. monocytogenes* for a wide range of environmental conditions. SSSP v. 3.1 can be used both for seafood and meat products to evaluate and document *L. monocytogenes* growth responses.

References

- Dalgaard, P., Buch P., S. Silberg 2002. Seafood Spoilage Predictor – development and distribution of a product specific application software. *International Journal of Food Microbiology* 73, 227-233.
- Le Marc, Y., Huchet, V., Bourgeois, C. M., Guyonnet, J. P., Mafart, P. and Thuault, D. (2002). Modelling the growth kinetics of *Listeria* as a function of temperature, pH and organic acid concentration. *International Journal of Food Microbiology*, 73 (2-3), 219-237.
- McMeekin, T. A., Baranyi, J., Bowman, J., Dalgaard, P., Kirk, M., Ross, T., Schmid, S., and Zwietering, M. H. 2006. Information systems in food safety management. *International Journal of Food Microbiology*, 112 (3), 181-194.
- Mejlholm O. and Dalgaard P. (2009). Development and validation of an extensive growth and growth boundary model for *Listeria monocytogenes* in lightly preserved and ready-to-eat shrimp. *Journal of Food Protection*, 72, October issue, In press.
- Mejlholm O., Le Marc, Y. and Dalgaard P. (2009a). Evaluation of growth boundary models – importance of data distribution and performance indices. The present proceedings.
- Mejlholm, O., Gunvig, A., Borggaard, C., Hansen, F., Mellefont, L., Ross, T., Leroi, F., Else, T., Visser, D. and Dalgaard, P. (2009b). Predicting growth and growth boundary of *Listeria monocytogenes* – an international validation study with focus on processed and ready-to-eat meat and seafood. The present proceedings.
- Tamplin, M. 2009. Accessible modelling software and databases. *Bulletin of the International Dairy Federation*, 433, 59-64.

Evaluation of the microbial growth for different transport conditions of warm raw pork carcasses

L. Guillier

Agence française de sécurité sanitaire des aliments, Direction de l'évaluation des risques nutritionnels et sanitaires (French food safety agency), 27-31 Avenue du Général Leclerc, F-94701 Maisons Alfort cedex, France. (l.guillier@afssa.fr)

Abstract

The European regulation provides for the possibility for the Member States to derogate from the 7°C core temperature for transport of warm raw pork carcasses from the slaughterhouse to a cutting plant. In France, raw pork carcasses must attain the temperature of 12°C in the core of carcass before transport and the duration of transport cannot be longer than two hours. This work aims at establishing alternative transport conditions based on two different performance criteria. Alternative conditions were assessed by the calculation of the growth potentials of different micro-organisms (*Aeromonas hydrophila*, *Escherichia coli*, *Listeria monocytogenes*, *Salmonella*, and *Yersinia enterocolitica*). For micro-organisms several secondary models proposed by the Pathogen Modeling Program, the Combase Modelling Toolbox, Sym'Previus and other published models were tested. Growth occurring at the surface and in the core of the carcasses were considered. It was shown, according to performance criteria and assumptions made, that a large easing of the transport conditions of the actual regulation cannot be proposed.

Keywords : cooling; hygiene package; time-temperature equivalent

Introduction

At the end of the slaughter process, the temperature of pig carcasses is approximately 30°C at the surface and 38-40°C in the core. These temperatures are very conducive to the growth of most bacteria that contaminate carcasses. Consequently, post-mortem chilling processes are aimed at bringing down the temperature of the carcass as rapidly as possible, in order to primarily protect the microbiological quality of the meat and also, but with less emphasis on maintaining sensory and technological quality of meat.

Regulation 853/2004 of the European Parliament and of the Council of 29 April 2004 laying down specific hygiene rules for food of animal origin, sets out the modalities for livestock slaughter and the preparation of carcasses. Food business operators must ensure that meat must attain the core temperature of 7°C before transport. However, the regulation provides for the possibility for the Member States to derogate from the 7°C core temperature for transport of warm raw pork carcasses from the slaughterhouse to a cutting plant, with the purpose of obtaining fresh cut or deboned meat. In France, the competent authority actually enforces that meat must attain the temperature of 12°C in the core of carcass before transport, and remain at that temperature during a two-hour transport. A substantial number of meat processors, find it difficult to operate to this standard and ask for an easing of the exemption.

The aim of this work is to provide information that will assist the competent authority for establishing alternative transport conditions.

Materials and Methods

Micro-organisms, growth models and assumptions

The growths of *Aeromonas hydrophila*, *E. coli*, *Listeria monocytogenes*, *Salmonella*, and *Yersinia enterocolitica* were considered. Predictive microbiology software packages, Pathogen Modeling Program (<http://pmp.arserrc.gov/PMPOne.aspx>), Combase Predictor (www.combase.cc), [MLA](#) [Refrigeration](#) [Index](#) [Calculator](#)

(<http://www.foodsafetycentre.com.au/refrigerationindex.php>) and Sym'Previus (www.symprevius.org) were used to assess the growth of selected bacteria.

Lag time was not taken into account. It was considered that carcass temperature remains constant during transport in refrigerated lorries. The pH value was fixed at 6.2 which corresponds to the initial pH of meat before cooling. Water activity (a_w) was set at 0.995, the value usually considered for fresh meat.

Performance criteria for establishing alternative transport conditions

Two criteria were used to set alternative duration and temperature of warm raw pork transport. The first was the one proposed by the scientific committee of the Belgian federal agency for food chain safety (Federal agency for the safety of food chain, 2008). They determined a performance criterion: less than a doubling of the bacterial population must be achieved during the transport of warm pork carcasses. The second criterion tested in this paper states that the alternative temperature conditions and transport times must generate microbial growths equivalent or lower than those predicted at the temperature and for the time defined in the actual exemption (12°C – 2 hours).

Results and discussion

In this study three of the main high risk hazards involved in foodborne infections caused by pork meat, *Y. enterocolitica*, *Salmonella* and *L. monocytogenes* were considered (Fosse *et al.*, 2008). *E. coli* has the advantage of having a minimum growth temperature close to 7°C (Ross *et al.*, 2003), which is a usual target temperature to be reached while cooling carcasses. *A. hydrophila*, which is potentially present in pork meat, has been selected due to its psychrotrophic nature. When several models were available the model giving the safest transport conditions was kept.

Even if the presence of bacteria in the core of meat is a possible phenomenon (Gill, 1979), particularly with *Salmonella*, surface is the main place where contamination is likely to arise and therefore is worth being considered.

Relationship between surface and core temperature

A relationship has been established (Figure 1) between temperatures taken at the surface and in the core of hams of 24 cooling carcasses (Anonymous, 2008). That relationship made it possible to determine the temperature at the surface. The calculated value was used to assess the bacterial growth on the meat surface.

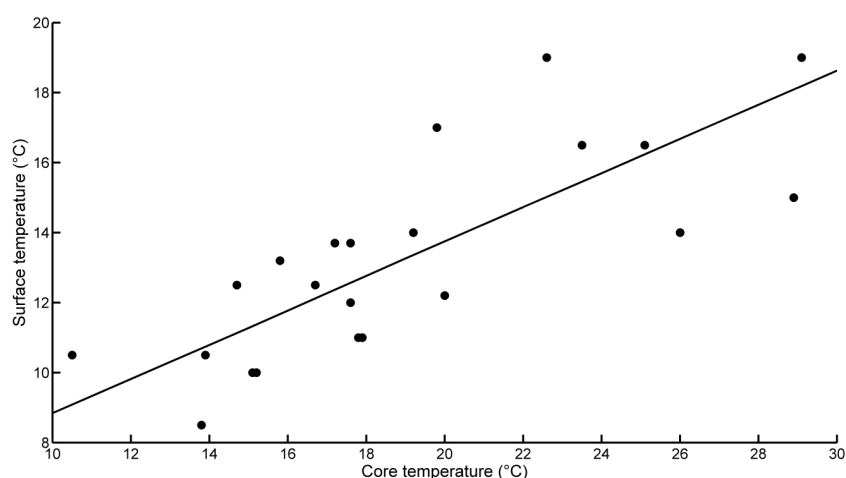


Figure 1: Surface temperatures (T_S) versus core temperatures (T_C) of hams at the time of loading (•). Major axis (—) : $T_S = 0.4866 T_C + 3.99$.

Alternative transport conditions according to performance criterion 1

Large differences are observed between bacteria to achieve the performance criterion of a maximum of one generation during refrigerated transport (Figure 2). As Belgian federal agency for food chain safety (2008) observed, the growth of *A. hydrophila* was found to have the lowest generation time both in deep meat and on surface.

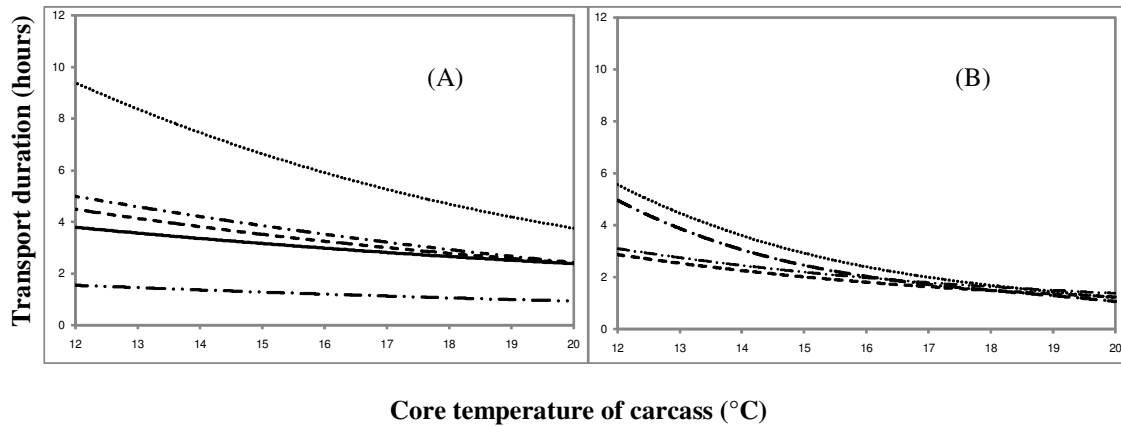


Figure 2: Maximum transport time depending on the core temperature of carcasses leading to a doubling on the surface (A) or in deep meat (B) of *A. hydrophila* (••-), *L. monocytogenes* (- • -), *Salmonella* (•••), *E. coli* (•-) and *Y. enterocolitica* (—).

Alternative transport conditions to verify equivalence of risk

To achieve the objective of risk equivalence with actual exemption, growth potentials for alternative transport conditions must not be higher than those corresponding to the actual regulation. Maximum transport times depending on the core temperature of the carcasses at the time of loading were calculated to achieve this criterion. Those maximum transport times are given in Figure 3. Logically, the increase of core temperature at loading implies a reduction of transport times below two hours. Contrary to the previous performance criterion, maximum transport durations are not limited by the fastest growing bacteria, but by *E. coli* and *Salmonella*. These bacteria have not the highest growth rates but the highest relative changes when temperature increases. Considering growth in deep meat would lead to shorter duration of transport than growth on surface.

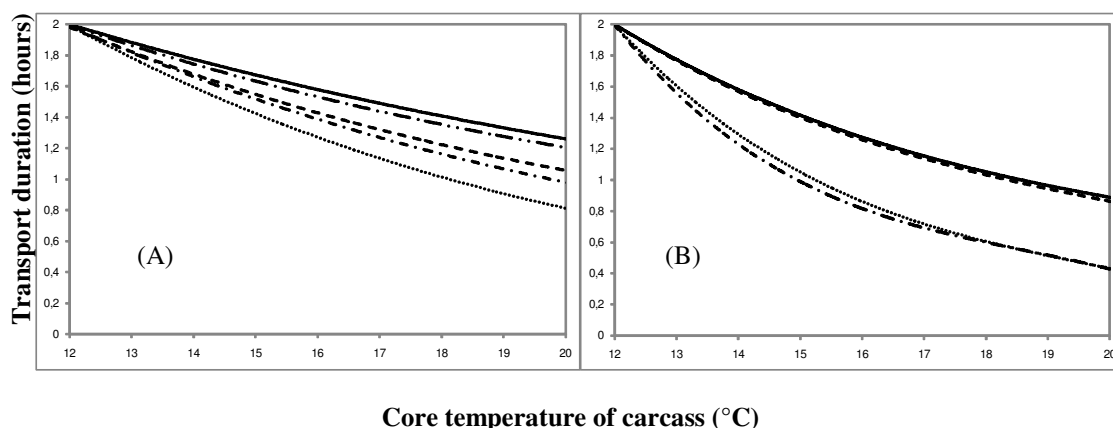


Figure 3: Maximum transport duration depending on the core temperature of carcasses leading to growths on the surface (A) or in deep meat (B) of *A. hydrophila* (••-), *L. monocytogenes* (- • -), *Salmonella* (•••), *E. coli* (•-) and *Y. enterocolitica* (—) equivalent to those with transport with a core temperature of 12°C for two hours.

It must be stressed that the different growth simulations are safe simulations. First, because temperature of meat was considered to be stable during transport in refrigerated lorries. A recent study (Anonymous, 2008) showed a decrease of surface temperature kinetics during transport in refrigerated lorries. The lag times were considered to be nil, even when it is likely that the bacteria contaminating the carcasses are in a physiological condition that requires adaptation before exponential growth (Ingham *et al.*, 2007). Most of the models tested have been established in liquid culture media and not in meat. The growth model used for *Salmonella* is an aerobic model, even though what is considered is growth in deep meat. Lastly, water activity has been considered to be optimal even at the surface, when partial drying is possible (Savell *et al.*, 2005).

An analysis of the bibliography dealing with the evolution of bacterial population during cooling confirms that that bacterial growths are certainly not as high as predicted. For example, on the basis of a statistical survey of the data from eight studies, Gonzales Barron *et al.* (2008) have shown that the prevalence of pork carcasses that are contaminated before refrigeration was 2.4 times greater than after cooling. That reduction of prevalence was observed regardless of the mode of cooling.

Conclusions

In the current state of knowledge, a large easing of the actual exemption cannot be proposed. Meanwhile, opportunities for customized chilling programs still exist. For this an approach similar to Australian Quarantine Inspection Service (2005) or the Meat Industry Research Institute and New Zealand Food Safety Authority (2004) should be adopted. They established process hygiene indexes based on temperature function integration techniques for assessing hygienic adequacy of cooling procedures. The establishment of such a criteria would provide a convenient way of determining the significance of the transport of warm carcasses in refrigerated lorries.

Acknowledgements:

Author thankfully acknowledges Pascal Garry for providing surface and core temperature datasets of pork carcasses.

References

- Anonymous (2008). Transport des carcasses n'ayant pas atteint la température réglementaire. Institut de la filière porcine. Technical report.
- Australian Quarantine Inspection Service (2005). Export control (meat and meat products) Orders 2005 (<http://www.comlaw.gov.au/ComLaw/Legislation/LegislativeInstrumentCompilation1.nsf/>).
- Federal agency for the safety of food chain. (2008) Advice 31-2008 of the Scientific Committee of the FASFC on the uncooled transport of pig carcasses. http://www.afsca.be/comitescientifique/avis/documents/AVIS31-2008_FR_DOSSIER2008-23.pdf.
- Fosse J., Seegers H. and Magras C. (2008). Prioritising the risk of foodborne zoonoses using a quantitative approach : application to foodborne bacterial hazards in pork and beef. *Revue scientifique et technique (International Office of Epizootics)* 27, 643-655.
- Gill C.O. (1979). Intrinsic bacteria in meat. *Journal of Applied Bacteriology* 47, 367-378.
- Gonzales Barron U., Bergin D. and Butler F. (2008). A meta-analysis study of the effect of chilling on prevalence of *Salmonella* on pig carcasses. *Journal of Food Protection* 71, 1330-1337.
- Ingham S.C., Fanslau M.A., Burnham G.M., Ingham B.H., Norback J.P. and Schaffner D.W. (2007). Predicting pathogen growth during short-term temperature abuse of raw pork, beef, and poultry products: use of an isothermal-based predictive tool. *Journal of Food Protection* 70(6), 1446-1456
- New Zealand Food Safety Authority (2004). Industry Standard 6 / Industry Agreed Standard 6 Processing of Edible Product.
- Ross T., Ratkowsky D.A., Mellefont L.A. and McMeekin T.A. (2003). Modelling the effects of temperature, water activity, pH and lactic acid concentration on the growth rate of *Escherichia coli*. *International Journal of Food Microbiology* 82, 33-43.
- Savell J.W., Mueller S.L. and Baird B.E. (2005). The chilling of carcasses. *Meat Science - 50th International Congress of Meat Science and Technology, (ICoMST), 8-13 August 2004, Helsinki, Finland* 70, 449-459.

Predictive modelling of *Escherichia coli* O157:H7 cross contamination during slaughter operations

E. Cummins¹, P. Nally¹, F. Butler¹, S. O' Brien¹ and G. Duffy²

¹ UCD School of Agriculture, Food Science and Veterinary Medicine, Belfield, Dublin 4, Ireland
(enda.cummins@ucd.ie)

² Food Safety Department, Ashtown Food Research Centre, Ashtown, Dublin 15, Ireland.

Abstract

The effect of abattoir slaughter operations on the prevalence and counts of *Escherichia coli* O157:H7 (*E. coli* O157:H7) was modelled by means of a second-order Monte Carlo simulation method. Contamination of beef trimmings may result in human exposure to *E. coli* O157:H7 as beef trimmings are processing into saleable products, such as beef burgers, for human consumption. The risk assessment model was developed in Microsoft Excel using the @RISK add-in (version 4, Palisade, New York). Distributions were used to model the slaughter operations that may influence the prevalence and counts of *E. coli* O157:H7 on beef carcasses. The operations modelled included de-hiding, evisceration, carcass washing, chilling and boning out/trimming. Data used in the model was based on a combination of results from extensive survey work and existing scientific literature. The mean simulated prevalence of *E. coli* O157:H7 in trimmings was 2.36% and the calculated mean counts on contaminated trimmings was approx. $-2.69 \log_{10}$ CFU/g. These simulated values were within the range estimated by survey results. A sensitivity analysis revealed the inputs having greatest effect on the prevalence and counts of *E. coli* O157:H7 on beef trimmings, these included: test sensitivity (correlation coefficient -0.27), hide to carcass transfer factor (correlation coefficient 0.26), and the initial hide prevalence (correlation coefficient 0.20). The model enables a closer analysis of the factors which contribute to beef contamination and resulting risks to consumers.

Keywords: Simulation, *Escherichia coli*, beef, cross contamination

Introduction

Verocytotoxigenic *Escherichia coli* (VTEC), in particular serogroup O157, has emerged as a pathogen of major public concern. High profile outbreaks have focused attention on outbreaks connected to food products, in particular, minced beef and beef burgers (CDC, 1993; Duffy *et al*, 2006a). Preliminary figures indicate that approximately 167 cases of VTEC occurred in Ireland during 2007 (HPSC, 2007), while other suspected cases in 2008 are currently under investigation. The current number of illnesses in Ireland represents a worrying trend. The *E. coli* O157 bacterium is present in faeces and the intestines of healthy bovines and can contaminate meat during the slaughter process (Chapman, 2000). Cross contamination can occur at multiple stages during the slaughter process resulting in potential contamination of meat destined for human consumption. The objective of this work was to develop a quantitative exposure assessment to model the contamination of beef trimmings at Irish abattoirs in an effort to identify critical points in the process and to assess the impact of process stages on the prevalence and counts of *E. coli* O157:H7.

Materials and methods

The focus of the model was within the slaughterhouse. The prevalence and counts of *E. coli* O157:H7 bacteria were modelled at various stages along the slaughter line. A flow diagram of the process is given in Figure 1. The model was created in Microsoft Excel 2000 with the add-on package @Risk (version 4.05, Palisade Corporation, New York, USA).

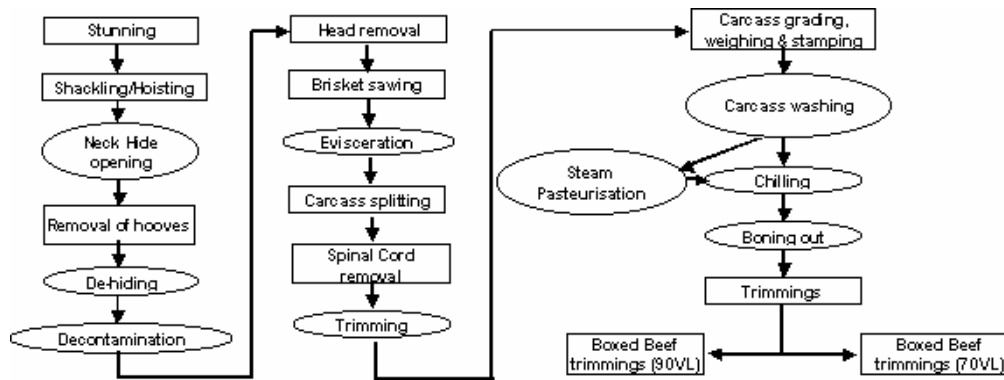


Figure 1: Flow diagram of the stages involved in bovine slaughter and subsequent production of beef trimmings. Ovals denote steps that may either increase or decrease contamination. Rectangles denote steps with little or no increase in contamination.

Distributions can be used to represent the effect each process stage has on microbial numbers by modelling intermediary processing stages (e.g. dehiding, evisceration, washing, chilling, boning out). As a result changes in microbial counts on the carcass can be simulated as the carcass moves through the plant. Model inputs were derived from Irish data where possible. A number of studies specific to Irish abattoir conditions (Sheridan, Lynch and Harrington, 1992; McEvoy *et al.*, 2000, 2001, 2003, Carney *et al.*, 2006; Duffy *et al.*, 2005; O'Brien *et al.*, 2005) provided valuable input data; alternatively, international data and scientific literature were consulted to improve the basis for the model where Irish specific data was not available. In a probabilistic risk assessment, the term “second-order” is often used to describe the use of probability distributions to represent variability and uncertainty in the input parameters (Vose, 2000). Variability and uncertainty in the input parameters were incorporated in the construction of a second-order model by means of probability distributions. Detailed analysis of the inputs and calculations are too exhaustive to provide here but are provided in detail in Cummins *et al.* (2008).

Results and discussion

The simulation was run with 10,000 iterations of the model using Latin Hypercube sampling. The observed prevalence of contaminated trimmings (2.36%) is similar to the prevalence reported for minced beef products i.e. 2.80% (Cagney *et al.*, 2004), which highlights the likely transfer of contaminated beef trimmings into the food chain in the form of comminuted beef products. The mean values for the prevalence of contaminated trimmings from the simulation and the commercial survey (Duffy 2006b) are also similar (Figure 2).

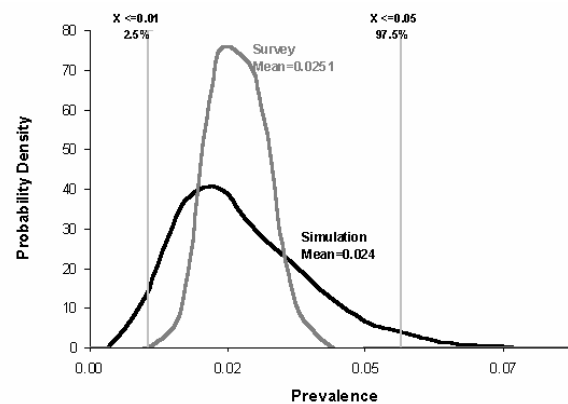
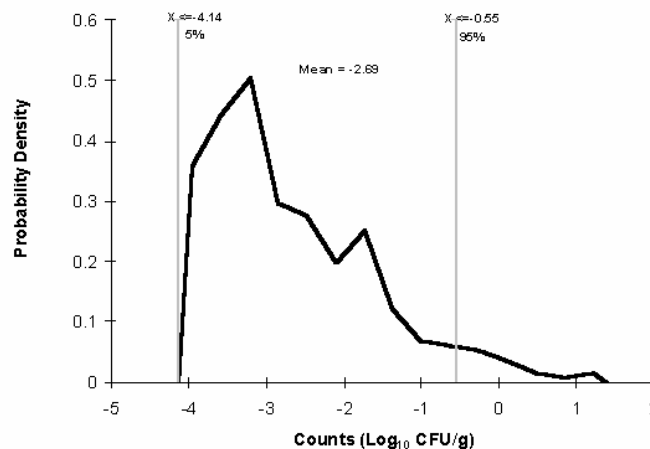


Figure 2: Simulation Vs. survey results (including uncertainty analysis) for the prevalence of *E. coli* O157:H7 on beef trimmings.

The simulated mean counts of *E. coli* O157:H7 on contaminated trimmings was $-2.69 \log_{10}$ CFU/g (Figure 3). Simulated counts include situations where the simulated value is less than the detection limit of the direct plate method (i.e. $< 0.70 \log_{10}$ units). Therefore, this has the effect of pulling the graph in Figure 3 to the left. The enumeration technique of direct plating onto CT-SMAC as used by Cagney *et al.* (2006) is not sensitive at low concentrations. As a result, in most samples (25/32 of the beef trimming samples) the pathogen was detectable by enrichment only, suggesting that the pathogen numbers are low i.e. $< 0.70 \log_{10}$ units. This substantiates the models low estimate for bacterial contamination on beef trimmings and provides some confidence in model results.



Figures 3: Simulated counts of *E. coli* O157:H7 on contaminated beef trimmings.

Given the estimated small dose required to cause illness resulting from the ingestion of *E. coli* O157:H77 these predictions may be a cause for concern. A sensitivity analysis (using correlation coefficient) revealed the parameters having the greatest impact on model predictions. The input having greatest impact on *E. coli* prevalence was the test sensitivity (-0.27), followed closely by the hide carcass transfer factor (0.26) and the initial hide prevalence (0.20). The initial count on the animal hide was the parameter having the greatest impact on count predictions in the model. The contaminated surface area and decrease from hide to carcass were also having an impact on model predictions. The analysis reveals the need for further research to reduce cross contamination at the hide removal stage. The fact that the initial microbial counts on animal hides and the initial prevalence on animal hides are ranked highly in the sensitivity analyses highlights the importance of having animals as free from microbial contamination as possible when presented for slaughter.

Conclusions

The model described in this paper predicted the prevalence and counts of *E. coli* O157:H7 in Irish beef trimmings and compared the results to a commercial survey carried out in Ireland. The model integrated predictive microbiology with quantitative risk assessment techniques. The model distinguishes between model inputs that are not well characterised because of lack of knowledge (uncertainty) and model inputs that are heterogeneous (variable). The model results indicate there may be cause for concern if *E. coli* counts are not reduced at a later stage in the processing process. Risk managers will be interested in the sensitivity analysis which revealed the effects the input parameters are having on model predictions and where further resources should be directed at reducing model uncertainty and improving model accuracy. The model can provide an appropriate decision support tool aiding risk mitigation strategies in the slaughter plant in an effort to protect human health. Model validation is an important component of this exercise; given the comparability between model predictions and survey results, the use of the input distributions seems justified. The model is an appropriate decision-support tool representing current scientific knowledge with regard to the slaughter

process. The model highlights the need for further research in the area of process simulation and microbial risk assessment.

Acknowledgements

The authors wish to acknowledge the Department of Agriculture for their funding of this project under the Food Institute Research Measure.

References

- Cagney, C., Crowley, H., Duffy, G., Sheridan, J.J., O'Brien, S.B., Carney, E., Blair, I.S., McDowell, D.A. and Bishop, R.H. (2004) Prevalence and numbers of *Escherichia coli* O157:H7 in minced beef and beef burgers from butchers shops and supermarkets in the Republic of Ireland. *Food Microbiology* 21, 203-212.
- Carney, E., O'Brien, S.B., Sheridan, J.J., McDowell, D.A., Blair, I.S. and Duffy, G. (2006) Prevalence and level of *Escherichia coli* O157 on beef trimmings, carcasses and boned head meat at a beef slaughter plant. *Food Microbiology* 23(1), 52-59.
- CDC (1993) Centre for Disease Control. Update: multistate outbreak of *Escherichia coli* O157:H7 infections from hamburgers- western United States, 1992-1993. *Morbidity and Mortality Weekly Report*, 42, 258-263.
- Chapman, P.A. (2000) Sources of *Escherichia coli* O157 and experiences over the past 15 years in Sheffield, UK. *Journal of Applied Microbiology Symposium Supplement* 88, 51S-60S.
- Cummins, E., Nally, P., Butler, F., Duffy, G. and O'Brien, S. (2008) Development and validation of a probabilistic second-order exposure assessment model for *Escherichia coli* O157:H7 contamination of beef trimmings from Irish meat plants. *Meat Science* 79, 139-154.
- Duffy, G., Butler, F., Cummins E., O'Brien S., Nally, P., Carney, E., Henchion M., Mahon D. and Cowan C. (2006b) *E. coli* O157:H7 in beef burgers produced in the Republic of Ireland: A quantitative microbial risk assessment. Ashtown Food Research Centre, Teagasc, Dublin 15, Ireland. ISBN: 184170461X.
- Duffy, G., Cummins, E., Nally, P., O'Brien S. and Butler F. (2006a) A review of quantitative microbial risk assessment in the management of *Escherichia coli* O157:H7 on beef. *Meat science* 74(1), 76-88.
- Duffy, G., O'Brien, S.B., Carney, E., Sheridan, J.J., McDowell, D.A. and Blair, I.S. (2005) Characterisation of *E. coli* O157 isolates from bovine hide and beef trimming in Irish abattoirs by pulsed field gel electrophoresis. *Journal of Microbiological Methods* 60(3), 375-382.
- HPSC (2007) Epidemiology of Verotoxigenic *E. coli* in Ireland, 2007. Health Protection Surveillance Centre, Ireland. Available from <http://www.ndsc.ie>
- McEvoy, J.M., Doherty, A.M., Finnerty, M., Sheridan, J.J., McGuire, L., Blair, I.S., McDowell, D.A. and Harrington D. (2000) The relationship between hide cleanliness and bacterial numbers on beef carcasses at a commercial abattoir. *Letters in Applied Microbiology* 30, 390-395.
- McEvoy, J.M., Doherty, A.M., Sheridan, J.J., Thomson-Carter, F.M., Garvey, P., McGuire, L., Blair, I.S. and McDowell, D.A. (2003) The prevalence and spread of *Escherichia coli* O157:H7 at a commercial beef abattoir. *Journal of Applied Microbiology* 95, 256-266.
- McEvoy, J.M., Doherty, A.M., Sheridan, J.J., Thomson-Carter, F.M., Garvey, P., McGuire, L., Blair, I.S. and McDowell D.A. (2001) The incidence and spread of *Escherichia coli* O157:H7 at a commercial beef abattoir. Epidemiology of verocytotoxigenic *E. coli*. In Proceedings of Concerted action, CT98-3935, hosted by Teagasc, The National Food centre, Malihide, Dublin, Ireland 8-10th February 2001.
- O'Brien, S.B., Duffy, G., Carney, E., Sheridan, J.J., McDowell, D.A. and Blair, I.S. (2005) Prevalence and numbers of *Escherichia coli* O157: on bovine hide at a beef slaughter plant. *Journal of Food Protection* 68(4), 660-665.
- Sheridan, J., Lynch, B., & Harrington, D. (1992) The effect of boning and plant cleaning on the contamination of beef cuts in commercial boning hall. *Meat Science* 32, 185-194.
- Vose, D. (2000) Risk Analysis: a Quantitative Guide, 2nd Ed: J Wiley Chichester, England, ISBN 0-471-99765-X.

Evaluation of primary models to predict microbial growth by plate count and absorbance methods

M.L. Pla¹, S. Oltra¹, M.D. Esteban², S. Andreu² and A. Palop²

¹ Departamento de Matemática Aplicada, EPSA, Universidad Politécnica de Valencia, Pza. Ferrandiz y Carbonell, s/n 03801 Alcoy, Spain

² Departamento de Ingeniería de Alimentos y del Equipamiento Agrícola, Universidad Politécnica de Cartagena, Pº Alfonso XIII, 48 30203 Cartagena, Spain

Abstract

There are a number of sigmoid equations and several models that have been used as growth functions. Probably, Gompertz, Baranyi, Richards, logistic and three-phase linear are the most preferred models among researchers. However, there is significant disagreement on which is the best fitting primary growth model and the selection is often based on convenience.

Microorganisms exposed to exactly the same favourable growth conditions, and with a similar precultural history should be in similar optimal physiological state and should behave in a similar way, so they should show the same growth parameters, growth rate and lag time.

The objective of this research was to check the performance of different mathematical models in predicting growth parameters, both by absorbance and plate count methods. For this purpose, growth curves of three different microorganisms (*Bacillus cereus*, *Listeria monocytogenes* and *Escherichia coli*) grown under the same conditions, but with several different initial concentrations each, were analyzed.

When measuring the microbial growth of each microorganism by optical density, almost all models provided quite high goodness of fit ($r^2 > 0.97$) for all growth curves. The growth rate remained approx. constant for all growth curves of each microorganism, when considering one growth model, but differences were found among models. Richards and logistic models failed to fit properly all the survival curves selected in a first stage and were disregarded. Three-phase linear model provide the lowest variation for growth rate values for all three microorganisms, closely followed by Baranyi model.

When measuring the microbial growth of each microorganism by plate count, again three-phase linear was the model to provide less variability for growth rates of microorganisms growing in the same conditions. So, in spite of being the model which provided worst goodness of fit (lowest correlation coefficient and highest residual mean square error values), it was considered the growth model which best performed.

Keywords: microorganisms, growth models, predictive modelling, growth curves

Introduction

There are a number of sigmoid equations and several models that have been used as growth functions. All they differ in 'ease of use' and number of parameters in the equation. Some authors have recently compared the behaviour of different growth models, from different viewpoints (Zwietering et al. 1990; Buchanan et al. 1997; Dalgaard and Koutsoumanis, 2001; Baty and Delignette-Muller, 2004; López et al. 2004; Perni et al. 2005). These studies have reached to different conclusions. Hence, there is significant disagreement in literature on which is the best fitting model for predictive microbiology. Probably, Gompertz, Baranyi, Richards, logistic and three-

phase linear are the most preferred models among researchers. Anyhow, the selection of a model in predictive food microbiology is often subjective and based on convenience. The objective of this research was to check the performance of different mathematical models in predicting growth parameters, both by absorbance and plate count methods. For this purpose, growth curves of three different microorganisms (*Bacillus cereus*, *Listeria monocytogenes* and *Escherichia coli*) grown under the same conditions, but with different initial concentrations each, were analyzed.

Material and methods

Microorganisms

B. cereus INRA-AVTZ415 was kindly provided by the Institut National de la Recherche Agronomique (INRA, Avignon, France). *L. monocytogenes* and *E. coli* type strains (CECT 4031 and CECT 515, respectively) were provided by the Spanish Type Culture Collection (CECT).

Optical density growth curves

100-well microtitre plates were filled with 400 μ L of the growth media (BHI for *B. cereus*, TSB+YE for *L. monocytogenes* and pH 5 TSB+YE for *E. coli*), inoculated with the microorganisms and incubated in a Bioscreen C analyzer. Incubation temperatures were 30°C for *B. cereus* and 37°C for *L. monocytogenes* and *E. coli*. At 20 min intervals, the optical density (OD) of the samples using a wideband filter (420-580 nm) was measured. A total of 345 individual growth curves were generated by absorbance measurements.

Plate count growth curves

50 mL flasks of the growth media were inoculated with the microorganisms and incubated with agitation at 500 rpm. Growth media and incubation temperatures were the same than for optical density growth curves. At preset time intervals, samples were taken, properly diluted in buffered peptone water and incubated in BHI agar for 24 h at 30°C for *B. cereus*, and in TSA+YE for 24 h at 37°C for *L. monocytogenes* and *E. coli*.

Mathematical models

Analyses of the growth curves were performed using five primary growth models. These growth models were based either on linear (derived from the Monod model) or non-linear (Gompertz, Logistic, Richards and Baranyi) equations and re-parameterized to reflect microbial growth parameters as derived by Zwietering et al. (1990).

Curve fitting of three-phase linear, Gompertz, logistic and Richards models were done using the curve fitting tool of Matlab 7.0. The curve fitting of the Baranyi's equation was done using DMFit 2.0 program and the model of Baranyi and Roberts (1994) as kindly provided by Dr. József Baranyi. Analysis of variance, medians and quartiles for box and whisker plots were calculated using StatGraphics.

Results and discussion

The slopes of all the optical density growth curves corresponding to one microorganism were parallel in the exponential growth phase, that is, the growth rates were similar, as it should correspond to different cultures of the same microorganism growing exactly in the same conditions. Three-phase linear, Gompertz and Baranyi models provided values that could be expected for growth parameters of the three growth curves selected of *E. coli*. However, Richards and logistic models were not able to fit properly these typical growth curves apparently easy to model, i.e. they gave abnormal values for growth parameters, and were disregarded.

Each model had a trend in providing higher or lower values, three-phase linear giving consistently the lowest values, followed by Baranyi and Gompertz models, in this order, for both the growth rate and the lag phase. In a previous comparison of these three models, Buchanan et al. (1997) already noticed and explained this effect on the basis of the nature of each model. Hence, depending on the predictive model chosen, values for growth rates and lag times will be consistently higher or lower and it is difficult to discern which model performs more adequately on the basis of the values provided for these parameters.

In this context, our viewpoint is that the best performing model would be that giving similar values for the growth parameters of different cultures of one microbial strain growing under exactly the same conditions and with the same precultural history. With this purpose, an extensive analysis of growth curves was performed with the three selected growth models. Only growth rate was considered for this study, since this parameter should be similar for all growth curves of the same microbial strain, even when starting from different initial inocula levels. A total of 345 growth curves were analysed.

With growth rate values obtained for all *E. coli*, *B. cereus* and *L. monocytogenes* growth curves with three-phase linear, Gompertz and Baranyi growth models, analyses of variance were performed for each microorganism. These analyses of variance showed that initial concentration did not influence growth rate, and that significant differences were found among growth rate values given by the different models, as already pointed out.

Table 1: Average \pm standard deviation of growth rate values (OD units/h) obtained with three-phase linear, Gompertz and Baranyi growth models for all the growth curves of *Bacillus cereus* INRA-AVTZ 415 at 30°C in BHI, *Listeria monocytogenes* CECT 4031 at 37°C in TSB+YE and *Escherichia coli* CECT 515 at 37°C in pH5 TSB+YE.

| Growth model | <i>B. cereus</i> | <i>L. monocytogenes</i> | <i>E. coli</i> |
|--------------------|-------------------|-------------------------|-------------------|
| Three-phase linear | 0.226 \pm 0.062 | 0.170 \pm 0.022 | 0.104 \pm 0.011 |
| Gompertz | 0.364 \pm 0.627 | 0.296 \pm 0.941 | 0.123 \pm 0.011 |
| Baranyi | 0.261 \pm 0.085 | 0.164 \pm 0.042 | 0.105 \pm 0.018 |

Table 1 shows average and standard deviation for growth rate of all three microorganisms and all three models, and Figure 1 shows box and whiskers plots for the three microorganisms. These plots are based on the median and withstand perturbations caused by outliers better than plots based on the average. These results clearly show that Gompertz model has a high degree of variation in the growth rate values provided, being three-phase linear and Baranyi the models that best performed. Three-phase linear model provided slightly less variation than Baranyi, so it should be the model of election.

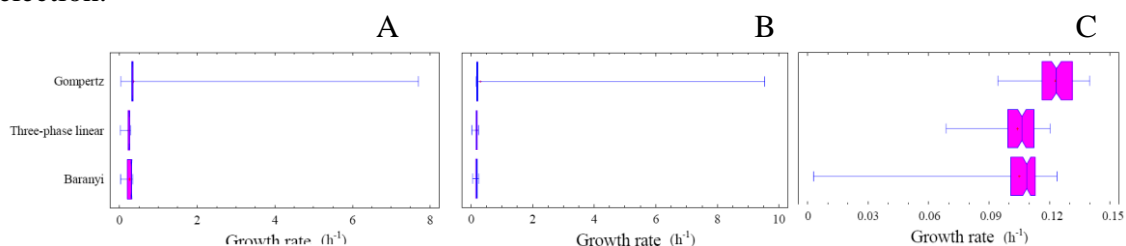


Figure 1: Box and whisker plots for growth rate values of *Bacillus cereus* INRA-AVTZ 415 at 30°C in BHI (A), *Listeria monocytogenes* CECT 4031 at 37°C in TSB+YE (B) and *Escherichia coli* CECT 515 at 37°C in pH5 TSB+YE (C).

In order to double check the results obtained, several plate-count growth curves of these same microorganisms were modelled with the three growth models. Similar results to those obtained with absorbance data were obtained when modelling the data from plate count growth curves.

Table 2 shows average and standard deviation for growth rate of all three microorganisms as obtained by three-phase linear, Gompertz and Baranyi models. Again, three-phase linear was the model which worse goodness of fit provided, with r^2 values as low as 0.92 and RMSE values as high as 0.49. But again, when comparing the similarities in the growth rate values (Table 2), three-phase linear was the model to give less variation (lower standard deviation) for the different growth curves.

Table 2: Average \pm standard deviation of growth rate values (log cycles/h) obtained with three-phase linear, Gompertz and Baranyi growth models for all the growth curves of *Bacillus cereus* INRA-AVTZ 415 at 30°C in BHI, *Listeria monocytogenes* CECT 4031 at 37°C in TSB+YE and *Escherichia coli* CECT 515 at 37°C in pH5 TSB+YE.

| Growth model | <i>B. cereus</i> | <i>L. monocytogenes</i> | <i>E. coli</i> |
|--------------------|-------------------|-------------------------|-------------------|
| Three-phase linear | 1.146 \pm 0.035 | 0.447 \pm 0.035 | 0.538 \pm 0.032 |
| Gompertz | 1.420 \pm 0.164 | 0.510 \pm 0.029 | 0.616 \pm 0.066 |
| Baranyi | 1.258 \pm 0.065 | 0.474 \pm 0.036 | 0.593 \pm 0.085 |

Buchanan et al. (1997) reported that the three-phase linear model was more robust than Gompertz or Baranyi models. López et al. (2004) found, from a statistical viewpoint, that three-phase linear was among those models showing best goodness of fit, at least for plate counts. Our results show that three-phase linear is also the model which provide less variability when analysing similar growth curves (closely followed by Baranyi model), hence being the most accurate model, even when it provides worse fitting to the data than most other primary growth models.

Conclusions

Three-phase linear model provide the lowest variation for growth rate values for all three microorganisms, closely followed by Baranyi model. So, in spite of providing worst goodness of fit, it was considered the growth model which best performed.

Acknowledgements

This research was financially supported by Ministerio de Ciencia y Tecnología of the Spanish Government and Fondo Europeo de Desarrollo Regional (FEDER) through the Projects AGL2003-00996 and AGL2006-10280.

References

- Baranyi J. and Roberts T.A. (1994) A dynamic approach to predicting bacterial growth in food. *International Journal of Food Microbiology* 23, 277-294.
- Baty F. and Delignette-Muller M.-L. (2004) Estimating the bacterial lag time: which model, which precision. *International Journal of Food Microbiology* 91, 261-277.
- Buchanan R.L., Whiting R.C. and Damert W.C. (1997) When is simple good enough: a comparison of the Gompertz, Baranyi and three-phase linear models for fitting bacterial growth curves. *Food Microbiology* 14, 313-326.
- Dalgaard P. and Koutsoumanis K. (2001) Comparison of maximum specific growth rates and lag times estimated from absorbance and viable count data by different mathematical models. *Journal of Microbiological Methods* 43, 183-196.
- López S., Prieto M., Dijkstra J., Dhanoa M.S. and France J. (2004) Statistical evaluation of mathematical models for microbial growth. *International Journal of Food Microbiology* 96, 289-300.
- Perni S., Andrew P.W. and Shama G. (2005) Estimating the maximum growth rate from microbial growth curves: definition is everything. *Food Microbiology* 22, 491-495.
- Zwietering M.H., Jongenburger I., Rombouts F.M. and van't Riet K. (1990) Modelling of the bacterial growth curve. *Applied and Environmental Microbiology* 56, 1875-1881.

A predictive model for the effect of temperature and water activity on the growth of pseudomonads in osmotically pretreated gilthead seabream fillets

T.N. Tsironi, P.S. Taoukis

National Technical University of Athens, School of Chemical Engineering, Laboratory of Food Chemistry and Technology, Iroon Polytechniou 5, 15780 Athens, Greece (ftsironi@chemeng.ntua.gr)

Abstract

The effect of temperature (0-15°C) and water activity (0.94-0.97) on the growth of *Pseudomonas* sp. in osmotically pretreated gilthead seabream fillets was studied and kinetically modeled using an Arrhenius type equation. Gilthead seabream fillets were treated at 37°C in osmotic solutions of 50:5 high dextrose equivalent maltodextrin (DE47):NaCl/100 g for different treatment times (0-120 min), in order to achieve water activity values between 0.94 and 0.97. Fish slices were aerobically packed in unsealed pouches and stored isothermally (0-15°C). *Pseudomonas* sp. were enumerated using selective media in appropriate time intervals to allow for efficient kinetic analysis of microbial deterioration. A mathematical model was developed, based on a modified Arrhenius-type equation, for predicting the combined effect of temperature and water activity on the growth rate of *Pseudomonas* sp. of osmotically pretreated gilthead seabream fillets. The nominal minimum water activity ($a_{w,min}$) for growth of *Pseudomonas* sp. was determined to be 0.941. The activation energy parameter of the model, 48 ± 4 kJ/mol, gives the measure of the dependence of *Pseudomonas* sp. growth on storage temperature. The applicability of the developed model was validated at different treatment conditions and storage temperatures.

Keywords

Pseudomonas sp., predictive modelling, chilled fish, osmotic dehydration

Introduction

Fresh fish is an extremely perishable food as compared to other food commodities. Spoilage of chilled fresh and minimally processed fish is attributed mainly to bacterial activity and it manifests itself as changes in the sensory characteristics (Gram and Huss, 1996). *Pseudomonas* sp. can be the dominant spoilage microorganism in aerobic storage of fresh, chilled fish (Gram and Huss, 1996; Kyrana et al., 1997). Koutsoumanis and Nychas (2000) proposed a spoilage model for aerobically stored gilthead seabream based on *Pseudomonas* sp. growth.

Partial dehydration of food products by an osmotic process has received increased attention as a pre-treatment to further processing to improve nutritional, sensorial and functional properties of food. By reducing the water activity of the food matrix, microbial growth is reduced or inhibited (Raoult-Wack, 1994). The preservative effect of osmotic pretreatment is greater as the water activity of the final product decreases. *Pseudomonas* sp. growth was as a good quality index for shelf life evaluation of aerobically stored osmotically pretreated gilthead seabream (*Sparus aurata*) fillets (Tsironi et al., 2009). Lowering the water activity to a value of 0.95, has a pronounced effect, especially on the growth rate of *Pseudomonas* sp. (Neumeyer et al., 1997). Under this context, osmotic treatment can extend the shelf life of gilthead seabream fillets, reducing the initial load and delaying microorganisms' growth. By developing a model that can predict the growth of *Pseudomonas* sp. in chilled fish, the rate of spoilage can be predicted by monitoring the temperature and measuring the water activity.

Gilthead seabream is a Mediterranean fish of high commercial value due to its desirable characteristics (aroma, taste, white flesh). Products like chilled fillets from marine cultured Mediterranean fish have high commercial potential if their shelf life can be extended through packaging or minimal processing. The objective of the study was to develop a predictive

model for the effect of temperature and water activity on the growth of *Pseudomonas* sp. in osmotically pretreated gilthead seabream fillets.

Materials and methods

Fresh gilthead seabream (*Sparus aurata*) fillets directly obtained in ice from the filleting line of a mariculture unit were cut into rectangular slices (3x3x1cm³, 10±1g) and treated at 37°C in osmotic solution, 50:50 maltodextrin(DE47):NaCl/100g for different times (0, 30, 60, 90 and 120 min), in order to achieve water activity values between 0.94-0.97. Untreated and treated slices were aerobically packed in unsealed pouches and stored at controlled isothermal conditions (0, 5, 10 and 5°C).

Pseudomonas sp. were enumerated on Cetrimide Agar (CFC, Merck, Darmstadt, Germany) in appropriate time intervals to allow for efficient kinetic analysis of microbial deterioration. The microbial growth was modeled using the Baranyi Growth Model (Baranyi and Roberts, 1995) and kinetic parameters such as the rate (k) of the microbial growth were estimated. The growth rate constants of *Pseudomonas* sp. for the different water activity and temperature conditions were fitted to an Arrhenius-type model, reparametrised to exhibit a minimum water activity value ($a_{w,min}$) for *Pseudomonas* sp. growth and an activation energy value (E_a), that indicates the temperature dependence of *Pseudomonas* sp. growth rates (Eq. 1)

$$k = k_{ref} \cdot \frac{a_w - a_{w,min}}{a_{w,o} - a_{w,min}} \cdot \exp \left[\frac{E_a}{R} \left(\frac{1}{T_{ref}} - \frac{1}{T} \right) \right] \quad (1)$$

where T is the absolute temperature (K), a_w is the water activity, E_a is the activation energy (kJ/mol), R is the universal gas constant, T_{ref} is a reference temperature (4°C), $a_{w,min}$ is the minimum water activity value for *Pseudomonas* sp. growth, $a_{w,o}$ is the water activity of the untreated samples and k_{ref} is the *Pseudomonas* sp. growth rate at $a_{w,o}$ and T_{ref} .

The model developed from the isothermal studies was validated at dynamic temperature conditions. *Pseudomonas* sp. growth was measured at a variable temperature distribution, that consisted of several cycles of three temperature steps: 2 h at 5°C, 2 h at 9°C and 2 h at 12°C, with T_{eff} =8.8°C at different a_w values in the range studied.

Results and discussion

Pseudomonas sp. were found to dominate the spoilage of gilthead seabream fillets. The results of the API 20NE test (Bio-Mérieux, Marcy L'Etoile, France) revealed that *P. fluorescens* and *P. luteola* were members of the microbial association as predominant bacteria in aerobically stored osmotically pretreated gilthead seabream fillets, while other types of gram-negative psychrotrophic bacteria, mainly *Aeromonas* sp., were also isolated. The parameters and statistics of the classical Arrhenius model for the exponential growth rate constants of *Pseudomonas* sp. at each studied water activity are illustrated in Table 1. Growth rate appeared similarly dependent on temperature, as the E_a values estimated were not significantly different ($P<0.05$), therefore allowing the expression of the combined effect of water activity and temperature in one equation (Eq.1).

Table 1. Parameters and statistics of the Arrhenius model for the growth rate constants of *Pseudomonas* sp. in osmotically pretreated gilthead seabream fillets

| a_w | E_a (kJ/mol) | $k_{ref(4^\circ C)}$ (d ⁻¹) | R ² |
|-------|----------------|---|----------------|
| 0.969 | 50.2 | 0.373 | 0.990 |
| 0.963 | 52.6 | 0.277 | 0.991 |
| 0.950 | 55.2 | 0.151 | 0.954 |
| 0.944 | 50.3 | 0.013 | 0.940 |
| 0.940 | 58.9 | 0.009 | 0.969 |

Eq. 1 described satisfactorily the dependence of *Pseudomonas* sp. growth rates on water activity and temperature (Table 2). The results of the studies under constant temperature conditions showed that the Arrhenius type model (Eq.1) describes successfully the growth of

Pseudomonas sp. on osmotically pretreated aerobically packed gilthead seabream fillets within a range from 0 to 15°C and water activity between 0.94-0.97.

Table 2. Parameters and statistics of the Arrhenius-type model (Eq.1) for the growth of *Pseudomonas* sp. in osmotically pretreated gilthead seabream fillets

| Parameter | Value \pm 95% CI* |
|-------------------------------------|---------------------|
| k_{ref} (d ⁻¹) | 0.382 \pm 0.020 |
| $a_{w,\text{min}}$ | 0.941 \pm 0.001 |
| E_a (kJ/mol) | 48.0 \pm 4.1 |
| R^2 | 0.986 |

*95% CI, 95% confidence interval

In order to evaluate the suitability of the model to predict the *Pseudomonas* sp. growth under nonisothermal conditions, the predicted growth rates derived from Eq.1 were compared to the observed by experiments under dynamic conditions. The experimental and the predicted by the model values are shown in Table 3. The % error is in all cases $\leq 11\%$, well below the 20% limit used in the literature as criterion of applicability (Dalgaard et al., 1997), showing that the model can predict satisfactorily the growth of *Pseudomonas* sp. on osmotically pretreated gilthead seabream fillets under nonisothermal conditions and can be applied reliably in the dynamic temperature conditions of the real chill chain.

Table 3. Predicted and experimental growth rate constants of *Pseudomonas* sp. in osmotically pretreated gilthead seabream fillets, at different a_w and variable temperature conditions ($T_{\text{eff}}=8.8^\circ\text{C}$)

| a_w | k_{pred} (d ⁻¹) | k_{exp} (d ⁻¹) | %error |
|-------|--------------------------------------|-------------------------------------|--------|
| 0.969 | 0.544 | 0.527 | -3.4 |
| 0.963 | 0.428 | 0.432 | 1.1 |
| 0.950 | 0.175 | 0.157 | -11.1 |
| 0.944 | 0.058 | 0.063 | 7.7 |

Conclusions

A mathematical model was developed, based on a modified Arrhenius-type equation, for predicting the combined effect of temperature and water activity on the growth rate of *Pseudomonas* sp. of osmotically pretreated gilthead seabream fillets. The results of the study showed that the developed model can be a reliable tool for predicting the shelf life of osmotically pretreated gilthead seabream fillets if the water activity and the temperature conditions are known. Advantages over existing models are its simplicity to fit data and its practical use.

References

- Baranyi J., Roberts T.A. (1995). Mathematics of predictive food microbiology. *International Journal of Food Microbiology* 26, 199-218.
- Dalgaard P, Mejlholm O, Huss HH. (1997). Application of an iterative approach for development of a microbial model predicting the shelf-life of packed fish. *International Journal of Food Microbiology* 38,169-179.
- Gram L., Huss H.H. (1996) Microbiological spoilage of fish and fish products. *International Journal of Food Microbiology* 33, 121-137.
- Kyrana V.R., Lougovois V.P., Valsamis D.S. (1997). Assessment of shelf-life of maricultured gilthead sea bream (*Sparus aurata*) stored in ice. *International Journal of Food Science and Technology* 32, 339-347.
- Koutsoumanis K., Nychas G.J.E. (2000) Application of a systematic experimental procedure to develop a microbial model for rapid fish shelf life predictions. *International Journal of Food Microbiology* 60, 171-184.
- Neumeyer K., Ross T., McMeekin T.A. (1997) Development of a predictive model to describe the effects of temperature and water activity on the growth of spoilage pseudomonads. *International Journal of Food Microbiology* 38, 45-54.
- Raoult-Wack A.L. (1994) Recent advances in the osmotic dehydration of foods. *Trends in Food Science & Technology* 5, 255-260.
- Tsironi T., Salapa I. and Taoukis P. (2009) Shelf life modelling of osmotically treated chilled gilthead seabream fillets. *Innovative Food Science and Emerging Technologies* 10, 23-31.

Quantification of the effect of factors involved in challenge-test assays on the growth rate estimation of *Listeria monocytogenes*

V. Stahl¹, H. Bergis², G. Bourdin³, M. Cornu², C. Denis⁴, B. Hezard¹, V. Huchet⁵, A.M. Jandos⁶, A. Lintz¹, V. Zuliani⁷, J.-C. Augustin⁸

⁽¹⁾ Aérial, Parc d'Innovation – rue Laurent Fries F-67412 Illkirch (v.stahl@aerial-crt.com)

⁽²⁾ Afssa LERQAP, 23 avenue du Général de Gaulle – F - 94706 Maisons Alfort Cedex (m.simon-cornu@afssa.fr)

⁽³⁾ Afssa LERPPE, Boulevard Bassin Napoléon – F-62200 Boulogne Sur Mer (g.bourdin@afssa.fr)

⁽⁴⁾ ADRIA NORMANDIE, bd 13 juin 1944 - F - 14310 Villers-Bocage (cdenis@adrianie.org)

⁽⁵⁾ ADRIA Développement Z.A Creac'h Gwen - F - 29196 Quimper Cédex (veronique.huchet@adria.tm.fr)

⁽⁶⁾ Institut Pasteur de Lille, 1 rue du Prof. Calmette - BP 245 F - 59019 Lille (anne-marie.jandos@pasteur-lille.fr)

⁽⁷⁾ IFIP-Institut du porc, pôle viandes fraîches et produits transformés, 7 avenue du Général de Gaulle -F-94704 Maisons Alfort Cedex (veronique.zuliani@ifip.asso.fr)

⁽⁸⁾ Unité MASQ, Ecole Nationale Vétérinaire d'Alfort, 7 Avenue du Général de Gaulle – F-94704 Maisons-Alfort Cedex (jcaugustin@vet-alfort.fr)

Abstract

This study describes an original interlaboratory trial relative to food challenge-tests conducted by eight French laboratories. The impact of several factors (linked to the type of foodstuff, to biological parameters and to experimental conditions as well as to the laboratory performing the test) on the growth rate of *Listeria monocytogenes* was quantified. The major factors influencing the growth rate variability were the “manufacturing origin of the product” and the “localization of the inoculum in food”. Others factors had effects from moderate to high according to the heterogeneity of the food matrix. The factor “laboratory which managed the challenge-test” was not statistically significant. Good laboratories practices, expertise/knowledge of food challenge-tests methodology permitted to control the laboratory effect on the growth rate estimation of *L. monocytogenes*.

Keywords: challenge-test, *Listeria monocytogenes*, growth rate variability, interlaboratory trial

Introduction

Direct evaluation of growth of artificially inoculated bacterial pathogens in foods using challenge-tests is an interesting tool for management of food safety. However, an issue is their ability to describe the growth of a food pathogen in conditions similar as possible to a naturally contaminated and routinely produced food. The laboratory performing a challenge-test must define, according to its expertise and knowledge, different experimental choices. Bacterial growth in food is known to be affected by many factors (Koutsoumanis *et al.*, 2004; Tienungoon *et al.*, 2000; Devlieghere *et al.*, 2001). Models developed in predictive microbiology quantify the effect of temperature, pH, water activity or lactic acid concentration (Zuliani *et al.*, 2007; Cornu *et al.*, 2006; Le Marc *et al.*, 2004). Other factors like competition with simultaneous growth of the food flora are modelled by the use of a new approach (Delignette *et al.*, 2006). Sources of variability such as food composition and experimental conditions may have a strong impact on the result of the growth rate estimation of *L. monocytogenes*. In this collaborative research, the objective was to quantify the impact of several factors linked to the type of foodstuff, to biological parameters and to experimental conditions as well as to the laboratory performing the test.

Materials and methods

Experimental design

Seven factors were studied:

Laboratories performing the challenge tests (factor 1). Eight French laboratories regularly performing challenge-tests.

Food matrices. Between-manufacturers variability (**factor 2**) and between-batches variability (**factor 3**).

Experimental conditions.

*Inoculation method of elaborated products (**factor 4**): in mixed product, on the ingredient the most sensitive to bacterial growth or at interface between ingredients.

*Food structure (**factor 5**): inoculation of the minced or not minced food matrix.

*Food portion sample for *L. monocytogenes* enumeration (**factor 6**): 10g to 270g

*Physiological state of the inoculum (**factor 7**): exponentially growing cells or cells with a nutritional stress (Guillier *et al.* 2006 ; Pinon *et al.* 2004).

Challenge- tests and determination of growth parameters

Experimental plans were designed in relation with specific descriptions of challenge-testing methodologies and were applied to five different foodstuffs: pâté, smoked herring, sliced cooked ham, cooked chicken included in sandwiches and surimi salad. The size of the *L. monocytogenes* inoculum was 100 CFU/g. Challenge-tests parameters, environmental conditions (pH, a_w , temperature 8°C), microbiological flora (total flora, lactic acid bacteria) and artificially inoculated *L. monocytogenes* were monitored along the incubation (shelf-life of the product). Each laboratory estimated the growth rate (μ_{\max}) of the obtained growth curves using a fitting tool, Sym'Previous software (www.symprevious.org) which was used by the majority (Pinon *et al.*, 2004).

Statistical analysis

An ANOVA was performed in order to determine which factors had a significant effect on the estimated growth rate.

Results and discussion

1-Laboratory impact

The laboratory which managed the challenge-test had a moderate effect: standard deviations (SD) of μ_{\max} range from 0 to 0.010 h⁻¹ (Table 1).

Table 1. Effect of the laboratory performing the challenge-test

| Food | Labo-ratory | Manu-facturer | Batch | Inoculum location | Portion sample | μ_{\max} (h ⁻¹) | SD |
|----------------|-------------|---------------|-------|--------------------------|----------------|---------------------------------|-------|
| Pâté | 1 | 1 | 1 | whole slice | 10 g | 0.042 | 0.003 |
| | 2 | 1 | 1 | whole slice | 10 g | 0.038 | |
| | 1 | 1 | 1 | stuffing | 10 g | 0.050 | 0.002 |
| | 3 | 1 | 1 | stuffing | 10 g | 0.047 | |
| | 2 | 1 | 1 | interface stuffing/jelly | 10 g | 0.048 | 0.005 |
| | 3 | 1 | 1 | interface stuffing/jelly | 10 g | 0.055 | |
| Smoked herring | 1 | 1 | 2 | surface | 10 g | 0.021 | 0.001 |
| | 2 | 1 | 2 | surface | 50 g | 0.023 | |
| Cooked ham | 1 | 1 | 1 | surface | 90 g | 0.015 | 0.007 |
| | 2 | 1 | 1 | surface | 270 g | 0.029 | |
| | 3 | 1 | 1 | surface | 90 g | 0.022 | |
| | 1 | 2 | 1 | surface | 90 g | 0.045 | 0.010 |
| | 2 | 2 | 1 | surface | 90 g | 0.030 | |
| | 3 | 2 | 1 | surface | 90 g | 0.048 | |
| | 1 | 3 | 1 | surface | 90 g | 0.000 | |
| | 2 | 3 | 1 | surface | 90 g | 0.000 | 0.000 |
| | 3 | 3 | 1 | surface | 90 g | 0.000 | |
| | 1 | 1 | 1 | surface | 25 g | 0.058 | |
| Cooked chicken | 2 | 1 | 1 | surface | 25 g | 0.049 | 0.004 |
| | 3 | 1 | 1 | surface | 25 g | 0.053 | |
| | 1 | 1 | 1 | surface | 25 g | 0.071 | |
| Surimi salad | 2 | 1 | 1 | surface | 25 g | 0.060 | 0.009 |
| | 3 | 1 | 1 | surface | 25 g | 0.055 | |

The Figure 1 shows growth curves obtained under repeatability conditions by different laboratories for the same foods. The average repeatability standard deviation of μ_{\max} was on average equal to 0.007 h^{-1} .

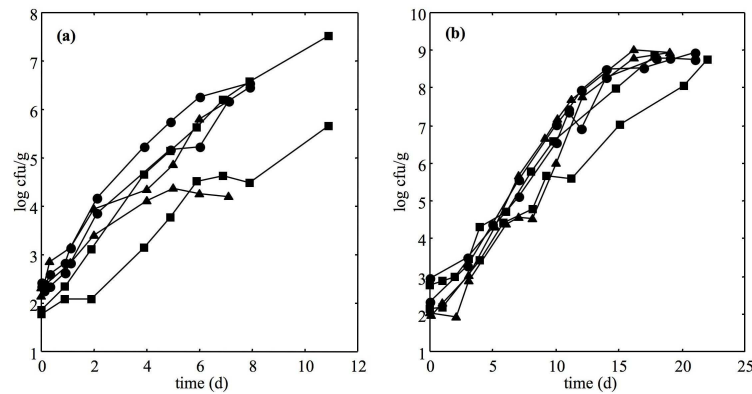


Figure 1. Observed data growth of *L. monocytogenes* at 8°C in (a) surimi salad (b) pâté, from three laboratories (●, ▲, ■) (two repetitions for each laboratory).

2- Food matrix impact

The manufacturer factor had a high impact, dependent on the food studied (SD of 0.001 for smoked herring, 0.021 for sliced cooked ham).

Table 2. Effect of the manufacturer factor

| Food | Laboratory | Manufacturer | Batch | Location | Portion sample | μ_{\max} (h^{-1}) | SD |
|----------------|------------|--------------|---------|----------|----------------|----------------------------------|-------|
| Smoked herring | 1 | 1 | 1 | surface | 10 g | 0.027 | 0.004 |
| | 1 | 1 | 2 | surface | 10 g | 0.021 | |
| | 1 | 2 | 1 | surface | 10 g | 0.024 | 0.002 |
| | 1 | 2 | 2 | surface | 10 g | 0.021 | |
| | 1 | 1 | 1 and 2 | surface | 10 g | 0.024 | 0.001 |
| | 1 | 2 | 1 and 2 | surface | 10 g | 0.022 | |
| Cooked ham | 1 | 1 | 1 | surface | 90 g | 0.015 | 0.004 |
| | 1 | 1 | 2 | surface | 90 g | 0.023 | |
| | 1 | 1 | 3 | surface | 90 g | 0.021 | |
| | 1, 2 and 3 | 1 | 1 | surface | 90 g | 0.022 | 0.021 |
| | 1, 2 and 3 | 2 | 1 | surface | 90 g | 0.041 | |
| | 1, 2 and 3 | 3 | 1 | surface | 90 g | 0.000 | |
| Cooked chicken | 1 | 1 | 1 | surface | 25 g | 0.053 | 0.006 |
| | 1 | 1 | 2 | surface | 25 g | 0.045 | |
| Surimi salad | 1 | 1 | 1 | surface | 25 g | 0.057 | 0.013 |
| | 1 | 1 | 2 | surface | 25 g | 0.045 | |
| | 1 | 1 | 3 | surface | 25 g | 0.071 | |

The variability linked to the batches was moderate. The SD was 0.006 on average with SD ranged from 0.002 for the smoked herring to 0.013 for the surimi salad.

3- Experimental conditions impact

The impact of the inoculation method of elaborated products, chosen by the laboratory, led to a SD values ranged from 0.006 to 0.036 h^{-1} . This effect was low for pâté: SD value of 0.006 for the three inoculated zones tested (slice, stuffing, jelly interface). The effect was high for sandwiches: indeed cooked chicken and yoghurt have significantly different physico-chemical characteristics (SD value of 0.036 between the two ingredients with growth on cooked chicken and no growth observed in the yogurt-based sandwich sauce). The respective effects

of food structure (SD of 0.005 h⁻¹ in pâté and smoked herring) and of food portion sample for *L. monocytogenes* enumeration were low (SD of 0.004 on average with a SD value of 0.002 for pâté (slice, stuffing) and a SD value of 0.005 for smoked herring).

Conclusion

This original interlaboratory trial relative to food challenge-tests, conducted by eight French laboratories, demonstrated that good laboratories practices, expertise/knowledge of food challenge-tests methodology permitted to control the **laboratory effect** on the growth rate estimation of *L. monocytogenes*. To assess the growth behaviour of *L. monocytogenes* in food, the between manufacturers variability must be considered and their choice explained. The between batches variability was moderate in regard to the objective of a routine challenge test. The impact of the experimental choices like inoculation method was potentially important, and dependent of the type and the heterogeneity of the food matrix. The impact of the food portion sample for enumeration of *L. monocytogenes* was low for the relatively homogeneous products we tested. It may be different for heterogeneous food products. The obtained results will also contribute to the enrichment of French Standard AFNOR NF V01-009 (2007) and the European Technical Guidance Document (Anonymous, 2008).

Acknowledgements

This work was supported by a grant from ACTIA (Paris, France) and the French Ministry of Agriculture, in collaboration with professionals. This project is part of the National French Technological Network (RMT) “Expertise on determination of microbial food products shelf-life”.

References

- AFNOR NF V01-009 (2007) describing the laboratory protocols for implementing challenge-tests.
- Anonymous (2008) Technical Guidance Document on shelf life studies for *Listeria monocytogenes* in ready-to-eat foods. (http://ec.europa.eu/food/food/biosafety/salmonella/docs/shelflife_listeria_monocytogenes_en.pdf)
- Cornu M., Beaufort A., Rudelle S., Laloux L., Bergis H., Miconnet N., Serot T., and Delignette-Muller M.L. (2006) Effect of temperature, WPS (water-phase salt) and phenolic contents on *Listeria monocytogenes* growth rates on cold-smoked salmon and evaluation of secondary models. *International Journal of Food Microbiology* 106, 161–170.
- Delignette-Muller M.L., Cornu M., Pouillot R., and Denis J.B. (2006) Use of Bayesian modelling in risk assessment: Application to growth of *Listeria monocytogenes* and food flora in cold-smoked salmon. *International Journal of Food Microbiology* 106, 195 – 208.
- Devlieghere F., Geeraerd A.H., Versyck K.J., Vanderwaetere B., Van Impe J., and Debevere J. (2001) Growth of *Listeria monocytogenes* in modified atmosphere packed cooked meat products: a predictive model. *Food Microbiology* 18, 53-66.
- Guillier L. and Augustin J.C. (2006) Modelling the individual cell lag time distributions of *Listeria monocytogenes* as a function of the physiological state and the growth conditions. *International Journal of Food Microbiology* 111 (3), 241-251
- Koutsoumanis K. P., Kendall P.A., and Sofos J.N. (2004) A comparative study on growth limits of *Listeria monocytogenes* as affected by temperature, pH and aw when grown in suspension or on a solid surface. *Food Microbiology* 21, 415-422
- Le Marc Y., Huchet V., Bourgeois C.M., Guyonnet J.P., Mafart P., and Thuault D. (2002) Combined effects of pH and organic acids on the growth rate of *Listeria innocua*. *International Journal of Food Microbiology* 73 (2-3), 219-237.
- Pinon A., Zwietering M., Membré J-M., Leporq B., Mettler E., Perrier L., Thuault D., Coroller L., Stahl V. and Vialette M. (2004) Development and validation of experimental protocols for use of cardinal growth models for prediction of microorganism in food products. *Applied and Environmental Microbiology* 70, 1081-1087.
- Tienungoon S., Ratkowsky D.A., Mcmeekin T.A., and Ross T. (2000) Growth limits of *Listeria monocytogenes* as a function of temperature, pH, NaCl, and lactic acid. *Applied and Environmental Microbiology* 66, 4979-4987.
- Zuliani V., Lebert I., Augustin J.C., Garry P., Vendeuvre J.L. and Lebert A. (2007) Modelling the behaviour of *Listeria monocytogenes* in ground pork as a function of pH, water activity, nature and concentration of organic acid salts. *Journal of Applied Microbiology* 103, (2007) 536–550.

Dynamic models for growth of *Salmonella* in ground beef and chicken at temperatures applicable to the cooking of meat

Vijay K. Juneja¹, Lihan Huang¹ and Harshavardhan Thippareddi²

¹ U.S. Department of Agriculture, Agricultural Research Service, Eastern Regional Research Center, 600 E. Mermaid Lane, Wyndmoor, PA 19038 (vijay.juneja@ars.usda.gov, lihan.huang@ars.usda.gov)

² Department of Food Science and Technology, University of Nebraska-Lincoln, Lincoln, NE 68583 (hthippareddi2@unl.edu)

Abstract

Growth kinetics of *Salmonella* in beef and chicken at several isothermal conditions ranging from 10 to 45°C was assessed. The data were then fitted into primary models, namely the logistic, modified Gompertz, Baranyi, and Huang models. Statistical analysis was done to evaluate the performances of these models using various criteria, namely mean square error (MSE), pseudo- R^2 , -2 log likelihood, Akaike's and Bayesian's information criteria. Based on these criteria, all the chosen models fitted well to the growth data of *Salmonella* in beef. In chicken, the modified Gompertz model described growth data the best, followed by the Baranyi model, and then the logistic model. The maximum growth rates (r_{\max} or μ_{\max}) at different isothermal conditions estimated from each primary model were then fitted as a function of temperature using the Modified Ratkowsky equation. It was observed that the lag phase duration was an inverse function of specific growth rates. Dynamic simulation of growth of bacterial growth was conducted by integrating the modified Ratkowsky equation with the primary models using a numerical method, and validated with linear heating temperature profiles. Performance of both isothermal and dynamic models were evaluated by using root mean square error, accuracy factor, bias factor and mean absolute relative residue, and were found to be satisfactory (within 0.5 logs). The comparison of computer simulation and experimental data will be presented. These dynamic models can be used to predict potential *Salmonella* growth in beef and chicken in case of process deviations or to set critical limits in HACCP plans for beef and chicken.

Keywords: Kinetic modeling, growth models, *Salmonella*

Introduction

Salmonella spp. are widely distributed in nature and are a major cause of foodborne illness in the United States. Salmonellosis, the illness caused by this bacterium, is reported to cause illnesses in approximately 40,000 people in the United States annually (CDC, 2005). While many different types of products are increasingly being implicated in *Salmonella* foodborne illnesses, red meat and poultry remain predominant products contributing to foodborne illnesses. Food products from these industries are the most vulnerable foods for the growth of *Salmonella*, particularly *S. enteritidis*. Improper cooking, cross contamination of cooked products and temperature abuse during processing and storage of these foods is the major cause of salmonellosis.

The growth of microorganisms in foods is significantly affected by time and temperature. Traditional microbial enumeration techniques are time-consuming, and may not be able to provide real-time information about the potential growth of foodborne pathogens in foods. Therefore, modeling the effect of temperature on the growth of *Salmonella* in meat and poultry products can help the industry and regulatory agencies to predict and estimate potential growth of *Salmonella* during processing, storage, and transportation. Such predictive models can also be useful in day to day decision making in the food processing operations in HACCP implementation and risk assessment in the event of temperature abuse and process deviation.

Therefore, the objective of this work was to conduct a systematic investigation into the growth kinetics of *Salmonellae* in beef, pork, and poultry meats under both isothermal and dynamic temperature conditions, and to develop mathematical models for estimating the growth of this pathogen in meats.

Materials and Methods

Primary models

Four different primary mathematical models of various complexities were evaluated. These models included modified Gompertz model, modified logistic model, Baranyi model, and Huang model.

Modified Gompertz/Logistic model

$$\begin{aligned} x(t) &= x_0 + (x_{\max} - x_0) \exp \left\{ -\exp \left[-\mu(t - M) \right] \right\} \\ \text{Gompertz: } r_{\max} &= \frac{x_{\max} - x_{\min}}{e} \times B, \quad \lambda = M - \frac{1}{B} \end{aligned} \quad \text{Eq. 1}$$

$$\begin{aligned} x(t) &= x_0 + \frac{(x_{\max} - x_0)}{1 + \exp \left[-\mu(t - M) \right]} \\ \text{Logistic: } r_{\max} &= \frac{x_{\max} - x_{\min}}{4} \times B, \quad \lambda = M - \frac{2}{B} \end{aligned} \quad \text{Eq. 2}$$

$$\begin{aligned} y(t) &= y_0 + \mu_{\max} F(t) - \ln \left\{ 1 + \frac{\exp \left[\mu_{\max} F(t) \right] - 1}{\exp(y_{\max} - y_0)} \right\} \\ \text{Baranyi: } F(t) &= t + \frac{1}{\nu} \ln \left[\exp(-\nu t) + \exp(-h_0) - \exp(-\nu t - h_0) \right] \end{aligned} \quad \text{Eq. 3}$$

$$\text{Huang: } y(t) = y_0 + \mu_{\max} \left\{ t + \frac{1}{25} \ln \frac{1 + \exp \left[-25(t - \lambda) \right]}{1 + \exp(25\lambda)} \right\} \quad \text{Eq. 4}$$

In Eqs. 1 and 2, x is the logarithm (base 10) of bacterial concentration, and r_{\max} is the maximum growth rate (based on x). In Eqs. 3 and 4, y is the natural logarithm of bacterial concentration, and μ_{\max} is the specific growth rate (based on y). To convert μ_{\max} to r_{\max} , μ_{\max} must be divided by 2.303. In all equations, λ is the duration of lag phase.

Secondary model

$$r_{\max} = a(T - T_{\min})^2 \{1 - \exp[b(T - T_{\max})]\} \quad \text{Eq. 5}$$

Dynamic analysis

The goal of dynamic analysis is to estimate the growth of bacteria under dynamic temperature conditions. For dynamic analysis, the differential form of primary model must be used. All primary models can be used for dynamic analysis, but Baranyi model (Eq. 6) was used in this study. This equation was numerically solved using 4th-order-Runge-Kutta method.

$$\frac{dy}{dt} = \frac{1}{1 + \exp[-Q(t)]} \mu_{\max} T(t) [1 - \exp(y - y_{\max})]$$

$$\frac{dQ}{dt} = \mu_{\max} T(t)$$

Eq. 6

Microbiological procedures

Bacterial cultures and isothermal studies

A five-strain cocktail, consisting of *Salmonella* Thompson FSIS 120; *Salmonella* Enteritidis Phage Type 4, H3502; *Salmonella* Hadar MF 60404; *Salmonella* Montevideo FSIS 051; and *Salmonella* Heidelberg F5038BG1, was used in growth studies. The bacteria were inoculated irradiated raw ground beef (95% lean), ground chicken, or ground pork, and incubated at 10, 15, 20, 25, 28, 32, 35, 37, 42, 45 or 47°C.

Dynamic studies

For dynamic studies, inoculated ground pork samples were incubated under different temperature profiles: linear - 45°C to 7°C in 10 h, 2 to 44°C in 24 h; exponential - 45°C to 4°C in 10 h, 2°C to 42°C in 10 h; and, sinusoidal - 0 and 24°C for 48 h (20 h/cycle), 0 and 10 °C for 240 h (50 h/cycle).

Results and Discussion

Isothermal studies and primary models

Most growth curves obtained in these studies were not complete with all three phases, and only contained from lag and exponential phases. Figure 1 demonstrates the suitability of each model for fitting the isothermal growth curves obtained from beef. Although the modified Gompertz/Logistic and Baranyi models are more suitable for growth curves completed with all three phase, they were capable of describing incomplete growth curve with a reasonable degree of accuracy. The reduced form of the Huang model (Eq. 4) was especially suitable for incomplete growth curves.

The analysis of fit statistics, including -2 log likelihood, Akaike's information criterion (AIC), and Bayesian information criterion (BIC), suggested that there were no significant difference in these parameters among all the models, indicating that all these models were equally suitable for fitting the growth curves and with similar accuracy.

Temperature dependence and secondary model

The growth of *Salmonella* in beef, pork, and chicken meats, were highly temperature dependent, and the growth rate can be expressed as a function of temperature using a modified Ratkowsky model (Figures 2 and 3). A high degree of correlation between λ and r_{\max} was observed (Figure 4).

Dynamic analysis

The differential form of Baranyi model was numerically solved to estimate the growth of *Salmonella* in pork under different temperature profile, and Figures 5 and 6 demonstrates the results of numerical analysis and their comparison with experimental observations. In general, the dynamic model could generally estimate the growth of bacteria within a 0.5 log accuracy for linear, exponential, and sinusoidal temperature profiles.

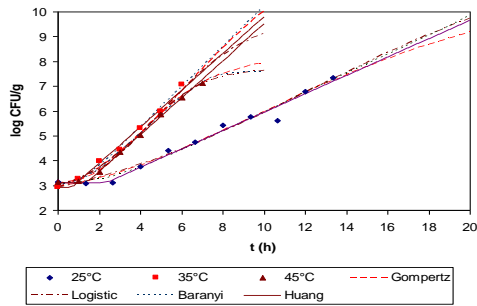


Figure 1: Selective growth curves fitted by modified Gompertz and logistic models, Baranyi model, and Huang model.

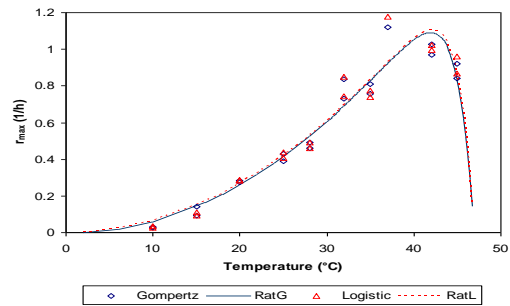


Figure 2: Specific growth rates (r_{\max}) and the Modified Ratkowski curves derived from modified Gompertz and logistic models (beef data).

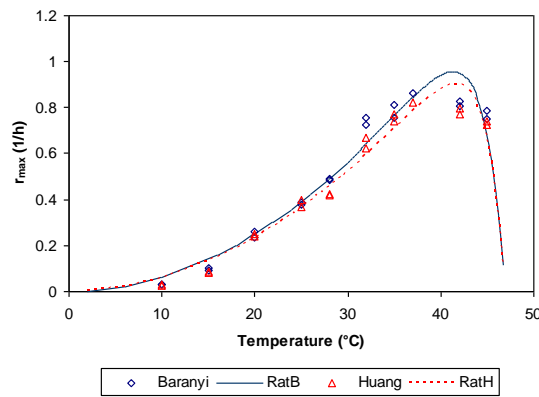


Figure 3: Specific growth rates (r_{\max}) and the Rajkowski curves derived from Baranyi and Huang models (beef data)

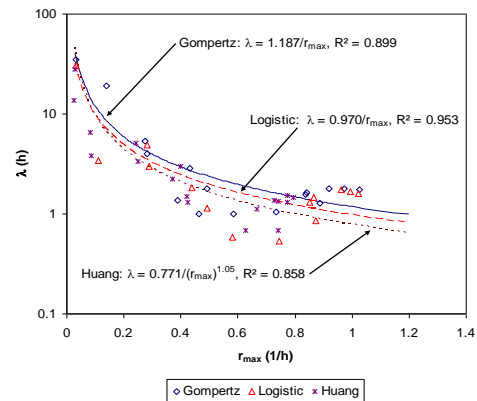


Figure 4: Relationship between the lag phase duration (λ) and specific growth rate derived from Gompertz, logistic, and Huang models (beef data)

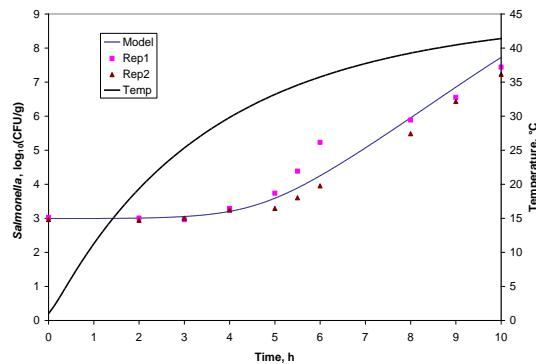


Figure 5: Validation of the dynamic model for *Salmonella* spp. in ground sterile pork under exponential heating profile (from 2 °C to 42 °C in 10 h).

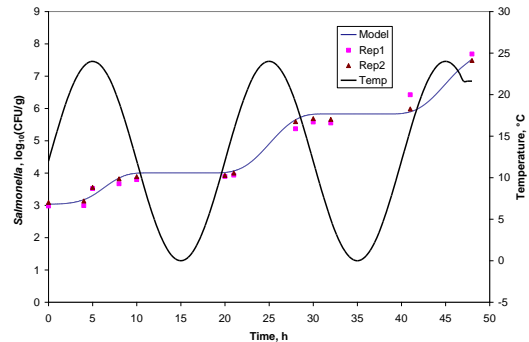


Figure 6: Validation of the dynamic model for *Salmonella* spp. in ground sterile pork under short sinusoidal temperature profile (between 0 °C and 24 °C for 48 h with a time period of 20 h/cycle).

References

CDC, (2005). Salmonellosis – General information. Division of bacterial and mycotic diseases. Centers for Disease Control and Prevention, Available at http://www.cdc.gov/ncidod/dbmd/diseaseinfo/salmonellosis_g.htm. Accessed on June 16, 2005.

Using ComBase Predictor and Pathogen Modeling Program as support tools in outbreak investigation: an example from Denmark

T.B. Hansen, C.O.A. Møller and J.K. Andersen

National Food Institute, Technical University of Denmark, Mørkhøj Bygade 19, DK-2860 Søborg, Denmark.
(tibha@food.dtu.dk)

Abstract

During a 20-case-outbreak of verocytotoxin-producing *Escherichia coli* O26:H11 in 2007 in Denmark, two of the cases were also found to be infected with *Yersinia enterocolitica*. The source was an organic semi-dried fermented sausage and the question was: “Could *Y. enterocolitica* have survived, or even multiplied, during the production of the suspected sausage?” To elucidate this, the ComBase Predictor (CBP) and the Pathogen Modeling Program (PMP) were used as support tools. From information on the company’s website, it was calculated that the water phase salt changed from 4.6% to 8.0% during production and pH changed from 5.5 to 4.7. No nitrite was used. Predictions of growth/reduction of *Y. enterocolitica* and *E. coli* in a matrix covering these pH- and WPS-values were compared at 24°C mimicking fermentation temperature, at 16 and 5°C mimicking drying and storage temperatures, respectively. The results showed that *Y. enterocolitica* would be able to multiply during the first part of the production. Compared to *E. coli* growth of *Y. enterocolitica* was predicted to be slower in the beginning of the fermentation but faster in the end with CBP and faster during the whole fermentation with PMP. CBP predicted that an increase of one log-unit took approx. 50 h at conditions in the beginning of the drying period and approx. 100 h in the middle. During storage growth of *Y. enterocolitica* would only be expected in case of production failures, such as insufficient drying or addition of a too low amount of salt to the batter. A deterministic model was constructed in Microsoft Excel using information on the production of the implicated sausage. This model predicted the level of *Y. enterocolitica* to increase 2.3, 4.2 and 7.8 log-units during fermentation, drying and storage, respectively. At the point of release of the sausage for sale, 1 *Y. enterocolitica* could have increased to 10⁶ and the sausage could, therefore, not be ruled out as the source of *Y. enterocolitica* found in two of the outbreak cases.

Keywords

Outbreak, *Yersinia enterocolitica*, *Escherichia coli*, VTEC, semi-dried fermented sausage.

Introduction

In February 2007, an outbreak of verocytotoxin-producing *Escherichia coli* O26:H11 was realized in Denmark. The outbreak involved 20 cases primarily children in the age from 2 to 3 years. Using a credit card traceability method, a possible source was traced to be an organic semi-dried fermented sausage. The source was later confirmed when the outbreak strain was recovered from raw material used in the sausage production. Besides *E. coli* O26:H11, *Yersinia enterocolitica* was also found in two of the cases and during the outbreak investigation the following question arose: “Could *Y. enterocolitica* have survived, or even multiplied, during the production of the suspected sausage?” To elucidate this, the ComBase Predictor (CBP) and the Pathogen Modeling Program (PMP) were used as support tools.

Methods

Environmental conditions of sausage

To determine intrinsic characteristics, such as concentration of water phase NaCl, concentration of NaNO₂ and pH, of the suspected semi-dried sausage the following information was collected from the company’s website and from the label. To produce 100 g

of the organic sausage 127 g meat, 4 g salt (NaCl), 2 g spices and 0.5 g dextrose were used. The ready-to-eat sausages contained 9 g fat, 22 g protein and 2 g carbohydrates per 100 g.

The weight reduction (WR) was calculated on the basis of the recipe of the used batter

$$WR = 100 * ((M + Nb + S + D) - 100) / (M + Nb + S + D) \quad (1)$$

where WR is the weight reduction in %, M is gram of meat, Nb is gram of NaCl, S is gram of spices and D is gram of dextrose used for the production of 100 g of sausage.

The NaCl content, measured in gram, in the ready-to-eat sausage, (Ns) was calculated on the basis of amount of NaCl in the batter (Nb) as well as WR

$$Ns = 100 * Nb / (100 - WR) \quad (2)$$

The water content in the ready-to-eat sausage (Ws) was calculated on the basis of the labelled content of fat, protein and carbohydrates as well as the calculated Ns

$$Ws = 100 - (F + P + C + Ns) \quad (3)$$

where Ws is water content in %, F is gram of fat, P is gram of protein and C is gram of carbohydrate in 100 g of ready-to-eat sausage.

The % water in the batter (Wb) was calculated using formulae (1) and (3)

$$Wb = 100 * Ws / (100 - WR) \quad (4)$$

The water phase NaCl concentrations in batter (WPSb) was calculated on the basis Nb from recipe and formula (4)

$$WPSb = 100 * Nb / (Wb + Nb) \quad (5)$$

The water phase NaCl concentrations in the ready-to-eat sausage (WPSs) was calculated on the basis of formula (2) and (3)

$$WPSs = 100 * Ns / (Ws + Ns) \quad (6)$$

Both WPSb and WPSs are measured in %.

Production of semi-dried sausages can be split into three major steps, fermentation, drying and storage. As there was no information available on the website concerning specific processing temperatures, a standard procedure was adopted. Thus, the widely used fermentation temperature of 24°C was chosen to mimic the fermentation step and 16°C to mimic the drying step. Storage temperature was set to 5°C as indicated on the label.

Predictions from CBP and PMP

Growth/reduction rates of *Y. enterocolitica* and *E. coli* were predicted using both ComBase Predictor (CBP) as well as Pathogen Modeling Program (PMP). The growth and reduction rates were defined as the time in hours to obtain 1 log-increase and 1 log-reduction of the microorganisms, respectively. In all predictions, lag was excluded. In PMP, the procedure for predicting time to 1 log-increase was to set the difference between 'level of concern' and 'initial level' equal to 1 log CFU. With regard to time to 1 log-reduction in PMP, time to obtain 5 log-reductions was predicted and divided by 5. In CBP, time to 1 log-increase was estimated from the predicted doubling time by division by 0.301 ($\ln(2) / \ln(10)$). No non-thermal inactivation models were available for *Y. enterocolitica* and *E. coli* in CBP.

Spreadsheet model

A deterministic model was constructed in Microsoft Excel for evaluating the fate of *Y. enterocolitica* and *E. coli* during production conditions similar to the sausage implicated in the outbreak. Interviewing the company collected the information on specific production conditions. Fermentation was carried out at 16°C for 48 h, drying from 16 to 13°C in 8 d, reducing the weight gradually, and chilled storage at 5°C for up to 4 months. Intrinsic characteristics of the ready-to-eat sausage were measured to be pH = 5.1 and $a_w = 0.96$. By conversion of the a_w to WPSs = 6.6% as described by (Resnik & Chirife, 1988) and using the formulae (1) to (6), WPSb was estimated to be 4%. The company informed that pH of the batter usually was around 5.5. Prediction of growth/survival was performed with CBP for *Y. enterocolitica* and PMP for *E. coli*. In all predictions, lag was excluded.

Results and discussion

Production of semi-dried sausages is a dynamic process where pH, temperature and WPS change with ongoing processing. From the website and label information, WPSb was calculated to be 4.6% and WPSs to be 8%. As there is no drying going on during the fermentation step, WPS will be equal to the WPSb during this processing step. WPS in the product after the drying step will be equal to WPSs, as the sausage is vacuum packaged during the storage period and no further loss of water can occur. There was no information on

Table 1: Time (h) to obtain 1 log-increase (**bold**) or 1 log-reduction (*italic*) at 24°C and 16°C of *Yersinia enterocolitica* and *Escherichia coli*.

| pH | NaCl (% w/v) | <i>Yersinia enterocolitica</i> | | | | <i>Escherichia coli</i> | | | |
|-----|-----------------|--------------------------------|-------------|-------------|-------------|-------------------------|-------------|-------------|------------|
| | | 24°C | | 16°C | | 24°C | | 16°C | |
| | | CBP | PMP | CBP | PMP | CBP | PMP | CBP | PMP |
| 6.0 | 4.5 | 8.7 | 4.4 | 19 | 9.1 | 7.2 | 6.0 | 22 | 17 |
| | 5.0 | 11 | 4.6 | 23 | 9.6 | 8.3 | 6.7 | 24 | 18 |
| | 6.0 | 16 | <i>o.m.</i> | 36 | <i>o.m.</i> | 11 | <i>181</i> | 32 | <i>455</i> |
| | 6.5 | 20 | <i>o.m.</i> | 45 | <i>o.m.</i> | 13 | <i>180</i> | 36 | <i>454</i> |
| | 7.0 | 25 | <i>o.m.</i> | 56 | <i>o.m.</i> | <i>o.m.</i> | <i>179</i> | <i>o.m.</i> | <i>453</i> |
| | 8.0 | <i>o.m.</i> | <i>o.m.</i> | <i>o.m.</i> | <i>o.m.</i> | <i>o.m.</i> | <i>176</i> | <i>o.m.</i> | <i>451</i> |
| 5.0 | 4.5 | 14 | 4.6 | 32 | 9.3 | 14 | 11.7 | 41 | 31 |
| | 5.0 | 17 | 4.7 | 39 | 9.6 | 15 | 13.0 | 46 | 34 |
| | 6.0 | 25 | <i>o.m.</i> | 59 | <i>o.m.</i> | 21 | <i>94</i> | 59 | <i>235</i> |
| | 6.5 | 32 | <i>o.m.</i> | 75 | <i>o.m.</i> | 24 | <i>94</i> | 67 | <i>238</i> |
| | 7.0 | 40 | <i>o.m.</i> | 94 | <i>o.m.</i> | <i>o.m.</i> | <i>95</i> | <i>o.m.</i> | <i>241</i> |
| | 8.0 | <i>o.m.</i> | <i>o.m.</i> | <i>o.m.</i> | <i>o.m.</i> | <i>o.m.</i> | <i>96</i> | <i>o.m.</i> | <i>247</i> |
| 4.5 | 4.5 | 21 | 5.0 | 48 | 9.9 | 23 | 18.0 | 70 | 47 |
| | 5.0 | 25 | 5.0 | 59 | 10 | 27 | 20.6 | 79 | 53 |
| | 6.0 | 38 | <i>o.m.</i> | 91 | <i>o.m.</i> | 35 | <i>59</i> | 102 | <i>147</i> |
| | 6.5 | 47 | <i>o.m.</i> | 114 | <i>o.m.</i> | 41 | <i>59</i> | 116 | <i>150</i> |
| | 7.0 | 59 | <i>o.m.</i> | 146 | <i>o.m.</i> | <i>o.m.</i> | <i>60</i> | <i>o.m.</i> | <i>153</i> |
| | 8.0 | <i>o.m.</i> | <i>o.m.</i> | <i>o.m.</i> | <i>o.m.</i> | <i>o.m.</i> | <i>62</i> | <i>o.m.</i> | <i>159</i> |

CBP: ComBase Predictor, PMP: Pathogen Modeling Program, o.m.: outside model.

the fermentation or pH conditions of the sausage on the website, but it was stated that dextrose was added to boost the fermentation. This information was used to estimate the final pH of the sausage to be around 4.7. Initial pH was assumed to be similar to pH of raw meat, *i.e.* around 5.5 – 6.0. As the suspected sausage was organic, no nitrite was added. It was decided to compare growth and survival of *Y. enterocolitica* and *E. coli* in a matrix covering pH-values from 4.5 to 6.0 and WPS from 4.5% to 8.0%. Subsequently, the growth/reduction rates of *Y. enterocolitica* and *E. coli* in this matrix were predicted, at 24°C mimicking fermentation, at 16°C mimicking drying and at 5°C mimicking storage. Both CBP as well as

PMP were used for the predictions (Table 1). The results showed that *Y. enterocolitica* would be able to multiply during the fermentation at 24°C as well as during the first part of the drying at 16°C (Table 1). Compared to *E. coli* growth of *Y. enterocolitica* was predicted to be slower in the beginning of the fermentation (24°C) but faster in the end with CBP and faster during the whole fermentation with PMP (Table 1). During drying and chilled storage only CBP covered WPS concentrations higher than 5% in the case of *Y. enterocolitica*. CBP predicted that an increase of one log-unit took approx. 50 h at conditions in the beginning of the drying period and approx. 100 h in the middle (Table 1). As multiplication of *Y. enterocolitica* is unlikely at WPS above 7% (ICMSF, 1996), no further growth during the rest of drying as well as storage would be expected. However, in case of a drying failure or addition of a too low amount of NaCl in the batter, growth of *Y. enterocolitica* could occur. In a semi-dried sausage with WPS of 7 %, CBP predicted a one log-increase of *Y. enterocolitica* in about 1 month at 5°C (results not shown).

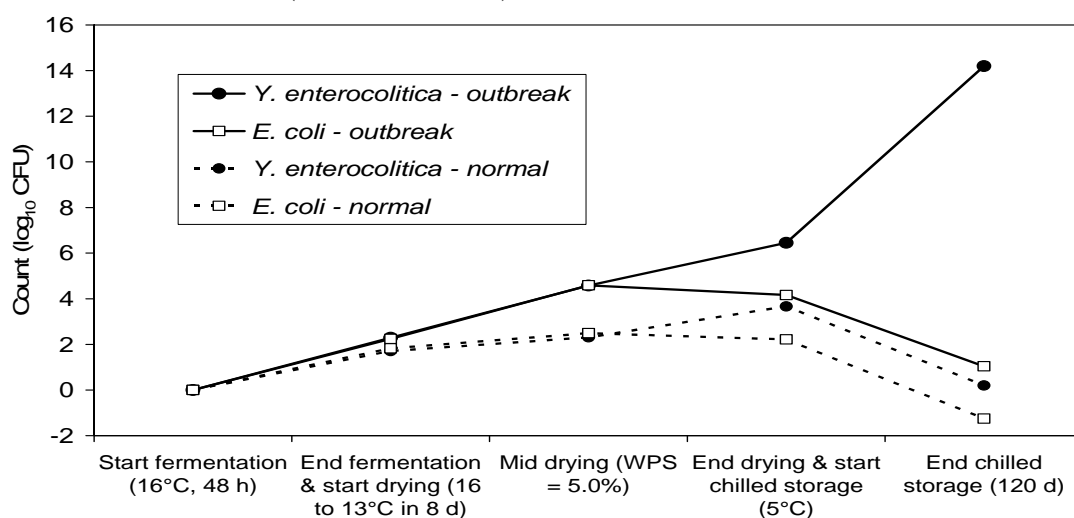


Figure 1: Predicted behaviour of *Yersinia enterocolitica* and *Escherichia coli* under normal production conditions and conditions similar to the semi-dried sausage implicated in the *Escherichia coli* O26:H11 outbreak in Denmark 2007.

When the outbreak source was finally confirmed, a model was constructed in Microsoft Excel that calculated the expected behaviour of *Y. enterocolitica* and *E. coli* during production of the implicated sausage. As shown in Figure 1, the model predicted the level of *Y. enterocolitica* to increase 2.3, 4.2 and 7.8 log-units during fermentation, drying and storage under outbreak production conditions. The corresponding numbers for *E. coli* were 2.2, 1.9 and -3.1 log-units. As can be seen from Figure 1, *E. coli* levels were expected to be highest in the beginning of the shelf-life period. This corresponded well with the fact that most of the cases occurred in the first month after release of the sausage for sale.

Conclusions

CBP and PMP were successfully used as support tools to evaluate whether two cases of infection with *Y. enterocolitica* could have originated from the same sausage that caused an outbreak of *Escherichia coli* O26:H11. Results showed that this was very likely because, at the point of release of the sausage for sale, production failures had led to an extra 3 log-increase of *Y. enterocolitica* as compared to normal production conditions.

References

- ICMSF (1996) Microorganisms in foods 5. Characteristics of microbial pathogens, Blackie Academic & Professional, London, UK (ISBN 0412 47350 X)
- Resnik, S. and Chirife, J. (1988) Proposed theoretical water activity values at various temperatures for selected solutions to be used as reference sources in the range of microbial growth. *Journal of Food Protection* 51 (5), 419-423.

Model for *Listeria monocytogenes* inactivation on dry-cured ham by high hydrostatic pressure processing

S. Bover-Cid¹, N. Belletti², M. Garriga¹ and T. Aymerich¹

¹ IRTA. Food Technology. Finca Camps i Armet, E-17121 Monells, Spain (sara.bovercid@irta.es).

² Dipartimento di Scienze degli Alimenti, Università degli Studi di Bologna, Sede di Cesena, Piazza G. Goidanich, 60, 47023 Cesena, Italy.

Abstract

The aim of the work was to develop a model of the inactivation of *Listeria monocytogenes* on dry cured ham by high hydrostatic pressure (HHP) processing, as a function of the technological parameters: intensity, length and fluid temperature. Dry-cured ham inoculated with *L. monocytogenes* was treated at different HHP conditions (at 347 – 852 MPa; for 138 to 945 seconds; at 7.6 to 24.4 °C) following a central composite design. Bacterial inactivation was assessed in terms of logarithmic reductions of *L. monocytogenes* counts on selective media. According to the best fitting and most significant polynomial equation, pressure and time were the most important factors determining the inactivation extent. The signification of the quadratic term of pressure and time indicated that little effect was observed below 450 MPa whereas holding time longer than 10 min did not result in a meaningful reduction of *L. monocytogenes* counts. Temperature showed not significant influence at the range assayed. The model was validated with data obtained from further experiments within the range of the experimental domain. The accuracy factor and bias factor were within the proposed acceptable values indicating the suitability of the model for predictive purposes.

Key words

High hydrostatic pressure, *Listeria monocytogenes*, Ready-to-eat meat, Dry cured ham, Response surface.

Introduction

Ready-to eat (RTE) meat products are highly appreciated by the consumers, however the manufacture of this type of food products increases the risk of microbial contamination, especially regarding *Listeria monocytogenes*. High-pressure processing (HPP) is an attractive preservation technology that is mild for food but inactivates pathogenic and spoilage microorganisms. This non thermal technology shows a promising potential as listericidal treatment for RTE products (HHS 2008), which could be particularly used for the meat industry as alternative to heat pasteurization.

The effectiveness of the HPP is known to depend on technological parameters, such as pressure, time and temperature, as well as the type and the physiological state of microorganisms. It is also known that food intrinsic factors can also affect the microbial resistance to high pressure. The ability of bacteria to survive HPP can be greatly increased when treated in nutritionally rich media, e.g. meat, containing substances like proteins, fat and carbohydrates (Simpson and Gilmour 1997). Since the results obtained in buffers or synthetic media cannot always be extrapolated and applied to real situations, it is important to assess the effect of HHP in real food matrixes.

Models quantifying the effect of HHP processing parameters in the pathogen inactivation on cured RTE meat products are not available. Therefore, the aim of the present work was to build and validate a model of the inactivation of *Listeria monocytogenes* on dry cured ham as a function of the intensity, length and fluid temperature of HHP treatment.

Materials and methods

Experimental design

Dry-cured ham ($a_w=0.88$ and $pH= 5.84$) was sliced (*c.a.* 25 g/slice) and inoculated with *L. monocytogenes* CTC1034 (originally isolated from dry-cured ham) to a final concentration of *c.a.* 10^7 CFU/g. Inoculated slices were vacuum packaged and treated at different HHP conditions according to a central composite design (Table 1). The equipments Wave6000 NC Hyperbaric (Burgos, Spain) and Thiot ingenierie – NC Hyperbaric (Bretenoux, France – Burgos, Spain) were used for pressures up to and above 600MPa, respectively. Samples for each treatment were prepared and sampled at least in duplicate.

Table 1: Variables and levels used for the central composite design.

| Factors / Levels | -1.68 | -1 | 0 | +1 | +1.68 |
|------------------|-------|-----|-----|------|-------|
| Pressure (MPa) | 347 | 450 | 600 | 750 | 852 |
| Time (minutes) | 2.3 | 5.0 | 9.0 | 13.0 | 15.5 |
| Temperature (°C) | 7.6 | 11 | 16 | 21 | 24.4 |

Analytical determinations

After diluting the samples in sterile saline solution, appropriate decimal dilutions were plated onto selective media, Chromogenic Listeria Agar (Oxoid), incubated at 37°C for 48h. Bacterial inactivation was assessed in terms of logarithmic reductions, i.e. $\log(N/N_0)$, as the difference between counts after the treatments and the initial inoculum.

Mathematical modelling

The models were fitted to the experimental data using the statistical package Statistica for Windows (Statsoft Inc., Tulsa, OK, USA). Backward stepwise linear regression was applied and the goodness of fit of the models was evaluated using the adjusted determination coefficients (R^2_{adj}), the significance *P*-values derived from the Fisher *F*-test and the significance of the Lack of Fit (*LoF*) test.

Model validation

To evaluate the suitability of the developed model, external data from experiments not included during model development as well as data from studies in real RTE meat product inoculated with *L. monocytogenes* have been used. The appropriate validation indexes were calculated according to Baranyi *et al.* (1999) to know the accuracy and the bias of the models developed.

Results and discussion

The pressure resistance of the *L. monocytogenes* CTC1034 on dry cured ham was considerably higher than the resistance shown in previous studies dealing with cooked ham (Jofré *et al.* 2007). Total inactivation was not achieved even after the most intense and long treatment. Most probably, the lower water activity of cured ham has a baroprotective effect. Therefore, models about the inactivation of *L. monocytogenes* in other meat products (Koseki *et al.* 2007) are not representative for dry-cured ham.

Modelling approach

The data relative to the Log of survivor ratio were fitted through the multiple regression analysis to obtain the polynomial equations describing the effects of the studied factors. Since the magnitude of pressure units (in MPa) was too high in comparison with the magnitude of the factors time (in min) and temperature (in °C), unsatisfactory statistical outputs were observed. Therefore, three different approaches were assessed: (i) \log_{10} transformation of the values for the factor pressure, i.e. P_{\log} ; (ii) rescaling the values of the factor pressure with a 1/100 ratio, i.e. $P_{0.01}$; (iii) using reference values from the central composite design levels for

all three studied factors (Table 1), which were summed of 5 in order to avoid negative and zero values and give the following five levels: 3.32, 4, 5, 6 and 6.68, respectively.

Table 2 shows the mathematical equations obtained with the three approaches. The high R^2_{adj} , all very significant, and the statistically no-significant LoF test indicate the goodness of fit of the mathematical equations to the experimental data. The surface response plots resulting from all three approaches were very similar, and Figure 1 shows the surface obtained with the Log transformed pressure. According to the best fitting and most significant polynomial equation (i.e. Log P approach), pressure and time were the most important factors determining the inactivation extent. The significance of the quadratic term of pressure pointed out that little effect was observed below 450 MPa. Cell death increases with pressure, but it does not follow a first order kinetics. In fact, the quadratic term of time was significant, showing that holding time longer than 10 min did not result in a meaningful reduction of *L. monocytogenes* counts. This finding agrees with the tailing phenomenon (Diels *et al.* 2007). Pressure and time showed a statistically significant interaction.

It has been reported that temperature of the treatment can play an important role in microbial inactivation by HPP. At optimal growth temperatures (i.e. 37°C for *L. monocytogenes*), lower inactivation is usually observed than at temperatures below or above the optimal value because membrane fluidity can be more easily disrupted at temperatures beyond optimal growth (Smelt 1998). However, at the range of temperature assayed in the present work, this factor was not significant and thus it was not included in the equation model.

Model validation

The three models obtained were validated with data obtained from further experiments within the range of the experimental domain, but not used to build the model and, whenever possible with data from international scientific literature. The accuracy factor and bias factor (Table 2) were within the proposed acceptable values (Baranyi *et al.* 1999, Ross *et al.* 2000). The best scores, close to the optimum value of 1, were obtained with the first approach (i), when the factor pressure was Log transformed, which was also the one giving the best statistical performance.

Table 2: Equations describing the influence of high hydrostatic pressure processing parameters (pressure, P and holding time, t) on the inactivation of *L. monocytogenes* on dry-cured ham.

| Approach | Mathematical equation | R^2_{adj} (P) | P_{LoF} | B_f | A_f |
|------------------------------|--|-------------------------|-----------|-------|-------|
| (i) Log P | $\text{Log}(N/N_0) = -380.3164 + 292.5942 \cdot [P_{\text{Log}}] - 56.1268 \cdot [P_{\text{Log}}]^2 + 1.4090 \cdot [t] + 0.0133 \cdot [t]^2 - 0.6423 \cdot [P_{\text{Log}}] \cdot [t]$ | 0.9884 (<0.0001) | 0.268 | 1.03 | 1.18 |
| (ii) P 0.01 rescaled | $\text{Log}(N/N_0) = -0.4698 + 1.0528 \cdot [P_{0.01}] - 0.1847 \cdot [P_{0.01}]^2 + 0.0115 \cdot [t]^2 - 0.0558 \cdot [P_{0.01}] \cdot [t]$ | 0.9855 (<0.0001) | 0.205 | 1.11 | 1.16 |
| (iii) reference levels | $\text{Log}(N/N_0) = -4.1777 + 3.5478 \cdot [P_{\text{ref}}] - 0.4273 \cdot [P_{\text{ref}}]^2 + 0.1268 \cdot [t_{\text{ref}}]^2 - 0.3351 \cdot [P_{\text{ref}}] \cdot [t_{\text{ref}}]$ | 0.9839 (<0.0001) | 0.203 | 0.84 | 1.57 |

R^2_{adj} (P): determination coefficient (significance level); P_{LoF} : significance of the lack of fit test; B_f : Bias factor; A_f : Accuracy factor.

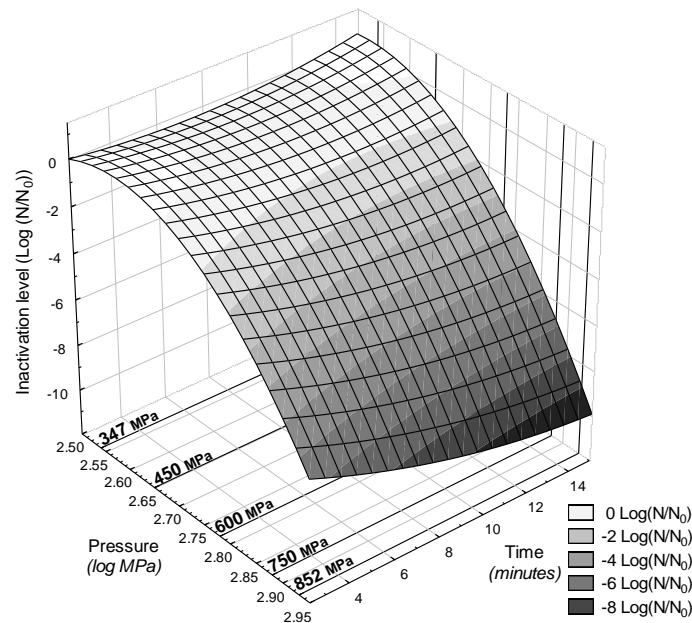


Figure 1: Response surface plot resulting from the model describing the effect of pressure (as Log transformed values) and time on inactivation of the *L. monocytogenes* on dry cured ham.

Conclusions

The present work provided the scientific data to build a mathematical model describing the behaviour of *L. monocytogenes* as a function of the technological parameters of the HHP treatment. Both the statistical performance and the validation parameters support the suitability of the model for predictive purposes.

The output of the present work will assist in the evaluation of the most determinant factors of the efficacy of high hydrostatic pressure to improve food safety. Moreover, the results could also be used by the food industries, for instance to evaluate the relation costs/benefits of a potential implementation of HHP technology in their production processes.

Acknowledgements

This work has been funded by the Spanish *Ministerio de Ciencia e Innovación* (RTA2007-00032 and CSD2007-00016).

References

- Baranyi J., Pin C. and Ross T. (1999) Validating and comparing predictive models. *International Journal of Food Microbiology* 48 (3), 159-166.
- Diels A., Van Opstal I., Masschalck B. and Michiels C.W. (2007) Modelling of high-pressure inactivation of microorganisms in foods. In: S. Brul, S. Van Gerwen and M. Zwietering (Eds.), *Modelling microorganisms in food*. Chapter 9, 161-197, Woodhead Publishing Limited, Cambridge, UK, 294 pp. (ISBN 1-84569-006-0)
- HHS (U.S. Department of Health and Human Services) (2008) *Guidance for industry: Control of listeria monocytogenes in refrigerated or frozen ready-to-eat foods*. Food and Drug Administration. Center for food Safety and Applied Nutrition. Available from: <http://www.fda.gov/Food/GuidanceComplianceRegulatoryInformation/GuidanceDocuments/FoodProcessingHACCP/ucm073110.htm>
- Jofré A., Garriga M. and Aymerich T. (2007) Inhibition of *listeria monocytogenes* in cooked ham through active packaging with natural antimicrobials and high pressure processing. *Journal of Food Protection* 70 (11), 2498-2502.
- Koseki S., Mizuno Y. and Yamamoto K. (2007) Predictive modelling of the recovery of *listeria monocytogenes* on sliced cooked ham after high pressure processing. *International Journal of Food Microbiology* 119 (3), 300-307.
- Ross T., Dalgaard P. and Tienungoon S. (2000) Predictive modelling of the growth and survival of *Listeria* in fishery products. *International Journal of food Microbiology* 62 (3), 231- 245.
- Simpson R. and Gilmour A. (1997) The effect of high hydrostatic pressure on *Listeria monocytogenes* in phosphate- buffered saline and model food systems. *Journal of Applied Microbiology* 83 (2), 181- 188.
- Smelt J.P.P.M. (1998) Recent advances in the microbiology of high pressure processing. *Trends in Food Science and Technology* 9, 152-158.

Simulation of human exposure to mycotoxins in dairy milk

E. Cummins and R. Coffey

UCD School of Agriculture, Food Science and Veterinary Medicine, Belfield, Dublin 4, Ireland
(enda.cummins@ucd.ie)

Abstract

Mycotoxins are secondary metabolites produced by fungi when cereals or animal feed are colonised by moulds. Toxins may be excreted from milk produced by bovines which have been fed mycotoxin contaminated feed; this may represent a human health risk. The objective of this study was to develop a quantitative risk assessment model for five mycotoxins (Aflatoxin, Ochratoxin, Deoxynivalenol, Fumonisin, Zearalenone, T-2) of potential human health concern and to assess the potential human exposure to mycotoxins through consumption of dairy milk. Probability distributions were used to account for parameter uncertainty and variability. The model indicated the simulated tolerable daily intakes (TDIs) from milk for males and females all fell below European Union guidelines. Aflatoxin M1 was the toxin of greatest concern as it had potential to exceed the EU limit of 0.05 lg/kg in milk. The sensitivity analysis identified the concentration of toxins in maize as the area which needs most attention in relation to crop management and agricultural practice. The sensitivity analysis also identified the carry over rate as a factor closely related to risk and as a factor which required further research.

Keywords: Mycotoxins, milk, exposure assessment.

Introduction

Monte Carlo simulation techniques were used to model the human exposure to mycotoxins resulting from mycotoxin contamination of dairy feed, subsequently carried over to dairy milk for human consumption. Mycotoxins are secondary metabolites of fungi and are produced when cereals or animal feed are colonised by moulds. Excretion of such toxins in bovine milk has been documented (Yiannikouris and Jouany, 2002; Blüthgen, Hammer, and Teufel, 2004) and their carryover to dairy produce represents a potential threat to human health. Studies have demonstrated that human dietary exposure to mycotoxins may lead to severe illness and can lead to liver cancer (Marquardt, 1996; Notermans, 2003). This assessment specifically focused on six mycotoxins of concern to humans (Aflatoxin B1/M1, Ochratoxin A, Deoxynivalenol, Fumonisin B1, Zearalenone and T-2 toxin) and involved analysing data on the occurrence of these mycotoxins in three dairy feed ingredients (barley, wheat and maize), inclusion rates in dairy feed, carryover rates to milk and subsequent human exposure. By combining the estimated individual mycotoxin concentrations in milk with available consumption data for the Irish population, the daily intake of mycotoxins from milk by individuals was calculated. The exposure was characterised by the probability that viable mycotoxin concentrations were in milk at the time of consumption.

Materials and methods

Information and data for the development of the model were obtained from Irish studies and expert opinion and, when not available, from research in other countries. The basic model structure is given in Figure 1. The model input data and calculations can be seen in Coffey *et al.* (2009). The model used Monte Carlo simulation techniques (Vose, 2000) to create the output distributions. Monte Carlo methods repeatedly select values randomly from distributions to create multiple scenarios of a problem. Together, these scenarios give a range of possible solutions, some of which are more probable and some less probable resulting in a probability distribution for the solution parameter. The exposure model used probability distributions to account for model uncertainty and variability. The @RISK software package,

version 4.0 (Palisade, USA), in combination with Microsoft Excel 2000 (Microsoft, USA) was used to run the simulation. The simulation was run for 10,000 iterations and reflects the inherent uncertainty in the production of bovine feed, in milk consumption and in the uncertainty of the mathematical process. The probability of a toxin in milk, the level of the toxin in milk and the probability of human exposure were outputs of the mathematical model. Monte Carlo simulation was also used to perform a sensitivity analysis of the model to assist in the identification of critical points in the process.

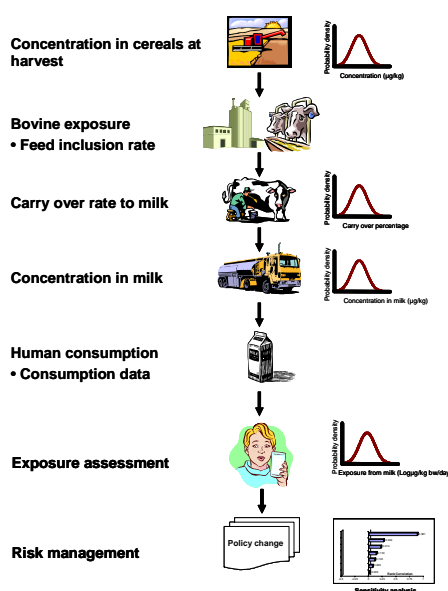


Figure 1: Model structure for simulating feed to food transfer of mycotoxins in bovine milk.

Results and discussion

For each toxin, the risk assessment model produced a probability density distribution representing the potential level of bovine milk contamination with mycotoxins. This represents the uncertainty about the true mean value. A summary of the simulation results, including uncertainty analysis and comparison with EU regulations for each analysed mycotoxin, is given in Table 1. A probability-exposure distribution for males and females was also produced in relation to milk consumption. Table 2 displays a summary of these results together with existing legislation in the EU.

A sensitivity analysis was subsequently conducted to provide a measure of the most important factors affecting the risk to human health from an individual mycotoxin in milk. This information was displayed on a bar chart and can be seen in Figure 2. The sensitivity analysis may be the most important result of the risk assessment. It can be used to identify factors for which risk management strategies can be based in order to reduce the overall exposure to mycotoxins.

Mean levels for the mycotoxins assessed in milk all fell below EU limits (Table 1). Aflatoxin M1 was singled out as the toxin of greatest concern. In certain circumstances its concentration exceeded the EU limit of 0.05 µg/kg in milk. This data was in line with the literature reviewed which also found Aflatoxin M1 occurring at potentially high levels in milk (EFSA, 2004). However, it should be noted that for all other mycotoxins assessed in this study, EU limits only exist for their presence in cereal based foods and are thus not strictly comparable to this risk model which focused on milk.

Table 1. Simulated uncertainty distribution about individual mycotoxin levels in milk

| | AFM1 (µg/kg) | OTA (µg/kg) | DON (µg/kg) | FB1 (µg/kg) | ZEN (µg/kg) | T-2 (µg/kg) |
|-----------------------------|-------------------|-----------------------|------------------|------------------|-----------------|-------------|
| Mean | 0.0161 | 0.0002 | 1.0000 | 0.3600 | 0.3900 | 0.0722 |
| 5 th percentile | 0.0002 | 8.84×10 ⁻⁷ | 0.0049 | 0.0093 | 0.0002 | 0.0006 |
| 95 th percentile | 0.0834 | 0.0009 | 4.0047 | 1.4391 | 2.5570 | 0.2881 |
| Limit | 0.05 ^a | 3 ^b | 500 ^c | 400 ^d | 50 ^e | |

a = EU limit for AFM1 in milk

(Commission Regulation 2003/2174/EC)

b = EU limit for cereal based food

(Commission Regulation (EC) 472/2002)

c = EU limits for cereal based foods (no limits exist for milk)

(Commission Regulation (EC) No 856/2005)

d = EU limits for maize based products (no limits exist for milk)

(Commission Regulation (EC) No 856/2005)

e = No limit for the presence of T-2 in milk/food products exists

(Commission Regulation (EC) No 856/2005)

Table 2. Simulated exposure to individual mycotoxins from milk for males and females.

| | AFM (pg/kg bw/day) | | OTA (pg/kg bw/day) | | DON (pg/kg bw/day) | | FB1 (pg/kg bw/day) | | ZEN (pg/kg bw/day) | | T-2 (pg/kg bw/day) | |
|---------------------------------------|-----------------------|---------|-----------------------|-------------------|-----------------------|----------------------|-----------------------|----------------------|-----------------------|---------------------|-----------------------|--------------------|
| | Male | Female | Male | Female | Male | Female | Male | Female | Male | Female | Male | Female |
| Mean | 8.619 | 9.371 | 0.046 | 0.049 | 608.520 | 650.738 | 327.097 | 351.125 | 43.558 | 46.827 | 32.492 | 34.992 |
| 5 th percentile | 0.356 | 0.381 | 0.002 | 0.002 | 9.961 | 10.293 | 16.960 | 18.253 | 0.478 | 0.479 | 0.927 | 0.988 |
| 95 th percentile | 212.559 | 238.037 | 2.353 | 2.426 | 13580.226 | 13833.657 | 4650.418 | 5021.668 | 6553.209 | 6895.027 | 973.727 | 1168.956 |
| Tolerable daily intake (pg/kg bw/day) | a | a | 5000 ^b | 5000 ^b | 1000000 ^b | 1000000 ^b | 2000000 ^b | 2000000 ^b | 200000 ^b | 200000 ^b | 60000 ^b | 60000 ^b |

a = No tolerable daily intake has been estimated (see text)

(UK food standard agency,2004)

b = Tolerable daily intake estimated by the EU

(Commission Regulation (EC) No 856/2005)

It has not been possible to estimate a Tolerable Daily Intake (TDI) for Aflatoxin which is a carcinogen. The estimated TDI's for all other mycotoxins by the exposure assessment model were below those estimated by the EU indicating negligible risk to humans. It is suggested that the regulatory limits for aflatoxin in milk are set to ensure that any risk from total dietary intake is very low. On examination of the sensitivity results for all the assessed mycotoxins, it was clear that in most cases risk estimates were very sensitive to the initial concentration of each toxin in maize followed by the level in barley and wheat. This concurs with the literature reviewed. The sensitivity analysis also singles out the concentration of toxins in maize as the area which needs most attention in relation to crop management and agricultural practice. The carry over rate also warrants further investigation.

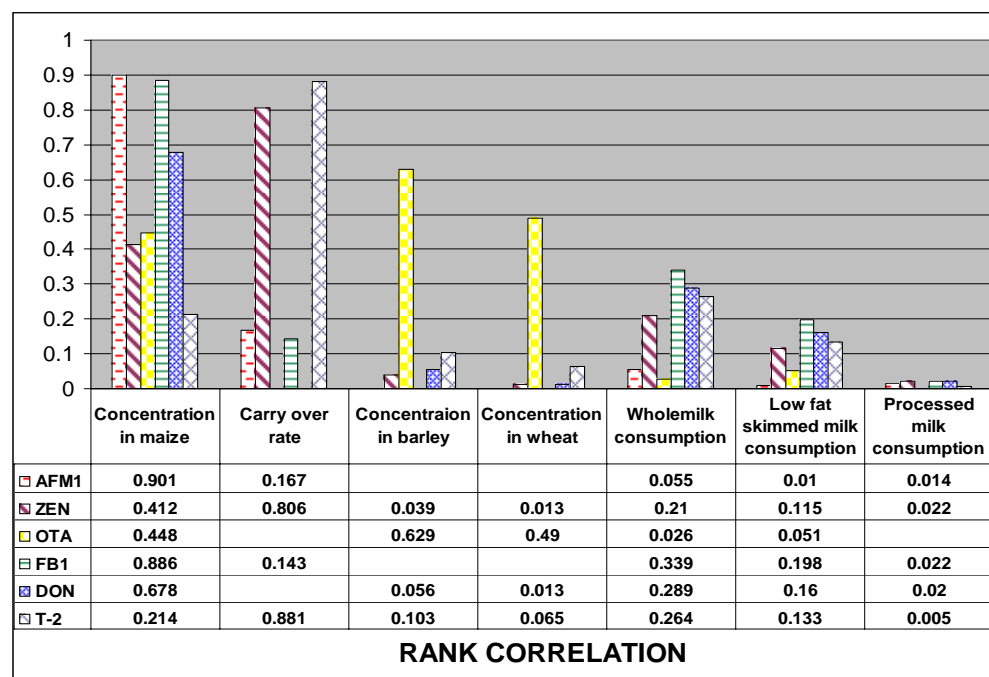


Figure 2. Sensitivity analysis for human exposure to mycotoxins in bovine milk.

Conclusions

Exposure modelling and risk assessment can be valuable tools in assessing risks to humans and animal from mycotoxins in the feed/food chain. The quantitative exposure assessment developed in this study tries to address the deficiency in scientific literature on the estimation of risk from feedborne hazards and serves as an initial attempt to link the animal feed chain and the human food chain. The model assesses the potential human exposure to six mycotoxins in dairy milk. Results fit well with observed data, suggesting that the mathematical approximations of all real life variables are justified. Simulated exposure levels for mycotoxins in milk are all below limits set by the EU except for Aflatoxin M1. Under certain conditions it exceeded EU limits. A sensitivity analysis also suggests that the key to reducing mycotoxin contamination is at the field level, prior to the harvesting of grain for feed production. Results from the exposure assessment model suggested that the presence of mycotoxins in bovine feed at normal contamination levels should not give rise to significant mycotoxin concentrations in milk. Evidence suggests that mycotoxins may never be completely removed from the feed-to-food chain but that current exposure levels are likely to be small in dairy milk and well below EU guidelines. It can be concluded that, from a risk perspective, the presence of mycotoxins in bovine milk poses little risk to man.

References

- Blüthgen, A., Hammer, P. and Teufel P. (2004) Mycotoxins in milk production. Occurrence, relevance and possible minimization in the production chain feeds-milk. *Kieler Milchwirtschaftliche Forschungsberichte* 56(4), 219-263.
- Coffey R., Cummins, E. and Ward S. (2009) Exposure assessment of mycotoxins in dairy milk. *Food Control* 20(3), 239-249.
- EFSA (2004) Opinion of the Scientific Panel on Contaminants in Food Chain on a request from the Commission related to Aflatoxin B1 as undesirable substance in animal feed. *The European Food Safety Authority Journal*, 39, 1-27.
- Marquardt, R.R. (1996) Effects of molds and their toxins on livestock performance: a western Canadian perspective. *Animal Feed Science and Technology* 58(1-2): 77-89.
- Notermans S. (2003) Food authenticity and traceability, ensuring the safety of animal feed. Available from: www.foodmicro.nl/ensuringsafety.pdf Accessed 23/11/08
- United Kingdom food standard agency, (2005) Survey of spices for aflatoxins and ochratoxin A. Available from: <http://www.food.gov.uk/multimedia/pdfs/fsis7305.pdf> (accessed: 19/06/05)
- Vose, D. (2000) *Risk Analysis: a Quantitative Guide*, 2nd Ed: J Wiley Chichester, England, ISBN 0-471-99765-X.
- Yiannikouris, A. and Jouany, J.P. (2002) Mycotoxins in feeds and their fate in animals: a review. *Animal research* 51, 81-9

Validation of a predictive model for the growth and survival of total *Vibrio parahaemolyticus* in post harvest shellstock Asian oysters

S. Parveen¹, C.L. White¹, L. DaSilva¹, A. DePaola², J. Bowers³, and M.L. Tamplin⁴

¹University of Maryland Eastern Shore, Princess Anne, MD (sparveen@umes.edu)

²U. S. Food and Drug Administration, Dauphin Island, AL (Angelo.Depaola@fda.hhs.gov)

³U. S. Food and Drug Administration, College Park, MD (John.Bowers@fda.hhs.gov)

⁴University of Tasmania, Tasmania, Australia (Mark.Tamplin@utas.edu.au)

Abstract

Vibrio parahaemolyticus is a naturally occurring halophilic bacterium that can cause gastroenteritis in seafood consumers. Gastroenteritis is usually associated with the ingestion of contaminated seafood, especially oysters. Recently, a predictive model for the growth and survival of total *V. parahaemolyticus* in post harvest American (*Crassostrea virginica*) oysters was developed and validated against independent data obtained with the same species of oysters harvested from the Chesapeake Bay and Gulf of Mexico. The bias (B_f) and accuracy (A_f) factors of the model with respect to these independent data were 1.06 and 1.08, respectively. However, it remains unknown whether or not the same model would be valid for, and predictive of, growth and survival of total *V. parahaemolyticus* in a different species of oysters, specifically, Asian (*C. ariakensis*) oysters. Therefore, the objective of this study was to address this data gap. Asian oysters were collected from Chesapeake Bay during the warmer months (June and July 2008) and then stored at 5, 10, 20, 25, and 30°C for selected time intervals. At each time interval, two samples consisting of six oysters each were analyzed separately for *V. parahaemolyticus* levels by a direct-plating colony hybridization method. The Baranyi D-model was fitted to the total *V. parahaemolyticus* growth and survival data to estimate the parameters of lag phase duration (LPD), the growth/inactivation rate (GR) and the maximum population density (MPD). Total *V. parahaemolyticus* was slowly inactivated at 5°C and 10°C with GRs of -0.0019, -0.0019 log CFU/h, respectively. Maximum GR (0.0699 log CFU/h) and MPD (6.20 log CFU/g) were observed at 30°C and 25°C, respectively. At 15 °C, 20°C and 25°C, the GR was 0.0155, 0.0246 and 0.0483 log CFU/h, respectively. No significant LPD was observed. The B_f and A_f of the secondary growth model in Asian oysters were 1.18 and 1.19, respectively. A comparison of GRs in Asian oysters to predictions of the FDA *V. parahaemolyticus* quantitative risk assessment was similarly discrepant, with GRs of total *V. parahaemolyticus* in Asian oysters consistently lower than the corresponding predictions for American oysters. A regression analyses of the GR estimates in Asian oysters versus harvest conditions suggested that harvest water conditions had no appreciable effect on GR. These results indicate that the model developed for the growth of total *V. parahaemolyticus* in American oysters would be protective for predicting total *V. parahaemolyticus* growth in Asian oysters. The results of this study also provided basic information necessary to assess the safety of Asian oysters in regard to the growth and survival of *V. parahaemolyticus*, and will assist health and regulatory officials in making decisions related to the release of Asian oysters into the Chesapeake Bay.

Keywords: *Vibrio parahaemolyticus*, predictive models, American and Asian Oysters

Introduction

Vibrio parahaemolyticus is a human pathogen that occurs naturally in estuarine environments and is transmitted to humans primarily through the consumption of raw or mishandled seafood, especially oysters. Gastroenteritis with occasional bloody diarrhea is the most common syndrome associated with *V. parahaemolyticus* infections, but primary septicaemia can occur in individuals

with underlying chronic illness (DePaola *et al.* 2003; Food and Drug Administration 2005). A number of significant *V. parahaemolyticus* illness outbreaks have been reported in the U. S. resulting in an increased interest in this pathogen (DePaola *et al.* 2003). Several investigators have reported that *V. parahaemolyticus* is found in the aquatic environments only during the warmer months, when water temperatures ranged from 15-22°C; densities of *V. parahaemolyticus* in shellfish at harvest positively correlated with harvest water temperature (DePaola *et al.* 2003; Parveen *et al.* 2007). The state of Virginia proposed the introduction of Asian oysters (*Crassostrea ariakensis*) into the lower Chesapeake Bay in the mid 1990s to aid the failing American oyster (*C. virginica*) industry which was declining due to oyster diseases. It has been reported that Asian oysters grow more rapidly than American (*Crassostrea virginica*) oysters and are more resistant to diseases (Calvo *et al.* 2000). A means for forecasting *V. parahaemolyticus* growth over a wide range of temperatures is via quantitative predictive models. Predictive modelling has been used to model the population dynamics of a number of pathogenic and spoilage bacteria of foods. Recently, Parveen *et al.* (2008) developed and validated a predictive model for the growth and survival of *V. parahaemolyticus* in American oysters. However, it is unknown whether a model for developed with respect to American oysters is valid for predicting growth and survival of *V. parahaemolyticus* in Asian oysters.

Materials and methods

Collection of samples

Asian Oysters (*C. ariakensis*) were collected from Chesapeake Bay experimental oyster rearing areas in Virginia in June and July 2008. During collection of samples, seawater temperature and salinity were measured in the upper 0.5 m of the surface water with a dissolved oxygen conductivity meter (Model 85, Yellow Springs Instrument Co., Yellow Springs, OH) (DePaola *et al.* 2003).

Analysis of samples

After sample collection, groups of oysters were stored at 5, 10, 15, 20, 25 and 30°C. At the selected time intervals, two samples of six oysters were analyzed separately by direct-plating colony hybridization method that have been previously described (DePaola *et al.* 2003; Kaysner and DePaola 2004).

Primary and secondary model development

For model development, colony-forming units (CFU) were transformed to log₁₀ values, and mean and standard deviation were plotted in an Excel spreadsheet. The dynamic model described by Baranyi and Roberts (1994) was used to fit curves to the experimental data and to estimate primary parameters including lag phase duration (LPD [h]), growth/inactivation rate (GR [log CFU/h]) and maximum population density (MPD [log CFU/g]) using DMFit curve-fitting software. The secondary model was produced using Table Curve 2D (SPSS Inc., Chicago, IL) with built-in and customized equations. The Ratkowsky square root model was used to model GR. Model performance was measured by bias (B_f) and accuracy (A_f) factors (Baranyi *et al.* 1999).

Statistical analysis

The potential effect of harvest conditions (temperature and salinity) on the growth and survival of *V. parahaemolyticus* in Asian oysters were evaluated by regression analysis.

Results and discussion

The growth and survival of total *V. parahaemolyticus* in oysters were measured at 18 days (432 h) for 5 and 10°C, 10 days (240 h) for 15°C, 7 days (168 h) for 20°C and 3 days (72 h) for 25 and

30°C. Parameters of the growth and survival of total *V. parahaemolyticus* in Asian oysters were estimated based on the Baranyi D-model. *Vibrio parahaemolyticus* was found to be slowly inactivated at 5 and 10°C (i.e. -0.0019 and -0.0019 log CFU/h, respectively). Maximum GR (0.0699 log CFU/h) was observed at 30°C. At 15, 20 and 25°C, the GR was 0.0155, 0.0246, and 0.0483 log CFU/h, respectively. MPD was 5.6, 5.9, 6.2, and 5.9 log CFU/g at 15, 20, 25 and 30°C, respectively. No LPD was observed at any storage temperature. Similar trends were obtained when predictive models were developed for the growth and survival of *V. parahaemolyticus* in American oysters (Parveen *et al.* 2008).

In comparison to these estimated GRs in Asian oysters, predictions of the previously determined model (Parveen *et al.* 2008) of GR versus temperature was found to have bias (B_f) and accuracy (A_f) factors of 1.18 and 1.19, respectively. Baranyi *et al.* (1999) have suggested that the A_f of an acceptable model should be less than or equal to 1.15 if the model has one independent variable. Therefore, the fit of the Ratkowsky square root growth model to the GR estimates meets the definition of acceptable. A comparison of the estimated GRs in Asian oysters to predictions of the FDA *V. parahaemolyticus* quantitative risk assessment (QRA) was similarly discrepant, with GR of total *V. parahaemolyticus* in Asian oysters consistently lower than the corresponding predictions for American oysters (Figure 1). These results indicate that the model developed for the growth of total *V. parahaemolyticus* in American oysters is fail-safe for predicting the growth rate of this bacterium in Asian oysters.

Scatterplots of the estimated GRs at each growth temperature (20, 25, and 30°C) versus harvest water temperature and salinity indicated no systematic pattern to the variation in GR attributable to the harvest conditions. This observation was confirmed by regression analyses of the GR estimates versus harvest conditions; effects of harvest site conditions on the parameters (slope and intercept) of the square root growth model were not significant. The lack of any substantial relationship between GR and harvest water temperature and salinity supports the assumptions made in the FDA *V. parahaemolyticus* QRA (Food and Administration 2005). In that assessment, only one study of *V. parahaemolyticus* growth in oysters was identified (Gooch *et al.* 2002), and extrapolation to other temperatures was accomplished by assuming that the relative GR in oysters versus broth (Food and Drug Administration 2005) was temperature independent. In addition, the results of this study are consistent with the results of a previous study in American oysters (Parveen *et al.* 2008).

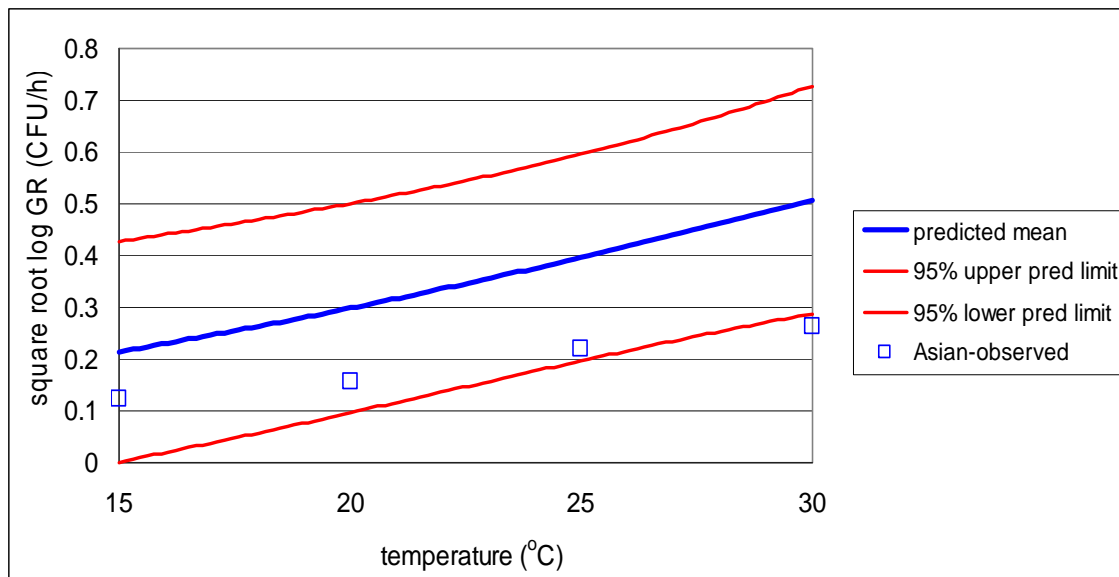


Figure 1: Observed GR of total *V. parahaemolyticus* in the Asian oyster compared to predicted GR based on American oyster *V. parahaemolyticus* model.

Conclusions

The model developed for the growth of total *V. parahaemolyticus* in American oysters was found to be protective (i.e. fail-safe) for predicting total *V. parahaemolyticus* growth in Asian oysters. In addition, the results of this study will assist regulatory officials with their decision to release the Asian oyster into the Chesapeake Bay.

Acknowledgements

We gratefully acknowledge S. Veprek, M. Mudoh, G. Rutto, S. Pagadala, R. Korir, and P. Sang for technical assistance and J. Schwarz, T. Rippen and C. Brooks for helpful suggestions. This project was supported by the National Research Initiative of the United States Department of Agriculture, Cooperative State Research, Education and Extension Service, grant # 2006-35201-16644 and University of Maryland Eastern Shore Advanced Curriculum Technology-Based Instructional Opportunities Network (ACTION).

References

- Baranyi, J. and Robert, T.A. (1994) A dynamic approach to predicting bacterial growth in food. *International Journal of Food Microbiology*. 23(3-4) :277-294.
- Baranyi, J., Pin, C. and Ross, T. (1999) Validating and comparing predictive models. *International Journal of Food Microbiology*. 48(3):159-166.
- Calvo, G.W., Luckenbach, M.W. Allen, S.K. and Bureson. E.M. (2000) A comparative field study of *Crassostrea ariakensis* and *Crassostrea virginica* in relation to salinity in Virginia. School of Marine Science, Virginia Institute of Marine Science, College of William and Mary.
- DePaola, A. Nordstrom, J.L. Bowers, J.C. Wells, J.G. and Cook. D.W. (2003) Seasonal abundance of total and pathogenic *Vibrio parahaemolyticus* in Alabama Oysters. *Applied and environmental Microbiology*. 69(3):1521-1526.
- Food and Drug Administration (FDA). (2005) Draft risk assessment on the public health impacts of *Vibrio parahaemolyticus* in raw molluscan shellfish. U.S. FDA, Washington, DC.
- Gooch, J. DePaola, A. Bowers, J.C. and Marshall, D.L. (2002) Growth and survival of *Vibrio parahaemolyticus* in postharvest American oysters. *Journal of Food Protection*. 65(6):970-974.
- Kaysner, C. A. and DePaola, A. (2004) *Vibrio cholerae*, *V. parahaemolyticus*, *V. vulnificus*, and other vibrio spp., Chapter 9. 8th edition, Bacteriological analytical manual (www.cfsan.fda.edu).
- Parveen, S., Hettiarachchi, K.A. Bowers, J.C. Nordstrom, J.L. Tamplin, M.L. McKay, R. Beatty, W. Brohawn, K. Dasilva. L. and DePaola, A. (2008) Seasonal distribution of total and pathogenic *Vibrio parahaemolyticus* in Chesapeake Bay oysters and waters. *International Journal of Food Microbiology*. 128(2):354-36.
- Parveen, S. Dasilva, L. DePaola, A. Bowers, J.C. White, C. Hettiarachchi, K.A. Rutto, G. Brohawn, K. and Tamplin, M.L. (2008) Development and validation of predictive models for the growth and survival of total *Vibrio parahaemolyticus* in post harvest shellstock American oysters. 108th General Meeting for ASM. June 1-5. 2007. Boston, MA.

Modelling contamination to build a sampling plan: application to French diced bacon industry and *Listeria monocytogenes*

N. Commeau^{1,2,3}, E. Parent², E. Billoir⁴, V. Zuliani⁵ and M. Cornu¹

¹ Microbiologie quantitative et estimation des risques (MQER), Agence française de sécurité sanitaire des aliments (Afssa), 23 avenue du Général de Gaulle, F-94706 Maisons Alfort Cedex, France (n.commeau@afssa.fr)

² UMR 518, Mathématiques et Informatique Appliquées, AgroParisTech/INRA, 16 rue Claude Bernard F-75005 Paris, France

³ AgroParisTech ENGREF, 19 avenue du Maine, F-75732 Paris, France

⁴ UR341 Mathématiques et Informatique Appliquées, INRA, Domaine de Vilvert, F-78350 Jouy-en-Josas, France

⁵ IFIP, Institut de la filière porcine, Pôle Viandes Fraîches et Produits Transformés, 7 avenue du Général de Gaulle, F-94704 Maisons Alfort Cedex, France

Abstract

We designed an experimental sampling plan to get knowledge on *L. monocytogenes* and on lactic acid bacteria (LAB) concentrations on pork breasts after tumbling in a French diced bacon plant. Then, we built a Bayesian model to estimate variability (including between batches-variability) and uncertainty. The results of the model are used to predict *L. monocytogenes* concentration on breasts after tumbling and could be useful to optimise a sampling plan for industrial own-checks.

Keywords

Bayesian modelling, sampling plan, *L. monocytogenes*, pork breasts

Introduction

Nowadays, food business operators who sell food products in Europe have to make sure the product they make is safe (regulation EC 2073/2005). In this context, a sampling plan is a commonly tool used in order to assess contamination of a given food borne pathogen in the plant and to take decisions (throw away a batch, clean the plant better...). Performances of different sampling plans cannot be compared in situ in a plant for cost and feasibility reasons whereas modelling makes it possible. Among all the elements needed to model a sampling plan, it is necessary to get knowledge about pathogen concentration during the process.

We worked with a French plant producing diced bacon. After studying the process from pork breasts to package units of diced bacon (i.e. arrival, tumbling-and-brining, steaming, dicing and packaging (see Billoir et al, same conference for more details)), we designed an experimental sampling plan to get detection and enumeration data on (1) *L. monocytogenes* concentration and enumeration data on (2) LAB on breasts after tumbling and on diced bacon after packaging. To use concentration information, a Bayesian model, using both detection and enumeration data, was built to assess variability and uncertainty of *L. monocytogenes* concentration during the process. This paper is focused on the results concerning breasts after tumbling and their modelling.

Experimental sampling plan construction

To get data, the simplest way was to make a random sampling plan on the breasts. A random sampling is a method of selecting n units out of N such that every one of all the possible samples has an equal chance of being drawn. In that case, we thought breast population was quite heterogeneous and that dividing it into homogeneous subpopulations could produce a gain in the estimates. Breasts can be tumbled 3 times longer during weekend than during week. Thus, we chose a random sampling (sampling where population of N units is divided into N_1, \dots, N_S subunits, here $S=2$, called strata) stratified on tumbling time. The drawing in each stratum is being made independently from the others. A simple random sampling is taken in each stratum.

To determine how many samples need to be taken in a stratified sampling, we used the method proposed by Cochran (1977) which consists of minimising the variance $V(\mu_{st})$ for a given cost C of taking the sample or of minimising the cost C for a given variance, where $V(\mu_{st})$ is the variance of the mean $\mu_{st} = \sum_{i=1}^2 W_i \mu_i$ with $W_i = \frac{N_i}{N}$, where N is the size of the population and N_i the size of the stratum i .

The chosen cost function is $C = c_0 + \sum n_i c_i$, where c_0 represents a overhead cost and c_i the cost of taking one sample from the stratum i . Here, we made the assumption that the cost per unit is the same in all strata ($c_i=c$) and that the variance of μ_i are equal. In that case, the variance V is minimum for a specified cost C , and the cost is minimum for a specified variance V when $n_i = nW_i$. In our case, there are 2 strata: breasts tumbled during week and breasts tumbled during week-end tumbling.

Considering (i) that the sampling plan was constrained to ca. 100 breasts analysed, (ii) that in this plant 12% of breasts are tumbled during week-end and (iii) assuming that the breasts tumbled in one single tumbler compose a batch, the optimised plan was to sample 12 batches (10 tumbled during the week and 2 during week-end), and 9 breasts from each of them.

Sampling plan results

Material and methods

From May to June 2009, 104 breasts (8 to 9 from 12 batches) were sampled just after tumbling, following the sampling plan justified above.

From each sample, 100 cm² of the lean surface were excised for *L. monocytogenes* analyses (detection and enumeration) and 100 cm² of the lean surface for LAB enumeration.

Detection and enumeration of *L. monocytogenes* were carried out on the same test portion. Each 100cm²-test portion was stomached with 100 mL of half Fraser broth, stored 1h at 20°C, and 5mL of this first dilution were pour-plated into 5 plates of ALOA (agar for *Listeria* according to Ottaviani and Agosti). Antibiotics were added to the remaining first dilution for the enrichment procedure of the standard ISO 11290-1/A1. For the analyses of LAB, enumeration was performed onto MRS (Mann-Rogosa-Sharpe), according to the standard ISO 15 214.

Results

LAB concentration was always greater than 10 cfu/cm² and under 3200 cfu/cm². Breast from the same batch have very similar LAB concentration, as it is shown on Figure 1. Usually, differences between the smaller and the higher concentration within batch were less than one log, clearly suggesting that cells concentration is homogenised during tumbling. Concentration for batches 2 and 5 are the highest ones and these two batches are the only ones tumbled during week-end. An ANOVA concluded to a significant week-end effect (p-value<10⁻¹⁶). The extended length of time breasts spend in the tumbler during week-end (3 times longer than the week) may explain this higher concentration: LAB has more time to grow.

L. monocytogenes was detected in 25 of the 104 analysed test portions (24%), with prevalences per batch ranging from 0% to 100%. Here, absence means absence in 100 cm², so the detection threshold is equal to 0.01 cfu/cm², which is much lower than in standard own-checks. In the 11th batch, all tested breasts were positive for detection and enumeration (0.6 to 5.8 cfu./cm²). Among the 11 other batches, only one other sample was positive for enumeration (at the threshold: 0.2 cfu/cm²). This between-batches difference and within-batch homogeneity is consistent with the results obtained with LAB: cells distribution among breasts taken from a single tumbler appears then very homogenous. No week end effect was observed on *L. monocytogenes* data.

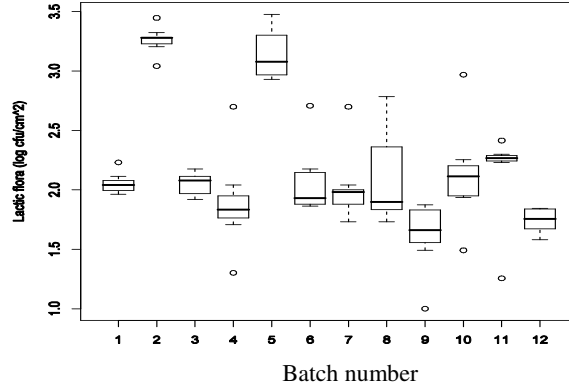


Figure 1: Boxplots of the LAB concentration in cfu/cm² per batch for pork breasts after tumbling

Modelling the *L. monocytogenes* contamination in breasts

Material and methods (model, priors, computation)

The Bayesian model used here to describe *L. monocytogenes* results is composed of two parts: the latent part and the data one. For the latent part, we considered every batch i has a mean concentration z_i which follows a lognormal distribution with mean μ and standard deviation σ .

$$z_i \sim \text{LogN}(\mu; \sigma)$$

Here, we used enumeration data expressed in colony counts (raw data). For the i^{th} batch, we considered that v_{ij} , the number of cells in the test portion j , follows a Poisson distribution with parameter $z_i * S$, where S is the surface of the test portion ($S=100 \text{ cm}^2$). The colony count y_{ij} (ie the number of cells in the volume plated onto the 5 ALOA plates for the j^{th} breast of the i^{th} batch) follows a Poisson distribution with parameter $v_{ij} * d$, where d is the ratio between the volume spread onto the 5 plates and the volume of the first dilution ($d=5/100$).

$$v_{ij} \sim P(z_i * S) \quad y_{ij} \sim P(v_{ij} * d)$$

Concerning detection results (expressed in a binary way: ‘absence’ or ‘presence’), we considered that ‘absence’ meant there was indeed no *L. monocytogenes* in the test portion (but the latter could have been elsewhere on the breast). Considering cells dispersion on the breast follows a Poisson distribution, then the detection result x_{ij} for the batch i and the test portion j follows a Bernoulli distribution with parameter $1 - \exp(-z_i * M)$.

$$x_{ij} \sim \text{Ber}(1 - e^{-(z_i * M)})$$

The directed acyclic graph (DAG) of the model is shown on figure 2.

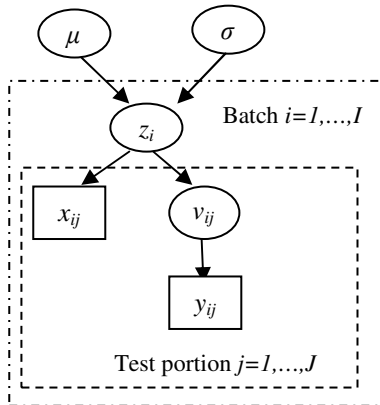


Figure 2: DAG of the model. The mean concentration of the batch i is noted z_i . For a test portion j , there are 2 kinds of data: colony count (y_{ij}) and detection result (x_{ij}). All the parameters are represented in ellipses and data are in rectangles. Arrows indicate a probabilistic dependence between parents and children. For example, z_i has two parents (μ and σ) and $2 * J$ children (all the y_{ij} and the x_{ij}). Given all its parents, a node is independent from all the other nodes, except its children. Nodes without parents are called hyperparameters.

Informative priors were based on outputs of Billoir et al. (same conference):

$$\mu \sim N(-2.94; 2) \quad \text{and} \quad \sigma^2 \sim IG(5.10^{-3}; 7.10^{-2})$$

Bayesian estimation of the posterior distributions were performed using OpenBugs (<http://mathstat.helsinki.fi/openbugs/>, 2007). 200,000 iterations were performed for each model. 1 value out of 10 was taken to avoid autocorrelation.

Results

Table 1: Descriptive statistics of empirical distributions of hyperparameters of the model expressed in log cfu/cm² (S.D. stands for standard deviation and perc. for percentile)

| Parameter | Mean | S.D. | 2.5 th perc. | 50 th perc. | 97.5 th perc. |
|-----------|-------|------|-------------------------|------------------------|--------------------------|
| μ | -2.95 | 0.41 | -3.80 | -2.93 | -2.19 |
| σ | 1.52 | 0.48 | 0.86 | 1.42 | 2.74 |

Descriptive empirical distributions of the hyperparameters are shown on table 1.

The posterior distribution of μ represents the remaining uncertainty on the mean log concentration of the breasts after tumbling and the posterior distribution of σ represents the remaining uncertainty on the between-batches variability. To assess the capacity of the model to replicate data, we chose 50 values of μ and σ from their posterior distributions and replicated 30,000 data y_{rep} for every observed datum y_{obs} . Then, we calculated the mean and the credibility interval at 95% of $y_{rep}=0$, $1 \leq y_{rep} < 10$ and $y_{rep} \geq 10$ colony counts. The result is shown on figure 3. Each time, observed data (black dots) are very close to the mean or, at least are within the credibility interval.

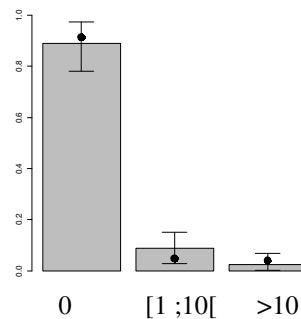


Figure 3: Mean (barplots) and 95% credibility interval (segments) of the replicated data, and real data (black points). Data are colony counts of *L. monocytogenes* measured in breasts after tumbling. Barplots for 0, [1;10[and >10 colony counts.

Conclusion

To optimise an industrial sampling plan for own-checks, the first step is to get knowledge about contamination of the considered hazard during the process. To do that, a way is to select an interesting step and to study the pathogen concentration. In the process of the diced bacon, tumbling is the chosen step. Both results of LAB and *L. monocytogenes* support the conclusion that cells are homogenized during tumbling.

In the considered plant, sampling of breasts is currently performed at the really start of the process. We suggest that sampling after the tumbling step could be more appropriate.

Our modelling of the concentration of *L. monocytogenes* can then be used to optimise the industrial sampling plan but also to calibrate the model describing the process of Billoir et al..

Acknowledgments

This work was supported by a grant from the Agence National de la Recherche (ANR) (France), as a part of the Quant'HACCP project.

References

- Cochran W. (1977) *Sampling techniques*, 3rd edition, John Wiley & Sons, New York, USA, 428pp. (ISBN: 047116240X)
- Billoir E., Denis J-B., Commeau N., Cornu M. and Zuliani V. Probabilistic modelling of *L. monocytogenes* behaviour in diced bacon along the manufacture process chain. *Submitted to the same conference.*

Comparative modelling study on the effect of ozone flow rate and concentration on the colour degradation of orange juice

V.P. Valdramidis¹, B.K. Tiwari², Colm P. O'Donnell² and P.J. Cullen¹

¹ School of Food Science & Environmental Health, Dublin Institute of Technology, Cathal Brugha Street, Dublin 1, Ireland (pjculen@dit.ie)

² Biosystems Engineering, UCD School of Agriculture, Food Science and Veterinary Medicine, University College Dublin, Belfield, Dublin 4, Ireland (brijesh.tiwari@ucd.ie)

Abstract

Colour degradation kinetics of orange juice ozonation at a range of gas flow rates (0.03-0.25 L/min) and ozone concentrations (2-10.0% w/w) are presented in this study. Different modelling approaches describing the effect of the colour rate constants, i.e., k_{TCD} , k_s , k_b , k_L , are evaluated in order to describe them with respect to the applied ozone treatments. For that purpose two modified Ratkowsky-type models and a polynomial model are developed. The polynomial model could accurately describe the changes of the rate constants and the construction of an iso-rate contour plot depicts that the impact that ozone has on the colour characteristics of orange juice has the following order (from the highest to the lowest): k_L (lightness) $> k_a$ (yellowness) $> k_b$ (redness). Current observations are important for further application of ozonation in the fruit juice industry.

Introduction

Colour is one of the most important attributes of food products as it affects sensory perception and consumer acceptance of foods. Additionally, it is an indicator of the cooking degree as well as the concentration of colorants. Fruit juice colour is principally attributed to various carotenoid compounds, including; a-, b-, f-carotene, antheraxanthin, auroxanthin, leutin, luteoxanthin, mutatoxanthin, violaxanthin, zeaxanthin, zeinoxanthin and b-cryptoxanthi (Melendez-Martinez *et al.*, 2007). A knowledge of the processing parameters combined with the kinetics of quality attributes such as the colour is of utmost importance for the design and optimisation of a food process.

Ozone is one of the most potent sanitizers as it appears to be effective against a wide spectrum of microorganisms at relatively low concentrations for treatments of drinking water, municipal wastewater and recently also of fruit juices (Patil *et al.*, 2009). Orange juice colour is a primary factor considered by the consumer in determining juice quality. It is therefore imperative to develop quantitative approaches that evaluate accurately the colour kinetics during ozonation in order to identify the desirable processing conditions for producing orange juice of high colour quality.

Previous studies have shown that L^* , a^* , and b^* colour values were significantly affected by gas flow rate, ozone concentration, and treatment time. The main objective of this research is the careful development of modelling approaches for evaluating the colour range constants as a function of ozonation processing parameters. Defining the standards for an effective process design in the context of quality process optimization is also addressed.

Materials and Methods

Colour data

Freshly orange juice was produced by filtering with a double layer of cheesecloth after purchase from a local market (Reilly Wholesale Ltd., Dublin, Ireland). Ozone treatments were carried out in a 250 mL bubble column with a built-in diffuser. Ozone was generated using an ozone generator (model OL80, Ozoneservices, Canada). Oxygen flow rate was controlled using a gas flow regulator. Data on the lightness (L^*), yellowness (a^*), redness (b^*) of ozonated freshly squeezed orange juice samples were obtained. Total colour difference (TCD) has been calculated as follows.

$$TCD = \sqrt{(L^* - L_o)^2 + (a^* - a_o)^2 + (b^* - b_o)^2} \quad (1)$$

where L_o , a_o and b_o are the colour values of untreated juice.

Rate constants for each of the colour parameters as previously calculated by Tiwari *et al.* (2008) were correlated with respect to the control variables of the gas flow rate (0.03-0.25 L/min) and the ozone concentration (2-10.0% w/w).

Model development

Initially the different rate constants with respect to the processing factors were tested for a number of models, i.e., second order polynomial, different types of Ratkowsky-type model. The second-order response surface model with an interaction factor reads as follows:

$$k_{TCD} = \beta_o + \beta_1 \cdot T + \beta_2 \cdot T^2 + \beta_3 \cdot A + \beta_4 \cdot A^2 + \beta_5 \cdot T \cdot A \quad (2)$$

where β_i are the polynomial coefficients. Only significant parameters ($P < 0.05$) have been retained by performing a stepwise fit. Two different types of the Ratkowsky type model (Ratkowsky *et al.*, 1983) have also been considered. These transformed equations appear as follows:

$$\sqrt{k_{TCD}} = \alpha_1 \cdot \sqrt{[Ozone]} - a_2 \cdot \sqrt{flow_{rate}} - a_3 \quad (3)$$

$$k_{TCD} = \alpha_1 \cdot ([Ozone] + a_2) \cdot (flow_{rate} + a_3) \quad (4)$$

Where [Ozone] is the ozone concentration expressed in %w/w and $flow_{rate}$ is the flow rate of ozone in the system expressed in L/min. The different secondary models are evaluated with respect to their performance (comparison of root mean squared error *RMSE*). For the best performing model contour plots of the combined ozone flow rate and concentration with respect to the iso-rate colour degradation rates were constructed.

Results and Discussion

The response surface models accurately described the studied kinetics. When the models were compared statistically (based on the estimation of the *RMSE*) it appeared that the polynomial model could describe more accurately the kinetics of all the colour constants.

Table 1. Statistical evaluation of all the studied models based on the estimation of the Root Mean Squared Error (*RMSE*).

| | <i>a</i> | <i>b</i> | <i>L</i> | TCD |
|--------------|----------|----------|----------|--------|
| Equation (2) | 0.0055 | 0.0013 | 0.0243 | 0.0615 |
| Equation (3) | 0.014 | 0.0055 | 0.0347 | 0.0433 |
| Equation (4) | 0.0086 | 0.0017 | 0.0329 | 0.1033 |

A monotonic increase for all the studied colour constants was evident for an increasing flow rate and increasing ozone concentration (see Figure 1). This proves the high oxidative capacity of ozone on the quality indices of orange juice. An analysis of ozone flow rate and ozone concentration diagrams was also performed based on the developed mathematical expressions (Figure 2). The developed iso-rate contour plots integrated the information of all the studied colour variables. The more intense the treatment (i.e., high flow rate, high concentration) the higher is the degradation of the lightness followed by the yellowness and

the redness of the orange juice. Flow rate as low as 0.03 L/min and ozone concentration of 2% w/w had the lowest effect on the colour of orange juice.

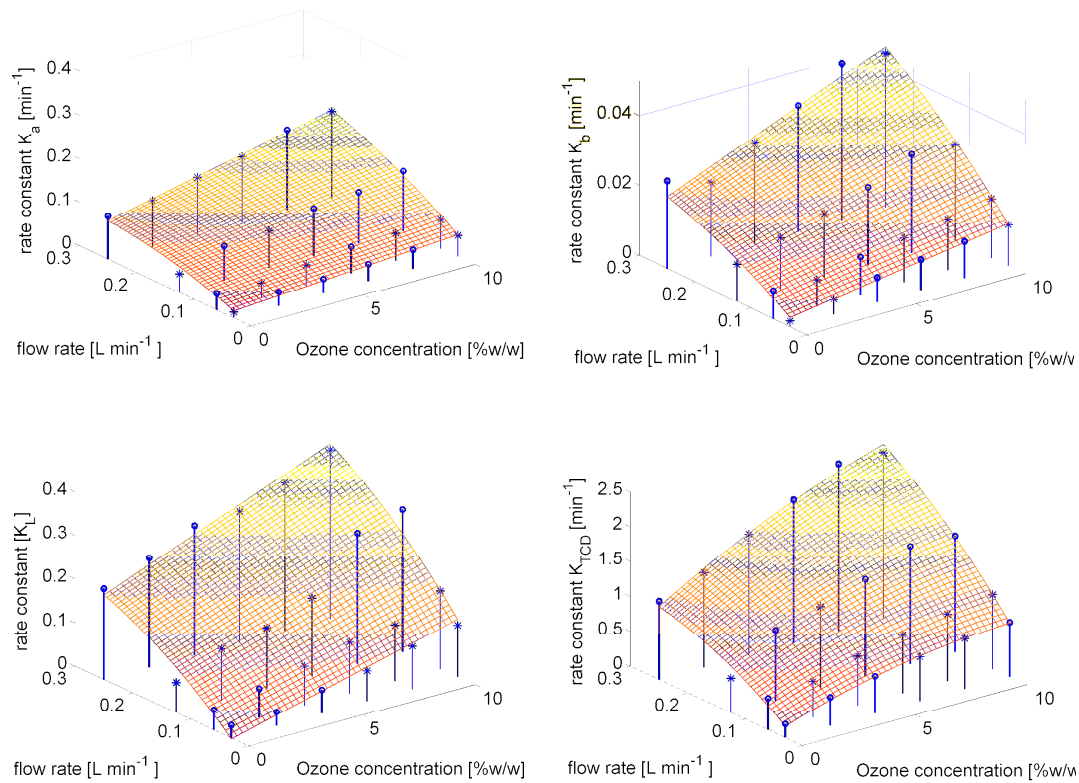


Figure 1. Modelling the colour rate constants as a function of the processing variables, i.e., ozone concentration, ozone flow rate. Top left : k_a rate constant, top right : k_b rate constant, bottom left : k_L rate constant and bottom right : k_{TCD} rate constant. (o): experimental data points above the surface, (*): experimental data points under the surface.

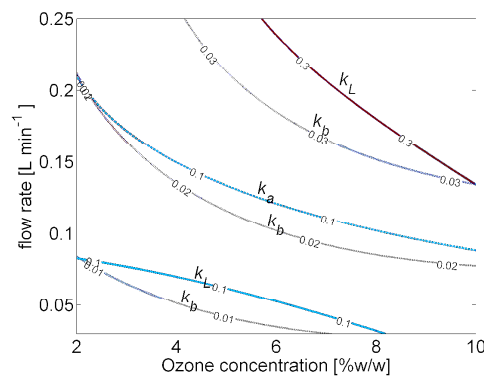


Figure 2. Iso-rate contour plots of the colour constants for the applied ozone treatments as presented with respect to the flow rate and the ozone concentration.

As it has been discussed in the literature, ozone has a high oxidation potential (2.07 V) resulting in the degradation of most organic compounds. The oxidizing ability of ozone is derived from the nascent oxygen atom. However it has been reported that ozonation of organic dyes results in loss of colour due to the oxidative cleavage of the chromophores

(Nebel 1975) due to attack on conjugated double bonds. Similarly the chromophore of conjugated double bonds of carotenoids is responsible for orange juice colour.

Conclusions

Quantitative studies focusing on the effect of processing variables to the quality attributes are essential for optimizing or designing any process. Application of mathematical modelling techniques during ozonation of orange juice was used as a driving force for identifying the effect of ozone flow rate and concentration during this non-thermal processing of orange juice. The output of this study could be considered for framing food industry guidelines that are of importance for non-thermal pasteurization of fruit juice by ozone.

Acknowledgements

Funding for this research was provided under the National Development Plan 2000-2006, through the Food Institutional Research Measure, administered by the Department of Agriculture, Fisheries & Food, Ireland.

References

- Melendez-Martinez, A. J., Vicario, I. M. and Heredia, F. J. (2007) Review: Analysis of carotenoids in orange juice. *Journal of Food Composition and Analysis* 20(7), 638-649.
- Nebel, C. (1975) Ozone decolorization of secondary dye laden effluents Second Symposium on Ozone Technology Montreal.
- Patil, S., Bourke, P., Frias, J. M., Tiwari, B. K. and Cullen, P. J. (2009) Inactivation of *Escherichia coli* in orange juice using ozone *Innovative Food Science & Emerging Technologies* in press.
- Ratkowsky, D. A., Lowry, R. K., McMeekin, T. A., Stokes, A. N. and Chandler, R. E. (1983) Model for bacterial culture-growth rate throughout the entire biokinetic temperature-range. *Journal of Bacteriology* 154(3), 1222-1226.
- Tiwari, B. K., Muthukumarappan, K., O'Donnell, C. P. and Cullen, P. J. (2008) Kinetics of Freshly Squeezed Orange Juice Quality Changes during Ozone Processing. *Journal of Agricultural and Food Chemistry* 56(15), 6416-6422.

Probability of survival and/or growth of *Listeria monocytogenes* cells exposed to heat-shock and essential oils treatments and proteomic analysis.

P.M. Periago^{1,2}, L. Guevara¹, M. Muñoz¹, P.S. Fernández^{1,2}

¹ Department of Food Engineering and Agriculture Equipment, Polytechnic University of Cartagena, Paseo Alfonso XIII 48, 30203 Cartagena,, Spain (paula.periago@upct.es)

² Laboratory of Microbial Food Safety, Institute of Plant Biotechnology, Polytechnic University of Cartagena, Campus Muralla del Mar, 30202 Cartagena, Spain (pablo.fernandez@upct.es)

Abstract

The antibacterial action of carvacrol and thymol on two *Listeria monocytogenes* strains (STCC4031 and NCTN4032) was studied. The compounds of essential oils, carvacrol or thymol, showed bactericidal effect on *L. monocytogenes* cells, which was more evident with increasing the exposition time. The combined treatment of mild heat (55°C) and carvacrol and/or thymol also decreased the survivors of *L. monocytogenes*, showing a synergistic antibacterial effect. The analysis of survival curves using the frequency distribution function of Weibull allowed an accurate prediction of the level of inactivation achieved. This study indicates the potential use of carvacrol and thymol applied simultaneously with a mild heat treatment for preservation of minimally processed foods.

Keywords: *Listeria monocytogenes*; predictive modelling; mild heat; essential oils compounds; cell injury.

Introduction

L. monocytogenes is a foodborne pathogen microorganism that causes listeriosis, which has been associated with outbreaks by ingestion of milk, cheese, vegetables, salads and meat (Jacquet *et al.*, 1995). The use of natural antimicrobial systems for food preservation could accomplish the demand of additive free food products from consumers. Carvacrol and thymol are compounds present in the essential oil fraction of *Oreganum* and *Thymus* plants and both compounds are classified as GRAS. They both have been shown to exhibit antibacterial activity including food pathogens (Sivropoulou *et al.*, 1996; Helander *et al.*, 1998; Ultee *et al.*, 2000; Periago and Moezelaar, 2001; Periago *et al.*, 2001, 2004, 2006; Delgado *et al.*, 2004). The microbial safety and stability of most minimally processed foods is based on application of combined preservative factors of which (mild) heating is the most common preservation technique in use these days (Leistner, 2000). As sublethal injury is supposed to be related to the higher sensitivity of survivors to stress conditions after treatment, the success of a combined treatment should be correlated with the degree of sublethal injury caused by the hurdles in the bacterial population (Wuytack *et al.*, 2003). Bacteria have evolved adaptive networks to face the challenges of changing environments and to survive under conditions of stress (Abee and Wouters, 1999). When microorganisms develop resistance to commonly used preservation methods, food quality and safety may be affected and therefore understanding of stress adaptive mechanisms plays a key role in designing safe food processing conditions (Bower and Daeschel, 1999). However, so far the combined effect of carvacrol, thymol and mild heat on the viability and the proteomic profile of *L. monocytogenes* cells are not well known.

In the present study, the viability and the sublethal injury of cells of two strains of *L. monocytogenes* (STCC 4031 and NCTN4032) to moderate heat and/or essential oils compounds of (carvacrol and thymol) treatments were studied. Then, protein extracts of cells were analysed by 2-D electrophoresis in order to investigate changes in the protein patterns when exposed to mild heat alone, to essential oils alone or to both treatments simultaneously.

Materials and methods

Bacterial strain

L. monocytogenes STCC4031 (type strain) and *L. monocytogenes* NCTN4032 (associated with case of meningitis after eating cheese) were provided by the Spanish Type Culture Collection (STCC). Cultures were maintained at -80°C in 30% glycerol until use.

Chemicals

Carvacrol (Fluka Chemie AG, Buchs, Switzerland) and thymol (Sigma Aldrich Chemie, Steinheim, Germany) stock solutions were held in 95% ethanol at 4°C .

Combined stresses

Suspensions cells were placed into tubes containing TSBYE medium (Trypticase Soy Agar with Yeast Extract). The treatments consisted of mild heat only (55°C), essential oils compounds only (0.3 mM of carvacrol, 0.3 mM of thymol, 0.3 mM of carvacrol and 0.3 mM of thymol) and mild heat combined with essential oils compounds (55°C and 0.3 mM of carvacrol, 55°C and 0.3 mM of thymol, 55°C and 0.3 mM of carvacrol and 0.3 mM of thymol). Treatments were performed during 30 min exposure and the viability was measured after 0, 5, 10, 15, 20, and 30 min.

Viable count and survival curves

After appropriate serial dilutions, samples were plated onto TSAYE (non selective medium) and onto TSAYE-NaCl (selective medium). Plates with TSAYE were incubated for 48 h at 37°C and those with TSAYE-NaCl for 72 h at the same temperature. After incubation, colony forming units (CFU) were counted. Survival curves were based on mean values obtained from at least three independent experiments.

Determination of degree of injury

The number of injured cells was determined by subtracting the CFU on TSAYE from those on TSAYE-NC (Muñoz *et al.*, 2007), and percent injury was calculated for each of triplicated samples using the following equation (Hansen and KnØchel, 2001).

$$\% \text{ injured cells} = 100 \times \frac{\text{cfu on TSAYE} - \text{cfu on TSA - NaCl}}{\text{cfu on TSAYE}}$$

Statistical data processing and distribution fitting

An ANOVA analysis was performed to establish significant differences among the different combinations of conditions tested using MATLAB[®] software. The interpretation of the parameters obtained and goodness of fit using frequency distributions of Weibull was evaluated. If the inactivation of microorganisms by antimicrobial exposure follows a Weibull distribution, the survival function will be: $S(t) = e^{-a^*(t)^n}$

Predictions for time to a certain decrease in the microbial population can be derived from eqn (1), the function would be: $t = \ln(S(t)/-a)^{1/n}$

Proteomic analysis of *L. monocytogenes*

Total cellular protein extractions were performed as described by Periago *et al.* (2002a,b). Subsequently, proteins in the homogenate were analysed by two-dimensional gel electrophoresis (2D-E). 2-DE separation of *L. monocytogenes* protein extracts was performed using immobilized pH gradient strips for isoelectric focusing and a vertical system for SDS-PAGE separation. The gels were silver stained and analyzed, integrated and normalized using PD-Quest software (Bio-Rad, Richmond, CA). Induction factors for each stress-induced protein were calculated as the ratio between the normalized value in 'stress'-gel and the normalized value in 'control'-gel.

Results and discussion

Survival curves

In the presence of compounds with essential oils survival curves presented a downwards concavity that was best fitted using the Weibull model since a linear model could not describe the experimental results (Figure 1). This was indicated by a “ β ” value lower than 1 in all cases (Table 1).

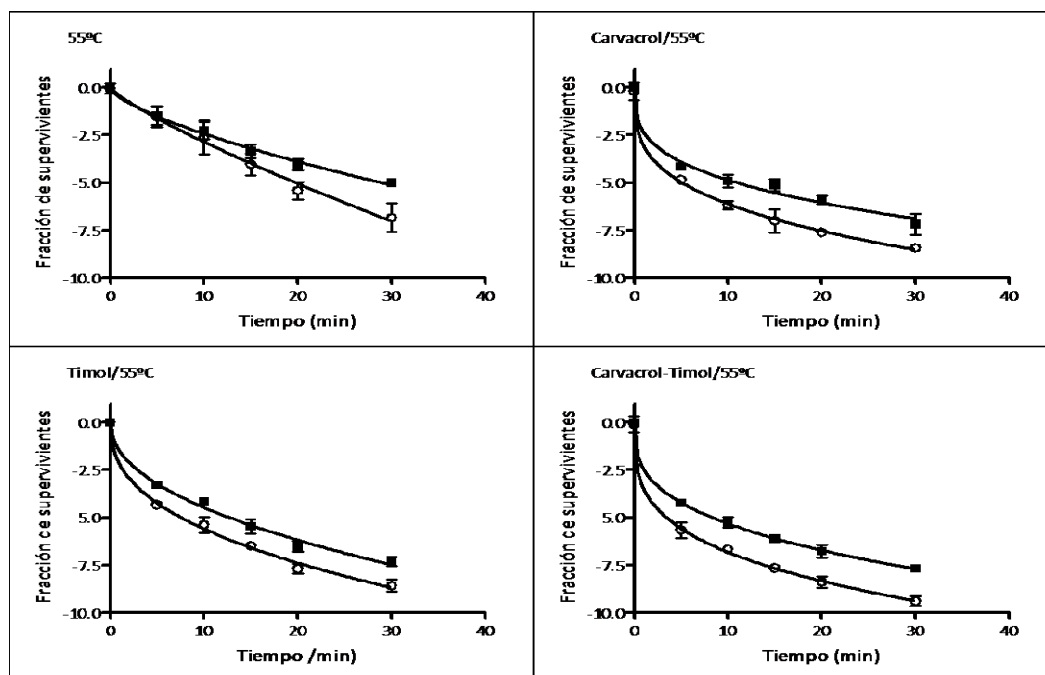


Figure 1. Survival curves of *L. monocytogenes* CECT 4031 exposed to a mild heat treatment alone (55°C) and combined with compounds of essential oils carvacrol and/or thymol (0.3 mmol/mL each one). ■ : nonselective medium and ○ : selective medium.

Table I. Growth parameters α y β of *L. monocytogenes* CECT 4031 exposed to a mild heat treatment alone (55°C) and combined with compounds of essential oils carvacrol and/or thymol (0.3 mmol/mL each one).

| <i>L. monocytogenes</i> CECT 4031 | | | | | |
|-----------------------------------|------------|------------|-------------|------------|-----------|
| Treatment | MNS | | MS | | R^2 |
| | α | β | α | β | |
| 55°C | 3.1±0.2 | 0.73±0.03 | 2.42±0.2 | 0.76±0.03 | 0.98/0.99 |
| Carvacrol | 0.074±0.01 | 0.32±0.008 | 0.032±0.005 | 0.32±0.007 | 1/0.99 |
| Thymol | 0.38±0.04 | 0.46±0.01 | 0.33±0.04 | 0.5±0.01 | 0.99/0.99 |
| Car-Thym | 0.08±0.005 | 0.34±0.004 | 0.02±0.004 | 0.31±0.009 | 0.99/0.99 |

MNS: nonselective medium. MS: selective medium.

Degree of injury

Injury increased with time of exposure for heat treated cells. However, in the presence of carvacrol, thymol or their combination this increase was evident up to 5 min of exposure, since afterwards they reached a level close to 99% that remained constant.

Proteomic analysis of L. monocytogenes

An important induction of several proteins was observed in 2D gels of cell extracts exposed to heat and heat combined with carvacrol and thymol compared to control.

Conclusions

The combination of mild heat, carvacrol and thymol caused an important inactivation of *L. monocytogenes* cells and, therefore, could contribute to extend the shelf-life of food products. Non linear models can be a useful tool to describe the behaviour of this microorganism exposed to hurdle technology including essential oils. Resistance against these compounds could be, at least partly explained, by the induction of stress induced proteins which can have implications in food safety.

Acknowledgements

The work was funded by the Spanish Ministry of Science and Innovation through project AGL 2006-13320-C03-02/ALI. Marina Muñoz acknowledges Fundacion Cajamurcia for her post-doc grant

References

- Abee, T., Wouters, J.A., 1999. Microbial stress response in minimal processing. *Int. J. Food Microbiol.* 50, 65-91.
- Bower, C.K., Daeschel, M.A., 1999. Resistance responses of microorganisms in food environments. *Int. J. Food Microbiol.* 50, 33-44.
- Delgado, B.; Fernández, P.S.; Palop, A.; Periago, P.M. 2004. Effect of thymol and cymene to establish safe conditions related to *Bacillus cereus* vegetative cells through the use of frequency distributions. *Food Microbiol.* 21: 327-334.
- Hansen, T. B. and Knøchel, S. 2001. Factors influencing resuscitation and growth of heat injured *Listeria monocytogenes* 13-249 in sous vide cooked beef. *Int J Food Microbiol.* 63. pp. 135 - 147.
- Helander I. M., Alakomi H.-L., Latva-Kala K., Mattila-Sandholm T., Pol I. E., Smid E. J., Gorris L. G. M. and von Wright A. 1998. Characterisation of the action of selected essential oil components on Gram-negative bacteria. *J. Agricul. Food Chem.* 46: 3590-3595.
- Jacquet, C., B. Catimel, R. Brosch, C. Buchrieser, P. Dehaumont, V. Goulet, A. Lepoutre, P. Veit, and J. Rocourt. 1995. Investigations related to the epidemic strain involved in the French listeriosis outbreak in 1992. *Appl. Environ. Microbiol.* 61:2242-2246.
- Leistner, L. 2000. Basic aspects of food preservation by hurdle technology. *Int. J. Food Microbiol.* 55:181-186.
- Muñoz, M., De Ancos, B., Sánchez-Moreno, C., and Cano, P. 2007. Effects of high pressure and mild heat on endogenous microflora and on the inactivation and sublethal injury of *Escherichia coli* inoculated into fruit juices and vegetables soup. *J Food Prot.* 70. pp. 1587 – 1593.
- Periago, P.M.; Abee, T.; Wouters, J.A. 2002a. Analysis of the heat-adaptive response of psychrotrophic *Bacillus weihenstephanensis*. *Int. J. Food Microbiol.* 79(1-2): 17- 26.
- Periago, P.M.; Conesa, R.; Delgado, B.; Fernández, P.S.; Palop, A. 2006. *Bacillus megaterium* spore germination and growth inhibition by a treatment combining heat with natural antimicrobials. *Food Technol. Biotechnol.* 44(1): 17-23.
- Periago, P.M.; Delgado, B.; Fernández, P.S.; Palop, A. 2004. Use of carvacrol and cymene to control growth and viability of *Listeria monocytogenes* cells and predictions of survivors using frequency distribution functions. *J. Food Prot.* 67: 1408-1416.
- Periago P. M. and Moezelaar R. 2001. Combined effect of nisin and carvacrol at different pH and temperature levels on the viability of different strains of *Bacillus cereus*. *Int. J. Food Microbiol* 68: 141-148.
- Periago, P. M., Palop, A. and Fernández, P. S. 2001 Combined effect of nisin, carvacrol and thymol on the viability of *Bacillus cereus* heat-treated vegetative cells. *Food Sci. Technol. Int.* 7(6), 487-492.
- Periago, P.M.; van Schaik, W.; Abee, T.; Wouters, J.A. 2002b. Identification of proteins involved in the heat-stress response of *Bacillus cereus* ATCC14579. *App. Environ. Microbiol.* 68(7): 3486-3495.
- Sivropoulou A., Papanikolaou E., Nikolaou C., Kokkini S., Lanaras. T. and Arsenakis M. (1996). Antimicrobial and cytotoxic activities of *Origanum* essential oils. *J. Agricul. Food Chem* 44(5): 1202-1205.
- Ultee A., Slump R. A., Steging G. and Smid E. J. 2000. Antimicrobial activity of carvacrol towards *Bacillus cereus* on rice. *J. Food Protec.* 63(5): 620-624.
- Wuytack, E.Y.; Duong Thi Phuong, L.; Aertsen, A.; Reyns, K.M.F.; Marquenie, D.; De Ketelaere, B.; Masschalck, B.; Van Opstal, L. et al. 2003. Comparison of sublethal injury induced in *Salmonella enterica* serovar *Typhimurium* by heat and by different nonthermal treatments. *J. Food Protec.* 66: 31-37.

A Predictive model for evaluating the effects of cultivation on oat β -glucan levels

E. Cummins and U. Tiwari

Biosystems Engineering, UCD School of Agriculture, Food Science and Veterinary Medicine, University College Dublin, Belfield, Dublin 4, Ireland (uma.tiwari@ucd.ie; enda.cummins@ucd.ie)

Abstract

Oat β -glucans have many positive health effects on human health by improving the nutritional value of food. This study aims to develop a farm-level baseline model using Monte Carlo simulation technique (including three scenario analysis) to compare and assess the impact of various cultivation and farm-level factors (including cultivar factors, environmental conditions, agronomic and storage factors) influencing β -glucan content in harvested oat grains and to identify potential parameters which influence β -glucan content. The simulated mean β -glucan level in harvested oat grain was 3.50 and 4.25 g/100g for hulled oats (HO) and naked oats (NO), respectively. A sensitivity analysis highlighted that cultivar selection was the most important input parameter compared to other inputs in determining the final β -glucan level (correlation coefficients of 0.64 and 0.79 for HO and NO, respectively). The analysis also indicated the positive effect of delayed sowing on β -glucan content (correlation coefficients of 0.32 and 0.25 for HO and NO, respectively). Germination and storage factors showed a negative impact on the final β -glucan levels. A scenario analysis highlighted the applicability of the proposed model for various agronomic practices. This study provides a simulation tool to assess critical factors influencing β -glucan content in harvested grain.

Introduction

Oats is an important cereal crop throughout the developing world, and in recent years, the amount of oats used for human consumption has increased because of the dietary benefits associated with phytochemicals, such as β -glucans, present in the grain (Food and Drug Administration, 1997). Many researchers showed the positive nutritional effect by incorporating oats β -glucan into various food products, including breakfast cereals, beverages, bread and infant foods (Flander *et al.*, 2007 ; Yao *et al.*, 2007). Oat β -glucan is a viscous and soluble dietary fibre component which can attenuate postprandial glucose levels and lower serum cholesterol levels (Theuvsen and Mensink, 2007 ; Tosh *et al.*, 2008). Variations in β -glucan content are influenced by various cultivar selections, environmental and agronomic practices. This study was used to quantify the variability and uncertainty in the level of β -glucans in harvested oats and, through a sensitivity analysis, assess the relative importance cultivation and management practices have on influencing the final β -glucan levels in harvested oats.

Materials and Methods

Model development

Data on thirty hulled oat (HO) and naked oat (NO) genotypes were collated from existing scientific and technical literature. In addition, data on the impact of various environmental conditions, agronomic practices and storage factors was collated. Monte Carlo simulation techniques were used to model uncertainty and variability using probability distribution functions (PDFs) resulting in an output distribution. The probability distributions used in the model are summarised in Table 1. Monte Carlo methods randomly select values from given distributions to create multiple scenarios of a problem. The scenarios developed used the same data as the

baseline model except where specified. No fertiliser application was assumed for scenario 1, to assess the predicted influence of fertilisation. For scenario 2, oats grains are harvested on the day of maturity (i.e. growth stage 92) and no storage of the grain was assumed in the scenario 3. The simulation was performed using the parameters and calculations and the model run for 10,000 iterations.

Results and Discussion

The baseline model found that the mean simulated β -glucan level in harvested oats grain was 3.50 and 4.25 g/100g for HO and NO, respectively (Figure 1). A sensitivity analysis showed that cultivar selection was the most important parameter in determining the final β -glucan level (correlation coefficients of 0.64 and 0.79 for HO and NO, respectively), when compared to other environmental and agronomical factors. The analysis also indicated that crops sown in the latter part of the sowing season may influence the final β -glucan levels (correlation coefficients of 0.32 and 0.25 for HO and NO, respectively), highlighting the importance of harvesting date. Germination time, storage days and temperature showed a negative impact on the final β -glucan levels (Figure 2). In addition to the baseline model, the scenario analysis also highlighted the impact of fertiliser application, harvest date and storage factors.

Scenario 1 showed the importance of fertiliser application with a potential 3 % decrease in β -glucan content when no fertiliser was applied. This highlights the small, but positive effect, of fertiliser application on the β -glucan levels. In contrast, scenario 2 showed the impact of harvesting date with a potential increase in β -glucan by approximately 6.4 % for both HO and NO cultivars, highlighting the importance of harvesting as close to growth stage 92 as possible. This optimises the retention of β -glucan in the harvested grain and reduces the possibility of germination and thereby controlling grain yield. By not storing oats grain after harvesting (scenario 3) β -glucan content significantly increased by 11 % for both HO and NO cultivars, highlighting the impact of storage on the level of β -glucan.

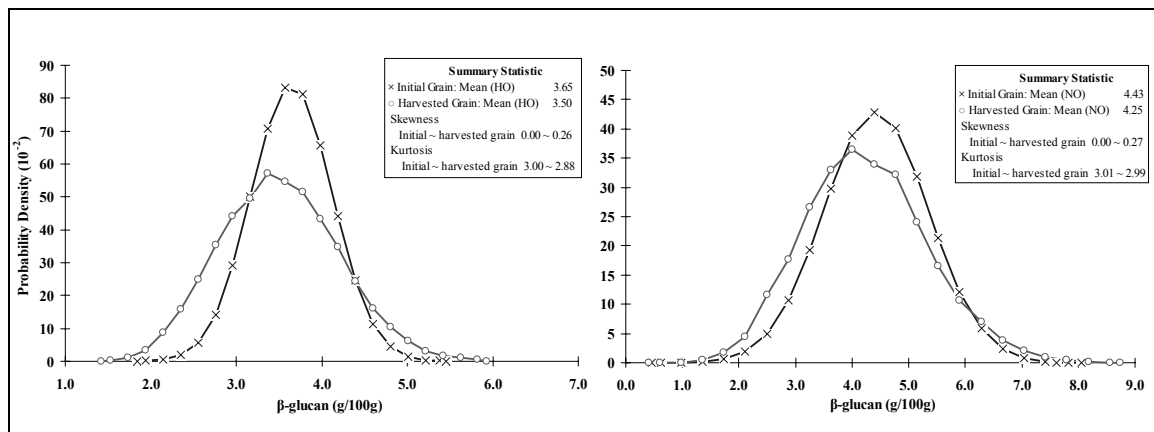


Figure 1. Simulated output (PDFs) of β -glucan in oats cultivars.

Table 1. Input distributions to model the β -glucan levels in oats

| Symbol | Description | Mean | Distribution | Units |
|---------------------------------|--------------------------------|-------|--|------------|
| Cultivar Data | | | | |
| HO | Hulled Oats | 3.65 | Normal (3.65, 0.47) | g/100g |
| NO | Naked Oats | 4.43 | Normal (4.43,0.92) | g/100g |
| Environmental Conditions | | | | |
| L | Location | 1 | Factor | |
| SoF | Soil factor | 1 | Versatile soil | |
| SpH | Soil pH | 1 | Factor | |
| <i>Climatic Condition</i> | | | | |
| SPr | Precipitation (spring oats) | 60 | Uniform (min 20, max 100) | mm / month |
| WPr | Precipitation (winter oats) | 95 | Uniform (min 40, max 150) | mm / month |
| ST | Temperature (spring oats) | 15 | Triangle (min 10, max 20) | °C |
| WT | Temperature (winter oats) | 7 | Triangle (min 5, max 10) | °C |
| Pr | Precipitation (growing period) | 95 | Discrete ({WPr, SPr}, {0.51, 0.49}) | mm / month |
| T | Temperature (growing period) | 7 | Discrete ({WT, ST}, {0.51, 0.49}) | °C |
| CF | Climatic factor | 0.951 | Prediction line, Function of Pr and T | |
| Agronomic Factors | | | | |
| SDD | Sowing Delay Days | 15 | Uniform (min 0, max 30) | days |
| SDF | Sowing date factor | 1.129 | Fixed factor | days |
| <i>Fertiliser application</i> | | | | |
| N | Nitrogen application | 110 | Triangle (min 40, max 140) | kg/ ha |
| Fu | Foliar Urea | 60 | Fixed | kg/ ha |
| FF | Fertiliser factor | 1.033 | Prediction line, Function of N and Fu | kg/ ha |
| <i>Irrigation</i> | | | | |
| IF | Irrigation factor | 1 | Fixed factor | |
| <i>Germination</i> | | | | |
| GTime | Germination Time | 1 | Exponential, beta 1.33 | days |
| GTemp | Germination Temperature | 10 | Fixed value | °C |
| GF | Germination factor | 0.952 | Prediction line, Function of GTime , Gtemp | |
| Storage | | | | |
| SDays | Storage days | 180 | Uniform (min 0, max 365) | days |
| STemp | Storage temperature | 10 | Triangle (min 5, max 20) | °C |
| SMo | Storage moisture | 12~25 | Prediction line, Function of STemp | % |
| SF | Storage factor | 0.730 | Prediction line, Function of SDays, Stemp | |

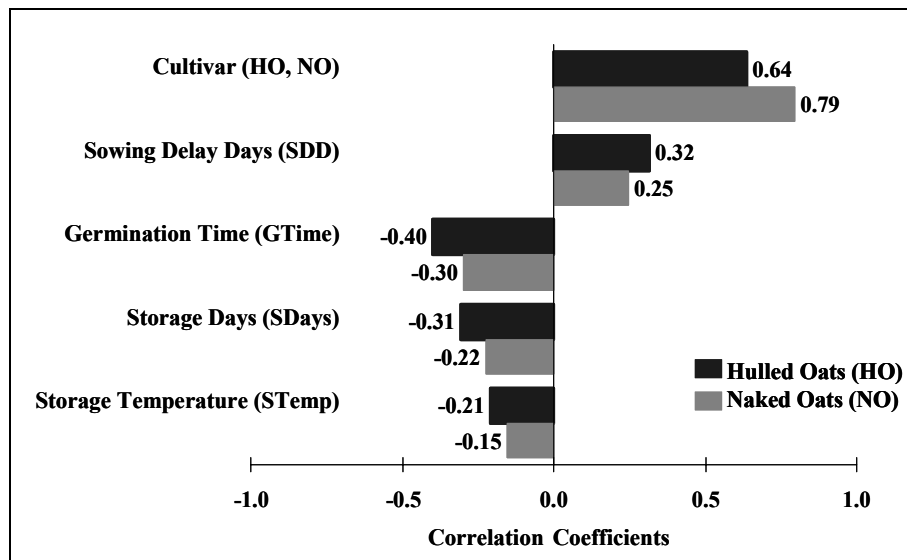


Figure 2 Sensitivity analysis for level of β -glucan in harvested oats cultivars

Conclusions

This study represents a preliminary effort to model various cultivation and storage conditions and their effects on β -glucan content in harvested oats grain. This is a novel approach to predict and assess the level of β -glucan content in oats grain. The model indicated a mean level of β -glucan in HO and NO of 3.50 g/100g and 4.25 g/100 g, respectively, which is within the range of reported values found in the literature. The scenario analysis highlights the importance of agronomic practices such as harvesting date and storage of harvested grains, although they are not as effective as the genotypic selection in effecting β -glucan content. This work contributes to current scientific knowledge and represents a new development in the understanding of the effects of various factors on β -glucan levels in oats.

Acknowledgements

The authors wish to acknowledge the Irish Department of Agriculture and Food for their funding of this project under the Food Institutional Research Measure.

References

- Flander, L., Salmenkallio-Marttila, M., Suortti, T., & Autio, K. (2007). Optimisation of ingredients and baking process for improved wholemeal oat bread quality. *LWT-Food Science and Technology*, 40, 860–870.
- Food and Drug Administration (1997). Final rule for food labelling: Health claims; Oats and coronary heart disease. *Federal Regulations*, 7 (62), 3584–3681.
- Theuwissen, E., & Mensink, R. P. (2007). Simultaneous intake of β -glucan and plant stanol esters affects lipid metabolism in slightly hypercholesterolemic Subjects. *The Journal of Nutrition*, 137, 583–588.
- Tosh, S. M., Brummer, Y., Wolever, T.M.S., & Wood, P.J. (2008). Glycemic response to oat bran muffins treated to vary molecular weight of β -glucan. *Cereal Chemistry*, 85 (2), 211–217.
- Yao, N., Jannink, J., & White, P. J. (2007). Molecular weight distribution of (1 \rightarrow 3)(1 \rightarrow 4)- β -glucan affects pasting properties of flour from oat lines with high and typical amounts of β -glucan. *Cereal Chemistry*, 84 (5), 471–479.

Growth Model of *Yersinia* species in Raw Ground Beef

Saumya Bhaduri* and Lihan Huang

Eastern Regional Research Center Agricultural Research Service, United States Department of Agriculture,
600 East Mermaid Lane, Wyndmoor, PA 19038 USA (saumya.bhaduri@ars.usda.gov,
lihan.huang@ars.usda.gov)

Abstract

Yersinia pestis (YP), the causative agent of bubonic and pneumonic plague, is a potential bio-threat agent in foods. Little is known about its growth behavior in intentionally contaminated foods. Therefore, the kinetics of growth of virulence plasmidless (pYV) YPKIM5 (lacking virulence determinants) in sterile and non-sterile raw ground beef (RGB) were studied. Since the chromosomal DNA sequence of YP and *Y. pseudotuberculosis* (YPST) harboring pYV are nearly identical, YPST was used to represent YP for investigation in foods. The growth kinetics of YPST harboring pYV (YPST⁺) was studied to develop growth models in sterile and non-sterile raw ground beef (RGB) at temperatures ranging from 0 to 30°C. The growth models were first developed in sterile RGB, and then validated in non-sterile RGB. In irradiated sterile RGB, YPST⁺ replicated from 0 to 30°C, with corresponding growth rates (GR) ranging from 0.023 to 0.622 log₁₀ CFU/h at 0-25°C, and 0.236 log CFU/h at 30°C. The maximum population densities (MPD) ranged from 8.7 to 11.0 log₁₀ CFU/g. The growth and MPD of YPST⁺ were reduced significantly at 30°C. Models for GR and MPD of YPST⁺ in sterile RGB as a function of storage temperatures were produced and displayed acceptable bias and accuracy. The models were validated with rifampicin resistant YPST⁺ (rif-YPST⁺) in non-sterile retail RGB stored at 4, 10, and 25°C. The observed GR and MPD of rif-YPST⁺ in non-sterile RGB were within 95% of the predicted values, and were similar to those of YPST⁺ in sterile RGB. Moreover, there was no loss of pYV in YPST⁺ during its growth in RGB, indicating that RGB contaminated with YPST⁺ and virulent YP could cause diarrhea and oro-pharyngeal plague, respectively due to refrigeration failure, temperature (10-25°C) abuse, and if the meat was not properly cooked.

Keywords: *Yersinia pestis*; *Yersinia pseudotuberculosis*; ground beef; growth, pYV stability

Introduction

The genus *Yersinia* consists of 11 species, but only *Y. pestis*, (YP) *Y. enterocolitica*, and *Y. pseudotuberculosis* (YPST) are considered to be pathogenic to humans. Among these three human pathogens, *Y. pestis*, the causative agent of bubonic plague in humans is considered the most invasive and virulent. *Yersinia pestis* has also been proposed to be ancestrally related to *Y. pseudotuberculosis*, but the latter exhibits similar behaviors and clinical symptoms to the more distantly related *Y. enterocolitica*. While rare, *Y. pestis* has been implicated as a foodborne pathogen causing foodborne outbreaks of oro-pharyngeal plague by the handling or consumption of inadequately cooked goat and camel meat. The risk, morbidity, and mortality of contracting plague through consumption of food deliberately contaminated with *Y. pestis* are currently unknown but potentially real. Furthermore, the identification of multidrug-resistant strains and the potential use of this pathogen in food for the deliberate contamination of food could cause plague in large populations.

All three pathogenic species of *Yersinia* carry a 70-kb virulence plasmid (pYV) which is directly involved with virulence of these organisms. However, the pYV is known to be

unstable. In general, cells lose pYV with subculture and during storage at refrigerator/freezing temperatures as well as at incubation temperatures over 30°C. Loss of this plasmid results in loss of virulence.

Ground beef is produced in large quantities and, if contaminated, could affect the health of numerous consumers. In ground beef processing plants, different portions of beef are combined and ground. The resulting ground product is then distributed throughout wholesale and retail markets in chubs and hamburger patties. In this regard, there are few available reports concerning the fate of *Y. pestis* in foods, and more specifically, in ground beef. In this report the behavior of pYVless avirulent YP in sterile RGB over a wide range of temperatures was described. However, the growth kinetics of plasmidless cells was shown to be different. Thus, it is important to study growth and model with plasmid-bearing cells.

Since the chromosomal DNA sequence of YP and YPST harboring pYV are nearly identical, experiments were conducted to develop a growth model of pYV-bearing YPST in sterile and non-sterile RGB over a range of temperatures where the virulence plasmid is not lost as a reference model for virulent YP. Moreover, to fully assess the potential risk of illness, it is necessary to know the effect of the endogenous microflora on the behavior/fate of YPST in raw ground beef. The stability of the virulence plasmid during the growth of YPST in ground beef was also studied. The growth model of YPST could be used to predict the growth of YP during processing, storage, transportation, and food serving of ground beef in canteens and fast food chains.

Materials and Methods

Bacterial strains and preparation

Yersinia pestis KIM5, a derivative of strain KIM (Kurdistan Iran Man) which lacks the chromosomally-encoded pigmentation (Pgm⁻) locus and pYV (KIM5YP⁻), a clinical isolate of pYV-bearing YPST (serotype O:1b; strain PB1/+) (YPST⁺), and rifampicin resistant (rif-YP⁻) and rif-YPST PB1/+ (rif-YPST⁺) were used in this study.

Sample inoculation

Irradiated sterile and non-sterile retail RGB were inoculated with YP⁻, rif-YP⁻ YPST⁺, and rif-YPST⁺ were inoculated and grown at temperatures ranging from 0 to 43°C.

Bacterial enumeration and Data analyses

At each time interval, three samples of inoculated RGB were diluted with 1% peptone water and were surface-plated on Congo red (CR) magnesium oxalate agar (CRMOX). The plates were incubated at 37°C for 24 h and colonies were counted. Red pin point colonies appearing on agar plates indicated the presence of YPST⁺ and rif-YPST⁺. DMFit, using the Baranyi dynamic growth model, was used to fit the data time-versus-log₁₀ CFU plots which were used to measure GR and MPD

Results and Discussion

Growth and Maximum Population Densities (MPD) of KIM5YP⁻ in RGB

There is no data concerning the growth of YP⁻ in RGB during storage over a range of temperatures. In sterile ground beef, YP⁻ replicated from 0 to 4°C, with corresponding GR ranging from 0.0014 to 0.2887 log CFU/h and MPD from 7.4 to 9.8 log CFU/g. However, at -20°C and at ≥ 41°C temperatures, the organism was inactivated. Models for

YP⁺ growth rate and MPD were reasonably close to the experimental values. The models were validated with rif-YP⁺ by using non-sterile retail GB containing native microflora.

Growth rate (GR) of YPST in RGB

Since growth at temperatures over 30°C facilitates the loss of pYV, the growth kinetics of YPST⁺ was studied at 0, 2, 4, 10, 15, 20, 25, and 30°C in sterile RGB. The Ratkowsky four parameter square root model was used to model the growth rate of plasmid-bearing virulent YPST from 0 to 30°C. This model assumes a homogeneous variance in the growth rates, which was observed in this study and takes the form: $GR = b^2(T - T_{min})^2(1 - \exp(c(T - T_{max})))^2$, where GR = growth rate, T = temperature, T_{min} is the theoretical minimum temperature below which no growth is possible, T_{max} is the theoretical maximum temperature beyond which growth is not possible, and b and c are scale parameters. A plot of GR versus temperature (Figure 1) shows that growth rate increased with temperature, reached a maximum at 22°C, and then declined. In irradiated sterile RGB YPST⁺ replicated from 0 to 30°C, with corresponding growth rates (GR) ranging from 0.023 to 0.622 log₁₀ CFU/h at 0-25°C, and the GR was 0.236 log CFU/h at 30°C. To validate the model, the observed growth rates of rif-YPST⁺ in non-sterile retail RGB were compared to the predicted growth rates from this model at 4, 10 and 25°C. It was found that the predicted and observed growth rates for rif-YPST⁺ in non-sterile retail RGB were statistically equivalent.

Maximum Population Densities (MPD) of YPST in RGB

The MPD can be influenced by limiting quantities of nutrients and/or by production of inhibitory substances. The MPD ranged from 8.65 to 11.86 log CFU/g. The MPD progressively increased from 8.65 at 10°C to 10.95 log CFU/g at 15°C to a maximum observed value of 11.86 log CFU/g at 20°C, with a slight reduction to 11.0 log CFU/g at 25°C and to 9.75 log CFU/g at 30°C. A logistic-type model was fitted to the MPD-temperature data and the following parameters estimated (Figure 2): $MPD = 4a \exp[-(T-b)/c] / [1 + \exp(-(T-b)/c)]^2$, where MPD = maximum population density, T = temperature, a = 11.79, b = 20.92, c = 9.82, $r^2 = 0.97$, and mean square for error = 0.84. Model performance measures for GR were calculated and yielded bias and accuracy factors of 1.00 and 1.01, respectively. Validation of this model was performed by comparing the observed MPD of rif-YPST in non-sterile retail RGB stored at 4, 10 and 25°C to predicted MPD in non-sterile RGB. At 10°C, the predicted MPD was lower than the observed MPD for rif-YPST, but at 25°C, the predicted and observed MPD values were statistically equivalent.

Stability of virulence plasmid in (pYV) YPST⁺ during its growth in RGB

Defining YPST growth kinetics in food is not the only relevant information for risk assessment. In addition, it is important to understand the stability of elements encoded by the chromosome and plasmids that are necessary for virulence of YPST. By using CR-uptake assay on CRMOX it was found that the pYV in YPST was stable during its growth in RGB at 0, 2, 4, 10, 15, 20, 25, and 30°C and indicated that cells were potential pathogen.

Conclusion

In conclusion, a reliable model was developed based on the data to predict the growth of YPST in RGB. Since YPST is closely related to YP and clinically related to

Y. enterocolitica, the model developed here may be used for both pathogens. The potential growth of virulence plasmid-bearing YPST at refrigerated temperatures could pose an increased health risk for contaminated retail RGB if commercial and consumer storage is extended for a longer period such as 4 to 6 weeks. It is of great significance that YPST retained the virulence plasmid during its growth at common storage and handling temperatures for RGB; therefore, contaminated RGB with YPST and YP are potentially capable of causing food poisoning and oro-pharyngeal plague respectively under appropriate conditions such as refrigeration failure, temperature (10-25°C) abuse, and if the meat was not properly cooked.

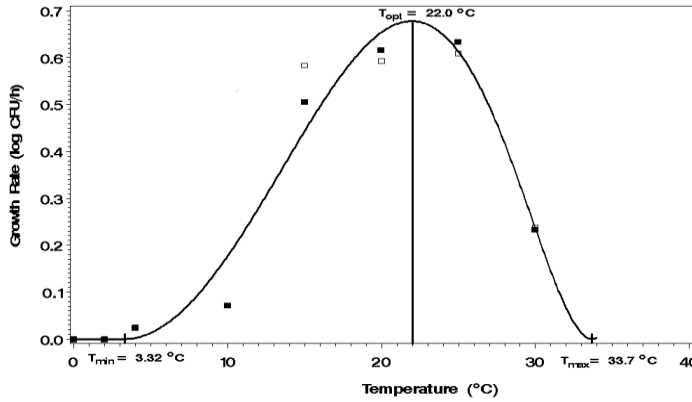


Figure 1: Growth rates of *Y. pseudotuberculosis* PB1/+ in sterile raw ground beef as a function of storage temperature. Trial 1 (□) and Trial 2 (■). A secondary model (expanded Ratkowsky) was fit to the growth rate data. The solid line is the prediction based on the *Y. pseudotuberculosis* PB1/+ model. T_{\min} (minimum temperature) = 3.32°C, T_{opt} (optimum temperature) = 22.0°C, and T_{\max} (maximum temperature) = 33.70°C.

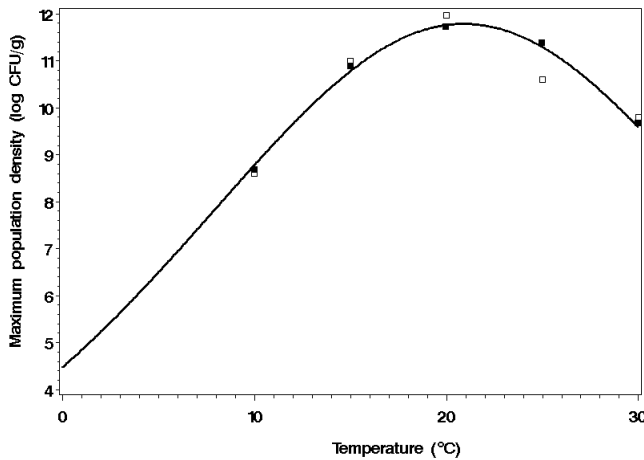


Figure 2: Maximum population density (MPD) of *Y. pseudotuberculosis* PB1/+ in sterile raw ground beef as a function of storage temperature. Trial 1 (□) and Trial 2 (■). A secondary logistic model was fit to the growth rate data. The solid line is the prediction based on the *Y. pseudotuberculosis* PB1/+ model.

Modeling the Transport of *Salmonella* into Whole-Muscle Meat Products during Marination and the Subsequent Lethality during Thermal Processing

B.P. Marks^{1,3}, J.A. Rochowiak², V. Tuntivanich⁴, E.T. Ryser³, A.M. Booren³

¹Dept of Biosystems and Agricultural Engineering, Michigan State University, 210 Farrall Hall, East Lansing, MI 48824-1323 (marksbp@msu.edu). *Corresponding author.*

²Formerly Dept of Biosystems and Agricultural Engineering, Michigan State University.

³Dept of Food Science and Human Nutrition, Michigan State University, East Lansing, MI 48824 (ryser@msu.edu; booren@msu.edu)

⁴Formerly Dept of Food Science and Human Nutrition, Michigan State University.

Abstract

The safety of marinated, whole-muscle, fully-cooked meat and poultry products depends both on the probability of bacteria entering the product interior and the effectiveness of the cooking process. Therefore, the objectives of this project were to: (1) develop a mechanistic mathematical model for the transport of *Salmonella* into intact whole-muscle meat products during marination, (2) compare the model to experimental data, and (3) quantify thermal inactivation of *Salmonella* in marinated, whole-muscle products, accounting for both internalization and product-specific inactivation parameters. For the transport model, turkey breast meat was assumed to be composed of intercellular capillaries of uniform size, computed from image analyses of bright-field micrographs. *Salmonella* transport into the muscle was modeled using a capsule-in-pipe formulation, coupled into a capillary diffusion model, and solved using a finite difference solution. Experimentally, irradiated whole-muscle turkey breasts were vacuum tumbled in marinade inoculated with an 8-serovar *Salmonella* cocktail (10^8 CFU/mL); thereafter, each sample was dissected to construct *Salmonella* concentration profiles. Lastly, thermal inactivation parameters for *Salmonella* in whole-muscle and ground turkey breast were applied to compare potential survivors. The numerical solution for the transport model was stable and yielded reasonable mass transport results, predicting that marinade uptake achieved steady-state concentration profiles at ~6 min. In experimental trials, significant numbers of *Salmonella* reached the core (>3.5 log CFU/g), with the concentration decreasing with increasing distance from the product surface ($P<0.0001$). Although the transport model also predicted *Salmonella* concentrations as high as 5 log CFU/g at 4 cm below the product surface, the shape of the concentration profile did not match the experimental results well (local deviations >3 log CFU/g). Although the worst-case concentration at the center of a whole-muscle product was significantly less than can occur in ground-and-formed product ($P<0.01$), thermal resistance was nearly double in the whole-muscle product. Accounting for these two opposite effects, the overall marination-cooking process outcome was much poorer (by 1.7 log) for whole muscle than for ground product. Overall, thermal process validations for these products should account for both the risk of internalization and the effect of product structure on thermal resistance.

Keywords

food safety, mass transfer, bacteria, pathogens, inactivation, poultry

Introduction

Ready-to-eat meat and poultry products have been increasing in popularity, and marination is one means to enhance product flavor, quality, and value. Food processors producing marinated whole-muscle meat products commonly operate under the assumption that the interiors of intact undamaged whole-muscle products are pathogen free. This belief is also reflected in federal regulations. Prior to 2005, FSIS distinguished between intact beef cuts (e.g., steaks and roasts) and non-intact cuts when establishing policies regarding *E. coli* O157:H7 contamination (USDA-FSIS 2002). An intact piece of beef is defined as “a cut of

whole muscle that has not been injected, mechanically tenderized, or reconstructed” (USDA-FSIS 1999). The FSIS justified this distinction by stating, “... the interior of intact products remains essentially protected from pathogens migrating below the exterior. Consequently, customary cooking of intact products will destroy any *E. coli* O157:H7” (USDA-FSIS 2002). However, due to growing concern regarding the sterility of marinated products, FSIS issued a notice requiring all whole-muscle products “injected with marinade” to be treated as mechanically tenderized products (USDA-FSIS 2005).

Recent research has confirmed that the assumption of interior sterility may not be valid (Tuntivanich 2008, Velasquez 2006, Warsaw et al. 2008). *Salmonella* can indeed migrate into the interior of *intact* products, particularly if the product has been vacuum tumbled. This interior contamination can be especially dangerous, because other tests have also shown that pathogens found inside whole-muscle products have a higher thermal resistance than those in ground products (Orta-Ramirez et al. 2005, Tuntivanich et al. 2008). Thus, current models may be ineffective at accurately predicting the time and temperature required to ensure adequate thermal processing, which depends on both the risk of contamination and the substrate-specific thermal resistance of *Salmonella*, which is the target organism in the United States Department of Agriculture (USDA) Food Safety Inspection Service (FSIS) lethality performance standards for ready-to-eat meat and poultry product (USDA-FSIS 1999).

Therefore, the objectives of this project were to: (1) develop a mechanistic mathematical model for the transport of *Salmonella* into intact whole-muscle meat products during marination, (2) compare the model to experimental data, and (3) quantify thermal inactivation of *Salmonella* in marinated, whole-muscle products, accounting for both internalization and product-specific inactivation parameters.

Materials and Methods

Marinade/Bacterial Transport Model

Given the complexity of marinade/bacterial transport in post-mortem muscle products, the proposed *Salmonella* transport model was built upon the following simplifying assumptions: (1) Capillary diffusion is the only driving force for marinade transport, (2) The meat is composed of a bundle of uniform cylindrical capillaries (i.e., intercellular space), (3) All liquid transported into the meat is immediately absorbed into the cells, causing them to expand and thereby reduce intercellular space, (4) When the intercellular space decreases below the diameter of a *Salmonella* cell, transport of the cells stops, (5) Physical properties of the marinade are equal to those of water, (6) The density of an individual *Salmonella* cell is equal to water, (7) All *Salmonella* cells are non-motile, inert capsules of equal size, and (8) There are no physicochemical effects of salts and phosphates in the marinade.

Given those assumptions, the initial size of the intercellular capillaries was computed from image analyses of bright-field micrographs subjected to a thresholding procedure (Fig. 1). *Salmonella* transport into the muscle was modeled using a capsule-in-pipe formulation (Latto and Chow 1982), coupled into the capillary diffusion model, and solved using a finite (central) difference solution. The full mathematical implementation of the above assumptions and principles can be found in the original thesis upon which this paper is based (Rochowiak 2007).

Marination Experiments

Fresh, whole muscle, boneless, skinless turkey breasts (1.5-2.0 kg, in triplicate) were obtained from a local processor, vacuum packaged,

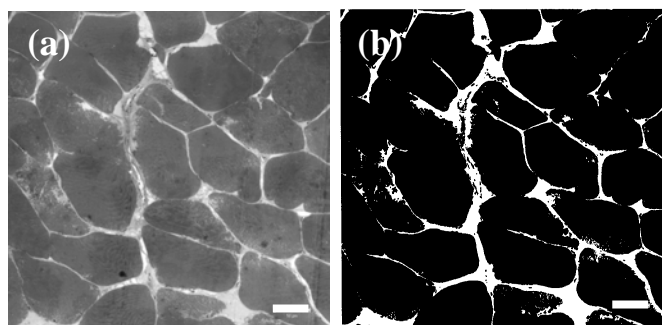


Figure 1. Utilization of thresholding technique (via Matlab™) on (a) a bright-field micrograph to quantify the intercellular space (b) after a given treatment. Bars 50 μ m.

frozen at -20°C, irradiated (>10 kGy), thawed (4°C, 48 h), and then vacuum tumbled (20 min; 4°C; 100 kPa) in marinade (3.2% salt, 0.8% phosphate) inoculated with an 8-serovar *Salmonella* cocktail (10⁸ CFU/mL) previously acquired from Dr. V. Juneja (USDA-ARS-ERRC; Wyndmor, PA). Thereafter, each sample was dissected to extract ~1 g subsamples at multiple depths in the interior of the turkey breast, using an electrosurgical cauterizing scalpel to prevent transfer of cells through the sample (Tuntivanich 2008). The subsamples were stomached, serially diluted in 0.1% peptone water, plated in duplicate on Petrifilm™ Aerobic Count Plates, which were incubated at 37°C for 48 h, to enumerate the *Salmonella* concentration at various locations in the turkey breast.

Thermal Inactivation

The *Salmonella* thermal inactivation parameters used in this study were previously reported for the same cocktail in whole muscle and ground turkey breast (Tuntivanich et al. 2008). In testing a Weibull model against those original isothermal data (55, 60, and 62.5°C), a null hypothesis that $n=1$ was not rejected ($\alpha=0.05$), so that log-linear inactivation kinetics were presumed. The resulting D_{ref} and z values for *Salmonella* in whole muscle and ground turkey breast were 1.91 min and 5.38 C°, and 1.03 min and 5.16 C°, respectively. These results showed that *Salmonella* was ~1.8 times more resistant in whole muscle than in ground product ($\alpha=0.05$).

Linking Bacterial Transport to Thermal Inactivation

Lastly, *Salmonella* survival probability was compared at the core of equivalent whole muscle or ground product. The difference between inoculum/contamination at the core of a whole muscle product and that in the ground product (i.e., assumed uniformly distributed) was treated as a reduction process. Then, the product-specific inactivation parameters were applied to core temperature data from a whole turkey breast cooked in a pilot-scale convection oven (93.3°C, 145 min, max humidity ~90%rh, cook-in-bag, $T_{core,max}=61.5^{\circ}\text{C}$) to quantify the difference in predicted survivors for the two product types.

Results and Discussion

Transport Model

The numerical solution for the transport model was stable and yielded reasonable mass transport results, predicting that marinade uptake achieved steady-state concentration profiles at ~6 min (Fig. 2). In experimental trials, *Salmonella* concentrations were ~7 log CFU/g just below the meat surface (for the higher inoculum), and significant numbers of *Salmonella* reached the core (~3 log CFU/g), with the concentration decreasing with decreasing inoculum level and distance from the product surface ($P<0.0001$). Although the transport model also predicted *Salmonella* concentrations as high as 5 log CFU/g at 4 cm below the product surface, the shape of the concentration profile (Fig. 3) did not match the experimental results well (local deviations >3 log CFU/g). These results indicate that the hypothesis about the underlying transport mechanism was not supported, and that mechanisms other than passive particle transport likely influence the process.

Process Outcomes

The application of product-specific inactivation parameters to actual core temperature data from a turkey product cooked in a pilot-scale, moist-air convection oven illustrates the relative impact of bacterial internalization and thermal resistance on the overall outcome of

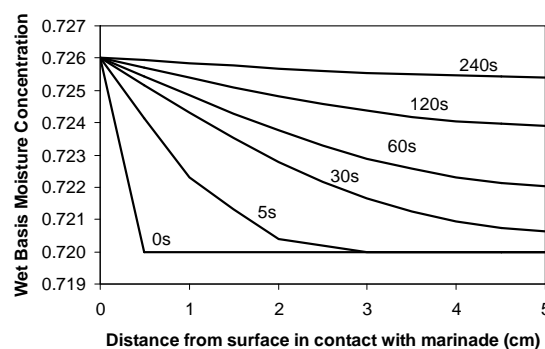


Figure 2. Predicted moisture profiles and extracellular space (i.e., effective gap radius) from the simplified, capillary-diffusion model for marinade transport.

the marination-cooking process (Table 1). Although the worst-case *Salmonella* concentration at the core of a whole muscle product (based on above experimental results) was significantly less than can occur in ground product ($P<0.01$), the enhanced thermal resistance of *Salmonella* in the whole muscle product caused an inferior overall process outcome (by 1.7 log) than for an equivalent ground product (presumed to have the same size, composition, and thermal history).

Conclusions

Salmonella can enter the interior of intact, marinated, whole-muscle products, and the transport mechanisms are more complex than passive fluid/particle flow. Additionally, thermal process validations for these products should account for both the risk of internal contamination and the effect of product structure on thermal resistance.

Table 1: Comparison of predicted process outcomes between whole muscle and ground turkey product for *Salmonella* lethality, based on worst-case scenario and pilot-scale cooking data.

| Product type | Worst case initial core <i>Salmonella</i> concentration (log CFU/g) | Computed process lethality (log reductions) | Net process outcome (log CFU/g) |
|--------------|---|---|---------------------------------|
| Whole muscle | 3.0 | 6.8 | -3.8 |
| Ground | 7.0 | 12.5 | -5.5 |

Acknowledgements

This study was partially supported by the Cooperative State Research, Education, and Extension Service, U.S. Department of Agriculture, under agreement 2003-35201-13796.

References

- Latto, B. and K.W. Chow (1982) Hydrodynamic transport of cylindrical capsules in a vertical pipeline. The Canadian Journal of Chemical Engineering, 60, 713-722.
- Orta-Ramirez, A., B.P. Marks, C.R. Warsow, A.M. Booren and E.T. Ryser (2005) Enhanced thermal resistance of *Salmonella* in whole muscle compared to ground beef. Journal of Food Science: 70 (7), M359-M362.
- Rochowiak, J. (2007) Modeling the Transport of *Salmonella* into Whole-Muscle Meat Products during Marination. In Biosystems and Agricultural Engineering, 109. East Lansing, MI: Michigan State University.
- Tuntivanich, V. (2008). Effects of Marination on *Salmonella* Penetration and Muscle Structure of Turkey Breast. In Food Science and Human Nutrition, East Lansing, MI: Michigan State University.
- Tuntivanich, V., A. Orta-Ramirez, B.P. Marks, E.T. Ryser and A.M. Booren (2008) Thermal inactivation of *Salmonella* in whole muscle and ground turkey breast. Journal of Food Protection: 71 (12), 2548-2551.
- USDA-FSIS (1999) Performance standards for the production of certain meat and poultry products. Federal Register, January 6, 1999, 732-749.
- USDA-FSIS (2002) Comparative risk assessment of intact (non-tenderized) and non-intact (tenderized) beef: Technical Report. United States Department of Agriculture, Food Safety Inspection Service. Washington, DC.
- USDA-FSIS (2005) Verification of establishment's reassessment of HACCP plans to address mechanically tenderized beef products. Notice. United States Department of Agriculture, Food Safety Inspection Service. Washington, DC.
- Velasquez, A. (2006) Thermal resistance and migration of *Salmonella* spp. into marinated pork products. In Food Science and Human Nutrition. East Lansing, MI: Michigan State University.
- Warsow, C.R., A. Orta-Ramirez, B.P. Marks, E.T. Ryser and A.M. Booren (2008) Single directional migration of *Salmonella* into marinated whole muscle turkey breast. Journal of Food Protection, 71, 153-156.

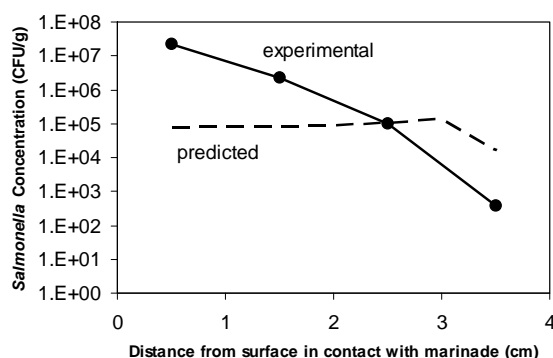
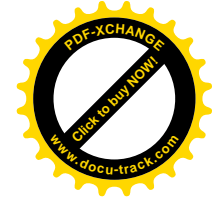


Figure 3. Comparison of predicted and experimental results for *Salmonella* concentration profile in turkey breast.



Effect of the temperature on the inhibition of *Escherichia coli* and *Listeria monocytogenes* by lactic acid bacteria

C. Aguilar and B. Klotz

Universidad de La Sabana, Campus Puente del Común, Autopista Norte Km 21, Chía (Cundinamarca), Colombia
(bernadette.klotz@unisabana.edu.co)

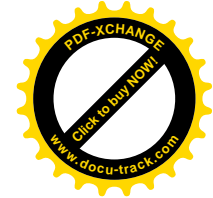
Abstract

In this study the effect of temperature on the dynamic of bacterial populations in pure and co-cultures was investigated. Cell numbers of pure and co-cultures at refrigeration, abusive and optimum growth temperatures (5, 20, and 37°C) were determined at regular intervals. The antagonistic activity of two lactic acid bacteria (LAB) strains, *Lactobacillus plantarum* WS4174 and *L. plantarum* LB279, with auto- and co-inducible bacteriocin-like inhibitory substance production respectively, against model strains of *Escherichia coli* and *Listeria monocytogenes* was quantified through the comparison of the estimated kinetic parameters of pure and mixed cultures. The Baranyi and Roberts model and a composite equation were fitted according to the experimental data. Temperature had an effect on the level of inhibition of the growth of the pathogens by LAB and the spectrum of action. Low and sub-optimal temperatures significantly reduced the antagonistic activity of the two LAB strains against the pathogenic bacteria. At refrigeration temperature only the growth of the Gram positive pathogenic strain was inhibited. The results obtained showed the importance to validate functionality when system-conditions are changed.

Keywords: Temperature, lactic acid bacteria, antagonism, functionality.

Introduction

It is recognized for more than hundred years that many fermented food stuffs guarantee their microbiological safety due to the antagonistic action of lactic acid bacteria (LAB) against foodborne pathogens. But still today there is a lack of knowledge on the dynamic of microbial populations involved in food fermentation processes. In recent years this bacterial antagonism has received more scientific attention as a consequence of the current trends toward less processed and healthy food. One of the main mechanisms used by LAB to avoid colonization and proliferation of potential pathogens is the production lactic acid and other functional metabolites, such as bacteriocins, that are potentially useful as natural substitutes for chemical preservatives in the context of biocontrolling the growth of pathogens and spoilage bacteria in food and hence enhancing food safety, quality and extending shelf life (Gálvez *et al.*, 2007). The antagonistic activity of LAB against *E. coli* and *L. monocytogenes* is well established. However the functionality of LAB strains under different food processing and storage conditions is still questioned. Production of biogenic metabolites, such as bacteriocins is closely associated with bacterial growth and strongly influenced by many physicochemical factors. Bacteriocins are produced generally during exponential cell growth, production ceased when cells enter the stationary phase (De Vuyst *et al.*, 1996), and activities decrease at the end of the growth phase as a result of proteolytic activity, adsorption to the producer cells and/or aggregation (De Vuyst and Vandamme, 1992; Joerger and Klaenhammer, 1986; Parente *et al.*, 1994). The bacteriocin activity and the amount produced per cell is cell density dependent and quorum sensing regulated (Quadri, 2002). Temperature is also an important factor influencing the bacteriocin production (Juarez-Tomas *et al.*, 2002; Mataragas *et al.*, 2004). Many studies reported that optimal cell growth not always resulted in high levels of bacteriocin and that the highest concentrations were obtained at sub-optimal temperature values (De Vuyst *et al.*, 1996; Krier *et al.*, 1998; Parente *et al.*, 1994). On the other hand, high bacteriocin titres were observed at optimum temperature range by Leroy and De Vuyst (2002 and 1999) and by Schillinger and Lucke (1989). It is known, that foods are often packaged and stored at abusive temperatures and that some LAB have difficulties to grow or to produce



bacteriocins at levels sufficiently high enough for microbial control at refrigeration temperatures. Therefore, the success of food preservation using in situ antimicrobial metabolites production requires more profound understanding between growth, microbial interactions, and production and performance of antagonistic metabolites as function of environmental conditions and medium composition.

The purpose of this study was (1) to measure the inhibitory potential of LAB against *E. coli* and *L. monocytogenes* and to elucidate the type of interaction present in broth co-cultures and (2) to assess the effective antagonistic efficacy of LAB at different incubation temperatures (refrigeration, abuse, and optimum temperatures). Under these growth conditions, mono- and co-cultures, growth curves were constructed and kinetic parameters were estimated and compared in order to accomplish these goals.

Materials and methods

Bacterial strains and inoculum preparation

Lactobacillus plantarum WS4174, *L. plantarum* LB279, *E. coli* ECO25, and *L. monocytogenes* LMO26 were isolated from dairy products. *Escherichia coli* ECO25 and *L. monocytogenes* LM26 were used as model microorganisms. The antimicrobial activity of the LAB against the indicator bacteria was determined by the spot-on-lawn method with un- and neutralized supernatant produced at 37°C. *Lactobacillus plantarum* WS4174 has an autoinducible and *L. plantarum* LB279 a co-culture inducible bacteriocin-like inhibitory-substance (BLIS) production, respectively. Strains were activated and subcultured in MRS broth at 37°C for 24 h without agitation, resulting in approximately 3×10^9 cells mL⁻¹.

Growth procedures and growth curves generation

The growth curves were constructed from three independent time course experiments in MRS broth at 5, 20, and 37°C ($\pm 1^\circ\text{C}$) and under aerobic conditions. Non-agitated pure and co-cultures (binary system 1:1) without pH regulation were started with an initial concentration for each bacterium of 2.55 ± 0.26 CFU mL⁻¹. There was no significant difference ($P \geq 0.05$) between the starting bacterial concentrations of all single and co-cultures. Colony forming units per mL of the pathogenic strains on plate count agar (PCA) and on MRS agar showed no significant difference ($P \geq 0.05$) after 48-h incubation under aerobic conditions. Pathogenic and LAB strains were plated on MRS agar showing colonies with different appearance.

Determination of microbial growth parameters

The Baranyi and Roberts (1994) model was fitted to growth data and parameters were estimated by non-linear least-squares regression using the DMfit curve-fitting program (available at <http://www.ifr.bbsrc.ac.uk>). By the presence of a death phase an additional lineal equation was fit.

$$N(t) = \begin{cases} \ln(N_t) = \ln(N_0) + \mu_{\max} A(t) - \ln\left(1 + \frac{\exp(\mu_{\max} A(t)) - 1}{N_{\max} / N_0}\right) & \text{when } 0 \leq t < 264 \text{ h} \\ \ln(N_t) = a - bt & \text{when } 264 \text{ h} \leq t < t_{\max} \end{cases}$$

$\ln(N_t)$ is the natural logarithm of the cell concentration (CFU mL⁻¹) at time t (h), $\ln(N_{\max})$ is the natural logarithm of the maximum cell concentration (CFU mL⁻¹), $\ln(N_0)$ is the natural logarithm of the inoculum level (CFU mL⁻¹), $A(t)$ is the lag function, μ_{\max} is the maximum specific growth rate (h⁻¹), a and b are the intersect and the slope of the line, respectively.

The goodness of fit of the fitted equation was assessed by standard error (SE), residual analysis, and coefficient of determination (R^2).

Statistical analysis

Data were analyzed by ANOVA at a level of significance of $P < 0.05$. The analyses were performed with the SPSS (Release 15.0, SSPS Inc, Chicago) statistical program.

Results and discussion

The growth of four bacterial strains and the dynamic of four types of binary bacterial systems (antagonist/pathogen) under different temperatures (refrigeration, abusive and optimum) were studied. Temperature had an effect on the level of inhibition of growth of the pathogens by LAB and the spectrum of action at 5 and 20°C. In pure cultures, *Escherichia coli* ECO25 showed increased sensitivity to cold temperatures reflected in decreased maximal cell concentration (N_{\max}) and the presence of a death phase (Table 1 and Fig. 1). All four strains presented a lag phase at 5°C and similar maximal growth rate (μ_{\max}) although significant difference (CI 95%) was observed between LAB and pathogenic strains. The Arrhenius plot showed a lineal behaviour between μ_{\max} of pure cultures and temperature with $r > 0.97$.

Table 1: Estimated kinetic parameters of pure and co-cultures at 5, 20, and 37°C. (1) *L. plantarum* WS4174, (2) *L. plantarum* LB279, (3) *E. coli* ECO25, and (4) *L. monocytogenes* LMO26.

| 5°C | | | | | | 20°C | | | | | | 37°C | | | | | |
|-------|--------|--------|-------|---------|----------------|-------|-------|-------|-------|---------|----------------|-------|-------|-------|-------|---------|----------------|
| C | rate | lag | yEnd | se(fit) | R ² | C | rate | lag | yEnd | se(fit) | R ² | C | rate | lag | yEnd | se(fit) | R ² |
| 1 | 0.037 | 48,040 | 8,404 | 0.166 | 0.993 | 1 | 0.156 | 0.000 | 9,132 | 0.154 | 0.993 | 1 | 0.324 | 2.889 | 9,039 | 0.219 | 0.991 |
| 1 + 3 | 0.037 | 46,700 | 8,396 | 0.160 | 0.993 | 1 + 3 | 0.153 | 0.000 | 9,148 | 0.157 | 0.992 | 1 + 3 | 0.317 | 2,523 | 9,120 | 0.224 | 0.991 |
| 1 + 4 | 0.037 | 49,110 | 8,746 | 0.201 | 0.991 | 1 + 4 | 0.160 | 0.000 | 9,124 | 0.146 | 0.993 | 1 + 4 | 0.320 | 2,518 | 9,125 | 0.209 | 0.992 |
| 2 | 0.037 | 48,630 | 8,999 | 0.154 | 0.995 | 2 | 0.140 | 3,325 | 9,077 | 0.126 | 0.995 | 2 | 0.252 | 0.000 | 9,262 | 0.205 | 0.991 |
| 2 + 3 | 0.037 | 48,530 | 8,928 | 0.159 | 0.995 | 2 + 3 | 0.140 | 3,014 | 9,077 | 0.124 | 0.995 | 2 + 3 | 0.253 | 0.000 | 9,276 | 0.219 | 0.990 |
| 2 + 4 | 0.038 | 50,940 | 8,644 | 0.202 | 0.991 | 2 + 4 | 0.139 | 2,728 | 9,101 | 0.119 | 0.996 | 2 + 4 | 0.257 | 0.000 | 9,357 | 0.222 | 0.990 |
| 3 | 0.030 | 19,870 | 7,404 | 0.139 | 0.994 | 3 | 0.090 | 0.000 | 8,653 | 0.211 | 0.986 | 3 | 0.251 | 0.000 | 8,733 | 0.192 | 0.991 |
| | -0.021 | | 1,723 | | 0.995 | | | | | | | | | | | | |
| 3 + 1 | 0.031 | 20,310 | 7,395 | 0.124 | 0.995 | 3 + 1 | 0.086 | 0.000 | 5,996 | 0.233 | 0.947 | 3 + 1 | 0.338 | 0.000 | 5,735 | 0.173 | 0.964 |
| | -0.022 | | 1,660 | | 0.991 | | | | | | | | | | | | |
| 3 + 2 | 0.029 | 18,900 | 7,126 | 0.328 | 0.964 | 3 + 2 | 0.084 | 0.000 | 6,246 | 0.297 | 0.930 | 3 + 2 | 0.184 | 0.000 | 5,331 | 0.132 | 0.974 |
| | -0.019 | | 2,288 | | 0.988 | | | | | | | | | | | | |
| 4 | 0.028 | 90,320 | 8,643 | 0.115 | 0.998 | 4 | 0.103 | 3,827 | 8,902 | 0.214 | 0.992 | 4 | 0.315 | 3,697 | 9,070 | 0.301 | 0.986 |
| 4 + 1 | 0.028 | 86,080 | 6,230 | 0.111 | 0.994 | 4 + 1 | 0.045 | 8,851 | 6,190 | 0.130 | 0.992 | 4 + 1 | 0.507 | 5,097 | 4,833 | 0.138 | 0.985 |
| 4 + 2 | 0.028 | 91,960 | 8,642 | 0.110 | 0.998 | 4 + 2 | 0.043 | 8,993 | 6,183 | 0.211 | 0.979 | 4 + 2 | 0.171 | 1,641 | 5,121 | 0.121 | 0.989 |

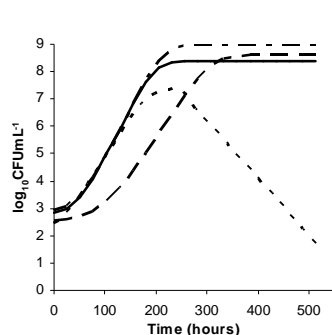


Figure 1: Pure cultures at 5°C. *L. plantarum* WS4174 (—), *L. plantarum* LB279 (---), *L. monocytogenes* (···) and with *L. plantarum* LB279 *E. coli* (—·—).

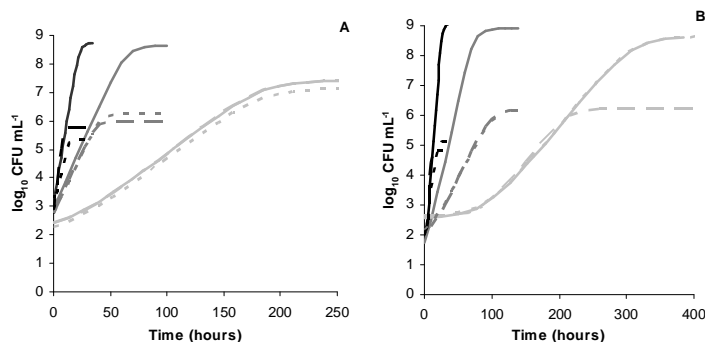
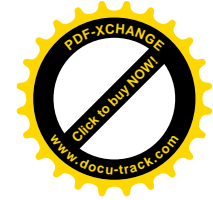


Figure 2: Pure and co-culture growth of *E. coli* (A) and *L. monocytogenes* (B) at different temperatures. Pure cultures (—), mixed cultures with *L. plantarum* WS4174 (---) and with *L. plantarum* LB279 (···). 5°C (light grey), 20°C (dark grey) and 37°C (black).

At 5°C, only the growth of *L. monocytogenes* LMO26 was affected by the simultaneous growth with *L. plantarum* WS4174 showing a decreased N_{\max} of almost 2 log-cycles (Fig. 2). Spot-on-lawn challenge studies showed that only the supernatant produced at 5°C by *L. plantarum* WS4174 was effective against *L. monocytogenes* LMO26. In pure cultures at 20°C, all strains increased their μ_{\max} in at least 300% and only *L. plantarum* LB279 and *L. monocytogenes* LMO26 continued to have lag phases of 3.3 and 3.8 h respectively (Table 1). The level of inhibitory interaction of the LAB strains against the pathogenic bacteria was more evident at 20 °C and reflected in reduced μ_{\max} and N_{\max} for *L. monocytogenes* LMO26 and diminished N_{\max} for *E. coli* ECO25 (Table 1 and Fig. 2). The N_{\max} of *L. monocytogenes* LMO26 and of *E. coli* ECO25 was reduced in approximately 3 log-cycles and the μ_{\max} of *L. monocytogenes* LMO26 decreased in 50%. At optimal temperature the inhibitory action of the



two LAB strains was stronger on both pathogenic strains. The two LAB strains reduced the N_{\max} of *L. monocytogenes* LMO26 more effectively in almost 4 log cycles (Table 1 and Fig. 2). The pH profile was determined by the LAB strains and the lowest value of approximately 4 units was not influenced by temperature and was not the inhibitory factor.

From parameter significance it was shown that physical factors, such as temperature, influenced the population dynamics in mixed cultures and the production of BLIS. Temperature-stress seemed to down-regulate the production of BLIS. However, the contribution of the cold stress response of the foodborne pathogens to their resistance to antimicrobial metabolites could not be discarded.

Conclusions

The results gathered in this work showed that the four bacterial strains were able to grow at the temperature range of 5 to 37°C. The LAB did not modify their growth pattern when grown as pure or mixed culture at all temperatures indicating an interaction of amensalism. However, low and sub-optimal temperatures reduced the antagonistic activity of the two LAB strains against the pathogenic bacteria demonstrating the importance of functionality validation. At refrigeration temperatures only the growth of the Gram positive pathogenic strain was inhibited by the LAB strain with auto-inducible BLIS production. With gradual increased of the temperature the spectrum of action was extended to the Gram negative strain.

Acknowledgements

Authors thank the Universidad de La Sabana for the financial support of this study.

References

- Baranyi J. and Roberts T.A. (1994) Review paper: A dynamic approach to predicting bacterial growth in food. *International Journal of Food Microbiology* 23, 277-294.
- De Vuyst L. and Vandamme E.J. (1992) Influence of the carbon source on nisin production in *Lactococcus lactis* subsp. *lactis* batch fermentations. *Journal of General Microbiology* 188, 571-578.
- De Vuyst L., Callewaert R. and Crabbé K. (1996) Primary metabolite kinetics of bacteriocin biosynthesis by *Lactobacillus amylovorus* and evidence for stimulation of bacteriocin production under unfavourable growth conditions. *Microbiology* 142, 817-827.
- Gálvez A., Abriouel H., Lucas-López R.L. and Omar N.B. (2007) Bacteriocin-based strategies for food biopreservation. *International Journal of Food Microbiology* 120, 51-70.
- Joerger M.C. and Klaenhammer T.R. (1986) Characterization and purification of helveticin J and evidence for a chromosomally encoded bacteriocin produced by *Lactobacillus helveticus* 481. *Journal of Bacteriology* 167, 439-446.
- Juárez -Tomás M.S., Bru E., Wiese B., de Ruiz Holgado A.A.P. and Nader-Macías M.E. (2002) Influence of pH, temperature and culture media on the growth and bacteriocin production of vaginal *Lactobacillus salivarius* CRL 1328. *Journal of Applied Microbiology* 93 (4), 714-724.
- Krier F., Revol-Junelles A.M. and Germain P. (1998) Influence of temperature and pH on production of two bacteriocins by *Leuconostoc mesenteroides* subsp. *mesenteroides* FR52 during batch fermentation. *Applied Microbiology and Biotechnology* 50, 359-363.
- Leroy F., Degeest B. and De Vuyst L. (2002) A novel area of predictive modelling: describing functionality of beneficial microorganisms in foods. *International Journal of Food Microbiology* 73, 251-259.
- Leroy F. and De Vuyst L. (1999) Temperature and pH conditions that prevail during fermentation of sausages are optimal for production of the antilisterial bacteriocin sakacin K. *Applied and Environmental Microbiology* 65, 974-981.
- Mataragas M., Metaxopoulos J., Galiotou M. and Drosinos E.H. (2003) Influence of pH and temperature on growth and bacteriocin production by *Leuconostoc mesenteroides* L124 and *Lactobacillus curvatus* L442. *Meat Science* 64, 265-271.
- Parente E., Ricciardi A. and Addario G. (1994) Influence of pH on growth and bacteriocin production by *Lactococcus lactis* subsp. *lactis* 140VWC during batch fermentation. *Applied Microbiology and Biotechnology* 41, 388-394.
- Quadri L.E.N. (2002) Regulation of antimicrobial peptide production by autoinducer mediated quorum sensing in lactic acid bacteria. *Antonie Van Leeuwenhoek* 82, 133-145.
- Schillinger U. and Lucke F.K. (1989) Antimicrobial activity of *Lactobacillus sake* isolated from meat. *Applied and Environmental Microbiology* 55, 1901-1906.

Effects of citral, carvacrol and (E)-2-hexenal on growth inactivation of *Listeria monocytogenes* during heat treatment

S.L. Sado Kamdem^{1,2}, N. Belletti¹, R. Lanciotti¹, and F. Gardini¹

¹ Dipartimento di Scienze degli Alimenti, Università degli Studi di Bologna, Sede di Cesena, Piazza G. Goidanich, 60, 47521 Cesena, Italy. www.foodsci.unibo.it

² Laboratoire de Microbiologie, Department of Biochemistry, University of Yaounde I, P.O. Box 812 Yaounde, Cameroon.

Abstract

The use of aroma compounds (AC) in combination with heat treatment against pathogenic microorganisms needs the comprehension of the effects as well as of the action mechanism. This comprehension can be obtained through the use of predictive modeling. The present work intends to understand, using the Weibull model, the effect of isothermal treatments in combination with AC on the inactivation kinetics of *Listeria monocytogenes*. Moreover the survival data were used to obtain an empirical model giving acceptable predictions of the antimicrobial efficacy of AC on the basis of their partition coefficient and vapor pressure. This approach could be useful in the screening of AC antimicrobial activity.

Keywords

Weibull, physical properties, *Listeria monocytogenes*, citral, carvacrol, (E)-2-hexenal

Introduction

The interest in the use of AC as natural alternatives to other preservatives is wide, still their use is limited. Their combination with other hurdles has been proposed as a promising strategy. The exploitation of such a strategy needs a comprehension on how these hurdles can interact for a more pronounced result. Modeling approach is a way to quantify combined effects of hurdles. Thus, the scope of the present work was to study the effect of isothermal heat treatments performed alone or in combination with sub-lethal concentrations of 3 different AC on the fate of *Listeria monocytogenes* 56 Ly. Another objective of the present work was to empirically evaluate a predictive approach to assess the behaviour of the AC used, on the basis of their physical parameters such as partition coefficient and vapour pressure. The bioactivity of AC can be linked to those physical properties.

Materials and methods

Compounds used and temperatures studied

Target compounds (citral, carvacrol, (E)-2-hexenal), were used at a sub-lethal level defined as 1/5 the minimal bactericidal concentration (MBC) able to kill an initial inoculum of 10^2 cells/ml of target strain *Listeria monocytogenes* 56 Ly (preliminary trials, data not shown). Final concentrations tested were: 50, 30 and 65 ppm for citral, carvacrol and (E)-2-hexenal respectively. Control samples were added with the same amount of ethanol used to dissolve AC. Seven different temperatures were considered in this study: 53, 55, 58, 63, 65, 68 °C, all trials were conducted under isothermal conditions.

Isothermal trials

A set of 10 ml vials containing 3 ml of brain heart infusion (BHI) added with the target aroma compound concentration were sealed and placed in a water bath set at treatment temperature until target temperature was reached inside the vial. Then, 25 µl of *L. monocytogenes* 56Ly (grown twice in BHI broth for 24 h at 37°C and centrifugated for 15 min at 4000 rpm) were aseptically inoculated in each sealed vial to a final concentration of 10^7 - 10^8 cells/ml. The treatments time was considered from cell inoculums in vials. At defined intervals vials were

removed from bath and placed in a cryogenic solution to rapidly cool. Vials were enumerated by plate count on BHI agar. Plate count data were expressed as survivors over time, $S(t)$.

Modelling

Use of Weibull model

The following equation (1) derived from Weibull distribution (Corradini and Peleg, 2004) was used:

$$\log_{10} S(t) = -b(T)t^{n(T)} \quad (1)$$

Where $S(t)$ is the ratio between survivors at time t and initial inoculum at time 0 ($N(t)/N(0)$), t is treatment time, $n(T)$ and $b(T)$ are the temperature depending parameters, characteristics of the Weibull model, to be estimated.

Definition of a model based on physical parameters of tested compounds

The approach used to build the empirical model based on physical properties (partition coefficient and vapour pressure) of AC was the following. Equations for the prediction of partition coefficient $K_{O/W}$ were obtained at 25 °C using Abraham coefficients (Kai-Uwe, 2005). Those coefficients were kindly calculated by Prof. Abraham using his model. The $K_{O/W}$ dependency on temperature was then obtained for each compound from equation (2) (Bahadur *et al.* 1997).

$$\log_{10} K_{o/w} = A - \frac{\Delta Ht}{2.303RT} \quad (2)$$

where A is a regression constant, ΔHt is transfer enthalpy of compound between phases, R is gas constant and T is temperature in Kelvin degrees.

For vapor pressure (Pv), data were collected from literature and converted in their respective value expressed in mmHg. Then the dependency on temperature was obtained using Clausius-Clapeyron equation. Only survival data of *L. monocytogenes* 56Ly obtained from the use of carvacrol and (E)-2-hexenal were used to build the empirical model, while data from citral were used for model validation. The model was built using data of the controls, the $K_{O/W}$ and Pv of the compounds at the different temperatures and performing a regression analysis.

Statistical analyses were performed using Microsoft Office Excel 2003, StatSoft Statistica 6.

Results and discussion

Results obtained with the Weibull model

The survival data were fitted with the Weibull model and b and n parameters were estimated for each aroma/temperature combination. Estimated parameters, sum of squared errors (SSE) and the predicted time needed to inactivate 7 log CFU are reported in Table 1.

The parameter $b(T)$ defines the rate of microbial inactivation (the higher is b the higher the rate of microbial inactivation). As can be observed in Table 1, this value has an increasing trend at increasing temperatures. With respect to the controls, it can be observed that sub-lethal concentrations of AC highly contribute to the reduction of the value of b parameter as well as the time needed to obtain a 7 log inactivation. This time (expressed in minutes) can be shortened to about 1/3 of the time necessary in the absence of AC. It is interesting to point out that this behaviour can be observed also at low temperatures (55°C), strengthening the importance of this approach for a possible industrial application.

Re-elaborating isothermal results using raw data (without logarithm transformation), the Weibull distribution parameters can be obtained in order to assess the distribution of thermal resistance of *L. monocytogenes* 56Ly in the different conditions studied. The distribution mean time of resistance of the population tends to decrease at increasing temperatures, passing from 84.92 for treatment at 53°C to 0.018 for treatment at 68 °C in control samples. It can be observed a general more pronounced decrease of distribution mean value with the addition of AC with respect to controls added only with ethanol. The addition of 30 ppm of carvacrol leads to a distribution mean value of 8.38 at 53 °C. Also the distribution mode can

be described by the same trend. This indicates that the addition of the AC contributed to the increase of the cells sensitivity to heat.

Table 1. Scale (b) and shape (n) parameters obtained after modelling with the Weibull model, the isothermal inactivation curves in the presence of 0 ppm of aroma compound (control), 50 ppm of citral, 30 ppm of carvacrol and 65 ppm of (E)-2-hexenal. Sum of Squared Errors (SSE) and the time (expressed in minutes) to inactivate 7 Log CFU are reported.

| Tested compounds | Param. | Tested temperatures | | | | | | |
|-------------------------------|--------|---------------------|---------|-------|-------|-------|--------|--------|
| | | 53 | 55 | 58 | 60 | 63 | 65 | 68 |
| Control (ethanol) | b | 6.9E-05 | 0.00844 | 0.131 | 1.147 | 3.545 | 7.392 | 15.316 |
| | n | 2.052 | 1.282 | 1.192 | 0.617 | 0.633 | 0.665 | 0.711 |
| | SSE | 2.83 | 0.64 | 0.18 | 1.18 | 0.06 | 19.36 | 0.22 |
| | -7 log | 274.90 | 189.40 | 28.10 | 18.78 | 2.94 | 0.92 | 0.33 |
| Citral (50 ppm) | b | 0.00047 | 0.205 | 0.468 | 1.993 | 6.518 | 12.761 | 21.103 |
| | n | 1.835 | 0.854 | 0.887 | 0.769 | 1.060 | 0.979 | 0.706 |
| | SSE | 0.20 | 0.48 | 0.72 | 0.26 | 0.17 | 0.65 | 0.13 |
| | -7 log | 189.00 | 62.36 | 21.13 | 5.13 | 1.07 | 0.54 | 0.21 |
| Carvacrol (30 ppm) | b | 0.131 | 0.200 | 0.839 | 1.711 | 6.043 | 8.828 | 13.377 |
| | n | 0.730 | 0.868 | 0.905 | 0.882 | 1.166 | 0.570 | 0.461 |
| | SSE | 0.44 | 0.87 | 1.43 | 1.29 | 0.63 | 1.23 | 0.67 |
| | -7 log | 233.50 | 60.07 | 10.43 | 4.94 | 1.14 | 0.67 | 0.25 |
| (E)-2-hexenal (65 ppm) | b | 2.8E-05 | 0.034 | 0.762 | 1.146 | 9.092 | 10.335 | 15.125 |
| | n | 2.666 | 1.353 | 0.885 | 1.348 | 1.191 | 0.812 | 0.471 |
| | SSE | 0.15 | 0.73 | 0.09 | 0.36 | 0.34 | 0.36 | 0.02 |
| | -7 log | 105.9 | 51.5 | 12.28 | 3.83 | 0.80 | 0.62 | 0.23 |

Model based on physical parameters of tested compounds and validation

The solubilization in cell membranes is the first step needed to EO constituents to determine damages to microorganisms and to reach the cell targets inside the cell or in the same cell membranes. For this reason, we decided to use partition coefficient and vapor pressure in the attempt to build a model able to predict the Weibull parameters for *L. monocytogenes* 56Ly inactivation in presence of AC and thermal treatment. Those two physical parameters can be considered an indirect measure of the hydrophobic characteristics of molecules which is linked to their bioactivity against microorganisms.

Given the impossibility to test all AC available, an empirical approach based only on the knowledge of physical parameters can help in the initial screening procedure of essential oils compounds. The resulting empirical models obtained, even though based on two molecules (carvacrol, (E)-2-hexenal), are reported in Table 2. The corresponding plots of fitted and observed values are represented in Figure 1. This empirical model was validated using the set of data obtained with citral. The observed and fitted values of n and b are reported in Figure 2.

Table 2: estimated parameters of the empirical model containing physical parameters (model for b , Eq1; model for n , Eq2).

| Eq1 | Constant | b_{cont} | $\ln P_v$ | $\log K_{O/W}$ | $(\ln P_v)^2$ | $(b_{\text{cont}})^2$ | $\ln T$ |
|-----|----------|-------------------|-----------|----------------|---------------|-----------------------|---------|
| | -22,208 | 1,721 | 6,090 | 19,199 | -0,00108 | -0,0524 | -14,163 |
| Eq2 | Constant | n_{cont} | $\ln P_v$ | $\log K_{O/W}$ | $(\ln P_v)^2$ | $(n_{\text{cont}})^2$ | $\ln T$ |
| | 23,855 | -2,146 | -1,577 | -5,201 | -0,000645 | 0,969 | -0,119 |

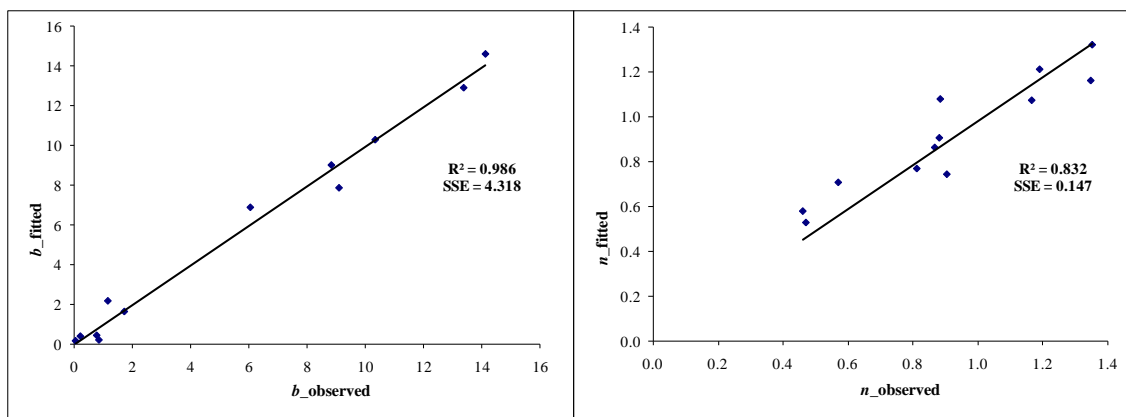


Figure 1: scatterplots of observed and fitted values obtained for the empirical model construction on the basis of carvacrol and (E)-2-hexenal; (a) b parameter, (b) n parameter.

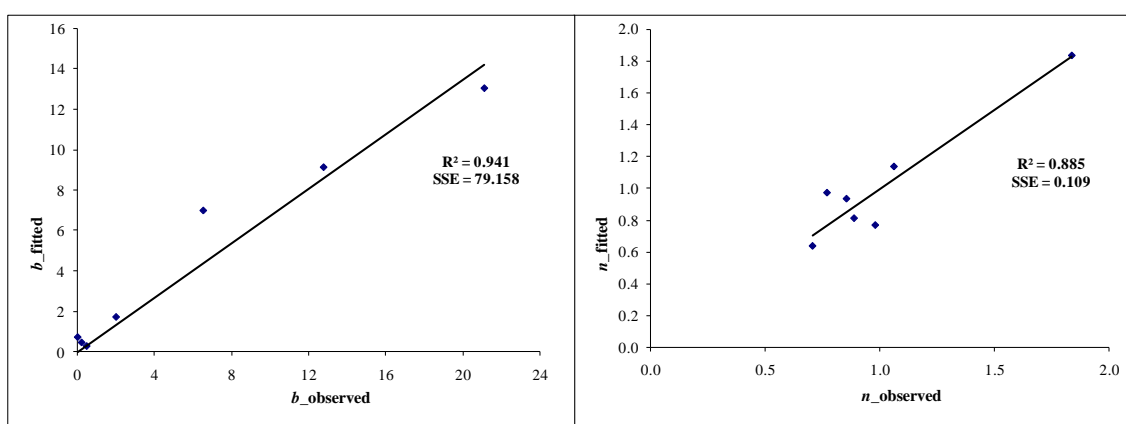


Figure 2: scatterplots of observed and fitted values obtained for the validation of the empirical model with citral; (a) b parameter, (b) n parameter.

Conclusions

The Weibull model resulted to be a good model for the fitting of survival data obtained by the combination of heat and AC. The empirical model approach proposed here can be of interest in the screening of antimicrobial activity of AC. The systematical use of this approach could shorten screening experimental times and could be of use to widen the knowledge of the behavior of these substances. One weak point of the empirical model proposed is the difficulty encountered to find reliable and experimental vapor pressure and partition coefficients. Furthermore, the existence of a more complete data base regarding AC could help also in the comprehension of their activity and mechanisms of action. Another weak point is the difficulty encountered in predicting b and n parameters using the same equation in a range of temperatures, great differences have been found at 53 and 68 °C.

Acknowledgments

The Authors wish to thank Prof. Abraham for the valuable help in the calculation of partition coefficient, and for the use of its model.

References

- Bahadur N. P., Wan-Ying Shiu, Boocock D. G. B., Mackay D. (1997). Temperature Dependence of Octanol-Water Partition Coefficient for Selected Chlorobenzenes. *J. Chemical Engineering Data*. 42, 685-688.
- Corradini, M. G., Peleg, M. (2004). Demonstration of the applicability of the Weibull-Log-Logistic survival model to the isothermal and nonisothermal inactivation of *E. coli* K-12 MG1655. *J. Food Protect.* 67, 2617-2621.
- Kai-Uwe, G. (2005). Predicting the equilibrium partitioning of organic compounds using just one linear solvation energy relationship (LSER). *Fluid Phase Equilibrium*. 233, 19-22.

Evaluation of growth boundary models – importance of data distribution and performance indices

O. Mejlholm^{1*}, Y. Le Marc² and P. Dalgaard¹

¹ DTU Aqua, Technical University of Denmark, Kgs. Lyngby, Denmark (ome@aqu.dtu.dk)

² Institute of Food Research, Norwich Research Park, Norwich, NR4 7UA, UK

Introduction

Various indices have been used to evaluate the performance of growth boundary models including the correct prediction percentage and the percentage of fail-dangerous or fail-safe predictions. These measures reflect the overall predictive ability of the model; however, they do not take into account the ‘distance’ between the environmental parameters and the growth boundary. Clearly, a high correct prediction percentage should be expected if the evaluation is performed on data located far from the growth boundary, unless the performance of the model is poor. From such data it is not possible to determine the performance of the evaluated model more precisely, and its ability to predict growth and no-growth might be overestimated if based exclusively on the correct prediction percentage (Fig. 1a).

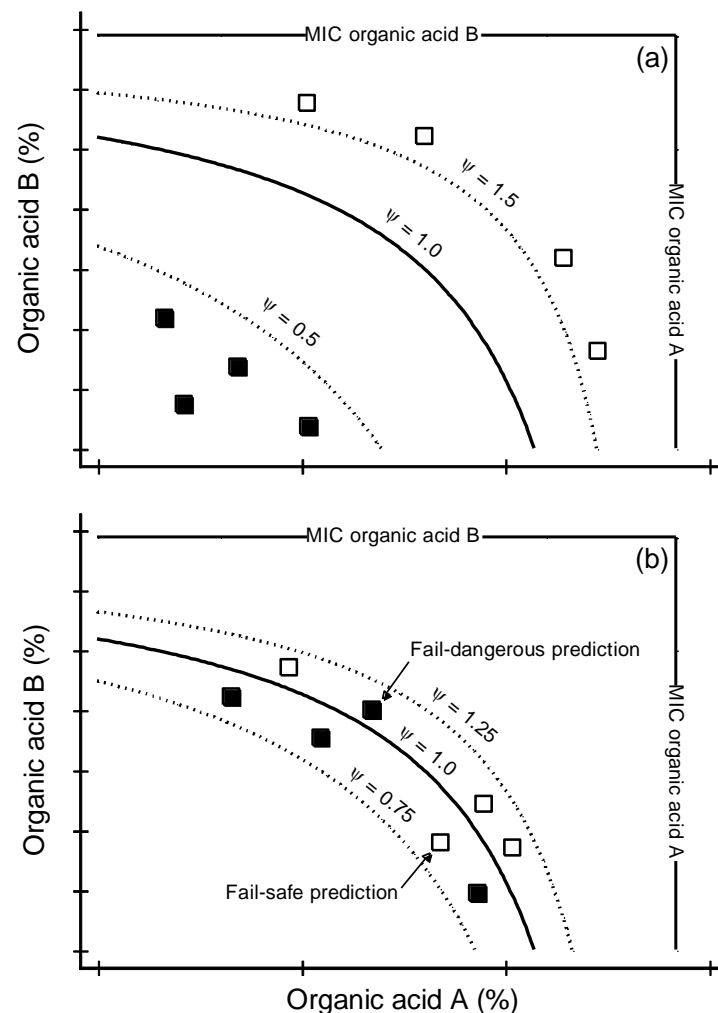


Figure 1: Predicted growth boundary (solid line) and interfaces (dotted lines) of *Listeria monocytogenes* depending on concentrations of organic acid A and B. A newly developed model for *L. monocytogenes* was used to predict the growth boundary ($\psi = 1.0$) and interfaces with ψ -values of 0.5, 0.75, 1.25 and 1.5. Theoretical growth (■) and no-growth (□) responses of *L. monocytogenes*

Data in the close range of the growth boundary are more appropriate for model evaluation but a lower correct prediction percentage and some fail-dangerous and/or fail-safe predictions should be expected, even for a good model (Fig. 1b).

Material and Methods

To demonstrate the importance of data distribution on performance indices, a newly developed growth boundary model for *L. monocytogenes* (Mejlholm and Dalgaard, 2009; <http://sssp.dtuqua.dk>) was evaluated on 156 growth and no-growth responses of the pathogen in seafood and meat products (Table 1). These data were divided into sub-groups based on their ‘distance’ to the growth boundary. To quantify the ‘distance’ between sets of environmental parameters (i.e. product characteristics and storage conditions) and the predicted growth boundary, the ψ -value was used (Le Marc et al. 2002). The growth boundary is defined by a ψ -value of 1.0 and predicted growth and no-growth responses has ψ -values lower and higher than 1.0, respectively (Fig. 1).

Table 1 Importance of data distribution on performance indices

| Range (ψ) | n^b | Percentage of predictions ^a | | |
|-------------------------------|-------|--|----------------|-----------|
| | | Correct | Fail-dangerous | Fail-safe |
| $\psi < 0.5$ and $\psi > 1.5$ | 66 | 92 | 6 | 2 |
| $0.75 < \psi < 1.25$ | 36 | 69 | 12 | 19 |
| Whole range | 156 | 87 | 8 | 5 |

^a Predicted by the model of Mejlholm and Dalgaard (2009)

^b n , number of experiments

For the full range of data, 136 out of 156 growth and no-growth responses of *L. monocytogenes* were correctly predicted by the newly developed model resulting in a correct prediction percentage of 87 (Table 1). Eight predictions were fail-dangerous (5%) and these data had an average ψ -value of 1.33 ± 0.22 (AVG \pm SD), whereas the 12 fail-safe predictions (8%) had an average ψ -value of 0.76 ± 0.16 (AVG \pm SD). When predictive microbiology growth boundary models are evaluated the average ψ -values for fail-dangerous and fail-safe predictions can be used to describe the performance of the examined model. The closer the incorrect predictions lie to the growth boundary ($\psi = 1.0$) the better the performance of the model. In the close range of the growth boundary, defined by ψ -values between 0.75 and 1.25 (Fig. 1), a correct prediction percentage of 69 were obtained (Table 1). Four fail-dangerous (12%) and seven fail-safe predictions (19%) were located within this range. Thus, more than half of the incorrect predictions (55%) were located close to the growth boundary where the difference between correct and incorrect predictions to a great extent can be explained by the inherent variability in the environmental parameters of the products. A correct prediction percentage of 92 were obtained when the model of Mejlholm and Dalgaard (2009) was evaluated on data with ψ -values < 0.5 and > 1.5 (Table 1). This support the assumption that the performance of growth boundary models might be overestimated if the evaluation is based on data located far from the growth boundary.

Conclusions

To improve transparency when growth boundary models are evaluated, we suggest that measures of model performance should be reported together with ψ -values to describe the ‘distance’ between the evaluated data and the growth boundary.

References

- Le Marc, Y., Huchet, V., Bourgeois, C. M., Guyonnet, J. P., Mafart, P. and Thuault, D. (2002). Modelling the growth kinetics of *Listeria* as a function of temperature, pH and organic acid concentration. *International Journal of Food Microbiology*, 73 (2-3), 219-237.

Mejlholm O. and Dalgaard P. (2009). Development and validation of an extensive growth and growth boundary model for *Listeria monocytogenes* in lightly preserved and ready-to-eat shrimp. *Journal of Food Protection*, In Press.

Predictive model for growth of *Clostridium perfringens* during cooling of cooked uncured meat and poultry

Vijay K. Juneja^{1*}, Harry Marks², Lihan Huang¹, and Harshavardhan. Thippareddi³

¹. Eastern Regional Research Center, Agricultural Research Service, U.S. Department of Agriculture, 600 E. Mermaid Lane, Wyndmoor, PA 19038 (vijay.juneja@ars.usda.gov*, lihan.huang@ars.usda.gov)

². U.S. Department of Agriculture, Food Safety Inspection Service, 14th and Independence S.W., Washington, DC 20250 (Harry.marks@fsis.usda.gov)

³. Department of Food Science and Technology, University of Nebraska-Lincoln, Lincoln, Nebraska 68583 (hthippareddi2@unl.edu)

Abstract

Comparison of *C. perfringens* spore germination and outgrowth in cooked uncured products during cooling for different species is presented. Cooked, uncured product was inoculated with *C. perfringens* spores and vacuum packaged. For the isothermal experiments, all samples were incubated in a water bath stabilized at selected temperatures between 10 – 51 °C and sampled periodically. For dynamic experiments, the samples were cooled from 54.4 to 27 °C and subsequently from 27 to 4 °C for different time periods, designated as x and y hours, respectively. The growth models used were based on a model developed by Baranyi and Roberts (1994), which incorporates a constant, referred to as the physiological state constant, q_0 . The value of this constant captures the cells' history before the cooling begins. To estimate specific growth rates, data from isothermal experiments were used, from which a secondary model was developed, based on a particular form of Ratkowsky's 4-parameter equation. The estimated growth kinetics associated with pork and chicken were similar, but growth appeared to be slightly greater in beef; for beef, the maximum specific growth rates estimated from the Ratkowsky curve was about $2.7 \log_{10}$ cfu/u, while for the other two species, chicken and pork, the estimate was about $2.2 \log_{10}$ cfu/h. Physiological state constants were estimated by minimizing the mean square error of predictions of the \log_{10} of the relative increase versus the corresponding observed quantities for the dynamic experiments: for beef the estimate was 0.007, while those for pork and chicken the estimates were about 0.011. For a hypothetical 1.5 h cooling from 54 °C to 27° and 5 h to 4°C, corresponding to USDA cooling guidelines, the predicted growth (\log_{10} of the relative increase) for each species was: 1.29 for beef; 1.07 for chicken and 0.86 \log_{10} for pork. However, it was noticed for pork in particular, the model using the derived q_0 had a tendency to over-predict relative growth when there was observed small amounts of relative growth, and under-predict relative growth when there was observed large relative growth. To provide more fail-safe estimate, rather than using the derived value of q_0 , a value of 0.04 is recommended for pork.

Keywords: *C. perfringens*, cooling, modeling, cooked uncured meats

Introduction

C. perfringens is an anaerobic, Gram-positive, non-motile, spore-forming, rod-shaped bacterium. The organism is ubiquitous in the environment and is found in soil, dust, and raw ingredients such as spices, used in food processing, and in the intestines of humans and animals. Thus, raw protein foods of animal origin are frequently contaminated with

C. perfringens. Proper cooling is critical to prevent the outgrowth of *C. perfringens* in cooked meat and poultry products.

The FDA (2001) Food Code dictates that cooked meats should be cooled from 60-21°C within 2 h, and from 60-5°C within 6 h. The USDA-FSIS also sets cooling compliance guidelines (USDA/F SIS, 2001) for chilling cooked meats that require cooling from 54.4-26.7°C to be < 1.5 h, and from 26.7-4.4°C < 5 h. Additional guidelines allow for the cooling of certain cured cooked meats from 54.4-26.7°C in 5 h, and from 26.7-7.2°C in 10 h (USDA/F SIS 2001). In the event of cooling deviation, meat processors must be able to document that the customized or alternative cooling regimen results in < 1 log₁₀ CFU increase in *C. perfringens*. Computer modeling can be used to estimate the growth of *C. perfringens* during cooling in the event of cooling deviation. Therefore, the objective of this research was to develop a predictive model for estimating growth of *C. perfringens* during cooling cooked uncured meat products.

Materials and methods

Test organisms, spore production, inoculation, and enumeration

Three strains of *C. perfringens*, NCTC 8238 (Hobbs serotype 2), NCTC 8239 (Hobbs serotype 3), and NCTC 10240 (Hobbs serotype 13) were used and prepared according to Juneja et al. (1993). The spore cocktail was inoculated to individually-packaged ground meats (~3.0 log₁₀ cfu/g, 5 g per package). To enumerate, samples were properly mixed, serially diluted, and surface-plated onto tryptose-sulfite-cycloserine agar plates. Samples were heat-shocked at 75 °C for 20 min prior to experiment.

Growth studies

For kinetic analysis, inoculated samples were incubated at selected temperatures between 10 and 51°C to obtain isothermal growth curves. The Baranyi model was used as primary model to fit the growth curves. Rajkowsky model was used to evaluate the effect of temperature on growth rate. For dynamic cooling experiments, samples were submerged in a water bath programmed to decrease linearly from 54.4°C to 27 °C and from 27 °C to 4 °C at different cooling rates. For $t < 0$ h (10 minutes) the temperature was assumed to be constant. To estimate dynamic growth, the differential form of the primary model was numerically solved for different temperature conditions.

Results

Specific growth rates – EGR, and Lag times from isothermal experiments

Figure 1 shows some of experimental growth curves and the results of curve fitting for cooked pork. Figure 2 illustrates the effect of temperature on maximum growth rates (log₁₀/h) for cooked beef, chicken, and pork. The minimum and maximum growth temperatures estimated by the Ratkowsky model were around 10 and 52°C, respectively.

Estimation of q_0 from dynamic experiments

The estimate of q_0 was made using the growth data generated from experiments, excluding those for which the final levels were near the levels indicating a stationary phase (~ 8 log₁₀). The value of q_0 was derived to be equal to the value that minimized the mean square errors of predictions: for beef $q_0 = 0.0699$; for chicken, $q_0 = 0.0105$, and for pork, $q_0 = 0.0111$. With q_0 estimated, the differential form of Baranyi model was solved numerically to estimate the growth of *C. perfringens* in various meats under varying temperature conditions.

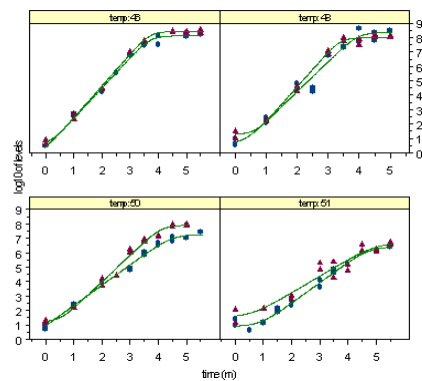


Figure 1: Growth of *C. perfringens* in pork

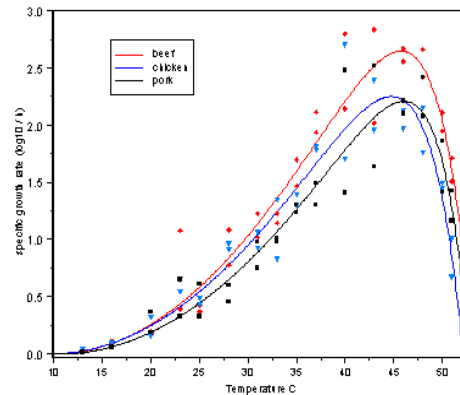


Figure 2: Effect of temperature on growth rate of *C. perfringens* in beef, pork, and chicken

Estimation of Dynamic growth

Tables 1 and 2 list the results of dynamic estimation of the relative growth of *C. perfringens* in cooked ground chicken and chicken, respectively.

Table 1. Estimation of relative growth of *C. perfringens* in cooked chicken

| Elapsed time (h) | | Initial log ₁₀ level | Estimated relative growth | Observed relative growth | | Difference (Observed- estimated) |
|------------------|-----------|---------------------------------------|---------------------------------|--------------------------|-----------------------|--|
| 54.4 – 27°C | 27 – 4 °C | | | Mean | Standard deviation | |
| 1.5 | 0.0 | 2.81 | 1.14 | 0.47 | 0.05 | -0.67 |
| 1.5 | 12.5 | 2.27 | 3.24 | 2.39 | 0.06 | -0.85 |
| 1.5 | 15.0 | 2.38 | 3.66 | 3.54 | 0.25 | -0.12 |
| 3.0 | 0.0 | 2.28 | 3.32 | 2.73 | 0.39 | -0.59 |
| 3.0 | 7.5 | 2.49 | 4.55 | 4.13 | 0.25 | -0.42 |
| 3.0 | 10.0 | 2.96 | 4.74 | 2.67 | 0.13 | -2.07 |
| 3.0 | 12.5 | 2.49 | 5.16 | 3.79 | 0.91 | -1.37 |
| 4.5 | 0.0 | 2.33 | 5.26 | 4.73 | 0.25 | -0.53 |

Table 2. Estimation of relative growth of *C. perfringens* in cooked beef

| Elapsed time (h) | | Initial log ₁₀ level | Estimated relative growth | Observed relative growth | | Difference (Observed- estimated) |
|------------------|-----------|---------------------------------------|---------------------------------|--------------------------|-----------------------|--|
| 54.4 – 27°C | 27 – 4 °C | | | Mean | Standard deviation | |
| 0.0 | 12.5 | 2.16 | 0.87 | 0.58 | - | -0.29 |
| 0.0 | 15.0 | 2.81 | 1.28 | 1.80 | - | 0.52 |
| 1.5 | 0.0 | 2.87 | 1.07 | 0.66 | 0.33 | -0.41 |
| 1.5 | 0.0 | 1.07 | 1.07 | -0.24 | 0.59 | -1.31 |
| 1.5 | 12.5 | 2.64 | 3.24 | 2.73 | 0.24 | -0.51 |
| 1.5 | 15.0 | 2.77 | 3.67 | 3.62 | 0.04 | -0.05 |
| 3.0 | 0.0 | 2.97 | 3.56 | 2.45 | 0.09 | -1.11 |
| 3.0 | 0.0 | 0.81 | 3.58 | 1.44 | 0.19 | -2.14 |
| 3.0 | 7.5 | 2.80 | 4.72 | 4.55 | 0.35 | -0.17 |
| 3.0 | 10.0 | 3.18 | 4.71 | 3.61 | 0.40 | -1.10 |
| 3.0 | 12.5 | 2.98 | 4.94 | 4.30 | 0.29 | -0.64 |
| 3.0 | 12.5 | 0.85 | 5.75 | 1.72 | 1.98 | -4.03 |
| 3.0 | 15.0 | 0.47 | 6.20 | 0.86 | 1.25 | -5.34 |
| 4.5 | 0.0 | 3.03 | 4.94 | 4.37 | 0.20 | -0.57 |
| 4.5 | 0.0 | 0.82 | 6.07 | 4.03 | 0.36 | -2.04 |
| 4.5 | 10.0 | 0.88 | 7.04 | 2.20 | 0.31 | -4.84 |
| 6.0 | 0.0 | 2.84 | 5.16 | 6.20 | 0.28 | 1.04 |
| 6.0 | 0.0 | 0.73 | 7.26 | 5.35 | 0.74 | -1.91 |

Discussion

The estimated growth of *C. perfringens* in cooked chicken meat was generally within 0.5 log₁₀ cfu/g from the observed values, except two temperature conditions (Table 1). More discrepancy between the estimated and observed growth of *C. perfringens* in cooked beef was observed (Table 2). The discrepancy was even more severe if the initial cell concentration was low or the samples were exposed to higher temperature conditions (54.4 – 27°C) for longer time. The growth of *C. perfringens* usually experiences the well known “Phoenix” phenomenon, during which some of the cells die before the cells adjust to the environment and the population starts to increase. The “Phoenix” phenomenon is more significant at higher temperature ranges. According to Table 2, the estimated bacterial growth was more accurate if the samples were exposed to shorter time at temperatures between 54.4 and 27°C and longer time between 27 and 4°C. In the work reported by Huang (2003), an adjustment coefficient was used in the numerical analysis procedures to factor in the “Phoenix” phenomenon. The estimated growth of *C. perfringens* was closer to the observed values with the adjustment factor in Huang (2003).

Conclusion

This paper presents a model for predicting the relative growth of *C. perfringens* in uncured meat and poultry products (beef, chicken and pork) under both isothermal and dynamic temperature conditions. Although the primary model was able to accurately describe the growth of *C. perfringens* in various meats, the results of dynamic analysis of the growth of this microorganism under changing temperature conditions may vary. The accuracy of dynamic analysis, affected by the “Phoenix” phenomenon, was influenced by initial cell condition and temperature history. An adjustment coefficient may be needed to improve the accuracy of dynamic analysis.

Reference

- Baranyi J. and Roberts T. (1994) A dynamic approach to predicting bacterial growth in food. *International Journal of Food Microbiology* 23, 277-294.
- FDA. 2001. Food Code. Part 3.5: Limitation of growth of organisms of public health concern. U.S. Food and Drug Administration, Rockville, MD.
- Juneja V.K., Call J.E. and Miller A.. (1993) Evaluation of methylxanthines and Related compounds to enhance *Clostridium perfringens* sporulation using a modified Duncan and Strong medium. *Journal of Rapid Methods and Automation in Microbiology* 2, 203-218.
- USDA/FSIS (2001) Performance standards for the production of certain meat and poultry products; final rule. *Federal Register* 64, 732-749.
- Huang, L. (2003). Dynamic computer simulation of *Clostridium perfringens* growth in cooked ground beef. *International Journal of Food Microbiology* 87, 319-332.

Fatty Acids Composition of Polish Commercial Cakes as Assessed by Standard Methods or by FT-IR Spectroscopy

P. Koczoń¹, M. Wirkowska¹, B. Kowalski¹

¹ Warsaw University of Life Sciences, Faculty of Food Sciences, Food Chemistry Department, ul. Nowoursynowska 159 C, 02-787 Warsaw, Poland (piotr_koczon@sggw.pl)

Abstract

A variety of types of polish commercial cakes, purchased in local markets and stored during 10 months were studied toward quality changes. Measurements of fat composition due to free fatty acids content and unsaturated trans acid content, the oxidative stability (rancimant), peroxide value, as well as polar fraction were performed for cakes from just-purchased and opened packets, and for those stored for 10 month, in one month intervals. Listed above characteristics were determined by conventional methods (e.g. gas chromatography or titration). On the other hand, FT-IR spectra of solid samples (KBr pressed pallets technique) of every type of cakes were registered. The values of only two measured parameters were correlated with spectral data at statistically significant level, and therefore two independent models, one for peroxide value (model I), and another one for unsaturated trans fatty acid content (model II) were successfully calibrated. Obtained characteristic parameters were: $R^2 = 0.89$, PRESS (Prediction Residual Error Sum of Squares) = 1.12, factors number = 2, and $R^2 = 0.92$, PRESS = 0.98, factors number = 4, for model I and II, respectively. Calibrated models correctly predict peroxide value and unsaturated trans fatty acid content of unknown samples of different type of cakes, and therefore can be used for rapid estimation of those parameters in cakes.

Keywords: cakes, unsaturated acid, FT-IR spectroscopy, PLS regression, predictive modeling, chemometrics

Introduction

There is a plenty assortment of cakes offered by confectionery market. Nowadays cereal cakes beside basic compositions contain nutritionally valuable compositions such as fruits, muesli, milk and so on. According to producers, presence of listed compositions justifies use of such cakes as a between meals snacks. Cakes containing fat at different level are products popular among children and young people. Although cakes are not significant source of fat in ordinary diet, fat delivered this way increases total number of consumed lipids. There is a fact, that fat beside carbohydrates and proteins is primary composition of diet and is necessary for humans, as plays important role in proper function and development of the organism. Beside fat quantity, its quality in terms of composition also plays a role in respect to human organism proper functionality.

Five different type of cakes present in polish market were studied: cakes with oat flakes; cakes with oat flakes, wheat flakes and dried fruits; cakes with oat flakes; cakes with oat flakes and sunflower seeds; cakes with oat flakes, sesame seeds and sunflower seeds, assigned in the text as A, B, C, D, E, respectively. Recently, the determination of PV (peroxide value) in commercial oils was assessed by the modern infrared spectroscopy (FT-IR) (Yildiz et al., 2002); which can also be extended to the determination of PV in cakes. The theoretical principles of IR had been reported earlier (Koczoń et al., 2006), and the technique finds application in the food analysis

(Tay et al., 2002) and significantly less number for monitoring of chemical changes in foods (Quilitzsch, 2005).

Herein we have monitored several characteristic parameters during cakes storage. Whereby, peroxide value, and trans fatty acid content were assessed by the conventional method and the FT-IR spectra were registered for each sample. The correlation of tested parameters as the quality status of the cakes with IR spectral data was the aim of this paper. We attempt to build a robust, reliable model for prediction and rapid determination of all studied parameters, while succeeded in peroxide value and trans unsaturated fatty acids content exclusively. Statistical technique of Partially Least Square (PLS) regression, with cross validation diagnostic was used to create proposed models.

Materials and methods

Infrared spectroscopy in MIR and NIR regions were applied to register spectra of solid state samples. Cake sample and KBr were mixed in a ratio of 1:300, to prepare pellets with press of 12T. In the hexan-cold extracted fat, acid value (AV) and peroxide value (PV) were determined by titration method; polar fraction (PF) and fatty acid composition were determined by gas chromatography (GC); oxidative stability by Rancimat. Data obtained by those methods were treated as standards. GRAMS AI software was used for all calculations and model calibrations/validations.

Results and discussion

Table 1 gathers selected data of all parameters measured for every studied cake at the very beginning of experiment (time “0”), and in the end of the experiment, ten months later (time “10”). Data presented in Table 1 are averages of five measurements and characterize studied cakes. As the fat is very important composition of cake which effects in proper cakes structure e.g. fragility, taste, or durability (Caponio et al., 2006) its characterization is of importance. Fat content and fat composition decide on usefulness of long-term expiration date products. Due to high temperature used during baking, fat used in production process might undergo unfavorable alterations. Those changes, mainly oxidation, might continue during storage, which usually leads to product spoilage. Secondary oxidation products (e.g. hexanal) are often themselves of low sensoric detection level, although significantly decrease sensoric features of product (Klensporf and Jeleń, 2005). Data gathered in Table 1 were used for building statistical model involving FT-IR spectral data. Exclusively PV out of all Table 1 parameters, correlates with infrared data at statistically significant level, therefore only model was created for this parameter (MODEL I, Table 2). In order to create robust model, with strong predictive ability, 55 experimental data were incorporated in the model calibration and validation (5 types of cakes, measured at 11 time intervals). Characteristics of developed model are as follows: $R^2 = 0.89$, Prediction Residual Error Sum of Squares (PRESS) = 1.12, factors number = 2. Spectral regions applied for this model were: 2872-2838; 1424-1408; 1390-1351; 1183-1154 cm^{-1} . It is worth to notice, that unexpectedly, application of spectral data from NIR region did not increased model quality in terms of R^2 , PRESS or predictive strength.

PV is used for evaluation of oxidative stability which is a parameter responsible for oxidation resistance of fat. Oxidative stability depends on fatty acid composition, content of pro-oxidants and antioxidants, and storage conditions (Kita et al., 2003). Proposed model can be used for rapid determination of PV and therefore for evaluation of oxidative stability, age and quality of any cake. Fortunately, spectral measurement is reliable, short, and there is no need for use of any chemicals.

Table 3 contains data for fatty acid (FA) composition at the beginning and last month of storage (column “0” and “10”, respectively). Heading “trans” of the bottom row stays for total content of 18:1, 18:2 and 18:3 trans fatty acids. Data from bottom row of Table 3 are statistically correlated with FT-IR data, which allows creation of the model for determination of trans fatty acid content. Again 55 data were incorporated in the model calibration and validation. Model obtained characteristics are as follows: $R^2 = 0.92$, PRESS = 0.98, factors number = 4. Spectral regions applied for this model were: 3507-3338; 1774-1712; 1686-1607; 1473-1452 cm^{-1} . Again, application of data from NIR region did not increase model quality in terms of R^2 , PRESS or predictive strength. Model II presented in Table 2 allows measurement of content of trans fatty acids in unknown cake. After calibration and validation, model was used to measure trans fatty acid level in four unknown cakes of the same type as studied. Data are presented in Table 4.

Trans isomers, especially those arising during technological processes (e.g. hydrogenation), are perceived similarly to saturated fatty acids, as unfavorable factors causing unfavorable effects (e.g. increase of total cholesterol level, as well as its LDL fraction in blood). Moreover, trans isomers contrary to saturated fatty acids, decrease level of cholesterol HDL fraction, and increase a risk for coronary heart disease (de Roos et al., 2001). Also blood vessels atherosclerosis (Dlouchy et al., 2003) as well as blood anemia resulting in heart attack (Oomen et al., 2001), occur more frequently in case of persons consuming products containing high level of trans fatty acids. Therefore, according to food safety politics, there is a need for rapid determination of trans fatty acids as well as oxidative stability of ready to use products such as cakes.

Conclusions

Two statistical models, one for peroxide value (model I), and another for unsaturated trans fatty acid content (model II) were successfully calibrated and validated based on traditional and spectral data obtained within this study. Both models can be applied for rapid evaluation of mentioned parameters.

Table 1: Free fatty acid (FFA), polar fraction (PF) content [%], oxidative stability value [hours] and peroxide value PV [mmol/O₂/kg] determined for all studied cakes assigned as A, B, C, D, E, respectively.

| Parameter | Type of the cake | | | | | | | | | |
|-----------------------------|------------------|-------|-----------------|------|-----------------|------|-----------------|------|-----------------|-------|
| | A | | B | | C | | D | | E | |
| | Time of storage | | Time of storage | | Time of storage | | Time of storage | | Time of storage | |
| | 0 | 10 | 0 | 10 | 0 | 10 | 0 | 10 | 0 | 10 |
| FFA (%) | 3.76 | 8.2 | 1.06 | 6.68 | 1.03 | 6.21 | 1.03 | 7.21 | 4.12 | 14.65 |
| PF (%) | 5.88 | 11.1 | 3.12 | 8.34 | 3.46 | 10.1 | 1.37 | 9.59 | 3.87 | 12.36 |
| Oxidative stability [h] | 3.75 | 0.21 | 7.75 | 2.11 | 7.1 | 2.08 | 11.6 | 3.58 | 2.72 | 0.19 |
| PV[mmol/O ₂ /kg] | 4.15 | 10.38 | 0.80 | 6.79 | 1.1 | 6.04 | 0.42 | 8.27 | 0.84 | 7.85 |

Table 2: Characteristics of MODEL I and MODEL II obtained for studied cakes

| | R ² | PRESS | FN |
|----------|----------------|-------|----|
| MODEL I | 0.89 | 1.12 | 2 |
| MODEL II | 0.92 | 0.98 | 4 |

Table 3: Content of fatty acids incorporated in fat extracted from studied cakes in first and last month of experiment. “Trans” in bottom row stays for sum of 18:1, 18:2, and 18:3 trans isomers.

| Fatty acid composition of fat extracted from cakes | | | | | | | | | | |
|--|------------------|-------|--------------|-------|--------------|-------|--------------|-------|--------------|-------|
| Fatty acid | Type of the cake | | | | | | | | | |
| | A | | B | | C | | D | | E | |
| | Storage time | | Storage time | | Storage time | | Storage time | | Storage time | |
| | 0 | 10 | 0 | 10 | 0 | 10 | 0 | 10 | 0 | 10 |
| 16:0 | 22.53 | 23.45 | 28.72 | 30.21 | 24.54 | 25.93 | 35.64 | 36.64 | 12.79 | 12.99 |
| 18:0 | 1.76 | 2.15 | 3.00 | 3.98 | 3.03 | 4.39 | 3.01 | 2.65 | 2.93 | 3.43 |
| 18:1(cis) | 38.82 | 37.89 | 46.33 | 44.1 | 48.33 | 45.75 | 24.94 | 23.21 | 40.12 | 38.83 |
| 18:2(cis) | 34.01 | 33.42 | 15.73 | 12.22 | 15.51 | 13.58 | 11.49 | 10.01 | 38.21 | 36.38 |
| 18:3(cis) | 1.15 | 0.56 | 3.46 | 2.25 | 3.07 | 2.86 | 0.23 | 0.12 | 2.83 | 2.21 |
| Trans | - | - | 1.45 | 1.49 | 1.32 | 1.21 | 2.63 | 2.49 | 2.54 | 2.68 |

Table 4: Content of trans fatty acids estimated by traditional method (real value) and predicted by developed model (predicted value).

| Trans fatty acid content | | | | |
|--------------------------|------|------|------|------|
| | B | C | D | E |
| Real value | 1.46 | 1.28 | 2.47 | 2.60 |
| Predicted value | 1.53 | 1.23 | 2.55 | 2.52 |

References:

- Caponio F., Summo C., Delcuratolo D. and Pasqualone A. (2006) Quality of the lipid fraction of Italian biscuits. *Journal of the Science of Food and Agriculture* 86, 356 – 361.
- Dlouhý P., Tvrzická E., Staňková B., Vecka M., Žak A., Straka Z., Fanta J., Páchl J., Kubisová D., Rambousková J., Bílková D. and Anděl M. (2003) Higher content of 18:1 trans fatty acids in subcutaneous fat of persons with coronographically documented atherosclerosis of the coronary arteries. *Annals of Nutrition and Metabolism* 47(6), 302 – 305.
- Kita A., Aniołowski K. and Włodarczyk E. (2003) Zmiany frakcji tłuszczowej w przechowywanych produktach przekąskowych. *Żywność. Nauka. Technologia. Jakość* 2(35), 87 – 95.
- Klensporf D., and Jeleń H. (2005) Analysis of volatile aldehydes in oat flakes by SPME – GC/MS. *Polish Journal of Food and Nutrition Science* 4 (14/55), 389 – 395.
- Koczoń, P., Piekut J., Borawska M., Świsłocka R. and Lewandowski W. (2006) Microbiological and vibrational study of selected picolinates and o-iodobenzoates. *Analytical and Bioanalytical Chemistry* 384, 302 – 308.
- Oomen M.C., Ocké M., Feskens E.J.M., Erp-Barat M.A., Kok F.J. and Kromhout D. (2001) Association between trans fatty acids intake and 10-years risk of coronary heart disease in the Zutphen Elderly Study: A prospective population –based study. *The Lancet* 357, 746 – 751.
- de Roos N.M., Schouten E.G. and Katan M.B. (2001) Consumption of a solid fat rich in lauric acids results in a more favourable serum lipid profile in healthy men and women than consumption of a solid fat rich in trans – fatty acids. *Human Nutrition and Metabolism, the Journal of Nutrition, American Society for Nutritional Sciences* 131(2), 242 – 245.
- Tay A., Singh R. K., Krishnan S.S. and Gore J. P. (2002) Authentication of olive oil adulterated with vegetable oils using Fourier Transform Infrared Spectroscopy. *Lebensmittel-Wissenschaft und-Technologie* 5, 99–103.
- Quilitzsch R., Baranska M., Schulz H. and Hoberg E. (2005) Fast determination of carrot quality by spectroscopy methods in the UV-VIS, NIR and IR range. *Journal of Applied Botany and Food Quality* 79, 163-167.
- Yildiz, G., R. L. Wehling, S. L. Cuppett, 2002. Monitoring PV in corn and soybean oils by NIR Spectroscopy. *Journal of American Oil Chemists' Society*, 11: 1085–1089.

Modelling aspects of orange juice quality kinetics during ultrasound processing

B.K. Tiwari¹, V.P. Valdramidis², Colm P. O'Donnell¹ and P.J. Cullen²

¹ Biosystems Engineering, UCD School of Agriculture, Food Science and Veterinary Medicine, University College Dublin, Belfield, Dublin 4, Ireland (brijesh.tiwari@ucd.ie)

² School of Food Science & Environmental Health, Dublin Institute of Technology, Cathal Brugha Street, Dublin 1, Ireland (pjculen@dit.ie)

Abstract

The objective of this study was to develop a deterministic modelling approach for non-enzymatic browning (NEB) and ascorbic acid (AA) degradation in orange juice during ultrasound processing. Freshly squeezed orange juice was sonicated using a 1500 W ultrasonic processor at a constant frequency of 20 kHz and processing variables of amplitude level (24.4 – 61.0 μm), temperature (5 – 30 °C) and time (0 – 10 min). The rate constants of the NEB and AA were estimated by a primary model (zero and first order) while their relationship with respect to the processing factors was tested for a number of models, i.e., second order polynomial, different types of Ratkowsky-type model, and an Arrhenius-type model. The non-monotonic behaviour of NEB has been described more accurately by the use of a polynomial model. The rate constants of AA were described by a similar type of model having a monotonic behaviour. A synergistic effect of temperature for different amplitudes on the rate constant of both the NEB and the AA was observed, while an antagonistic effect of amplitude on the rate of NEB was evident. Constructed contour plots illustrate that low temperatures and intermediate amplitudes result in lower NEB and AA deterioration and consequently improved quality orange juice.

Introduction

The use of ultrasound within the food industry has been a subject of research and development for many years with applications in both food analysis (diagnostic ultrasound) and food processing (power ultrasound). Ultrasound is one of the non-thermal technologies that has been identified as a potential technology to meet the FDA requirements of a 5 log reduction in pertinent microorganisms found in fruit juices. Advantages of sonication include reduced processing time, higher throughput and lower energy consumption while reducing thermal effects (Knorr *et al.*, 2004). Various research groups have demonstrated the inactivation of pathogenic and spoilage microorganisms (*E coli*, *Listeria*), enzymes (pectin methyl esterase, polyphenol oxidase) with reduced effects on quality or nutritional parameters including ascorbic acid (Tiwari *et al.*, 2008).

Among the main quality parameters that identify the processing efficiency and based on which different processes of orange juices are designed, are the non-enzymatic browning (NEB) and the ascorbic acid (AA) content. Kinetic models can be used for an objective, fast and economic assessment of food quality. Kinetic modelling may also be employed to predict the influence of processing on critical quality parameters. The objective of this study was to develop integrated deterministic modelling approaches of both quality indices, i.e., AA and NEB, to identify the optimal conditions for producing orange juice with minimal quality deterioration. Therefore, the kinetics of the quality indices of NEB and AA are described quantitatively in order to evaluate the combined effect of the extrinsic parameters of amplitude and temperature on them. The developed deterministic modelling approaches of both quality indices are integrated in order to identify the optimal conditions for producing an orange juice with minimal quality deterioration.

Materials and Methods

Juice preparation and ultrasound processing

Oranges (*Citrus sinensis* cv. *Valencia*) were purchased from a local fruit supplier (Reilly Wholesale Ltd., Dublin Ireland). Fresh juice was squeezed and filtered using a double layer cheese cloth to remove pulp. A 1,500 W ultrasonic processor (VC 1500, Sonics and Materials Inc., Newtown, USA) with a 19 mm diameter probe was used for sonication. Samples were processed at a constant frequency of 20 kHz. The energy input was controlled by setting the amplitude of the sonicator probe. Extrinsic parameters of temperature (5, 10, 15, 20, 25, 30 °C), amplitude (24.4, 42.7, 61.0 μ m) and time (2, 4, 6, 8, 10 min) were varied with pulse durations of 5 s on and 5 s off. 80 mL orange juice samples were placed in a 100 mL jacketed vessel through which water with a flowrate of 0.5 L/min was circulated. All treatments were carried out in triplicate.

Determination of non-enzymatic browning and ascorbic acid

Non-enzymatic browning was measured using the method of (Meydavi *et al.*, (1977) including orange juice centrifugation, removal of coarse particles, addition of ethyl alcohol to juice supernatant and a final step of centrifugation. The absorbance of the supernatant was obtained at 420 nm using a Unicam UV-VIS (UV2) spectrophotometer with distilled water as blank. Measurements were taken in triplicate and mean value reported.

Ascorbic acid content was determined following the HPLC (Shimadzu Model no: SPD - M10AVP, Shimadzu Co., Japan) analytical procedure outlined by (Lee *et al.*, (1999)). The mobile phase was 25 mM KH_2PO_4 (adjusted to pH 3.0 with phosphoric acid) while eluate was monitored by UV detection at 245 nm. Chromatograms were recorded and processed with EZStart Chromatography Software V.7.2.1. Results were reported as g of ascorbic acid/L of tomato juice.

Model development

The rate constants of the NEB and AA were estimated by a primary model describing the evolution of the concentration of a component, i.e., NEB and AA, with respect to the time. A zero order and a first order model were employed for this purpose.

$$C(t) = C(0) + k \cdot t \quad (1)$$

$$C(t) = C(0) \cdot \exp(k \cdot t) \quad (2)$$

where $C(t)$ represents the AA concentration [mg/ 100 mL of orange juice] and the NEB level, respectively, at time t and k is the rate constant. The relationship of the rate constant, k , with respect to the processing factors was tested for a number of secondary models, i.e., second order polynomial, different types of Ratkowsky-type model, and an Arrhenius-type model. The second-order response surface model with an interaction factor reads as follows:

$$k = \beta_0 + \beta_1 \cdot T + \beta_2 \cdot T^2 + \beta_3 \cdot A + \beta_4 \cdot A^2 + \beta_5 \cdot T \cdot A \quad (3)$$

where β_i are the polynomial coefficients. Only significant parameters ($P < 0.05$) have been retained by performing a stepwise fit. An Arrhenius type equation inspired by the model of Cerf (Cerf *et al.*, 1996) was developed, in which the effect of the temperature and amplitude on the rate constants of NEB and ascorbic acid was investigated. The model is:

$$k = C_0 + C_1 \cdot A^2 + \frac{C_2}{T} \quad (4)$$

Where C_0 , C_1 , C_2 are the coefficients of the Arrhenius type model. Two different types of the Ratkowsky type model (Ratkowsky et al., 1983) have also been considered. These transformed equations appear as follows:

$$\sqrt{k} = \alpha_1 \cdot (A + \alpha_2) \cdot (T + \alpha_3) \quad (5)$$

$$\sqrt{k} = \alpha_1 \cdot (A + \alpha_2)^2 \cdot (T + \alpha_5) \quad (6)$$

In case of the kinetics of NEB the following equation was employed:

$$\sqrt{k} = \alpha_1 \cdot (A + \alpha_2) \cdot (1 + \exp(\alpha_3 \cdot (\alpha_4 - A))) \cdot (T + \alpha_5) \quad (7)$$

Where α_i are the coefficients of determination for these models. Observe that Eq. (7) has been transformed in such a way that takes into account the antagonistic effect of amplitude for different temperatures on the non-enzymatic rate constants (see constant rates of NEB at Fig. 2). The different secondary models are evaluated with respect to their performance (comparison of root mean squared error *RMSE*) and the best fitted models are used to construct iso-rate contour plots that integrate the NEB and AA kinetics for the combined amplitude and temperature treatments.

Results and discussion

Non-enzymatic browning (NEB)

The browning index of NEB followed a zero order reaction (Eq. (1) was employed) with respect to the time for the different studied amplitudes and temperatures. Eq. (7) of the modified Ratkowsky model could better describe the observed non-linearities (*RMSE* = 0.0031) when compared with Eqs. (5), (6) but resulted in non-accurate parameters, i.e., SE errors were much higher than the estimated parameters. This could be attributed to the fact that a limited amount of data describes the observed antagonistic behaviour of amplitude on non-enzymatic browning. Among all the tested secondary models the polynomial model (Eq. (3)) gave the best regression performance for describing the non-monotonic behaviour of the effect of amplitude on the NEB constants (Fig. 1, left). At amplitude levels of 42.7 μm the NEB rate appeared to be lower than at higher or lower amplitude levels for the same temperatures. The observed monotonic increase of the NEB rate with respect to temperature has also been reported for the browning kinetics of apple juice and apple cider (Ugarte-Romero et al., 2006; Vaikousi et al., 2008).

Ascorbic acid degradation (AA)

A significant ($p < 0.05$) reduction in orange juice ascorbic acid content (mg/100 mL) was observed as a function of time. The degradation kinetics of ascorbic acid followed first order kinetics (Eq. (2)) and the estimated rate constants for each of the replicates are illustrated in Fig. 3. At the highest processing conditions of amplitude (61.0 μm) and processing temperature (30 °C) the largest reduction in ascorbic acid after sonication was observed. The ascorbic acid rate constant with respect to the amplitude and the temperature was described more accurately by employing the polynomial model (Eq. (3)). Fig. 1 (middle) illustrates that increase of temperature and increase of amplitude resulted in increase of the ascorbic acid loss. This indicates a synergistic effect of temperature for different amplitudes and temperatures on the rate constant of AA.

Contour design

An analysis of amplitude and temperature diagrams was performed based on the best fitted mathematical expressions (see previous Sections). Thereafter, iso-rate contour plots integrating non enzymatic browning and ascorbic acid information were developed (Fig. 1, right). The constructed contour plots illustrate that low temperatures and intermediate

amplitudes, i.e., 42.7, result in lower NEB and AA deterioration and consequently better quality of orange juice. Non enzymatic browning effects appear to be more sensitive to ultrasound processing than ascorbic acid degradation (Fig. 2). It is therefore suggested that NEB could be more appropriate to determine the intensity of an ultrasound processing during commercial applications.

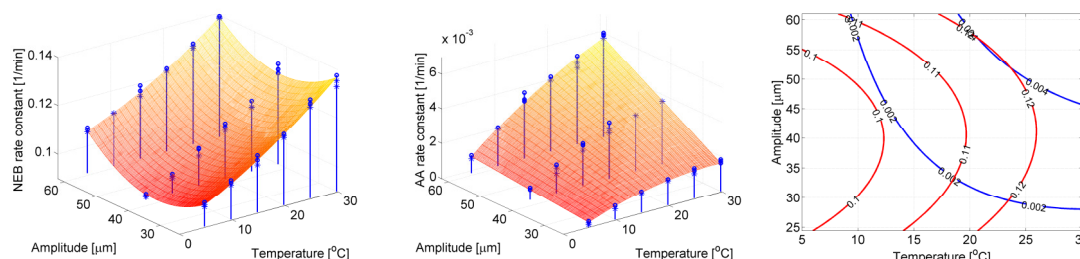


Figure 1. Left figure: Modelling the non enzymatic browning rate constant, k (Eq. (3)). Middle figure: Modelling the ascorbic acid rate constant, k (Eq. (3)). (o): experimental data points above the surface, (*): experimental data points under the surface. Right figure: Non enzymatic browning and ascorbic acid iso-rate contour plots for $k = 0.1, 0.11, 0.12$ [1/min] and $k = 0.004, 0.004$ [1/min], respectively.

Conclusions

Non-enzymatic browning reactions involve caramelization and formation of Maillard reaction. Ascorbic acid levels determine the shelf life of the orange juice. The developed modelling approaches exploit quality data to identify the optimal processing regions for minimising quality deterioration of orange juice during ultrasound processing which is of high relevance to food industry. Ultrasound was found to have more drastic effect on NEB than AA degradation of orange juice therefore the inactivation rate of the former could serve as indicator for the adequacy of this process.

Acknowledgements

Funding for this research was provided under the National Development Plan 2000-2006, through the Food Institutional Research Measure, administered by the Department of Agriculture, Fisheries & Food, Ireland.

References

- Cerf, O., Davey, K. R. and Sadoudi, A. K. (1996) Thermal inactivation of bacteria - A new predictive model for the combined effect of three environmental factors: Temperature, pH and water activity. *Food Research International* 29(3-4), 219-226.
- Knorr, D., Zenker, M., Heinz, V. and Lee, D. U. (2004) Applications and ultrasonics in food potential of processing. *Trends in Food Science & Technology* 15(5), 261-266.
- Lee, H. S. and Coates, G. A. (1999) Measurement of total vitamin C activity in citrus products by HPLC: A review. *Journal of Liquid Chromatography & Related Technologies* 22(15), 2367-2387.
- Meydavi, S., Saguy, I. and Kopelman, I. J. (1977) Browning determination in citrus products. *Journal of Agricultural and Food Chemistry* 25(3), 602-604.
- Ratkowsky, D. A., Lowry, R. K., McMeekin, T. A., Stokes, A. N. and Chandler, R. E. (1983) Model for bacterial culture-growth rate throughout the entire biokinetic temperature-range. *Journal of Bacteriology* 154(3), 1222-1226.
- Tiwari, B. K., Muthukumarappan, K., O'Donnell, C. P. and Cullen, P. J. (2008) Effects of sonication on the kinetics of orange juice quality parameters. *Journal of Agricultural and Food Chemistry* 56(7), 2423-2428.
- Ugarte-Romero, E., Feng, H., Martin, S. E., Cadwallader, K. R. and Robinson, S. J. (2006) Inactivation of *Escherichia coli* with power ultrasound in apple cider. *Journal of Food Science* 71(2), E102-E108.
- Vaikousi, H., Koutsoumanis, K. and Biliaderis, C. G. (2008) Kinetic modelling of non-enzymatic browning of apple juice concentrates differing in water activity under isothermal and dynamic heating conditions. *Food Chemistry* 107(2), 785-796.

Behavioural noise and colonial growth dynamics of single microbial cells

K. Koutsoumanis and A. Lianou

Department of Food Science and Technology, School of Agriculture, Aristotle University of Thessaloniki, Thessaloniki 54124, Greece * Tel/Fax: +30 2310991647, e-mail: kkoutsou@agro.auth.gr

Abstract

In this work we developed a time-lapse microscopy method for monitoring colonial growth of single cells. The colonial growth of 160 *Salmonella* Typhimurium single cells on tryptone soy agar at 25 °C was monitored. Images were taken at 5-min intervals for six hours after inoculation. After counting, data were transformed to the respective growth curves showing the exact number of cells in each colony over time with each separate colony originating from a single cell. The obtained growth curves (160 curves in total) were then fitted to a primary model for the estimation of the lag phase and growth rate. Fitting trials of growth curves corresponding to the same colony with different final populations ranging from 4 to 100 cells showed that the calculated lag and rate is getting constant when the final number of cells reaches 15-20. The lag phase of single cell colonial growth ranged from 0 to 5.13 h (mean=1.66 h) with a percent coefficient of variation (CV) of 46.3. The growth rate (mean=0.77 h⁻¹) showed less but still significant variability with a percent CV of 16.6. The latter variability in the growth rate reflects a corresponding variability in the distribution of single cell division times among individual colonies. The method presented in this work allows for monitoring and modeling the colonial growth of single cells simulating bacterial growth on solid foods. Using Monte Carlo simulation it is also shown that beyond the scientific interest in understanding single cell growth dynamics, the data provided are valuable for quantitative microbial risk assessment purposes.

Keywords: single-cell; colonial growth dynamics; *Salmonella*

Introduction

For many years predictive microbiology deals with the development of deterministic models based on studies with large microbial populations. Traditional mathematical models describe the growth of microbial populations as a whole, without considering the individual cells. In “real life” however, contamination of foods with pathogens usually occurs at very low numbers and the probability that their multiplication results in an infectious level at the time of consumption depends greatly on the kinetics of the contaminating cells as well as on whether they are able to grow. Recently, the importance of stochastic models which are able to predict the effects of more “realistic” contamination events (low microbial numbers) in food safety has been stressed. Thus, predictive microbiology studies have focused on monitoring microbial kinetics at a single cell level.

Individual cells within clonal microbial populations exhibit a marked phenotypic variation which refers to epigenetic sources of population variation that do not involve changes in the genome (Avery, 2006). For example, the production of a specific protein in genetically identical cells in an essentially identical environment can differ among cells owing to stochastic fluctuations (or noise) during transcription and translation, leading to differences in protein levels. The observable consequence of the above variation is the behavioral noise of single cells including the noise in the division time.

In the recent years several studies have focused on monitoring the kinetics of single microbial cells. Elfving et al. (2004) and Wakamoto et al. (2001) developed novel automated microscopic methods that enabled the user to monitor the division times of individual cells. Both of the above methods however, only allow for monitoring of one cell alone with the daughter cell being

removed after division. This approach does not take into account the “community effect”. Indeed, in “real life”, interactions among cells of a forming colony may occur during growth of an initially single cell on a solid food.

The objective of the present study was to develop a time-lapse microscopy method for monitoring colonial growth of single cells simulating bacterial growth on solid foods. The population dynamics of microbial colonies originating from a single cell were studied and the extent of variation in individual colony growth kinetics was evaluated.

Materials and Methods

The bacterial strain used in the study was *Salmonella enterica* serotype Typhimurium FSL S5-520 (bovine isolate), kindly provided by Dr. Martin Wiedmann (Cornell University, Ithaca, New York). Twenty microliters of a 24-h culture of the isolate, after two 10-fold serial dilutions in quarter-strength Ringer’s solution (Lab M Limited), were added to 500 µl of tryptone soy agar (TSA; Lab M Limited) solidified on a glass slide, and were left to dry in a biological safety cabinet for 5 min. A z-motorized microscope (Olympus BX61) equipped with a ×100 objective (Olympus) and a high-resolution device camera (Olympus DP71) was used for monitoring growth of single cells. The quality of the images was improved by developing an auto-focus procedure with an Extended Depth of Focus (EDF) system using the ScopePro module of ImageProPlus software. Each final image was a result of 20 images captured in different z-axis planes. The EDF system allowed the combination of the z-stack images of multi-level focal planes into a single in-focus image. The above procedure provided high quality images of bacterial colonies in which cells can be counted either manually or by the image analysis software. In this study the colonial growth of 160 *Salmonella* Typhimurium single cells on TSA at 25 °C was monitored. Images were taken at 5-min intervals for 6 h after inoculation. Using the ×100 objective the colonial growth of 15-30 single cells to a final number of 100 cells per colony could be monitored in each experiment. After counting, data were transformed to the respective growth curves showing the exact number of cells in each colony over time with each separate colony originating from a single cell. The obtained growth curves (160 curves in total) were then fitted to the primary model of Baranyi and Roberts (1994) for the estimation of lag phase and maximum specific growth rate (μ_{\max}).

Results and Discussion

Figure 1 shows a representative colonial growth of a *S. Typhimurium* single cell and the formation of a colony on TSA during 6 h at 25 °C.

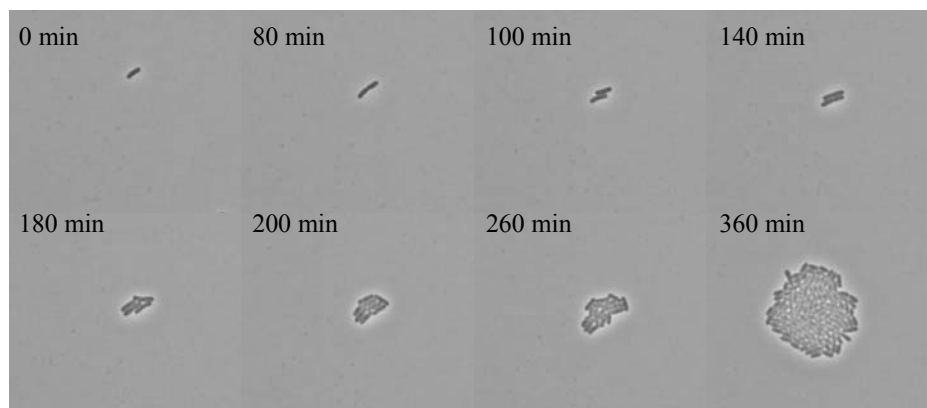


Figure 1: Representative colonial growth of a *S. Typhimurium* single cell on tryptone soy agar during 6 hours at 25 °C

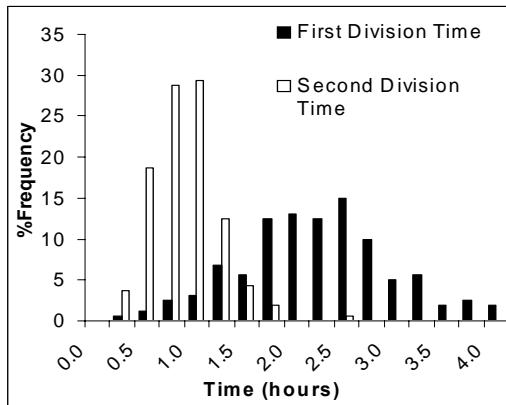


Figure 2: Growth curves of 160 cells of *Salmonella* Typhimurium grown on tryptone soy agar at 25 °C.

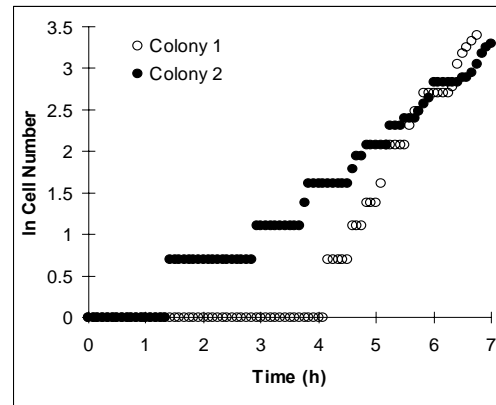


Figure 3: Growth curves of two representative colonies of *Salmonella* Typhimurium grown on tryptone soy agar at 25 °C.

The first division time (FDT), which is the sum of the lag time and the first generation time, and second division time (SDT) of 160 cells are presented in Figure 2. The average FDT value was 2.15 h with SD=0.81 h. As expected the SDT was significantly shorter with an average value of 0.81 h and SD=0.33 h. The growth curves of two representative colonies are shown in Figure 3.

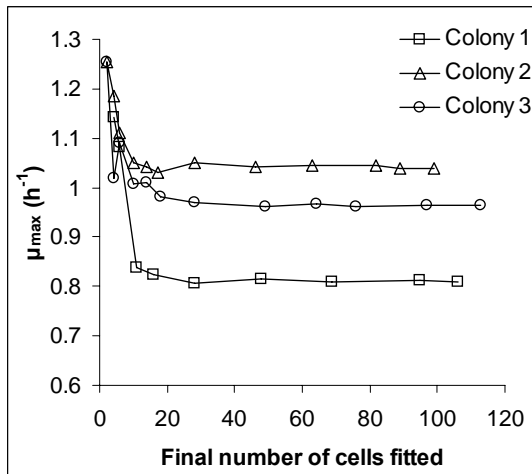


Figure 4: Effect of the final number of cells in a colony fitted to the primary model on the calculated μ_{\max} for 3 representative colonies.

Fitting trials of growth curves for the same colony with different final populations ranging from 4 to 100 cells showed that the calculated lag and μ_{\max} are getting constant when the final number of cells reaches 15-20 (Figure 4). Based on the above results growth curves with a final population of 25-30 cells for each colony were fitted.

The lag phase of single cell colonial growth ranged from 0 to 5.13 h (mean=1.66 h) with a percent coefficient of variation (CV) of 46.3. The μ_{\max} (mean=0.77 h⁻¹) showed less but still significant variability with a percent CV of 16.6. No correlation was observed between the lag phase and the μ_{\max} indicating variability in the physiological state of the single cells. The mean value of the physiological state parameter h_0 (=lag* μ_{\max}) was 1.24 (CV=57.2%). The variability in the

μ_{\max} reflects a corresponding variability in the distribution of single cell division times among individual colonies. This can be also seen in Figure 3 where the mean division time of cells in colony 1 is significantly shorter compared to colony 2. It needs to be noted that the variability of μ_{\max} among individual colonies cannot be attributed to the low number of cells (25-30) since as it is shown in Figure 4, the μ_{\max} of a colony is constant for colonial populations above 20 cells. The distributions of μ_{\max} and lag times of single cell colonial growth (Figure 5) were used to evaluate the variability in the growth dynamics *S. Typhimurium* populations as affected by the inoculum level. For this purpose, the colonial growth of a single cell was calculated by introducing the distributions of μ_{\max} and lag times to the primary model using Monte Carlo simulations, and then the total growth of the population was estimated as the sum of individual cells in each colony.

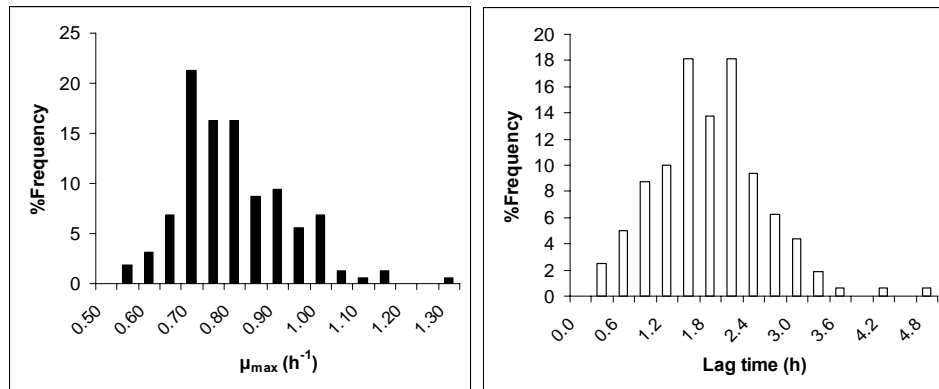


Figure 5: Distributions of μ_{\max} and lag times of *Salmonella* Typhimurium colonial growth for 160 single cells.

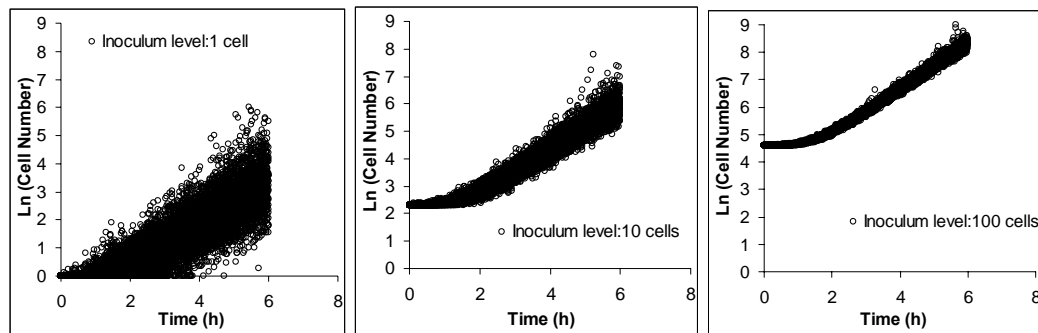


Figure 6: Effect of inoculum level on the variability of population growth.

The results of the simulation are shown in Figure 6. For an inoculum level of 1 cell, the population after 6 h varies from 5 to 265 cells. The variability of single cell growth however, is masked as the inoculum level increases. Considering that in “real life” contamination of foods with pathogens usually occurs at very low numbers (close to 1 cell), the results of the present study, beyond the scientific interest in understanding the behaviour of single cell colonial growth, can be used for more realistic microbial risk assessments.

Acknowledgements

This study has been carried out with the financial support of the Commission of the European Communities, Project ProSafeBeef “Food-CT-2006-36241”.

References

- Avery S.V. (2006) Microbial cell individuality and the underlying sources of heterogeneity. *Nature Reviews* 4, 577-587.
- Baranyi, J. and Roberts T. A. (1994) A dynamic approach to predicting bacterial growth in food. *International Journal of Food Microbiology* 23, 277-294.
- Elfwing, A., LeMarc Y., Baranyi J. and Ballagi A. (2004) Observing growth and division of large numbers of individual bacteria by Image Analysis. *Applied Environmental Microbiology* 70, 675-678.
- Wakamoto, Y., Inoue I., Morguchi H. and Yasuda K. (2001) Analysis of single-cell differences by use of an on-chip microculture system and optical trapping. *Fresenius' Journal of Analytical Chemistry* 371, 276-281.

Use of Time Temperature Indicators as Risk Management Tools for *L. monocytogenes* in Ready-To-Eat foods

Koutsoumanis, K., Vaikousi H., and Biliaderis C. G.

Department of Food Science and Technology, School of Agriculture, Aristotle University of Thessaloniki, Thessaloniki 54124, Greece* Tel/Fax: +30 2310991647, e-mail: kkoutsou@agro.auth.gr

Abstract

The objective of the present work was to evaluate the effectiveness of Time Temperature Indicators as risk management tools for *Listeria monocytogenes* in RTE foods. In a previous study we presented a microbial Time Temperature Indicator (TTI) system based on the growth and metabolic activity of a *Lactobacillus sakei* strain. In the latter system, an irreversible color change of a chemical chromatic indicator (from red to yellow) progressively occurs due to the pH decline as a result of *L. sakei* growth and metabolism in a selected medium. In this study we show that both the *L. sakei* growth and colour change of the microbial TTI system exhibit similar kinetic responses with the growth of *L. monocytogenes*. With an appropriate selection of the initial level of *L. sakei* in the system, the TTI end point (time at which a distinct visual color change to the final yellow was observed) can be adjusted in order to indicate a certain level of *L. monocytogenes* growth in the food during distribution and storage. Thus, the use of the microbial TTI can assure a maximum limit in the growth of the pathogen from production to consumption time by informing the consumers when this limit is exceeded in a product unit. The latter limit, which we call Growth Tolerance Criterion (GTC), can be considered as a performance criterion for the growth of *L. monocytogenes* during distribution and storage. The applicability of the microbial TTI in reducing consumer exposure to *L. monocytogenes* from the consumption of pate was evaluated in a simulation study. The TTI was appropriately adjusted to provide a GTC=3 logs CFU/g. The concentration of the pathogen and the colour of the TTI at the time of consumption were estimated with a probabilistic approach using Monte Carlo simulation. The simulation results showed that the application of the TTI resulted in a significant reduction of consumer exposure to *L. monocytogenes*. Assuming that packages in which the TTI end point has been reached before consumption are discarded, the predicted percentage of consumed products contaminated with *L. monocytogenes* concentrations above 10^3 CFU/g was reduced from 5% to 0.2% with the use of TTI.

Keywords: Time Temperature Indicators, *L. monocytogenes*, Risk Management

Introduction

The available risk assessment models for *Listeria monocytogenes* in Ready-To-Eat (RTE) foods predict that nearly all cases of listeriosis result from the consumption of high numbers of the pathogen. These models have also stressed the great impact of the growth between manufacture and consumption on the rates of listeriosis and indicated that storage time and temperature during distribution, retail and domestic storage are among the most important risk factors. The above indicate that application of an optimized safety assurance system for *Listeria monocytogenes* in Ready-To-Eat (RTE) foods requires continuous monitoring and control of storage conditions, from production to consumption. Time Temperature Integrators (TTI) allow such control down to product unit level. TTI can show an easily measurable, time and temperature dependent change that cumulatively reflects the time-temperature history of the food product.

In a previous study we developed a microbial TTI prototype, based on the growth and metabolic activity of a *Lactobacillus sakei* strain (Vaikousi et al. 2008). In this particular TTI system, an irreversible colour change of a chemical indicator from red to yellow progressively occurs due to the pH decline, as a result of microbial growth and metabolism of a selected growth medium.

Furthermore, experiments conducted on the effect of inoculum level showed a negative linear relationship between the level of *L. sakei* inoculated in the system medium and the end point of the TTI. The above relationship provides the ability of easily adjusting the TTI end point by using an appropriate inoculum level of *L. sakei*. The complete kinetic study conducted for the effect of temperature on the TTI response (colour change), showed that the developed TTI can be used as an effective tool for monitoring shelf life during distribution and storage of food products that spoil by the growth and metabolic activity of lactic acid bacteria or other bacteria of similar kinetic behavior (Vaikousi et al. 2009).

The objective of the present study was to evaluate the potential of the microbial TTI as a risk management tool for *L. monocytogenes* in Ready-To-Eat foods. The applicability of the microbial TTI to monitor the growth of *L. monocytogenes* during distribution and storage was evaluated through a case study on pate products. Furthermore, the effectiveness of the TTI in reducing consumer exposure to the pathogens was studied with a probabilistic approach using Monte Carlo simulation.

Materials and Methods

The applicability of a microbial Time Temperature Indicator, based on the growth and metabolic activity of a *L. sakei* strain developed in a previous study (Vaikousi et al. 2008), in monitoring growth of *L. monocytogenes* was evaluated. Growth data of *L. monocytogenes* in pate from Combase (<http://www.combase.cc/>) were compared with the growth of *L. sakei* in the TTI system and the colour response of the TTI. The initial level of *L. sakei* in the TTI was adjusted appropriately in order to provide an end point (time at which a distinct visual color change to the final yellow was observed) which corresponds to time-temperature conditions allowing a 3 logs CFU/g growth of *L. monocytogenes*. The effectiveness of the TTI in reducing consumer exposure to the pathogen was evaluated in a simulation study. The initial contamination level of the *L. monocytogenes* in pate was described with a Normal distribution with mean=-9.0 log CFU/g, SD=3.5, and a minimum value of -2.3 log CFU/g assuming pate packages of 200g. The storage temperature (°C) and the storage time until consumption (days) of pate were described with a Normal (4.98, 2.93-°C) and a Normal (7, 1.5-days) distribution, respectively, based on literature data. The concentration of the pathogen and the colour of the TTI at the time of consumption were estimated using Monte Carlo simulation.

Results and Discussion

Growth of *L. monocytogenes* in pate was very close to the growth of *L. sakei* in the TTI at storage temperatures from 0 to 15 °C (Figure 1a) while the temperature dependence of the pathogen's growth in pate was similar to that of the TTI end point. This can be seen from the parallel position of the respective Arrhenius plots in Figure 1b. In particular, the activation energies of *L. monocytogenes* growth in pate and the reverse of the TTI end point were 131.9 and 129.3 kJ/mole, respectively. With an appropriate selection of the initial level of *L. sakei* in the system, the TTI end point (time at which a distinct visual color change to the final yellow was observed) can be adjusted in order to indicate a certain level of *L. monocytogenes* growth in the product during distribution and storage. For example, with an initial *L. sakei* level close to 10⁵ CFU/ml, the end point of the TTI is reached when it is exposed to time-temperature conditions allowing 3 logs CFU/g growth of *L. monocytogenes* in pate. An example for 10 °C is shown in Figure 2. Based on the above, the use of the TTI can assure a maximum limit in the growth of the pathogen from production to consumption time by informing the consumer when this limit is exceeded in a product unit. In fact, the latter limit, which we call Growth Tolerance Criterion (GTC), can be considered as a performance criterion for the growth of *L. monocytogenes* during distribution and storage.

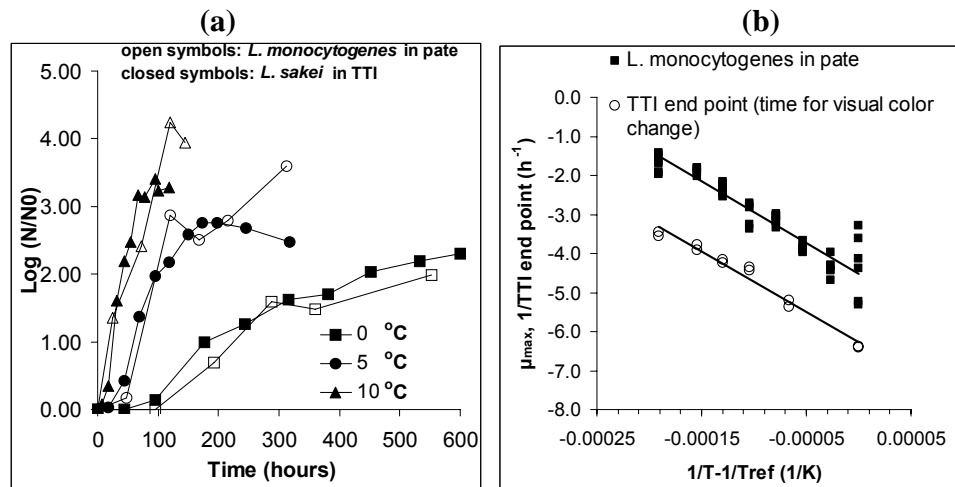


Figure 1. Comparison between growth (a) and Arrhenius plots (b) of *L. monocytogenes* in pate and *L. sakei* in the TTI system.

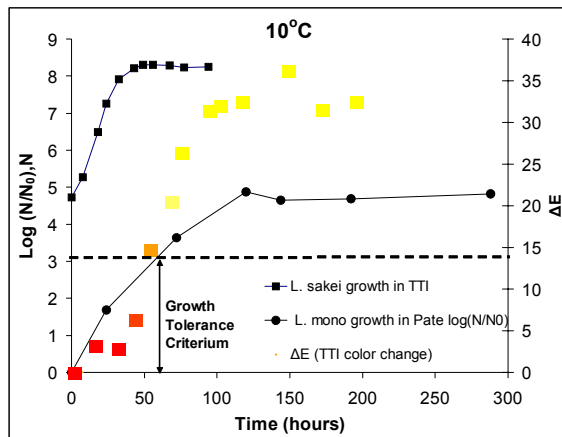


Figure 2 Comparison between growth of *L. monocytogenes* in pate and response of a TTI system adjusted to provide a Maximum Growth Criterion of 3 logs CFU/g

It needs to be noted that without the use of the TTI, meeting a performance criterion related to microbial growth during distribution and storage is almost impossible due to the variability of the chill chain conditions and the fact that conditions of domestic storage is beyond producer's or retailer's control. The use of the TTI however, can provide an indication that cumulatively reflects the time-temperature history of the food down to a product unit level and inform the consumer when the performance criterion is not met.

The applicability of TTI in reducing consumer exposure to *L. monocytogenes* was further evaluated in a simulation study. The microbial TTI was adjusted for providing a GTC=3 logs CFU/g. The

concentration of the pathogen and the colour of the TTI at the time of consumption were estimated based on the Arrhenius models presented in Figure 1b using Monte Carlo simulation. Figure 3a presents the predicted concentration *L. monocytogenes* in contaminated pate packages in relation to the time distance between the TTI end point and the time to consumption. In the x-axis of the latter figure negative values indicate packages in which the TTI end point has been reached before consumption. As it is shown the concentration of the pathogen in these packages at the time of consumption is significantly higher compared to packages in which the TTI end point has not been reached.

The predicted percentage of packages in which the TTI end has been reached before consumption time was 10.6%. It needs to be noted that this percentage depends on both the time-temperature conditions of the chill chain and the chosen GTC level. For example, a better control of storage temperature during distribution and storage or an increase of the GTC level would results to a significant reduction of the packages in which TTI end point is reached before consumption.

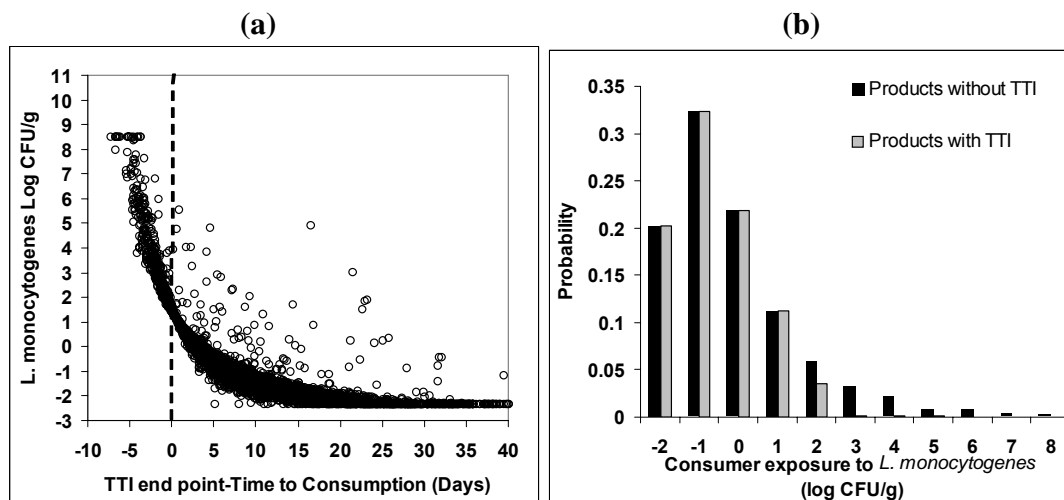


Figure 3. (a): *L. monocytogenes* concentration in contaminated pate packages in relation to the distance between TTI end point and time to consumption. Negative values in the x-axis indicate packages in which the TTI end point has been reached before consumption. (b): Effectiveness of TTI use on consumer exposure to *L. monocytogenes* for pate consumption assuming that packages in which the TTI end point has been reached are not consumed (i.e. 10.6% of packages are discarded due to TTI colour change).

The use of the TTI designed to provide a GTC of 3 logs CFU/g resulted in a significant reduction of consumer exposure to *L. monocytogenes* (Figure 3b). Indeed, assuming that packages in which the TTI end point has been reached are discarded, the percentage of consumed packages contaminated with *L. monocytogenes* concentrations above 10^3 CFU/g was reduced from 5% to 0.2% with the use of TTI.

Conclusions

In conclusion, the results of the present study indicate that the developed microbial Time Temperature Indicator can be used as an effective risk management tool for *L. monocytogenes* in Ready-To-Eat foods. The TTI can be adjusted in order to indicate the compliance to a selected Growth Tolerance Criterion (GTC). The GTC can be considered as a performance criterion for the growth of *L. monocytogenes* during distribution and storage and it can be defined according to the respective Food Safety Objective (FSO).

Acknowledgements

This study has been carried out with the financial support of the Commission of the European Communities, Project ProSafeBeef “Food-CT-2006-36241”

References

- Vaikousi, H., C.G. Biliaderis K. and Koutsoumanis (2009) Applicability of a microbial Time Temperature Indicator (TTI) for monitoring spoilage of modified atmosphere packed minced meat, *International Journal of Food Microbiology*, 133, 272-278
- Vaikousi, H. C.G. Biliaderis, and K.P. Koutsoumanis (2008) Development of a Microbial Time/Temperature Indicator Prototype for Monitoring the Microbiological Quality of Chilled Foods *Appl. Envir. Microbiol.* 74: 3242-3250.

Effect of the growth environment on the strain variability of *Salmonella enterica* kinetic behavior

A. Lianou and K.P. Koutsoumanis

Laboratory of Food Microbiology and Hygiene, Department of Food Science and Technology, School of Agriculture, Aristotle University of Thessaloniki, Thessaloniki 54124, Greece (alianou@agro.auth.gr; kkoutsou@agro.auth.gr)

Abstract

Aiming at the evaluation of the strain-to-strain growth variation of *Salmonella enterica* as affected by growth conditions, the kinetic behavior of 60 isolates of the pathogen was assessed at 37°C under different pH (4.3-7.0) and a_w (0.964-0.992) conditions. Maximum specific growth rate (μ_{max}) values corresponding to each isolate and growth condition were estimated by means of absorbance detection times of serially diluted cultures using the automated turbidimetric system Bioscreen C. The intra-specific variability of μ_{max} among the *Salmonella* isolates was important and greater than that observed within the isolates (i.e. among replicates). Moreover, strain variability increased as the growth conditions became more stressful, with a_w demonstrating a stronger effect on variability than pH. The coefficient of variation among the tested isolates at pH 7.0- a_w 0.992 was 6.1%, while at pH 4.3- a_w 0.992 and pH 7.0- a_w 0.964 was 12.0% and 23.5%, respectively. For each tested strain, the effect of pH and a_w on μ_{max} was modeled and the strain variability of pH_{min} and a_{wmin} was determined. Beyond the scientific interest in understanding strain variability, the results of the present study provide quantitative information for integrating strain variability in microbial risk assessment.

Keywords: *Salmonella*, growth environment, strain variability, kinetic behavior

Introduction

The strain-dependent character of the growth behavior of foodborne pathogens has been well documented and has been acknowledged as an issue of major importance in quantitative microbiology, particularly with regard to risk assessment approaches (Juneja et al., 2000; Lianou et al., 2006; Lindqvist, 2006). Although the implications of strain variability for microbial risk assessment have been recognized and efforts to be controlled have been made, the validity of assumptions commonly embraced by risk assessors warrants further investigation if inaccurate risk estimates are to be avoided. An assumption commonly used in microbial risk assessment is that strain variability is not affected by growth conditions (Ross and McMeekin, 2003). Nevertheless, there are research data indicating that the impact of growth conditions on the observed strain variability of foodborne pathogens may be considerable (De Jesús and Whiting, 2003; Lianou et al., 2006). Given the above and that the strain variability of *Salmonella enterica* has been less studied compared to other foodborne pathogens, the objective of this study was to evaluate the effect of growth conditions (i.e. pH and a_w) on the strain variability of the kinetic behavior of the organism.

Materials and methods

Sixty *S. enterica* isolates were evaluated in the present study, and were primarily isolates of human or animal (i.e. bovine) origin belonging to various serotypes (i.e. Typhimurium, Enteritidis, Newport, Heidelberg, Montevideo, Seftenberg, Infantis, Agona and Derby). Stock cultures of the isolates were stored frozen (-70°C) onto Microbank™ porous beads (Pro-Lab Diagnostics, Ontario, Canada). Working cultures were stored refrigerated (5°C) on tryptone soy agar (TSA; Lab M Limited, Lancashire, United Kingdom) slants, and were activated (24 h at 37°C) and subcultured (18 h at 37°C) in tryptone soy broth (TSB; Lab M Limited). Aliquots of five 10-fold serial dilutions of each culture were added to TSB of the following characteristics dispensed in 100-well microtiter plates: (i) pH 7.0 and a_w 0.992; (ii) pH 7.0 and

a_w 0.983; (iii) pH 7.0 and a_w 0.977; (iv) pH 7.0 and a_w 0.964; (v) pH 5.5 and a_w 0.992; (vi) pH 5.0 and a_w 0.992; (vii) pH 4.5 and a_w 0.992; or (viii) pH 4.3 and a_w 0.992. The pH of TSB was adjusted to the above values using HCl (Sigma-Aldrich, Seelze, Germany), while the above a_w values were measured in TSB containing NaCl (Merck, Darmstadt, Germany) at the following concentrations (w/v): 0.5% (a_w 0.992; NaCl contained in TSB as part of its basal composition), 3.5% (a_w 0.983), 4.5% (a_w 0.977) or 6% (a_w 0.964). The initial concentrations of the inocula were determined on TSA and the range of bacterial concentrations obtained in the microtiter plates was approximately 10 – 10^5 cfu/well. The microtiter plates were placed in the automated turbidimetric system Bioscreen C (Oy Growth Curves Ab Ltd., Raisio, Finland) at an incubation temperature of 37°C , and optical density (OD) measurements were taken at regular time intervals using a wide-band filter (420–580 nm). In total, 9,600 OD curves were generated.

The maximum specific growth rate (μ_{\max}) of each isolate at each growth condition was estimated from absorbance detection times (DT: time required for a specific OD increase to be recorded) as described previously (Dalgaard and Koutsoumanis, 2001). Briefly, plots of the DTs corresponding to the five 10-fold serial dilutions of each culture against ln cfu/well were generated, and μ_{\max} values were estimated from the slope of these plots using the equation $\mu_{\max} = -1/\text{slope}$. The experiments were conducted twice and two samples (i.e. two microtiter plate-wells per dilution) per isolate were analysed at each replication ($n=4$).

Results and discussion

Important growth variability among the tested isolates was demonstrated (Figure 1). The estimated μ_{\max} (h^{-1}) ranged from 1.51 to 2.13 at pH 7.0- a_w 0.992, from 0.96 to 1.39 at pH 7.0- a_w 0.983, from 0.74 to 1.10 at pH 7.0- a_w 0.977, from 0.12 to 0.59 at pH 7.0- a_w 0.964, from 1.27 to 1.95 at pH 5.5- a_w 0.992, from 1.02 to 1.67 at pH 5.0- a_w 0.992, from 0.78 to 1.37 at pH 4.5- a_w 0.992 and from 0.70 to 1.28 at pH 4.3- a_w 0.992.

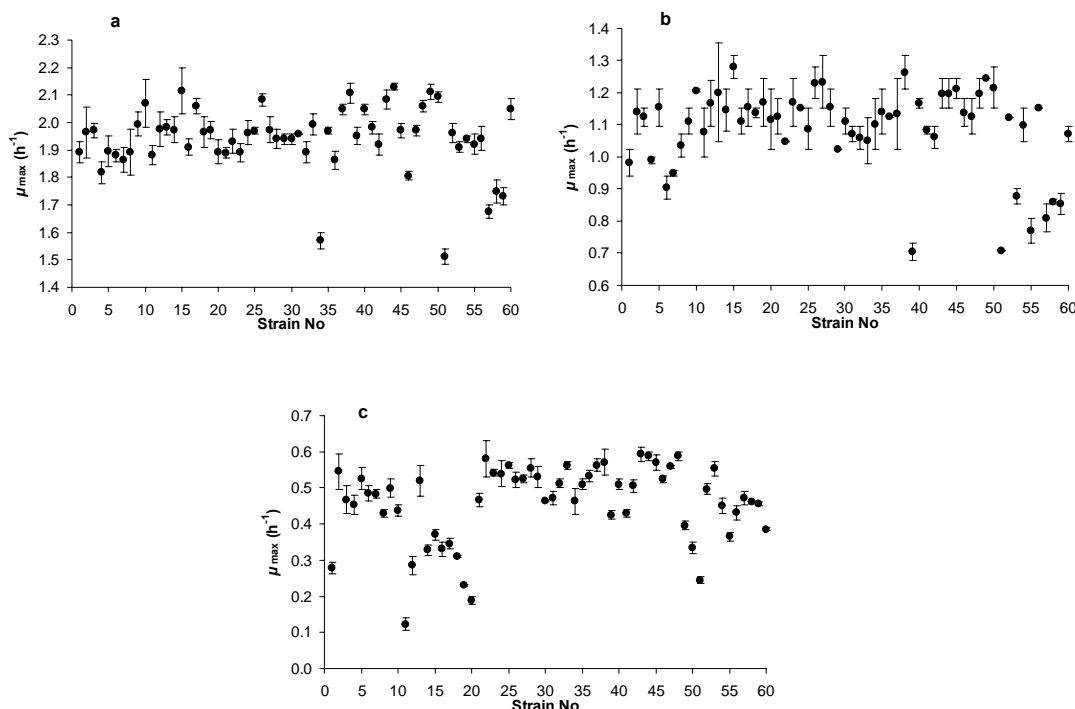


Figure 1: Estimated values of the maximum specific growth rate (μ_{\max}) for 60 *Salmonella enterica* isolates in tryptone soy broth at pH 7.0 and a_w 0.992 (a), at pH 4.3 and a_w 0.992 (b), and at pH 7.0 and a_w 0.964 (c). Values are means \pm standard errors ($n=4$).

As demonstrated by the estimated μ_{\max} values, and given that pH 4.3 is expected to be very close to the minimum pH allowing *Salmonella* growth (no growth of none of the tested isolates was observed at pH 4.0 in preliminary experiments), decreasing a_w (achieved by increasing NaCl concentrations) appeared to have a stronger effect on *Salmonella* growth than decreasing pH (Figures 1 and 2).

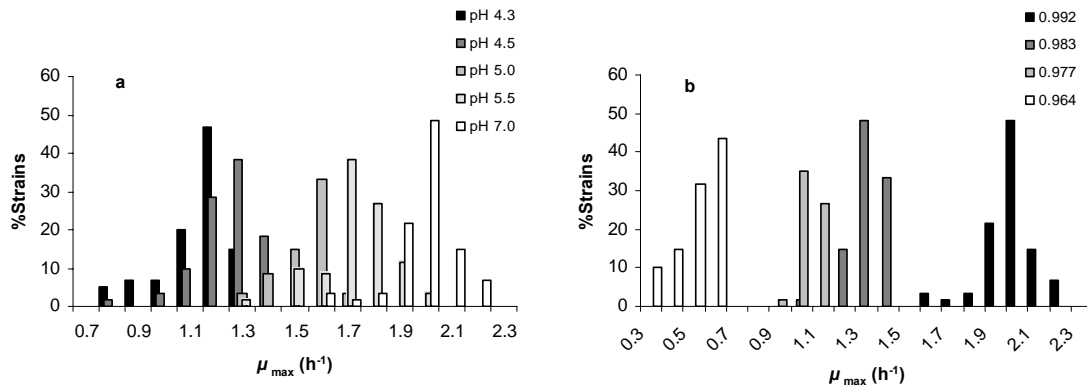


Figure 2: Frequency distribution of the maximum specific growth rate (μ_{\max}) for 60 *Salmonella enterica* isolates in tryptone soy broth at pH 4.3-7.0 (a), and at a_w 0.964-0.992 (b).

Although some of the tested isolates demonstrated a similar growth behavior (i.e. low, intermediate or high μ_{\max}) at pH 4.3 and at a_w 0.964, no clear relationship between the kinetic behavior of the isolates at these two growth conditions (i.e. low pH and low a_w) was evident. Furthermore, no serotype-related trends associated with the estimated μ_{\max} of the tested isolates, at none of the growth conditions evaluated, were observed.

The coefficient of variation of μ_{\max} was larger among strains than within strains, demonstrating that the variability of μ_{\max} among the tested isolates was greater than that among replicates. Moreover, strain variability increased as the growth conditions became more stressful, and a_w appeared to exert a stronger effect on variability than pH (Figure 3). The coefficient of variation among the tested isolates at pH 7.0- a_w 0.992 was 6.1%, while at pH 4.3- a_w 0.992 and pH 7.0- a_w 0.964 was 12.0% and 23.5%, respectively.

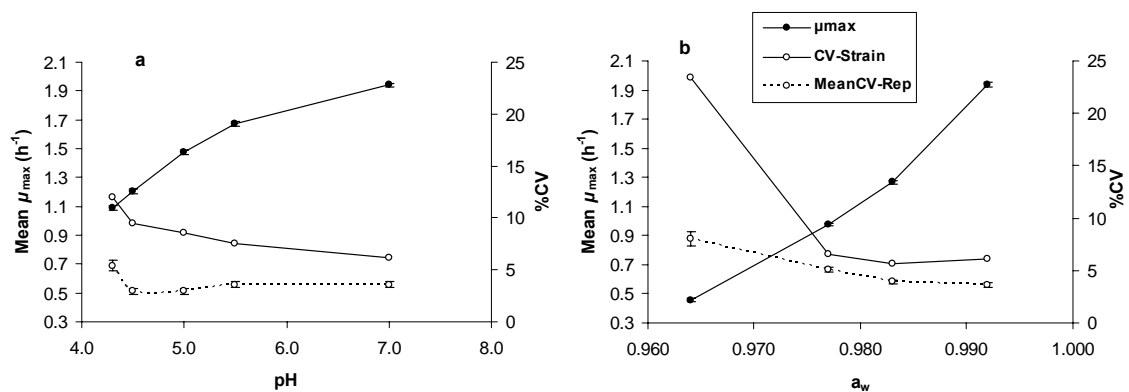


Figure 3: Mean (\pm standard error, $n=60$) maximum specific growth rate (μ_{\max}) of *Salmonella enterica* isolates, coefficient of variation of μ_{\max} among isolates (CV-Strain), and mean (\pm standard error, $n=60$) coefficient of variation among replicates (MeanCV-Rep) at pH 4.3-7.0 (a), and at a_w 0.964-0.992 (b).

A next step towards the exploitation of the above data in risk assessment approaches is to model the estimated μ_{\max} for each strain as a function of pH and a_w . For instance, the frequency distribution of the parameter $a_{w\min}$ for the tested isolates, with the latter being estimated by modelling the μ_{\max} for each isolate as a function of a_w using the secondary square

root model and the curve-fitting program TableCurve 2D (Systat Software Inc., San Jose, CA, United States), is given in Figure 4.

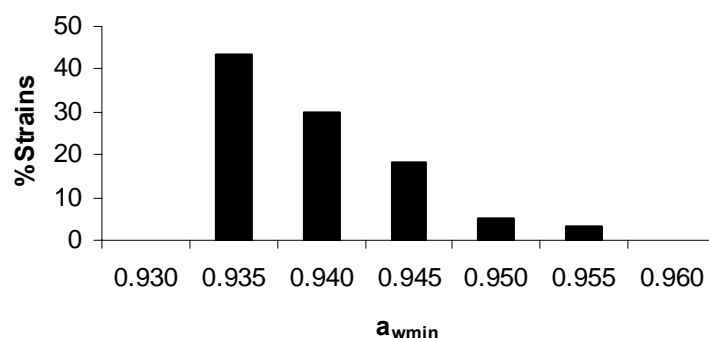


Figure 4: Frequency distribution of the parameter a_{wmin} for 60 *Salmonella enterica* isolates, as estimated by modelling the maximum specific growth rate (μ_{max}) for each isolate as a function of a_w using the secondary square root model.

The development of a stochastic approach for describing strain variability based on the estimated distributions of the parameters pH_{min} and a_{wmin} using Monte Carlo simulation would be of great value in microbial risk assessment. Such an approach is expected to be more appropriate for taking into account strain variability in exposure assessment compared to the previously used relative rate approach (Ross and McMeekin, 2003) which assumes no effect of the growth environment on the variability among strains.

Conclusions

This study demonstrates that the effect of the growth environment on the strain variability of *S. enterica* kinetic behavior is not negligible. Thus, such an effect needs to be evaluated, ascertained and taken into account in the development of stochastic approaches for use in quantitative microbiology and particularly in microbial risk assessment.

Acknowledgements

This study has been carried out with the financial support of the Commission of the European Communities, Project ProSafeBeef “Food-CT-2006-36241”.

References

- Dalgaard P. and Koutsoumanis K. (2001) Comparison of maximum specific growth rates and lag times estimated from absorbance and viable count data by different mathematical models. *Journal of Microbiological Methods* 43, 183-196.
- De Jesús A.J. and Whiting R.C. (2003) Thermal inactivation, growth, and survival studies of *Listeria monocytogenes* strains belonging to three distinct genotypic lineages. *Journal of Food Protection* 66, 1611-1617.
- Juneja V.K., Marks H.M. and Huang L. (2003) Growth and heat resistance kinetic variation among various isolates of *Salmonella* and its application to risk assessment. *Risk Analysis* 23, 199-213.
- Lianou A., Stopforth J.D., Yoon Y., Wiedmann M. and Sofos J.N. (2006) Growth and stress resistance variation in culture broth among *Listeria monocytogenes* strains of various serotypes and origins. *Journal of Food Protection* 69, 2640-2647.
- Lindqvist R. (2006) Estimation of *Staphylococcus aureus* growth parameters from turbidity data: characterization of strain variation and comparison of methods. *Applied and Environmental Microbiology* 72, 4862-4870.
- Ross T. and McMeekin T.A. (2003) Modeling microbial growth within food safety risk assessments. *Risk Analysis* 23, 179-197.

Modelling growth of *Penicillium expansum* and *Aspergillus niger* under dynamic temperature conditions

M. Gougouli and K. Koutsoumanis

Laboratory of Food Microbiology and Hygiene, Department of Food Science and Technology, Faculty of Agriculture, Aristotle University of Thessaloniki, Greece. (gougouli@agro.auth.gr) & (kkoutsou@agro.auth.gr)

Abstract

The objective of the present work was to study and model fungal growth at both static and dynamic temperature conditions. The growth of *Penicillium expansum* and *Aspergillus niger* was investigated on malt extract agar, at isothermal conditions. The radial growth rate (μ) and lag phase (λ) of mycelium growth were modelled as a function of temperature using a Cardinal Parameter Model (CPM). The results showed that the CPM can describe successfully the effect of temperature on fungal growth within the entire biokinetic range for both isolates. The Cardinal Model (CM) parameters for μ were very close to the respective parameters for $1/\lambda$ indicating a similar temperature dependence for μ and $1/\lambda$. The derived models were further validated under non-isothermal conditions using various time-temperature scenarios. The results showed that when temperature shifts occurred before the end of the lag, they did not cause any significant additional lag and the observed total lag was very close to the cumulative lag predicted by the model. In experiments with temperature shifts after the lag phase, μ was adopted instantaneously to the current temperature when the temperature profile included temperatures which were inside the region of growth. In contrast, for scenarios with temperatures close to the growth limits or outside the growth region the models overestimated growth, indicating that fungi were stressed by this type of temperature shifts.

Keywords: mycelium growth, temperature, kinetic models, dynamic conditions

Introduction

Advance of predictive microbiology has allowed a significant progress in the development of effective validated models pertinent to food safety and quality. Despite this progress, fungal growth models remain a research tool rather than an effective application. In addition, most of the available mathematical models predicting fungal growth refer to isothermal conditions. However, studies on the chill chain have shown that temperature during distribution and storage of foods is not constant. Such temperature abuses during any stage of the chill chain, in the case of contamination of food products with fungal spores and/or conidia, may result in an unexpected appearance of visible mycelium, and further production of unpleasant and hazardous metabolites. Numerous published models have dealt with the prediction of bacterial growth under dynamic temperature conditions (Koutsoumanis, 2001) but reports for fungal behavior under temperature fluctuations are still missing.

The objective of the present work was to study and model growth of *Penicillium expansum* and *Aspergillus niger*, isolated from yogurt, at both static and dynamic temperature conditions. Models for the effect of storage temperature on the growth of *P. expansum* and *A. niger* were developed and further validated under non-isothermal conditions. The time-temperature scenarios studied included single temperature shifts before or after the end of lag phase and continuous periodic temperature fluctuations.

Material and methods

The growth of *P. expansum* and *A. niger*, isolated from spoiled yogurt, was investigated on malt extract agar (LAB M, United Kingdom) (a_w 0.997) adjusted to pH 4.2 with lactic acid. Aliquots (1- μ l) of conidia suspensions (final concentration 10^6 conidia/ml) were inoculated in the centre of the Petri dishes containing the solidified growth medium. Two independent

experiments at each storage temperature were performed and for each one the perpendicular diameters of three mycelia were measured at appropriate time intervals to allow for an efficient kinetic analysis at isothermal conditions. The storage temperature tested ranged from -3 to 35°C for *P. expansum* and from 0 to 42.5°C for *A. niger*. The radial growth rate (μ) and lag phase (λ) of mycelium growth were estimated using the linear model (Equation (1)):

$$r - r_0 = \mu(t - \lambda) \quad (1)$$

where r the mycelium diameter (mm), r_0 the average diameter of inoculum (mm) at time $t = 0$, μ the radial growth rate (mm/h), t the time (h) and λ the lag time (h).

The obtained estimates μ and λ for the two fungi stored under isothermal conditions were further expressed as a function of temperature using the Cardinal Parameter Model (CPM) (Rosso and Robinson, 2001):

$$\mu = \frac{\mu_{\text{opt}}(T - T_{\text{max}})(T - T_{\text{min}})^2}{(T_{\text{opt}} - T_{\text{min}})[(T_{\text{opt}} - T_{\text{min}})(T - T_{\text{opt}}) - (T_{\text{opt}} - T_{\text{max}})(T_{\text{opt}} + T_{\text{min}} - 2T)]} \quad (2)$$

where μ_{opt} the radial growth rate at optimum conditions (mm/h), T the temperature (°C), T_{max} and T_{min} the maximum and the minimum temperature (°C), respectively, and T_{opt} the optimum temperature for growth (°C). In the case of λ , the $1/\lambda$ value was used in the model. Table Curve 2D (Systat Software Inc., CA, United States) was used for fitting the data to the models.

The models were further validated against observed fungal growth under non-isothermal conditions. The time–temperature scenarios studied included single temperature shifts before or after the end of lag phase and continuous periodic temperature fluctuations. Mycelium growth at fluctuating temperatures was predicted using the method described by Koutsoumanis (2001). The prediction of growth was based on the assumption that after a temperature shift, the radial growth rate is adopted instantaneously (Equation (4)). For the prediction of the lag phase a cumulative approach was applied (Equation (3)). Based on the above, growth under non-isothermal temperature was predicted using the tested time–temperature conditions, $T(t)$, recorded by the temperature monitoring devices and the CPMs for the estimation of the “momentary” $\lambda_{(T)}$ and $\mu_{(T)}$.

$$\int_0^{\lambda} \frac{1}{\lambda_{(T)}} dt = 1 \quad (3)$$

$$r_{t_i} = r_{t_{i-1}} + \mu_{(T)} dt \quad (4)$$

where λ is the total lag, $\lambda_{(T)}$ and $\mu_{(T)}$ are the lag time and the radial growth rate, respectively, at temperature T , corresponding to a short, assuming constant-temperature time interval dt_i , and r_{t_i} is the diameter of the mycelium.

Results and discussion

The linear model described satisfactory mycelium radial growth with correlation coefficients ranging between 0.991 and 1 for *P. expansum*, and 0.971 and 1 for *A. niger*. The CPMs described successfully the effect of temperature on fungal growth kinetic parameters within the entire biokinetic range for both isolates (Figure 1). The CM parameters for μ were very close to the respective parameters for $1/\lambda$ (Table 1) indicating a similar temperature dependence for μ and $1/\lambda$.

Validation at changing temperatures is of great importance for evaluating the performance of the derived models in predicting fungal growth, in order to reveal potential effects of varying time–temperature on fungal behaviour. Figures 2, 3 and 4 present the comparison between predicted and observed growth at six representative dynamic temperature scenarios. In the first scenario, when the temperature shifts occurred before the end of the lag, the observed total lag was very close to the cumulative lag predicted by the *P. expansum* and *A. niger* dynamic models (Figure 2). The latter observation indicates that the time required for each fungus to reach the end of the lag at changing temperature conditions is cumulative and it can be calculated according to Equation (3).

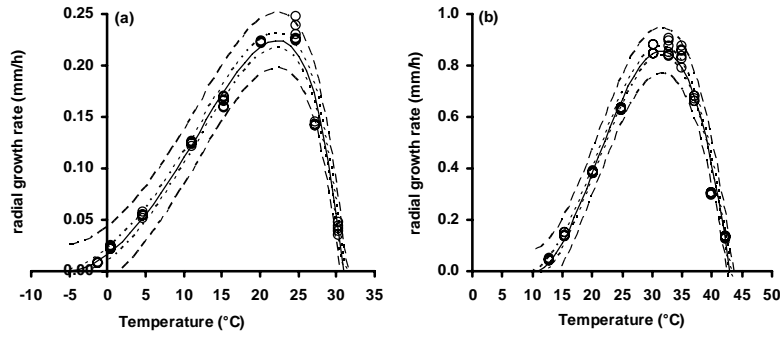


Figure 1: CPM (solid line) for the effect of storage temperature on the radial growth rate of *P. expansum* (a) and *A. niger* (b). The dotted and the discontinuous lines depict the 95% confidence and prediction limits of the effect of storage temperature on the radial growth rate, respectively.

Table 1: Estimated values for the parameters of CM describing the effect of temperature on μ and $1/\lambda$ of *P. expansum* and *A. niger*.

| Fungus | Parameter ^a | Estimated value ^b | R ^c | Parameter ^d | Estimated value ^b | R ^c |
|--------------------|---------------------------|------------------------------|----------------|--------------------------------|------------------------------|----------------|
| <i>P. expansum</i> | T_{\min} (°C) | -5.44 ± 0.83 | 0.974 | T_{\min} (°C) | -3.41 ± 0.93 | 0.979 |
| | T_{\max} (°C) | 30.88 ± 0.11 | | T_{\max} (°C) | 30.76 ± 0.08 | |
| | T_{opt} (°C) | 22.18 ± 0.24 | | T_{opt} (°C) | 24.97 ± 0.27 | |
| | μ_{opt} (mm/h) | 0.224 ± 0.004 | | $1/\lambda_{\text{opt}}$ (1/h) | 0.069 ± 0.001 | |
| <i>A. niger</i> | T_{\min} (°C) | 10.40 ± 0.53 | 0.982 | T_{\min} (°C) | 6.47 ± 0.95 | 0.964 |
| | T_{\max} (°C) | 42.93 ± 0.10 | | T_{\max} (°C) | 47.13 ± 0.51 | |
| | T_{opt} (°C) | 31.61 ± 0.20 | | T_{opt} (°C) | 33.45 ± 0.31 | |
| | μ_{opt} (mm/h) | 0.857 ± 0.009 | | $1/\lambda_{\text{opt}}$ (1/h) | 0.078 ± 0.001 | |

^a parameters of CM describing the effect of temperature on μ

^b \pm : standard error

^c coefficient of determination

^d parameters of CM describing the effect of temperature on $1/\lambda$

In experiments with temperature shifts after the end of lag time the radial growth rate was adopted instantaneously to the current temperature (Figure 3a). In all the experiments with temperature shifts within the growth region of the tested fungi the observed growth data fell inside the prediction confidence limits, independently from the tested temperatures, showing that the dynamic models were successfully validated at the tested conditions.

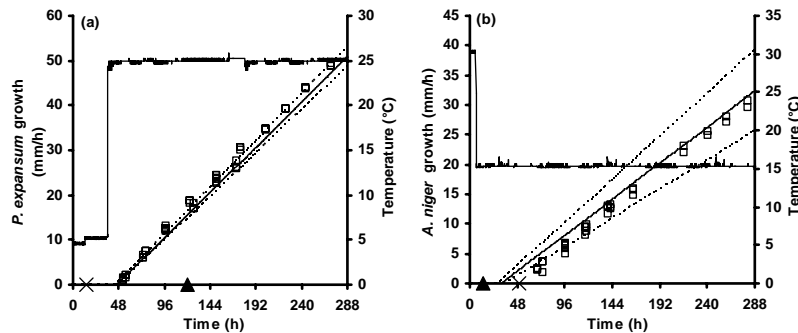


Figure 2: Comparison between observed (points) and predicted (lines) growth of *P. expansum* and *A. niger* under dynamic temperature conditions, with the temperature shift occurring before the end of the lag (a: 36h at 5°C and then at 25°C, b: 6h at 30°C and then at 15°C). (▲: predicted lag time at the initial temperature before the temperature shift, X: predicted lag time at the final temperature after the temperature shift). The dotted lines depict the 95% confidence limits of the predicted growth.

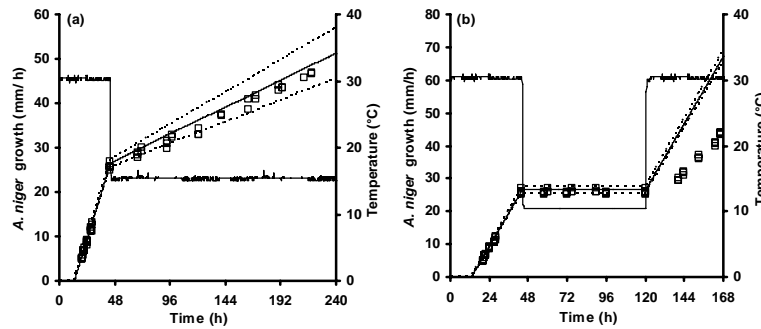


Figure 3: Comparison between observed (points) and predicted (lines) growth of *A. niger* under dynamic temperature conditions, with the temperature shift occurring after the end of the lag (a: 44h at 30°C and then 196h at 15°C, c: 48h at 30°C, 72h at 10°C and then 48h at 30°C). The dotted lines depict the 95% confidence limits of the predicted growth.

However, in the case of Figure 3b, where the temperature profile included a downshift below the minimum temperature for growth of *A. niger* (10°C), a significant overprediction was observed which could be attributed to a potential stress imposed by the low temperature. These results were confirmed in experiments with periodic temperature shifts in which the models satisfactory predicted growth when the temperature profiles included temperatures inside the growth region (Figure 4a). In contrast, in scenarios with temperature close to the growth limits or outside the growth region (Figure 4b), the models overestimated growth.

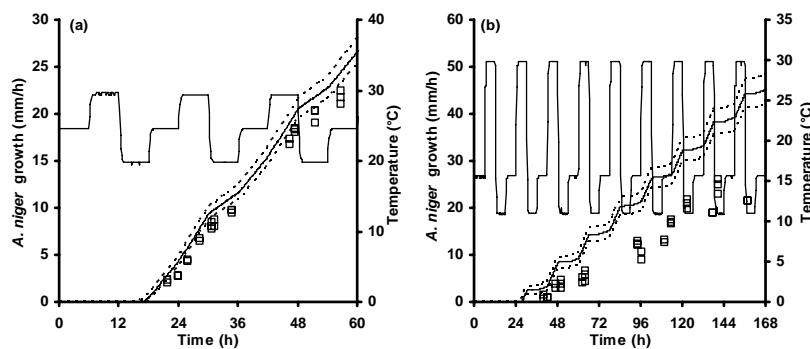


Figure 4: Comparison between observed (points) and predicted (lines) growth of *P. expansum* and *A. niger* under continuous periodic temperature fluctuations (a: 6h at 25°C, 6h at 30°C, and 6h at 20°C, b: 6h at 15°C, 6h at 30°C, and 6h at 10°C). The dotted lines depict the 95% confidence limits of the predicted growth.

Conclusions

The mycelium growth of *Penicillium expansum* and *Aspergillus niger* was studied and modelled at static and dynamic temperature conditions. The developed models predicted adequately the growth of the tested fungi at dynamic conditions when the temperature shifts fell within the region of their growth. However, when the temperature profile included a downshift below the minimum temperature for growth, a significant overprediction was observed which could be attributed to a potential stress imposed by the low temperature.

References

- Koutsoumanis K. (2001) Predictive modeling of the shelf life of fish under nonisothermal conditions. *Applied and Environmental Microbiology* 67, 1821-1829.
- Rosso L. and Robinson T.P. (2001) A cardinal model to describe the effect of water activity on the growth of moulds. *International Journal of Food Microbiology* 63, 265-273.

Estimating the probability of undetected failure of pasteurization process control using Fault Tree Analysis

J. Hein M. van Lieverloo¹, Cornelis P. Willig², Martijn B. Fox¹ and Marjon H.J. Wells-Bennik¹

¹ NIZO food research, Kerhemseweg 2, 6718 ZB Ede, the Netherlands (hein.van.lieverloo@nizo.nl)

² Dependable Industrial Automation Consultancy, Herman Heijermanslaan 2, 21056 ES Heemstede, the Netherlands (cornelis.willig@diac.nl)

Keywords: Process control; Boolean Monte Carlo analysis; process optimization, cost-benefit analysis.

Abstract

Dairies rely on process control to warrant the temperatures and holding times required for pasteurization. It is possible to quantify the probability of simultaneous failure of primary as well as process safety control components, using Fault Tree Analysis (FTA), thus quantitatively validating this Critical Control Point. FTA of a case study pasteurization process using generic component failure rate data showed that a former configuration on average would lead to the top event ‘undetected contamination’ every 5 years. The five base events most contributing to this failure rate all concerned milk flow control. The failure rate dropped to once every 1050 years when a second flow meter was installed, serving as a flow guard that automatically initiates recirculation to the raw milk tank when flow deviates from set point values. After this cost-effective change of process control, other base events (leaking regenerative heaters, PLC cards) became most important. The failure rates are estimates from a basic model excluding so-called ‘common cause failures’ (e.g. PLC failure) that usually increase failure rates. Fault Tree Analysis is a tool well applicable to quantify the low probabilities of calamities in pasteurization and other critical food processing, to identify the most important process components and to find the optimal balance of costs, safety and quality.

Introduction

Most strains of *L. monocytogenes* are very sensitive to regular pasteurization conditions (Van Asselt & Zwietering, 2006). However, if pasteurization fails undetected (and therefore unchecked), milk may be contaminated. Growth models show that some bacteria, e.g. *Listeria monocytogenes*, readily grow in pasteurized milk (Te Giffel and Zwietering, 1996) and any contamination during or after pasteurization will lead to a high probability of exceeding the EU food safety objective of < 100 cfu/g at the time of consumption (Van Lieverloo et al., 2007). Contamination incidents such as the USA Whittier Farms post-pasteurization outbreak end of 2007 show the need for rigorous control of any post-pasteurization recontamination (Anonymous, 2008). The dairy industry strives for undetectably low probabilities of recontamination of milk, preferably zero. This poses the challenge of estimating actual levels of recontamination. Other industries (aircraft, nuclear, petrochemical) that accept extremely low probabilities of barely unacceptable events (explosions, contamination) use Fault Tree Analysis (FTA) to estimate probabilities of both primary as well as secondary safety systems failing at the same time.

Materials and methods

FTA is a Boolean Monte Carlo Analysis where known probabilities of base events (failing valves, thermometers, computers etc.) are used to calculate the probability of the top event (Andrews and Moss, 2002), in this case the undetected contamination of milk. This FTA focused on cross-contamination between raw and pasteurized milk, low temperature and low heating time. The basics of an FTA are the simulation of the effects of failures of base components ('base events') by linking these events using AND and OR gates. When either of two or more events occurring lead to another event, these events are linked using an OR gate. When two or more events must occur simultaneously or consecutively to lead to another event, this occurrence is described by an AND gate. Figure 1 shows the symbols used to present a fault tree in a diagram.

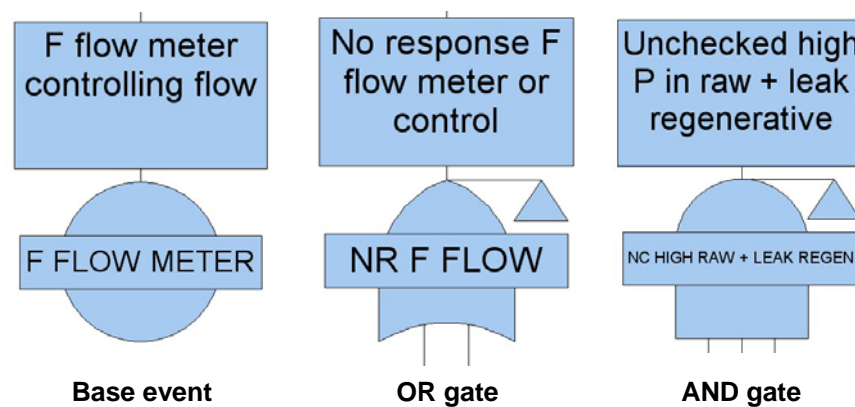


Figure 1: Most common symbols in a fault tree. The triangles are used to indicate replicated branches.or to indicate a link within the fault tree paging display.

Boolean algebra rules apply to calculations of probabilities of events described by an OR or AND gate. Roughly, the probabilities of base events connected by an OR gate are added and probabilities of base events connected by an AND gate are multiplied, but actual Boolean algebra is more complex (Andrews and Moss, 2002) and was performed by the software (FaultTree+ by Isograph Ltd). Several models can be used to describe the probabilities of base events. Most commonly used are fixed models, assuming equal failure probability during the lifetime of the component (excluding burn-in and wear-out periods). Another common model applies to components and personnel (operators) that may only fail 'on demand' as they are not continuously operating. The failure models can either be point estimates or probability density functions, the latter case allowing for a Boolean Monte Carlo analysis.

The results of the model include the failure rate (reciprocal of Mean Time To Failure MTTF) and the unavailability ('down-time') of the system. The relative contribution of base events to the unreliability was calculated as the Fussel-Vesely importance ranking (Andrews and Moss, 2002), corrected to 100%. In this basic FTA, no variability was included and calculations were performed using point estimates of failure rates. It is important to emphasize that these values are not actual failure data, as the actual component failure rates probably most likely are lower than then generic failure data used. Maintenance data will be used to optimize the data of important components.

Results and discussion

The case study fault tree of the pasteurization process with the top event ‘undetected contamination’ is shown in Figure 2. Calculating the model results in a mean failure rate of the top event of once every 5 years. In the Fussel-Vesely importance ranking, five basic events concerning flow control top the list (Table 1). The base event with the highest importance, ‘No response to failure of flow meter or flow control’ occurs four times in the fault tree (Figure 2). In the former configuration of the process, the flow was controlled by one flow meter, leaving the detection of flow failures (failing pump, failing flow meter or failing PLC cards) to observing operators. The failure rate dropped to once every 1050 years when a second flow meter was installed, serving as a flow guard that automatically initiates recirculation to the raw milk tank when flow deviates from set point values (Figure 3). After this change, other base events (PLC cards, leak of regenerative heat exchanger) became most important (Table 2) and the configuration became more balanced from a cost-benefit point-of-view.

Table 1: Importance ranking of base events for top event ‘undetected contamination’ of the **former configuration** of the case study pasteurization process (using generic failure rate data)

| Relative importance | Base event |
|---------------------|---|
| 49.9 % | No response to failure of flow meter or flow control (some operator experience). Failure on demand rate set fixed at 0.5. |
| 12.47 % | Failure of PLC input card responding to flow meter input ^a |
| 12.47 % | Failure of the speed control unit of the raw milk pump ^a |
| 12.47 % | Failure of the PLC output card controlling raw milk pump speed ^a |
| 12.47 % | Failure of the flow meter controlling flow via the raw milk pump ^a |

^a failure rate fixed at once in 10 years, MMTR 8 hours
MTTR = mean time to repair (from failure to running)

Table 2: Importance ranking of base events for top event ‘undetected contamination’ of the **new configuration** of the case study pasteurization process (using generic failure rate data)

| Relative importance | Base event |
|---------------------|--|
| 18.47% | Failure of PLC output card initiating recirculation to raw milk ^a |
| 12.35% | Leakage of regenerative (dormant failure rate of once per three years, inspection interval three years, MTTR 8 hours) |
| 8.22% | Failure of PLC output card relaying high temperature differences between start and end of the holding section ($> 1\text{ }^{\circ}\text{C}$) ^a |
| 6.44% | Failure of the steam kettle ^b |
| 4.29% | Failure of the flow guard meter ^a |
| 4.29% | Failure of PLC input card flow guard meter ^a |
| 3.99% | Block of flow after regenerative (raw side) fixed at once per year |
| 3.22% | Failure of the speed control on the raw milk pump ^a |
| 3.22% | Failure of flow meter ^a |
| 3.22% | Failure of PLC input card flow ^a |
| 3.22% | Failure of PLC output card flow meter ^a |

^a failure rate fixed at once in 10 years, MMTR 8 hours

^b failure rate fixed at once in 10 years, MMTR 8 hours

MTTR = mean time to repair (from failure to running)

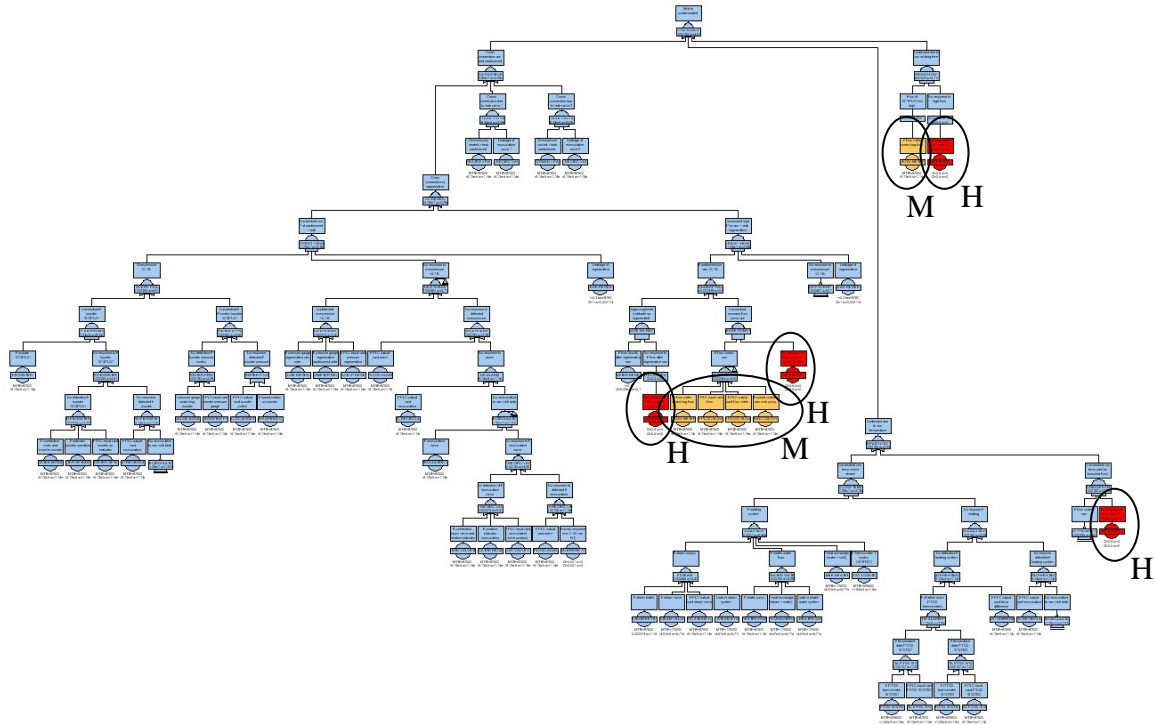


Figure 2: Fault tree of the former case study pasteurization process configuration. The most important base events (see Table 1) are marked H (high = ‘No response to failure of flow meter or flow control’, occurring four times in the tree) and M (middle).

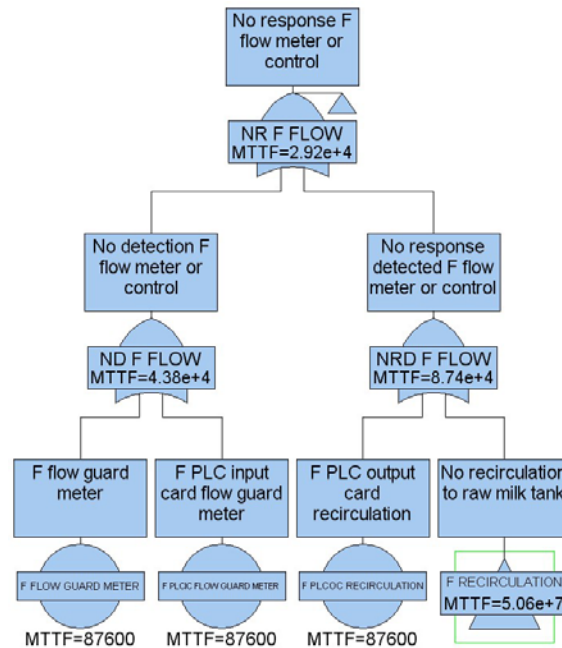


Figure 3: Fault tree branch of the optimized part of the case study pasteurization process configuration. A guarding flow meter automatically initiates recirculation to the raw milk tank when the flow control system (pump, flow meter, PLC cards) fails. MMTF (mean time to failure) is the reciprocal of the failure rate. The triangle bottom right refers to a deeper branch.

The actual failure rate of the new configuration probably is higher than once every 1000 years, as this failure rate is estimated by a basic model. Common cause failure models will be added to the model to account for the effect of e.g. a PLC failing entirely or the effect of common age, brand and maintenance plans for similar parts (valves, thermometers etc.).

The failure rates of the events with the highest importance rankings will be varied to evaluate the effect of variability and uncertainty on the model results, thus turning the model into a Boolean Monte Carlo analysis.

Conclusion

It is possible to estimate the probability of pasteurization process control failure with an acceptable level of certainty. Moreover, it is possible to pin-point the weakest link in the safety control, prioritizing it for optimization if the level contamination needs to be lowered. It is also possible to assess whether the relative contribution to unreliability (and unavailability) of all safety systems are consistent with their relative capital and operational expenditures. Thus, FTA provides companies with a tool to optimize the safety as well as the cost-effectiveness of their pasteurization process.

Literature

- Andrews, J.D. and Moss, T.R. (2002) Reliability and risk assessment. 2nd ed. Professional Engineering Publishing Ltd. London and Bury St Edmunds, United Kingdom, 540 p.
- Anonymous (2008) Environmental and milk products test positive for *Listeria*. Milk processing plant will remain closed until cleared by health officials. Press release January 17, 2008. The Official Website of the Office of Health and Human Services (EOHHS), Commonwealth of Massachusetts.
http://www.mass.gov/?pageID=eohhs2pressrelease&L=1&L0=Home&sid=Eeohhs2&b=pressrelease&f=080117whittier_farms&csid=Eeohhs2
- Te Giffel, M.C. and Zwietering M.H. (1999) Validation of predictive models describing the growth of *Listeria*. Int. J. Food Microbiol. 46: 135-149
- Van Asselt ED, Zwietering MH (2006) A systematic approach to determine global thermal inactivation parameters for various food pathogens – Int. J. Food Microbiol 107(1), 73-82
- Van Lieverloo, J.H.M., Fox, M., Schutyser, M., Te Giffel, M.C. and De Jong, P. (2007) Evolving from high through low uncertainty risk assessments for dairy products using kinetic, stochastic and fault tree modelling. Proc. 5th Int. Conf. Predictive Modeling in Foods, Athens, 16-19 September 2007.

Estimating undetectably low post-pasteurization recontamination levels of milk with pathogens using surrogate microbial variables

J. Hein M. van Lieverloo, J. Meeuwisse, A. Wagendorp, Martijn B. Fox and Marjon H.J. Wells-Bennik

NIZO food research, Kerhemseweg 2, 6718 ZB Ede, the Netherlands

Abstract

A model was constructed to estimate maximum recontamination probability via air during packaging of milk products. Based on ratios of Plate Count (PC) to estimated maximum (none found) *Listeria* levels in air samples and PC levels in the air in the filling machine, the estimated mean *Listeria* spp. contamination probability via air would be less than $3.4 \cdot 10^{-6}$ per carton. The air contamination model was validated using concentrations of Gram-negative bacteria in air samples and the frequency of spoilage with Gram-negative bacteria in daily test samples of 12 cartons taken from the filling machine. The validation shows that on some days more cartons are contaminated with Gram-negative bacteria than expected from the air contamination model, indicating the need for modeling other contamination routes.

Based on the ratios of PC to estimated maximum (none found) *Listeria* levels in surface swab samples and PC levels in the air in the filling machine, the most likely estimated maximum *Listeria* spp. contamination probability via air would be less than $1.7 \cdot 10^{-8}$ per carton. As no *Listeria* spp. was found in any of the samples, the actual probability of contamination is lower.

Keywords Packaging, air, Monte Carlo analysis, *Listeria monocytogenes*, total plate counts, Gram-negative bacteria..

Introduction

Recontamination of processed foods may form an important contribution to spoilage and the presence of pathogens in food. Few risk assessments and research projects however include the probability of recontamination (Reij & Den Aantrekker, 2004). Growth models show that *Listeria monocytogenes* readily grows in pasteurized milk (Te Giffel and Zwietering, 1996) and any contamination after pasteurization will lead to a high probability of exceeding the EU food safety objective of < 100 cfu/g at the time of consumption (Van Lieverloo et al., 2007). Contamination incidents such as the USA Whittier farm post-pasteurization outbreak end of 2007 show the need for rigorous control of any post-pasteurization recontamination (Anonymous, 2008). The dairy industry strives for extremely low probabilities of recontamination of milk, preferably zero. This poses the challenge of determining actual levels of recontamination. As it is not feasible to ever test for such low probabilities of finding *L. monocytogenes* in milk or milk products, a model for indirect assessment was constructed. From the possible points of recontamination identified during HACCP, two priorities were selected; (i) failing pasteurization control (as presented in another abstract of this conference) and (ii) recontamination via the air during packaging.

Materials and method

Air samples

The contamination routes were mapped for the oldest model of packaging machines available in the company (Figure 1). On 10 days from September to December 2008, air samples were collected on the roof (air-inlet into factory and filling machine), the environment of the filling machine, the mandrel compartment of the machine (blank folding and bottom sealing), the filling compartment and the top sealing compartment. Air samples were either analyzed for total plate counts (PC agar, Tritium Veldhoven, the Netherlands, 100-250 L air samples), Gram-negative bacteria (Tritium EC broth agar, 500-1000 L) and *Listeria* spp (Tritium PALCAM agar, 1000 L) using the Merck MAS-100[®] air sampler.

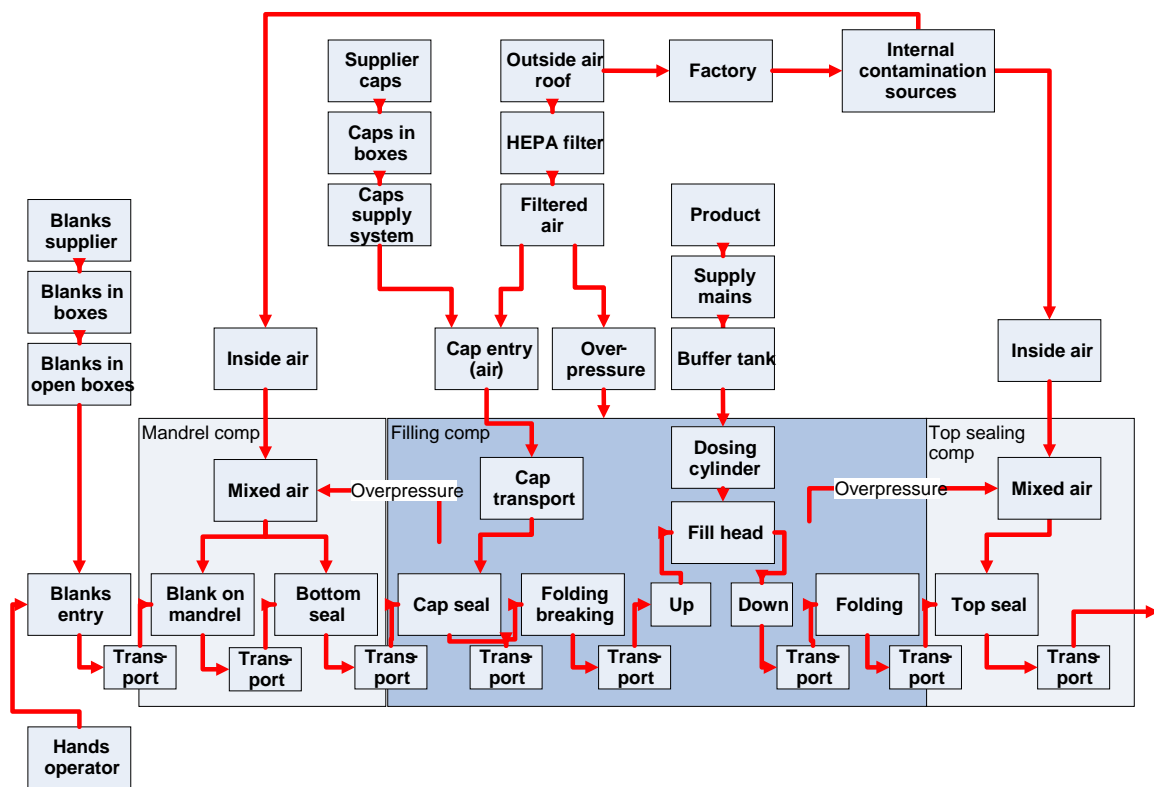


Figure 1: Schematic overview of the milk carton packaging machine and the possible contamination routes (only contamination via air was investigated).

Surface samples

In July 2009, surfaces (c. 100 cm²) in the factory were swabbed with a sterile cotton swab (wetted in 1.5 ml sterile water) and samples were kept on melting ice and in a 4 °C refrigerator before analysis (within 24 hours). After vortexing, sub-samples were transferred to agar plates to determine total plate count (PCA medium) and *Listeria* spp. (PALCAM agar, three plates with each 0.1 ml). The detection limit for *Listeria* spp. was 1 cfu per 20 cm².

Model

The model is described as

$$Lspp_{tot} = Poisson \sum_{i=1}^n \left(\frac{PC_{comp,i}}{PC_{ref,i}} * Lspp_{ref,i} * V_{comp,i} \right)$$

where

- Lspp = concentration of *Listeria* spp. (cfu/l)
- PC = concentration of plate count (cfu/l)
- V_{comp} = volume (l) of air that entered the carton per compartment
- tot = in carton
- comp = in compartment
- ref = on reference site

Three compartments and reference sites were distinguished

- Mandrel compartment with the filling machine environment as reference site
- Filling compartment with the roof as reference site
- Top seal compartment with the filling machine environment as reference site

Although the air in the mandrel and top seal compartment is a mixture of (HEPA filtered) air from the filling compartment and the filling machine environment, most of the bacteria in the air are likely to originate from the filling machine environment. The volume of air and deposition of air particles into the milk carton was calculated:

- 1225 ml of air: when the open carton is released from the bottom sealer (mandrel)
- equivalent of 7.9 ml of air (particles) deposited in the mandrel compartment
- equivalent of 15.9 ml of air (particles) deposited in the filling compartment
- equivalent of 6.6 ml of air (particles) deposited in the top seal compartment.

The deposition of particles in the open carton was calculated based on the deposition rate of 0,027 m/s determined by Den Aantrekker et al (2003) and the mean residence time in the parts of the filling machine. The model was validated using the frequency of milk carton contaminated with Gram-negative bacteria in daily test series.

The model was calculated in two forms, one using PC and *Listeria* spp. ratios from air samples in the filling machine environment and the other using PC and *Listeria* spp. ratios from swab samples in the filling machine environment.

The model based on air samples was validated using concentrations of Gram-negative bacteria in air samples and the frequency of Gram-negative contamination of 12 milk (product) cartons tested daily (and more often during air sampling days).

In the models, independence between all variables was assumed, probably overestimating contamination probabilities as high levels of plate counts probably are associated with the highest probability of finding *Listeria* spp.. As no *Listeria* spp. were found in any of the samples, the model is valid for a homogeneous air composition and therefore can not be used to estimate contamination during incidents.

Calculations

Data analysis was performed using @RISK 5.5 (Palisade) and Microsoft® Excel® 2002 (XP). The air model was calculated for the 10 individual sampling days in 2008 (100 simulations of 10,000 iterations each).

Results and discussion

Air samples

No *Listeria* spp. has been found in any of the 1000 L air samples on the roof (12), in the factory (46) and in the carton bottom sealing compartment (21). Assuming a homogeneous air composition and excluding any incident conditions, the concentration of *Listeria* spp. in the factory air is less than $2 \cdot 10^{-5}$ cfu/l ($\text{beta}(1;47)/1000$; Vose, 2008).

Using the ratios of *Listeria* spp. to plate counts in the air and the plate counts in air in the filling machine, the mean probability *Listeria* spp. contamination via air in the filling machine was estimated to be less than $3.4 \cdot 10^{-6}$ per carton. The model predicts a daily variation of the contamination probability of less than 1 in 10.000 cartons in 81% to 99% of 100 simulations and less than 2 in 10.000 cartons in 98 %. Actual frequencies of contamination of 12 carton test series with Gram-negative bacteria on 4 of 10 sampling days were low but (statistically) significantly higher than predicted with the air contamination model, suggesting that other contamination routes remain to be evaluated.

Surface swab samples

Supplemental sampling for plate counts and *Listeria* spp. on surfaces in factories shows that on no site *Listeria* spp. was found, although high plate counts (PC; up to $2.1 \cdot 10^{-6}$) were found on sites where *Listeria* spp. was most likely to be found (floors, drains and wet conveyor belt housings). Based on the ratios of the highest PC to (theoretical maximum) *Listeria* levels in surface swab samples and PC levels in the filling machine, the most likely estimated mean *Listeria* spp. contamination probability would be less than $1.7 \cdot 10^{-8}$ per carton. As no *Listeria* spp. was found in any of the samples, the actual probability of contamination is lower. It also means that it is difficult to estimate the distribution of the recontamination probability.

Conclusion

This investigation shows that it is possible to estimate recontamination levels after pasteurization, although the absence of *Listeria* spp. in the filling machine environment leaves uncertainty about the actual contamination levels. The mean estimated frequencies of recontamination via air after pasteurization are around one in a million to one in 100 million cartons, but uncertainty about the probability distribution remains.

Literature

- Anonymous (2008) Environmental and milk products test positive for *Listeria*. Milk processing plant will remain closed until cleared by health officials. Press release January 17, 2008. The Official Website of the Office of Health and Human Services (EOHHS), Commonwealth of Massachusetts. http://www.mass.gov/?pageID=eohhs2pressrelease&L=1&L0=Home&sid=Eeohhs2&b=pressrelease&f=080117_whittier_farms&csid=Eeohhs2
- Den Aantrekker, E.D., Beumer, R.R., Van Gerwen, S.J., Zwietering, M.H., Van Schothorst, M. and Boom R.M. (2003) Estimating the probability of recontamination via the air using Monte Carlo simulations – Int. J. Food Microbiol. 87(1-2), 1-15
- Reij, M.W., Den Aantrekker, E.D. and ILSI Europe Risk Analysis in Microbiology Task Force (2004) Recontamination as a source of pathogens in processed foods. Int. J. Food Microbiol. 91, 1– 11
- Te Giffel, M.C. and Zwietering M.H. (1999) Validation of predictive models describing the growth of *Listeria*. Int. J. Food Microbiol. 46: 135-149
- Van Lieverloo, J.H.M., Fox, M., Schutyser, M., Te Giffel, M.C. and De Jong, P. (2007) Evolving from high through low uncertainty risk assessments for dairy products using kinetic, stochastic and fault tree modelling. Proc. 5th Int. Conf. Predictive Modeling in Foods, Athens, 16-19 September 2007.
- Vose, D. (2008) Risk analysis: a quantitative guide. 3rd edition. J. Wiley & Sons, Chichester, United Kingdom, 735 p.

Application of Network science to analyse the proteome of *Escherichia coli* during the lag phase under acid stress

Heather Haines^{1,2}, Tom Ross¹, John Bowman¹ and Carmen Pin³

¹ Tasmanian Institute of Agricultural Research, University of Tasmania, Hobart, Australia

² new address: Department of Human Services, Victoria, Australia.

³ Institute of Food Research, Norwich, NR4 7UA, United Kingdom

Abstract

The aim of this work was to investigate the mechanism of acid resistance in *E. coli*. To do this, the synthesis of proteins during the lag time of acid habituated and non acid habituated populations was compared under acid-stress conditions. A network compiling all metabolic reactions, functional roles and predictive operons was developed for the genome of *E. coli*. The sub networks of the synthesised proteins during the lag of habituated and non-acid habituated cells were extracted and compared. Global topological network measurements were applied to explore the functional significance of the protein biosynthesis during the lag. The networks of the acid habituated cells and non-acid habituated cells inoculated at pH 4.6 were different from each other and from that of the control culture, i.e. non-acid habituated cells inoculated at pH 7. The inferred intracellular activity during the lag period involves energy and amino acid metabolism in acid habituated cells inoculated at pH 4.6 and in the control culture. In non-acid habituated cells inoculated at low pH, enhanced proteins during the lag are related to transport of macromolecules through the membrane and DNA repair.

Keywords

Lag time, microarray, networks, *Escherichia coli*.

Introduction

The lag phase is a period of adjustment and adaptation in bacteria in response to a sudden change in their environment. During this period the bacterial population “gets ready” to grow in the new conditions. Low (acid) pH is commonly used to minimise bacterial growth in foods but bacteria, including *Escherichia coli*, have been found to develop phenotypes highly resistant to low pH after an initial ‘habituation’ process. Analysis of protein biosynthesis by bacteria during the lag phase due to acid stress, could contribute to understanding the biochemical and physiological strategies of bacteria as they adapt and grow at low pH.

Network science is an emerging, highly interdisciplinary research area that aims to develop theoretical and practical approaches and techniques to increase the understanding of natural and man made networks.

The purpose of this work is the integration of the proteome data in a network constructed according to the metabolic pathways, functional roles and predicted operon composition of *E. coli*. With this approach we aim to handle the complexity of the protein biosynthesis that occur during lag time of acid habituated and non-acid habituated cells.

Materials and Methods

Bacterial Strain and proteome analysis of lag time samples

Non-acid habituated enterohemorrhagic *E. coli* O111:H was grown at 37°C and pH 7 in nutrient broth (NB). Acid stressed cells were inoculated at pH 4.6 acidified with glacial acetic acid and incubated at 37°C. These cultures were used to inoculate fresh tanks of NB at pH 7 and 4.6. Samples were obtained during the lag time after 1, 2, 3 and 4 hours of incubation at 37°C. Protein extracts were resolved by two-dimensional gel electrophoresis. Differential protein spots were identified using either pre-existing proteomic reference maps or experimentally using MALDI or Q-tof mass spectroscopy.

Network construction

A bi-partite network was constructed for the genome of *E. coli* O111:H- as follows. Genes constituted nodes of type 1. The genome composition was obtained from the EcoCyc database (<http://ecocyc.org/> (Keseler, *et al.*, 2005)). Type 2 nodes were transcription and sigma factors and operons (RegulonDB v6.0 database (Gama-Castro, *et al.*, 2008)), metabolic pathways (KEGG maps: <http://www.genome.ad.jp/kegg/pathway.html>) and functional role categories (CMR-TIGR:

<http://cmr.tigr.org/tigr-scripts/CMR/CmrHomePage.cgi>). The information was completed and revised according to the EcoCyc database.

Accordingly, five classes were defined for the type 2 nodes: operons, transcription factors (TFs), sigma factors, TIGR functional categories and KEGG metabolic pathways. Genes were linked to type 2 nodes if they were regulated by them or associated with them. Thus, the edges of the network connected genes to KEGG pathways, TIGR categories, operons and also transcription and sigma factors, if genes encoded them. Arcs connected transcription and sigma factors to genes whose transcription was regulated by them.

Results and Discussion

The detection of enhancement of protein synthesis increased with the incubation time. Most of proteins were detected after 3-4 hours of incubation. In general, enhanced expression was not reduced in posterior samples. The number of proteins detected in non-acid habituated cells at pH 4.6 was similar to that of the control culture (Figure 1). Slightly smaller numbers of proteins were detected for the acid habituated cells inoculated at pH 4.6.

The network derived from the non-acid habituated culture inoculated at pH 4.6 was different from that of the acid habituated culture. There was not any protein in common detected during the lag of both cultures. When comparing with the proteins enhanced in the control culture, the translation elongation factors, EF-Tu, that binds aminoacylated tRNAs to form the ternary complex, and the α subunit of the RNA polymerase were enhanced in both the non-acid habituated cells inoculated at pH 4.6 and in the control culture. The phosphoglycerate kinase, P_{gk}, involved in glycolysis was detected in both the acid habituated and the control culture.

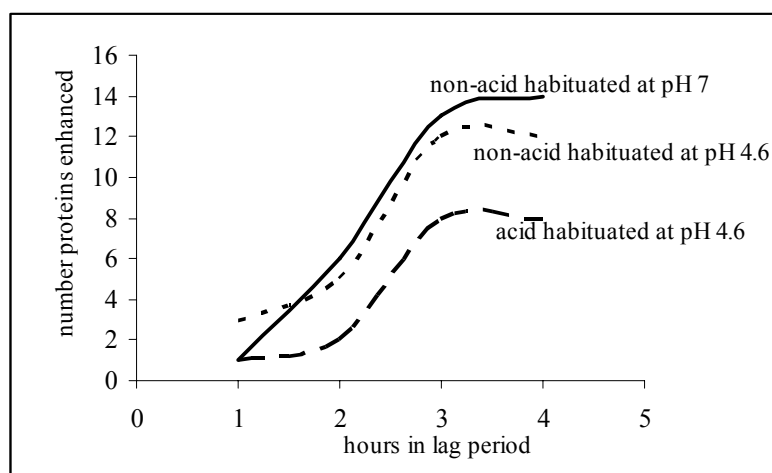


Figure 1. Number of proteins with enhanced synthesis during the lag period of acid and non-acid habituated cells inoculated at pH 4.6 and in a control culture non-acid habituated inoculated at pH 7

Figure 2 shows the main cellular functions and pathways associated to the proteins enhanced during the lag period. In non-acid habituated cells inoculated at pH 4.6, enhanced proteins were associated with transcription factors, membrane transporters for carbohydrates, alcohol and organic acids, DNA repair and components of the 'general secretory pathway'.

The proteins detected in acid habituated cells inoculated at pH 4.6 were associated to glycolysis, the TCA cycle, alanine and aspartate metabolism and chaperon systems involved in folding and stabilization of proteins. There was not any function in common during the lag period of acid and non-acid habituated cells inoculated at pH 4.6. In general, acid habituated cells enhanced proteins related to energy and anabolic metabolism, being these activities more similar to the control culture than to the non-acid habituated cells inoculated at pH 4.6.

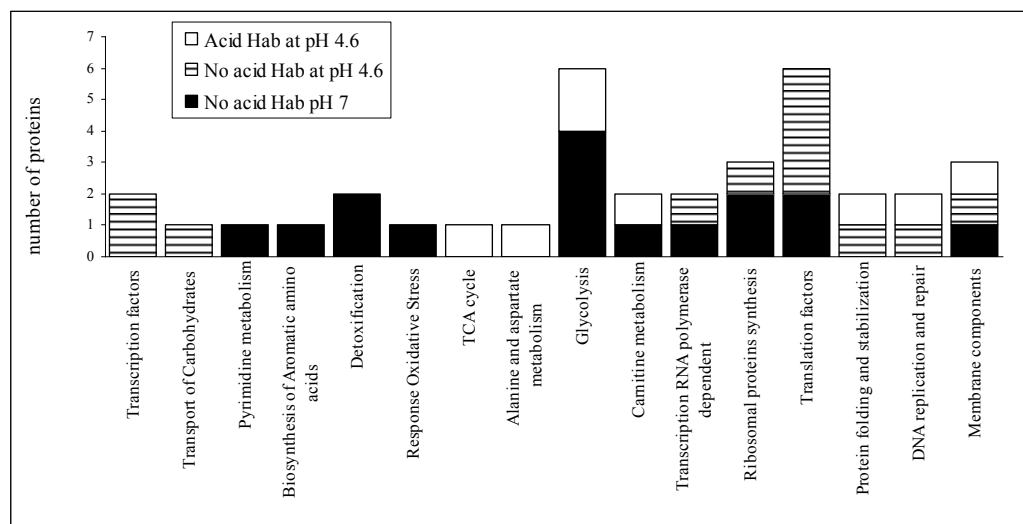


Figure 2. Cellular functions and metabolic pathways associated to the proteins enhanced during the lag period of acid and non-acid habituated cells inoculated at pH 4.6 and in a control culture non-acid habituated inoculated at pH 7

Proteins enhanced in the control culture were related to the metabolism of nucleotides and amino acids, glycolysis, ribosomal proteins, transcription and translation factors. Also a detoxification system for the maintenance of the redox potential was enhanced.

Proteins associated to translation, mainly elongation factors were detected in all cultures during lag time.

Conclusions

Integrating high-throughput and computational data in bacterial networks enables biologists to reconcile heterogeneous data types, find inconsistencies and generate systematic hypothesis. The functional roles and metabolic paths associated to the proteins synthesised during lag period at pH 4.6 were different in acid and non-acid habituated cells. The inferred intracellular activity during the lag period includes energy and amino acid metabolism in acid habituated cells inoculated at pH 4.6 and in the control culture. In non-acid habituated cells inoculated at low pH, activity is related to transport of macromolecules through the membrane and DNA repair.

Acknowledgements

CP thanks the fellowship from the OECD Co-operative Research Programme: Biological Resource Management for Sustainable Agricultural Systems funding her stay at the School of Agricultural Science, University of Tasmania and the support from the BBSRC core strategic grant 42230A

References

Gama-Castro, S., Jimenez-Jacinto, V., Peralta-Gil, M., Santos-Zavaleta, A., Penaloza-Spinola, M.I., Contreras-Moreira, B., Segura-Salazar, J., Muniz-Rascado, L., Martinez-Flores, I., Salgado, H., Bonavides-Martinez, C., Abreu-Goodger, C., Rodriguez-Penagos, C., Miranda-Rios, J.,

- Morett, E., Merino, E., Huerta, A.M., Trevino-Quintanilla, L., Collado-Vides, J., 2008. RegulonDB (version 6.0): gene regulation model of Escherichia coli K-12 beyond transcription, active (experimental) annotated promoters and Textpresso navigation. *Nucleic Acids Res* 36, D120-124.
- Keseler, I.M., Collado-Vides, J., Gama-Castro, S., Ingraham, J., Paley, S., Paulsen, I.T., Peralta-Gil, M., Karp, P.D., 2005. EcoCyc: a comprehensive database resource for Escherichia coli. *Nucleic Acids Res* 33, D334-337.